Programa de Doctorado en Salud Pública, Ciencias Médicas y Quirúrgicas

MEDICINA REGENERATIVA DEL ESTROMA CORNEAL PARA EL TRATAMIENTO DEL QUERATOCONO AVANZADO: RESULTADOS CLÍNICOS Y EVOLUCIÓN DE LA MICROSCOPÍA CONFOCAL

TESIS DOCTORAL EN COTUTELA

Realizada y defendida por

MONA EL ZARIF

Director de la tesis

DR. JORGE L. ALIÓ SANZ

Director de la tesis

DR. NEHMAN MAKDISSY

Codirector de la tesis

DR. JORGE L. ALIÓ DEL BARRIO

UNIVERSIDAD MIGUEL HERNÁNDEZ DE ELCHE

2021

Doctoral Program in Public Health, Medical and Surgical Sciences

REGENERATIVE MEDICINE OF THE CORNEAL STROMA FOR ADVANCED KERATOCONUS: CLINICAL OUTCOMES AND CONFOCAL MICROSCOPY EVOLUTION

DOCTORAL THESIS UNDER JOINT SUPERVISION

REALIZED AND DEFENDED BY

MONA EL ZARIF

Director of the thesis

DR. JORGE L. ALIÓ SANZ

Director of the thesis

DR. NEHMAN MAKDISSY

Codirector of the thesis

DR. JORGE L. ALIÓ DEL BARRIO

UNIVERSIDAD MIGUEL HERNÁNDEZ DE ELCHE

2021

ESTA TESIS DOCTORAL SE BASA EN SEIS ARTÍCULOS CIENTÍFICOS Y CUATRO CAPITULOS DE LIBROS. SE PRESENTA A TRAVÉS DE UN COMPENDIO DE PUBLICACIONES.

THIS DOCTORAL THESIS IS BASED ON SIX SCIENTIFIC ARTICLES AND FOUR BOOK CHAPTERS. IS PRESENTED THROUGH A COMPENDIUM OF PUBLICATIONS.

ESTA TESIS DOCTORAL SE BASA EN SEIS ARTICULOS CIENTIFICOS PUBLICADOS Y CUATRO CAPITULOS DE LIBROS. SE PRESENTA MEDIANTE UN COMPENDIO DE PUBLICACIONES:

1. Alió del Barrio, J.L., Arnalich-Montiel, F., De Miguel, M.P., El Zarif, M., Alió, J.L., 2021. **Corneal stroma regeneration: preclinical studies**. Exp. Eye Res. 202, 108314. https://doi.org/10.1016/j.exer.2020.108314

- Factor de impacto y cuartil de Exp. Eye Res. En JCR.: FI (3,011), (Q1), y Rango = 12/60.

Año 2019

- Cuartil de Exp. Eye Res. en SJR: (Q1) en 2020.

Este artículo científico del compendio de publicaciones con referencia (240) de la publicación científica acreditada para esta tesis, es un artículo de revisión, consiste de un resumen de toda la evidencia científica existente en la etapa experimental preclínica de nuestro equipo de investigación en el campo de la medicina regenerativa del estroma corneal. Está vinculado con la justificación de esta tesis doctoral.

2. Alió, J., Alió Del Barrio, J., El Zarif, M., Azaar, A., Makdissy, N., Khalil, C., Harb, W., El Achkar, I., Jawad, Z., De Miguel, M., 2019. **Regenerative surgery of the corneal stroma for advanced keratoconus: 1-year outcomes**. Am J Ophthalmol 203, 53–68. https://doi.org/10.1016/j.ajo.2019.02.009

- Factor de impacto y cuartil de Am J Ophthalmol en JCR: FI (4,013), (Q1), y Rango = 7/60. Año 2019.
- Cuartil de Am J Ophthalmol en SJR: (Q1) en 2019.

Este artículo científico del compendio de publicaciones, con referencia (177) de la publicación científica acreditada para esta tesis doctoral. Presenta los resultados a los 12 meses de la implantación de **ADASCs** autólogos en **G-1** y la implantación de injertos estromales descelularizados con o sin **ADASCs** autólogas para pacientes con queratocono avanzado en **G-2 y G-3**. Está vinculado con la hipótesis, objetivos, material y métodos, resultados, discusión y conclusiones de esta tesis doctoral.

3. El Zarif, M, Alió, J., Alió del Barrio, J., Abdul Jawad, K., Palazón-Bru, A., Abdul Jawad, Z., De Miguel, M., Makdissy, N., 2021. **Corneal stromal regeneration therapy for advanced keratoconus: long-term outcomes at 3 years**. Cornea 40, 741–754. https://doi.org/10.1097/ICO.0000000000002646

- Factor de impacto y cuartil de Cornea en JCR: FI (2,215), (Q2), Rango = 25/60 Año 2019.
- Cuartil de Cornea en SJR: (Q1) en 2020.

Este artículo científico del compendio de publicaciones, con referencia (180) de la publicación científica acreditada para esta tesis doctoral. Presenta los resultados a los tres años de la implantación de las **ADASCs** autólogas y la implantación de injertos estromales descelularizados con o sin **ADASCs** autólogas para pacientes con queratocono avanzado en los grupos 1, 2 y 3. Está

vinculado con la hipótesis, objetivos, material y métodos, resultados, discusión y conclusiones de esta tesis doctoral.

4. El Zarif, M, Abdul Jawad, K., Alió del Barrio, J., Abdul Jawad, Z., Palazón-Bru, A., De Miguel, M., Saba, P., Makdissy, N., Alió, J., 2020. **Corneal stroma cell density evolution in keratoconus corneas following the implantation of adipose mesenchymal stem cells and corneal laminas: an in vivo confocal microscopy study**. IOVS 61, 22. https://doi.org/10.1167/iovs.61.4.22

- Factor de impacto y cuartil de IOVS en JCR: FI (3,470), (Q1), y Rango = 10/60. Año 2019
- Cuartil de IOVS en SJR: (Q1) en 2020.

Este artículo científico del compendio de publicaciones, con referencia (179) de la publicación científica acreditada para esta tesis doctoral. Presenta los resultados de la biomicroscopía confocal al año tras la implantación de **ADASCs** autólogas y la implantación de injertos estromales descelularizados con o sin **ADASCs** autólogas para pacientes con queratocono avanzado en los grupos 1, 2 y 3. Está vinculado con la hipótesis, objetivos, material y métodos, resultados, discusión y conclusiones de esta tesis doctoral.

5. El Zarif, Mona, Alió del Barrio, J.L., Arnalich-Montiel, F., De Miguel, M.P., Makdissy, N., Alió, J.L., 2020. **Corneal stroma regeneration: new approach for the treatment of cornea disease**. APJO 9, 571–579. https://doi.org/10.1097/APO.0000000000000337

- Factor de impacto y cuartil de APJO en SCI: FI (2.62), (Q2). Año 2021.

Este artículo científico del compendio de publicaciones con referencia (241) de la publicación científica acreditada para esta tesis, es un artículo de revisión que presenta un resumen integrado de la metodología y los resultados, basado en la evidencia de los estudios clínicos experimentales realizados por nuestro grupo de investigación en el tema de la regeneración del estroma corneal para el tratamiento de enfermedades corneales, particularmente en el queratocono. Este artículo está vinculado con los métodos, resultados, discusión y conclusiones de esta tesis doctoral.

6. El Zarif, Mona, Alió, J.L., Alió del Barrio, J.L., De Miguel, M.P., Abdul Jawad, K., Makdissy, N., 2021. **Corneal stromal regeneration: a review on human clinical studies for treatement of keratoconus**. Front Med 8, 650724. https://doi.org/10.3389/fmed.2021.650724

- Factor de impacto y cuartil de Front Med en JCR: FI (3,90), (Q1), y Rango = 29/165. Año 2019.
- Cuartil de Front Med en SJR: (Q1) en 2019.

Este artículo científico del compendio de publicaciones con referencia (242) de la publicación científica acreditada para esta tesis, es un artículo de revisión que presenta un resumen integrado de la metodología y los resultados de los estudios clínicos en humanos informados en la literatura revisada sobre el tema "regeneración del estroma corneal humano" y "terapia de mejora de la córnea". Además, esta revisión ofrece una comparación de los resultados entre los diferentes estudios recientes realizados por otros autores y nuestro estudio. Este artículo está vinculado con los métodos, resultados, discusión y conclusiones de esta tesis doctoral.

7. El Zarif, M., Abdul Jawad, K., Alió, J.L., 2019. **Confocal microscopy of the cornea in a clinical model of corneal stromal expansion using adipose stem cells and corneal decellularized laminas in patients with keratoconus.** In: Alió JL, Alió del Barrio JL, Arnalich-Montiel F, (Eds.), Corneal Regeneration therapy and surgery. 1st ed. Springer, pp. 363–386. https://doi.org/10.1007/978-3-030-01304-2_24

Este capítulo científico del compendio de publicaciones con referencia (105) de la publicación científica acreditada para esta tesis. Está vinculado con material y métodos, resultados y discusión de esta tesis doctoral.

8. Alió J.L., **El Zarif M**, Alió del barrio J.L., **Cellular therapy of the corneal stroma: a new type of corneal surgery for keratoconus and corneal dystrophies a translational research experience.** 1st ed. Elsevier. (Accepted in 2020. Ahead of print).

Este capítulo científico del compendio de publicaciones con referencia (41) de la publicación científica acreditada para esta tesis. Está vinculado con la introducción, métodos, resultados, discusión y conclusión de esta tesis doctoral.

9. Alió del barrio JL, **El Zarif M**, Alió JL., 2021**. Anterior segment OCT: observations in corneal stroma regeneration**, In: Alió J.L., Alio del Barrio J.L., (Eds.), Text and Atlas of Anterior Segment OCT. Springer Nature, pp. 207–210. https://doi.org/10.1007/978-3-030-53374-8_9

Este capítulo científico del compendio de publicaciones con referencia (254) de la publicación científica acreditada para esta tesis. Está vinculado con material y métodos, resultados y conclusión de esta tesis doctoral.

10. El Zarif M, Alió J.L., Alió del Barrio J.L., **Advanced therapy of the human corneal stroma in keratoconus with stem cells.** (Accepted in 2021. Ahead of print).

Este capítulo científico del compendio de publicaciones con referencia (251) de la publicación científica acreditada para esta tesis. Está vinculado con la introducción, materiales y métodos, resultados, discusión y conclusión de esta tesis doctoral.

PATENTE

Una de las producciones importantes de nuestro estudio que pudimos registrar una Patente en el Líbano *Nº 1115.* Registrado como producto médico.

Título: "New Cornea: Medication for the Treatment of Corneal Dystrophies, Leukomas and Related Opacities of the Human Eye".

VINCULACIÓN DE LA PATENTE

La patente que pudimos registrar está vinculada a la técnica y procedimiento metodológico, incluye todo el procedimiento completo del procesamiento de laboratorio previo a la cirugía de las láminas y las **ADASCs**.

EL TEXTO PRINCIPAL DE LA PATENTE

REPÚBLICA LIBANESA

El Ministerio de Economía y Comercio
Dirección General de Economía y Comercio
Departamento de Propiedad y Protección Intelectual

PATENTE

11155

El Director General de Economía y Comercio, en virtud de la Ley N°240 del 08/07/2000 y en particular a sus artículos 16 y 17, relativos a las patentes y de conformidad con la Resolución N°152 del 16 de julio del 1939 (en aplicación al Acuerdo de la Unión de París relativo a la Protección de la Propiedad Industrial a fecha del 20/03/1883),

Y en virtud de la solicitud presentada a fecha del 29/03/2017 por Dña. Mona Hussein Al-Zarif, domiciliada en: Al-Makassed building, Riad El-Solh, Sidón, Líbano, y el Profesor Jorge Luciano Alió Y Sanz, residente en España. En virtud del acta de petición reseñada y dispuesta por la Autoridad de Protección de la Propiedad Intelectual del 29/03/2017,

SE LE OTORGA A

Dña. **Mona Hussein El-Zarif**, domiciliada en: Al-Makassed Building, Riad Al-Solh Street, Sidon, Líbano y al Profesor **Don Jorge Luciano Alió Y Sanz**, residente en España, **la Patente relativa a:** Distrofias Corneales de Leucoma. Un fármaco para el tratamiento de la Distrofia Corneal y todo lo relacionado con las opacidades de la córnea humana "Leucoma". Se otorga por un período de veinte años desde la fecha de presentación de su petición solicitada a fecha del 29/03/2017 y registrada bajo el número #11155.

PUBLICACIONES PREDOCTORALES DIRECTAMENTE RELACIONADAS CON ESTA TESIS DOCTORAL

1. Alió Del Barrio, J., El Zarif, M., De Miguel, M., Azaar, A., Makdissy, N., Harb, W., El Achkar, I., Arnalich-Montiel, F., Alió, J., 2017. **Cellular therapy with human autologous adipose-derived adult stem cells for advanced keratoconus**. Cornea 36, 952–960. https://doi.org/10.1097/ICO.0000000000001228

- Factor de impacto y cuartil de Cornea en JCR: FI (2,464), (Q2), Rango = 19/59. Año 2017
- Cuartil de Cornea en SJR: (Q1) en 2017.

Este artículo con referencia (30) en esta tesis doctoral, presenta los resultados a los seis meses de la primera aplicación en **G-1** de la implantación autóloga de células madre mesenquimales adultas autólogas derivadas del tejido adiposo (**ADASCs)** dentro del estroma corneal en pacientes con queratocono avanzado. Está vinculado con la hipótesis, objetivos, material y métodos, resultados, discusión y conclusiones de esta tesis doctoral.

2. Alió Del Barrio, J., El Zarif, M., Azaar, A., Makdissy, N., Khalil, C., Harb, W., El Achkar, I., Jawad, Z., de Miguel, M., Alió, J., 2018. **Corneal stroma enhancement with decellularized stromal laminas with or without stem cell recellularization for advanced keratoconus**. Am J Ophthalmol 186, 47–58. https://doi.org/10.1016/j.ajo.2017.10.026

- Factor de impacto y cuartil de Am J Ophthalmol en JCR: FI (4,483), (Q1), Rango = 6/60. Año 2018.
- Cuartil de Am J Ophthalmol en SJR: (Q1) en 2018.
- Este artículo es: **UNO DE LOS ARTÍCULOS DE AJO MÁS CITADOS DESDE 2018**.

Este artículo con referencia (31) en esta tesis doctoral, presenta los resultados a los seis meses para la segunda y tercera aplicación en **G-2** y **G-3** mediante la implantación de láminas estromales descelularizadas con o sin **ADASCs** autólogas para pacientes con queratocono avanzado. Está vinculado con la hipótesis, objetivos, material y métodos, resultados, discusión y conclusiones de esta tesis doctoral.

THIS DOCTORAL THESIS IS BASED ON SIX PUBLISHED SCIENTIFIC ARTICLES AND FOUR BOOK CHAPTERS. IT IS PRESENTED THROUGH A COMPENDIUM OF PUBLICATIONS:

1. Alió del Barrio, J.L., Arnalich-Montiel, F., De Miguel, M.P., El Zarif, M., Alió, J.L., 2021. **Corneal stroma regeneration: preclinical studies**. Exp. Eye Res. 202, 108314. https://doi.org/10.1016/j.exer.2020.108314

- Impact factor and quartile of Exp. Eye Res. in JCR: FI (3,011), (Q1), and Rank = 12/60. Year-2019.
- Quartile of Exp. Eye Res. in SJR: (Q1) in 2020.

This scientific article of the compendium of publications with reference (240) of the scientific publication accredited for this thesis, is a review article, it consists of a summary of all the scientific evidence existing in the preclinical experimental stage of our research team in the field of corneal stromal regenerative medicine. It is linked to the justification of this doctoral thesis.

2. Alió, J., Alió Del Barrio, J., El Zarif, M., Azaar, A., Makdissy, N., Khalil, C., Harb, W., El Achkar, I., Jawad, Z., De Miguel, M., 2019. **Regenerative surgery of the corneal stroma for advanced keratoconus: 1-year outcomes**. Am J Ophthalmol 203, 53–68. https://doi.org/10.1016/j.ajo.2019.02.009

- Impact factor and quartile of Am J Ophthalmol in JCR: FI (4,013), (Q1), and rank = 7/60. Year-2019.
- Quartile of Am J Ophthalmol in SJR: (Q1). Year-2019.

This scientific article of the compendium of publications, with reference (177) of the accredited scientific publication for this doctoral thesis. It presents the twelve-month outcomes of the implantation of autologous **ADASCs** in **G-1**, and the implantation of decellularized stromal grafts with or without autologous **ADASCs** for patients with advanced keratoconus in **G-2**, and **G-3**. It is linked to the hypothesis, objectives, material and methods, results, discussion, and conclusions of this doctoral thesis.

3. El Zarif, M, Alió, J., Alió del Barrio, J., Abdul Jawad, K., Palazón-Bru, A., Abdul Jawad, Z., De Miguel, M., Makdissy, N., 2021. **Corneal stromal regeneration therapy for advanced keratoconus: long-term outcomes at 3 years**. Cornea 40, 741–754. https://doi.org/10.1097/ICO.0000000000002646

- Impact factor and quartile of Cornea in JCR: FI (2,215), (Q2), and Rank= 25/60. Year-2019
- Quartile of Cornea in SJR: (Q1). Year-2020.

This scientific article of the compendium of publications, with reference (180) of the accredited scientific publication for this doctoral thesis. It presents three-year outcomes of the implantation of autologous **ADASCs**, and the implantation of decellularized stromal grafts with or without autologous **ADASCs** for patients with advanced keratoconus in groups 1,2, and 3. It is linked to the hypothesis, objectives, material and methods, results, discussion, and conclusions of this doctoral thesis.

4. El Zarif, M, Abdul Jawad, K., Alió del Barrio, J., Abdul Jawad, Z., Palazón-Bru, A., De Miguel, M., Saba, P., Makdissy, N., Alió, J., 2020. **Corneal stroma cell density evolution in keratoconus corneas following the implantation of adipose mesenchymal stem cells and corneal laminas: an in vivo confocal microscopy study**. IOVS 61, 22. https://doi.org/10.1167/iovs.61.4.22

- Impact factor and quartile of IOVS in JCR: FI (3,470), (Q1), and Rank = 10/60. Year-2019
- Quartile of IOVS in SJR: (Q1). Year-2020.

This scientific article of the compendium of publications, with reference (179) of the scientific publication accredited for this doctoral thesis. It presents one-year confocal biomicroscopy outcomes following the implantation of autologous **ADASCs,** and the implantation of decellularized stromal grafts with or without autologous **ADASCs** for patients with advanced keratoconus in groups 1,2 and 3. It is linked to the hypothesis, objectives, material and methods, results, discussion, and conclusions of this doctoral thesis.

5. El Zarif, Mona, Alió del Barrio, J.L., Arnalich-Montiel, F., De Miguel, M.P., Makdissy, N., Alió, J.L., 2020. **Corneal stroma regeneration: new approach for the treatment of cornea disease**. APJO 9, 571–579. https://doi.org/10.1097/APO.0000000000000337

- Impact factor and quartile of APJO in SCI: FI (2.62), (Q2). Year-2021

This scientific article of the compendium of publications with reference (241) of the scientific publication accredited for this thesis, is a review article that presents an integrated summary of the methodology and the results, based on the evidence of the experimental clinical studies carried out by our research group on the issue of corneal stroma regeneration for the treatment of corneal diseases, particularly in keratoconus. This article is linked to the methods, results, discussion, and conclusions of this doctoral thesis.

6. El Zarif, Mona, Alió, J.L., Alió del Barrio, J.L., De Miguel, M.P., Abdul Jawad, K., Makdissy, N., 2021. **Corneal stromal regeneration: a review on human clinical studies for treatement of keratoconus**. Front Med 8, 650724. https://doi.org/10.3389/fmed.2021.650724

- Impact factor and quartile of Front Med in JCR: FI (3,900), (Q1), Rank = 29/165. Year-2019.
- Quartile of Front Med in SJR: (Q1). Year-2020.

This scientific article of the compendium of publications with reference (242) of the scientific publication accredited for this thesis, is a review article that presents an integrated summary of the methodology and results of clinical studies in humans reported in the reviewed literature on the topic "human corneal stroma regeneration" and "corneal enhancement therapy". Furthermore, this review offers a comparison of the results between the different recent studies carried out by other authors and our study. This article is linked to the methods, results, discussion, and conclusions of this doctoral thesis.

7. El Zarif, M., Abdul Jawad, K., Alió, J.L., 2019. **Confocal microscopy of the cornea in a clinical model of corneal stromal expansion using adipose stem cells and corneal**

decellularized laminas in patients with keratoconus. In: Alió JL, Alió del Barrio JL, Arnalich-Montiel F, (Eds.), Corneal Regeneration therapy and surgery. 1st ed. Springer, pp. 363–386. https://doi.org/10.1007/978-3-030-01304-2_24

This scientific chapter of the compendium of publications with reference (105) of the scientific publication accredited for this thesis. It is linked to material and methods, results and discussion of this doctoral thesis.

8. Alió J.L., **El Zarif M**, Alió del barrio J.L., **Cellular therapy of the corneal stroma: a new type of corneal surgery for keratoconus and corneal dystrophies a translational research experience.** 1st ed. Elsevier. (Accepted in 2020. Ahead of print).

This scientific chapter of the compendium of publications with reference (41) of the scientific publication accredited for this thesis. It is linked to the introduction, methods, results, discussion, and conclusion of this doctoral thesis.

9. Alió del barrio JL, **El Zarif M**, Alió JL., 2021**. Anterior segment OCT: observations in corneal stroma regeneration**, In: Alió J.L., Alio del Barrio J.L., (Eds.), Text and Atlas of Anterior Segment OCT. Springer Nature, pp. 207–210. https://doi.org/10.1007/978-3-030-53374-8_9

This scientific chapter of the compendium of publications with reference (254) of the scientific publication accredited for this thesis. It is linked to material, methods, results, and conclusion of this doctoral thesis.

10. **El Zarif M**, Alió J.L., Alió del Barrio J.L., 2021 **Advanced therapy of the human corneal stroma in keratoconus with stem cells.** (Accepted in 2021. Ahead of print).

This scientific chapter of the compendium of publications with reference (251) of the scientific publication accredited for this thesis. It is linked to the introduction, materials, and methods, results, discussion, and conclusion of this doctoral thesis.

PATENT

One of the importante productions of our study that we could register a *Patent in Lebanon nº 11155. Registrated as medical product.*

Title: "New cornea: Medication for the Treatment of Corneal Dystrophies, Leukomas and Related Opacities of the Human Eye".

PATENT LINK

The patent is linked to the technique and methodological procedure, it includes the entire procedure of the laboratory processing before the implantation surgery of the **ADASCs** and the decellularized/recellularized laminas with **ADASCs.**

THE MAIN TEXT OF THE PATENT

Lebanese Republic
The Ministry of Economy and Trade
General Directorate of Economy and Trade
Intellectual Property and Protection Department
PATENT

The General Director of Economy and Trade, in accordance with Law No.240 of 07/08/2000 in particular articles 16 and 17 related to patents. In accordance with Resolution No. 152 of 16th July 1939 (in application of the Paris Union Agreement on the Protection of Industrial Property of 03/20/1883), based on the request submitted on 29th March 2017, by Ms. Mona Hussein Al-Zarif, resident in the Al Makassed Building, Riad El-Solh street, Sidon, Lebanon, and Professor Jorge Luciano Alió Y Sanz, resident in Spain. Based on the act of presentation of the aforementioned application organized by the Head of the Intellectual Property Protection Authority on 29th March 2017.

GRANTS:

Mrs. Mona Hussein El-Zarif, whose address is at: Al-Makassed Building, Riyadh Al-Solh Street, Sidon, Lebanon, and Professor Jorge Luciano Alió y Sanz, resident in Spain, **the Patent** related to Leucoma Corneal Dystrophies. A drug for the treatment of Corneal Dystrophy and everything related to opacities of the human cornea "Leucoma". This is for a period of twenty years from the presented date of the application submitted on 03/29/2017 and registered under number # 11155.

PREDOCTORAL PUBLICATIONS DIRECTLY RELATED TO THIS DOCTORAL THESIS

1. Alió Del Barrio, J., El Zarif, M., De Miguel, M., Azaar, A., Makdissy, N., Harb, W., El Achkar, I., Arnalich-Montiel, F., Alió, J., 2017. **Cellular therapy with human autologous adipose-derived adult stem cells for advanced keratoconus**. Cornea 36, 952–960. https://doi.org/10.1097/ICO.0000000000001228

- Factor de impacto y cuartil de Cornea en JCR: FI (2,464), (Q2), Rango = 19/59. Año 2017
- Cuartil de Cornea en SJR: (Q1) en 2017.

The scientific article with reference (30) in this doctoral thesis, presents the six-month outcomes for the first application in **G-1** of the implantation of autologous adipose-derived adult mesenchymal stem cells (**ADASCs**) within the corneal stroma in patients with advanced keratoconus. It is linked to the hypothesis, objectives, material and methods, results, discussion, and conclusions of this doctoral thesis.

2. Alió Del Barrio, J., El Zarif, M., Azaar, A., Makdissy, N., Khalil, C., Harb, W., El Achkar, I., Jawad, Z., de Miguel, M., Alió, J., 2018. **Corneal stroma enhancement with decellularized stromal laminas with or without stem cell recellularization for advanced keratoconus**. Am J Ophthalmol 186, 47–58. https://doi.org/10.1016/j.ajo.2017.10.026

- Factor de impacto y cuartil de Am J Ophthalmol en JCR: FI (4,483), (Q1), Rango = 6/60. Año 2018.
- Cuartil de Am J Ophthalmol en SJR: (Q1) en 2018.
- Este artículo es: **UNO DE LOS ARTÍCULOS DE AJO MÁS CITADOS DESDE 2018**.

The scientific article with reference (31) in this doctoral thesis, presents the Six-month outcomes for the second and third applications in **G-2**, and **G-3** by the implantation of decellularized stromal laminas with or without autologous **ADASCs** for patients with advanced keratoconus. It is linked to the hypothesis, objectives, material and methods, results, discussion, and conclusions of this doctoral thesis.

El Dr. "Jorge L. Alió Sanz" director, el Dr. "Nehman Makdissy" director, y el Dr. "Jorge L. Alió del Barrio" codirector de la tesis doctoral titulada **"**MEDICINA REGENERATIVA DEL ESTROMA CORNEAL PARA EL TRATAMIENTO DEL QUERATOCONO AVANZADO: RESULTADOS CLÍNICOS Y EVOLUCIÓN DE LA MICROSCOPÍA CONFOCAL**"**

Informan:

Que Dña. "Mona El Zarif" ha realizado bajo nuestra supervisión el trabajo titulado **"**MEDICINA REGENERATIVA DEL ESTROMA CORNEAL PARA EL TRATAMIENTO DEL QUERATOCONO AVANZADO: RESULTADOS CLÍNICOS Y EVOLUCIÓN DE LA MICROSCOPÍA CONFOCAL**"**

Conforme a los términos y condiciones definidos en su Plan de Investigación y de acuerdo al Código de Buenas Prácticas de la Universidad Miguel Hernández de Elche, cumpliendo los objetivos previstos de forma satisfactoria para su defensa pública como tesis doctoral.

Lo que firmamos para los efectos oportunos, en Alicante a 22 de Julio de 2021

Directores/a de la tesis Codirector/a de la tesis

Dr. "Jorge L. Alió Sanz", Dr. "Nehman Makdissy" directores.

Dr. "Jorge L. Alió del Barrio" codirector

The Dr . “Jorge L. Alió Sanz” director, the Dr. “Nehman Makdissy” director, and the Dr. “Jorge L. Alió del Barrio” codirector of the doctoral thesis titled *“***REGENERATIVE MEDICINE OF THE CORNEAL STROMA FOR ADVANCED KERATOCONUS: CLINICAL OUTCOMES AND CONFOCAL MICROSCOPY EVOLUTION***”*

Inform:

That Mrs. “Mona El Zarif” has carried out under our supervision the work entitled *“***REGENERATIVE MEDICINE OF THE CORNEAL STROMA FOR ADVANCED KERATOCONUS: CLINICAL OUTCOMES AND CONFOCAL MICROSCOPY EVOLUTION***”*

In accordance with the terms and conditions defined in its Research Plan and in accordance with the Code of Good Practices of the Miguel Hernández de Elche University, fulfilling the objectives set satisfactorily for its public defense as a doctoral thesis.

What we sign for the appropriate purposes, in Alicante on July 22, 2021

Directors/of the thesis

Codirector/ of the thesis

Dr. “Jorge L. Alió Sanz”, Dr. “Nehman Makdissy” directors.

Dr.M. “Jorge L. Alió del Barrio” codirector

PROGRAMA DE DOCTORADO EN SALUD PÚBLICA, CIENCIAS MÉDICAS Y QUIRÚRGICAS

D. Vicente Francisco Gil Guillén, Coordinador del Programa de Doctorado en Salud Pública, Ciencias Médicas y Quirúrgicas de la Universidad Miguel Hernández de Elche,

AUTORIZA:

La presentación y defensa como tesis doctoral del trabajo "MEDICINA REGENERATIVA DEL ESTROMA CORNEAL PARA EL TRATAMIENTO DEL QUERATOCONO AVANZADO: RESULTADOS CLÍNICOS Y EVOLUCIÓN DE LA MICROSCOPÍA CONFOCAL" realizado por Dña. Mona El Zarif bajo la dirección del Dr. Jorge Luciano Alió Sanz, la codirección del Dr. Jorge Alió del Barrio en la Universidad Miguel Hernández y el director D. Nehman Makdissy en la Lebanese University. De acuerdo a la información recibida sobre las evaluaciones previas realizadas en cumplimiento de la normativa general vigente y la propia de la Universidad Miguel Hernández y según lo certificado por las personas que han realizado la tutoría y dirección, la tesis cumple los requisitos para proceder a su defensa pública.

En Sant Joan d' Alacant, a 22 de julio de 2021

The Academic Committee of the Doctoral School of Sciences and Technology of the Biotechnology program of the Lebanese University, represented by the Dean of the doctoral school **Prof. Dr. Fawaz EL OMAR**

AUTHORIZES:

The presentation and defense as a Doctoral Thesis ¨ **REGENERATIVE MEDICINE OF THE CORNEAL STROMA FOR ADVANCED KERATOCONUS: CLINICAL OUTCOMES AND CONFOCAL MICROSCOPY EVOLUTION ¨,** carried out by Ms. Mona El Zarif under the direction of Dr. Jorge Luciano Alió Sanz, the co-direction of Dr. Jorge Alió del Barrio at the Miguel Hernández University, and the director Dr. Nehman Makdissy at the Lebanese University. According to the information received on the previous evaluations carried out in compliance with the general regulations in force and that of the Miguel Hernández University, and the Lebanese University as certified by the doctors who have carried out the tutoring and direction, the thesis completes the requirements to proceed with its public defense.

What I sign in Beirut on July 22, 2021

Dr. Fawaz EL OMAR, the Dean of the Doctoral School of Sciences and Technology of the Biotechnology program of the Lebanese University.

LA HISTORIA DE NUESTRO PROYECTO

Una fuerza extraña me atrae de la otra punta del Mediterráneo. ¿Una noche en el verano del 2011, me llamó una persona misteriosa, me decía por qué no implantamos células madre derivadas del tejido adiposo en la córnea de pacientes con queratocono avanzado? Digamos es como cuando se calló la manzana sobre la cabeza del sabio Isaac Newton, entonces descubrió la ley de la gravedad…

Esta idea no dejaba de llamarme intensamente, me puse entonces a buscar en internet sobre un científico que había iniciado el implante de células madre en la córnea, me salía información sobre el Prof. Jorge Alió y Sanz, que reside en Alicante y trabaja en la Clínica de Vissum. Él realizó con su equipo en un estudio experimental el trasplante de células madre adiposas humanas en la córnea de los conejos.

¡Yo conozco a Vissum, claro que sí, es una clínica moderna y preciosa de oftalmología, la miraba de fuera cuando era estudiante de optometría en la Universidad de Alicante con mucha admiración, cada uno de nosotros soñaba con pasar por allí, hacer prácticas o trabajar con este equipo maravilloso!

Ha querido el destino misterioso en marzo del 2012 que viajásemos, nuestro amigo el doctor biólogo Nehman Makdissy, mi marido Ziad y yo a la otra punta del Mediterráneo. Quedamos con el Prof. Jorge Alió, nos reunimos con el mismo Dr. Alió para explicarle nuestra idea de proyecto en implementar el estudio experimental realizado por él y su equipo con pacientes que padecen queratocono con el fin de sustituir el trasplante corneal clásico en cirugía regenerativa de la córnea. ¡Entonces, todo era un sueño en aquella reunión, no pensaba ninguno de nosotros que estábamos sembrando la semilla de un proyecto científico pionero, y que esta semilla iba a crecer y salir a la vida, con su tallo tan tierno, que pudiera abrir el camino de las dificultades y las imposibilidades!

¿Quién desencadenó el misterio yo o el profesor Alió? Realmente no lo sé, pero sí que estoy segura de que nosotros dos somos personas muy resistentes, fuertes, con mucha decisión y voluntad, nunca nos rendimos, cuando iba a caerme me sostenía él con mucha fuerza, me empujaba a seguir y a avanzar, quizás yo como soy una mujer más tierna que él, me sentía a veces debilitada, pero él siempre era el maestro, el animador, la luz en la obscuridad, nunca se cansaba en contestar a mis dudas, escuchar mis ideas, y respetar mis opiniones.

¡Si ha querido el destino que conocieramos al Profesor Alió! ¡A esta persona única y extraordinario en este mundo!

Hoy, han crecido completamente las plumas sobre mis alas, mi Profesor me suelta diciéndome: Vuela a lo más alto mi doctoranda, ¡las águilas solo viven en los picos de las cimas! Le contesto a mi Profesor: Volaré, pero seguiré influida por ti, ¡siguiendo siempre tu sombra!

! Gracias a Dios, gracias a ALLAH que me ha dado esta oportunidad en esta vida, junto con mi profesor, nuestro equipo, el apoyo de mi extraordinaria familia, especialmente de mi encantador esposo Ziad, mis dos queridos y adorables hijos Karim y Sima, mis amigos ¡He podido pasar en este camino glorioso del conocimiento y la ciencia, he podido dejar mis pequeñas y modestas huellas en este mundo!

THE HISTORY OF OUR PROJECT

I feel a strange power draws me from the other end of the Mediterranean. One night in the summer of 2011, a mysterious person called me and asked me why we not try implanting stem cells derived from adipose tissue in the cornea of patients with advanced keratoconus? Let's say it was like when the apple fell on the head of the wise Isaac Newton and he then discovered the law of gravity.

This idea kept calling me intensely, so I started searching on the internet for a scientist who had started been experimenting in this field. I got information about Prof. Jorge Alió y Sanz, who lives in Alicante and works in the Vissum Clinic. He conducted with his team an experimental study on the transplantation of human adipose stem cells into the cornea of rabbits.

I knew Vissum. Of course, I did. It is a modern and beautiful ophthalmology clinic. I looked at it from the outside with much admiration when I was an optometry student at the University of Alicante, each of us dreamed to be there, doing an internship or working with this wonderful team!

Destiny wanted Ziad my husband, and our friend and biologist doctor Nehman Makdissy and I to travel to the other end of the Mediterranean in March 2012, where we met Prof. Jorge Alió. We explained to him our project idea to implement the experimental study carried out by him and his team with patients suffering from keratoconus in order to replace the classic corneal transplant with regenerative corneal surgery. So, everything was a dream in that meeting and little did we know that we were sowing the seed of a pioneering scientific project and that this seed was going to grow and come to life, with its so tender stem, it could open the way for many possibilities!

Who triggered the mystery me or Professor Alió? I do not know! But I am sure that both of us are very persistent, strong people, with a lot of dedication and will. We never gave up, when I was going to fall, he would grab me with great force, he would push me to continue and move forward. Perhaps since I am a more lenient woman than he is, I sometimes felt weakened, but he was always the teacher, the animator, the light in the dark, he was never tired of answering my questions, listening to my ideas, and respecting my opinions.

¡Yes, destiny wanted us to meet Professor Alió! ¡This unique and extraordinary person in this world!

Today, thank to my Professor, my wings have fully grown. He lets go of me saying: Fly to the top, my doctoral student, eagles only live on the peaks! I answer my Teacher: I will fly, but I will continue to be influenced by you, always following your shadow!

Thank you, God, thank you ALLAH who has given me this opportunity in my life, together with my Professor, our team, the support of my extraordinary family, especially my lovely husband Ziad, my two dear, and adorable children Karim and Sima, and my friends. I have been able to pass on this glorious path of knowledge and sciences. I have been able to leave my small and modest footprint in this world!

AGRADECIMIENTOS

En primer lugar me gustaría agradecer al Profesor Jorge L. Alió y Sanz director y tutor de esta tesis doctoral, quien ha contribuido a mi formación como optometrista e investigadora y que continuamente me ha guiado, orientado, inspirado durante el desarrollo de este trabajo tan pionero, por los apoyos morales que siempre me daba para seguir adelante y superar todos los obstáculos. Profesor Alió es una persona única en este mundo, es un ejemplo a seguir.

A mi marido, Ziad Abdul Jawad, por su constante apoyo en mi formación y por su lucha para ayudarme a crecer profesionalmente. Además, por el tiempo que le he robado a él y a nuestros adorables hijos Karim y Sima para que yo pudiese dedicarme a esta tesis, mi familia me daba un apoyo continuo, recibía de ellos mucho cariño y entendimiento, juntos lo hemos conseguido.

A mis padres que descansan en paz, seguro que están orgullosos por haber hecho sus sueños realidad al obtener el título de doctora e interesante investigadora.

A mi Director del Líbano Prof. Nehman Makdissy que me ha acompañado desde la idea inicial hasta la implementación del proyecto en el Líbano, por su apoyo moral continuo y por su trabajo tan meticuloso. Juntos sembramos la semilla de este proyecto innovador.

A mi codirector de tesis Dr. Jorge L. Alió del Barrio porque él es el que inició una parte importante del trabajo pre-clínico, y siguió con nuestro grupo todos los procedimientos clínicos.

A María Asunción por la gran labor y apoyo que llevaba a cabo con todos los doctorandos. A toda la comisión de profesores que se interesaban mucho y nos daban consejos para mejorar nuestros trabajos de investigación hasta la elaboración de la tesis.

Al Prof. Fawaz el Omar, por el apoyo profesional que me daba siempre.

A Dr. Samar por su apoyo.

A los coautores de los distintos artículos científicos, por compartir sus conocimientos y por su colaboración, sobre todo Dr. Ibrahim Achkar que fue quién me inspiró la primera idea del implante de células madre adiposas, Dra. Maria P De Miguel por su gran labor en el traslado del know how, y por su continuo apoyo, he ganado además de este proyecto una gran amiga, y Dr. Antonio Palazón por su gran profesionalidad, amabilidad y paciencia.

A Óptica General (Saida-Líbano) por haber financiado este proyecto de investigación.

Al Instituto Oftalmológico de Alicante, Vissum (Grupo Miranza) por haberme facilitado la transferencia del proyecto.

A laser Vision (Hazmyeh-Libano) por haberme facilitado todos los estudios diagnósticos en su centro, sobre todo a Peggy Saba que se ofrecía continuamente para este proyecto.

A Reviva (Bsalim-Líbano) por haber facilitado y participado en el trabajo de laboratorio.

A todos los pacientes de esta aplicación clínica porque han creído en nuestro trabajo y responsabilidad, colaboraban de una forma ideal. Gracias a ellos también se ha podido realizar esta etapa clínica importante.

A mi hermana Rola de quién he estado ausente mucho tiempo que no he podido pasar con ella ni con su familia, a mis hermanos Hassan, Ghassan y Mohammed El Zarif, y a todos mis familiares El Zarif y Abdul Jawad, sobre todo a los sobrinos y sobrinas, especialmente las que viven en España a Dina y Aurora ya que he recibido todo su apoyo durante mi tiempo de solitud en el extranjero, a los sobrinos Riwa, Yasmine, Hour, Ray, Abdul-Rahman…. por el apoyo que me ofrecían, y a mis queridas primas Racha, Thouraya, Roa, Zakya, Nour, Samar, Souhair, Mohammad, Mahmoud, Souheil, Talal and Houssam….

A todas mis tías Khayrya, Fatima y Bader que me rodean con tanto cariño e interés para recuperarme de la perdida tan dura de mi madre!

A mi gran amiga Olena por su apoyo de todo tipo.

A todos mis amigos y queridos, Basma, Nahed, Yolla, Souhayla, Rola, Maya, Ana, Hiba, Samer, Wissam, Louay and Salim… siempre he recibidode ellos muchos ánimos.

A mí maestro en la vida Mahmoud, y a mí maestro de conocimiento tecnológico Haytham.

A todos los empleados de Óptica General que me apoyaban siempre precisamente Rasha.

Un agradecimiento especial al Instituto Alicantino de Cultura, Juan Gil-Albert por haberme valorado y ofrecido un premio y ayuda tan importante para mi investigación.

A todos los que me desean el continuo éxito.

¡Dedico este trabajo a los ojos tan preciosos de mi familia pidiendo de Allah que las proteja!

¡A los ojos de mi país el Líbano que no cesan de llorar del destrozo continuo y el sufrimiento interminable que recibe!

¡A los ojos de mi madre y mi padre que se descansan en paz y me miran desde el horizonte tan lejano!

¡A los ojos de mi profesor que no cesa de sacrificar y salvar a los miles de ojos de pacientes, que Dios le bendiga a él y a toda su familia!

¡A todos los que viven en la oscuridad y sueñan con un rallo de luz que ilumine sus ojos!

ACKNOWLEDGEMENT

First of all, I would like to thank Professor Jorge L. Alió y Sanz, the director and tutor of this doctoral thesis, who has contributed to my training as an optometrist and researcher and who has continuously guided, oriented, inspired me during the development of this pioneering work and for the moral support that kept me going and overcome all the obstacles. Professor Alió is a unique person in this world. He is an example to follow.

To my husband, Ziad Abdul Jawad, for his constant support, care and affection, and for his struggle to help me grow professionally. Also, for the time I have stolen from him and our adorable children Karim and Sima so that I could dedicate myself to this thesis. My family gave me continuous and unwavering support. They were very understanding and together we have achieved it.

To my parents who rest in peace, they are surely proud of me for having achieved their dream of obtaining the title of doctor and a researcher.

To my Lebanese Director Prof. Nehman Makdissy who has accompanied me from the initial idea to the implementation of the project in Lebanon, for his continuous moral support and his meticulous work. Together we sow the grains of this innovative project.

To my co-director of thesis Dr. Jorge L. Alió Del Barrio because he is the one who initiated an important part of the preclinical work, and followed all the clinical procedures with our group.

To María Asunción for the great work and support she did for all of us doctoral students. To the entire committee of professors who gave us a lot of interest and advice to improve our research work all the way to the preparation of the thesis.

To Prof. Fawaz el Omar, for the professional support he always gave me.

To Dr. Samar for his support.

To the co-authors of the different scientific articles, for sharing their knowledge and for their collaboration, especially Dr. Ibrahim Achkar, who was the one who had inspired me with the first idea of the adipose stem cell implant, and Dr. Maria P Demiguel for her great work in transferring the know-how, and for her continuous support. I have also gained a great friend from this project. In addition to Dr. Antonio Palazón for his great professionalism, kindness and patience.

To Optica General (Saida-Libano) for having financed this research project.

To the Ophthalmological Institute of Alicante, Vissum (Grupo Miranza) for having facilitated the transfer of the project.

To laser Vision (Hazmyeh-Lebanon) for having provided me with all the diagnostic tools at their center, especially to Peggy Saba who continuously volunteered for this project.

To Reviva (Bsalim-Lebanon) for having facilitated and participated in the laboratory work.

To all the patients of this clinical application, for their belief in our work and responsibility, they collaborated in an ideal way. Thanks to them it was possible to carry out this important clinical stage.

To my sister Rola who I have been absent from for a long time to and her family, my brothers Hassan, Ghassan, and Mohammed El Zarif, and all my relatives El Zarif and Abdul Jawad, especially the nephews and nieces precisely those who live in Spain Dina and Aurora because I have received all the support from them during my time of solitude abroad. For the nephews Riwa, Yasmine, Hour, Ray, Abdul-Rahman… for the support they offered me, and my lovely cousins Racha, Thouraya, Roa, Zakya, Nour, Samar, Souhair, Mohammad, Mahmoud, Souhail, Talal, and Houssam….

To all my aunts Khayrya, Fatima, and Badre who surrounded me with such affection and interest to recover the hard loss of my mother!

To my great friend Olena for her support of all kinds of her.

To all my friends and loved ones, Basma, Nahed, Yolla, Souhayla, Rola, Maya, Ana, Hiba, Samer, Wissam, Louay and Salim… I have always received from them a lot of encouragement.

To my teacher in life Mahmoud, and to my teacher of technological knowledge Haytham.

To all my employees of Optica General who always supported me, especially Rasha.

To everyone who wishes me the continued success.

A special thanks to the Instituto Alicantino de Cultura, Juan Gil-Albert for having valued me and offered me such an important award and help for my research.

¡I dedicate this work to the precious eyes of my family asking Allah to protect them!

¡To the eyes of my country, Lebanon, who do not stop crying from the continuous destruction and endless suffering that it receives!

¡To the eyes of my mother and father who rest in peace and look at me from the far horizon!

¡To the eyes of my professor who does not stop sacrificing and saving thousands of patients' eyes, may God bless him and all his family!

¡To all those who live in darkness and dream of a ray of light that illuminates their eyes!

RESUMEN EN CASTELLANO

INTRODUCCIÓN. La terapia celular del estroma corneal ha ido ganando interés en los últimos años como un tratamiento alternativo potencial para las enfermedades del estroma corneal, como cicatrices, distrofias y ectasias corneales. Las ectasias corneales, como el queratocono, se caracterizan por un adelgazamiento progresivo, abombamiento y distorsión de la córnea, con pérdida secundaria de la visión por el alto astigmatismo irregular. La rehabilitación visual de las ectasias corneales avanzadas requiere técnicas de trasplante corneal penetrante o lamelar, que presentan varias inconvenientes, como el rechazo del injerto, el fracaso y la lenta recuperación visual debido a los altos niveles de astigmatismo postoperatorio inducido en relación con la sutura. La ingeniería tisular de la córnea tiene como objetivo solucionar este problema, aunque la estructura altamente compleja del estroma corneal limita la utilidad en la práctica clínica real de sustitutos corneales estromales que se han intentado crear en el laboratorio, debido a su falta de propiedades de transparencia o resistencia adecuadas.

Por otro lado, nuestro grupo demostró en estudios con animales que las células madre mesenquimales de fuentes extraoculares son capaces no solo de sobrevivir y diferenciarse *in vivo* en queratocitos humanos adultos, sino también de producir nuevo colágeno dentro del estroma del huésped. También, han demostrado ser capaces de mejorar cicatrices corneales preexistentes o la transparencia corneal en modelos animales para distrofias corneales.

Además, se han descrito varias técnicas de descelularización corneal, capaces de proporcionar una matriz extracelular corneal acelular (**ECM**). Estos constructos que actúan a modo de “andamios” se han vuelto más populares en los últimos años, ya que proporcionan un entorno natural para el crecimiento y la diferenciación de las células, son bien tolerados incluso por receptores

xenogénicos, ya que los componentes de la **ECM** generalmente se conservan incluso entre diferentes especies.

Teniendo en cuenta toda esta evidencia, nuestro grupo informó por primera vez en un ensayo clínico de fase 1 de los posibles beneficios de la terapia celular del estroma corneal con células madre mesenquimales extraoculares en pacientes con queratocono avanzado, con o sin un "transportador" coadyuvante compuesto de estroma corneal de donante humano descelularizado, demostrando excelentes niveles de seguridad y una moderada eficacia.

OBJETIVOS. Esta investigación, innovadora y pionera en su campo, tiene como objetivo a largo plazo el poder reemplazar la necesidad de trasplante de córnea clásico en estos pacientes con queratocono terminal. Consideramos que las células madre mesenquimales adultas derivadas del tejido adiposo humano pueden ser una fuente ideal de células madre para la regeneración del estroma corneal. Además de eso, hemos demostrado que las láminas de matriz corneal humana acelular sembradas con estas células madre autólogas mesenquimales derivadas de tejido adiposo humano no causan reacciones de inflamación ni rechazo. Los resultados de esta terapia celular avanzada se estudiarán en esta tesis durante un período de 3 años.

DISEÑO. El diseño del estudio se trató de una serie de casos prospectivo, intervencionista con aleatorización entre los diferentes grupos, y no enmascarado por la imposibilidad del mismo (el tipo de intervención en visible en el postoperatorio por parte del observador).

MÉTODOS. Se distribuyeron catorce ojos consecutivos de pacientes con queratocono avanzado (grado IV según clasificación dela RETICS) en 3 grupos experimentales. Los pacientes del grupo-1 (**G-1**) se sometieron a la implantación de células madre mesenquimales adultas autólogas derivadas del tejido adiposo (**ADASCs**) de forma aislada (3×10^6 células/1 ml de **PBS**) (n = 5). Grupo-2 (**G-2**), los pacientes recibieron el implante intraestromal de una lámina de estroma corneal

humano donante descelularizada (n = 5) de 120 micras (**µm**) de grosor y sin células madre acompañantes. Grupo-3 (**G-3**), los pacientes recibieron la implantación intraestromal de una lámina de estroma corneal humano donante descelularizada (también de 120 **µm** de grosor) posteriormente recelularizada con **ADASCs** autólogas de tejido adiposo ($1x10^6$ células/1 ml de **PBS**) (n = 4). Las **ADASCs** se obtuvieron mediante liposucción electiva de la parte inferior de la nalga con pacientes mujeres, y de la misma parte o de la cadera con los hombres. Se realizó la implantación de **ADASCs** y láminas corneales de donantes humanos descelularizadas / **ADASCs** -relelularizadas dentro de un bolsillo realizado por femtosegundo bajo anestesia tópica.

SEGUIMIENTO. Los seguimientos de los pacientes se efectuaron al primer día, una semana y 1, 3, 6, 12 y 36 meses. Todos los resultados principales y segundarios se registraron a lo largo de la evaluación preoperatoria, así como al primer mes, 3, 6, 12 y 36 meses postoperatorios y eran: Agudeza visual a distancia sin ayuda (**UDVA**), agudeza visual a distancia corregida (**CDVA**), agudeza visual a distancia corregida con lentes de contacto rígidas (**CLDVA**) en (decimal equivalente a la escala logMar), esfera refractiva (**Rx Sphr**) en dioptrías (**D**), cilindro refractivo (**Rx Cyl**) (**D**), el grosor corneal central (**CCT**) (**µm**) medido mediante el segmento anterior de tomografía de coherencia óptica **(AS-OCT)**, topografía corneal de Scheimpflug del punto más delgado (**Thinnest point**) (**µm**), volumen de la córnea (**CV**) (mm^3), aberrometría corneal, queratometría media anterior (**Anterior Km**) (**D**), queratometría media posterior (**Posterior Km**) (**D**), queratometría máxima (**Kmax**) (**D**), cilindro topográfico (**Topo Cyl**) (**D**), biomicroscopía con lámpara de hendidura, fundoscopía, presión intraocular (**IOP**), y finalmente la evolución de las células y la densidad de queratocitos, así como la evolución de las láminas implantadas descelularizadas/recelularizadas con **ADASCs** se estudiaron mediante la microscopía confocal con Rostock Cornea Module, durante un período de 12 meses.

RESULTADOS. No se observaron complicaciones como turbidez o infección durante el seguimiento de los 3 años. Se Obtuvo una mejora de casi 1 línea en la escala LogMar en **UDVA**, 2 líneas en **CDVA** y 2,3 líneas en la escala LogMar en **CLDVA** en todos los casos. Se obtuvo una disminución estadísticamente significativa en la agudeza visual a distancia corregida **CDVA** en los **G-2** y **G-3** [P < 0,001] en comparación con el **G-1**. La **CLDVA** mostró un empeoramiento estadísticamente significativo en el **G-2** [P < 0,001] en comparación con el **G-1**. Se observó un aumento estadísticamente significativo en el grosor corneal central **CCT** en el **G-2** [P = 0.012] y en el **G-3** [P < 0.001], en el punto más delgado de la topografía corneal de Scheimpflug en el **G-2** [P = 0.007] y el **G -3** [P = 0,001] en comparación con el **G-1**. Se observó un aumento significativo [P < 0,001] en la densidad celular en el estroma corneal anterior y posterior con todos los grupos, en el estroma medio con el **G-1**, en las superficies anterior y posetriores de las y dentro del tejido implantado. No hubo una asociación significativa entre la recelularización y la presencia de tejido fibrótico.

CONCLUSIONES. La implantación intraestromal de **ADASCs** y láminas de estroma corneal humano descelularizado /**ADASCs**-recelularizado no tuvo complicaciones durante el período de 3 años. La técnica mostró una mejoría moderada en **UDVA** y **CDVA** en queratocono avanzado, y una mejoría estadísticamente significativa en todos los casos que recibieron implante intrastromal de una lámina de estroma corneal humano donante descelularizada/recelularizadas con **ADASCs**. Esta innovadora técnica de regeneración del estroma corneal puede proporcionar a los pacientes adecuados una solución alternativa al trasplante de córnea clásico, en una recuperación menos invasiva, más segura y fácil con un período postoperatorio mucho menos prolongado.

Estas innovadoras técnicas de regeneración del estroma corneal pueden proporcionar a los pacientes adecuados una solución alternativa al trasplante de córnea clásico, de una forma menos invasiva, más segura y con un postoperatorio mucho menos prolongado.

PALABRAS CLAVES: medicina regenerativa, bioingeniería corneal, terapia con células madre, queratocono, células madre adultas derivadas de tejido adiposo (**ADASCs**), queratocitos, microscopía confocal corneal, terapia corneal avanzada.

SUMMARY IN ENGLISH

INTRODUCTION. Cellular therapy of the corneal stroma, with either ocular or extraocular stem cells, has been gaining a lot of interest over the last decade as a potential alternative treatment for corneal stroma diseases such as corneal dystrophies, scarring, and ectasias. Corneal ectasias, such as keratoconus, are characterized by progressive thinning, bulging, and distortion of the cornea, with secondary loss of vision due to high irregular astigmatism. Visual rehabilitation of advanced corneal ectasias requires penetrating or lamellar corneal transplantation techniques, which present several drawbacks, such as graft rejection, failure, and slow visual recovery due to high levels of induced postoperative astigmatism concerning the suturTissue engineering of the cornea aims to solve this problem, although the highly complex structure of the corneal stroma limits the usefulness of these corneal substitutes in real clinical practice, to date, in the laboratory, due to a lack of either transparency or strength properties.

On the other hand, our group previously demonstrated in animal studies that mesenchymal stem cells from extraocular sources are capable to not only survive and differentiate *in vivo* into adult human keratocytes but also producing new collagen within the host stroma**.** They improve preexisting scars or corneal transparency in animal models for corneal dystrophies.

Besides, several corneal decellularization techniques have been described, which provide an acellular corneal extracellular matrix (**ECM).** These scaffolds have become more popular in the last few years as they provide a natural environment for the growth and differentiation of cells and are tolerated well even by xenogeneic recipients, as components of the **ECM** are generally preserved among species.

Considering all this evidence, we report herein the thesis for the first time in phase 1 clinical trial the possible benefits of cellular therapy of the corneal stroma with extraocular mesenchymal stem

cells in patients with advanced keratoconus, with or without a carrier (scaffold) composed of decellularized human donor corneal stroma, demonstrating excellent safety levels and a promising efficacy.

OBJECTIVES. This research study is innovative and pioneer, its objective is to replace classical corneal transplant in these patients with end-stage keratoconus. We believe that human adult mesenchymal stem cells derived from adipose tissue can be a source of cells for the regeneration of the corneal stroma**.** In addition to that, acellular human corneal matrix laminas seeded with autologous human adipose-derived mesenchymal stem cells will not cause any inflammation or rejection**.** The outcomes of this advanced cell therapy will be studied in this thesis for a period of 3 years.

DESIGN. The design of this study is prospective series of cases, interventional with randomization among the different groups, and no masked (the type of intervention is visible in the postoperative period by the observer).

METHODS. Fourteen consecutive patients with advanced keratoconus (grade IV according to RETICS classification) were enrolled into 3 experimental groups: Group-1 (**G-1**) of patients underwent intrastromal implantation of autologous adipose-derived adult stem cells (**ADASCs)** alone (3x 10^6cells/1 mL of **PBS**) (n = 5), Group 2 (**G-2**) of patients received the intrastromal implantation of a decellularized donor human corneal stroma lamina (120 **µm** thick) (n =5) without **ADASCs**, and Group 3 (**G-3**) of patients received intrastromal implantation of a decellularized donor human corneal stromal lamina (120 **µm** thick) subsequently recellularized with autologous **ADASCs** (1x10^6cells/1 ml of **PBS**) (n = 4). Autologous **ADASCs** were obtained by elective liposuction from the lower part of the cleft with female patients, and with men from the lower part

of the cleft or the hip. Implantation of **ADASCs**, and decellularized/**ADASCs**-recellularized human donor corneal laminas was performed into a femtosecond pocket under topical anesthesia.

FOLLOW-UP. The patients were followed at 1 day, 1 week, and at 1, 3, 6, 12, and 36 months. The assessment of all the main and secondary outcomes were recorded throughout the preoperative assessment, as well as the 1^{st}, 3^{rd}, 6^{th}, 12^{th}, and 36 postoperative months, and were: Unaided distance visual acuity (**UDVA**), corrected distance visual acuity (**CDVA**), rigid contact lens distance visual acuity (**CLDVA**) in (decimal equivalent to the logMar scale), refractive sphere (**Rx Sphr**) in diopters (**D**), refractive cylinder (**Rx Cyl**) (**D**), central corneal thickness (**CCT**) (**µm**) measured by the anterior segment optical coherence tomography (**AS-OCT**), Scheimpflug corneal topography thinnest point (**Thinnest point**) (**µm**), cornea volume (**CV**) (mm^3), corneal aberrometry, anterior mean keratometry (**Anterior Km**) (**D**), posterior mean keratometry (**Posterior Km**) (**D**), maximum keratometry (**Kmax**) (**D**), topographic cylinder (**Topo Cyl**) (**D**), slit-lamp biomicroscopy, fundoscopy, intraocular pressure, and finally the evolution of the cells and the keratocytes density, as well as the evolution of the implanted decellularized/recellularized laminas with **ADASCs** were studied by confocal microscopy with Rostock Cornea Module, for a period of 12 months.

RESULTS. No complications such as haze or infection were observed during the 3-year follow-up. We obtained an improvement of almost 1 line in the LogMar scale in **UDVA**, 2 lines in **CDVA**, and 2.3 lines in the LogMar scale in **CLDVA** in all cases. A statistically significant decrease in corrected distance visual acuity **CDVA** was obtained in **G-2** and **G-3** [$P < 0.001$] when compared to **G-1**. The **CLDVA**, showed a statistically significant worsening in **G-2** [$P < 0.001$] compared to **G-1**. A statistically significant increase in central corneal thickness **CCT** was observed in **G-2** [$P = 0.012$] and **G-3** [$P < 0.001$], in the Scheimpflug corneal topography **Thinnest point** in **G-2** [$P = 0.007$] and **G-3** [$P = 0.001$] when compared to **G-1**. A significant increase [$P < 0.001$] was observed

in the cell density in the anterior and posterior corneal stroma with all the groups, in the mid stroma with **G-1**, on the anterior, and posterior surfaces of the laminas, and within the implanted tissue. There was not a significant association between recellularization and the presence of fibrotic tissue.

CONCLUSIONS. Intrastromal implantation of **ADASCs** and decellularized/**ADASCs**-recellularized human corneal stroma laminas did not have complications for a period of. The technique showed a moderate improvement in **UDVA**, and **CDVA** in advanced keratoconus, and statistically significant improvement in all the cases that received intrastromal implantation of a decellularized/ recellularized laminas with **ADASCs** from human corneal stromal donor. This innovative corneal stromal regeneration technique can provide suitable patients with an alternative solution to classic corneal transplantation, in a less invasive, safer, and easy recovery with a much less prolonged postoperative period.

KEYWORDS: regenerative medicine, corneal bioengineering, stem cell therapy, keratoconus, adipose-derived adult stem cells (**ADASCs**), keratocytes, corneal confocal microscopy, advanced corneal therapy.

GLOSARIO DE ABREVIATURAS

3D: Tres dimensiones
3rdorder RMS: RMS de aberración de tercer orden.
4thorder RMS: RMS de aberración de cuarto orden.
ADASCs: Células madre adultas derivadas del tejido adiposo.
AHS: Suero humano autólogo.
ALDH: Aldehído deshidrogenasa.
Anterior Km: Queratometría media anterior.
AS-OCT: Segmento anterior de tomografía de coherencia óptica.
BM: Membrana de Bowman.
BM-MSCs: Células madre mesenquimales derivadas de la médula ósea.
CCT: Espesor corneal central.
CDVA: Agudeza visual a distancia corregida.
CECs: Células epiteliales de la córnea.
CL: lentes de contacto.
CLDVA: Lente de contacto rígida para agudeza visual a distancia.
CSA: Ciclosporina-A.
CSSCs: Células madre del estroma corneal.
CV: Volumen de la córnea.
CXL: Cross-linking.
D: Dioptría.
DALK: Queratoplastia lamelar anterior profunda.
DM: Membrana de Descemet.
DMEM: Medio de Eagle modificado por Dulbecco.
DNA: Ácido desoxirribonucleico.
ECD: Densidad de células endoteliales.
ECM: Matriz extracelular corneal.
ESCs: Células madre embrionarias.
GAGs: Glucosaminoglicanos.
h-ADASCs: Células madre humanas adultas derivadas del tejido adiposo.
h-CSSCs: Células madre humanas del estroma corneal.
HGF: Factor de crecimiento de hepatocitos.
HOA RMS: RMS de aberración de alto orden.
ICRS: Segmentos de anillos intracorneales.
IFATS: Federación Internacional de Terapias Adiposas.
IGF-I: Factor de crecimiento similar a la insulina-I.
IHC: Inmunohistoquímico.
IL: Interleuquina.
IOP: Presión intraocular.
iPSCs: Células madre pluripotentes inducidas.

G-CSF: Factor estimulante de colonias de granulocitos.
KC: Quimioatrayente de queratinocitos.
Kmax: Queratometría máxima.
LESCs: Células madre epiteliales limbares.
LIF: Factor inhibidor de leucocitos.
LKP: Queratoplastia lamelar.
LOA RMS: RMS de aberración de bajo orden.
Mip: Proteína inflamatoria de macrófagos.
miRNA: Microácido ribonucleico.
MCP: Proteína quimioatrayente de monocitos.
MMP: Metaloproteinasas de matriz.
mRNA: Ácido ribonucleico mensajero.
MSCs: Células madre mesenquimales.
OCT: Tomografía de coherencia óptica.
PAX6: Genhomeótico de caja emparejada 6, un factor de transcripción
PBS: Solución tampón fosfato salino.
PDGF: Factor de crecimiento derivado de plaquetas.
PKP: Queratoplastia penetrante.
Posterior Km: Queratometría media posterior.
PRK: Queratectomía fotorrefractiva.
RA: Ácido retinoico.
RGP: Rígido permeable al gas.
RMS: Raíz cuadrada media.
RNA: ácido ribonucleico.
Rx Cyl: Cilindro refractivo.
Rx Sphr: Esfera refractiva.
SD: Desviación Estándar.
SDS: Dodecil sulfato de sodio.
SVF: Fracción vascular del estroma.
TEM: Microscopía electrónica de transmisión.
TGF: Factor de crecimiento transformante.
TGFβ1: Factor de crecimiento transformante beta 1.
TNF: Factor de necrosis tumoral.
Topo Cyl: Cilindro topográfico.
TSG6: Gen estimulado por el factor de necrosis tumoral α 6.
TUNEL: Marcado terminal de desoxinucleotidiltransferasa biotina-dUTP.
UCMSCs: Células madre mesenquimales del cordón umbilical.
UDVA: Agudeza visual a distancia sin ayuda.
UMSCs: Células madre mesenquimales umbilicales.
UV: Ultravioleta.
VEGF: Factor de crecimiento endotelial vascular.
µm: Micra.

GLOSSARY OF ABBREVIATIONS

3D: Three dimensions.
3rd order RMS: Third order aberration RMS.
4th order RMS: Fourth order aberration RMS.
ADASCs: Adipose-derived adult stem cells.
AHS: Autologous human serum.
ALDH: Aldehyde dehydrogenase.
Anterior Km: Anterior mean keratometry.
AS-OCT: Anterior segment optical coherence tomography.
BM: Bowman's membrane.
BM-MSCs: Bone marrow mesenchymal stem cells.
CCT: Central corneal thickness.
CDVA: Corrected distance visual acuity.
CECs: Corneal epithelial cells.
CL: Contact lenses.
CLDVA: Rigid contact lens distance visual acuity.
CSA: Cyclosporine-A.
CSSCs: Corneal stroma stem cells.
CV: Cornea volume.
CXL: Cross-linking.
D: Diopter.
DALK: Deep anterior lamellar keratoplasty.
DM: Descemet membrane.
DMEM: Dulbecco's modified eagle medium.
DNA: Deoxyribonucleic acid.
ECD: Endothelial cell density.
ECM: Extracellular corneal matrix.
ESCs: Embryonic Stem Cells.
GAGs: Glycosaminoglycans.
h-ADASCs: Human adipose-derived adult stem cells.
h-CSSCs: Human Corneal stroma stem cells.
HGF: Hepatocyte growth factor.
HOA RMS: High order aberration RMS.
ICRS: Intracorneal ring segments.
IFATS: International Federation of Adipose Therapeutics.
IGF-I: Insulin-like growth factor-I.
IHC: Immunohistochemical.
IL: Interleukin.
IOP: Intraocular pressure.
iPSCs: Induced pluripotent stem cells.

G-CSF: Granulocyte colony-timulating factor**.**
KC: Keratinocyte chemoattractant.
Kmax: Maximum keratometry.
LESCs: Limbal epithelial stem cells.
LIF: Leukocyte inhibitory factor.
LKP: Lamellar keratoplasty.
LOA RMS: Low order aberration RMS.
Mip: Macrophage inflammatory protein.
miRNA: micro ribonucleic acid.
MCP: Monocyte chemoattractant protein.
MMP: Matrix metalloproteinases.
mRNA: Messenger ribonucleic acid.
MSCs: Mesenchymal stem cells.
OCT: Optical coherence tomography.
PAX6: Paired box homeotic gene 6, a transcription factor.
PBS: Phosphate-buffered solution.
PDGF: Platelet-derived growth factor.
PKP: Penetrating keratoplasty.
Posterior Km: Posterior mean keratometry.
PRK: Photorefractive keratectomy.
RA: Retinoic acid.
RGP: Rigid gas permeable.
RMS: Root mean square.
RNA: Ribonucleic acid.
Rx Cyl: Refractive cylinder.
Rx Sphr: Refractive sphere.
SD: Standard deviation.
SDS: Sodium dodecyl sulfate.
SVF: Stromal vascular fraction.
TEM: Transmission electron microscopy.
TGF: Transforming growth factor.
TGFβ1: Transforming growth factor beta 1.
TNF: Tumor necrosis factor.
Topo Cyl: Topographic cylinder.
TSG6: Tumor necrosis factor-α-stimulated gene 6.
TUNEL: Terminal deoxynucleotidyl transferase biotin-dUTP nick end labeling.
UCMSCs Umbilical Cord Mesenchymal Stem Cells.
UDVA: Unaided distance visual acuity.
UMSCs: Umbilical mesenchymal stem cells.
UV: Ultraviolet.
VEGF: Vascular endothelial growth factor.
µm: Micron.

TABLA DE CONTENIDO: VERSIÓN EN ESPAÑOL

LISTA DE TABLAS

LIST OF TABLES

LISTA DE FIGURAS

LIST OF FIGURES

VERSIÓN EN ESPAÑOL

1. INTRODUCCIÓN

La terapia celular del estroma corneal ha ganado interés en los últimos años como una posible opción de tratamiento alternativo para las enfermedades del estroma corneal, como las cicatrices, distrofias y ectasias corneales. Estas enfermedades inducen la distorsión de la anatomía y fisiología de la córnea y conducen a la pérdida de su transparencia y la consiguiente pérdida de visión. El queratocono es la distrofia corneal más común con una prevalencia diversa en la población de 0.05-2.3%. Al ser una enfermedad relativamente prevalente, se observa más hoy que antes debido a las herramientas de diagnóstico más avanzadas que están disponibles para el diagnóstico de queratocono temprano (1). Se caracteriza por adelgazamiento progresivo, abultamiento y distorsión de la córnea, y causa cambios progresivos en la visión con aumento de miopía y astigmatismo miópico, irregularidad corneal y pérdida visual (2).

El estroma corneal constituye más del 90% del grosor corneal. Muchas características de la córnea, incluida su fuerza, morfología y transparencia, son atribuibles a la anatomía y propiedades del estroma corneal (3). La matriz extracelular del estroma corneal está compuesta por colágeno que forma más del 70% del peso de la córnea deshidratada, siendo el más abundante es el tipo I (75%), y proteoglicanos, incluido el queratán sulfato, que es el más abundante (65%), cuyo núcleo proteico está compuesto por lumicán, queratocán y mimecán (3). El queratocán se expresa solo en el estroma corneal, por lo que se considera en la ingeniería de tejidos como un marcador específico de diferenciación queratocítica (4). El componente celular del estroma corneal ocupa solo el 2-3% del volumen del estroma, siendo las células predominantes los queratocitos, que son células mesenquimales que derivan de la cresta neural, que se distribuyen entre las laminillas de colágeno. Los queratocitos se encuentran en estado de quiescencia en la córnea normal, y son los responsables

del recambio constante de la matriz extracelular estromal mediante la producción de colágeno, que es fundamental para el mantenimiento de la transparencia corneal. Cuando los queratocitos activan su metabolismo, se transdiferencian en fibroblastos y miofibroblastos, que participan en la curación del estroma corneal. La capacidad de renovación de los queratocitos estromales se debe a las células precursoras del estroma corneal limbar anterior, que expresa marcadores de células madre adultas (5).

El queratocono se caracteriza por una pérdida progresiva de queratocitos: su número disminuye del estroma anterior al posterior (6), que conduce a un adelgazamiento progresivo del estroma (1,6), y una disminución de la fuerza corneal (7). Esta definición es válida para la mayoría de los pacientes con queratocono, aunque pueden existir algunas variaciones en la expresión fenotípica de la enfermedad (8). La mayoría de los casos de queratocono tienen córneas delgadas y una débil resistencia mecánica relacionada con la pérdida progresiva de la densidad de los queratocitos (9). La apoptosis de queratocitos (6,10) o la liberación de enzimas que puedan ser la causa de la pérdida de queratocitos y, en consecuencia, la pérdida del estroma corneal con el tiempo (6,10). La proporción de queratocitos en el estroma corneal disminuye con la progresión de la enfermedad (6). En las etapas finales del queratocono, los aspectos clínicos de la córnea delgada y debilitada se asocian con una fuerte disminución en el número de queratocitos. Se asocia a una deformación corneal severa (6), y alteración en la ubicación del ápice corneal (11), causando una pérdida visual severa.

La prevalencia y el carácter progresivo del queratocono han llevado a proponer diferentes terapias alternativas, que en este momento se encuentran en uso, incluyendo el cross-linking (**CXL)** de colágeno, anillos y segmentos intracorneales, trasplante de córnea, y más recientemente, implante de membrana de Bowman (**BM**) (2). Por su parte, la rehabilitación visual de las ectasias

corneales avanzadas requiere técnicas de trasplante de córnea penetrantes o lamelares, las cuales presentan varios inconvenientes, como rechazo del injerto, falla y recuperación visual lenta debido a altos niveles de astigmatismo postoperatorio inducido por las suturas (2). Además, se debe considerar que en muchos países el acceso al tejido corneal del donante está limitado, aproximadamente el 53% de la población mundial no tiene acceso al trasplante de córnea (12). Por lo tanto, la demanda de córneas de donantes adecuadas está aumentando más rápido que el número de donantes, dejando a miles de pacientes curables en todo el mundo esperando un posible tratamiento (13,14). La cuantificación de la gran escasez de tejido de injerto corneal mostró que una córnea solo está disponible para 70 casos necesarios (12).

Para resolver el problema de salud global, estudios de investigación recientes se han centrado en desarrollar en el laboratorio un sustituto de la córnea que podría imitar las características de la córnea humana *in vivo* y posteriormente, ser una alternativa al tejido de un donante humano, para encontrar una alternativa al trasplante de córnea clásico, pero esto aún no se ha logrado debido a la extrema dificultad de imitar la ultraestructura altamente compleja del estroma corneal, obteniendo sustitutos que no logran suficiente transparencia o resistencia (15,16). Además, los diseños basados en andamios sintéticos han planteado algunas preocupaciones importantes, como las fuertes respuestas inflamatorias inducidas en su biodegradación o las respuestas inflamatorias crónicas inespecíficas (17). Por otro lado, recientemente se han descrito varias técnicas de descelularización corneal, que proporcionan una matriz corneal acelular (**ECM)** (18). Estos andamios han ganado un interés cada vez mayor, como proporcionan un entorno natural ideal para el crecimiento y la diferenciación de células (ya sean células de donantes trasplantadas o células del huésped en migración) (19). Además, los componentes de la **ECM** generalmente se conservan entre las especies, y la eliminación de todos los componentes celulares inmunogénicos podría abrir el

campo del xenotrasplante a los receptores humanos mediante el uso de tejido de donantes de otros animales como el cerdo, que comparte importantes similitudes con la córnea humana (20).

En los últimos años, el interés en la terapia celular del estroma corneal utilizando células madre mesenquimales (**MSCs**) de fuentes oculares o extraoculares ha ganado mucho interés; Los estudios demostraron que las **MSCs** son capaces de diferenciarse en queratocitos adultos in *vitro* e *in vivo* (3). Varios autores, incluyendo informes de nuestro grupo de investigación, han demostrado (17,19,21) que estas células madre no solo pueden sobrevivir y diferenciarse en queratocitos humanos adultos en escenarios xenogénicos sin inducir una reacción inflamatoria, sino que también: i) producen nuevo colágeno dentro del estroma del huésped (21,22), ii) modular las cicatrices preexistentes mediante la remodelación del estroma corneal (23,24), y iii) mejorar la transparencia corneal en modelos animales con distrofias corneales, reorganizando el colágeno así como en modelos animales para metabolopatías por catabolismo de proteínas acumuladas (25–28). Las células madre mesenquimales también han mostrado propiedades inmunomoduladoras en escenarios singénicos, alogénicos e incluso xenogénicos (28,29). Actualmente, están disponibles los primeros datos clínicos sobre la seguridad y la eficacia preliminar de la terapia celular del estroma corneal de los ensayos clínicos en humanos de fase 1 (30,31), que pronto pueden proporcionar una opción de tratamiento alternativa real para las enfermedades de la córnea.

Considerando la evidencia científica existente, parece que todos los tipos de las **MSCs** tienen un comportamiento similar *in* vivo (Tabla 1), y por lo tanto pueden lograr la diferenciación en queratocitos y modular el estroma corneal con propiedades inmunomoduladoras (32). También se ha informado recientemente que las **MSCs** secretan factores paracrinos como el factor de crecimiento endotelial vascular (**VEGF**), el factor de crecimiento derivado de plaquetas (**PDGF**), el factor de crecimiento de hepatocitos (**HGF**) y el factor de crecimiento transformante beta 1

(**TGFβ1**). Aunque las acciones precisas de los diferentes factores de crecimiento para la cicatrización de heridas en la córnea no se comprenden completamente, en general, parecen promover la migración celular, la supervivencia de los queratocitos mediante la inhibición de la apoptosis y regular positivamente la expresión de los genes del componente de la **ECM** en los queratocitos, lo que posteriormente mejora la reepitelización corneal y cicatrización de heridas estromales (33). Las **MSCs** se pueden obtener de muchos tejidos humanos, incluido el tejido adiposo, la médula ósea, el cordón umbilical, la pulpa dental, la encía, el folículo piloso, la córnea y la placenta (34,35).

Las células madre del estroma corneal (**CSSCs**) forman una fuente prometedora para la terapia celular, ya que la técnica de aislamiento y los métodos de cultivo se han optimizado y refinado (36); presumiblemente, deberían ser eficaces para diferenciarse en queratocitos, ya que están comprometidos con el linaje corneal. Por otro lado, aislar **CSSCs** de forma autóloga es más exigente técnicamente considerando la pequeña cantidad de tejido del que se obtienen. Además, esta técnica todavía requiere un ojo sano contralateral, que no siempre está disponible (por enfermedad bilateral). Por tanto, estos inconvenientes pueden limitar su uso en la práctica clínica. El uso alogénico de las **CSSCs** requiere tejido corneal de un donante vivo o cadavérico.

El tejido adiposo humano adulto es una buena fuente de células madre extraoculares autólogas, ya que satisface muchos requisitos: fácil acceso al tejido, alta eficiencia de recuperación celular y la capacidad de sus células madre adultas derivadas del tejido adiposo humano (**h-ADASCs**) para diferenciarse en múltiples tipos de células (queratocitos, osteoblastos, condroblastos, mioblastos, hepatocitos, neuronas, etc.) (21). Esta diferenciación celular se produce por efecto de factores o ambientes estimulantes muy específicos para cada tipo de célula, evitando la mezcla de múltiples tipos de células en distintos nichos.

Las **MSCs** derivadas de la médula ósea (**BM-MSCs**) son las más estudiadas entre las células madre mesenquimatosas, presentando un perfil similar a las células madre adultas derivadas del tejido adiposo (**ADASCs)**, pero su extracción requiere una punción de la médula ósea, que es un procedimiento complicado y doloroso que requiere anestesia general.

Las **MSCs** umbilicales (**UCMSCs**) presentan una buena alternativa, pero su uso autólogo es actualmente limitado porque el cordón umbilical generalmente no se almacena después del nacimiento.

Las células madre embrionarias (**ESCs**) tienen un gran potencial, pero también presentan importantes problemas éticos. Sin embargo, el uso de la tecnología de células madre pluripotentes inducidas (**iPSCs)** (37) podría resolver tales problemas, y su capacidad para generar queratocitos adultos ya ha sido probada *in vitro* (38).

Por último, es importante señalar que el efecto terapéutico de las **MSCs** en un tejido dañado no siempre está relacionado con la diferenciación potencial de las **MSCs** en el tejido del huésped, ya que múltiples mecanismos pueden contribuir simultáneamente a esta acción terapéutica, por ejemplo, la secreción de tróficos paracrinos. Además los factores de crecimiento son capaces de estimular las células madre residentes, producen una reducción de la lesión tisular y una activación de los efectos inmunomoduladores, en cuyo caso la diferenciación celular directa de las **MSCs** podría no ser relevante e incluso podría ser inexistente (32,39,40).

En esta tesis vamos a resumir la enfermedad del queratocono, la patogénesis moderna, la epidemiología y los diferentes factores que influyen en su aparición y desarrollo. También retomar los diferentes tipos de células madre (mesenquimales y otras) que se han propuesto para la regeneración del estroma corneal, así como la evidencia actual *in vitro* o *in vivo*, los diferentes protocolos de descelularización. Finalmente, revisar los diferentes abordajes quirúrgicos que se han

sugerido (*in vivo*) para la aplicación de la terapia con células madre para regenerar el estroma corneal.

Tabla 1. Células madre analizadas para la regeneración del estroma corneal: evidencia de diferenciación *de queratocitos o similar a queratocitos y su posible aplicación autóloga.*

	CSSCs	**BM-MSCs**	**ADASCs**	**UMSCs**	**ESCs**	**iPSCs**
Demostración de la diferenciación de queratocitos *in vitro*	Sí	Sí	Sí	Sí	Sí	Sí
Demostración de la diferenciación de queratocitos *in vivo*	Sí	Sí	Sí	Sí	No	No
Posible uso autólogo	Sí /No	Sí	Sí	Sí /No	No	Sí

CSSCs, células madre del estroma corneal; **MSCs**, células madre mesenquimatosas; **BM-MSCs**, células madre mesenquimales derivadas de la médula ósea; **ADASCs**, células madre adultas derivadas de tejido adiposo; **UMSCs**, umbilical **MSCs**; (**ESCs)**, células madre embrionarias; **iPSCs**, células madre pluripotentes inducidas. Tabla extraída del capítulo científico de Alió JL y cols. (41).

1.1. EL QUERATOCONO

1.1.1 EL QUERATOCONO NO ES UNA ENFERMEDAD TAN RARA

Desde finales de la década de 1950, las lentes de contacto (**CL**) se convirtieron en una solución parcial para la pérdida visual de los pacientes con queratocono, mientras que otros enfoques no existían, esta enfermedad potencialmente cegadora no tenía esperanzas de un tratamiento adecuado. Los pacientes con queratocono tenían la misma categoría que cualquier distrofia corneal sin tratamiento potencial y sin recomendaciones terapéuticas para realizar. Desde aquellos históricos "días negros", ha habido un tremendo progreso en el diagnóstico y tratamiento de esta enfermedad (42). De hecho, el primer injerto de córnea para el queratocono avanzado fue realizado por Edward Zirm en Praga en 1906 (43).

En las últimas décadas, debido a factores ambientales y genéticos, estamos experimentando un brote epidémico de casos de queratocono, ya que depende de lograr capacidades de diagnóstico mejoradas, precisas y más accesibles. Ahora hay un futuro mejor y pronto habrá más mejoras para estos pacientes. La enfermedad que antes era intratable ahora está comenzando a ser tratada con éxito y está dando buenos resultados visuales.

Ahora hay un futuro prometedor y pronto habrá más mejoras para estos pacientes (42). Este incremento en el número de casos ha propiciado el desarrollo de expertos en queratocono, unidades especializadas en centros oftálmicos, e incluso unas nuevas revistas especializadas (International Journal of Keratoconus and Corneal Ectatic Diseases), con tantas publicaciones dedicadas exclusivamente a esta enfermedad corneal (42).

1.1.2 TEORÍAS MODERNAS SOBRE LA PATOGENIA DEL QUERATOCONO

La patogenia del queratocono sigue siendo desconocida a pesar de numerosos estudios intensivos. Los únicos factores comúnmente identificados parecen ser el frotarse los ojos y la presencia de alergias (44).

Se han descrito formas de transmisión autosómica dominante y autosómica recesiva (45). Varios estudios sugieren la existencia de formas subclínicas dentro de los familiares de pacientes queratocónicos (46,47).

Los estudios han demostrado una distribución desigual de la enfermedad en individuos caucásicos que viven en áreas geográficas similares. También se demostró que la incidencia del queratocono es cuatro veces mayor entre los asiáticos en comparación con los caucásicos (48). Otros estudios informan que se observan diferencias relacionadas con la etnia en el curso y la gravedad de la enfermedad, lo que proporciona un fuerte argumento a favor de la presencia de un componente genético (49,50). Se observan variaciones extremas en la prevalencia del queratocono en cuanto a la etnia, este componente sin duda tiene un papel importante (46,51).

El enfoque del gen candidato se basa en el conocimiento de la bioquímica y patología de la enfermedad, que consiste en identificar mutaciones en los genes que codifican las proteínas del tejido afectado (44). Se desconoce el grado de heterogeneidad genética de esta enfermedad hasta el momento. La prueba de mutaciones de varios genes que codifican la familia puede desempeñar un papel en el desarrollo de la enfermedad del queratocono (52,53). Se intentó identificar mutaciones en genes que codifican componentes de interleucina-I **(ILI**) (54), proteasas (55,56), Inhibidores de la proteasa (57,58), y colágenos de tipo I, III, IV, V, VI, VII y VIII están presentes en la córnea. El primer gen que codifica el colágeno probado fue COL6A1, pero no hubo una relación significativa

con el queratocono (59). Se desconoce el grado de heterogeneidad genética en esta enfermedad, y las mutaciones en varios genes codificadores de familias que aún no se han probado que puedan desempeñar un papel en el desarrollo del queratocono (44). Un estudio del gen VSX1 mutado condujo a la identificación de mutaciones relacionadas entre pacientes afectados por el queratocono. Este gen codifica un factor de transcripción legítimo y también se elabora en la distrofia polimorfa posterior (52), sin embargo, solo tiene un papel entre el 0,1% y el 0,4% del queratocono familiar y, por lo tanto, su importancia en la patogénesis del queratocono sigue siendo baja (44).

Por otro lado, los estudios han demostrado que existe una fuerte concordancia de niveles elevados de interleucina 6 (**IL6**), factor de necrosis tumoral α (**TNFα**) y metaloproteinasas de matriz (**MMP9**) que se encuentran en las lágrimas de pacientes queratocónicos (60–63). **MMP9** es una de las enzimas que degradan la matriz producida por el epitelio corneal humano y regulada por la citocina **IL6**. El **TNFα** además de **IL6** se considera un factor patogénico principal en la inflamación sistémica y corneal, induce la expresión de **MMP9**, no se encontró una mayor concentración de **MMP9** estadísticamente significativa en los ojos con lágrimas queratocónicas (60). **TNFα**, **MMP9** e **IL6** estaban fuertemente y altamente regulados en el nivel de ácido ribonucleico mensajero (**mRNA**) en el epitelio de pacientes con queratocono (63). Sin embargo, los autores podrían deducir que los mediadores de la inflamación están presentes en las córneas queratocónicas. El queratocono podría ser un trastorno inflamatorio, ya que muchos estudios indican la presencia de niveles elevados de marcadores inflamatorios pero aún con hallazgos contradictorios (63–65).

En general, se piensa que el queratocono probablemente sea causado por eventos fuera de la córnea y que estos eventos son por último los responsables de la inducción de esta ectasia. El frotamiento de ojos, la atopia, el desgaste de **CL**, estrés oxidativo (61,66,67), y asociado con factores genéticos que causan la enfermedad de la córnea (68).

Además, otros estudios basados en ácido ribonucleico (**RNA**) encontraron apoptosis de queratocitos corneales. Mace y cols. demostraron que el queratocono podría estar relacionado con una desregulación de las vías de proliferación y diferenciación celular (69).

Por lo tanto, el equilibrio inadecuado entre las citoquinas (pro y antiinflamatorias, como **IL6** / **TNFα** / **IL12** / **IL17** e **IL4** / **IL10**, respectivamente) puede llevar a una función y estructura corneal patológica, lo que conduce a un aumento de la apoptosis de los metaloproteinasas y los queratocitos. Los mecanismos moleculares subyacentes exactos quedan por dilucidar. Estos estudios han demostrado que en el queratocono existe un desequilibrio estructural corneal, asociado con el estrés metabólico y un desequilibrio entre la apoptosis y la proliferación. Sin embargo, estos estudios aún no han logrado identificar un biomarcador clínicamente utilizable para detectar el queratocono o evaluar su grado de gravedad (44).

1.1.3 EPIDEMIOLOGÍA DEL QUERATOCONO

La incidencia y la prevalencia del queratocono están determinadas por su carga y, a su vez, por la prestación de servicios y programas de detección y atención médica. Además, los factores genéticos y ambientales afectan la incidencia y prevalencia de la enfermedad. La evaluación preoperatoria identificó casos de queratocono subclínico no diagnosticado previamente, y por lo tanto protegieron los pacientes del empeoramiento iatrogénico de la ectasia. Además, los casos que antes se pensaba que eran unilaterales han demostrado de ser bilaterales con las imágenes de diagnóstico modernas. Se acepta que no existe un queratocono verdaderamente unilateral, la mejora de nuestra comprensión de la epidemiología del queratocono ha aumentado enormemente nuestra comprensión de la patogenia (70).

1.1.3.1 Incidencia y prevalencia.

Una revisión de los primeros estudios entre 1936 y 1966 sobre la prevalencia del queratocono encontró un rango de 50 a 230 casos por 100,000 (0.05 a 0.23%) (71). Una revisión de estudios posteriores (1959-2011) (72) encontraron unas estimaciones de prevalencia que varían de 0,3 por 100.000 (0,0003%) en Rusia a 2340 por 100.000 (2,3%) en Maharashtra, India (73). El artículo de Kennedy de 1986, en el que utilizaron queratoscopia y queratometría para estimar la prevalencia en Minnesota, EE. UU., En 54,5 / 100.000 (0,0545%) (74).

Unos estudios recientes demuestran que la etnia del Oriente Medio y Asia Central se considera un factor de riesgo para el queratocono (75). Otros estudios recientes realizados con topógrafos proporcionan estimaciones más sensibles, aportaron un resumen de los estudios de prevalencia publicados y enfatizaron las importantes diferencias metodológicas entre los informes basados en hospitales o clínicas y los estudios basados en la población (Tabla 2, Tabla 3) (76). Un estudio realizado en el Líbano por Waked N. y cols. de trabajo resultó en una prevalencia de queratocono del 3,3% (77). Este resultado estuvo de acuerdo con el estudio de los árabes israelíes, se registró una prevalencia del 3,18% en la población (78). Se obtuvieron resultados similares en Irán en Mashhad, la prevalencia de queratocono fue del 2.5% (79), sin embargo, la prevalencia en la población de Shahroud fue menor, se encontró un resultado entre 0,72% - 0,79% en hombres y mujeres respectivamente (80).

El rango de variación de las estimaciones en la incidencia anual del queratocono en Arabia Saudita varía de 1,4 a 600 casos por 100.000 habitantes (81). Las diferencias étnicas influyen con una incidencia de 25 / 100.000 / año para los asiáticos en comparación con 3,3 / 100.000 / año para los caucásicos en una única zona de captación (82). La revisión de McMonnies destacó y discutió la detección de casos de queratocono subclínico antes de la cirugía refractiva. Durante las últimas

décadas, debido a la tecnología de imagen moderna y la sensibilidad diagnóstica, las estimaciones de prevalencia han aumentado dramáticamente (83).

Tabla 2. Estudios epidemiológicos del queratocono realizados en hospitales / clínicas (Gordon-Shaag et al. BioMed Research International 2015 —reproducido con el amable permiso de los autores)

Autor	Localización	Edad en años	Tamaño de muestra	Incidencia/ 100,000	Prevalencia/ 100,000	Método
Tanabe y cols. (1985)	Muroran, Japón	10–60	2601-P		9	Queratometria
Kennedy y cosl. (1986)	Minnesota, Estados Unidos	12–77	64-P	2	54.5	Queratometria + retinoscopia
Ihalainen (1986)	Finlandia	15–70	294-P	1.5	30	Queratometria + retinoscopia
Gorskova y Sevost'ianov (1998)	Urales, Rusia				0.2–0.4	Queratometria
Pearson y cols. (2000)	Midlands, Reino Unido	10–44	382-P	4.5-W 19.6-A	57 229	Queratometria + retinoscopia
Ota y cols. (2002)	Tokio, Japón		325-P	9		Queratometria?
Georgiou y cols. (2004)	Yorkshire, Reino Unido		74-P	3.3-W 25-A		Exámen clinico
Assiri y cols. (2005)	Asir, Arabia Saudita	8–28	125-P	20		Queratometria
Nielsen y cols. (2007)	Dinamarca		NA	1.3	86	Índices clínicos + topografía
Ljubic (2009)	Skopje, Macedonia		2254		6.8	Queratometria
Ziaei y cols. (2012)	Yazd, Irán	25.7 ± 9	536	22.3		Topografía

Un paciente asiático (indio, paquistaní y bangladesí), blanco, P, NA no disponible. Reproducido con permiso del Libro Keratoconus: Recent Advances in Diagnosis and Treatment of Alió y cols. (70).

Tabla 3. Estudios epidemiológicos poblacionales del queratocono (Gordon-Shaag et al. BioMed Research International 2015 — reproducido con el amable permiso de los autores).

Autor	Localización	Edad en años (media)	Tamaño de muestra	Prevalencia/ 100,000 (cases)	Método	Método de muestreo
Hofstetter (1959)	Indianápolis, EE.UU	1–79	13345	120	Disco de placido [a]	Voluntarios rurales
Santiago y cols. (1995)	Francia	18–22	670	1190	Topografía	Reclutas del ejército
Jonas y cols. (2009)	Maharashtra, India	>30 (49.4 ± 13.4)	4667	2300	queratometria [a]	Voluntarios rurales (8 pueblos)
Millodot y cols. (2011)	Jerusalén, Israel	18–54 (24.4 ± 5.7)	981	2340	Topografía	Voluntarios rurales (1 facultad)
Waked y cols. (2012)	Beirut, Líbano	22–26	92	3300	Topografía	Voluntarios rurales (1 facultad
Xu y cols. (2012)	Beijing, China	50–93 (64.2 ± 9.8)	3166	900	Reflectometría óptica de baja coherencia [a]	Rural+ Voluntarios urbanos
Hashemi y cols. (2013)	Sharud, Irán	50.83 ± 0.12	4592	760	Topografía	Voluntarios rurales de un grupo aleatorio
Hashemi y cols. (2013)	Teherán, Irán	14–81 (40.8 ± 17.1)	426	3300	Topografía	Voluntarios urbanos (grupo estratificado)
Shneor y cols. (2014)	Haifa, Israel	18–60 (25.05 ± 8.83)	314	3180	Topografía	Voluntarios urbanos (1 facultad)
Hashemi y cols. (2014)	Mashhad, Irán	20–34 (26.1 ± 2.3)	1073	2500	Topografía	Voluntarios urbanos (grupo estratificado en 1 universidad)

[a] los métodos para detectar el queratocono utilizados en estos estudios ahora se consideran inadecuados y los resultados deben interpretarse con precaución. Reproducido con permiso del Libro Keratoconus: Recent Advances in Diagnosis and Treatment de Alió y cols. (70).

1.1.3.2 Factores ambientales y genéticos.

Si bien se atribuye el aumento en las estimaciones de prevalencia en parte debido principalmente a los avances tecnológicos en imágenes, y en otra parte debido al diagnóstico subclínico. Se cree que el queratocono es causado por una interacción compleja entre factores genéticos y ambientales, así como trastornos bioquímicos y biomecánicos (46,75,84,85). Se encontró una asociación significativa con la consanguinidad de la base genética de la enfermedad (86), se observaron patrones autosómicos dominantes de herencia familiar (87). Se detectó una mayor concordancia entre gemelos monocigóticos que dicigóticos (88). En el estudio de Rabinowitz, el 10% de los pacientes con queratocono tenían antecedentes familiares de la enfermedad, mientras que en el grupo control solo había un 0,05% (89). La mayoría de los casos de queratocono se consideran esporádicos (90). Actualmente se cree que las variaciones geográficas en la prevalencia están relacionadas con factores ambientales específicos que promueven la expresión de factores genéticos relacionados con la etnia (83).

1.1.3.3 Exposición a la luz ultravioleta.

Se ha identificado una mayor prevalencia de queratocono en áreas con alta exposición a la luz ultravioleta **(UV)** (83). La luz ultravioleta puede aumentar la producción de especies reactivas de oxígeno dentro de la córnea (91), y que las córneas queratocónicas no pueden procesar este exceso de especies reactivas de oxígeno (92), que conduce a un mayor estrés oxidativo, citotoxicidad y, por lo tanto, adelgazamiento de la córnea (66). Sin embargo, existe un argumento que contradice esta suposición de que es el **CXL** del colágeno corneal inducida por la luz ultravioleta, lo que podría esperarse que reduzca la prevalencia y la tasa de progresión de la ectasia (93).

1.1.3.4 Frotamiento de ojos y alergia.

El frotamiento de los ojos y su relación con enfermedades alérgicas o atópicas es otro factor de estrés ambiental relacionado con la enfermedad del queratocono, esta asociación se describió por primera vez en 1956 (94). Hoy en día, la asociación con el frotamiento ocular y el queratocono está ampliamente aceptada (76), los estudios han demostrado que la duración del frotamiento ocular en pacientes con queratocono parece más larga que la asociada solo con una enfermedad ocular alérgica (95), esto puede explicar que la mayoría de los ojos atópicos no desarrollen queratocono. En climas cálidos y secos, los altos niveles de polvo pueden inducir a frotarse los ojos con frecuencia y pueden causar una alta prevalencia del desarrollo de queratocono en estas áreas (76). Bawazeer y cols. encontraron que el queratocono se asoció con antecedentes familiares, atopia y frotarse los ojos (96).

1.1.3.5 Género y edad.

Los resultados sobre la preponderancia de género varían entre los estudios: algunos autores demostraron preponderancia femenina, mientras que otros demostraron preponderancia masculina. Otros autores no demostraron diferencias de género significativas. No se considera que el queratocono general favorezca a un género sobre el otro (1).

En cuanto a la edad, el queratocono es típicamente una enfermedad de la adolescencia y la edad adulta joven, presentándose entre las edades de 20 y 30 años (97). Ihalainen en (1986) informó que la edad media de los pacientes queratocónicos era de 18 años, y el 73% de los pacientes tenían 24 años o menos (98). Una progresión más rápida induce un tiempo más corto para la realizar la queratoplastia penetrante. La edad más temprana de aparición predice una mayor gravedad de la

enfermedad. El **CXL** de colágeno corneal ahora puede detener o ralentizar la progresión de la enfermedad (70).

1.1.4 HISTOPATOLOGÍA DEL QUERATOCONO

El queratocono es una enfermedad humana, y la falta de un modelo animal ha llevado a pensar que esta enfermedad aparece solo en seres humanos, y el acceso al trasplante de córnea en la etapa terminal de la enfermedad ha permitido la disponibilidad de tejido para estudios histopatológicos. Dichos hallazgos pueden informarnos de la patogénesis subyacente de la enfermedad y también pueden conducir a una hipótesis sobre el por qué el queratocono puede progresar (99).

Cambios estructurales en el queratocono: el adelgazamiento característico y otros signos biomicroscópicos de progresión de la enfermedad en el queratocono se correlacionarían con la alteración de los elementos estructurales de la córnea queratocónica.

1.1.4.1 Epitelio.

El epitelio superficial de las córneas queratocónicas mostraba una morfología celular normal en la periferia, pero se presentaban células muy alargadas en el vértice del cono (100). Los métodos recientes para el análisis del espesor epitelial incluyeron la tomografía de coherencia óptica de dominio espectral (**OCT**), que confirmó la presencia de una desviación pronunciada en el espesor epitelial (101,102). Las investigaciones de la microscopía confocal de pacientes queratocónicos mostraron que las células epiteliales corneales (**CECs)** superficiales están alargadas en una dirección oblicua y altamente reflectantes con un área evidente con falta de células, las alteraciones patológicas se encuentran en principio en la cuarta etapa de la enfermedad en el área central de la córnea (103–105). Los nuevos dispositivos de segmento anterior de tomografía de coherencia óptica

(AS-OCT) capturan instantáneamente una topografía de la superficie frontal con datos de paquimetría, proporcionando mapas de espesor corneal total y epitelial. En el caso del queratocono, se sabe que el epitelio es más delgado en la zona que recubre el cono (106–108). En el queratocono avanzado, podría haber un adelgazamiento epitelial excesivo que podría conducir a la ruptura del epitelio y la consiguiente cicatrización (109). En el queratocono, el epitelio se vuelve más delgado en el vértice del cono, mientras que está rodeado por un anillo de epitelio engrosado, que muestra un espesor de epitelio conocido como patrón epitelial en forma de "donut" (109).

La presencia de tinción del marcado terminal de desoxinucleotidiltransferasa biotina-dUTP (**TUNEL**), es un indicador de la presencia de células apoptóticas, con un patrón general de apoptosis que continúa hasta el epitelio basal (110,111). En las córneas queratocónicas, la membrana basal parece irregular y contiene desgarros localizados, mostrando un patrón errático de tinciones de laminina 1 y 5 con colágeno tipo VII localizado en anomalías de la membrana basal (112). Los estudios inmunohistoquímicos (**IHC**) en casos de queratocono avanzado demostraron una ruptura en la membrana celular, que puede conducir a una reducción significativa en el número de células epiteliales basales, lo que conduce a la presencia de algunas capas de epitelio superficial aplanado que se encuentran sobre una membrana basal anormal (65,89).

1.1.4.2 Membrana de Bowman (BM).

Se han observado anomalías estructurales en la **BM** en la parte central de la córnea queratocónica. El examen por microscopía electrónica de barrido de la organización del colágeno en el tejido queratocónico mostró unos defectos en los bordes y diversos grados de roturas en la capa de Bowman (113). Otros estudios informaron discontinuidades en la **BM** y con la presencia de un estroma distorsionado debajo de estos defectos, incluida la presencia de regiones fibróticas con áreas de contacto directo del epitelio con el estroma corneal (113,114). Los estudios de

microscopía confocal mostraron la presencia de rupturas en la **BM** con tejido cicatricial altamente reflectante (104). También, la presencia de estrías se ha descrito en otros estudios en los cuales encontraron que hay un reflejo de iluminación de fondo brillante debajo de la **BM** debido a un desorden de las fibras de colágeno (103).

1.1.4.3 Estroma.

- **Láminas de colágeno.**

Los estudios de microscopía electrónica de transmisión (**TEM**) del estroma queratocónico revelaron que el grosor de las láminas de colágeno en el queratocono no se altera, pero el número de láminas parece estar significativamente menor que en el estroma corneal normal (115). Los estudios de difracción de rayos X de sincrotrón indicaron que no había diferencia en el espaciamiento interfibrilar entre los colágenos de las córneas con queratocono y las córneas de control, se demostró que el adelgazamiento del estroma corneal en el queratocono no es el resultado de un empaquetamiento más apretado de las fibras de colágeno en el estroma corneal, Sin embargo, se demostró que hubo una reducción en el volumen de proteoglicanos a lo largo de las fibras de colágeno en la córnea queratocónica (116). Estos datos suponen una pérdida progresiva de láminas de colágeno dentro del estroma corneal, pero se desconoce el papel de los queratocitos y el destino del colágeno. La dispersión de rayos X de ángulo bajo ha mostrado una alteración en la orientación de las fibrillas de colágeno dentro de las láminas en la córnea patológica (117). Se sugiere que la pérdida de la integridad estructural, la degradación o los mecanismos de reparación insuficientes pueden ser importantes en la enfermedad (118).

Además, los estudios de microscopía confocal mostraron la presencia de micro estrías que es evidente en todo el estroma de la córnea, que también aparece como múltiples líneas oscuras y delgadas en comparación con la reflectividad estromal más brillante. Estas micro estrías podrían

resultar del proceso degenerativo que conduce a cambios en las laminillas de colágeno extracelular de la córnea (104). Estas micro estrías pueden aparecer como líneas horizontales, verticales, oblicuas o reticulares, y parecen extenderse desde el estroma más anterior hasta la membrana de Descemet (**DM**) (104). La presencia de estrías de Vogt en la reflectividad del estroma posterior es consistente con procesos patológicos del estroma corneal (100).

- **Deposición de matriz colágena y formación de cicatrices.**

Los datos proteómicos del queratocono muestran la presencia de disminuciones generalizadas en los proteoglicanos que forman las proteínas de la matriz extracelular, y son del colágeno tipos I, III, V, VI y XII, así como proteínas lumicán y queratocán (64,97,119).

La expresión de **TGFβ1**, **IL-1**, vimentina y tenascina (proteína de matriz asociada a cicatrices) se detectó aumentada en la córnea afectada (120). Se encontró un aumento en el colágeno tipo IX y hubo un patrón alterado en la endostatina (anti-angiogénico) que induce la apoptosis de las células endoteliales (121).

La presencia de fibronectina, colágeno tipo III, tenascina y laminina se localizó más intensamente en áreas de defectos en córneas queratocónicas. La presencia de estos componentes son signos de respuesta de cicatrización de heridas y formación de cicatrices (122–124). En la hidropesía asociada al queratocono, se puede observar la deposición de pocas cantidades de fibronectinina en la **DM** una tinción puntiforme con el marcado más intenso de colágeno III en todo el estroma posterior adyacente a la **DM**. Además, se observó tinción similar para la laminina en córneas queratocónicas con hidropesía en el estroma adyacente a las membranas de Bowman y Descemet. La deposición de **ECM** localizada en el estroma se encontró únicamente en áreas afectadas de hidropesía corneal (123).

- **Queratocitos**

Los queratocitos del huésped del estroma corneal muestran unas alteraciones en su morfología y su número en pacientes con queratocono. Se ha demostrado que la densidad de queratocitos es menor en las córneas queratocónicas que en las normales (110,111,125). La apoptosis de queratocitos parece estar aumentada en la córnea queratocónica y este hecho conduce a una reducción general en el número de queratocitos (111). En estudios recientes, al comparar la densidad de queratocitos en el estroma corneal, la densidad celular parecía ser menor en la parte más anterior del estroma en comparación con las regiones más posteriores. Estas observaciones reforzaron la sugerencia de que el queratocono es principalmente una enfermedad de la córnea anterior. El análisis histoquímico del estroma queratocónico informó una reducción general de los queratocitos en el estroma anterior en comparación con las córneas normales (126). En otro informe, se observó que las células estromales más anteriores, siendo queratocitos activados o de origen no queratocítico, enviaban procesos celulares (pseudópodos) dentro de la **BM** y hacia la lámina epitelial basal (127). Por tanto, se planteó la hipótesis de que esta actividad celular es responsable de la degradación del tejido corneal en la parte anterior del estroma y que puede contribuir al colapso de las células epiteliales hacia la **BM** (126,128,129).

Los estudios de microscopía confocal mostraron cambios en la morfología de los queratocitos desde el estroma anterior al posterior. Los queratocitos tenían núcleos delgados y consistentes en el estroma anterior y núcleos más consistentes y de mayor tamaño en la mitad del estroma. La morfología de los queratocitos en el estroma posterior era similar a la del estroma medio, pero eran más pequeños y menos brillantes (104,105).

1.1.4.4 Membrana de Descemet (DM).

Las roturas y los pliegues en la **DM** son una característica común en las córneas queratocónicas (130). Los cambios estructurales provocados por estas rupturas no están muy claros. Diferentes estudios de proteínas de la matriz extracelular no revelaron diferencias en la detección de colágeno tipo I, III, IV, V, VI o VIII entre córneas queratocónicas o normales, ni con laminina, ni con entactina y perlecano (113,131).

1.1.4.5 Endotelio.

El endotelio en muchas córneas queratocónicas mantiene una apariencia normal. Pero en algunos casos se pudo observar un desprendimiento de las capas anteriores. Sin embargo, se han observado algunas anomalías celulares como células pleomórficas alargadas que contienen estructuras intracelulares oscuras y pérdida de células endoteliales (132,133). Con los hallazgos de la microscopía confocal, la capa de células endoteliales puede mostrar cambios como un aumento en un área celular y una disminución en la densidad celular, polimegatismo y pleomorfismo dependiendo de la progresión de la enfermedad (104,105). Esta pérdida celular puede estar asociada con la apoptosis cellular (110), pero en general, se acompaña con una ruptura de la **DM** que parece ser responsable de una degradación significativa de las células endoteliales (132) en córneas que padecen el queratocono.

1.1.5 CLASIFICACIÓN DEL QUERATOCONO

Debido a la gran variabilidad entre los pacientes con queratocono, es muy importante clasificar esta enfermedad para proporcionar una guía general para los clínicos con respecto al nivel de progresión y las opciones de tratamiento que se pueden ofrecer. Existen varias clasificaciones del queratocono dependiendo de qué factores principales se consideren:

1.1.5.1 Clasificación de Amsler-Krumeich.

La clasificación más utilizada es la escala de **Amsler-Krumeich** (1946) (134). Esta escala se basa principalmente en criterios queratométricos, pero también incluye otros factores, como la refracción y la paquimetría. La clasificación del grado según la escala de Amsler-Krumeich (1946) se distribuye en 4 grados:

Grado 1

- Incurvamiento excéntrico.
- Lecturas queratométricas medias <48,00 dioptrías (**D**).
- Miopía y astigmatismo menores de 5,00 (**D**).

Grado 2

- Lecturas queratométricas medias: 48,00 a 53,00 (**D**).
- Miopía y astigmatismo entre 5,00 y 8,00 (**D**).
- Ausencia de cicatrices o estrías.
- Paquimetría> 400 micras (**µm**) en el punto más delgado.

Grado 3

- Lecturas queratométricas medias: 53,00 a 55,00 (**D**).
- Miopía y astigmatismo entre 8,00 y 10,00 (**D**).
- Ausencia de cicatrices o estrías.
- Paquimetría entre 300 y 400 **µm** en el punto más delgado.

Grado 4

- Lecturas queratométricas medias:> 55,00 (**D**).
- Refracción no medible.
- Estrías o cicatrices.
- Paquimetría entre 200 y 300 **µm** en el punto más delgado.

1.1.5.2 Clasificación morfológica.

Los métodos topográficos pueden proporcionar datos aberrométricos corneales, se desarrolló la escala Alio-Shabayek (2006) (135). Esta escala se adapta mejor a los métodos de diagnóstico actuales. Además de los factores mencionados anteriormente, incluye la aberrometría de la superficie anterior de la córnea, con especial énfasis en las aberraciones comáticas. Estos

parámetros se utilizan porque los valores de aberración de tipo coma (y, en general, aberraciones de orden superior) tienden a aumentar con el aumento de la protrusión del cono y, por tanto, con la progresión de la enfermedad.

Esta clasificación de la escala de Alió-Shabayek (2006) establece los siguientes 4 grados:

Grado 1

- Lectura queratométrica central media: menor o igual a 48,00 (**D**).
- Raíz cuadrada media (**RMS**) de aberraciones tipo coma: entre 1,50 y 2,50 **µm**.
- Ausencia de cicatrices o estrías.

Grado 2

- Lecturas queratométricas centrales medias: entre 48,00 y 53,00 (**D**).
- **RMS** de aberraciones tipo coma: entre 2,50 y 3,50 **µm**.
- Ausencia de cicatrices o estrías.
- Paquimetría superior a 400 **µm** en el punto más fino.

Grado 3

- Lecturas queratométricas centrales medias: entre 53,00 y 55,00 (**D**).
- **RMS** de aberraciones tipo coma: entre 3,50 y 4,50 **µm**.
- Ausencia de cicatrices o estrías.
- Paquimetría entre 300 y 400 **µm** en el punto más delgado.

Grado 4

- Lecturas queratométricas medias: Más de 55,00 (**D**).
- **RMS** de aberraciones de tipo coma: más de 4,50 **µm**.
- Estrías o cicatrices.
- Paquimetría entre 200 y 300 **µm** en el punto más delgado.

1.1.5.3 Clasificación RETICS

Como resultado del trabajo cooperativo multicéntrico de la red temática, finalmente se desarrolló una escala funcional basada principalmente en la agudeza visual a distancia corregida (**CDVA**) y se tituló la clasificación RETICS (8,136). Hasta el momento, se han propuesto muchos sistemas de clasificación para determinar la gravedad de la enfermedad ectásica corneal, pero la

mayoría se han desarrollado teniendo en cuenta la morfología topográfica de la enfermedad sin considerar otras variables clínicas que están estrechamente relacionadas con la función visual del paciente. Por este motivo, el sistema de clasificación que utilizamos determina la gravedad de la enfermedad, teniendo en cuenta parámetros funcionales y no puramente geométricos. Se consideran variables que presentan una correlación altamente significativa, como la presencia del astigmatismo interno, pérdida visual, **RMS** en coma, queratometría central media, asfericidad a 8 mm de diámetro corneal y que también están directamente relacionadas con el grado de limitación visual.

Las principales características de la clasificación **RECTIS** se presentan en 5 grados:

Grado 1

- **CDVA**: > 0.9 (decimal).
- Astigmatismo interno: entre 1,59 y 2,14 (**D**).
- **RMS** de tipo coma: entre 1,16 y 1,52 **µm**.
- Lecturas queratométricas centrales medias: entre 44,75 y 45,40 (**D**).
- $Q_{8\ mm}$: entre –0,22 y –0,05.
- Paquimetría: entre 495 y 510 **µm**.

Grado 2

- 0.6 < **CDVA** ≤ 0.9.
- Astigmatismo interno: entre 2,18 y 2,79 (**D**).
- **RMS** de tipo coma: entre 1,82 y 2,31 **µm**.
- Lecturas queratométricas centrales medias: entre 46,03 y 46,93 (**D**).
- $Q_{8\ mm}$: entre –0,48 y –0,22.
- Paquimetría: entre 475 y 493 **µm**.

Grado 3

- 0.4 < **CDVA** ≤ 0.6.
- Astigmatismo interno: entre 3.04 y 4.17.
- **RMS** de tipo coma: entre 2,65 y 3,32 **µm**.
- Lecturas queratométricas centrales medias: entre 48,21 y 49,27 (**D**).
- $Q_{8\ mm}$: entre –0,95 y –0,58.
- Paquimetría: entre 451 y 470 **µm**.

Grado 4

- **CDVA** ≤ 0.4.
- Astigmatismo interno: entre 3,68 y 4,58 (**D**).
- **RMS** de tipo coma: entre 3,45 y 4,42 **µm**.
- Lecturas queratométricas centrales medias: entre 51,42 y 53,12 (**D**).
- $Q_{8\ mm}$: entre –1,21 y –0,83.
- Paquimetría entre 433 y 454 **µm**.
- Estrías o cicatrices corneales en el 60% de los casos.

Grado PLUS

- **CDVA** < 0.2.
- Astigmatismo interno: más de 5,50 (**D**).
- **RMS** de tipo coma: más de 5,50 **µm**.
- Lecturas queratométricas centrales medias: más de 57,00 (**D**).
- $Q_{8\ mm}$: menos de –1,50.
- Paquimetría entre 360 y 420 **µm**.
- Estrías o cicatrices.

1.1.6 TRATAMIENTO Y MANEJO CLINICO DEL QUERATOCONO

El queratocono en muchos casos se acompaña de cambios morfológicos en el tejido corneal donde se origina un astigmatismo irregular progresivo y severo; En las etapas iniciales, la corrección de las gafas es adecuada en pacientes que pueden alcanzar no menos de 20/40 (137); Cuando la visión no se puede corregir con gafas y conduce al deterioro del rendimiento visual y la calidad óptica de los pacientes (133), La rehabilitación visual favorable de los pacientes con queratocono

son las lentes de contacto rígidas permeables a los gases (**RGP**), ya que son ajustables a los cambios de forma corneal y proporcionan una rehabilitación visual superior. El manejo de esta ectasia incluye otras técnicas como los procedimientos de termoqueratoplastia (hoy en día desatendidos), el **CXL** de colágeno corneal, segmentos de anillo intracorneal (**ICRS**), queratoplastia penetrante (**PKP**) y queratoplastia lamelar como la queratoplastia lamelar anterior profunda (**DALK**), con modalidades de trasplante recientemente propuestas del trasplante de capa de Bowman descrito por Melles (2,138–144).

1.1.6.1 Manejo del queratocono en pacientes con lentes de contacto.

Recordando la primera **CL** moderna, fue presentada por Edwin Theodor Saemisch. Fue el primero en insertar una **CL** en el ojo con fines de protección. Más tarde, a finales de la década de 1880, Adolph Eugen Fick, Eugene Kalt y August Müller trabajaron de forma independiente en la primera **CL** con la idea de corregir ópticamente la miopía del ojo humano (145,146).

En los últimos años, los avances en la fabricación y diseño de las **CL** para adaptar lentes más ajustadas al tipo de cono, han sido apoyados por el desarrollo y creación de topografía corneal y **OCT**, haciendo más segura y más efectiva la adaptación de diferentes tipos de **CL** para el queratocono (147,148). Las **CL** es la principal opción de tratamiento para la corrección visual del queratocono y uno de los primeros tratamientos de elección en el 90% de los pacientes que padecen una irregularidad de la superficie corneal (138,147–149).

En el contexto de los procedimientos no quirúrgicos, la adaptación de **CL** se basará en los mismos criterios de selección de cualquier adaptación de **CL**, y es una alternativa favorable para el manejo de las córneas queratocónicas, para restaurar la calidad de la visión, retrasar los procedimientos quirúrgicos y mejorar la calidad de vida de estos pacientes (150). Las **CL**, especialmente las **RGP**, se consideran el método más común y exitoso para tratar el querartocono

leve y moderado (151), pero la **CL** no detiene la progresión del cono en comparación con otros procedimientos quirúrgicos invasivos. El ajuste de la **CL** depende también de la gravedad de la progresión de la enfermedad ectática, la edad, la demanda visual, la tolerancia a la **CL** y la estabilidad corneal. Actualmente, existen varias opciones de compensación, dado que no existe un diseño de **CL** único adecuado para todos los casos de queratocono (138,150,152–154):

- **CL** blandas y **CL** tóricas blandas.
- **CL** rígidas permeables al gas (**RGP**).
- Sistema Piggyback (lente rígida y detrás una lente blanda).
- Lentes híbridas (centro rígido y faldón hidrofílico periférico suave).
- **CL** miniescleral, escleral y corneoescleral.

En resumen, debido a los diversos diseños disponibles, el manejo de las **CL** en el queratocono proporciona la mejor rehabilitación visual y mejora la calidad de vida de los pacientes (150).

1.1.6.2 Cross-Linking de colágeno corneal.

El término **CXL**, en las ciencias biológicas, se utiliza para describir la formación de puentes químicos tras una reacción química entre proteínas y otras moléculas. Estos puentes químicos pueden formarse a partir de reacciones químicas iniciadas por calor, presión o radiación, de esta manera se cambian las propiedades físicas de la materia. Este procedimiento puede generar rigidez o provocar una pérdida de elasticidad de las fibras de colágeno corneal, inducir **CXL** corneal que fue realizado por un grupo de investigación del Dresden Technic (155), utilizaron riboflavina (vitamina B2) y radiación ultravioleta (**UVA**) para aumentar la formación de enlaces cruzados entre las fibras de colágeno en el estroma corneal, produciendo un efecto de rígidez capaz de detener la progresión de la ectasia. Siguiendo esta línea de pensamiento, durante la última década, esta técnica

se ha introducido en la práctica clínica para el tratamiento de trastornos ectásicos corneales, como el queratocono, la degeneración corneal marginal pelúcida y la ectasia corneal después de la cirugía refractiva. Por lo tanto, los pacientes diagnosticados con trastornos ectásicos corneales ahora tienen la posibilidad de detener la progresión de la enfermedad evitando tratamientos más complejos y severos como el trasplante de córnea (156). Luego, los pacientes diagnosticados con trastornos corneales ectásicos pueden detener la progresión de la enfermedad mediante el tratamiento con **CXL**, para reducir el riesgo de progresión en pacientes con una córnea central clara y con queratocono progresivo con un grosor corneal más delgado > 400 **µm**. Se recomienda a los pacientes con córnea más delgada que realicen el **CXL** hipoosmolar (138).

1.1.6.3 Segmentos de anillo intracorneal.

La **CL** es la opción favorable para rehabilitar la visión de las córneas queratocónicas, pero son propensas a tener riesgos como la queratitis, ya sea no infecciosa o infecciosa. El manejo se vuelve más desafiante cuando los pacientes son intolerantes a las lentes rígidas, híbridas o esclerales o por la inestabilidad de la **CL** debido a córneas extremadamente incurvadas. Por este motivo, el control de esta ectasia además del **CXL** del colágeno corneal, los **ICRS** forman una solución antes de proceder a la **PKP** y la queratoplastia lamelar (**LKP**) (139–143).

Junto con el **CXL** de colágeno y las técnicas termoplásticas, los **ICRS** también se han utilizado en pacientes con queratocono (128,130,145). Esta técnica permite a los cirujanos remodelar la córnea con fines terapéuticos y refractivos. El uso de esta técnica fue introducido por Colin y cols. (141).

Teóricamente, se propone que las fibras de colágeno del tejido corneal estén separadas por **ICRS** (157). Por tanto, la córnea se aplanará por un efecto de acortamiento del arco de la geometría corneal inducida por los **ICRS**. La fuerza de tracción generada por el extremo de cada segmento de

anillo puede inducir un aplanamiento adicional en un eje de referencia, corrigiendo así el astigmatismo. Algunos modelos teóricos basados en el análisis de elementos finitos han demostrado que el efecto de aplanamiento de los **ICRS** es inversamente proporcional al diámetro corneal de implantación y directamente proporcional al grosor del segmento. En otras palabras, cuanto menor sea el diámetro y más grueso el segmento, mayor será el efecto del aplanamiento inducido (158).

Para obtener el mejor resultado posible después de la implantación de los **ICRS**, el clínico debe conocer las siguientes indicaciones preoperatorias (159): 1) Mejor agudeza visual corregida <0,9 (escala decimal). 2) El astigmatismo interno es menor que 3D. 3) Espesor corneal superior a 250-300 **µm** en el sitio del túnel corneal (dependiendo del espesor del **ICRS** a implantar). 4) Ausencia de cicatrización corneal central.

Considerando los tipos de segmentos intracorneales (156)**,** actualmente existen cuatro tipos principales de segmentos intracorneales: 1) Keraring, 2) Intacs, 3) Ferrara, y 4) Myoring.

Los **ICRS** presentan una opción importante y valiosa para el tratamiento de enfermedades ectásicas corneales, especialmente el queratocono. Sin embargo, es fundamental discutir con el paciente sus limitaciones y la incapacidad de predecir con precisión sus resultados postoperatorios.

1.1.6.4 Trasplante de córnea.

La mayoría de los especialistas estarían de acuerdo en que un paciente con queratocono avanzado es elegible para un trasplante de córnea cuando la corrección de las gafas es insuficiente, el uso continuo de **CL** es intolerable (160), las cicatrices estromales están presentes en el eje visual, o cuando otras modalidades de tratamiento como **UV-CXL** (160), La queratectomía fotorrefractiva guiada por topografía (**PRK**) o la **ICRS** pueden no mejorar la **CDVA** (138), y posteriormente la agudeza visual cae a niveles inaceptables y se vuelve deficiente para las necesidades del paciente.

Por lo tanto, el trasplante de córnea se describe para el queratocono avanzado con adelgazamiento/incurvamiento extremo (138,144). Aproximadamente entre el 12 y el 20% de los pacientes con queratocono pueden requerir un trasplante de córnea si no se aplica ningún otro tratamiento antes (137).

Ramón Castroviejo, oftalmólogo español, realizó el primer **PKP** para queratocono en 1936 (161). Varios años después, concluyó que la queratoplastia era el único procedimiento quirúrgico que cumplía con los siguientes requisitos para el tratamiento de las córneas queratocónicas: la cirugía debía limitarse a la córnea, y todo el abultamiento corneal debía ser eliminado y reemplazado por tejido normal de curvatura y grosor, dejando la zona pupilar libre de cicatrices. Según su experiencia, cuando se aplicó una técnica adecuada, el porcentaje de mejora permanente de la visión estaba entre 75-90% (161).

LKP se describió antes que **PKP**. Arthur von Hippel realizó la primera **LKP** exitosa en humanos en 1888, décadas antes de que Edward Zinn realizara la primera **PKP** humana exitosa, pero esta técnica fue abandonada en 1914 y no se reintrodujo hasta la década de 1940. Sin embargo, el concepto de queratoplastia lamelar profunda que se extendió a la **DM** es relativamente nuevo (2). El término **DALK** se atribuye a la disección del tejido del huésped cerca de la **DM** y fue introducido por primera vez por Archilla en 1984, quien también mostró el uso de inyección de aire intraestromal para opacificar la córnea y facilitar la extracción del tejido del huésped (162). En las últimas dos décadas, **DALK** ha ganado popularidad gracias a la mejora de las técnicas quirúrgicas y la disponibilidad de nuevos dispositivos e instrumentos quirúrgicos. Probablemente las dos técnicas más relevantes fueron las de Melles y Anwar (2). En 1999, Melles describió una técnica para visualizar el grosor de la córnea y la profundidad de la disección durante la cirugía creando una interfase óptica en la superficie posterior de la córnea llenando la cámara anterior con aire por

completo (163). En 2002, Anwar describió su popular técnica de "gran burbuja" para desnudar la **DM** inyectando aire en el estroma profundo para crear una gran burbuja entre el estroma y la **DM** (164). El porcentaje de trasplante de córnea lamelar en queratocono en el que se utilizó **DALK** aumentó con los años (160,165). Actualmente, un **PKP** electivo se usa para casos de queratocono avanzado solo si hay daños en **DM** y en el endotelio, debido a un hidrops corneal previo, o cuando se observan cicatrices estromales profundas que involucran a la **DM** (2).

En general, **PKP** ofrece una buena rehabilitación visual a largo plazo para pacientes con queratocono. Se ha informado que la tasa de rechazo es del 5,8 al 41% con un seguimiento a largo plazo (166–170). La mayoría de los estudios encontraron resultados refractivos y visuales equivalentes entre **PKP** y **DALK** siempre que la disección del estroma alcance el nivel o se acerque a la **DM** (165,171–175). Sin embargo, **DALK** se prefiere en pacientes con queratocono debido a la ausencia de riesgo de rechazo endotelial, disminución temprana de los esteroides, menor riesgo de glaucoma secundario y mejor aumento de la fuerza corneal.

1.2 PROGRESANDO HACIA UN NUEVO TIPO DE TERAPIA CORNEAL AVANZADA DEL QUERATOCONO

La terapia celular de la córnea debe considerarse como un enfoque terapéutico avanzado y prometedor para las enfermedades de la córnea. Sin embargo, el uso de queratocitos oculares humanos autólogos tiene muchas desventajas, como dificultades en su aislamiento, limitaciones en la disponibilidad de células con poblaciones elevadas y subcultivo celular ineficiente (176)**.** Las células madre del estroma corneal tienen la misma limitación de requerir tejido donante de córnea sano. Mientras tanto, las células madre de fuentes extraoculares han demostrado que pueden ser una fuente más favorable y adecuada para la regeneración del estroma corneal humano (21,22,30,31,177–180). En la actualidad, la terapia corneal avanzada podría ser un enfoque prometedor para superar estas limitaciones, ciertamente cuando las células madre se combinan con el uso de andamios; aquí, en este proyecto de tesis, discutiremos la aplicación de células madre mesenquimales combinadas con láminas descelularizadas obtenidas de donantes sanos.

1.2.1 FUENTES DE CÉLULAS MADRE UTILIZADAS PARA LA REGENERACIÓN DEL ESTROMA CORNEAL

La córnea proporciona dos tercios del poder refractivo del ojo y está compuesta por cinco capas bien definidas (Figura. 1 A), incluidas tres capas celulares separadas por dos membranas acelulares. El fenotipo de las enfermedades de la córnea se observa cuando se ven afectadas una o más capas de la córnea. La pérdida de las **CECs**, el factor director de muchas enfermedades de la córnea, se debe principalmente a la pérdida de células madre epiteliales del limbo que reponen el epitelio (**LESCs**). Otros factores pueden afectar la regeneración del estroma corneal (**CS**), como las células endoteliales corneales (**CEnCs**), donde tanto **CS** como **CEnCs** derivan de las células de la

cresta neural **NCCs** que se elevan desde las **MSCs**. A continuación, analizaremos brevemente las principales fuentes de **MSCs** y su participación en la regeneración del estroma corneal.

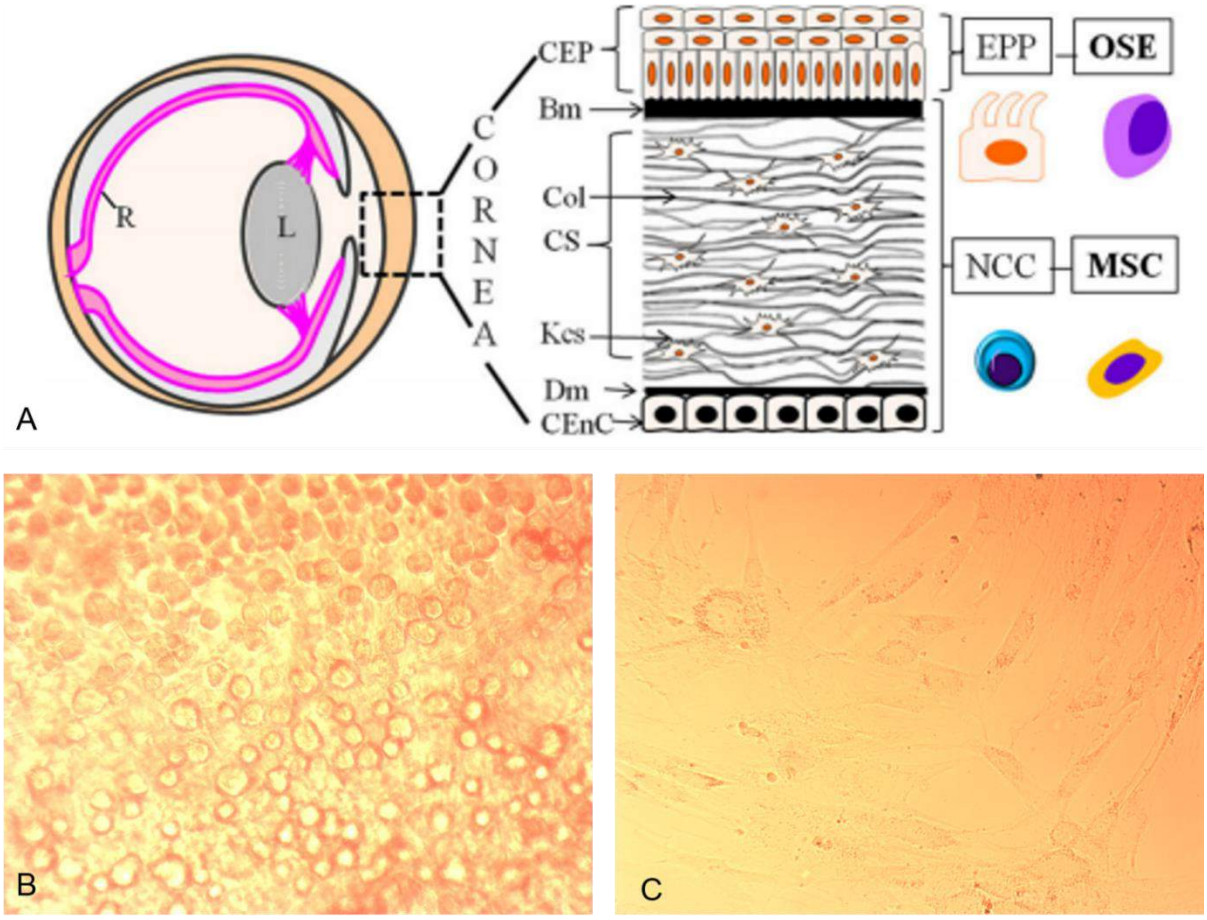

Figura 1. Microanatomía de la córnea. Aspecto de **ADASCs** humanas en cultivo.
(A) Esquema de capas en la córnea y su desarrollo. La córnea se compone de tres capas: las células epiteliales corneales: **CECs**, estroma corneal: **CS** y endotelio corneal: **CEn**, y dos membranas acelulares. La membrana de Bowman: **BM** que separa el epitelio corneal: **CEP** y **CS**. Membrana de Descemet: **DM**, intercalada entre **CS** y células endoteliales corneales: **CEnCs**. El CEP se deriva del EPP: precursores epiteliales que se originan en las células del ectodermo de la superficie ocular: **OSEs**. Tanto las **CS** como las **CEnCs** se derivan de las células de la cresta neural: **las NCCs** que surgen de las **MSCs**. La figura está tomada del artículo científico con referencia Chakrabarty y cols. (181). **(B)** Aspecto microscópico (fotografía de contraste de fase) de las **ADASCs** humanas (aumento de 10 ×). **(C) ADASCs** humanas en cultivo. La figura está extraída del capítulo científico con referencia Alió JL y cols. (41).

1.2.1.1 Células madre mesenquimales adultas derivadas de tejido adiposo (ADASCs).

Las células madre adultas derivadas del tejido adiposo **ADASCs** han despertado un gran interés en la medicina regenerativa y se utilizan ampliamente en la terapia celular. Su baja inmunogenicidad y su capacidad para autorrenovarse, diferenciarse, migrar a sitios dañados y actuar a través de rutas autocrinas y paracrinas se han establecido en conjunto como los principales mecanismos por los que se produce la reparación y regeneración celular. La fracción vascular del estroma (**SVF**) recién aislada del tejido adiposo se consideró para una regeneración tisular satisfactoria más adecuada, ya que contiene células madre/estromales multipotentes (llamadas células madre derivadas del tejido adiposo **ADASCs**, ampliamente conocidas por su comportamiento proliferativo y de diferenciación. a los elementos estromales, la **SVF** contenía un alto porcentaje de múltiples linajes de origen endotelial, hematopoyético y pericítico (182–185). Como se describió anteriormente, después del aislamiento y cultivo de la **SVF** (186,187), las células adherentes indican la presencia de homogeneidad o heterogeneidad de **ADASCs** indiferenciadas.

El análisis de la citometría de flujo proporcionó una evidencia de la ***inmunofenotipificación*** de las **ADASCs**; las pautas para su caracterización mostraron que ciertos marcadores se expresan positivamente por contrario a otros que no se expresan (187):

- **<u>Marcadores positivos:</u>**
  - **Marcadores positivos primarios:** Marcadores estables como CD13, CD29, CD44, CD73, CD90, CD105 (>80% en **ADASCs**), y marcadores inestables como CD34 (presente en niveles variables).
  - **Marcadores secundarios positivos:** CD10, CD26, CD36, CD49d, CD49e.
- **<u>Marcadores negativos:</u>**
  - **Marcadores negativos primarios**: CD31, CD45, CD235a (<2%).

- **Marcadores secundarios bajos o negativos**: CD3, CD11b, CD49f, CD106, PODXL.

Sin cultivo, se reveló que las **ADASCs** recién aisladas eran altamente positivas para CD34 y positivas para CD117 y antígeno leucocitario humano - isotipo DR **(HLA-DR)**. Mientras tanto, las **ADASCs** cuando se obtienen por cultivo son en su mayoría negativas para CD34 y **HLA-DR**. Esto indica claramente que las células primarias son significativamente más prometedoras en caso de que necesitemos mantener un cierto nivel de CD34 en el injerto (186,188); Sin embargo, para un impacto significativo de las células mesenquimales, las **ADASCs** cultivadas deben considerarse especialmente para la diferenciación.

Además, las **ADASCs** tienen ***efectos inmuno-moduladores*** y características proliferativas: En primer lugar, un estudio preclínico reciente sugirió que las **MSCs**, especialmente las **ADASCs**, regulaban negativamente numerosos marcadores de inflamación en cuanto a **mRNA** como **IL-1α**, **IL-1β**, **IL-6**, **IL- 10, TNF-α**, factor estimulante de colonias de granulocitos (**G-CSF**), proteína quimioatrayente de monocitos-1 (**MCP**-1), proteína inflamatoria de macrófagos-1α (**Mip**-1α), quimioatrayente de queratinocitos (**KC**), factor inhibidor de leucocitos (**LIF**), y regulan positivamente el factor de crecimiento proangiogénico **VEGF** (189)**.** Se pueden implantar las **ADASCs** cuando las citocinas inflamatorias se reducen a un nivel de máximo de 500 pg / ml de **IL**-6 y 30 pg / ml de **IL**-8 (30). Las **ADASCs** estimulan la inmunidad, se producen cambios en los macrófagos y se inhiben las células T y dendríticas, induciendo angiogénesis, disminución de la apoptosis y fibrosis con un aumento del proceso antiinflamatorio. Además, las **ADASCs** mostraron tasas más altas de proliferación cuando se expandieron *in vitro* (190). Estas características de las **ADASCs** en conjunto parecía que se promuevan durante la reparación de tejidos, donde se esperaba que la proliferación celular, la angiogénesis y los procesos antiinflamatorios ocurrieran rápidamente

en los sitios dañados. Para usos de trasplante en aplicaciones de queratocono, las **ADASCs** deben estar en un estado de inactividad donde se detiene la proliferación y se inicia el proceso de diferenciación (21).

Las **h-ADASCs** cultivadas *in vitro* (Figuras. 1B, 1C) en condiciones de ***diferenciación*** de queratocitos expresan colágenos y otros componentes de la matriz específicos de la córnea. Esta expresión es cuantitativamente similar a la lograda por las células madre humanas del estroma corneal (**h-CSSCs)** diferenciadas (191). La diferenciación de las **h-ADASCs** en queratocitos humanos funcionales también se ha demostrado *in vivo*, por primera vez, en un estudio previo de nuestro grupo utilizando el conejo como modelo (21). Antes del trasplante, se debe establecer la multipotencia de las **h-ADASCs** induciendo su diferenciación hacia linajes mesodérmicos, endodérmicos y ectodérmicos (190). Estas células, una vez implantadas en el estroma, expresan no solo colágenos de tipo I y VI (los componentes principales de la matriz extracelular corneal), sino también marcadores específicos de queratocitos como el queratocán y el aldehído deshidrogenasa (**ALDH)**. Un estudio reciente *in vitro* informó que un suplementario con ácido retinoico (**RA**) mejoraba la diferenciación de las **ADASCs** hacia un fenotipo de queratocitos. Las **ADASCs** diferenciadas mostraron una regulación positiva del queratocán, aumentaron la cantidad de colágeno tipo I y **ECM**, y mejoraron la expresión de queratocán, aldehído deshidrogenasa 3A1, lumicán y decorina. Mientras tanto, suplementar **RA** redujo la formación de tejido fibrótico, este hecho recientemente investigado es interesante para nuestro estudio (192).

1.2.1.2 Células madre mesenquimales de la médula ósea (BM-MSCs).

Park y cols. informaron que las **BM-MSCs** humanas se diferencian *in vitro* en células similares a los queratocitos cuando se cultivan en condiciones específicas de diferenciación de queratocitos (193). Demostraron una fuerte expresión de marcadores de queratocitos como lumicán

y aldehído deshidrogenasa (**ALDH**) junto con la pérdida de expresión de marcadores de **MSCs** como α-actina del músculo liso. Sin embargo, no pudieron demostrar una expresión evidente de queratocán en estas células diferenciadas (193). Trosan y cols. demostraron que las **BM-MSCs** de ratones cultivadas en extractos de córnea y factor de crecimiento similar a la insulina-I (**IGF-I**), se diferencian de manera eficiente en células similares a la córnea con expresión de marcadores específicos de la córnea, como la citoqueratina 12, el queratocán y el lumicán (194). La supervivencia y diferenciación de las **BM-MSCs** humanas en queratocitos también se ha demostrado *in vivo* cuando estas células se trasplantan dentro del estroma corneal. Se observó expresión de queratocano sin ningún signo de respuesta inmunitaria o inflamatoria (195).

1.2.1.3 Células madre mesenquimales del cordón umbilical (UCMSCs).

Las **MSCs** humanas aisladas del cordón umbilical neonatal han mostrado un comportamiento de diferenciación similar a otros tipos de **MSCs** cuando se trasplantan dentro del estroma corneal *in vivo*, expresando marcadores específicos de queratocitos como el queratocán sin inducir respuestas inmunitarias o de rechazo (196). Liu y cols. informaron que la inyección de estas células dentro del estroma corneal de ratones nulos lumicán mejoró la transparencia corneal y aumentó el grosor del estroma con láminas de colágeno reorganizadas, y también mejoró la función de los queratocitos del huésped a través de una mayor expresión de queratocán y **ALDH** en estos ratones (26). Estos datos son alentadores, aunque hasta la fecha, el uso autólogo de células madre mesenquimales del cordón umbilical (**UCMSCs**) no es posible, ya que el cordón umbilical de los nuevos nacimientos no se almacena sistemáticamente con las limitaciones de tiempo para un almacenamiento prolongado.

1.2.1.4 Células madre embrionarias (ESCs).

La experiencia actual con estas **ESCs** humanas para la regeneración del estroma corneal es mucho más limitada. Chan y cols. informaron que la diferenciación de estas células en un linaje de queratocitos se puede inducir *in vitro*, lo que demuestra una regulación positiva de los marcadores de queratocitos, incluido el queratocán (197).

Hasta donde sabemos, no se han realizado estudios *in vivo* con estas células en el campo de la medicina regenerativa para el estroma corneal. El uso de estas células también plantea muchos problemas éticos y, junto con la falta de datos *in vivo*, desanima su uso actual en un entorno clínico.

1.2.1.5 Células madre pluripotentes inducidas (iPSCs).

Como ya se mencionó, el uso de **ESCs** se ha abandonado parcialmente debido a preocupaciones éticas y especialmente desde el descubrimiento de las **iPSCs** (37), que se derivan de células adultas. En 2012, Shinya Yamanaka de Japón y John B. Gurdon del Reino Unido recibieron el Premio Nobel de Medicina por descubrir que las células maduras especializadas se pueden reprogramar a un estado inmaduro o de células madre y luego redirigir al linaje celular requerido utilizando factores específicos y estímulo ambiental. Las **iPSCs** prometen ser el futuro de la ingeniería celular y de tejidos (37,198,199).

En cuanto a su aplicación en la regeneración del estroma corneal, las **iPSCs** humanas han demostrado la capacidad de diferenciarse en células de la cresta neural (el precursor embrionario de los queratocitos). Al cultivarlos en el tejido corneal cadavérico, promueve su diferenciación de queratocitos al adquirir una morfología similar a los queratocitos y que expresan marcadores similares a los queratocitos corneales (38,181). También se ha demostrado que las **MSCs** derivadas de **iPSCs** ejercen propiedades inmunomoduladoras en la córnea similares a las observadas con las

BM-MSCs (200). Hasta donde sabemos, no se han publicado estudios que informen sobre la capacidad de las **iPSCs** para diferenciarse en queratocitos adultos *in* vivo en el modelo animal.

1.2.1.6 Células madre del estroma corneal (CSSCs).

Las empalizadas limbares de Vogt forman un nicho que contiene tanto las **LESCs** y **CSSCs** (201). Las **CSSCs** expresan genes típicos de los descendientes del ectodermo neural como el gen homeótico de la caja pareada 6 (**PAX6)**, marcadores de células madre adultas como **ABCG2**, y **MSCs** marcadores como **CD73** y **CD90** (5,201), exhiben el crecimiento clonal, las propiedades de autorrenovación y el potencial de diferenciación en múltiples tipos de células distintos. A diferencia de los queratocitos, **h-CSSCs** experimentan una expansión extensa *in vitro* sin perder su capacidad para adoptar un fenotipo de queratocito (5,201). Estas **MSCs** corneales tienen un potencial demostrado de diferenciación en el epitelio corneal y en queratocitos adultos *in vitro* (201,202). Cuando se cultivan en un sustrato de nanofibras poliméricas alineadas en paralelo, las **h-CSSCs** producen capas de fibras de colágeno muy paralelas con un empaquetamiento y un diámetro de fibrillas indistinguibles de los de las láminas del estroma humano (203). La habilidad de **h-CSSCs** para adoptar una función de queratocitos ha sido aún más sorprendente *in vivo*. Cuando se inyecta en el estroma corneal del ratón, las **h-CSSCs** expresan **mRNA** de queratocitos y proteína, reemplazando la **ECM** del ratón con componentes de la matriz humana. Estas células inyectadas permanecen viables durante muchos meses, aparentemente convirtiéndose en queratocitos inactivos (25).

Todos estos datos experimentales han despertado el interés en esta novedosa terapia basada en células para las enfermedades del estroma corneal, sin embargo, antes de su aplicación en la práctica clínica, su eficacia y seguridad deben estar bien probadas en ensayos clínicos en humanos, mientras que otras limitaciones como el alto nivel de los costes del laboratorio y las posibles

diferencias de eficacia terapéutica entre los diferentes donantes deben considerarse de una forma seria.

1.2.2 TÉCNICAS DE REGENERACIÓN DEL ESTROMA CORNEAL: APLICACIÓN TEMPRANA EN LA PRÁCTICA CLÍNICA

Todos estos tipos de células madre se han utilizado de diversas formas en varios proyectos de investigación para encontrar el procedimiento óptimo para regenerar el estroma corneal humano. La implantación de las **MSCs** de córnea se ha ensayado y estudiado mediante el trasplante intraestromal directo o después de la implantación desde la superficie ocular, por vía intravenosa y en la cámara anterior donde se espera la migración celular dentro del estroma. Se han analizado diferentes portadores celulares para potenciar los posibles beneficios de esta terapia.

1.2.2.1 Implantación de células madre en la superficie ocular.

La implantación superficial de las **MSCs** sería el enfoque óptimo para la reconstrucción de la superficie ocular y la regeneración del nicho de las **LESCs**. Sin embargo, la implantación superficial de las **MSCs** seguiría desempeñando un papel en la prevención o modulación de las cicatrices del estroma anterior después de una lesión en la superficie ocular (como una quemadura química). Como se discutió anteriormente, las **MSCs** secretan factores paracrinos que mejoran la reepitelización corneal y la cicatrización de heridas estromales (33). Por tanto, el beneficio de las **MSCs** en la superficie ocular puede estar más justificado por estos efectos paracrinos que por la diferenciación directa de las **MSCs** en células epiteliales, ya que la evidencia de estas últimas es controvertida. A este respecto, Di y cols. ensayaron *inyecciones subconjuntivales* de **BM-MSCs** en ratones diabéticos y reportaron un aumento de la proliferación de células epiteliales corneales, así

como una respuesta inflamatoria atenuada mediada por el gen estimulado por el factor de necrosis tumoral-α 6 (**TSG6)** (204).

Holan y cols. sugirieron la aplicación de **MSCs** en la superficie ocular utilizando andamios de nanofibras. Informaron que las **BM-MSCs** cultivadas en estos andamios pueden mejorar la reepitelización, suprimir la neovascularización y la reacción inflamatoria local cuando se aplican en un ojo lesionado por álcali en un modelo de conejo, y estos resultados fueron comparables a los obtenidos con células madre epiteliales del limbo, y ambos fueron mejores que los obtenidos con **ADASCs** (205). El mismo grupo sugirió que estos resultados se pueden mejorar cuando estos andamios de nanofibras sembrados con **BM-MSCs** de conejo cubiertos con andamios de nanofibras cargados con ciclosporina-A (**CSA**), observando una supresión de cicatrices aún mayor y resultados de curación con la combinación de ambas nanofibras con **MSCs** y **CSA** (206).

La aplicación tópica de una suspensión de **ADASCs** autólogas se ha informado en un informe de caso clínico aislado en cual los autores describen la curación de una úlcera neurotrófica que no responde al tratamiento convencional (207). La falta de más evidencia científica para este método de administración desde 2012 plantea dudas sobre su eficacia real.

Finally, Basu y cols. sugirieron la liberación de **MSCs** usando pegamento de fibrina (36). La resuspension de **CSSCs** en una solución de fibrinógeno humano se añadió a una superficie ocular herida con trombina en el lecho de la herida y posteriormente los geles de fibrinógeno. Usando esta aplicación, demostraron la prevención de la cicatrización corneal en el modelo de ratón junto con la generación de un nuevo estroma con una organización del colágeno indistinguible de la del tejido nativo. Actualmente, este grupo está involucrado en un ensayo clínico para validar estos hallazgos, utilizando **CSSCs** autólogas y heterólogas de biopsias limbares para casos de quemaduras químicas, úlceras neurotróficas y cicatrices establecidas. El informe preliminar mostró

una mejora en los parámetros visuales, la epitelización corneal, la neovascularización corneal y la claridad corneal (208).

1.2.2.2 Implantación intraestromal de células madre solas.

En algunos estudios se ha ensayado la inyección directa *in* vivo de células madre dentro del estroma corneal, se demostró la diferenciación de las células madre en queratocitos adultos sin signos de rechazo inmunológico. En nuestro estudio, también demostramos la producción de **ECM** humana por inmunohistoquímica cuando se trasplantaron unas **h-ADASCs** dentro de la córnea del conejo (Figuras. 1B, 1C, 2A, 2B) (21). Como era de esperar, se encontró que los tipos de colágeno I y VI se expresaban en el estroma corneal de los conejos, así como en las **h-ADASCs** trasplantadas. Los tipos de colágeno III y IV, que normalmente no se expresan en el estroma corneal, no se detectaron ni en el estroma corneal del huésped ni en las **h-ADASCs** trasplantadas (Figura. 2C). Du y cols. (25) informaron sobre la restauración de la transparencia y el grosor de la córnea en ratones nulos lumicán (córneas delgadas, neblina y alteración de la organización normal del estroma) tres meses después del trasplante intraestromal de **CSSCs** humanas. También confirmaron que el sulfato de queratán humano se depositó en el estroma del ratón y se reorganizaron las láminas de colágeno del huésped, concluyendo que la administración de **h-CSSCs** al estroma humano cicatrizado puede aliviar las cicatrices corneales sin necesidad de cirugía (25). Liu y cols. informaron hallazgos muy similares que utilizaron **h-UMSCs** utilizando el mismo modelo animal (26). Coulson-Thomas y cols. encontraron que, en un modelo de ratón para mucopolisacaridosis, las **h-UMSCs** trasplantadas participan tanto en el recambio de glicosaminoglicanos extracelulares (**GAGs**) como permiten a los queratocitos del huésped catabolizar los productos de **GAGs** acumulados (27).

Recientemente, nuestro grupo ha publicado el primer ensayo clínico en el que se reporta la seguridad y eficacia preliminar de la terapia celular del estroma corneal humano (30,177). En este ensayo clínico piloto, implantamos **ADASCs** autólogas (obtenidos mediante liposucción electiva) dentro de un bolsillo lamelar asistido por láser de femtosegundo en la mitad del estroma en pacientes con queratocono avanzado (Figuras 1B, 1C). No se observaron signos de inflamación o rechazo, lo que confirma toda la evidencia previa reportada en el modelo animal (30,177).

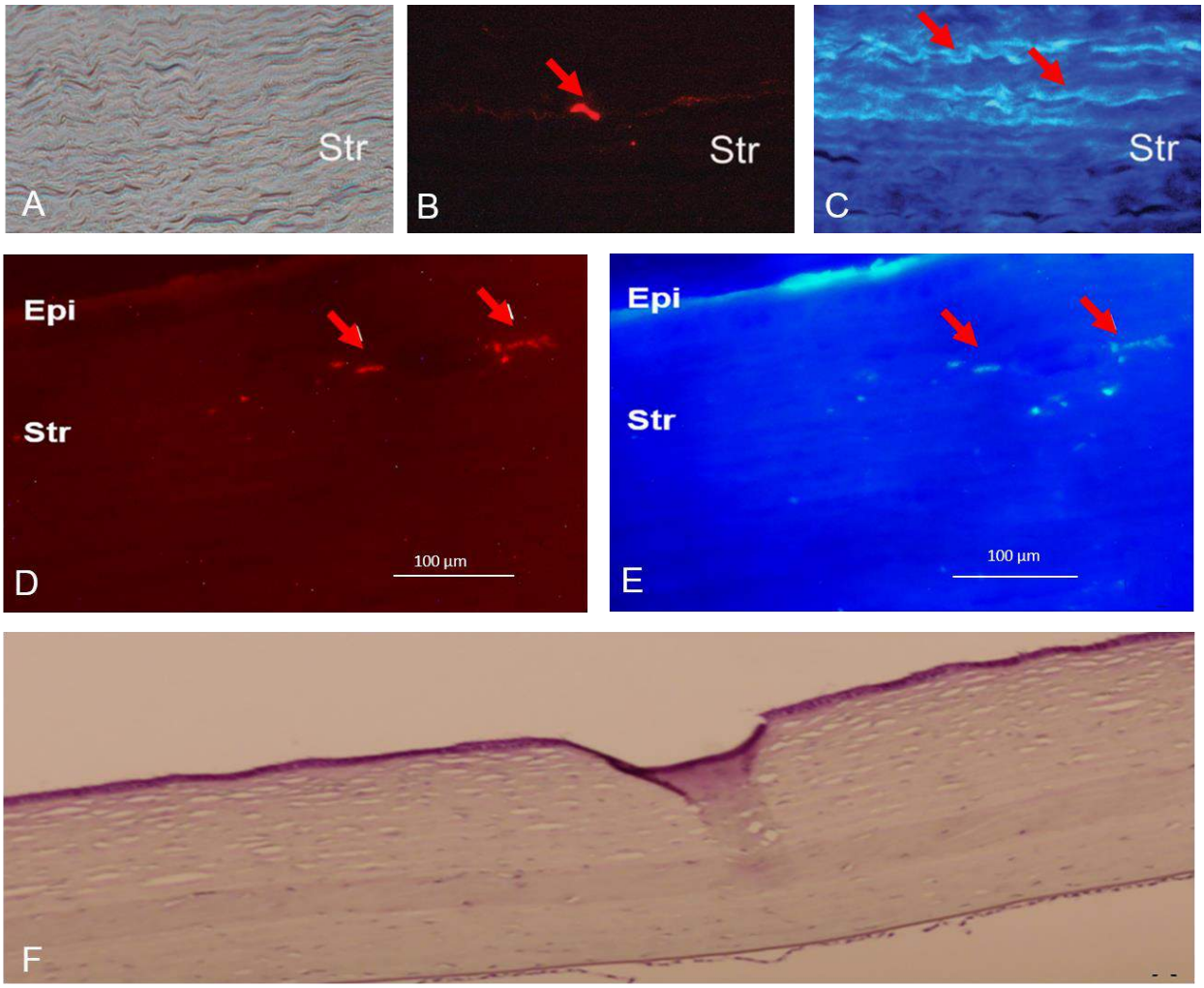

Figura 2. Observación de **ADASCs** humanas *in* vivo en el estroma corneal de conejo. **(A, B, C)** Trasplante de **ADASCs** humanas en el espesor del estroma de conejo *in* vivo. **(A)** Fotografía de contraste de fase que muestra un estroma morfológicamente intacto tres meses después del trasplante. **(B)** la misma sección que muestra la supervivencia de las células implantadas detectando el colorante Vybrant CM-DiL (flecha roja). **(C)** La misma sección que muestra la

expresión de nuevo colágeno de tipo I humano dentro del estroma del conejo (Str: estroma; Ampliación, 400X) (flechas rojas). Foto cortesía del Dr. Arnalich Montiel. Abreviatura: Str: estroma **(D, E, F)** Mejora del estroma corneal con el implante del estroma corneal humano descelularizado/recelularización con **h-ADASCs** en el modelo animal de conejo. **(D)** Células humanas (flechas rojas), marcadas con CM-DiI, alrededor y dentro del implante, lo que confirma la presencia de células humanas vivas dentro del estroma corneal del conejo. **(E)** Misma sección que muestra el queratocán humano y su eventual diferenciación en queratocitos humanos (flechas rojas) (aumento de 400 ×); Abreviatura: Epi: epitelio. **(F)** Tinción con hematoxilina-eosina de una córnea de conejo con un injerto implantado de estroma corneal humano descelularizado con colonización por **h-ADASCs** (aumento 200 ×). Figura extraída del capítulo científico con referencia Alió JL y cols. (41).

1.2.2.3 Implantación intraestromal de células madre junto con un andamio biodegradable.

Para potenciar el crecimiento y desarrollo de las células madre inyectadas en el estroma corneal, se ha realizado un trasplante junto con **ECM** sintético biodegradable. Espandar y cols. inyectaron **h-ADASCs** con un hidrogel de ácido hialurónico semisólido en el estroma corneal del conejo e informaron una mejor supervivencia y diferenciación de queratocitos de las **h-ADASCs** en comparación con su inyección sola (Figuras 3A, 3B) (22). Ma y cols. utilizaron **ADASCs** de conejo con un andamio biodegradable poliláctico-co-glicólico en un modelo de conejo de lesión del estroma en el que observaron tejido recién formado con remodelación exitosa del colágeno y menos cicatrices estromales (Figuras 3A-3C) (209). A los tres meses se observó una alta tasa de extrusión del implante (Figuras 3D, 3E). Los datos iniciales muestran que estos andamios podrían mejorar los efectos de las células madre en el estroma corneal, aunque se requiere y se justifica más investigación.

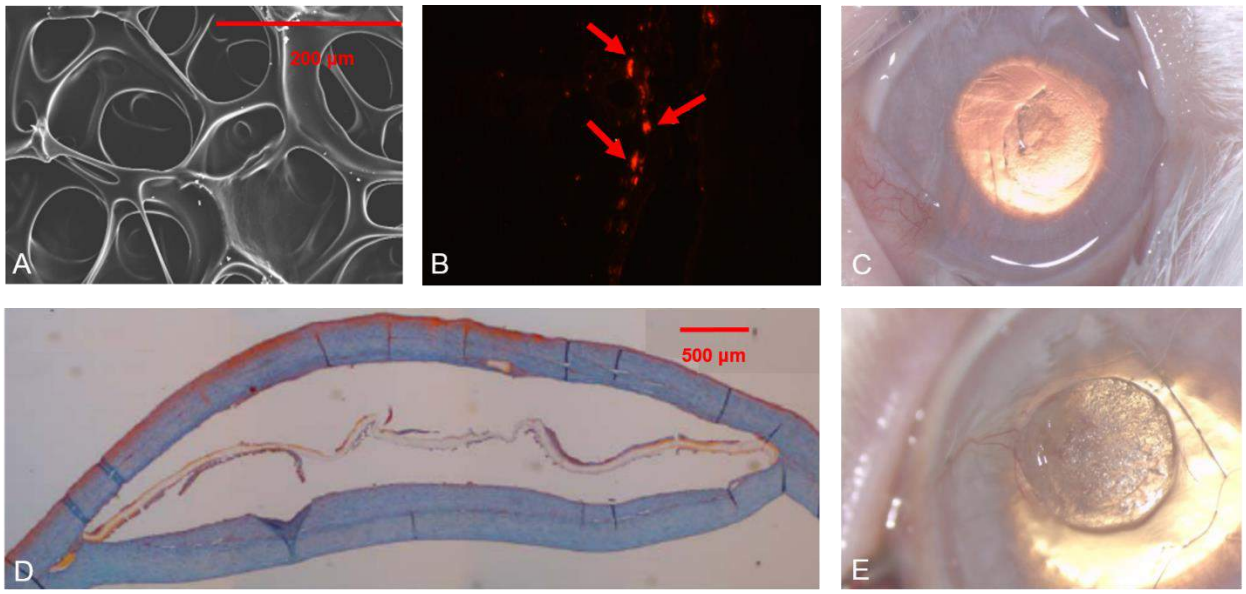

Figura 3. Trasplante de membranas macroporosas de membranas de polietilacrilato (**PEA**) junto con **ADASCs** humanas en el estroma de conejo *in* vivo.
(A) Imagen de microscopía electrónica de la **PEA**. **(B)** Supervivientes de las **ADASCs** después de tres meses (flechas rojas). **(C)** Implante intraestromal *in* vivo, nótese su transparencia. **(D)** La ausencia de una biointegración real conduce al desprendimiento de la de **PEA** del estroma circundante en las secciones histológicas. **(E)** Se observó una alta tasa de extrusión del implante. Figura extraída del capítulo científico con referencia Alió JL y cols. (17,41).

1.2.2.4 Implantación intraestromal de células madre con un andamio de estroma corneal descelularizado.

La compleja estructura del estroma corneal aún no se ha replicado y existen inconvenientes bien conocidos en el uso de diseños sintéticos basados en andamios: i) fuertes respuestas inflamatorias inducidas en su biodegradación y ii) casi todos los materiales poliméricos causan una respuesta inflamatoria inespecífica (17).

Recientemente, se han descrito varias técnicas de descelularización corneal, que proporcionan un **ECM** corneal acelular (18). El protocolo de descelularización ideal debe verificar:

- Eliminar el contenido celular y las moléculas de antígeno del xenoinjerto para reducir la reacción inmune del huésped (210).

- Conservar las proteínas estructurales y funcionales de la **ECM** sin alterar la matriz tisular general (211).
- Mantener la transparencia corneal (212).
- Apoyar el crecimiento de las células del huésped y de la córnea (213).

Todos los métodos de descelularización pueden resultar en alguna alteración de la ultraestructura del **ECM**, sin embargo, el proceso de descelularización debe optimizarse tratando de minimizar estos efectos indeseables (214). La descelularización completa se logra mediante combinaciones de métodos químicos, físicos y enzimáticos (215,216).

Estudios recientes realizaron diferentes métodos para la descelularización, resumimos brevemente estas metodologías:

1. **Tratamientos físicos**: Incluyen procesos de agitación, presión y congelación/descongelación que sirven para lisar las células, facilitar su enjuague y la eliminación del contenido celular del **ECM** (216).

2. **Métodos químicos**: Consta de diferentes metodologías entre ellas:

Los tratamientos con ácidos o bases se utilizan a menudo en combinación con otros métodos, como detergentes y alcoholes (211,217).

- Los detergentes iónicos y no iónicos se han utilizado en protocolos de descelularización con diversos grados de éxito. Los detergentes iónicos, como la solución de dodecilsulfato de sodio (**SDS**), son extremadamente efectivos en la solubilización de las membranas celulares, pero pueden causar la desnaturalización de las proteínas y, a veces, afectan la estructura de la **ECM** (218). Los detergentes no iónicos generalmente se consideran suaves y relativamente no desnaturalizantes, ya que rompen las interacciones lípido-lípido y lípido-proteína en lugar de las interacciones proteína-proteína (218).

- Los tratamientos hipotónicos e hipertónicos con agua desionizada y soluciones de cloruro de sodio pueden hacer que las células se lisen dentro de un tejido u órgano (216).
- Los alcoholes, como el etanol, eliminan los lípidos de los tejidos y, por lo tanto, alteran la membrana celular (211). Este método logró la eliminación completa de las células y conservó la estructura y la transparencia del tejido corneal original.
- Los agentes quelantes, como el ácido etilendiaminotetraacético **EDTA**, se utilizan a menudo en combinación con otros agentes descelularizantes, incluido el **SDS** (219).

3. **Métodos biológicos**: Los agentes enzimáticos, como las nun-cleasas y la fosfolipasa A2, se suelen utilizar en combinación con otras técnicas para alcanzar la descelularización completa. La aprotinina, un inhibidor competitivo de la serina proteasa, se usa habitualmente en combinación con un tratamiento con detergente para evitar la degradación enzimática de las proteínas de la matriz extracelular (215,220).

4. **Radiación con haz de electrones (haz-e)**: el tejido de la córnea se ha tratado con radiación con haz de electrones (haz-e) y se ha almacenado en albúmina sérica humana recombinante. El uso de (e-beam) mostró un gran éxito en muchos procedimientos oftálmicos porque aumenta la esterilidad de los tejidos corneales (221).

El tejido descelularizado ha ganado atención en los últimos años, ya que proporciona un entorno más natural para el crecimiento y la diferenciación de las células en comparación con los andamios sintéticos. Además, los componentes de la **ECM** generalmente se conservan entre las especies y son bien tolerados por los receptores xenogénicos. Además, los queratocitos son esenciales para remodelar el estroma corneal y para la fisiología epitelial normal (222). Esto resalta

la importancia de trasplantar un sustituto celular junto con el soporte estructural (**ECM** acelular) para realizar estas funciones críticas en la homeostasis corneal.

Hasta donde sabemos, todos los intentos de repoblar los andamios corneales descelularizados han utilizado células corneales (213,217,223), pero como ya se ha comentado, estas células tienen importantes inconvenientes que limitan su uso autólogo en la práctica clínica (daño al tejido donante, falta de células y subcultivos celulares más difíciles), reorientando así los esfuerzos para encontrar una fuente extraocular de células autólogas. En un estudio previo de nuestro grupo, mostramos la perfecta biointegración de láminas estromales corneales humanas descelularizadas de (100 **µm** de espesor) con y sin colonización por **h-ADASCs** dentro de la córnea del conejo (Figuras 2D, 2F), y no observamos respuesta de rechazo a pesar de que el injerto sea xenogénico (17). También demostramos la diferenciación de **h-ADASCs** en queratocitos funcionales dentro de estos implantes *in vivo*, que luego lograron su biofuncionalización adecuada (Figuras 2D, 2E). En nuestra experiencia, la descelularización de todo el estroma corneal (~ 500 µm) (utilizando detergente aniónico de dodecilsulfato de sodio) carece de eficacia, ya que no es posible eliminar por completo el componente celular. Sin embargo, demostramos que este método elimina completamente el componente celular y preserva la integridad del tejido del estroma corneal cuando se tratan lentículos más delgados; un método que luego ha sido confirmado por otros autores con el uso de la microscopía electrónica (19,224,225). Otros también han ensayado la integración de **ECM** de cartílago articular de cerdo descelularizado colonizado con **BM-MSCs** de ratón en el estroma corneal de conejo y han informado hallazgos similares, aunque la transparencia de estos andamios descelularizados no se informó claramente (226).

En nuestra opinión, la implantación de **MSCs** junto con **ECM** corneal descelularizada sería la mejor técnica para restaurar de una manera efectiva el grosor de una córnea humana patológica

y severamente debilitada porque la implantación de las **MSCs** por sí sola solo logra una nueva formación de **ECM** limitada y una restauración del espesor (21,30). Además, mediante esta técnica, y mediante el uso de las **MSCs** autólogas de un paciente determinado, teóricamente es posible transformar injertos alogénicos en injertos autólogos funcionales, evitando así cualquier riesgo de rechazo. Los tejidos descelularizados tienen el inconveniente de requerir equipos de laboratorio específicos, aunque los bancos de ojos podrían potencialmente hacerlo y entregar dichos injertos a diferentes centros clínicos. La queratofaquia (inserción intraestromal de un lentículo alogénico) fue descrita por Barraquer en 1964, pero se abandonó debido a la imprevisibilidad del resultado refractivo y la frecuencia relativamente alta de desarrollo de neblina de la interfase (227). La falta de turbidez observada en nuestro ensayo clínico piloto podría estar relacionada con la ausencia de queratocitos de donantes que podrían activarse potencialmente en el postoperatorio y generar tejido cicatricial. Además, ya se han descrito episodios de rechazo tras la implantación de lentículas alogénicas, riesgo que teóricamente se evita con el uso de injertos descelularizados (225). Debemos considerar que mientras se utilice tejido descelularizado humano, no habrá riesgo de enfermedades zoonóticas.

1.2.2.5 Inyección de células madre en la cámara anterior.

Demirayak y cols. informaron que las **BM-MSCs** y **ADASCs**, suspendidas en solución tamponada con fosfato (**PBS**) e inyectadas en la cámara anterior después de una lesión corneal penetrante en un modelo de ratón, pueden colonizar el estroma corneal y aumentar la expresión de marcadores específicos de queratocitos como el queratocán, con un aumento demostrado en la densidad de los queratocitos por microscopía confocal (24). Por el contrario, los posibles efectos secundarios de esta inyección de **MSCs** en la cámara anterior para el epitelio del cristalino y

la trabécula son muy cuestionables, ya que pueden inducir cicatrices y glaucoma posterior. Teniendo esto en cuenta, el uso clínico potencial de este enfoque, en nuestra opinión, es limitado.

1.2.2.6 Inyección intravenosa de células madre.

También se ha probado el uso sistémico, por inyección intravenosa, de **MSCs**. La inyección intravenosa de **BM-MSCs** en ratones después de un trasplante de córnea de aloinjerto pudo colonizar la córnea y la conjuntiva trasplantadas (tejidos oculares inflamados) pero no la córnea no injertada contralateral, disminuyendo simultáneamente la inmunidad y mejorando significativamente la tasa de supervivencia del aloinjerto (228). Yun y cols. informaron recientemente hallazgos similares con la inyección intravenosa de **MSCs** derivadas de **iPSCs** y **BM-MSCs** después de una lesión química superficial, donde observaron que la opacidad corneal, la infiltración inflamatoria y los marcadores inflamatorios en la córnea disminuyeron notablemente en los ratones tratados, sin diferencias significativas entre ambos tipos de **MSCs** (200). Por el contrario, nuestro grupo no observó ningún beneficio en las tasas de supervivencia y rechazo del aloinjerto corneal después de la inyección sistémica de **ADASCs** de conejo antes de la cirugía, durante la cirugía y en varios momentos después de la cirugía en conejos con córneas vascularizadas (modelo más similar a los trasplantes de córnea humana que los reportados con los ratones). Se observó una supervivencia del injerto más corta en comparación con los injertos de córnea no tratados (229).

1.2.3 MSCs AUTÓLOGAS VERSUS ALOGÉNICAS

Una cuestión fundamental para los ensayos clínicos futuros para evaluar más a fondo la viabilidad de la terapia celular del estroma corneal es si el uso de las **MSCs** autólogas es realmente necesario, y si las **MSCs** alogénicas podrían lograr el mismo beneficio sin ningún riesgo de inflamación o rechazo. Si consideramos toda la evidencia publicada en el modelo animal donde se implantaron **MSCs** humanas en el estroma corneal, a pesar de ser un trasplante xenogénico, nunca se han reportado signos de rechazo o inflamación (17,19,21–28). Esto coincide con la fuerte evidencia con respecto a las propiedades inmunomoduladoras e inmunosupresoras de las **MSCs**, que las ayudan a evadir el rechazo inmunológico del huésped y a sobrevivir inhibiendo la adhesión e invasión e induciendo la muerte celular de las células inflamatorias, en parte debido a un rico glucocáliz extracelular que contiene **TSG6** (29,230). Se ha demostrado que **TSG6** juega un papel crítico en las propiedades inmunosupresoras exhibidas por las **MSCs** (28,200,204). En conjunto, el uso de las **MSCs** alogénicas simplificaría enormemente la aplicación clínica de las **MSCs**, ya que los centros de aplicación clínica no necesitarían ningún equipo específico porque los posibles bancos de las **MSCs** podrían almacenar y suministrar células madre para su uso en pacientes. Ya existen sistemas de bajo costo disponibles que son capaces de mejorar la preservación de las **MSCs** a temperaturas hipotérmicas mientras mantienen su función normal, ampliando de esta manera el marco de tiempo para la distribución entre el sitio de fabricación y la clínica, y reduciendo los desechos asociados con la vida útil limitada de las células almacenadas en su estado líquido (231). Funderburgh y cols. informaron recientemente que las **MSCs** de diferentes donantes pueden tener diferentes propiedades inmunosupresoras y, en consecuencia, diferentes capacidades para regenerar y aliviar las cicatrices del estroma (232). Teniendo en cuenta este importante hallazgo, los bancos de las **MSCs** podrían seleccionar los mejores donantes para expandir y suministrar solo aquellas

MSCs con la mayor capacidad inmunosupresora y regenerativa, por lo que las células autólogas no serían necesarias. También debemos considerar que los queratocitos adultos obtenidos de las **MSCs** autólogas pueden tener el mismo defecto genético que condujo a la enfermedad corneal, como en el caso de la distrofia corneal. En este escenario, sería interesante el uso de las **MSCs** alogénicas en lugar de las autólogas. Un estudio reciente observó diferencias en la expresión génica entre los queratocitos derivados de **iPSCs** generados a partir de fibroblastos del estroma corneal humano normal y queratocónico, influyendo en el crecimiento y la proliferación celular, lo que confirma que, al menos en los casos de queratocono, las células adultas obtenidas de las **MSCs** aún pueden no ser funcionalmente normales (233).

1.2.4 EXOSOMAS DE MSCs

Los exosomas son vesículas extracelulares de tamaño nanométrico que se originan a partir de la fusión de cuerpos multivesiculares intracelulares con membranas celulares y se liberan en espacios extracelulares (230). Se les ha implicado en la capacidad de las **MSCs** para reparar el tejido dañado. Basu S. y cols. demostraron recientemente que los exosomas aislados de los medios de cultivo de **CSSCs** humanas tenían propiedades inmunosupresoras similares y también redujeron significativamente la cicatrización del estroma en las córneas heridas *in vivo* (208). Este hallazgo sugiere que para algunas enfermedades, como la prevención o reducción de cicatrices corneales, los exosomas de las **MSCs** pueden proporcionar una terapia no basada en células (232). Zhang y cols. sugirieron que los exosomas liberados por las **UCMSCs** trasplantadas en la córnea patológica pueden entrar dentro de los queratocitos y las células endoteliales de la córnea del huésped, con el papel de mejorar sus funciones (230). Los autores experimentaron *in vitro* con ratones con

mucopolisacaridosis VII y descubrieron que los exosomas secretados por las **UCMSCs** ayudaron en el proceso de reciclaje de los **GAGs** en los lisosomas de las células afectadas (27). Estos hallazgos abren un nuevo y emocionante campo para la investigación, ya que el uso de exosomas puede superar algunas de las limitaciones y riesgos asociados con la inyección celular intraestromal, dado que los exosomas se pueden aplicar potencialmente por vía tópica (196).

2. JUSTIFICACIÓN DE LA TESIS DOCTORAL

En la última década, la queratoplastia penetrante de espesor total ha sido parcialmente sustituida por técnicas lamelares donde solo se reemplazan las capas alteradas, como la técnica **DALK** para el estroma corneal (234). Esta técnica evita el rechazo endotelial, que es la causa más común de falla del injerto, pero aún presenta algunas desventajas como el rechazo del estroma inmune primario o el alto astigmatismo postoperatorio relacionado con las suturas (235,236)**.** Para evitar estos inconvenientes, hemos desarrollado un nuevo modelo de queratoplastia lamelar autóloga, que parte de un tejido de donante alogénico.

La terapia celular del estroma corneal es un enfoque terapéutico prometedor, pero el uso de queratocitos humanos autólogos tiene muchas desventajas, como causar daño a la córnea del donante, las células son insuficientes y el subcultivo celular es ineficiente (176). Basándose sobre estudios previos y exitosos en animales realizados en parte por nuestro equipo, se ha investigado una fuente extraocular de células abundantes y más accesibles para este propósito (21,22)**.** Se ha demostrado que el tejido adiposo humano adulto es una fuente ideal de células madre autólogas, ya que satisface muchos requisitos: Es de fácil acceso a este tejido, tiene una alta eficiencia de recuperación de células, y sus células madre conocidas como "células madre adultas derivadas del tejido adiposo humano" **h-ADASCs**, pueden diferenciarse en diferentes linajes celulares como queratinocitos, osteoblastos, condroblastos, mioblastos, hepatocitos, neuronas, entre otros (21,176)**.**

Además, estas células han mostrado propiedades inmunomoduladoras incluso en escenarios xenogénicos (17,19). Descubrimos que las **ADASCs** humanas trasplantadas en las córneas de conejo dañadas podían diferenciarse en queratocitos corneales y producir colágeno corneal y queratocán que son característicos del estroma corneal humano (21)**.**

En los últimos años, se han utilizado protocolos para obtener matrices corneales descelularizadas porque proporcionan un entorno más natural para el crecimiento y diferenciación de las células en comparación con los andamios sintéticos. También se ha demostrado previamente la eficacia de la descelularización con **SDS** en la córnea humana. En nuestro estudio utilizamos **h-ADASCs** para repoblar nuestros andamios, los cuales han mostrado excelentes resultados durante el seguimiento, la transparencia corneal se ha conservado completamente sin ningún signo de cicatrización (19). Hemos podido demostrar que las **h-ADASCs** trasplantadas en una lámina humana descelularizada sobrevivieron al menos 12 semanas después del trasplante *in vivo* en el modelo animal, y también se diferenciaron en queratocitos humanos, por lo tanto, con este modelo podríamos potencialmente ser capaces de obtener un injerto autólogo utilizando tejido adiposo del paciente y una córnea de donante alogénico, evitando teóricamente el riesgo de rechazo del estroma asociado con las opciones de trasplante lamelar alogénico (19)**.** Además, la ventaja de nuestro protocolo es la posibilidad de obtener varios injertos de un único donante alogénico, aumentando la disponibilidad de tejido del donante y acortando las listas de espera.

El objetivo de la actual tesis doctoral e investigación es llevar a cabo la investigación realizada por nuestro grupo y aplicarla a pacientes humanos que padecen el queratocono. Un sencillo procedimiento de liposucción y una córnea de donante no viable para el trasplante pueden proporcionar un injerto de estroma autólogo ópticamente transparente, con biocompatibilidad demostrada. Con la nueva técnica quirúrgica no invasiva, se pueden evitar muchas complicaciones asociadas a las técnicas habituales, con el fin de mejorar el pronóstico visual y la calidad de vida de los pacientes.

Estos estudios experimentales abrieron la traslación de este concepto a la terapia de enfermedades de la córnea humana, utilizando la enfermedad del queratocono avanzado como modelo para este tipo de

terapia avanzada. Este estudio tiene como objetivo construir una terapia con células madre alternativa a las técnicas clásicas de trasplante de córnea para regenerar el estroma corneal, evitando las complicaciones y limitaciones frecuentemente observadas con las técnicas actuales.

3. HIPÓTESIS

La implantación intraestromal de células madre adiposas en córneas queratocónicas, ya sea sola o con un portador compuesto por una lámina del estroma corneal humano acelular, puede transformarse en queratocitos humanos adultos y mejorar la condición clínica de dichos pacientes al promover la regeneración del estroma de la córnea patológica in *vivo*. La evolución de estas células, así como la evolución de las láminas acelulares implantadas, se observará mediante la microscopía confocal.

4. OBJETIVOS DE LA TESIS

4.1 OBJETIVOS PRINCIPALES

El objetivo principal del presente estudio es evaluar el potencial de la terapia celular del estroma corneal en pacientes con queratocono avanzado, mediante:

1. **Analizar la seguridad/eficacia de la implantación intraestromal de:**
   - Células madre adultas autólogas derivadas del tejido adiposo (**ADASCs**) solas.
   - Láminas de estroma corneal humano descelularizado.
   - Láminas del estroma corneal humano recelularizadas con **ADASCs** autólogas.
2. Demostrar que la implantación de **ADASCs** mesenquimales aisladas o embebidas en una lámina corneal acelular humana, va seguida de proliferación celular y no genera ninguna respuesta clínica o histológica de inflamación o rechazo.
3. Demostrar que las láminas corneales acelulares (sin células) son bien toleradas en el huésped de la córnea afectada con queratocono, sin obtener complicaciones clínicas.
4. Demostrar que las láminas estromales descelularizadas, con o sin **ADASCs**, son capaces de mejorar el grosor de la córnea así como la ectasia corneal e irregularidades secundarias.

4.2 OBJETIVOS SECUNDARIOS

1. Explorar los resultados visuales y refractivos mediante la implantación de **ADASCs** y la implantación de láminas corneales descelularizadas o recelularizadas.

2. Describir la respuesta biológica del tejido corneal tras la implantación de **ADASCs,** y la implantación de láminas corneales descelularizadas o recelularizadas mediante el análisis del tejido corneal con métodos de imagen no invasivos como la **OCT** del segmento corneal anterior.

3. Demostrar que el implante de **ADASCs** en el bolsillo corneal provoca una modesta mejora en los parámetros paquimétricos, y la implantación de láminas corneales descelularizadas o recelularizadas provoca una mejora significativa en los parámetros corneales paquimétricos y volumétricos corneales, utilizando la topografía corneal de Scheimpflug.

4. Investigar la respuesta clínica tras la implantación de **ADASCs** y la implantación de láminas corneales descelularizadas o recelularizadas con **ADASCs** mediante la biomicroscopía con lámpara de hendidura.

5. Evaluar la evolución celular (densidad, etc.) así como la evolución de las láminas acelulares mediante el desarrollo de abordaje técnico de la **microscopía confocal**:

- Valorar la evolución de las **ADASCs** una vez implantadas en el bolsillo estromal y monitorizar su evolución.
- Evaluar la evolución de las láminas descelularizadas implantadas sin **ADASCs** y la evolución biológica de las láminas hacia la recelularización.

- Evaluar la evolución de las **ADASCs** implantadas en las láminas corneales descelularizadas y la evolución del tejido descelularizado con la transformación y evolución de las células.
- Definir un método basado en el análisis cuantitativo subjetivo de las células estromales de la córnea y establecer este análisis para monitorizar la evolución de la densidad celular de las **ADASCs** implantadas con lámina o sin lámina durante el experimento.
- Investigar la evolución tanto cuantitativa como cualitativa de la densidad celular en el estroma anterior, medio y posterior de los pacientes.

5. MATERIAL Y MÉTODOS

5.1 APROBACIÓN, DISEÑO Y SUJETOS DEL ESTUDIO

Serie de casos prospectivos, de intervención, aleatorizados, no enmascarados, basados en la cooperación entre el Departamento de Investigación, de desarrollo e Innovación de Vissum Instituto Oftalmológico de Alicante, Universidad Miguel Hernández, Alicante (España), Óptica General (Saida, Líbano), el Centro de Laser Vision (Beirut, Líbano) y el Centro de Investigación y Aplicación REVIVA (Hospital de Oriente Medio, Beirut, Líbano). El Comité Ético de la Junta de Revisión Institucional (IRB) del Centro de Investigación y Aplicación Reviva (Universidad Libanesa, Beirut, Líbano), aprobó este estudio de manera prospectiva. Todos los pacientes firmaron un consentimiento informado por escrito para todos los procedimientos descritos en este estudio. El estudio se realizó en estricto cumplimiento de los principios de la Declaración de Helsinki y se registró oficialmente en el ***ClinicalTrials.gov*** (Código: NCT02932852).

Se inscribieron catorce pacientes en el estudio una vez seleccionados siguiendo los criterios de inclusión (ver más abajo), la edad media de los pacientes fue de 33,28 años (rango: 24-49 años; media de 34,2 años para **G-1**, 32,2 años para **G-2** y 36,25 años para **G-3**). La muestra del estudio estuvo compuesta por 9 mujeres y 5 hombres (proporción mujer / hombre de 2/3 para el grupo 1, 4/1 para el grupo 2 y 3/1 para el grupo 3), así como 10 ojos derechos y 4 ojos izquierdos. Los pacientes se distribuyeron aleatoriamente en tres grupos de estudio: A los pacientes del Grupo-1 (**G-1**) se les implantó células madre adultas autólogas derivadas de tejido adiposo (**ADASCs** solas, 3x 10^6 células/1 mL de **PBS**) (n = 5 pacientes); El grupo-2 (**G-2**) recibió implantes de láminas de estroma corneal humano descelularizado de 120 **µm** de espesor (n = 5 pacientes), y el grupo-3 (**G-3**) recibió láminas de estroma corneal humano recelularizado de 120 **µm** de espesor (**ADASCs**,

$1x10^6$ células/1 ml de **PBS**) (n = 4 pacientes). Las **ADASCs** se obtuvieron mediante liposucción electiva. Se distribuyeron aleatoriamente las láminas superficiales con **BM** láminas profundas sin **BM** entre los pacientes del **G-2** y **G-3** después del procedimiento de descelularización.

El seguimiento clínico del estudio de los pacientes se estableció por motivos de seguridad a la semana, 1, 3, 6, 12 y 36 meses postoperatorios, con informes intermedios cada 6 meses. Trece pacientes completaron completamente los tres años de seguimiento clínico. Solo un paciente del **G-1** se perdió después del primer mes postoperatorio debido a la imposibilidad de asistir a un seguimiento adicional por razones personales no relacionadas con el estudio (30,31,177,180).

5.2 JUSTIFICACIÓN DEL NÚMERO TOTAL DE PACIENTES

El pequeño número de pacientes (un total de 14 pacientes) que participaron en este experimento, es justificable en el sentido de que esta es la primera aplicación clínica de células **ADASCs** en ojos humanos, por lo tanto este número de pacientes no se guía por las reglas de un estudio genérico. Nuestro principal objetivo es determinar la seguridad de este innovador abordaje quirúrgico y confirmar los hallazgos demostrados previamente con estudios en animales, en pacientes humanos con queratocono avanzado.

5.3 CRITERIOS DE INCLUSIÓN Y EXCLUSIÓN

- **Criterios de inclusión:** Pacientes con queratocono avanzado definido como estadio ≥ IV; según la clasificación **RETICS** del queratocono (8), ya candidatos al trasplante de córnea por el estado avanzado de la enfermedad y la presencia de comorbilidades asociadas; Edad ≥ 18

años; Serología negativa del virus de la inmunodeficiencia humana (**VIH**), hepatitis B (**VHB**), hepatitis C (**VHC**) (30,31,177,180).

- **Criterios de exclusión:** Pacientes con **CDVA** < 0,1 en el ojo contralateral, hidropesía corneal previa o cicatrices corneales centrales, enfermedades oculares inflamatorias concomitantes activas; cualquier otra comorbilidad ocular que ponga en peligro la vista, procedimientos quirúrgicos corneales previos, incluido el colágeno **CXL**, embarazo o lactancia, y antecedentes de malignidad sistémica (30,31,177,180).

5.4 SELECCIÓN DE PACIENTES

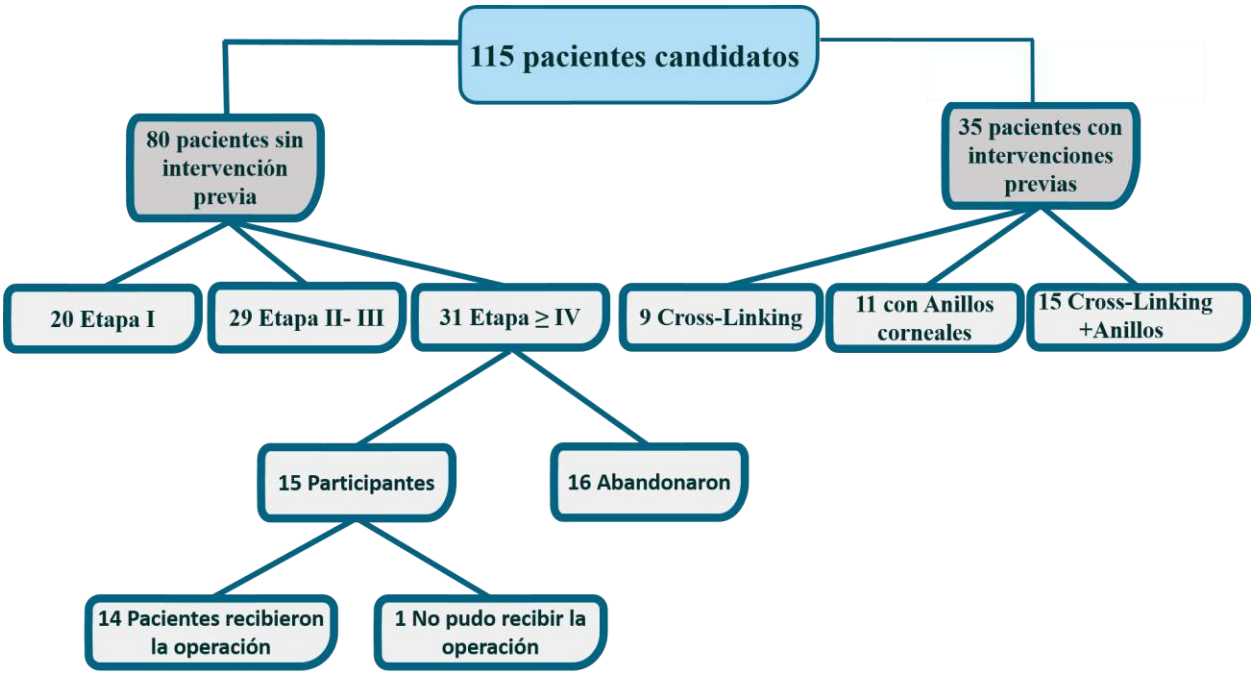

5.5 AISLAMIENTO, CARACTERIZACIÓN Y CULTIVO DE ADASCS AUTÓLOGAS

Se obtuvieron con anestesia local aproximadamente 250 ml de grasa mezclada mediante liposucción estándar de cada paciente. El tejido adiposo se procesó de acuerdo con los métodos descritos en nuestros informes anteriores (19,21,183,187,237). Brevemente, el tejido se digirió en colagenasa I durante 40 minutos a 37ºC y luego se inhibió la colagenasa agregando suero humano autólogo (**AHS**). Los eritrocitos se lisaron con el tampón de lisis de eritrocitos (Gibco-Life Technologies, EE.UU.). Luego, las células sedimentadas se cultivaron en medio de águila modificado de Dulbecco (**DMEM**) con Glutamax y piruvato de sodio (Gibco), **AHS** al 10%, Penicilina-estreptomicina al 1% (Gibco) y anfotericina B al 0,2% (Gibco). La caracterización celular se realizó mediante marcado CD34 + CD45-CD105 + mediante un análisis de citometría de flujo siguiendo las recomendaciones de la Federación Internacional de Terapias Adiposas (**IFATS**) (187). 60 a 80 horas antes de la cirugía se indujo la inactividad celular reduciendo la cantidad de suero al 0,5%, para trasplantar las **ADASCs** en un estado fisiológico más cercano a los queratocitos estromales no proliferativos naturales, ya que las células madre proliferativas dentro del estroma corneal podrían potencialmente inducir cicatrices estromales o "haze". La quiescencia, así como la ausencia de apoptosis y aneuploidía, se verificaron mediante marcaje con yoduro de propidio (Invitrogen, EE. UU.) Y análisis de citometría de flujo del ciclo celular, como se describió en artículos publicados por nuestro grupo (19,21). Justo antes de la inyección intraestromal, las células se recolectaron mediante tripsinización (Sigma) y se prepararon (3×10^6 células en 1 ml de **PBS**) por paciente (Figura. 1 B). Dicha concentración se estableció basándose en la evidencia observada en estudios experimentales previos y dada la pérdida celular esperada después de la implantación debido a la fuga de la solución celular fuera de la córnea (17,19,21,30,31,177,180). En el **G-3**, las

ADASCs se recolectaron mediante tripsinización (Sigma-Aldrich), 24 horas antes de la implantación y ($0,5 \times 10^6$ células por 1 ml de **PBS**) se cultivaron durante 24 y 12 horas en cada superficie de la lámina del estroma corneal descelularizado, respectivamente (30,31,177,180).

5.6 LÁMINAS

Para esta investigación se seleccionó un estroma corneal humano de córneas donantes con endotelio no viable (sin cicatrices) pero con serología viral negativa y útil para uso humano. Las córneas fueron proporcionadas por el banco de ojos "Banco de ojos para el tratamiento de la ceguera, Centro de Oftalmología Barraquer (Barcelona, España) siguiendo las Directivas reguladoras españolas 2004/23 / CE y 206/17 / CE" sobre estándares de calidad y seguridad para la donación, obtención, análisis, procesamiento, preservación, almacenamiento y distribución de células y tejidos humanos.

Las córneas del donante se montaron en una cámara anterior artificial (Barron, Katena Products, EE. UU.), El epitelio se eliminó mecánicamente con esponjas quirúrgicas y el estroma corneal anterior se cortó con el láser de femtosegundo IntraLase iFS de 60 Khz (AMO Inc, Irvine, Calif) en dos láminas consecutivas de 120 µm de espesor y 9,0 mm de diámetro, posteriormente se lavaron en **PBS** (Sigma) suplementado con 1% de antibiótico-antimicótico (Gibco). Los ajustes de los parámetros del láser de femtosegundo fueron equivalentes a los utilizados para una disección de colgajo **LASIK** estándar, excepto por un ángulo de corte del lado anterior de 360º. Con este procedimiento se obtuvieron dos láminas, una superficial que contiene la **BM** y otra más profunda sin esta capa. Se descartó la córnea posterior restante (31,177,180). El protocolo de descelularización se basó en publicaciones anteriores (19,31,177,180,211), brevemente, las láminas se sumergieron en **SDS** (Sigma) al 1% (peso/volumen) con un cóctel inhibidor de proteasa (P8340,

Sigma) y se incubaron en un agitador orbital (75 rpm) durante 24 horas a temperatura ambiente. Posteriormente, las láminas se lavaron 8 veces en **PBS** con antibiótico-antimicótico al 1% en las mismas condiciones durante 15 min, cada una a temperatura ambiente. Para eliminar el ácido desoxirribonucleico (**DNA**), las láminas se incubaron en **DNA** sa (Benzonase® Nuclease 6.5 U / mL, Merck) en **PBS** con el mismo cóctel inhibidor de proteasas y en las mismas condiciones a 37ºC durante 72 horas. Finalmente, las láminas se lavaron 8 veces durante 15 min cada una en **PBS** y con antibiótico-antimicótico al 1% (Figura 4A). 24 horas antes del trasplante, esas láminas para los pacientes que recibieron tejido recelularizado, se colocaron en pocillos de cultivo de tejidos para recelularización con **ADASCs** autólogas (se cultivaron $0,5x10^6$ células en cada lado de la lámina) de cada paciente del **G-3** (Figura 4B). Una vez finalizado el proceso de recelularización, las láminas se trasladaron al quirófano en **PBS** a temperatura ambiente para su implantación.

La eficacia de la descelularización y por tanto, la eliminación de células se controló en una lámina nueva de cada lote mediante tres métodos: análisis histológico con tinción nuclear 4 ', 6-diamidino-2-fenilindol (**DAPI**), y tinción con microscopía de fluorescencia con hematoxilina y eosina, y bioquímicamente mediante digestión en proteinasa K, extracción del **DNA** y cuantificación de **DNA** mediante el uso de un kit de ensayo Picogreen como en las publicaciones anteriores (Figura 4C) (19,180,211).

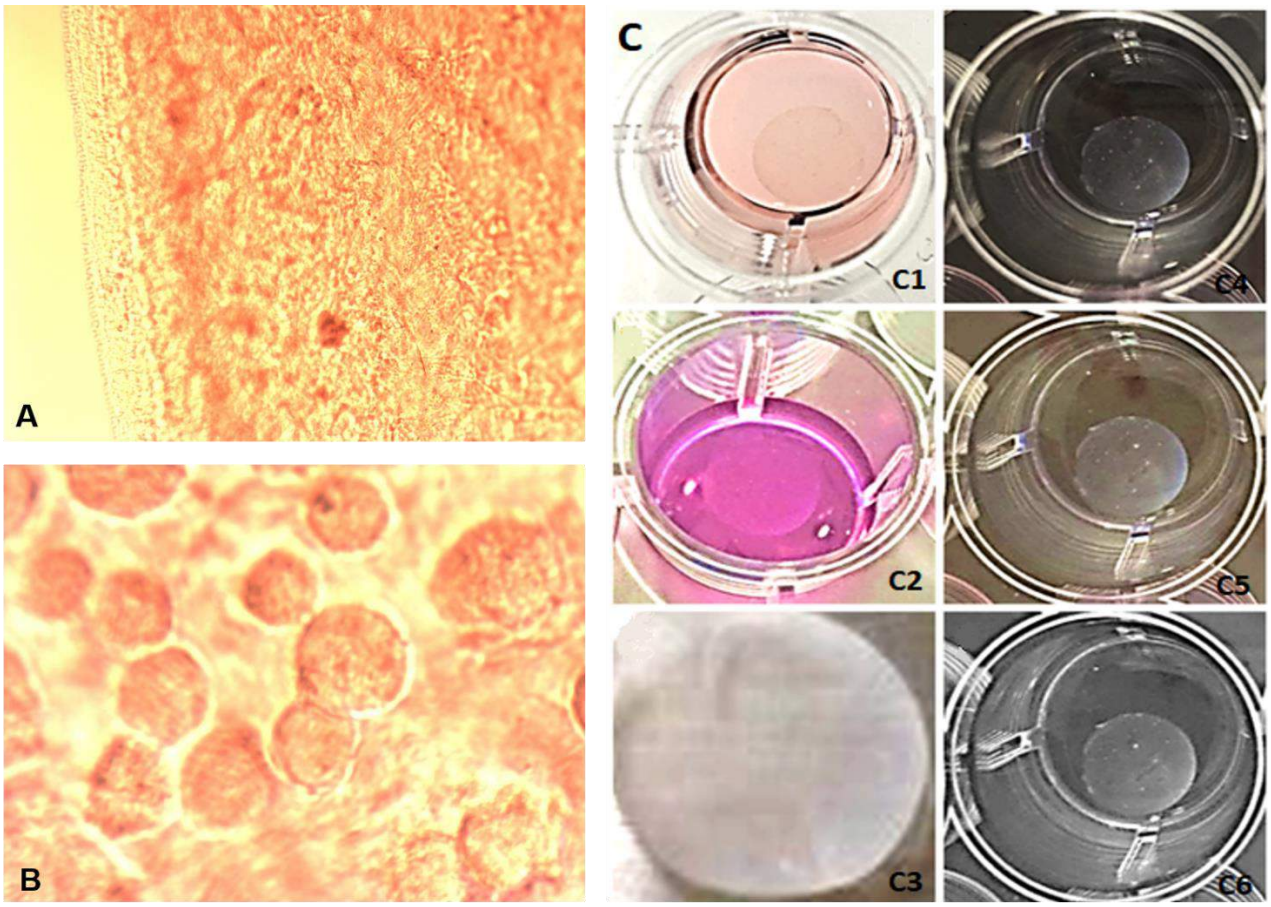

Figura 4. Observación de láminas descelularizadas y recelularizadas y proceso de descelularización/recelularización.
(**A**) Lámina corneal humana descelularizada (aumento de 10 ×). (**B**) Lámina corneal humana recelularizada con **ADASCs** (se cultivaron 0,5 x 10^6 células en cada lado de las láminas) (aumento de 10 x). Figura extraída del capítulo científico referido a Alió JL y cols. (41). (**C**) (**C1,2,3**) Lámina mantenida en medio de cultivo durante 2 horas luego transferida a **PBS**: observamos que el color del medio de cultivo como se esperaba se volvió más rojo correspondiente a un PH más básico, esto afecta a las láminas y las células, y que fue más significativa después de 26 horas (láminas tiene el aspecto de gelatina y más viscosa). (**C4,5,6**) lámina transferida directamente a **PBS** y mantenida en **PBS** hasta el final del procedimiento: la lámina permanece en buen estado, firme, con mantenimiento de espesor y no se observó aspecto viscoso.

5.7 PROCEDIMIENTOS QUIRÚRGICOS

5.7.1 IMPLANTACIÓN DE ADASCs AUTÓLOGAS

Se utilizó anestesia tópica. Se utilizó un láser de femtosegundo IntraLase iFS de 60 kHz (AMO Inc, Irvine, CA) en un modo de paso único para la disección lamellar corneal del receptor mediante la creación de un bolsillo lamellar intraestromal de 9,5 mm de diámetro a una profundidad media del punto más delgado de paquimetría preoperatorio medido por el Visante **AS-OCT** (Carl Zeiss, Alemania) (30,177,180). La disección corneal asistida por láser de femtosegundo terminó con un corte lateral anterior de 30^0 como una incisión corneal, la incisión de la longitud del arco fueron de 3 mm y se utilizaron ajustes de parámetros similares a los de la cirugía de **LASIK** en el láser de femtosegundo. Los ajustes de los parámetros del láser de femtosegundo se resumen en la publicación de nuestro grupo (Tabla 4) (30). A continuación, se abrió el bolsillo intraestromal corneal mediante la disección roma con el disector lamelar de Morlet (Duckworth & Kent, Inglaterra) y posteriormente, se inyectaron tres millones de **ADASCs** autólogas en 1 ml de **PBS** en el bolsillo a través de una cánula de 25-G. Previo a la inyección celular se realizó una paracentesis corneal de 1 mm para reducir la presión intraocular (**IOP**) y permitir inyectar lo más alto volumen en bolsillo estromal. Se aplicaron antibióticos tópicos y esteroides (Tobradex, Alcon) al final de la cirugía. Ningún paciente recibió suturas corneales (30,177,180).

Tabla 4. Especificaciones del láser para la preparación de la córnea receptora

Corte lamelar		**Corte del lado anterior**	
Parámetro	**Valor**	**Parámetro**	**Valor**
Diámetro (mm)	9.5	Diámetro (mm)	9.5
Profundidad (µm)	Más delgado/2	Profundidad posterior (µm)	Más delgado/2 +10
Energía (µJ)	1.50	Energía (µJ)	1.7
Sep Tang Puntos (µm)	5	Posición de corte (º)	90
Sep Rad Puntos (µm)	5	Ángulo de corte (º) **G-1**	30
		Ángulo de corte (º) **G-2 & G-3**	50
		Incisión de la longitud del arco **G-1**	3 mm
		Incisión de la longitud del arco **G-2& G-3**	4 mm
		Sep Puntos (µm)	3
		Sep Capas (µm)	3

Tang = Tangencial; Sep = Separación; Rad = Radial. Sep Tang Puntos: Separación tangencial entre puntos; Sep Rad Puntos: Separación radial entre puntos; Sep Puntos: Separación de puntos; Sep Capas: Separación entre capas. La tabla está tomada en parte de los artículos científicos de Alió Del Barrio y cols. (30,31).

5.7.2 IMPLANTACIÓN DE LENTICULOS

Se utilizó anestesia tópica con sedación oral para todas las cirugías. El láser de femtosegundo IntraLase iFS de 60 Khz se utilizó en un modo de un solo paso para la disección lamelar corneal del receptor mediante la creación de un corte lamelar intraestromal de 9,5 mm de diámetro a la mitad de la profundidad del punto de paquimetría más delgado preoperatorio, medido por el Visante **AS-OCT** (Carl Zeiss, Alemania). La disección corneal asistida por láser de femtosegundo terminó con un corte lateral anterior de 50^0 como una incisión corneal, y la incisión de la longitud del arco fue de 4 mm (Tabla 4). Los ajustes de los parámetros láser fueron equivalentes a los reportados recientemente por nuestro grupo para este tipo de disección (30). A continuación, se abrió el bolsillo intraestromal de la córnea mediante disección roma con el disector lamelar de Morlet (Duckworth & Kent, Inglaterra) y, posteriormente, se insertó, centró y desplegó la lámina mediante suaves golpecitos y masajes desde la superficie epitelial del huésped. Se realizó una paracentesis del limbo temporal justo antes de la implantación para reducir la **IOP**. En esos casos, al recibir una

lámina recelularizada con **ADASCs** del **G-3**, para compensar el daño celular esperado a lo largo del proceso de implantación del injerto, el bolsillo fue irrigado inmediatamente antes y después del trasplante con una solución que contenía 1 millón de **ADASCs** autólogas en 1 mL de **PBS** a través de una Cánula de 25-G. La incisión se cerró con una sutura de nailon 10/0 interrumpida que se retiró una semana después de la operación. Se aplicaron antibióticos tópicos y esteroides (Tobradex, Alcon) al final de la cirugía (31,177,180).

Todas las cirugías fueron realizadas por los mismos cirujanos en Laser Vision Center (Beirut, Lebanon) (30,31,177–180).

5.8 DISPOSITIVO DE MICROSCOPIO CONFOCAL IN VIVO

Se utilizó el microscopio confocal HRT3 con un módulo de córnea de Rostock (RCM) (Heidelberg Engineering, Heidelberg, Alemania). La fuente de luz de este microscopio confocal es un tipo coherente de diodo láser, con una longitud de onda de 670 nm y una resolución mínima de 1024 x 768 (16 bits) (238). Se utilizó luz coherente para mejorar el contraste y la calidad de las imágenes del estroma corneal, particularmente las células (6).

5.8.1 USO DEL MICROSCOPIO CONFOCAL

Se obtuvo un consentimiento informado firmado de los pacientes para el estudio de la microscopía confocal. Se aplicó una gota de anestésico tópico (oxibuprocaína al 0,4%) en el ojo a examinar. El microscopio confocal se fijó a 12 D. Se aplicó una gota de un gel de alta viscosidad (2,0 mg / g de carbómero) a la superficie frontal de la lente del microscopio del RCM. Luego, se colocó un RCM TomoCap encima del objetivo RCM. También se aplicó una gota del mismo gel

viscoso en la parte superior de la superficie exterior del TomoCap y en el ojo del paciente a examinar. Se colocó al paciente en una posición estable y cómoda, con el ojo alineado con la lente del microscopio confocal, y se le indicó que siguiera mirando la luz dentro de la lente. La posición focal se restableció a 0 en las células epiteliales superficiales del ojo examinado. A continuación, se giró el RCM en sentido horario o antihorario 0 ± 50 µm, y el plano focal se ajustó a la capa celular deseada. Finalmente, se obtuvieron al menos cuatro imágenes por cada 50 **µm** de profundidad y se almacenaron siguiendo un protocolo descrito previamente (238). Las imágenes analizadas en este estudio se encontraban de hecho a diferentes profundidades del estroma, pero siempre pertenecían a un diámetro central ≤ de 9 mm y estaban por debajo de la medida de diámetro del bolsillo intraestromal (30,31,105,177,179).

5.8.2 MÉTODO DE CONTEO DE CÉLULAS ESTROMALES

Las imágenes que tenían una mejor calidad de contraste e iluminación fueron seleccionadas de las imágenes capturadas y almacenadas durante la experiencia. Se determinó un área conocida como región de interés (ROI) y se utilizó casi la misma región ROI (0,1000 mm^2) para todos los recuentos de células en todas las capas del estroma corneal (6,105,179,238). Los criterios morfológicos utilizados en el presente estudio para diferenciar las células del estroma corneal de las células inflamatorias se describen en nuestra publicación (179).

Usamos el ajuste al 50% de brillo y contraste (Figura 5A) para todas las imágenes. Las células más iluminadas y más refringentes (9,10,105,179) fueron seleccionadas y marcadas en azul (238), estas celdas eran blancas o de color gris claro y tenían bordes claros y bien definidos (6,105,179). No se tuvieron en cuenta las celdas de color gris oscuro, ya que no pertenecían al plano

de 50 **µm** elegido (105,179). El brillo celular confocal se atribuye al contenido nuclear de estas células (6,9,30,31,104,105,125,177,179,239). Debido a sus cuerpos irregulares de forma ovalada (9), las diferencias de brillo entre ellos pueden atribuirse a diferentes direcciónes de incidencia del rayo de láser, o bien a sus diferentes actividades metabólicas (9). Solo los núcleos celulares que se identificaron con el método mencionado anteriormente se definieron como células del estroma corneal y se incluyeron en el proceso de recuento celular. Para simplificar en toda la tesis, cuando hablamos de densidad o morfología celular, nos referimos a la densidad o morfología del núcleo celular y no a la membrana celular que se observó mediante la microscopía confocal (6,9,30,31,104,105,125,177,179,239).

El material altamente reflectante no se consideró en el recuento celular siempre que el tamaño de la morfología reflectante excediera el tamaño que consideramos similar al queratocito estromal, ya sea en córneas normales o queratocónicas (6,9,30,31,104,105,125,177,179,239). Por ello, hemos considerado que esta estructura corresponde a un material fibrótico (179).

Después de que el primer recuento fue realizado, el contraste se incrementó al máximo y el brillo se redujo al mínimo. Cualquier célula del estroma que desapareció del plano elegido fue eliminada, y solo las células que quedaron en el plan de conteo se usaron para el resultado de recuento celular final, incluso si estaban débilmente identificadas en la imagen observada (Figura. 5B) (105,179).

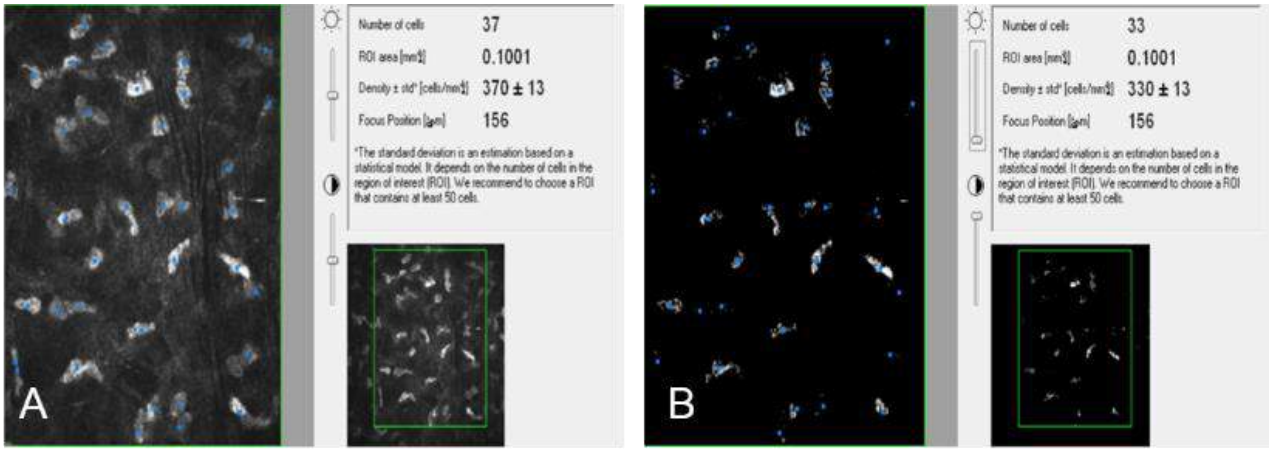

Figura 5. Método de recuento celular realizado por microscopía confocal.
(**A**) Recuento de células realizado con brillo y contraste medios. Se contaron las células más iluminadas y más refringentes y los queratocitos se marcaron en azul. (**B**) La eliminación de queratocitos que no pertenecen al plano bajo observación es posible utilizando configuraciones de bajo brillo y alto contraste. La figura está tomada del artículo científico con referencia El Zarif M et al. (179) acreditado por esta tesis.

5.8.3 CONTEO CELULAR DE ADASCs

El método de recuento de las **ADASCs** trasplantadas se realizó de manera similar. Las **ADASCs** tenían una forma redondeada, voluminosa y refringente (Figura. 6A) (30,105,179). La morfología y evolución de las **ADASCs** a lo largo del tiempo se describen más adelante en la parte 6 de la sección de resultados (Figura. 6B) (179).

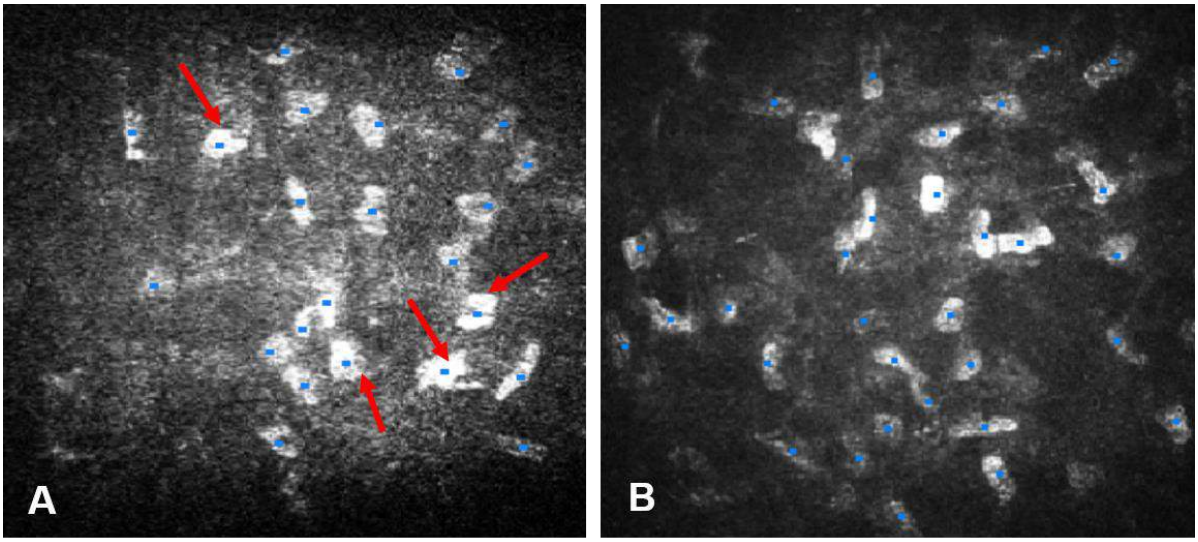

Figura 6. Conteo de **ADASCs** en el **G-1**.
(**A**) Recuento de **ADASCs** (flechas rojas) y de los queratocitos al primer mes después de la cirugía de un paciente queratocónico; las celdas están marcadas en azul. Las **ADASCs** tienen una forma redondeada y son más grandes, más luminosos y más refringentes que los queratocitos normales. (**B**) Recuento de células de un paciente con queratocono al año después de la implantación de las **ADASCs**; todas las células del estroma corneal muestran una forma similar. La figura está extraída del artículo científico con referencia El Zarif M y cols. (179) acreditado para esta tesis.

5.8.4 RECUENTO CELULAR EN LAS LÁMINAS DESCELULARIZADAS Y RECELULARIZADAS

Cuando aparecieron las láminas descelularizadas del **G-2** y recelularizadas del **G-3** sin estructuras celulares bien definidas, se consideraron totalmente acelulares en el área de 0.1 mm^2 que delimitamos en nuestro estudio (Figura. 7A) (31,105,177,179). Todas las estructuras que aparecieron en la superficie anterior, en la superficie posterior o en el estroma medio de la lámina; que mostraban bordes bien definidos que eran de color blanco o gris claro; y que tenían una morfología similar a la de un núcleo de un queratocito se contabilizaron como una célula (Figuras. 7B, 7C, 8A-8E) (105,179).

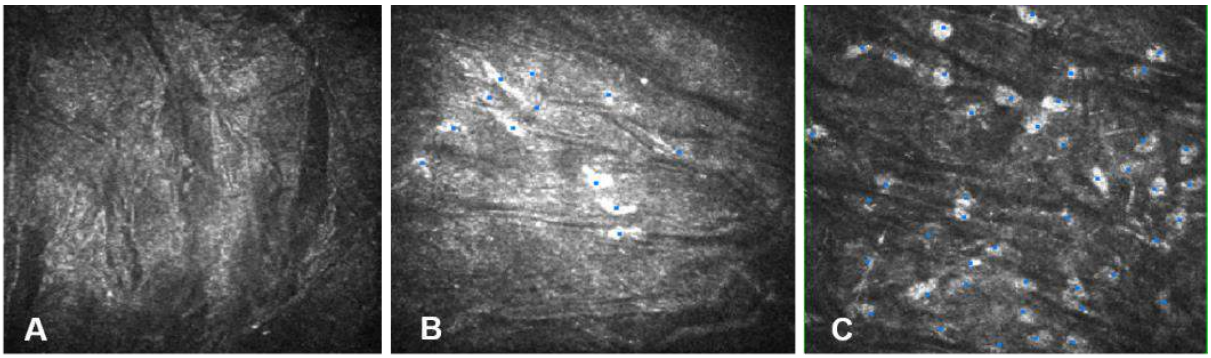

Figura 7. Recuento de células en láminas descelularizadas para el caso-9 del **G-2**.
(**A**) La superficie anterior de una lámina descelularizada aparece sin células al primer mes después de la cirugía. (**B**) Recuento de células en la superficie posterior de una lámina a los tres meses después de la cirugía. Las células muestran una morfología diferente de las células estromales de la córnea del huésped. Estas celdas son más pequeñas. (**C**) Recuento de células en la superficie posterior de una lámina al año postoperatorio. Todas las células muestran una morfología idéntica a la de los queratocitos estromales corneales normales. La figura está tomada del artículo científico referido a El Zarif M y cols. (179) acreditado para esta tesis.

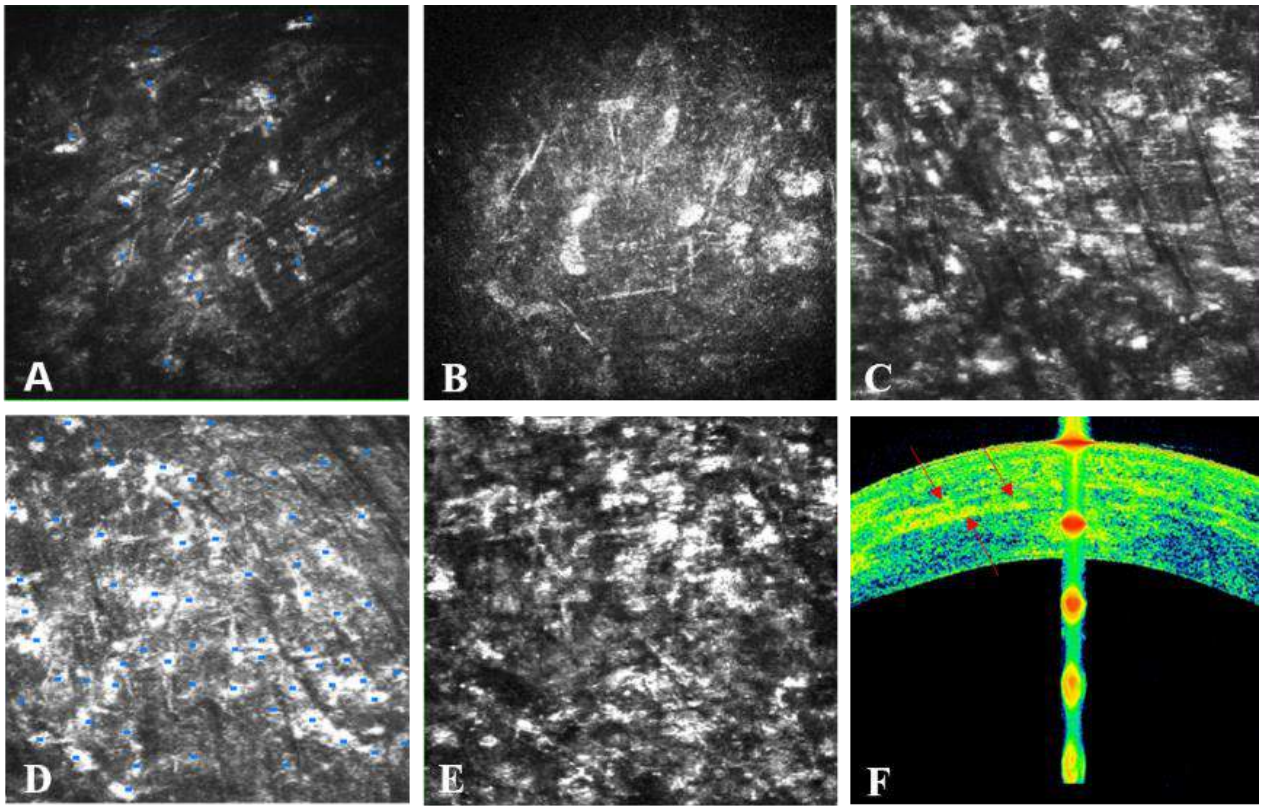

Figura 8. Recuento de células en la lámina recelularizada para el caso-13 del **G-3**.
(**A**) La superficie anterior de una lámina recelularizada al primer mes después de la operación; se pueden ver pocas **ADASCs** (marcadas en azul). (**B**) La superficie posterior de la lámina recelularizada al primer mes postoperatorio; nótese la presencia de algunas **ADASCs** similares en morfología a los queratocitos. (**C**) La superficie anterior de la lámina recelularizada a los 12 meses después de la cirugía muestra un número abundante de células estromales. (**D**) Estroma medio de la lámina a los 12 meses después de la cirugía que muestra un número elevado de células estromales. (**E**) La superficie posterior de la lámina recelularizada a los 12 meses postoperatorios muestra un alto número de células estromales. (**F**) Imagen de **OCT** donde las flechas rojas representan las superficies anterior y posterior, así como el estroma medio, de la lámina recelularizada a los 12 meses después de la cirugía. La figura está tomada del artículo científico referido a El Zarif M y cols. (179) acreditado para esta tesis.

5.8.5 CÁLCULO DE LA DENSIDAD CELULAR CORNEAL

Para obtener la densidad celular, primero definimos la región ROI (mm^2) (238) y luego se procedió a contar las celdas con la metodología descrita anteriormente. La densidad celular para el

área elegida se calculó mediante el software del microscopio confocal como el número de células multiplicado por 10 células/mm^2 ± desviación estándar (**SD**) (10,238).

Para calcular la densidad celular del estroma corneal entre los tres grupos, dividimos las medidas del estroma en tres zonas: estroma anterior, medio y posterior. El estroma medio coincidió con el plano quirúrgico (calculado como la mitad del punto más delgado de la córnea obtenido por **OCT** ± 50 **µm**) (30,31,105,177,179). El estroma anterior es el estroma ubicado debajo de la **BM** y el estroma posterior es el estroma ubicado por encima de la **DM** (30,31,177,179). Para aquellas mediciones en las que había una lámina (postoperatorio en el **G-2** y **G-3**), dividimos la lámina en tres áreas: superficie anterior, superficie posterior de la lámina y estroma medio de la lámina (Figura. 8F) (179).

Las principales medidas de resultados de este estudio son los cambios y la evolución de la densidad celular del estroma corneal durante un período de seguimiento de 1 año, analizados mediante la microscopía confocal corneal. Se estudió la densidad celular antes de la cirugía y a los 1, 3, 6 y 12 meses después de la cirugía. Se midió la densidad celular preoperatoria en el estroma anterior, medio y posterior en el **G-1**, así como en el **G-2** y **G-3**. Se estudió la densidad celular postoperatoria en el **G-2** y **G-3** en el estroma anterior y posterior y a través de la lámina, para explorar la evolución de su componente celular durante el tiempo de estudio (179).

5.9 CUIDADOS POSTOPERATORIOS Y PLAN DE SEGUIMIENTO

En el postoperatorio, los pacientes fueron evaluados mensualmente por el director médico y la monitora clínica del estudio para asegurar la correcta evolución de los pacientes. Los pacientes

fueron seguidos al primer día, una semana y a los 1, 3, 6, 12 meses (30,31,177). El seguimiento clínico después del año se realizó cada seis meses hasta los 36 meses del postoperatorio (180). Los siguientes datos se registraron preoperatoriamente y durante la evaluación postoperatoria, a los 1, 3, 6, 12 y 36 meses: La agudeza visual a distancia sin ayuda (**UDVA**), **CDVA**, agudeza visual a distancia con lentes de contacto rígidas (**CLDVA**) en (equivalente decimal a la escala logMar). La esfera refractiva (**Rx Sphr**) en dioptrías (**D**) y cilindro refractivo (**Rx Cyl**) (**D**). El grosor corneal central (**CCT**) (**µm**) se midió mediante la **AS-OCT** (Visante, Carl Zeiss Scheimpflug), la topografía corneal del punto más fino (**Thinnest point**) (**µm**), el volumen de la córnea (**CV**) (mm^3) y la aberrometría corneal (Pentacam; Oculus Inc., Wetzlar, Alemania), los análisis de Zernike de la superficie corneal anterior se realizaron con un diámetro pupilar máximo de 6 mm en todos los casos, independientemente del diámetro pupilar de los pacientes. La queratometría anterior media (**Anterior Km**) (**D**), la queratometría posterior media (**Posterior Km**) (**D**), la queratometría máxima (**Kmax**) (**D**) y el cilindro topográfico (**Topo Cyl**) (**D**) (Pentacam; Oculus Inc., Wetzlar, Alemania). La biomicroscopía con lámpara de hendidura, fundoscopía, **IOP** (mmHg) (Tonometría de aplanación de Goldmann) y la densidad de células endoteliales (**ECD**) (células/mm^2) medida por microscopía especular (Nidek, Aichi, Japón) (30,31,177,180). El estudio de microscopía confocal se completó hasta 12 meses utilizando el **microscopio confocal** HRT3 RCM (Heidelberg) con módulo Rostock de Cornea (179).

5.10 ANÁLISIS DE CONCORDANCIA ENTRE LOS EXPERTOS

Las medidas de las variables a lo largo del tiempo: Agudeza visual, refracción manifiesta, estudio de biomicroscopía con lámpara de hendidura, topografía corneal, aberrometría corneal, **AS-**

OCT y la microscopía confocal siempre se han realizado con los mismos dispositivos y con las mismas condiciones. Se quedaron en obtener el acuerdo sobre los mismos resultados, es decir, la concordancia es absoluta en nuestro estudio.

5.11 ANÁLISIS ESTADÍSTICO

1. El análisis estadístico del artículo científico publicado con anterioridad a esta tesis doctoral con la referencia (30): (Alió del Barrio J, **El Zarif M**, De Miguel M, Azaar A, Makdissy N, Harb W, et al. **Cellular therapy with human autologous adipose-derived adult stem cells for advanced keratoconus.** Cornea 2017; 36(8)952-60), fue un análisis descriptivo de los resultados clínicos.

2. El análisis estadístico del artículo científico publicado con anterioridad a esta tesis doctoral con la referencia (31): (Alió del Barrio JL, **El Zarif M**, Azaar A, Makdissy N, Khalil C, Harb W, et al. **Corneal stroma enhancement with decellularized stromal laminas with or without stem cell recellularization for advanced Keratoconus**. Am J Ophthalmol. 2018;186: 47-58), se realizó con el software de SPSS de la versión 20.0 para Windows (SPSS Inc., USA). La normalidad de los datos del estudio fue confirmada por la prueba de Kolmogorov-Smirnov, que determinó que todas las variables siguieron una distribución normal [$P < 0.05$]. Debido a la muestra del estudio (n: 9), se realizó la prueba del signo de Wilcoxon para probar las diferencias estadísticamente significativas (valor de P menor que 0.05).

3. El análisis estadístico del artículo científico con la referencia (177) acreditada para esta tesis: (Alió JL, Alió del Barrio JL, **El Zarif M**, Azaar A, Makdissy N, Khalil C et al. **Regenerative surgery of the corneal stroma for advanced keratoconus: 1-Year outcomes**. Am J Ophthalmol.

2019; 203:53-68), se realizó con el software de SPSS versión 20.0 para Windows (SPSS Inc., EE. UU.). Debido a la muestra de estudio de (n: 14), se utilizó la estadística no paramétrica. Se aplicó la prueba de suma de rangos de Wilcoxon para evaluar la importancia de las diferencias entre los datos preoperatorios y posoperatorios. Para todas las pruebas estadísticas se utilizó el mismo nivel de significación [$P < 0.05$].

4. El análisis estadístico del artículo científico con la referencia (180) acreditada para esta tesis: **(El Zarif M**, Alió JL, Alió del Barrio JL, Abdul Jawad K, Palazón-Bru A, Abdul Jawad Z, et al. **Corneal stromal regeneration therapy for advanced keratoconus: long-term outcomes at 3 years**. Cornea. 2021;40(6):741–54), se obtuvo mediante modelos lineales mixtos generalizados con variables de Poisson que incluyen resultados, tiempo y el grupo como efectos fijos, e individuos como efectos aleatorios. Una distribución de Poisson se caracteriza por una tasa media (la **SD** es igual a esta media o lambda) e indica el número de eventos para el resultado. Estimamos lambda a través de estos modelos, teniendo en cuenta toda la información recopilada. Los resultados de este estudio estadístico no representaron en ningún momento el resultado de un paciente de los diferentes grupos, pero representaron el total de datos recolectados de todos los pacientes de cada grupo en el tiempo continuo y proporcionan toda la información necesaria para comprender el impacto de la intervención. Se desarrollaron diagramas de dispersión para ayudar a interpretar los resultados, y la bondad de ajuste de los modelos se obtuvo mediante la prueba de razón de verosimilitud. El nivel de significancia del error tipo I se estableció cuando el valor de P [$P < 0.05$], y el software estadístico que usamos fue R 3.5.1. (180).

5. El análisis estadístico del artículo científico con la referencia (179) acreditada para esta tesis: : (**El Zarif M**, Abdul Jawas K, Alió del Barrio JL, Abdul Jawad Z, Palazón-Bru A, De Miguel MP, et al. **Corneal stroma cell density evolution in keratoconus corneas following the**

implantation of adipose mesenchymal stem cells and corneal laminas: an in vivo confocal microscopy study. IOVS. 2020;61(4)22), se realizó mediante modelos lineales mixtos generalizados con una variable de Poisson como resultado (efectos fijos, tiempo y grupo; efectos aleatorios, individual). Esta variable de Poisson correspondía a las densidades de los núcleos de los queratocitos (distribución de Poisson), indicando las medias de los núcleos celulares que aparecen en las figuras capturadas en diferentes niveles del estroma corneal (anterior, intermedio y posterior) o en la superficie anterior, estroma medio, y superficie posterior del tejido implantado para los intervalos de tiempo estudiados. Una variable de Poisson, a diferencia de una que sigue una distribución normal, se expresa mediante un único parámetro, que es solo el número promedio de eventos. La **SD** de la variable de Poisson (generalmente conocida como lambda) no se muestra en las figuras, pero es la misma que el parámetro promedio, en comparación con una distribución normal que se expresa por la media y la **SD**. Por otro lado, este parámetro promedio (obtenido a través de modelos lineales generalizados mixtos) toma en cuenta todas las medidas de todos los individuos y evalúa la variabilidad entre individuos y dentro de ellos. En consecuencia, los resultados presentados aquí son en respecto a cada grupo y proporcionan toda la información necesaria para comprender el impacto de la intervención. Se desarrollaron diagramas de dispersión para ayudar a interpretar los resultados, y la bondad de ajuste de los modelos se obtuvo mediante la prueba de razón de verosimilitud. El nivel de significancia del error tipo I se estableció en 0.05 y el software estadístico que usamos fue R 3.5.1 (179).

Se recopiló el número máximo de imágenes de cada paciente para calcular la densidad celular. Para no alterar los resultados, se utilizaron modelos matemáticos de medidas repetidas para controlar la variabilidad de cada individuo. Consideramos los recuentos promedios de células de dos observadores que los realizaron por separado siguiendo los mismos estándares científicos;

cuando existía una discrepancia entre ellos de más del 20%, se repetía el conteo o se tomaban otras imágenes, si era posible, hasta lograr acuerdo entre ellos (179).

5.12 MEDIDAS DE RESULTADOS

5.12.1 MEDIDAS DE RESULTADOS PRINCIPALES

Las principales medidas de resultado de esta investigación se dividieron en primarias y secundarias:

5.12.1.1 Medidas de resultados primarias.

Las medidas de resultados primarias fueron **UDVA**, **CDVA** y **CLDVA** (en decimal equivalente a la escala logMar). **Rx Sphr** (D), **Rx Cyl** (D). **CCT** (**µm**). Punto más fino **(Thinnest point)** (**µm**) y **CV** (mm^3). **RMS** de aberración de tercer orden (**3rdorder RMS**) (**µm**), **RMS** de aberración de cuarto orden (**4thorder RMS**) (**µm**), **RMS** de aberración de alto orden (**HOA RMS**) (**µm**) y **RMS** de aberración de bajo orden (**LOA RMS**) (**µm**) (30,31,177,180).

5.12.1.2 Medidas de resultados secundarias.

Las medidas de resultados secundarias fueron **Anterior Km** (D), **Posterior Km** (D), **Kmax** (D) y **Topo Cyl** (D) (30,31,177,180).

5.12.2 RESULTADOS DE LA MICROSCOPÍA CONFOCAL

5.12.2.1 Resultados morfológicos y de densidad celular.

Con pacientes implantados solo con **ADASCs G-1**, pacientes implantados con láminas corneales descelularizadas **G-2** y pacientes implantados con láminas corneales recelularizadas **G-3**. Los resultados de la densidad celular se calcularon en el estroma anterior, medio y posterior en **G-1**. En el estroma anterior y posterior en **G-2** y **G-3**, y en las superficies anterior, media y posterior del tejido implantado (179).

5.12.2.2 Resultados morfológicos del tejido fibrótico. (179)

6. RESULTADOS

LOS RESULTADOS DE ESTE ESTUDIO SE MUESTRAN EN FORMA DE INFORMES CIENTÍFICOS COMO SE INDICA A CONTINUACIÓN:

6.1 En este artículo de revisión resumimos toda la evidencia existente de experimentos preclínicos en el campo de la medicina regenerativa del estroma corneal. Esta evidencia fue la base del ensayo clínico descrito en la tesis actual. Los resultados demostrados en el artículo con referencia (240) de la publicación científica acreditada para esta tesis: Alió del Barrio JL, Arnalich-Montiel F, De Miguel MP, **El Zarif M**, Alió JL. **Corneal stroma regeneration: Preclinical studies**. Exp Eye Res. 2021;202:108314.

6.2 Resultados a los seis meses de la primera aplicación en **G-1** de la implantación autóloga de **ADASCs** dentro del estroma corneal en pacientes con queratocono avanzado. Fueron publicados con anterioridad a esta tesis doctoral en el siguiente artículo con referencia (30): Alió del Barrio J, **El Zarif M**, De Miguel M, Azaar A, Makdissy N, Harb W, et al. **Cellular therapy with human autologous adipose-derived adult stem cells for advanced keratoconus.** Cornea 2017; 36(8)952-60.

6.3 Resultados a los seis meses para la segunda y tercera aplicación en **G-2** y **G-3** mediante la implantación de láminas estromales descelularizadas con o sin **ADASCs** autólogas para pacientes con queratocono avanzado. Fueron publicados con anterioridad a esta tesis doctoral en el siguiente artículo con referencia (31): Alió del Barrio JL, **El Zarif M**, Azaar A, Makdissy N, Khalil C, Harb W, et al. **Corneal stroma enhancement with decellularized stromal laminas with or without stem cell recellularization for advanced Keratoconus**. Am J Ophthalmol. 2018;186: 47-58.

6.4 Resultados a los 12 meses de la implantación de **ADASCs** autólogos en **G-1** y la implantación de injertos estromales descelularizados con o sin **ADASCs** autólogas para pacientes con queratocono avanzado en **G-2 y G-3**. Fueron publicados en el siguiente artículo con referencia (177) de la publicación científica acreditada para esta tesis: Alió JL, Alió del Barrio JL, **El Zarif M**, Azaar A, Makdissy N, Khalil C et al. **Regenerative surgery of the corneal stroma for advanced keratoconus: 1-Year outcomes**. Am J Ophthalmol. 2019; 203:53-68.

6.5 Resultados a los tres años de la implantación de las **ADASCs** autólogas y la implantación de injertos estromales descelularizados con o sin **ADASCs** autólogas para pacientes con queratocono avanzado en los grupos 1, 2 y 3. Se publicaron en el siguiente artículo con referencia (180) de la publicación científica acreditada para esta tesis: **El Zarif M**, Alió JL, Alió del Barrio JL, Abdul Jawad K, Palazón-Bru A, Abdul Jawad Z, et al. **Corneal stromal regeneration therapy for advanced keratoconus: long-term outcomes at 3 years**. Cornea. 2021;40(6):741–54.

6.6 Resultados de la biomicroscopía confocal al año tras la implantación de **ADASCs** autólogas y la implantación de injertos estromales descelularizados con o sin **ADASCs** autólogas para pacientes con queratocono avanzado en los grupos 1, 2 y 3. Se publicaron en el siguiente artículo con referencia (179) de la publicación científica acreditada para esta tesis: **El Zarif M**, Abdul Jawas K, Alió del Barrio JL, Abdul Jawad Z, Palazón-Bru A, De Miguel MP, et al.**Corneal stroma cell density evolution in keratoconus corneas following the implantation of adipose mesenchymal stem cells and corneal laminas: An in vivo confocal microscopy study.** IOVS. 2020;61(4)22.

6.7 En la siguiente publicación presentamos un resumen integrado de los resultados, basado en la evidencia de los estudios clínicos experimentales realizados por nuestro grupo de investigación en el tema de la regeneración del estroma corneal para el tratamiento de enfermedades corneales, particularmente en el queratocono. Este resumen se publicó en el siguiente artículo con referencia (241) de la publicación científica acreditada para esta tesis: **El Zarif M**, Alió del Barrio JL, Arnalich-Montiel F, De Miguel MP, Makdissy N, Alió JL. **Corneal stroma regeneration: New approach for the treatment of cornea disease**. APJO. 2020;9(6):571–9.

6.8 Esta revisión resumió los resultados de los estudios clínicos en humanos informados en la literatura revisada por pares sobre el tema "regeneración del estroma corneal humano" y "terapia de mejora de la córnea". Además, esta revisión ofrece una comparación de los resultados entre los diferentes estudios recientes realizados por otros autores y nuestro estudio. Los resultados se publicaron en la siguiente revisión con referencia (242) de la publicación científica acreditada para esta tesis: **El Zarif M**, Alió JL, Alió del Barrio JL, De Miguel MP, Abdul Jawad K, Makdissy N. **Corneal stromal regeneration: A review on human clinical studies for treatment of keratoconus.** Front Med. 2021; 8:650724.

7. DISCUSIÓN

El tema de la regeneración del estroma corneal se ha desarrollado en los últimos cinco años y ha logrado importantes avances basados en el desarrollo de nuevos enfoques quirúrgicos como las cirugías intralamelares del estroma corneal y el uso de terapias avanzadas de bioingeniería y la terapia con células madre corneales para imitar y sustituir el estroma corneal humano.

A continuación en esta discusión se van a incluir comentarios referentes a publicaciones científicas que se realizaron en la época previa a esta tesis doctoral, directamente relacionados con la misma, pero cuyo contenido merece ser debatido en esta discusión para mejor comprensión de los resultados de esta tesis doctoral (30,31).

Nuestro grupo de investigación demostró por primera vez la viabilidad de las cirugías regenerativas del estroma corneal para el queratocono avanzado, utilizando **ADASCs** autólogas inyectadas en el bolsillo del estroma corneal en casos con queratocono avanzado, confirmando también la aparición de nuevo colágeno en las áreas inyectadas, que podrían Ser útil para el tratamiento de distrofias corneales, cicatrices y también podría aumentar ligeramente el grosor de la córnea (30,177,179,180,240–242).

Además, demostramos por primera vez que las láminas descelularizadas de un estroma corneal humano, colonizadas o no por **ADASCs** autólogas, pueden implantarse con fines terapéuticos en bases con fundamento a nivel clínico (31,177,179,180,240–242).

A lo largo de las diferentes etapas de este estudio, hay que reconocer los siguientes debates científicos correspondientes a cada una de las etapas de esta investigación:

7.1 Discusión de la revisión con referencia (240) de la publicación científica acreditada para esta tesis: Alió del Barrio JL, Arnalich-Montiel F, De Miguel MP, **El Zarif M**, Alió JL. **Corneal stroma regeneration: Preclinical studies**. Exp Eye Res. 2021;202:108314.

7.2 Discusión del artículo publicado con anterioridad a esta tesis doctoral con referencia (30): Alió del Barrio JL, **El Zarif M**, De Miguel M, Azaar A, Makdissy N, Harb W, et al. **Cellular therapy with human autologous adipose-derived adult stem cells for advanced keratoconus.** Cornea 2017; 36(8)952-60.

7.3 Discusión del artículo publicado con anterioridad a esta thesis doctoral con referencia (31): Alió del Barrio JL, **El Zarif M**, Azaar A, Makdissy N, Khalil C, Harb W, et al. **Corneal stroma enhancement with decellularized stromal laminas with or without stem cell recellularization for advanced Keratoconus**. Am J Ophthalmol. 2018;186: 47-58.

7.4 Discusión del artículo con referencia (177) de la publicación científica acreditada para esta tesis: Alió JL, Alió del Barrio JL, **El Zarif M**, Azaar A, Makdissy N, Khalil C et al. **Regenerative surgery of the corneal stroma for advanced keratoconus: 1-Year outcomes**. Am J Ophthalmol. 2019; 203:53-68.

7.5 Discusión del artículo con referencia (180) de la publicación científica acreditada para esta tesis: **El Zarif M**, Alió JL, Alió del Barrio JL, Abdul Jawad K, Palazón-Bru A, Abdul Jawad Z, et al**. Corneal stromal regeneration therapy for advanced keratoconus: long-term outcomes at 3 years**. Cornea. 2021;40(6):741–54.

7.6 Discusión del artículo con referencia (179) de la publicación científica acreditada para esta tesis: **El Zarif M**, Abdul Jawas K, Alió del Barrio JL, Abdul Jawad Z, Palazón-Bru A, De Miguel MP, et al**. Corneal stroma cell density evolution in keratoconus corneas following the**

implantation of adipose mesenchymal stem cells and corneal laminas: an in vivo confocal microscopy study. IOVS. 2020;61(4)22.

7.7 Discusión de la revisión con referencia (241) de la publicación científica acreditada para esta tesis: **El Zarif M**, Alió del Barrio JL, Arnalich-Montiel F, De Miguel MP, Makdissy N, Alió JL. **Corneal stroma regeneration: New approach for the treatment of cornea disease**. APJO. 2020;9(6):571–9.

7.8 Discusión de la revisión con referencia (242) de la publicación científica acreditada para esta tesis: **El Zarif M**, Alió JL, Alió del Barrio JL, De Miguel MP, Abdul Jawad K, Makdissy N. **Corneal stromal regeneration: a review on human clinical studies for treatment of keratoconus.** Front Med. 2021;8:650724.

7.1 Alió del Barrio JL, Arnalich-Montiel F, De Miguel MP, **El Zarif M,** Alió JL. **Corneal stroma regeneration: Preclinical studies.** Exp Eye Res. 2021;202:108314

Este estudio es la base fundamental de todos los estudios clínicos, en la medida en que contiene la base de la investigación experimental que es la base de este proyecto clínico realizado por nuestro grupo de investigación en los años anteriores. La primera aplicación clínica se logró a partir del experimento básico realizado por nuestro grupo de investigación. En este artículo, adaptamos los experimentos clínicos a los fundamentos necesarios para la primera aplicación clínica de este nuevo abordaje quirúrgico, utilizando técnicas de terapia avanzada por primera vez en el tratamiento del queratocono, y cómo dichos fundamentos experimentales se aplicaron transnacionalmente al ser humano (17,19,21,240).

En este estudio revisamos las evidencias planteadas en los estudios experimentales de nuestro grupo de investigación para su aplicación clínica, y el uso de células madre para la terapia celular del estroma corneal. Las **CSSCs** son una fuente prometedora para la terapia celular, ya que la técnica de aislamiento y los métodos de cultivo se han optimizado y refinado (36); presumiblemente, muestran un mayor potencial de diferenciación en queratocitos, ya que ya están comprometidos con el linaje corneal (243). Por otro lado, aislar **CSSCs** de forma autóloga es más exigente técnicamente considerando la pequeña cantidad de tejido del que se obtienen. Además, esta técnica todavía requiere un ojo sano contralateral, que no siempre está disponible (enfermedad bilateral). Por tanto, estos inconvenientes pueden limitar su uso en la práctica clínica. El uso de **CSSCs** alogénico requiere tejido corneal de un donante vivo o cadavérico.

El tejido adiposo humano adulto es una buena fuente de células madre extraoculares autólogas, ya que satisface muchos requisitos: fácil acceso al tejido, alta eficiencia de recuperación de células y la capacidad de sus células madre **h-ADASCs** para diferenciarse en múltiples tipos de células (queratocitos, osteoblastos, condroblastos, mioblastos, hepatocitos, neuronas, etc.) (21). Esta diferenciación celular se produce por efecto de factores o ambientes estimulantes muy específicos para cada tipo de célula, evitando la mezcla de múltiples tipos de células en distintos nichos.

Las **MSCs** de médula ósea (**BM-MSCs**) son probablemente las **MSCs** más estudiadas, presentando un perfil similar a las **ADASCs**, pero su extracción requiere una punción de la médula ósea, que es un procedimiento complicado y doloroso que requiere anestesia general.

Las **UMSCs** presentan una alternativa atractiva, pero su uso autólogo es actualmente limitado, ya que el cordón umbilical generalmente no se almacena después del nacimiento.

Las **ESCs** tienen un gran potencial, pero también presentan importantes problemas éticos. Sin embargo, el uso de **iPSCs** podría resolver estos problemas (37), y su capacidad para generar queratocitos adultos ya ha sido probada *in vitro* (38): las células adultas especializadas pueden reprogramarse a un estado de células madre o inmaduras y luego redirigirse al linaje celular requerido utilizando factores específicos y estímulos ambientales. Se ha demostrado que las **MSCs** derivadas de **iPSCs** ejercen propiedades inmunomoduladoras en la córnea similares a las observadas con las **BM-MSCs** (200). Hasta donde sabemos, no se han publicado estudios que informen sobre la capacidad de las **iPSCs** para diferenciarse en queratocitos adultos *in vivo* en el modelo animal.

Como se comentó anteriormente, es importante resaltar que el efecto terapéutico de las **SCs** en un tejido dañado no siempre está relacionado con la potencial diferenciación de las **SCs** en el tejido del huésped, ya que múltiples mecanismos pueden contribuir simultáneamente a esta acción terapéutica, La secreción de factores de crecimiento paracrinos capaces de estimular el tejido del huésped, en cuyo caso la diferenciación celular directa de las **SCs** puede no ser relevante e incluso puede ser inexistente (32,39,40).

Por otro lado, se han ideado muchos métodos físicos/de ingeniería para intentar controlar la organización del colágeno para su uso en ingeniería o para replicar tejidos, incluyendo electrohilado, transporte electrogradiente, magnético, flujo de tensiones, nano-litografía de pluma de inmersión, hilado húmedo, cristalización inducida por flujo, y densificación a un estado cristalino líquido. Ninguno de ellos ha podido recapitular la estructura del tejido corneal nativo. En general, no pueden igualar las propiedades mecánicas ni recrear organizaciones locales a nanoescala.

Hasta el momento se han desarrollado diferentes métodos para imitar la estructura del estroma corneal, entre ellos: cortes corneales descelularizados, vitrificación de colágeno, bioimpresión de colágeno en tres dimensiones (**3D**), compactación de colágeno por **3D**-RAFT y

plástico. El enfoque más prometedor ha sido desarrollado previamente por nuestro grupo, utilizando secciones de córnea humana descelularizadas que fueron recelularizadas con células madre mesenquimales adultas **h-ADASCs** derivadas del tejido adiposo humano en estudios experimentales con animales (Figuras. 2D,2E) (17,19,21), y lo que es más importante, también en pacientes que padecen enfermedades debilitantes del estroma corneal (31,177,244).

7.2 Alió del Barrio JL, **El Zarif M**, De Miguel M, Azaar A, Makdissy N, Harb W, et al. **Cellular therapy with human autologous adipose-derived adult stem cells for advanced keratoconus.** Cornea 2017; 36(8)952-60.

En este trabajo reportamos por primera vez la implantación de **ADASCs** en el estroma corneal humano en casos con queratocono, muchos casos aún se diagnostican en un estado avanzado donde el trasplante de córnea clásico (ya sea por técnicas de espesor total o lamelares) es la única opción de tratamiento. Nuestro grupo tuvo como objetivo encontrar una terapia alternativa al trasplante de córnea clásico para regenerar el estroma corneal, evitando así los importantes riesgos inter y postoperatorios asociados a esas técnicas (2). La terapia celular del estroma corneal mediante el uso de células madre ha ganado un interés científico relevante en los últimos años. Todas las **MSCs** parecen tener un comportamiento similar *in vivo*, pudiendo lograr una diferenciación de queratocitos y modular el estroma corneal con propiedades también inmunomoduladoras (3). Las **CSSCs** pueden tener funciones mejoradas, ya que son células corneales con un potencial de diferenciación más dirigido. Sin embargo, el número de **CSSCs** que se pueden obtener de las córneas humanas es bastante limitado y muy exigente técnicamente, con un subcultivo celular ineficaz y no siendo posible obtenerlas sin dañar la córnea donante. Todos estos importantes inconvenientes han limitado significativamente su uso para la práctica clínica e impiden su aplicación autóloga, por lo que es necesaria una fuente extraocular de células que pueda reemplazar

a las **CSSCs** para resolver todas estas limitaciones. Se ha demostrado que el tejido adiposo humano adulto es una fuente ideal de células madre autólogas, ya que satisface todos los requisitos: fácil acceso al tejido, alta eficiencia de recuperación de células y la capacidad de sus células madre **ADASCs** para diferenciarse en múltiples tipos de células (21). Las **BM-MSCs** tienen el mismo perfil que las **ADASCs**, pero su extracción mediante punción de la médula ósea es un procedimiento más complicado y doloroso que requiere anestesia general. Las **MSCs** umbilicales presentan una alternativa atractiva, pero su uso autólogo sería costoso y actualmente imposible. Las **ESCs** también presentan importantes problemas éticos. Las **iPSCs** de células madre pluripotentes inducidas, obtenidas de células adultas, ofrecen una nueva y emocionante posibilidad, ya que recientemente se ha demostrado su capacidad para diferenciarse en queratocitos corneales con propiedades inmunomoduladoras similares a las células madre mesenquimales (38,200).

Hasta la fecha, muchos estudios en modelos animales para diferentes anomalías corneales han demostrado los posibles beneficios de la terapia celular para mejorar la transparencia corneal por su capacidad para reorganizar las laminillas de colágeno del estroma, así como la producción de nuevo colágeno (3,16,27–29,17,19,21–26). Sin embargo, hasta donde sabemos, todavía no se han publicado datos *in vivo* en humanos que estudien la seguridad y eficacia de tales terapias. Este estudio fue la primera aplicación humana lograda con queratocono avanzado. Para ello, seleccionamos pacientes con queratocono avanzado ya candidatos a un trasplante de córnea clásico debido a una función visual insatisfactoria e intolerancia a las lentes de contacto, ya que, en caso de fallo, se podría realizar un tratamiento estándar para estos pacientes. La inyección de células madre al estroma corneal se realizó a través de un bolsillo laminar asistido por láser de femtosegundo a la media profundidad del estroma corneal medida por la **AS-OCT** (30). Aunque se trata de córneas con queratocono avanzado y con adelgazamiento severo, no observamos complicaciones

intraoperatorias como desgarros corneales. No obstante, para poder realizar esta técnica de forma segura, probablemente se requiera un punto paquimétrico mínimo más fino de 250 **µm** (ese grosor dejaría un casquete anterior cerca de un colgajo **LASIK**). Pueden surgir algunas preocupaciones sobre el posible efecto debilitante de esta disección corneal en una córnea ya severamente debilitada y patológica. Sin embargo, según los importantes hallazgos de John Marshall, los cortes laterales verticales a través de las laminillas corneales en lugar de las incisiones de delaminación horizontal contribuyen a la pérdida de la integridad estructural durante la creación del colgajo **LASIK** (245). En nuestro estudio solo se realizó un corte lateral anterior de 30º, por lo que, considerando estos hallazgos, el efecto debilitante de esta disección debería ser marginal.

Se prepararon tres millones de **ADASCs** autólogas (contenidos en 1 ml) para inyección en el bolsillo estromal. Esta alta concentración celular se decidió, ya que se esperaba una alta pérdida celular durante la inyección debido a la fuga de solución fuera de la córnea. Antes de la inyección, realizamos una paracentesis corneal para reducir la **IOP** y permitir más volumen dentro del bolsillo, aunque se esperaba que no quedara más del 10-30% del volumen inyectado dentro del estroma. Se necesitan más estudios para evaluar con precisión la cantidad real de células que quedan inmediatamente después del trasplante (30).

La función visual mejoró en todos los pacientes hasta los seis meses. Este beneficio fue modesto, pero se observó en los cuatro pacientes del estudio. Este hallazgo postoperatorio temprano teóricamente debe atribuirse al procedimiento quirúrgico en sí y no a la presencia de células madre, ya que aún no se han diferenciado en queratocitos adultos (30). No pudimos observar cambios tempranos en la refracción manifiesta o en la queratometría topográfica que puedan explicar esta mejora visual temprana (30).

Los datos queratométricos y paquimétricos obtenidos por topografía corneal (Pentacam) mostraron una estabilidad general (Figura. 9), con una posible progresión de la ectasia en el caso-2, los resultados queratométricos se han mantenido casi estables entre un mes postoperatorio y seis meses sin una verdadera progresión de la ectasia, este caso puede tener una redistribución de la superficie corneal anterior como consecuencia de la creación del bolsillo, lo que condujo a una reducción del astigmatismo y se asoció con una ganancia visual. Por tanto, parece que hubo un efecto "remodelador" posoperatorio del bolsillo corneal, un seguimiento futuro demostrará la posibilidad o no de una progresión ectásica.

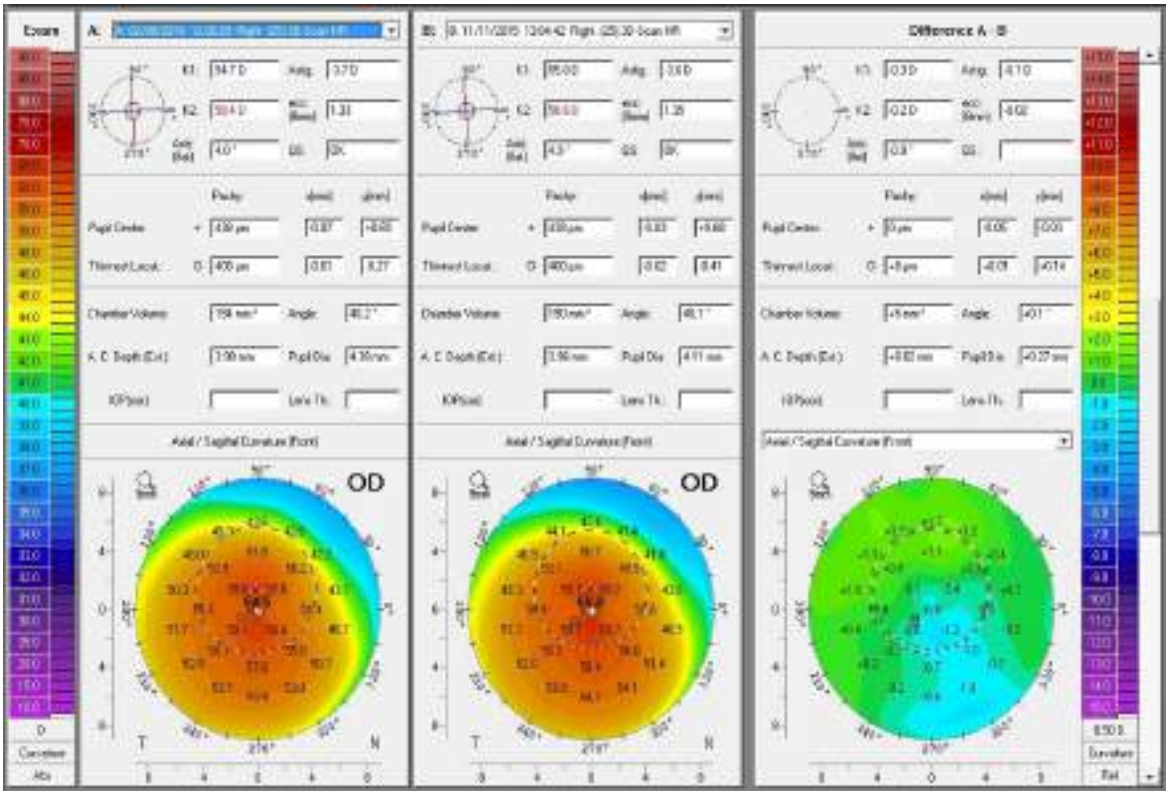

Figura 9. Comparación de la topografía corneal (Pentacam) entre el preoperatorio y los seis meses en el caso-1.
Observar la estabilidad de los parámetros queratométricos. La figura está extraída del artículo científico referido a Alió del Barrio y cols. (30).

La medición de la paquimetría por la **AS-OCT** en nuestro estudio demostró una mejora leve pero real del **CCT** (valor medio de 16,5 **µm** al sexto mes) (30), correlacionado con la presencia de áreas parcheadas de nueva producción de colágeno en la mayoría de los pacientes. Esta nueva producción de colágeno aparece en cantidades bajas y no distribuida homogéneamente a lo largo del plano quirúrgico, por lo tanto, este procedimiento no es capaz de restaurar grandes cantidades de tejido, como en las alteraciones de adelgazamiento de la córnea. Como se observó anteriormente en modelos animales, la adición de andamios derivados del ácido hialurónico o estroma corneal acelular puede ayudar a lograr este objetivo (19,22).

No observamos ninguna complicación inter o postoperatoria hasta los seis meses (30), siendo la cirugía bien tolerada en todos los casos con una restauración completa de la transparencia corneal en 24 horas. También pudimos observar una mejora clínica significativa de las opacidades corneales en el caso-2 (Figura. 10) (30), como se ha sugerido en estudios previos en modelos animales (23). Sin embargo, se requieren series de casos más grandes con opacidades corneales para demostrar este hallazgo.

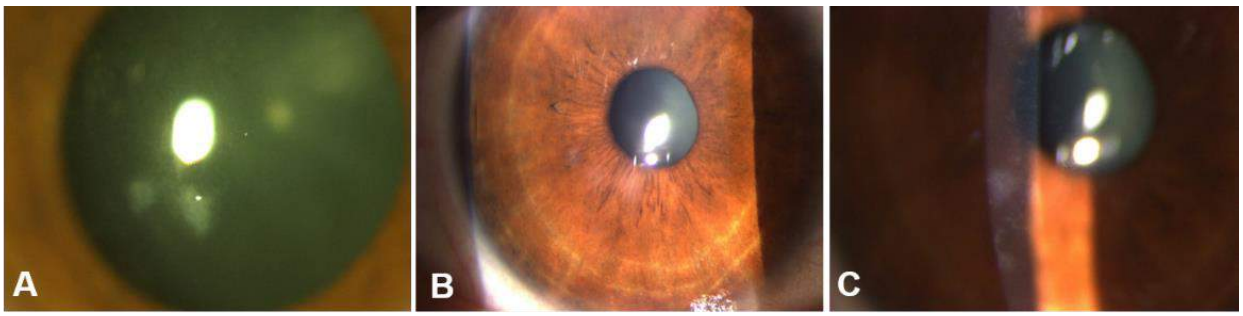

Figura 10. Imágenes con lámpara de hendidura del caso-2 en G-1.
(**A**) Preoperatoriamente. (**B** y **C**) en el sexto mes postoperatorio. Observe la mejoría postoperatoria en la densidad y severidad de las cicatrices del estroma anterior paracentral inferior. La figura está extraída del artículo científico referido a Alió del Barrio y cols. (30).

Dentro de los estudios experimentales, es fácil demostrar, mediante análisis post mortem, la supervivencia de las células marcadas previamente trasplantadas (mediante análisis de inmunofluorescencia) y su diferenciación en queratocitos adultos (detectando la expresión del queratocán) (19,21). Sin embargo, los estudios en humanos *in vivo* tienen el importante inconveniente de estar limitados a hallazgos de biomicroscopía confocal (vulnerables a interpretaciones subjetivas). Pudimos observar la presencia de células de forma redondeada en el plano quirúrgico en todos los pacientes que recibieron el implante **ADASCs**, mostrando posteriormente un cambio progresivo de forma dendrítica hasta llegar a no ser posible en diferenciarlos de los queratocitos normales al final del seguimiento de los seis meses (30).

7.3 Alió del Barrio JL, **El Zarif M**, Azaar A, Makdissy N, Khalil C, Harb W, et al. **Corneal stroma enhancement with decellularized stromal laminas with or without stem cell recellularization for advanced Keratoconus**. Am J Ophthalmol. 2018;186: 47-58.

En este artículo describimos la implantación de **ADASCs** en el estroma corneal en córneas con queratocono avanzado, es una línea de terapia novedosa y prometedora para el queratocono y otras distrofias corneales (30), a pesar de que su eficacia aún se requiere establecer adecuadamente, así como mejorar la técnica de administración de las células madre. Sin embargo, la producción demostrada de una nueva **ECM** humana, trasplantando las células madre mesenquimales en el estroma corneal *in vivo* en modelos animales (21–27), y en humanos (30) no se espera que sea suficiente para rehabilitar una córnea muy adelgazada. En este escenario, postulamos que la adición de tejido estromal corneal descelularizado podría mejorar los resultados previamente observados con la terapia celular sola, ya que proporciona un soporte tectónico y un ambiente ideal para las células madre (19,224).

La implantación de láminas descelularizadas o recelularizadas presenta una novedosa línea de tratamiento para casos de queratocono avanzado, donde a través de una técnica quirúrgica sencilla y rápida que se puede realizar bajo anestesia tópica, logramos una rehabilitación funcional parcial de la córnea ectásica avanzada y una recuperación casi completa del espesor, permitiendo potencialmente que estas córneas sean nuevamente candidatas para otras técnicas quirúrgicas no invasivas de rehabilitación visual. Cada córnea de donante puede generar fácilmente una donación de hasta tres láminas siguiendo este modelo, lo que podría resolver parcialmente la escasez mundial de córneas de donantes, mejorando el acceso del paciente al trasplante de córnea en muchas partes del mundo. Además, la técnica de descelularización por **SDS** es un método no complejo y económico que permite la eliminación de todo el componente celular donante alogénico del injerto, evitando cualquier riesgo de rechazo, mientras que el resto de la matriz extracelular aún conserva su arquitectura normal tal y como ha sido ya demostrado *in vitro* y en el modelo animal por nuestro grupo y otros autores (18,19,224).

En esta fase de este ensayo clínico piloto, informamos por primera vez hasta donde sabemos, el trasplante de tejido estromal corneal descelularizado en la córnea humana *in vivo*. Todos los parámetros visuales mejoraron moderadamente en más de una línea, logrando diferencias estadísticamente significativas en la **UDVA** a pesar de la pequeña muestra del estudio. Esto se correlaciona bien con la mejora significativa de la esfera refractiva y la aberración esférica. Sin embargo, todos los parámetros queratométricos anteriores, coma y las **HOA RMS** totales mejoraron sistemáticamente. Basándose sobre nuestros resultados se pudo esperar una mejora media del **Anterior Km** y la **Kmax** de 1,5 y 3,5D respectivamente. Todos los parámetros de espesor mejoraron significativamente por encima de 100 **µm**, logrando una casi una normalización del espesor de la córnea (31). Como se postuló inicialmente, no hemos observado ningún signo clínico

inflamatorio durante el seguimiento, así como tampoco células inflamatorias evidentes en la biomicroscopía confocal (179), observándose solo una leve "haze" del injerto a lo largo del primer mes postoperatorio, recuperándose completamente al tercer mes postoperatorio en todos los pacientes.

Por otro lado, dentro de los seis meses de seguimiento, no hemos podido demostrar las ventajas potenciales de agregar células madre mesenquimales al injerto estromal descelularizado. Los injertos recelularizados no mostraron una recuperación visual más rápida, mejores resultados o áreas de nueva producción de colágeno en la **OCT** corneal. Se requieren más estudios con un seguimiento más prolongado y muestras más grandes para aclarar el posible papel de la terapia celular además de este tipo de injerto corneal.

Además, en nuestro estudio, algunos pacientes recibieron aleatoriamente una lámina descelularizada o recelularizada con o sin **BM**. Melles y cols. describió recientemente los resultados con el trasplante de **BM** en el estroma medio de ojos con queratocono avanzado de una manera similar a la del presente estudio (246), obtuvieron un decrecimiento en la queratometría máxima en promedio de 77 ± 26.2 (D) a 69.2 ± 3.7 D, la mejor **CDVA** mejoró solo de 1.27 a 0.9 en LogMar, la mejor **CLDVA** se mantuvo estable, la paquimetría de punto más delgado promedio aumentó solo de 332 ± 59 µm antes de la cirugía hasta 360 ± 50 µm. Mientras tanto, en nuestro estudio obtuvimos una mejora equivalente a 1-2 líneas en escala LogMar en **CDVA**, y también **CLDVA** en todos los grupos, una mejora estadísticamente significativa en el **CCT** y del **thinnest point** con los grupos de láminas descelularizadas y recelularizadas, como bien en **CV** (31,177,180). Teniendo en consideración las limitaciones de nuestra pequeña muestra de estudio, no encontramos diferencias entre los pacientes que recibieron láminas que contenían o no **BM**. Si este hallazgo preliminar se confirma en estudios posteriores, sugeriría que podemos obtener varias láminas con potencia óptica

neutra de córneas no válidas para un injerto corneal. Nuestros resultados clínicos tienen al menos los mismos que los reportados con el trasplante de **BM** como capa aislada, pudimos demostrar no solo la viabilidad de esta cirugía, sino que pudimos mejorar los resultados visuales, así como la aberración corneal, además que la la adición de estroma permite una restauración completa del espesor (hecho que no se consigue solo con **BM**). Nuestros resultados abren un campo interesante para la investigación para explorar cómo las técnicas de rehabilitación visual alternativas y bien establecidas, como el colágeno corneal **CXL** y los segmentos del anillo intracorneal, se comportan en el ojo con queratocono avanzado con una restauración del grosor del estroma.

Un hallazgo importante mostrado en el estudio actual es el hecho de que se han observado signos tempranos de recelularización por los queratocitos del huésped a los seis meses después de la cirugía en todos los pacientes. No pudimos demostrar esta recelularización del huésped de los injertos descelularizados en nuestros estudios anteriores en animales con un solo seguimiento de tres meses (19). Otros autores han informado previamente de esta infiltración de queratocitos del huésped en injertos descelularizados en modelos animales para queratoplastia lamelar anterior (247), aunque, hasta donde sabemos, informamos por primera vez de este hallazgo para injertos descelularizados intraestromales. Esta recelularización del huésped permite una funcionalidad completa del tejido injertado, lo que debería garantizar el mantenimiento de la transparencia a largo plazo de la córnea.

Un tema relevante que no se ha aclarado en la fase actual de este estudio es si la implantación intraestromal de tejido estromal descelularizado o recelularizado podría detener la condición progresiva natural de esta enfermedad. Los pacientes del estudio eran ojos con queratocono avanzado que ya eran candidatos para un trasplante de córnea y el estado progresivo preoperatorio de la enfermedad no estaba bien determinado, por lo que se requerirán más estudios de la

biomecánica corneal para responder a este asunto. Sin embargo, todos los pacientes presentaron estabilidad o mejoría progresiva de los parámetros visuales y queratométricos.

7.4 Alió JL, Alió del Barrio JL, **El Zarif M**, Azaar A, Makdissy N, Khalil C et al. **Regenerative surgery of the corneal stroma for advanced keratoconus: 1-Year outcomes**. Am J Ophthalmol. 2019; 203:53-68.

Este documento informa sobre los resultados de 12 meses de la primera experiencia humana de terapia con células del estroma corneal hasta un año. Nuevamente, lo que se demuestra en este estudio es la ausencia de complicaciones del procedimiento observada en este estudio clínico de un año. El uso de un láser de femtosegundo para crear un bolsillo estromal en el estroma medio de los casos de queratocono avanzado se muestra en la experiencia como factible y sin consecuencias negativas, hasta un año de observación (177).

El primer tema importante que se demuestra en este estudio es la ausencia de complicaciones del procedimiento observada en este estudio clínico de un año. El uso de un láser de femtosegundo para crear un bolsillo estromal en el estroma medio de los casos de queratocono avanzado se muestra en la experiencia como factible y sin consecuencias negativas, hasta un año de observación. Este hallazgo es coherente con estudios previos reportados por nuestro groupo en los que una gran disección laminar corneal asistida por femtosegundo realizada aproximadamente a la profundidad de los seguidos de la implantación de un anillo circular intraestromal, demostró no verse afectada por complicaciones visuales, ni de la topografía, ni de las perspectivas queratométricas o anatómicas (248).

En este estudio se ofrecen los datos más representativos sobre la seguridad de la cirugía. La única inyección de células en el bolsillo corneal fue seguida de una mejora inmediata, aunque modesta, pero significativa, que se mantuvo durante todo el año de seguimiento. Esta respuesta inicial de la córnea indica la tolerancia a este tipo de cirugía, ya que no se observó deterioro en ningún caso del **G-1** ni en los demás grupos. A este nivel inicial de la experiencia, la diferenciación de queratocitos y la eventual producción de colágeno pueden no tener una influencia significativa en la respuesta mecánica de la córnea, por lo que estudios posteriores deberían garantizar la viabilidad de este tipo de cirugía desde la perspectiva biomecánica. Sin embargo, se crearon bolsillos asistidos por láser de femtosegundo en estas dimensiones para la implantación de segmentos anulares intracorneales sin impacto negativo, ya sea inmediato o tardío, en las córneas queratocónicas intervenidas, aunque en esta experiencia se implantó un cuerpo extraño intracorneal con fines terapéuticos (249). Además, según informes anteriores (245), Los cortes laterales verticales a través de las laminillas corneales en lugar de las incisiones de lamelación horizontal contribuyen a la pérdida de la integridad estructural durante la creación del colgajo **LASIK**, por lo que se puede esperar un impacto mínimo en la biomecánica corneal después de la creación de un bolsillo laminar como el realizado en este estudio clínico. Serán necesarios más estudios para estudiar la biomecánica de las córneas en pacientes con diferentes estadios de queratocono tras la implantación de **ADASCs**, láminas descelularizadas sin o con **ADASCs**, y comparar los resultados de los tres tipos de implantes.

En la experiencia actual confirmó hasta el año la buena tolerancia y la posibilidad de incrementar el grosor corneal mediante la implantación de láminas descelularizadas de estroma corneal creadas por láser de femtosegundo. Inducir un aumento calculado en el grosor de la córnea es factible mediante el uso de estas láminas femto-disecadas y descelularizadas que pueden

implantarse sin ningún impacto negativo en la biomecánica, visión y especialmente, anatomía corneal. Se ha demostrado que la irregularidad corneal mejora, aunque modestamente, mediante la reducción de la aberrometría corneal, como se observa en este estudio. Así, podemos deducir que el aumento calculado del grosor corneal inducido por el uso de estas láminas puede ser utilizado de forma terapéutica sin riesgo para la transparencia corneal y beneficia la regularidad y topografía corneal. La esfera refractiva de estos pacientes también mejoró, lo que está en coherencia con el aplanamiento de la córnea que se observa en el análisis queratométrico (177).

Probablemente, la característica más relevante es el mantenimiento de la transparencia corneal como un hecho. En ningún caso se observó el "haze" corneal relevante o cicatrización corneal al año de seguimiento, y ni siquiera durante la experiencia (salvo la neblina temprana observada a lo largo del primer mes tras la implantación de la lámina en **G-2** y **G-3**) (177). Esta cuestión es extremadamente importante porque la introducción de tejido corneal manipulado heterólogo podría ser seguida de cicatrización corneal y, finalmente, pérdida permanente de la visión. Las razones de esta transparencia corneal probablemente estén relacionadas con el carácter descelularizado de las láminas, ya que no se produce ninguna interacción biológica entre este tejido extraño de origen alogénico y las células del tejido huésped local. Estos hallazgos demuestran nuestros estudios experimentales previos en los que las láminas del estroma corneal descelularizado humano fueron bien toleradas en el modelo animal experimental (19). Además de esto, la presencia de las **ADASCs** autólogas en las láminas del tercer grupo podría ser de mayor relevancia para el mantenimiento no solo de la transparencia corneal sino también para la disminución de cicatrices corneales previas que pudieran estar presentes en estos casos, hecho que se ha descrito anteriormente en el modelo animal experimental (23–28), y que también lo pudimos observar en un paciente del **G-1** (30). Esta observación aislada de una disminución significativa por biomicroscopía

en las cicatrices presentes en la córnea antes de la operación podría estar relacionada con la capacidad de las células madre para mejorar la transparencia corneal por su capacidad para reorganizar el tejido enfermo anterior y la producción de un nuevo colágeno normal (177). Es necesario de realizar más estudios en córneas no transparentes y con cicatrices para confirmar la posibilidad terapéutica de esta nueva cirugía.

También es de particular relevancia la observación de una respuesta biológica positiva de los queratocitos del huésped a las láminas descelularizadas, especialmente en aquellas implantadas con **ADASCs** autólogas. En el **G-2** (láminas descelularizadas sin adición de **ADASCs**) el aumento del grosor corneal manteniendo la transparencia corneal fue paralelo a la observación de un aumento en la celularidad de las partes anterior y posterior del estroma corneal. Entonces la lámina corneal descelularizada no solo fue capaz de mantener condiciones transparentes aumentando el grosor corneal, sino que también hubo una respuesta celular positiva de los queratocitos del huésped al proliferar e incluso invadir el tejido implantado, lo que indica su activación biológica (Figuras. 7B, 7C). Este hallazgo fue aún más pronunciado en aquellas láminas implantadas con **ADASCs** (Figuras. 8A-8E) (177).

En el **G-1** (**ADASCs** solo), los hallazgos de la biomicroscopía confocal también son notables. Inicialmente, las **ADASCs** pudieron identificarse como redondeadas y de forma regular, mientras que más tarde durante la experiencia estas células se transformaron progresivamente en una forma fusiforme y mostraron una apariencia idéntica a los queratocitos normales de la córnea humana (Figura. 6) (30,177). También podría observarse un aumento en la densidad de queratocitos del estroma anterior y posterior en pacientes del **G-1**, por lo que no solo la presencia de la lámina corneal induce una respuesta biológica positiva en la córnea, sino que también esta respuesta de curación puede mejorarse mediante la inclusión de células **ADASCs**, lo que podría contribuir no

solo a la tolerancia biológica de la lámina corneal descelularizada sino también al mantenimiento de su transparencia e integración en la córnea huésped.

Como demuestran los datos del primer año de este estudio, estamos abriendo una nueva área de investigación y cirugía corneal. El uso de partes de la córnea para un aumento terapéutico del grosor corneal en córneas queratocónicas debilitadas y delgadas es un nuevo concepto para la investigación. Todos los parámetros clínicos corneales se mantuvieron o mejoraron y no se observó deterioro en ninguno de los casos del presente estudio (177).

7.5 <u>El Zarif M</u>, Alió JL, Alió del Barrio JL, Abdul Jawad K, Palazón-Bru A, Abdul Jawad Z, et al**. Corneal stromal regeneration therapy for advanced keratoconus: long-term outcomes at 3 years**. Cornea. 2021; 40(6):741–54.

En este artículo, informamos los resultados de tres años del primer estudio clínico sobre la terapia de regeneración del estroma corneal para el tratamiento del queratocono avanzado (30,31,177,180,241,242,250,251). Hemos podido constatar en este informe la ausencia de complicaciones como ectasia corneal, inflamación corneal o cualquier inducción significativa de cicatrización o turbidez corneal durante el seguimiento, la córnea mostró transparencia desde el primer día postoperatorio en el **G-1** y hasta los tres meses con el **G-2** y el **G-3**. En un estudio reciente con casos de queratocono progresivo leve a moderado, se demostró que la disección manual del estroma medio es eficaz, no hubo complicaciones en ningun caso operado e incluso fue eficaz para lograr la estabilización de la ectasia corneal en el 50% de los casos, estos hallazgos están en concordancia con nuestro estudio en el sentido en que la disección lamelar es factible en casos de queratocono progresivo (252).

Además, a los tres años después de la cirugía, obtuvimos una mejora de casi una línea en la escala LogMar en **UDVA**, 2 líneas en **CDVA** y 2,3 líneas en la escala LogMar en **CLDVA** en todos los casos (Figuras. 11A-11C; Tabla 5). Además, los valores medios de **Rx Sphr** mostraron una mejora en todos los grupos y se observó un cambio en **Rx Cyl** (Figuras. 11D, 11E; Tabla 5). En estudios posteriores, al aumentar el número de pacientes, se debe tomar la opinión del paciente sobre su satisfacción (como el cuestionario de la encuesta de satisfacción NAVQ-10), y su calidad de visión (con el cuestionario de Calidad de la Visión QOV de McAlinden y cols.) (253). Además, de tomar la opinión de los pacientes sobre la experiencia (con la prueba de detección de satisfacción del paciente de MacAlinson).

También, un aumento fue obtenido en el grosor del punto corneal más delgado **CCT** y **CV** (Figuras. 11F-11H; Tabla 5), hubo una mejora en todas las aberraciones corneales, especialmente en la de **3rdorder RMS,** y **HOA RMS** (Figura. 12), y una mejora en las variables secundarias, en **Anterior Km,** y en **Kmax** obtuvimos una mejora en los valores medios de 2 D y 3 D respectivamente hasta el seguimiento de tres años (Figura. 13; Tabla 6). Con el estudio realizado por Birbal y cols. (252) la **CDVA** con gafas se mantuvo estable en el 58% de los casos, y mejoró 2 líneas de Snellen en el 42%. La **CLDVA** se mantuvo estable en 44% de los casos, y mejoró de ≥ 2 líneas de Snellen en 33% y se deterioró en 22% de los casos, pero aunque la disección lamelar es factible no se puede lograr una mejora en el espesor ni la aberrometría corneal como lo fue en nuestro estudio, por los tanto los casos con queratocono con > 60 D mostraron una progresión continua.

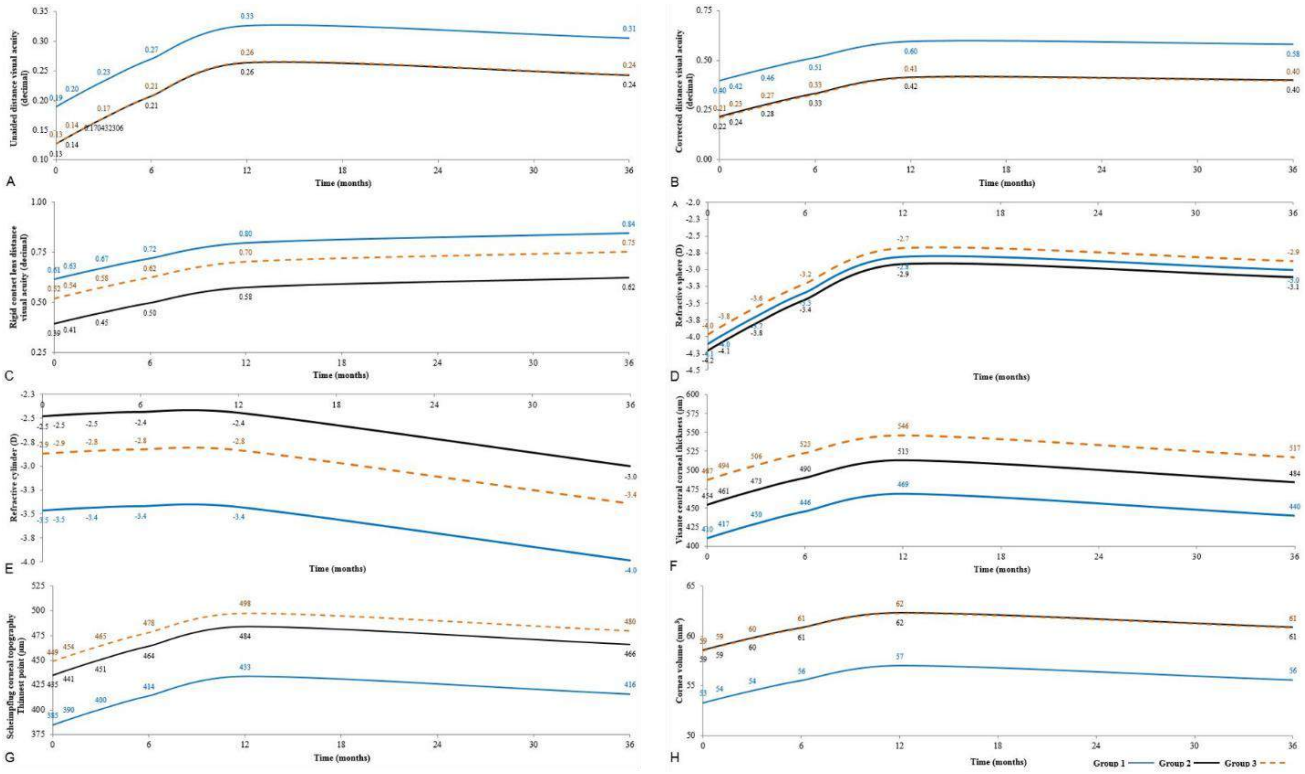

Figura 11. Resultados clínicos medios estadísticos a lo largo de 3 años de seguimiento en **G-1**, **G-2** y **G-3**.

(**A, B**) Muestran la mejora en la agudeza visual sin ayuda (**UDVA**) y la agudeza visual a distancia corregida (**CDVA**) (decimal) (equivalente a la escala de LogMar) desde el preoperatorio hasta los 36 meses. (**C**) Muestra una mejora en la agudeza visual con las lentes de contacto rígidas (**CLDVA**) (decimal) desde el preoperatorio hasta alcanzar un máximo a los 36 meses. (**D**) Muestra una mejoría con la esfera refractiva (**Rx** Sphr) en (D) desde el preoperatorio hasta los 12 meses, luego se observa una leve disminución hasta los 36 meses. (**E**) El cilindro refractivo (**Rx Cyl**) en (D) permaneció casi estable desde el preoperatorio hasta los 12 meses, seguido de un aumento en los valores medios hasta los 36 meses. (**F, G, H**) Presentan el grosor corneal central (**Visante CCT**) (µm), Pentcam Punto más fino (**Thinnest point**) (µm), Volumen de la córnea (**CV**) (mm^3) respectivamente. Observe el aumento de los valores medios desde el preoperatorio, hasta alcanzar un máximo a los 12 meses y luego se establecieron con un descenso lento hasta los 36 meses. La figura está tomada del artículo científico de El Zarif M y cols. (180) acreditado para esta tesis.

Tabla 5. Resultados estadísticos de las variables principales y secundarias entre **G-1**, **G-2** y **G-3** junto con el seguimiento hasta los tres años.

	Valor-P (G-2) / (G-1)	**Valor-P (G-3) / (G-1)**	**Valor-P (G-2) / (G-3)**	**σ**	**Valor-P** (trayectorias de las variables)
UDVA	[P = 0.054]	[P = 0.069]	[P = 0.986]	0.116	[P = 0.0021]
CDVA	[P < 0.001]	[P < 0.001]	[P = 0.900]	0.151	[P < 0.001]
CLDVA	[P < 0.001]	[P = 0.090]	[P = 0.010]	0.180	[P < 0.001]
Rx Sphr (D)	[P = 0.892]	[P = 0.863]	[P = 0.747]	2.691	[P = 0.649]
Rx Cyl (D)	[P < 0.001]	[P = 0.014]	[P = 0.086]	0.824	[P = 0.015]
Visante CCT (µm)	[P = 0.012]	[P < 0.001]	[P = 0.055]	62.940	[P = 0.004]
Thinnest point (µm)	[P = 0.007]	[P = 0.001]	[P = 0.465]	67.966	[P = 0.021]
CV (mm^3)	[P < 0.001]	[P < 0.001]	[P = 0.948]	3.757	[P = 0.001]
3^{rd} order RMS	[P < 0.001]	[P = 0.009]	[P = 0.376]	4.571	[P = 0.087]
4thorder RMS	[P = 0.074]	[P = 0.817]	[P = 0.004]	2.515	[P = 0.117]
HOA RMS (µm)	[P < 0.001]	[P = 0.038]	[P = 0.091]	4.530	[P = 0.061]
LOA RMS (µm)	[P = 0.617]	[P = 0.870]	[P = 0.491]	27.299	[P = 0.866]
Anterior Km (D)	[P = 0.085]	[P = 0.909]	[P = 0.062]	6.436	[P = 0.351]
Posterior Km (D)	[P = 0.001]	[P = 0.636]	[P = 0.004]	1.326	[P = 0.118]
Kmax (D)	[P = 0.949]	[P = 0.387]	[P = 0. 0.391]	8.250	[P = 0.643]
Topo Cyl (D)	[P = 0.091]	[P = 0.190]	[P = 0.753]	2.383	[P = 0.525]

Valor-P de las (trayectorias de las variables), desviación estándar (**σ**). Agudeza visual sin ayuda (**UDVA**), agudeza visual a distancia corregida (**CDVA**), agudeza visual a distancia con lentes de contacto rígidas (**CLDVA**) en (decimal equivalente a la escala logMar). Esfera refractiva (**Rx** Sphr) en (D) y cilindro refractivo (**Rx Cyl**) en (D). **OCT**-Visante del segmento anterior: Espesor corneal central (**Visante CCT**) (**µm**) (Carl Zeiss). Topografía corneal de Scheimpflug punto más delgado (**Thinnest point**) (**µm**), volumen de la córnea (**CV**) (mm^3). Aberrometría corneal (Pentacam; Oculus Inc., Wetzlar, Alemania): aberración de tercer orden **RMS** (**3rdorder RMS**) (**µm**), aberración de cuarto orden **RMS** (**4thorder RMS**) (**µm**), aberración de alto orden **RMS** (**HOA** RMS) (**µm**) y aberración de orden bajo **RMS** (**LOA RMS**) (**µm**). Queratometría media anterior (**Anterior Km**) en (D), queratometría media posterior (**Posterior Km**) en (D), queratometría máxima (**Kmax**) en (D) y cilindro topográfico (**Topo Cyl**) en (D) (Pentacam; Oculus Inc., Wetzlar, Alemania). La tabla está tomada del artículo científico de El Zarif M y cols. (180) acreditado para esta tesis.

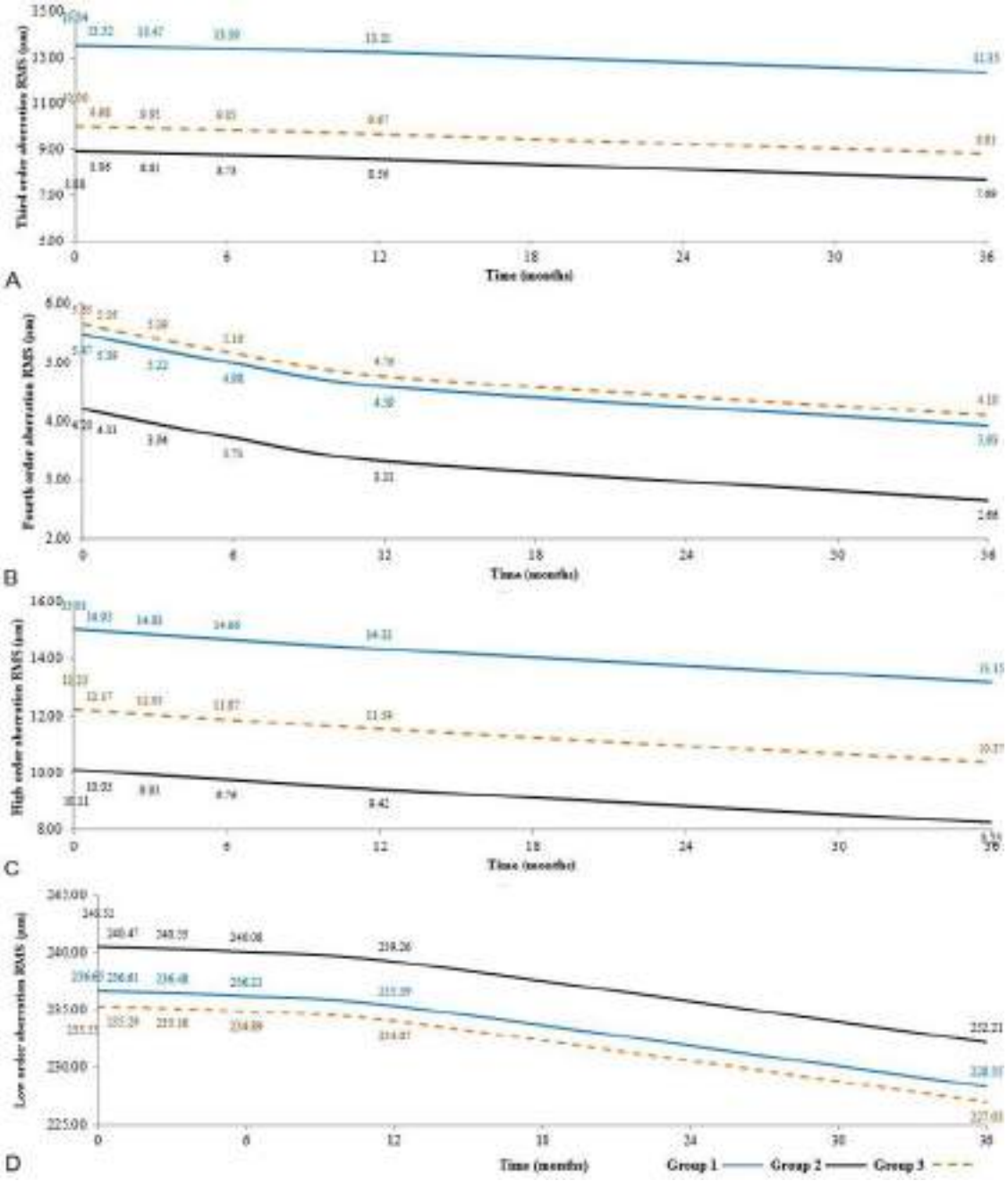

Figura 12. Resultados medios estadísticos de la aberrometría corneal a lo largo de tres años de seguimiento en **G-1**, **G-2** y **G-3.**

Observe la mejora en los valores medios estadísticos de aberrometría corneal en comparación con los valores medios preoperatorios. (**A**) Muestra la aberración **RMS** de tercer orden (**3rdorder RMS**) (**µm**). (**B**) Muestra la aberración **RMS** de cuarto orden (**4thorder RMS**) (**µm**). (**C**) Presenta la aberración de orden alto **RMS** (**HOA** RMS) (**µm**) (**D**) Ilustra la aberración de orden bajo **RMS** (**LOA RMS**) (**µm**). Observe la mejora en todos los valores medios de aberraciones hasta los 36 meses postoperatorios en comparación con los valores medios preoperatorios. La figura está tomada del artículo científico de El Zarif M y cols. (180) acreditado para esta tesis.

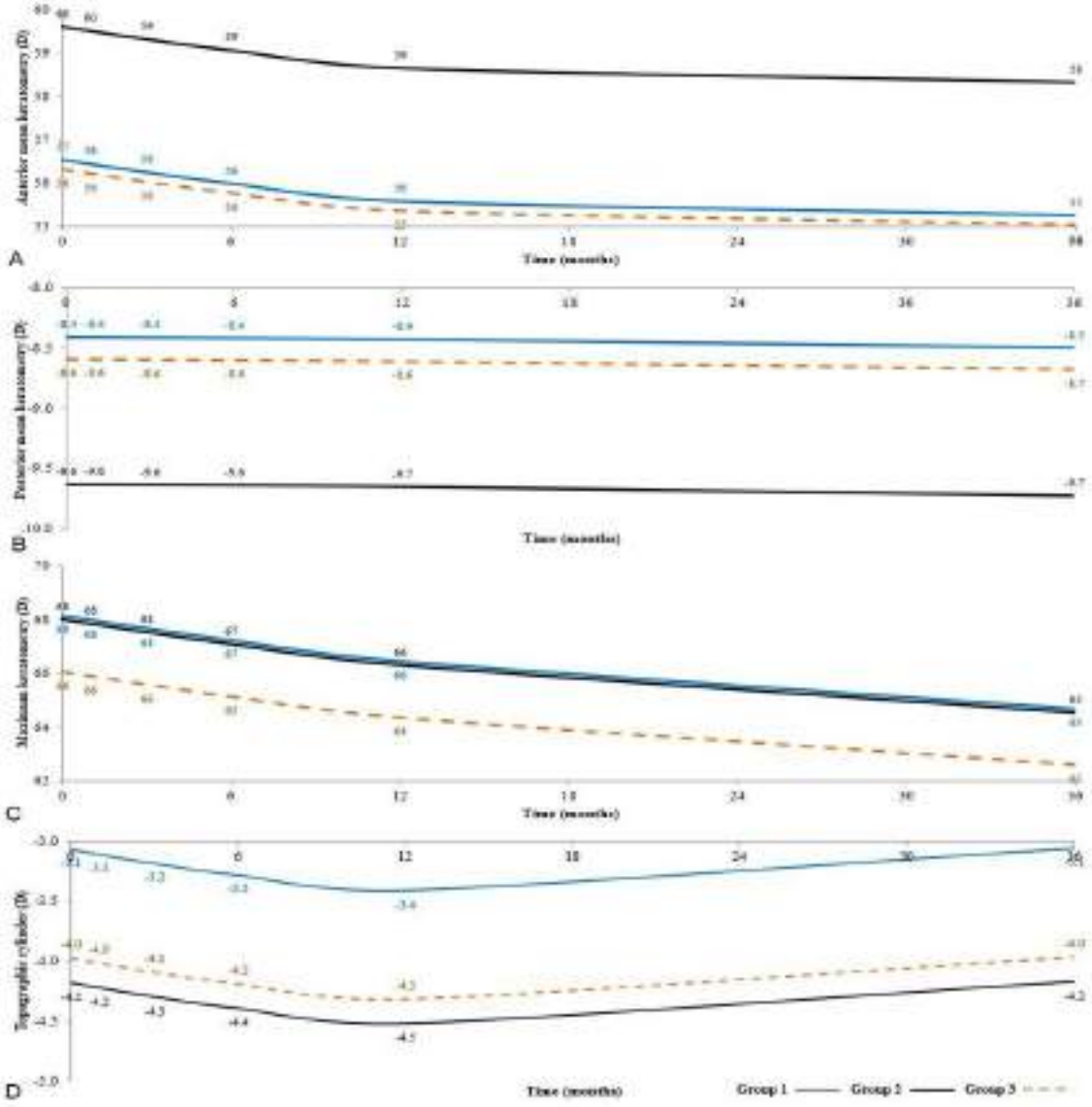

Figura 13. Resultados medios estadísticos de las variables secundarias a lo largo de tres años de seguimiento en **G-1**, **G-2** y **G-3/** preoperatorio.
(**A**) Muestra los valores medios de la queratometría media anterior (**Anterior Km**) en (D), observe la mejora de 1 dioptría a los 12 meses, seguida de otra 1 dioptría de aplanamiento hasta los 36 meses. (**B**) Muestra la queratometría media posterior (**Posterior Km**) en (D), los valores medios fueron casi estables en todos los grupos a los 36 meses con una única diferencia media de (0,1) (D). (**C**) Observe la queratometría máxima (**Kmax**) en (D), hubo un valor medio de 2 dioptrías de aplanamiento a los 12 meses, seguido de otra 1 dioptría de aplanamiento hasta los 36 meses. (**D**) Nótese el cilindro topográfico (**Topo Cyl**) en (D), cambio de -0,3 (D) a los 12 meses, mientras que a los 36 meses los valores medios subieron hasta los mismos resultados preoperatorios iniciales. La figura está tomada del artículo científico de El Zarif M y cols. (180) acreditado para esta tesis.

Tabla 6. Valores medios queratométricos de **Anterior Km** en (D) y queratometría máxima **Kmax** en (D) en **G-1**, **G-2** y **G-3**.

Grupo	Tiempo/mes	Anterior Km (D) Valores medios	Kmax (D) Valores medios
G-1	0	57.00	68.00
G-1	36	55.00	65.00
G-2	0	60.00	68.00
G-2	36	58.00	65.00
G-3	0	56.00	66.00
G-3	36	55.00	63.00
(G-1) – (G-2)	0	-3.00	0.00
(G-1) – (G-2)	36	-3.00	0.00
(G-1) – (G-3)	0	1.00	2.00
(G-1) – (G-3)	36	2.00	5.00
(G-2) – (G-3)	0	4.00	5.00
(G-2) – (G-3)	36	3.00	2.00

La diferencia en los valores medios entre los grupos: (**G-1**) - (**G-2**), (**G-1)** - (**G-3**) & (**G-2**) - (**G-3**). Queratometría media anterior (**Anterior Km**) en (D), queratometría máxima (**Kmax**) en (D) (Pentacam; Oculus Inc., Wetzlar, Alemania). La tabla está tomada del artículo de El Zarif M y cols. (180) acreditado para esta tesis.

El progresivo aplanamiento de la córnea explica la mejora observada en la esfera refractiva y los parámetros visuales. La mejora aberrométrica que se observa es consistente con tales mejoras en los parámetros visuales. Consideramos que estos resultados son relevantes para los ojos seleccionados para la investigación por tratarse de casos de queratocono avanzado con indicación

de injerto de córnea como única alternativa terapéutica. Curiosamente, la producción de neocolágeno y el aumento del grosor de la córnea se observaron después de la implantación de **ADASCs** y láminas descelularizadas o recelularizadas con **ADASCs** (Figura. 14). Si este hallazgo tiene alguna influencia en la biomecánica debilitada de la córnea con queratocono avanzado, se garantizara con futuras investigaciones (8).

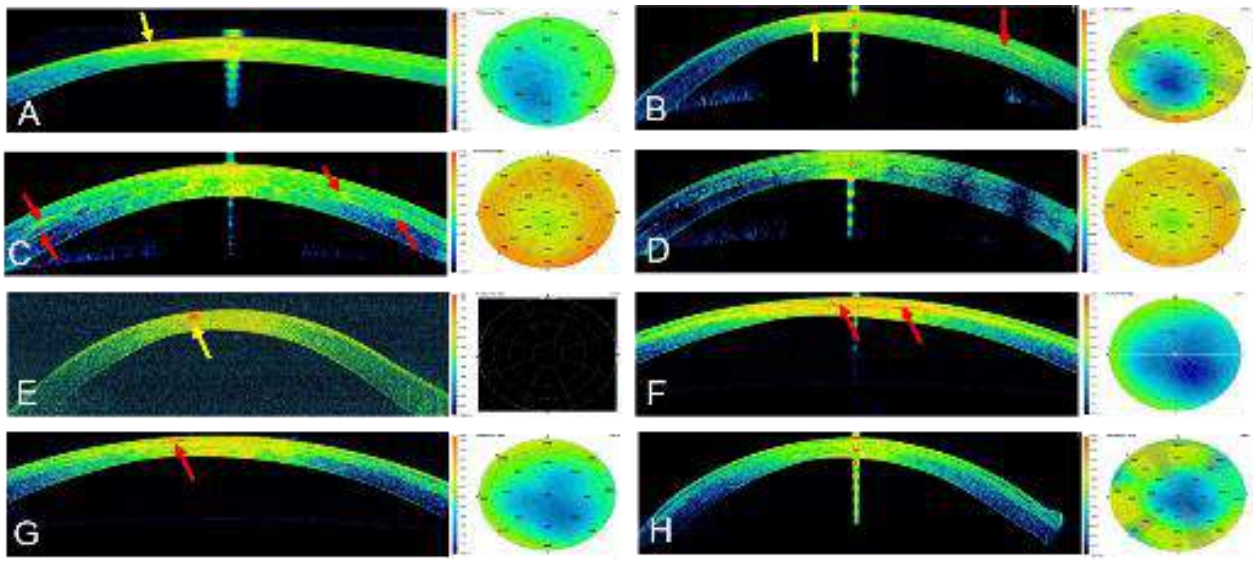

Figura 14. Imágenes de tomografía de coherencia óptica de la córnea con el Visante (Visante **OCT**) y mapas paquimétricos.
(**A, B**) Paciente **G-**1, caso-2. (**A**) Un mes después de la operación, observe la cicatriz paracentral reflectante (flechas amarillas). (**B**) A los tres años del postoperatorio, muestra una mejoría en la banda reflectante de neocolágeno (flecha roja). (**C, D**) Paciente **G-2**, caso-6. (**C**) A los seis meses, observe la alta reflectancia de la banda de neo-colágeno (flecha roja) y la mejoría en el mapa paquimétrico (lado derecho). (**D**) A los tres años, observe la mejora de la banda reflectante de neocolágeno (lado derecho) y la estabilidad del mapa paquimétrico. (**E, F, G, H**) Paciente **G-3**, caso-11. (**E**) En el preoperatorio se aprecia la cicatriz paracentral reflectante (flecha amarilla). No se capturó el mapa paquimétrico debido a la córnea muy delgada. (**F**) Al primer mes se aprecia la alta reflectancia de la banda de neocolágeno (flecha roja). (**G**) A los 12 meses se aprecia la mejoría de la banda reflectante de neocolágeno (flecha roja) y el mapa paquimétrico. (**H**) Casi a los tres años. Nótese la mejora de la integración de la lámina. La cicatriz paracentral reflectante ha desaparecido y se aprecia la estabilidad del mapa paquimétrico. La figura está tomada del artículo científico referido a El Zarif M y cols. (180) acreditado por esta tesis.

El modesto aumento observado en el grosor corneal en el **G-1** no fue significativo durante los tres años de seguimiento, mientras que en **G-2** y **G-3** el aumento de grosor fue estadísticamente significativamente mejor. Las láminas implantadas mostraron evidencia de biointegración del tejido implantado en el estroma del huésped por biomicroscopía así como por el estudio de la **AS-OCT**. La luz altamente reflectante observada en los resultados de la **OCT** y la nubosidad temprana observada por la luz oblicua de la lámpara de hendidura disminuyó gradualmente a partir del tercer mes postoperatorio (31,177,254) hasta el final de los tres años de seguimiento, cuando la lámina estaba bien integrada en el estroma corneal. Dicha biointegración puede estar relacionada con la leve disminución de los parámetros paquimétricos y volumétricos observados en los **G-2** y **G-3**.

El examen biomicroscópico demostró que todas las córneas a los tres años tenían un eje visual completamente transparente (Figuras. 15-17). Algunas cicatrices paracentrales preoperatorias presentes en algunos casos mostraron una mejora progresiva como en el caso-2, **G-1**, y el caso-11, **G-3**, esto podría estar relacionado con la implantación de **ADASCs** y la producción del neocolágeno como se demostró previamente en el modelo animal (Figuras. 15C, 15D, 15F, 17A-17E) (30,31,177–180). Además, la transparencia del tejido implantado mejoró durante el seguimiento (Figuras. 16B-16E, 17B-17E). No obstante, se observó la presencia de tejido fibrótico paracentral leve en todos los casos en **G-2** y **G-3** (Figuras. 16D, 16F, 17C-17E, 17F lado derecho). Este tejido fibrótico se localizó en la interfase paracentral de la lámina. No se encontró correlación significativa entre la recelularización de la lámina y la presencia de este tejido fibrótico (179), este hecho también se correlacionó con la transparencia corneal observada a partir de los 3 meses y hasta los tres años de seguimiento en los grupos tratados con láminas. Su formación puede evitarse en el futuro controlando la activación de los queratocitos del huésped, así como los queratocitos diferenciados de las **ADASCs** implantadas. Unos estudios publicados apoyan la hipótesis (255) que

la cicatrización de la herida corneal está mediada por vesículas extracelulares secretadas (**EVs**) que contienen microácido ribonucleico (**miRNA**). Estas vesículas podrían disminuir la expresión de genes inductores de fibrosis y restaurar la morfología del tejido normal transfiriendo **miRNA** específico al tejido diana.

Sin embargo, a pesar de las limitaciones relacionadas con el número limitado de casos incluidos en esta investigación piloto, consideramos que los resultados a los tres años demuestran la seguridad y el potencial terapéutico de nuestro método. Sin embargo, los resultados deben interpretarse con cautela.

Los resultados descritos en este documento muestran que nuestro enfoque ofrece un nuevo tipo de cirugía para aumentar el grosor de la córnea en casos de queratocono avanzado. Los parámetros visuales, topográficos y de aberrometría mejoraron en casi todos los casos de estudio. Se necesitan estudios futuros con cohortes más grandes y seleccionando casos con grados menos severos de queratocono con diferentes fenotipos para obtener más evidencia científica que apoye la aplicación clínica de este nuevo tipo de cirugía corneal.

La posible influencia de la implantación de células madre mesenquimales y láminas corneales sobre la naturaleza progresiva de la enfermedad merece más estudios para ser confirmada. Sin embargo, consideramos que los resultados a los tres años dan lugar a un nuevo potencial de aplicación clínica y tal vez un nuevo horizonte para el uso clínico de **ADASCs** mesenquimatosas y un nuevo tipo de terapia del estroma corneal en cirugía corneal.

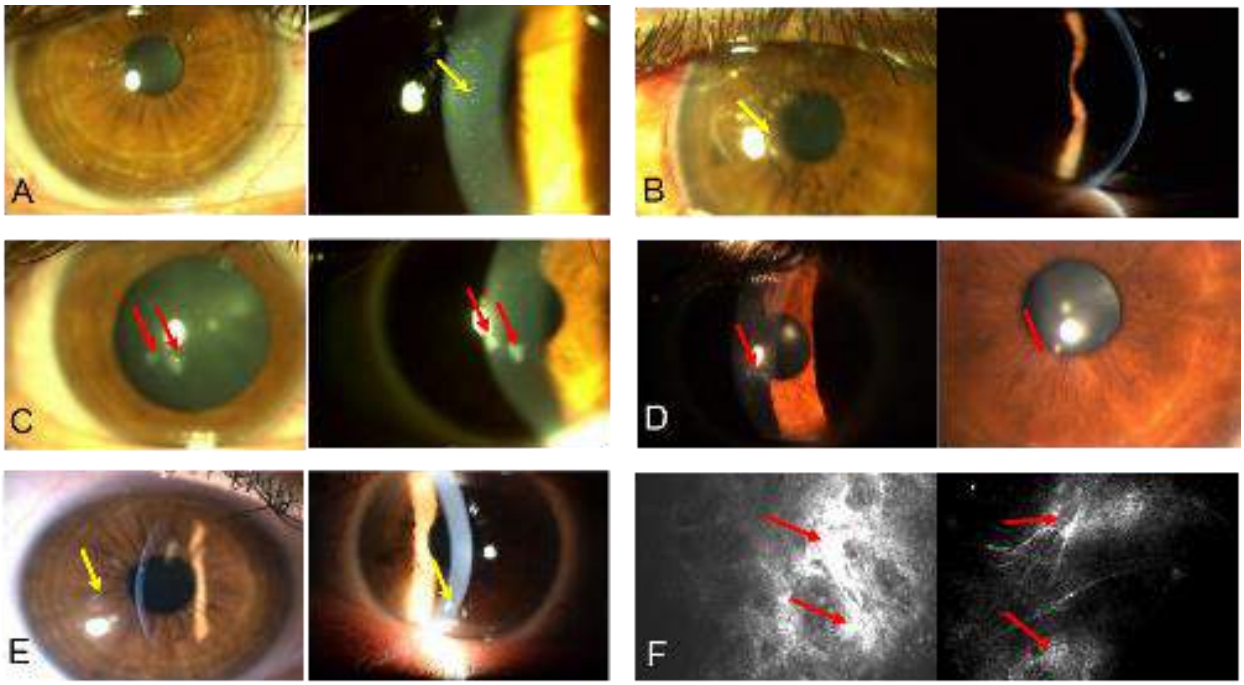

Figura 15. Cambios biomicroscópicos clínicos en **G-1** entre el estado preoperatorio y 36 meses. (**A**) Caso-1: muestra transparencia corneal al primer día posoperatorio (izquierda). Se pueden observar pequeños precipitados grisáceos dentro del plano quirúrgico (derecha) (flecha amarilla) pero sin ningún impacto en el rendimiento visual. (**B**) Caso-4, Observe la transparencia corneal al primer día postoperatorio (izquierda) y los pequeños precipitados grisáceos dentro del plano quirúrgico (flecha amarilla). Transparencia corneal normal a los seis meses (derecha). (**C**) Caso-2: observe la presencia de cicatrices paracentrales (flechas rojas) a nivel preoperatorio (izquierda) y al primer mes postoperatorio (derecha). (**D**) En el mismo caso-2, a los 12 meses (izquierda) y 36 meses (derecha): observe la marcada mejoría de las cicatrices paracentrales (flechas rojas). (**E**) Caso-1 (izquierda) y Caso-4 (derecha) 36 meses: se pudieron observar algunas "islas" dispersas, débiles e irregulares de neblina (flechas amarillas) sin ningún impacto en el rendimiento visual. (**F**) Hallazgos de microscopía confocal en el caso-2: observe los depósitos altamente reflectantes y el tejido fibrótico en el estroma anterior de la córnea a nivel preoperatorio (flechas rojas; izquierda), que corresponden a las cicatrices paracentrales. A los 12 meses (derecha) se pudo observar una mejoría del tejido fibrótico del estroma anterior (flechas rojas). La figura está tomada del trabajo referido a El Zarif M y cols. (180) acreditado para esta tesis.

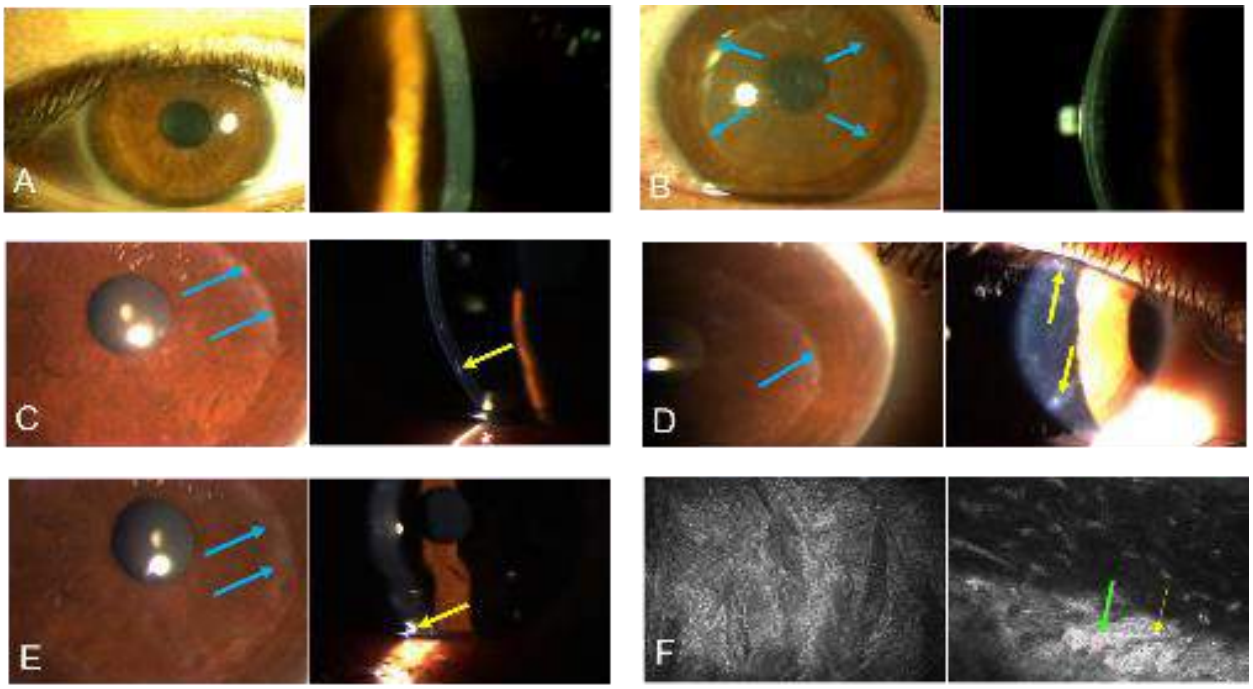

Figura 16. Cambios biomicroscópicos entre el preoperatorio y 36 meses en el **G-2** caso-5.
(**A**) Preoperatorio. (Izquierda y derecha). (**B**) Al primer día postoperatorio (izquierda y derecha): reducción de la transparencia por edema de la lámina implantada. (Flechas azules) muestran los bordes de la lámina. (**C**) A los seis meses: (las flechas azules; izquierda) y la (flecha amarilla; derecha) apuntan a la periferia de la lámina. (**D**) A los 12 meses: borde de la lámina implantada (flecha azul, izquierda). Tejido fibrótico paracentral en el plano quirúrgico (flechas amarillas; hacia la derecha). (**E**) Mejora de la transparencia del tejido implantado a los 36 meses (flechas azules). Tejido fibrótico paracentral en el plano quirúrgico (flechas amarillas; hacia la derecha). (**F**) Imagen de microscopía confocal en **G-2** caso-5: al mes (izquierda) podemos observar la superficie anterior acelular de la lámina descelularizada. A los 12 meses (derecha), podemos observar la acumulación de núcleos de queratocitos migratorios desde el estroma del huésped hacia la superficie posterior de la lámina descelularizada (flecha verde), y la presencia de algún tejido fibrótico paracentral en la periferia de la lámina (flecha amarilla). La figura está tomada del artículo de El Zarif M y cols. (180) acreditado para esta tesis.

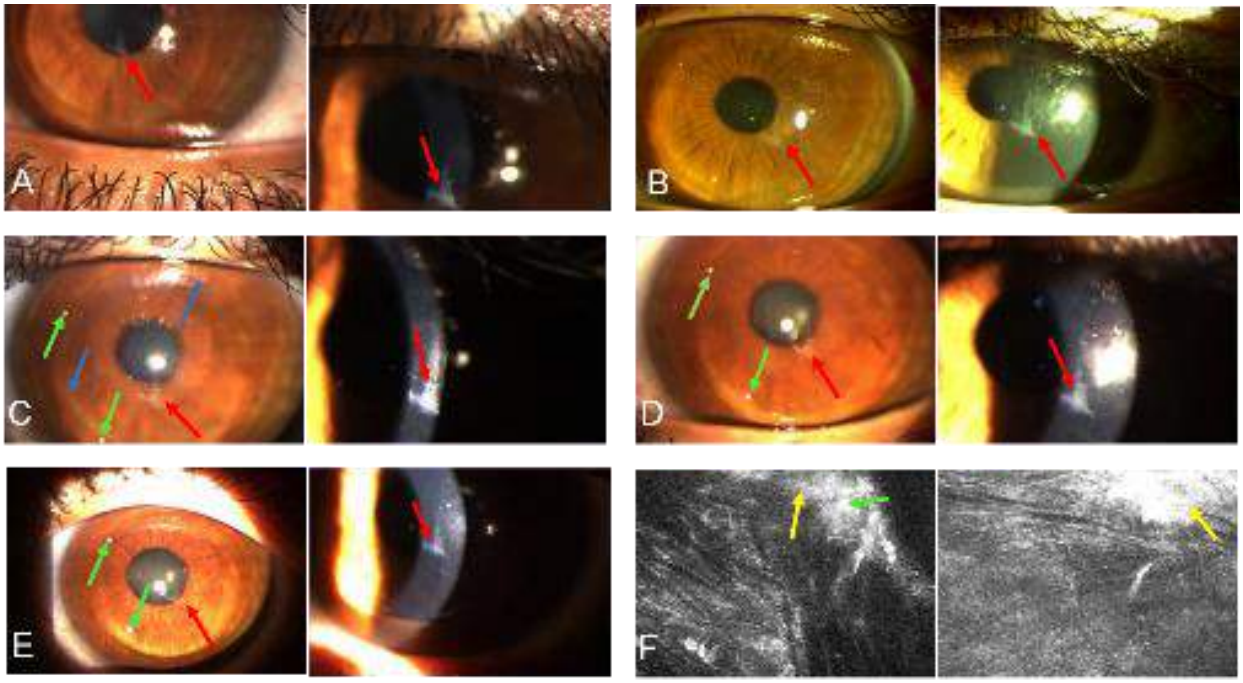

Figura 17. Cambios en la biomicroscopía en **G-3**, caso-11 desde el preoperatorio hasta los 36 meses. (**A**) Preoperatorio. (Flechas rojas) muestran la presencia de una cicatriz paracentral. (**B**) Al primer mes. (Flechas rojas) muestran la cicatriz paracentral. (**C**) A los seis meses. (Flechas azules) muestra la periferia de la lámina recelularizada, (flechas rojas) indican la cicatriz paracentral y las (flechas verdes) muestran la presencia de tejido fibrótico paracentral con una acumulación de queratocitos migratorios hacia el borde de la lámina. (**D**) 12 meses: observe la leve mejoría de la cicatriz paracentral (flechas rojas). Tenga en cuenta que el borde de la lámina no es notable. (Flechas verdes) indican la presencia del mismo tejido fibrótico paracentral. (**E**) A los 36 meses: observe la mejoría de la opacificación paracentral (flechas rojas). (Flechas verdes) muestran el mismo tejido anterior fibrótico. (**F**) Microscopía confocal en **G-3** caso-11: (flecha verde) acumulación puntual de queratocitos migratorios en la periferia de la superficie posterior de la lámina recelularizada (izquierda), mientras que la (flecha amarilla) muestra la presencia de algún tejido fibrótico. 12 meses después (izquierda), se detecta un tejido fibrótico altamente reflectante (flecha amarilla) en la superficie anterior de la lámina recelularizada. La figura está tomada del trabajo referido a El Zarif y cols. (180) acreditado para esta tesis.

7.6. **El Zarif M**, Abdul Jawad K, Alió del Barrio JL, Abdul Jawad Z, Palazón-Bru A, De Miguel MP, et al**. Corneal stroma cell density evolution in keratoconus corneas following the implantation of adipose mesenchymal stem cells and corneal laminas: An in vivo confocal microscopy study.** IOVS. 2020;61(4)22.

En este innovador estudio clínico, describimos por primera vez la evolución de las células madre mesenquimales implantadas en el estroma corneal humano utilizando microscopía confocal corneal *in vivo*. Los resultados informados aquí completan los resultados clínicos anteriores publicados en otra parte en relación con este estudio clínico en humanos (30,31,177,179).

Según los resultados de este estudio confocal, después de la inyección de solo **ADASCs** en los bolsillos corneales creados con un láser de femtosegundo en el **G-1**, hubo un aumento estadísticamente significativo en la densidad de queratocitos corneales en el estroma anterior, medio y posterior [$P < 0,001$] (Figura. 18). Esto se correlaciona bien con la producción ya informada de un nuevo colágeno, que resultó en mejorar el grosor corneal (30). También observamos en **G-1** cambios relevantes en la morfología de las células implantadas desde el momento de su implantación en los bolsillos corneales, ya que la morfología de las **ADASCs** era de forma redondeada hasta el tercer mes. Este hallazgo sugiere la supervivencia de las células madre implantadas después de su implantación. Más tarde, las células mostraron cambios que iban desde la formación de grupos alrededor de las células individuales hasta el desarrollo de la apariencia vista por el confocal de las células corneales estromales adultas a los 12 meses después de la cirugía (179).

En **G-2** y **G-3**, donde se implantaron láminas corneales con o sin impregnación con **ADASCs**, observamos que la implantación de dichas láminas, colonizadas o no por **ADASCs**,

favoreció un aumento en el número de células del estroma corneal en el estroma anterior y posterior de la córnea en un nivel estadístico altamente significativo [P < 0,001] (Figuras. 18A, 18C).

La microscopía confocal *in vivo* ofrece la posibilidad de estudiar la morfología normal de la córnea y los cambios microestructurales que pueden ocurrir en la densidad de queratocitos y la morfología de los queratocitos en la córnea queratocónica (6,9,104,125,238,239). Varios autores han estudiado los queratocitos humanos normales en el espesor central total de la córneas (125,239) utilizando una tecnología diferente (Tandem Scanning Corporation, Reston, VA, EE. UU.) y diferentes métricas (células/mm^3) con microscopios confocales. Otros autores en publicaciones más recientes utilizaron un microscopio confocal in vivo de barrido láser (Heidelberg Retina Tomograph II/RCM) y encontraron que la densidad media de queratocitos en el grupo de control era 786 ± 244 células/mm^2 en el estroma anterior y 293 ± 35 células/mm^2 en el estroma posterior. En el grupo de queratocono que no usó lentes de contacto, los valores fueron 662 ± 193 células/mm^2 y 236 ± 32,6 células/mm^2 en el estroma anterior y posterior, respectivamente (6).

En nuestro estudio, aumentamos la densidad celular en el estroma anterior medio y posterior a los 12 meses en comparación con el nivel preoperatorio (Figura. 18; Tabla 7), pero no detectamos ninguna nueva formación de estructuras fibróticas en el **G-1** (Figuras. 15A, 15B). La presencia del tejido fibrótico parecía estar relacionada con los grupos que recibieron solo láminas (con o sin **ADASCs**). Esto fue más evidente en el **G-3**, mientras que en el **G-1** las estructuras fibróticas estuvieron ausentes hasta los 12 meses después de la cirugía. Notamos una mejora de la cicatrización corneal para el caso-2 del **G-1** a los 12 meses después de la cirugía. (Figuras. 15C, 15D, 15F, 19C, 19D) (30,31,177,179). Sin embargo, en los **G-2** y **G-3** las estructuras fibróticas estaban presentes con los pacientes casi en la periferia de las láminas implantadas (Figuras. 16D, 16E, 16F lado derecho, 17C-17F, 20B, 20D, 20E, 20G; Tabla 8). Se ha postulado que las células

madre mesenquimales pueden evitar o mejorar las cicatrices preexistentes; aunque en las zonas no periféricas de las láminas implantadas no notamos diferencias en la transparencia corneal entre los tres grupos, ni la observación del "haze" corneal (Figuras. 19C, 19D, 20A, 20C) (30,177,179).

Además, también se observaron cambios en el interior de las láminas acelulares implantadas en el **G-2**. Este hallazgo demuestra que la lámina descelularizada fue colonizada por los queratocitos del paciente, proceso que se inició en el primer mes. Después de los 12 meses, se encontró que la lámina estaba completamente recelularizada (Figuras. 7B, 7C, 21).

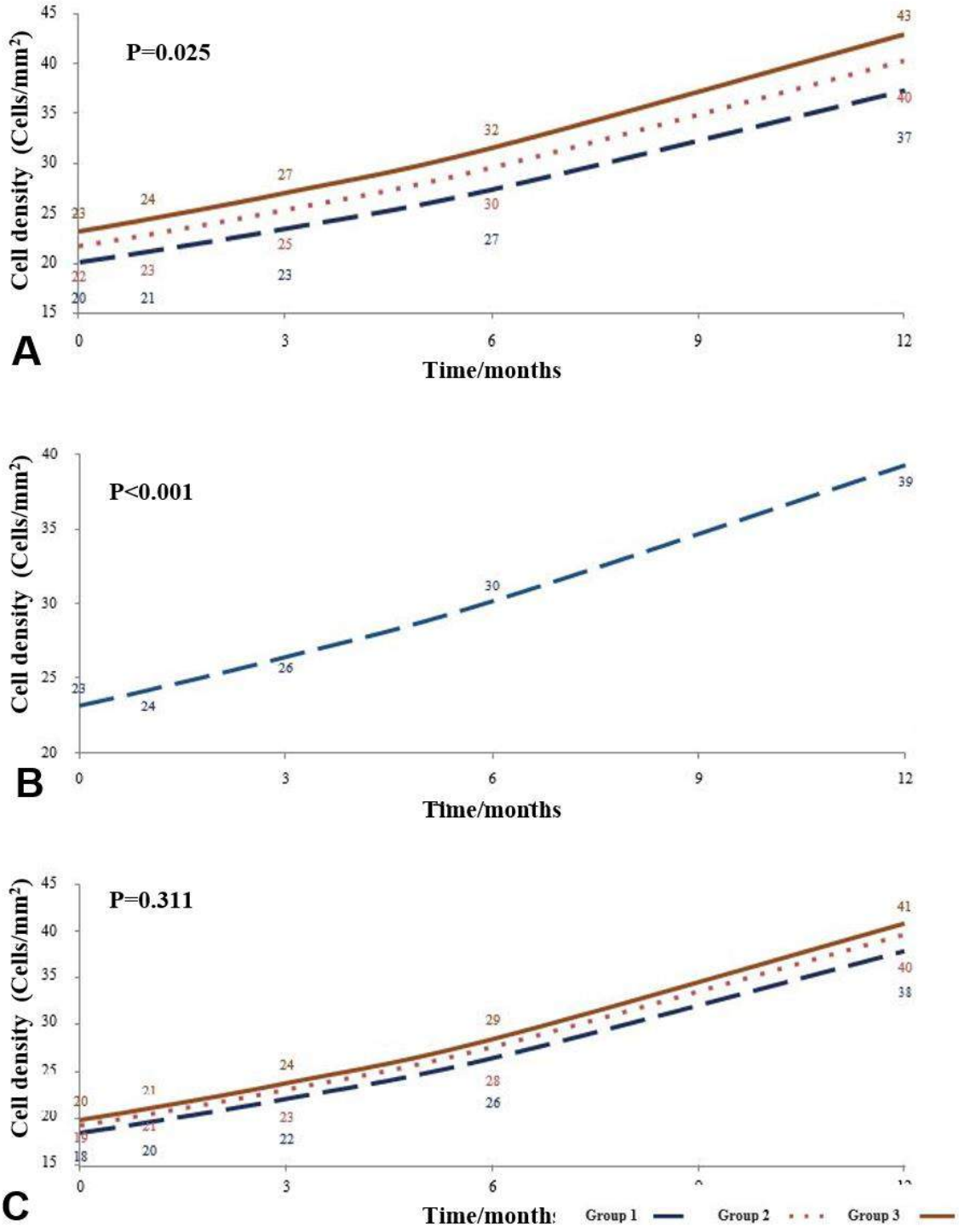

Figura 18. Resultados estadísticos de los cambios de densidad celular en el estroma corneal de **G-1**, **G-2** y **G-**3 a lo largo de 12 meses de seguimiento.
(**A**) Aumento de la densidad celular a lo largo del tiempo en el estroma anterior de la córnea en **G-1**, **G-2** y **G-3** desde el período preoperatorio hasta los 12 meses posteriores a la cirugía. Se detectó una diferencia estadística significativa [P = 0,025] entre los grupos. (**B**) Aumento estadísticamente significativo de la densidad celular [P < 0,001] a lo largo del tiempo en el estroma medio de la

córnea en **G-1** desde el período preoperatorio hasta 12 meses después de la cirugía. (**C**) Aumento de la densidad celular a lo largo del tiempo en el estroma posterior de la córnea en **G-1**, **G-2** y **G-3** desde el período preoperatorio hasta los 12 meses posteriores a la cirugía. No hubo diferencia significativa entre los tres grupos [P = 0.311]. La figura está extraída del artículo científico referido a El Zarif M y cols. (179) acreditado por esta tesis.

Tabla 7. Ratio de células de núcleos contados

	Estoma anterior	**Estroma medio**	**Estroma posterior**	**Superficie ant. de la lámina**	**Dentro de la lámina**	**Superficie post. de la lámina**
Grupo-1	372/201=1.850	393/232=1.693	379/185=2.048	----	----	----
Grupo-2	403/217=1.857	-------	396/193=2.051	102/28=3.642	95/14=6.785	165/43=3.837
Grupo-3	430/232=1.853	-------	408/199=2.050	251/69=3.637	254/38=6.684	328/86=3.813

Los ratios de células de núcleos contados son la proporción de densidades celulares a los 12 meses después de la cirugía en comparación con los valores preoperatorios en los **G-1**, **G-2** y **G-3**. La tabla está tomada del artículo científico de El Zarif M y cols. (179) acreditado para esta tesis.

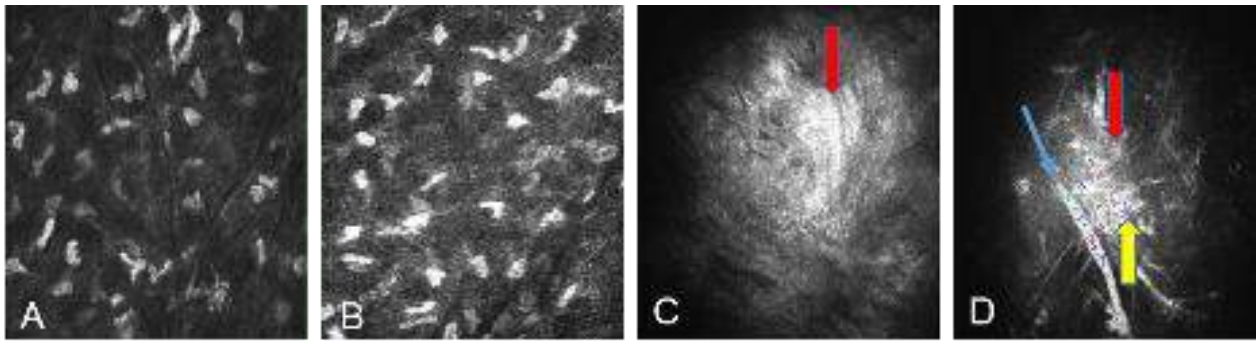

Figura 19. Hallazgos de la microscopía confocal a lo largo de los 12 meses postoperatorios.
(**A**, **B**) Recuento de células del estroma corneal anterior y posterior para el caso-10 del **G-3**, 12 meses después de la operación. (**A**) Estroma corneal anterior con abundantes células estromales corneales. El número y la morfología de las células del estroma corneal son muy similares a los del estroma normal. (**B**) Estroma corneal posterior con un número elevado de células de estroma corneal. La imagen muestra que las células del estroma corneal del estroma posterior son similares en número y morfología a las células del estroma de una córnea normal. (**C**) La presencia de depósitos hiperreflectantes (flecha roja) se correspondió con la cicatrización corneal paracentral preoperatoria observada en el preoperatorio del caso-2 en el **G-1**. (**D**) Se observa mejoría del tejido fibrótico (flecha roja) al mismo nivel con el mismo caso-2 del **G-1**. Nótese la presencia de fibroblasto (flecha amarilla). Se puede observar una parte del nervio corneal superficial (flecha azul). La figura está tomada del artículo científico de El Zarif M y cols. (179) acreditado por esta tesis.

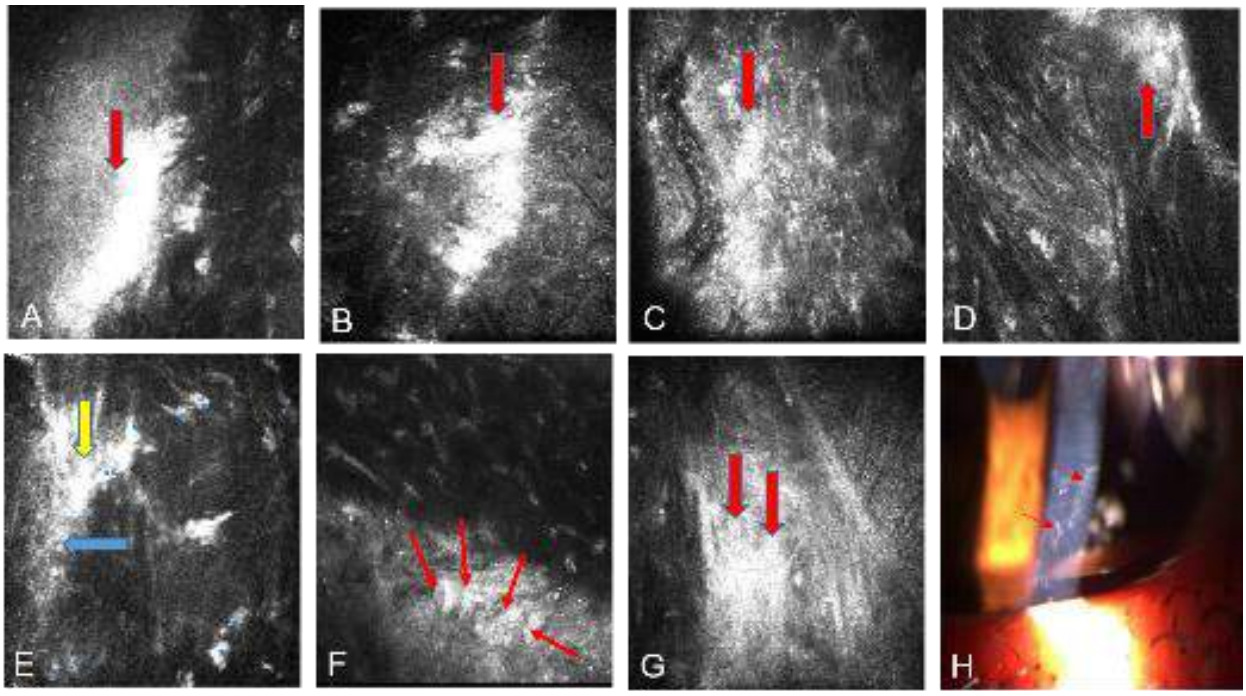

Figura 20. Hallazgos del tejido fibrótico obtenidos por la microscopía confocal y el biomicroscopio. Cambios morfológicos de los queratocitos corneales.
(**A**) La presencia de tejido fibrótico altamente reflectante (flecha roja) en el **G-3** caso-11 con queratocono se corresponde con la cicatriz preoperatoria en el estroma anterior paracentral observada a los tres meses de la cirugía. (**B**) La presencia de tejido fibrótico (flecha roja) es altamente reflectante en la periferia de la superficie posterior de la lámina a los tres meses para el mismo caso. (**C**) Mejoría del tejido fibrótico preoperatorio paracentral (flecha roja) en el estroma anterior del mismo caso-11 a los seis meses después de la operación. (**D**) Mejora del tejido fibrótico (flecha roja) en la periferia de la superficie posterior de la lámina recelularizada del mismo caso queratocónico, a los 12 meses de la cirugía. (**E**) Presencia de fibroblasto o miofibroblasto (flecha amarilla) y tejido fibrótico (flecha azul) en la superficie posterior de la lámina descelularizada de un paciente queratocónico a los tres meses después de la cirugía. (**F**) La zona de transición entre la superficie posterior de la lámina descelularizada y el estroma del huésped que muestra varias células estromales corneales migratorias (¿posiblemente queratocitos?) Con formas dendríticas (marcadas con flechas rojas) en un paciente queratocónico, a los 12 meses después de la cirugía. (**G**) Presencia de tejido fibrótico altamente reflectante (flecha roja) en la periferia en el estroma medio de la lámina descelularizada de un paciente queratocónico a los seis meses después de la cirugía. (**H**) Imagen con lámpara de hendidura de un paciente queratocónico que muestra tejido cicatricial periférico a los seis meses después de la cirugía. La figura está extraída del artículo científico referido a El Zarif M y cols. (179) acreditado por esta tesis.

Tabla 8. Representa la presencia o ausencia de tejido fibrótico en los **G-1**, **G-2** y **G-3**.

	Grupo	0 mes	1 mes	3 meses	6 meses	12 meses
Caso-1	1	-	-	-	-	-
Caso-2	1	+++ *	++ *	++ *	+ *	+ *
Caso-3	1	-	-	+ †	-	-
Caso-4	1	-	-	+ †	-	-
Caso-5	2	-	-	+/++ †	+/+ + †	+/++
Caso-6	2	-	-	-	+/++ †	+/++ †
Caso-7	2	-	-	-	+/++ †	+/++/+++ †
Caso-8	2	-	+ †	+/+++ †	+/++ †	-
Caso-9	2	-	+ †	+/++ †	+/++ †	+/++ †
Caso-10	3	-	+ †	+/++ †	+/++/+++ †	+ †
Caso-11	3	+++ *	++ † +++ *	+++ † +++ *	+/++/+++ † ++ *	+/++ † + *
Caso-12	3	-	-	-	+/++/+++ †	+/++/+++ †
Caso-13	3	-	-	+/++ †	+/++/+++ †	+/++ †

Nota: +, tejido fibrótico menor; ++, tejido fibrótico moderado; +++, tejido fibrótico elevado; –, ausencia de tejido fibrótico.

* Presencia de cicatriz paracentral con tejido fibrótico en el período preoperatorio; observamos una mejoría de las cicatrices y una disminución de la fibrosis.

† Presencia de tejido fibrótico durante el seguimiento postoperatorio.

La tabla está tomada del artículo científico de El Zarif M y cols. (179) acreditado por esta tesis.

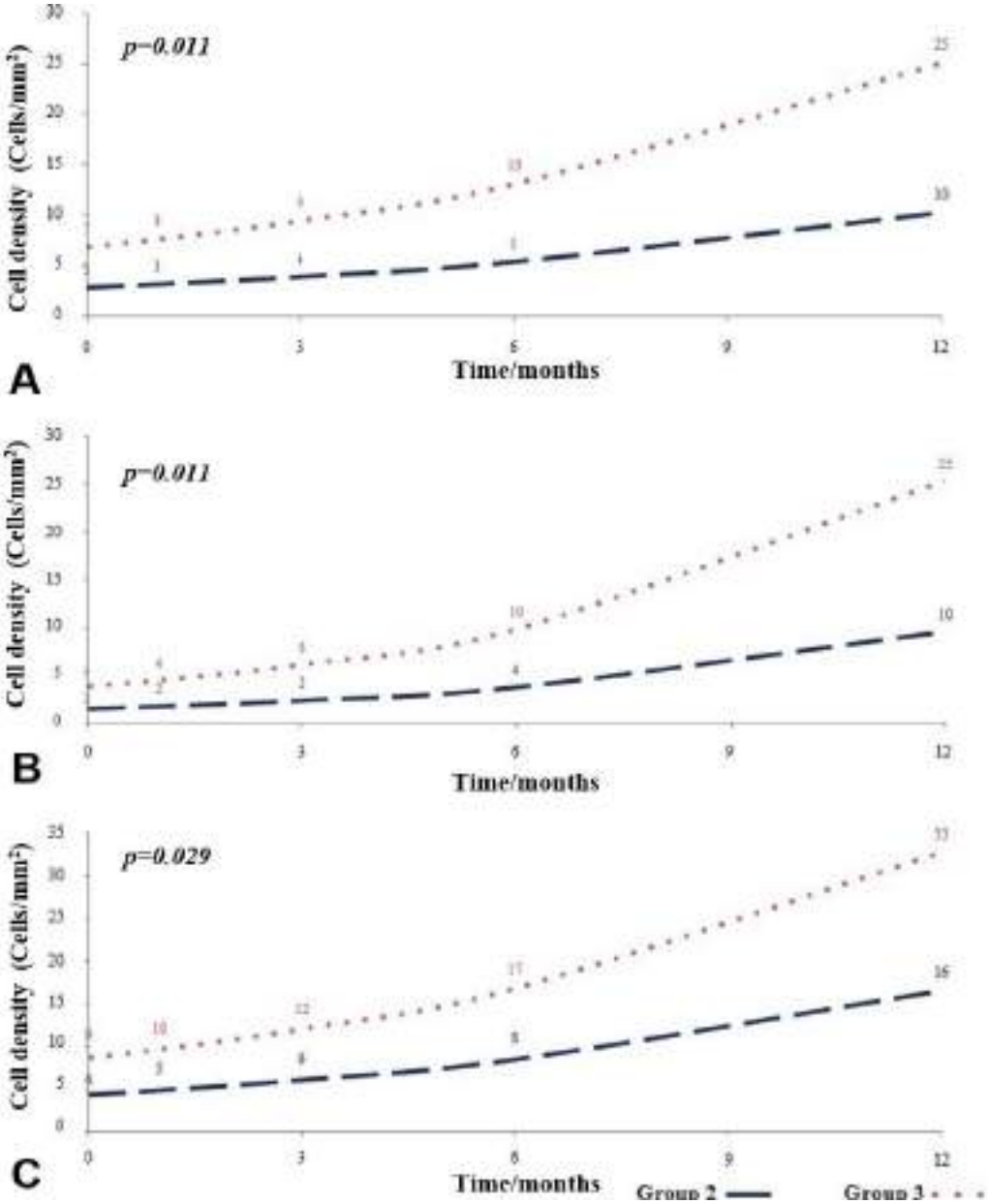

Figura 21. Resultados estadísticos de la densidad celular en las superficies anterior, media y posterior de las láminas a lo largo de 12 meses de seguimiento.
(**A**) Aumento de la densidad celular a lo largo del tiempo en la superficie anterior de la lámina en el **G-2** y el **G-3** desde el período preoperatorio hasta los 12 meses posteriores a la cirugía. Existe una diferencia estadística significativa [P = 0.011] entre el **G-2** y el **G-3**. (**B**) Aumento de la densidad celular a lo largo del tiempo en el estroma medio de la lámina en el **G-2** y el **G-3** desde el período preoperatorio hasta los 12 meses posteriores a la cirugía. Se detectó una diferencia estadísticamente significativa [P = 0,011] entre el **G-2** y el **G-3**. (**C**) Aumento de la densidad celular a lo largo del tiempo en la superficie posterior de la lámina en el **G-2** y el **G-3** desde el período preoperatorio hasta los 12 meses posteriores a la cirugía. Se detectó una diferencia estadísticamente significativa [P = 0,029] entre el **G-2** y el **G-3**. La figura está tomada del artículo científico de El Zarif M y cols. (179) acreditado para esta tesis.

Por otro lado, también hemos observado que a partir del primer mes postoperatorio en las láminas recelularizadas del **G-3** se produjo una disminución en las agrupaciones de células mesenquimales implantadas sobre las láminas. Se observó que tales cambios morfológicos celulares ocurren primero en la superficie posterior y luego en la superficie anterior (Figuras. 8A, 8B), y el número de células aumentó estadísticamente y significativamente desde el primer mes después de la cirugía hasta los 12 meses después de la cirugía (Figuras. 8C-8E, 21). Este hallazgo puede sugerir la supervivencia y diferenciación de las células implantadas hacia los queratocitos y/o la repoblación de estas láminas, estimulándose la migración de los queratocitos del estroma corneal del huésped para que proliferen hacia el tejido corneal descelularizado (256). Como las células no se pudieron etiquetar antes de la implantación debido a una posible interferencia con la transparencia y, por lo tanto, debido a problemas éticos, la distinción entre ambas poblaciones no es posible. Este hallazgo se correlaciona bien con otro informe (256) que demostró que la propagación y migración de los fibroblastos corneales ocurren en paralelo con los surcos alineados con las laminillas de colágeno. Durante la migración de estas células, las pistas de propagación se establecen mediante la alineación de las fibrillas mediante la generación de una fuerza mecánica. También es posible que las **ADASCs** liberen factores quimioatrayentes durante la evolución posterior a la implantación (257).

Además, en este estudio observamos que las células del estroma, que probablemente sean queratocitos, fibroblastos o miofibroblastos, han migrado desde el estroma corneal hacia el borde de la lámina en los casos en que no se inyectaron células (Figuras. 20E, 20F). Estas células estromales (queratocitos) muestran prolongaciones periféricas y transformaciones morfológicas con formas dendríticas, lo que indica que se han diferenciado en fibroblastos y miofibroblastos durante su período de actividad y que son capaces de deslizarse sobre las fibras de colágeno del tejido descelularizado o recelularizado (Figuras. 16F lado derecho, 17F lado izquierdo, 20E, 20F) (256).

También observamos, hasta los 12 meses después de la cirugía, el desarrollo de tejido fibrótico paracentral en la parte superior del estroma fotoablado del tejido implantado (Figuras. 20B, 20D, 20E, 20G) (256).

Hemos informado en este documento de una evolución en la morfología de las células del estroma corneal, se presume que son queratocitos. Se ha informado que estas células son normalmente de forma ovalada e irregular y sin forma dendrítica. En cuando migran o se activan es cuando asumen una forma dendrítica (125,256). Debido a que la evolución de la morfología de las células estromales en nuestro estudio no siguió ese patrón, nuestra observación no respalda los informes anteriores (21), que han descrito que en el tejido adulto los queratocitos están mitóticamente inactivos y tienen una morfología dendrítica plana (258).

Además, sería importante en estudios futuros establecer diferencias entre las distintas morfologías que se observan en las células estromales para comparar la evolución de las que tienen forma no dendrítica con las que tienen forma dendrítica, y las implicaciones biológicas que pueden tener tales cambios morfológicos.

Un tema relevante del presente estudio es la metodología utilizada para el recuento de células estromales, que fue un método manual específico. Esto puede introducir una cierta cantidad de subjetividad y sesgo de interpretación (Figura. 5); Sin embargo, este método nos proporcionó un recuento de células más preciso y discriminatorio que los recuentos de células automatizados del microscopio confocal, que se ven afectados por una gran variabilidad, inexactitudes y malas interpretaciones. La presencia de tejido fibrótico altamente reflectante en las áreas estudiadas podría dificultar la discriminación de los bordes de los núcleos de queratocitos que fueron el foco principal de nuestro estudio (Figuras. 16F lado derecho, 17F, 19C, 19D, 20).

Creemos que es necesario establecer un método de recuento celular más objetivo basado en programas de procesamiento de imágenes y algoritmos específicos en los que se puede editar el contraste y la iluminación, y se utilizan diversos filtros especializados para optimizar la visualización de las células queratocíticas y calcular mejor su tamaño.

7.7 El Zarif M, Alió del Barrio JL, Arnalich-Montiel F, De Miguel MP, Makdissy N, Alió JL. **Corneal stroma regeneration: New approach for the treatment of cornea disease**. APJO. 2020; 9(6):571–9.

En este informe presentamos un resumen integrado, basado en la evidencia, sobre la etapa actual de los estudios clínicos experimentales realizados por nuestro grupo de investigación en el tema de la regeneración del estroma corneal e integrados en estudios humanos en el tratamiento de enfermedades corneales, y particularmente en queratocono.

El estroma corneal ideal construido por bioingeniería debería ser capaz de imitar la córnea humana natural y mantener la homeostasis del estroma corneal. Para estos fines, debe contener tanto una fuente celular como un andamio de colágeno (8,15,16). Para el componente celular, se han investigado varios tipos de células tanto de origen ocular como extraocular, siendo las **MSCs** humanas las más probadas hasta ahora. Sin embargo, un mayor desarrollo de técnicas estandarizadas y más baratas de **iPSCs** puede superar el uso de las **MSCs** (200). El uso de secciones de córnea descelularizadas podría ser el más relevante clínicamente (17–19). Sin embargo, todavía está en desventaja por la necesidad de tejido corneal donado. El uso de exosomas de **MSCs** (sin su componente celular) revela un campo de investigación apasionante, ya que su uso podría superar

algunas de las limitaciones y riesgos asociados con la entrega directa de células madre a humanos in vivo si los exosomas pudieran aplicarse tópicamente (232).

Se demostró por primera vez la viabilidad y seguridad de la terapia con células del estroma corneal para córneas queratocónicas avanzadas. También se observó la aparición de una nueva formación de colágeno dentro del plano quirúrgico cuando se implantaron las **MSCs** (30), Aunque el colágeno no fue suficiente para restaurar el grosor de las córneas patológicas, juega un papel en la remodelación del estroma de las distrofias corneales y las cicatrices corneales para mejorar la transparencia corneal (Figuras. 14A, 14B). Además, la implantación de láminas de estroma corneal humanas descelularizadas o recelularizadas restaura eficazmente el grosor de la córnea (Figuras. 14C, 14D, 14F-14H), y potencialmente evita cualquier riesgo de rechazo del injerto (mientras que este riesgo todavía está presente por el uso de implantes estromales alogénicos). Hasta ahora, después de tres años de seguimiento, ningún paciente mostró inflamación, rechazo o cualquier evidencia de cicatrización o "haze" (30,31,177,179,180).

La popularización de **SMILE** como una opción de cirugía refractiva está proporcionando una gran cantidad de tejido de donante de córnea que podría potencialmente usarse para trasplantes humanos. Recientes Estudios realizados por Liu R y cols., y Zhao y cols. (259,260) demostraron después de 2 años de seguimiento que la implantación de lentículos intraestromales alogénicos con una incisión pequeña es factible y segura para remodelar la córnea. La cicatrización corneal se mantuvo estable y sus resultados fueron confirmados por biomicroscopía con lámpara de hendidura y por microscopía confocal *in vivo* y mediciones de densitometría corneal. Además, los autores observaron signos de reinervación corneal dentro del lentículo. La adición estromal de **SMILE** creó lentículos que se probaron ex vivo e *in vivo* (su viabilidad, seguridad y eficacia en el tratamiento de trastornos por adelgazamiento como el queratocono) (261–263). Este procedimiento aumenta el

grosor de la córnea proporcionando fuerza adicional a la córnea debilitada, así como el aplanamiento corneal anterior cuando se utiliza un lentículo negativo en forma de menisco (262).

Los andamios de colágeno sintético son, por definición, una fuente prometedora de tejido del estroma del donante, ya que no necesitan tejido de un donante humano y, por lo tanto, pueden estar potencialmente disponibles en todo el mundo. Sin embargo, sus dificultades que aún hoy están presentes, son mimetizar la transparencia y la fuerza de la córnea humana, junto con los altos gastos para su producción en el laboratorio, imposibilitan su presencia en la práctica clínica real durante los próximos años.

7.8 **El Zarif M**, Alió JL, Alió del Barrio JL, De Miguel MP, Abdul Jawad K, Makdissy N. **Corneal stromal regeneration: a review on human clinical studies for treatment of keratoconus.** Front Med. 2021; 8:650724.

En esta revisión, resumimos el estado actual de los estudios clínicos en humanos informados en la literatura revisada por pares sobre el tema de la regeneración del estroma corneal humano, la terapia de mejora corneal y las tendencias inmediatas de que dichos estudios han abierto nuevas perspectivas en la terapia de las enfermedades del estroma corneal, particularmente en el queratocono. Además, esta revisión ofrece una comparación entre los diferentes estudios recientes realizados con otros grupos y nuestro estudio, siendo que hasta donde sabemos, nuestro estudio clínico es el único que ha llevado a regenerar el estroma corneal mediante la implantación de **ADASCs** autólogas solas en el bolsillo del estroma corneal, o con lámina corneal humana acelular colonizada.

En nuestros artículos anteriores debatimos la viabilidad de las cirugías regenerativas del estroma corneal para el queratocono avanzado. Además, demostramos que las láminas descelularizadas de un estroma corneal humano, colonizadas o no por **ADASCs** autólogas, pueden implantarse con fines terapéuticos con un fundamento a nivel clínio (30,31,177,179,180).

Otros informes demostraron que el lentículo corneal alogénico refractivo inlay utilizando un lentículo **SMILE** combinado o no con colágeno acelerado **CXL** (241,242,262,264–267), es una cirugía prometedora, no se registraron inflamación, complicación, opacificación, vascularización o infección. Jorge Alio y cols. (268) realizaron con otro grupo un estudio prospectivo reciente en Teherán, informaron sobre un método novedoso para el tratamiento de la ectasia avanzada, con implantación personalizada de lentículos **SMILE** con 22 casos de queratocono avanzado (la forma del lentículo era compuesta o en forma de collar). El grosor de la córnea mostró un aumento medio de 100,4 **µm** en el **thinnest point** medido por la **AS-OCT**. Se obtuvo una mejora en los parámetros visuales, mejor **CDVA** mejoró de 0,70 (rango 0,4-1) a 0,49 (rango 0,3-0,7) a los seis meses con todos los pacientes, lo que estuvo en coherencia con la disminución de la aberración corneal, también la queratometría disminuyó de 54,68 ± 2,77 a 51,95 ± 2,21 (D).

Otros estudios recientes con adición estromal de lentículos de **SMILE** han demostrado ex vivo e *in vivo* su viabilidad, seguridad y eficacia en el tratamiento de trastornos por adelgazamiento como el queratocono (261–263). **SILK** indujo en **Kmax** un aplanamiento de 7,34 (D) y el uso de la adición de lentículos negativos en forma de menisco indujo también cierto aplanamiento del cono, la mejora fue (5.1 D a los 6 meses) en **Anterior Km,** mejor que la observada con Ganesh y cols. (264), y más plana que con los lentículos implantados por nuestro grupo (180).

Los procedimientos quirúrgicos comparativos **SFII** y **PKP** dieron como resultado un volumen corneal estable y una mejor agudeza visual durante el período de estudio de 24 meses. **SFII** fue menos invasivo y más eficiente en comparación con **PKP**. El uso de la implantación de lentículos cóncavos mejoró la queratometría central máxima de (-4,65 ± 2,04) (D), este resultado dio más aplanamiento que las láminas implantadas con nuestros estudios (180,266).

Sin embargo, el grosor de la córnea incrementado con las láminas planas (31,177,180) es más alto que el grosor del implante de los lentículos corneales alogénico **SMILE** combinado o no con colágeno **CXL** (262,264,266), además, los lentículos negativos en forma de menisco lograron un mayor aplanamiento, pero solo están disponibles para los conos centrales puros, ya que para los conos excéntricos (los que se ven comúnmente en el queratocono) generarían aberraciones inaceptables dentro del eje visual, a diferencia de las láminas planas, los parámetros de aberrometría mejoraron en casi todos los casos del estudio. Por otro lado, la mejora de la agudeza visual ha sido ligeramente mejor con el implante de lentículos de meniscos negativos que con el implante de láminas planas de nuestro grupo (180,262,264,266), pero el objetivo del implante estromal debería ser mejorar la agudeza visual y al mismo tiempo aumentar significativamente el grosor corneal en pacientes con queratocono avanzado.

Los estudios de endoqueratofaquia utilizando lentículas regulares de **SMILE** han demostrado ser una opción factible no solo para corregir ametropías como la hipermetropía y la presbicia, sino también para aumentar el grosor de la córnea queratocónica (269). Sin embargo, el uso de lentículos de meniscos positivos personalizados en córneas con queratocono es debatible (264,268), ya que teóricamente podría empeorar la miopía que se encuentra habitualmente con estos pacientes, por lo que los lentículos de meniscos planos o negativos son siempre preferibles para tal fin.

El uso de colágeno humano recombinante, sintetizado en levadura y entrecruzado químicamente, demostró ser factible (14,270), mejoró la agudeza visual, sin embargo, se obtuvo una gran variación del grosor corneal entre los casos de este estudio hasta los 24 meses de seguimiento, y se observó alta presencia de fibrosis, hecho que no se observó en nuestro estudio, el tejido fibrótico detectado se correspondía únicamente en la zona paracentral de las láminas corneales implantadas descelularizada o recelularizada (179).

Todos los estudios descritos anteriormente tienen la limitación de que fueron realizados con un número muy reducido de pacientes, en nuestro estudio demostramos que el uso de láminas acelulares (31,177,179,180), en el que la ausencia de células hace que la experiencia sea considerada como un injerto corneal, y mediante el uso de **MSCs** autólogas de un paciente determinado, fue posible transformar injertos alogénicos en injertos autólogos funcionales, evitando así cualquier riesgo de rechazo. Hasta el momento, el seguimiento a largo plazo no mostró complicaciones en todos los casos (180). Mientras que el trasplante en los casos de lentículos corneales alogénicos y material no estructurado en el caso del **CXL** recombinante de colágeno ha demostrado inicialmente ser potencialmente efectivo para el tratamiento del queratocono avanzado, pero aún teniendo células estromales heterólogas, se debe considerar como una nueva forma de trasplante de estroma corneal. Serán necesarios estudios futuros para incrementar el número de casos y aumentar la evidencia de la efectividad de estas cirugías corneales.

Serán necesarios estudios futuros para incrementar el número de casos y aumentar la evidencia de la efectividad de estas cirugías corneales.

FUTURAS PERSPECTIVAS

Con esta investigación piloto, nuestro principal objetivo era demostrar la seguridad de la implantación de las **ADASCs** y láminas descelularizadas o recelularizadas con células madre derivadas del tejido adiposo humano autólogo. Con base en los resultados de la presente investigación, podemos anticipar el desarrollo de nuevas áreas prometedoras de investigación traslacional y aplicaciones futuras de la siguiente manera:

1. El uso de las MSCs autólogas, en particular las ADASCs con fines terapéuticos: la enfermedad más relevante que podría beneficiarse de los resultados de este estudio es de hecho el queratocono, las distrofias corneales o incluso las cicatrices corneales, ya que estas células se comportan bien en el estroma corneal, no se produjo opacidades tampoco ninguna reacción inflamatoria. Las **MSCs** pueden sustituir a los queratocitos corneales enfermos y producir colágeno que podría restaurar el grosor corneal, además la activación biológica provocada por las **MSCs** comprobada en la presente tesis sugiere que podrían ser útiles para mejorar las primeras etapas de las distrofias corneales y los procesos de cicatrización corneal.

2. El uso de las MSCs del banco de células de donantes genéticamente perfectos para tratamientos corneales: Considerando toda la evidencia publicada en el modelo animal donde se implantaron **MSCs** humanas en el estroma corneal, a pesar de ser un trasplante xenogénico, nunca se han reportado signos de rechazo o inflamación (17,19,21–28). También debemos considerar que el queratocito adulto obtenido de **MSCs** autólogas puede tener el mismo defecto genético que condujo a la patología de la cornea, como en el caso de la distrofia corneal. Además, se ha observado que existe una diferencia de expresión génica entre los queratocitos derivados de **iPSCs** generados a partir de fibroblastos del estroma corneal humano normal y queratocónico, lo que influye en el

crecimiento y la proliferación celular, lo que confirma que, al menos en los casos de queratocono, las células adultas obtenidas de las **MSCs** pueden todavía no ser funcionalmente normal (233). En este escenario, sería interesante el uso de las **MSCs** alogénicas en lugar de las autólogas. Si las **MSCs** alogénicas podrían lograr el mismo beneficio sin ningún riesgo de inflamación o rechazo. El uso de las **MSCs** alogénicas simplificaría enormemente la aplicación clínica de las **MSCs**, ya que los centros de aplicación clínica no necesitarían ningún equipo específico porque los posibles bancos de las **MSCs** podrían almacenar y suministrar células madre para su uso en pacientes. Ya existen sistemas de bajo costo disponibles que son capaces de mejorar la preservación de las **MSCs** a temperaturas hipotérmicas mientras mantienen su función normal, ampliando así el marco de tiempo para la distribución entre el sitio de fabricación y la clínica, y reducir el desperdicio asociado con la vida de duración limitada de las células almacenadas en su estado líquido (231).

3- El uso de láminas corneales acelulares personalizadas moldeadas activadas biológicamente con MSCs normales en queratocono en estadios moderados y avanzados: En estadios moderados de las córneas patológica, implantación de láminas corneales humanas descelularizadas moldeadas con técnicas **3D** (271,272), involucraría láminas de colágeno tratadas de acuerdo con las características ópticas del ojo, y sembradas con **MSCs** alogénicas, tal implante dentro del estroma corneal, puede producir soluciones biológicas y ópticas, y puede mejorar los parámetros topográficos, paquimétricos y visuales de la córnea. Es una cirugía no invasiva, con anestesia local, y solo una sutura, el epitelio y el endotelio de la córnea se conservan intactos.

4- El uso de estroma corneal acelular para la sustitución completa del estroma corneal: La implantación intralamelar de injerto autólogo puede sustituir las técnicas habituales de trasplante de córnea como **PKP** o **DALK** en pacientes con enfermedad terminal. Estamos planeando implantar un estroma descelularizado mediante láser de femtosegundos asistido, el estroma corneal

descelularizado donado podría incluso personalizarse utilizando el programa de **3D** de acuerdo con las necesidades visuales, topográficas y aberrométricas de cada paciente (271,272). La propuesta de una cirugía tan innovadora y muy avanzada conserva el epitelio y el endotelio corneal intactos, es una cirugía mucho menos invasiva y podría incrementar en un nivel muy significativo el grosor de la córnea patológica. Además, el estroma descelularizado implantado se bioactivaría con las **MSCs** alogénicas que recelularizarían el colágeno recién implantado.

FASE DE APLICACIÓN CLÍNICA II

La segunda aplicación clínica se aplicará a otra población, etnia y raza para validar estos resultados preliminares y aumentar la muestra del estudio.

Este estudio tiene su siguiente fase en el FIS, el número del estudio: 2018-000523-14, está liderado por la Universidad Miguel Hernández **UMH** en aplicaciones multicéntricas en España, los objetivos del estudio son realizar una aplicación clínica de fase II, en córneas de 25 pacientes con diferentes etapas de queratocono, se implantará con células madre autólogas adultas, derivadas del tejido adiposo **ADASCs**, láminas descelularizadas o recelularizadas embebidas con **ADASCs**, el estudio ha sido aprobado según los protocolos del fondo de investigación de salud del gobierno español (el código de protocolo español: EI17-00523), empezará una vez obtenido el permiso de la Agencia Nacional de Drogas. El investigador principal es el Prof. Jorge L. Alió.

LIMITACIONES DEL ESTUDIO

Las conclusiones de este estudio piloto deben considerarse cuidadosamente, ya que son vulnerables al sesgo porque el estudio incluyó una pequeña muestra de pacientes. Las

investigaciones pioneras clínicas de las nuevas terapias son difíciles de realizar y tienen muchas limitaciones en términos de base administrativa, aprobatoria y ética. Por lo tanto, estudios futuros con una muestra más amplia y un seguimiento más prolongado deberían confirmar los resultados preliminares obtenidos (30,31,177,179,180,241,242).

No hubo un grupo de control en el que solo se realizara un bolsillo corneal, ya que se consideró poco ético, como no se podía ofrecer ningún beneficio al paciente de ese procedimiento. Como este estudio se realizó en voluntarios humanos vivos, no hubo posibilidad de realizar análisis post-mortem, ya que ninguno de los casos hasta el momento ha requerido trasplante de córnea, y en consecuencia falta una muestra de tejido para realizar la histopatología. Dentro de los estudios experimentales, es fácil demostrar, mediante análisis post-mortem, la supervivencia de las células marcadas previamente trasplantadas (mediante análisis de inmunofluorescencia) y su diferenciación en queratocitos adultos (mediante detección de expresión de queratocán) (240). Sin embargo, los estudios en humanos *in vivo* tienen la desventaja significativa de estar limitados a hallazgos de biomicroscopía confocal (vulnerables a interpretaciones subjetivas) para observar el comportamiento de trasplante de las células *in vivo* (105,179). Siempre es necesaria una perfecta colaboración del paciente, pero no siempre es el caso de todos los pacientes, lo que implica reducir la precisión de la medición de profundidad en el plano evaluado. Además, la metodología utilizada para el recuento de células estromales se realizó con un método manual específico. Esto puede introducir una cierta cantidad de subjetividad y sesgo de interpretación. Sin embargo, este método actualmente nos proporciona un recuento de células más preciso y discriminativo que el recuento de células automatizado del mismo microscopio, que se ve afectado por una gran variabilidad, inexactitudes y malas interpretaciones (105,179). La presencia de tejido fibrótico altamente reflectante en las áreas estudiadas podría generar dificultades en la discriminación de los bordes de

los núcleos de queratocitos que han sido el principal objetivo de nuestro estudio (Figuras. 17F lado derecho, 20B, 20G) (179). Dadas todas estas limitaciones, pudimos observar la presencia de células redondas en el plano quirúrgico en todos los pacientes, compatibles con las **ADASCs** trasplantadas, mostrando posteriormente un cambio dendrítico progresivo hasta tener una morfología no diferenciable de los queratocitos normales a los 12 meses de seguimiento postoperatorio.

En nuestro estudio de muestra reducida, no hemos podido comparar los resultados de los pacientes que han recibido láminas que contienen o no la **BM**. Son necesarios futuros estudios para mostrar la diferencia en resultados biomecánicos, curvatura sagital, aberrometría, recelularización de las láminas implantadas y correlacionarlo con la mejora de la agudeza visual (31,177,180).

En el presente estudio no hemos podido obtener una diferencia relevante entre pacientes con implantación intraestromal de tejido estromal descelularizado (con o sin células madre). En el futuro se esperan estudios más masivos para poder estudiar más resultados que estén relacionados con la biomecánica de la córnea. Por tanto, más allá de los estudios biomecánicos será necesario dar respuesta a esta pregunta (31,177,180).

FORTALEZAS DEL ESTUDIO

En este estudio, observamos que la inyección de células madre en el estroma corneal se realizó a través de un bolsillo laminar asistido por un láser de femtosegundo a profundidad media del estroma corneal. Aunque las córneas operadas estaban en estado de queratocono muy avanzado, y con un adelgazamiento severo, no observamos complicaciones intraoperatorias como la presencia de desgarros corneales (30,31,177,179,180,241,242). Además, este estudio ha demostrado una buena tolerancia y se confirmó la posibilidad de aumentar el grosor corneal mediante la implantación de láminas descelularizadas/recelularizadas de estroma corneal creadas por el láser de femtosegundo

sin ningún impacto negativo en la biomecánica, la visión y especialmente la anatomía y transparencia de la córnea (30,31,177,179,180,241,242).

Además, este es el primer ensayo clínico en humanos disponible con seguimiento a largo plazo. Los datos del primer y tercer año de este estudio muestran que estamos abriendo una nueva área de cirugía e investigación corneal. El uso de láminas corneales para un aumento terapéutico del grosor corneal en córneas queratocónicas debilitadas y delgadas es un nuevo concepto para la investigación. Todos los parámetros clínicos corneales se conservaron e incluso mejoraron; no se observó deterioro en ninguno de los casos del presente estudio. Además, en el caso-2 del grupo con implantación de **ADASCs** observamos una mejora de la cicatrización corneal paracentral preexistente, así como una mejora similar de las cicatrices paracentrales preexistentes, con el caso-11 del grupo de implantación de láminas recelularizadas. Basándose en los resultados del presente, las distrofias corneales o incluso las cicatrices corneales podrían ser relevantes, ya que estas células sobreviven en el estroma corneal y se diferencian en queratocitos. No provocan opacidades y no inducen ninguna reacción inflamatoria o rechazo y pueden mejorar las opacidades corneales (30,31,177,179,180,241,242).

8. CONCLUSIONES

LAS CONCLUSIONES DE ESTE TRABAJO SE PUEDEN RESUMIR EN LOS SIGUIENTES PUNTOS:

8.1 CONCLUSIONES CORRESPONDIENTES A LOS OBJETIVOS PRINCIPALES

1. Pudimos demostrar la seguridad y eficacia del implante en los siguientes tres grupos de cirugía:

   ▪ De las células madre adultas autólogas derivadas del tejido adiposo (**ADASCs** solas). Conclusión demostrada en los artículos científicos con referencias (30,177,179,180,240–242) de las publicaciones científicas acreditadas para esta tesis

   ▪ De láminas estromales corneales humanas descelularizadas. Conclusión demostrada en los artículos científicos con referencias (31,177,179,180,240–242) de las publicaciones científicas acreditadas para esta tesis.

   ▪ De láminas estromales corneales humanas recelularizadas con **ADASCs**. Conclusión demostrada en los artículos científicos con referencias (31,177,179,180,240–242) de las publicaciones científicas acreditadas para esta tesis.

2. Pudimos demostrar que la implantación de **ADASCs** aisladas o sembradas en una lámina corneal acelular humana, fue seguida de proliferación celular y no generó ninguna respuesta clínica o histológica de inflamación o rechazo en ninguno de los casos estudiados en nuestro estudio a lo largo del seguimiento posoperatorio.
3. Pudimos demostrar que las láminas corneales acelulares fueron bien toleradas por la córnea queratocónica, sin ningunas complicaciones.

4. Demostramos que las láminas descelularizadas o recelularizadas con **ADASCs** fueron capaces de aumentar (a un nivel estadísticamente significativo) el grosor de la córnea patológica y mejorar el estado clínico y la función visual de estos pacientes.

8.2 CONCLUSIONES CORRESPONDIENTES A LOS OBJETIVOS SECUNDARIOS

1. El estudio demostró que todos los pacientes mejoraron su función visual de una forma moderada (pero significativa). Además, el estudio demostró que todos los pacientes mejoraron significativamente su esfera refractiva, mientras que el cilindro refractivo permaneció estable en general. Conclusión demostrada en los artículos científicos con referencias (30,31,177,180,241,242) de las publicaciones científicas acreditadas para esta tesis.

2. La córnea respondió de manera positiva a la implantación de **ADASCs**, se observó con la **AS-OCT** por la formación de neocolágeno en el bolsillo corneal en el grupo donde solo se implantaron **ADASCs**, y la formación de neocolágeno en las superficies anterior y posterior de la lámina. Con el tiempo hubo una notable integración de la lámina dentro del estroma del huésped. Conclusión demostrada en los artículos científicos con referencias (30,31,177,180,241,242) de las publicaciones científicas acreditadas para esta tesis.

3. El estudio demostró que todos los pacientes mejoraron sus parámetros de grosor corneal paquimétrico y volumétrico, siendo esta mejora significativamente mejor en aquellos grupos con láminas descelularizadas o recelularizadas. Conclusión demostrada en los artículos científicos con referencias (30,31,177,180,241,242) de las publicaciones científicas acreditadas para esta tesis.

4. El examen biomicroscópico con lámpara de hendidura demostró la ausencia de complicaciones posoperatorias. No se registraron signos de inflamación o rechazo durante el

seguimiento en todos los pacientes. Conclusión demostrada en los artículos científicos con referencias (30,31,177,180,241,242) de las publicaciones científicas acreditadas para esta tesis.

5. El estudio de microscopía confocal demostró ser una herramienta extremadamente útil y necesaria para:

- La observación de la evolución de las **ADASCs** una vez implantadas en el bolsillo estromal y monitorizar su evolución.
- La observación de la evolución de las láminas descelularizadas implantadas sin **ADASCs**.
- La observación de la evolución de las **ADASCs** implantadas con las láminas corneales descelularizadas.
- El método basado en el análisis cuantitativo subjetivo de las células corneales estromales nos permitió monitorizar la evolución de la densidad celular de las **ADASCs** implantadas con lámina o sin lámina durante el experimento.
- Con microscopía confocal, pudimos investigar la evolución cuantitativa y cualitativa de la densidad celular en el estroma anterior, medio y posterior de los pacientes.

Conclusiones demostradas en el artículo científico con referencia (179) de la publicación científica acreditada para esta tesis.

8.3 CONCLUSIONES DE LAS PUBLICACIONES CIENTÍFICAS

8.3.1 Conclusión de la revisión con referencia (240) **de la publicación científica acreditada para esta tesis:** Alió del Barrio JL, Arnalich-Montiel F, De Miguel MP, **El Zarif M**, Alió JL. **Corneal stroma regeneration: Preclinical studies**. Exp Eye Res. 2021;202:108314.

En conclusión, para lograr una estructura de estroma adecuada, que imite la natural, de modo que mantenga la homeostasis del estroma corneal, se deben desarrollar en conjunto una fuente de células y un andamio de colágeno. En cuanto al componente celular, se han estudiado varios tipos de células, tanto de origen ocular como extraocular, siendo hasta ahora el uso de **h-ADASCs** el más prometedor clínicamente. Sin embargo, a largo plazo, probablemente el desarrollo de técnicas de **iPSCs** estandarizadas y más baratas también superará el uso de las **MSCs** (181). En cuanto a las láminas de colágeno, el uso de secciones de córnea descelularizadas es clínicamente el más relevante hasta el momento, pero aún tiene el inconveniente de necesitar una córnea donante. En los próximos años, los avances en nuevas técnicas de impresión **3D** con una resolución de celda única como **LIFT** (PreciseBiohttps: www.precisebio.com), bioimpresión asistida por láser (273), litografía basada en la polimerización de dos fotones (274), fabricación de filamentos fundidos (275), y otros métodos para lograr haces paralelos laminares de colágeno, como apiñamiento molecular (16) Impulsará rápidamente el desarrollo de un estroma corneal biomimético.

8.3.2 Conclusión del artículo científico publicado con anterioridad a esta tesis doctoral con referencia (30**):** Alió del Barrio JL, **El Zarif M**, De Miguel M, Azaar A, Makdissy N, Harb W, et al. **Cellular therapy with human autologous adipose-derived adult stem cells for advanced keratoconus.** Cornea 2017; 36(8)952-60.

Como conclusión de la implantación de **ADASCs** hasta los 6 meses, con el presente estudio de fase 1 mostramos de manera preliminar la seguridad del trasplante de estroma corneal de células madre adultas autólogas derivadas del tejido adiposo en humanos, su supervivencia *in vivo* y su capacidad para producir una cantidad baja de nuevo colágeno. Este estudio incluye una pequeña muestra de pacientes, por lo que se requieren estudios futuros con muestras más grandes para confirmar finalmente la seguridad del procedimiento, aclarar su eficacia, así como la relevancia de los hallazgos observados.

8.3.3 Conclusión del artículo científico publicado con anterioridad a esta tesis doctoral con referencia (31**):** Alió del Barrio JL, **El Zarif M**, Azaar A, Makdissy N, Khalil C, Harb W, et al. **Corneal stroma enhancement with decellularized stromal laminas with or without stem cell recellularization for advanced Keratoconus**. Am J Ophthalmol. 2018;186: 47-58.

En conclusión, la mejora del estroma corneal mediante el trasplante de injerto de estroma corneal descelularizado es una técnica novedosa que podría plantearse como una alternativa para los ojos queratocónicos avanzados a las técnicas clásicas de trasplante de córnea. Aún se necesitan más estudios con un mayor seguimiento y muestras de estudio para confirmar los resultados preliminares mostrados en este ensayo clínico piloto. El posible papel de la adición de células madre mesenquimales a dichos injertos sigue aún no estar tan claro.

8.3.4 Conclusión del artículo con referencia (177**) de la publicación científica acreditada para esta tesis:** Alió JL, Alió del Barrio JL, **El Zarif M**, Azaar A, Makdissy N, Khalil

C et al. **Regenerative surgery of the corneal stroma for advanced keratoconus: 1-Year outcomes**. Am J Ophthalmol. 2019; 203:53-68.

En conclusión, el tratamiento temprano de las córneas patológicas con células madre de origen autólogo o alogénico podría ser una opción incluso en las primeras etapas de la enfermedad. En etapas avanzadas, el trasplante de córnea podría ser eliminado como tiene muchos problemas involucrados en la disponibilidad de tejido corneal, el largo tiempo de recuperación y los resultados impredecibles. Las cicatrices corneales podrían tener una opción con el uso de estas células madre mesenquimales como tratamiento alternativo. De hecho, la enfermedad más relevante que podría beneficiarse de los resultados de este estudio es el queratocono. El queratocono es la distrofia corneal más frecuente e importante por su impacto sociológico. La frecuencia del queratocono es realmente relevante y es la primera causa de trasplante de córnea en la población joven (2). Todos estos pacientes podrían beneficiarse de este nuevo tipo de terapia quirúrgica que puede ser más accesible, no depende del tejido corneal humano viable y no presenta los peligros biológicos relacionados con el tejido alogénico con células alogénicas.

8.3.5 Conclusión del artículo con referencia (180**) de la publicación científica acreditada para esta tesis: <u>El Zarif M</u>**, Alió JL, Alió del Barrio JL, Abdul Jawad K, Palazón-Bru A, Abdul Jawad Z, et al**. Corneal stromal regeneration therapy for advanced keratoconus: long-term outcomes at 3 years**. Cornea. 2021;40(6):741–54.

En conclusión, en el presente informe, confirmamos los resultados de seguridad a 3 años de este enfoque de terapia avanzada para el tratamiento del queratocono. La córnea mostró transparencia hasta 3 meses con todos los casos tratados. La mejora del grosor corneal en las

córneas implantadas solo con células parece ser insuficiente para restaurar el grosor corneal normal, mientras que la implantación en el bolsillo etromal mostró un excelente resultado en la restauración del grosor corneal con mejor densidad celular en el grupo implantado con láminas recelularizadas. Las modestas, pero significativas mejoras visuales y refractivas encontradas en el estudio, con una total ausencia de complicaciones, confirman la viabilidad de este enfoque terapéutico como una potencial técnica novedosa para el tratamiento del queratocono. Futuros estudios con series más amplias y en casos menos avanzados de queratocono establecerán el potencial terapéutico de este nuevo tipo de cirugía.

8.3.6 Conclusión del artículo con referencia (179) **de la publicación científica acreditada para esta tesis:** **El Zarif M**, Abdul Jawas K, Alió del Barrio JL, Abdul Jawad Z, Palazón-Bru A, De Miguel MP, et al.**Corneal stroma cell density evolution in keratoconus corneas following the implantation of adipose mesenchymal stem cells and corneal laminas: an in vivo confocal microscopy study.** IOVS. 2020; 61(4)22.

En conclusión, la microscopía corneal confocal combinada con la tecnología utilizada en nuestra investigación ha demostrado ser una herramienta muy eficaz para la evaluación *in vivo* y el seguimiento de córneas implantadas con células madre mesenquimales con fines de regeneración corneal. Hemos informado los resultados de la microscopía confocal después de la implantación de **ADASCs** en el plano quirúrgico seleccionado, lo que permitió una evaluación cualitativa y cuantitativa de los mismos durante el experimento. Además, la microscopía corneal confocal permitió monitorear los cambios morfológicos progresivos que ocurrieron en las láminas descelularizadas y recelularizadas a lo largo del período de observación y ayudó a determinar los cambios en las densidades celulares en el tejido injertado, así como en todo el estroma corneal.

Las células estromales aumentaron significativamente en el nivel de la implantación inyectada en el estroma corneal. Además, indujeron un aumento significativo del nivel de células estromales cuando se implantan conjuntamente con una lámina corneal impregnada en la superficie con **ADASCs**. Este aumento era mayor que el observado cuando se implantan láminas corneales acelulares, incluso cuando le sigue a la implantación una repoblación de la lámina acelular por las células estromales de la córnea receptora. Si estos hallazgos indican la supervivencia de las **ADASCs** mesenquimales y su diferenciación en queratocitos o que dichas células mesenquimales provocan un estímulo biológico para la proliferación de las células del huésped, estos resultados deberan ser confirmados en futuros estudios sobre este tema.

8.3.7 Conclusión de la revisión con referencia (241) **de la publicación científica acreditada para esta tesis: El Zarif M**, Alió del Barrio JL, Arnalich-Montiel F, De Miguel MP, Makdissy N, Alió JL. **Corneal stroma regeneration: New approach for the treatment of cornea disease**. APJO. 2020; 9(6):571–9.

En conclusión, la terapia celular con implantación de **ADASCs** autólogas, estroma corneal humano descelularizado, y el transplante de lentículo corneal alogénico refractivo inlay es una terapia potencialmente eficaz para el queratocono. Estos hallazgos prometedores abren una nueva perspectiva en la terapia para el estroma corneal basada en la regeneración del estroma corneal y la mejora de su grosor, parámetros topográficos y visuales. Se necesitan estudios futuros para ampliar la aplicación potencial de estas nuevas terapias para el tratamiento del estroma en córneas patológica.

8.3.8 Conclusión de la revisión con referencia (242) **de la publicación científica acreditada para esta tesis: El Zarif M**, Alió JL, Alió del Barrio JL, De Miguel MP, Abdul Jawad K, Makdissy N. **Corneal stromal regeneration: a review on human clinical studies for treatment of keratoconus.** Front Med. 2021; 8:650724.

En conclusión, en esta revisión se discutió la terapia celular con implantación de **ADASCs** autólogas, estroma corneal humano descelularizado, lentículo **SMILE** alogénico, corneal Inlay, y en menor medida, el colágeno recombinante **CXL**. Como este procedimiento de hecho informó complicaciones de la topografía refractiva y corneal, también mostró inicialmente ser potencialmente efectivo para el tratamiento del queratocono avanzado. Estos hallazgos prometedores abren una nueva perspectiva de la terapia del estroma corneal basada en la mejora y regeneración del estroma corneal. Los estudios futuros ampliarán el potencial de la aplicación de estas nuevas terapias en el tratamiento de las enfermedades del estroma corneal.

RESUMEN Y CONCLUSIÓN GENERAL

Si bien este estudio involucró una pequeña muestra de estudio y se presentaron algunas otras limitaciones, al mismo tiempo las fortalezas de esta aplicación clínica podrían abrir una nueva vía para el manejo del queratocono, así como otras patologías corneales como distrofias o cicatrices corneales. Tales técnicas regenerativas podrían ofrecer un plan de tratamiento mucho menos agresivo que las técnicas regulares de trasplante penetrante o lamelar y aliviar la creciente demanda de tejido corneal del donante. La creación de bancos de células madre e incluso el almacenamiento de sus exosomas podría simplificar aún más estas técnicas y evitar algunas de las limitaciones asociadas con la implantación intraestromal directa de células.

ENGLISH VERSION

1. INTRODUCTION

Cellular therapy of the corneal stroma has been gaining interest in the last few years as a potential alternative treatment option for corneal stroma diseases such as corneal scarring, dystrophies, and ectasias. Such diseases induce distortion of the anatomy and physiology of the cornea and lead to loss of its transparency and subsequent loss of vision.

Keratoconus is the most common corneal dystrophy with a diverse prevalence in the population from 0.05-2.3 %. Being a relatively prevalent disease, it is more observed today than before due to the more advanced diagnostic tools that are available for the diagnosis of early keratoconus (1). It is characterized by progressive thinning, bulging, and distortion of the cornea, and causes progressive changes in vision with increased myopia and myopic astigmatism, corneal irregularity, and visual loss (2).

The corneal stroma constitutes more than 90% of the corneal thickness. Many features of the cornea including its strength, morphology, and transparency are attributable to the anatomy and properties of the corneal stroma (3). The extracellular matrix of the corneal stroma is composed of collagen, which forms for more than 70% of the weight of the dehydrated cornea, the most abundant being type I (75%), and proteoglycans including keratan sulfate which is the most abundant (65%) whose protein nucleus is composed of lumican, keratocan and mimecan (3). Keratocan is expressed only in the corneal stroma, therefore it is considered in tissue engineering as a specific marker of keratocytic differentiation (4). The cellular component of the corneal stroma occupies only 2-3% of the stromal volume, and in it, the predominant cells are keratocytes, mesenchymal cells that derive from the neural crest, which are distributed among the collagen lamellae. Keratocytes are in a quiescent state in the normal cornea, and they are responsible for the constant replacement of the

stromal extracellular matrix through the production of collagen, essential for the maintenance of corneal transparency. When keratocytes activate their metabolism, they transdifferentiate into fibroblasts and myofibroblasts, which participate in the healing of the corneal stroma. The capacity for renewal of stromal keratocytes is due to precursor cells in the anterior limbal corneal stroma, which expresses adult stem cell markers (5).

Keratoconus is characterized by a progressive loss of keratocytes: their number decreases from anterior to posterior stroma (6), leading to the progressive thinning of the stroma (1,6), and a decrease in corneal strength (7). This definition is valid for most patients with keratoconus, although some variations in the phenotypic expression of the disease might be present (8). Most keratoconus cases have thin corneas and a weak mechanical resistance related to the progressive loss of keratocyte density (9). Apoptosis of keratocytes (6,10) or, of enzymes are thought to be the cause of keratocyte loss and consequently loss of corneal stroma over time (6,10). The proportion of keratocytes in the corneal stroma is decreased with the progression of the disease (6). In the end stages of keratoconus, the clinical aspects of the thin and debilitated cornea are associated with a sharp decrease in the number of keratocytes. There is severe corneal deformation (6), and alteration in the location of the corneal apex (11), causing severe visual loss.

The prevalence and progressive character of keratoconus have led to the proposal of different alternative therapies, which at the moment are in use, including collagen crosslinking (**CXL)**, intracorneal rings and segments, corneal transplantation, and more recently, Bowman's membrane (**BM**) implantation (2). Meanwhile, visual rehabilitation of advanced corneal ectasias requires penetrating or lamellar corneal transplantation techniques, which present several drawbacks, such as graft rejection, failure, and slow visual recovery due to high levels of induced postoperative astigmatism related to the sutures (2). Also, it should be considered that in many

countries access to donor corneal tissue is limited, approximately 53% of the world's population has no access to corneal transplantation (12). Therefore, the demand for adequate donor corneas is increasing faster than the number of donors, leaving thousands of curable patients around the world waiting for possible treatment (13,14). The quantification of the great shortage of corneal graft tissue showed that a cornea is only available for 70 cases needed (12).

To solve the global health problem, recent research studies have focused on developing in the laboratory corneal substitutes that could mimic human cornea features *in vivo*, and subsequently be an alternative to human donor tissue, to find an alternative to classical corneal transplantation, but this has still not been yet accomplished due to the extreme difficulty in mimicking the highly complex ultrastructure of the corneal stroma, obtaining substitutes that either does not achieve enough transparency or strength (15,16). Moreover, synthetic scaffold-based designs have raised some important concerns such as strong inflammatory responses induced on their biodegradation, or chronic nonspecific inflammatory responses (17). On the other hand, recently several corneal decellularization techniques have been described, which provide an acellular corneal matrix (**ECM)** (18). These scaffolds have gained increasing interest as they provide an ideal natural environment for the growth and differentiation of cells (either transplanted donor cells or migrating host cells) (19). Also, components of the **ECM** are generally preserved among species, and the removal of all immunogenic cellular component could open the field of xenotransplantation to human recipients by using donor tissue from other animals such as the pig, that shares important similarities with the human cornea (20).

In the last few years, interest in cellular therapy of the corneal stroma using mesenchymal stem cells (**MSCs**) from either ocular or extraocular sources has gained a lot of interest; studies showed that **MSCs** are capable of differentiating into adult keratocytes *in vitro* and *in vivo* (3).

Several authors, including reports from our research group, have demonstrated (17,19,21) that these stem cells can not only survive and differentiate into adult human keratocytes in xenogeneic scenarios without inducing an inflammatory reaction, but also: i) produce new collagen within the host stroma (21,22), ii) modulate preexisting scars by corneal stroma remodeling (23,24), and iii) improve corneal transparency in animal models for corneal dystrophies by collagen reorganization, as well as in animal models for metabolopathies by the catabolism of accumulated proteins (25–28). Mesenchymal stem cells have also shown immunomodulatory properties in syngeneic, allogeneic, and even xenogeneic scenarios (28,29). The first clinical data regarding the safety and preliminary efficacy of cellular therapy of the corneal stroma from Phase 1 human clinical trials are now available (30,31), which may end up providing a real alternative treatment option for corneal diseases soon.

Considering existing scientific evidence, it seems that all types of **MSCs** have similar behavior *in vivo* (Table 1), and thus can achieve keratocyte differentiation and modulate the corneal stroma with immunomodulatory properties (32). It has also been recently reported that **MSCs** secrete paracrine factors such as vascular endothelial growth factor (**VEGF**), platelet-derived growth factor (**PDGF**), hepatocyte growth factor (**HGF**), and transforming growth factor-beta 1 (**TGFβ1**). Although the precise actions of the different growth factors for cornea wound healing are not fully understood, overall, they seem to promote cell migration, keratocyte survival by apoptosis inhibition, and upregulate the expression of the **ECM** component genes in keratocytes, subsequently enhancing corneal re-epithelialization and stromal wound healing (33). **MSCs** can be obtained from many human tissues, including adipose tissue, bone marrow, umbilical cord, dental pulp, gingiva, hair follicle, cornea, and placenta (34,35).

Corneal stromal stem cells (**CSSCs**) are a promising source for cellular therapy as the isolation technique and culture methods have been optimized and refined (36); presumably, they should be efficient in differentiating into keratocytes as they are already committed to the corneal lineage. On the other hand, isolating **CSSCs** autologously is more technically demanding considering the small amount of tissue that they are obtained from. Furthermore, this technique still requires a contralateral healthy eye, which is not always available (bilateral disease). Therefore, these drawbacks may limit its use in clinical practice. Allogeneic **CSSC** use requires living or cadaveric donor corneal tissue.

Human adult adipose tissue is a good source of autologous extraocular stem cells as it satisfies many requirements: easy accessibility to the tissue, high cell retrieval efficiency, and the ability of its human adipose-derived adult stem cells (**h-ADASCs**) to differentiate into multiple cell types (keratocytes, osteoblasts, chondroblasts, myoblasts, hepatocytes, neurons, etc) (21). This cellular differentiation occurs due to the effect of very specific stimulating factors or environments for each cell type, avoiding the mix of multiple kinds of cells in different niches.

Bone marrow **MSCs** (**BM-MSCs**) are the most widely studied **MSCs**, presenting a similar profile to adipose-derived adult stem cells (**ADASCs)**, but their extraction requires a bone marrow puncture, which is a complicated and painful procedure requiring general anesthesia.

Umbilical **MSCs** (**UMSCs**) present an attractive alternative, but their autologous use is currently limited as the umbilical cord is not generally stored after birth.

Embryonic stem cells (**ESCs**) have great potential, but also present important ethical issues. However, the use of Induced pluripotent stem cells (**iPSCs)** technology (37) could solve such problems, and their capability to generate adult keratocytes has already been proven *in vitro* (38).

Finally, it is important to remark that the therapeutic effect of **MSCs** in a damaged tissue is not always related to the potential differentiation of the **MSCs** in the host tissue as multiple mechanisms might contribute simultaneously to this therapeutic action, for example, secretion of paracrine trophic, and growth factors capable of stimulating resident stem cells, reduction of tissue injury and activation of immunomodulatory effects, in which case the direct cellular differentiation of the **MSCs** might not be relevant and could even be non-existent (32,39,40).

We will summarize the keratoconus disease, the modern pathogenesis, epidemiology, and different factors that influence their appearance and development. We will resume the different types of stem cells (mesenchymal and others) that have been proposed for the regeneration of the corneal stroma as well as the current *in vitro* or *in vivo* evidence, the different decellularization protocols. Finally, we will review the different surgical approaches that have been suggested (*in vivo*) for the application of stem cell therapy to regenerate the corneal stroma.

Table 1. Stem cells assayed for corneal stroma regeneration: evidence of keratocyte or keratocyte-like differentiation and their potential autologous application.

	CSSCs	**BM-MSCs**	**ADASCs**	**UMSCs**	**ESCs**	**iPSCs**
Keratocyte differentiation *in vitro* demonstrated	Yes	Yes	Yes	Yes	Yes	Yes
Keratocyte differentiation *in vivo* demonstrated	Yes	Yes	Yes	Yes	No	No
Possible autologous use	Yes/No	Yes	Yes	Yes/No	No	Yes

CSSCs: corneal stroma stem cells; **MSCs**: mesenchymal stem cells; **BM-MSCs:** bone marrow mesenchymal stem cells; **ADASCs**: adipose-derived adult stem cells; **UMSCs**: umbilical **MSCs**; (**ESCs)**: embryonic stem cells; **iPSCs**: induced pluripotent stem cells. The table is taken from the scientific chapter of Alió JL et al. (41).

1.1 KERATOCONUS

1.1.1 KERATOCONUS IS NOT A SO RARE DISEASE

Since the late 1950s, contact lenses (**CL**) became a partial solution for the visual loss of keratoconus patients, while other approaches were nonexistent, and this potentially blinding disease had no hope for adequate treatment. Keratoconus patients had the same category as any corneal dystrophy with no potential treatment and no therapeutic recommendations to perform. Since those historical "black days", there has been tremendous progress in the diagnosis and treatment of this disease (42). The first corneal graft for advanced keratoconus was performed by Edward Zirm in Prague in 1906 (43).

In the last few decades, due to environmental and genetic factors, we are experiencing an epidemic outbreak of keratoconus, as it relies on achieving improved, accurate, and more accessible diagnostic capabilities. There is a better future now, and there will be more improvements for these patients soon. The previously untreatable disease is now beginning to be treated successfully and is leading to good visual outcomes.

There is a promising future now, and there will be more improvements for these patients soon (42). This increase in the number of cases has led to the development of experts in keratoconus, specialized units in ophthalmic centers, and even a new specialized journal (International Journal of Keratoconus and Corneal Ectatic Diseases), with so many publications dedicated exclusively to this corneal disease (42).

1.1.2 MODERN PATHOGENESIS OF KERATOCONUS

The pathogenesis of keratoconus remains unknown despite numerous intensive studies. The only commonly identified factors seem to be eye rubbing and the presence of allergies (44).

Autosomal dominant and autosomal recessive transmission forms have been described (45). Several studies suggest the existence of subclinical forms within the relatives of keratoconic patients (46,47).

Studies have shown an uneven distribution of the disease in Caucasian individuals living in similar geographic areas. It was also shown that the incidence of keratoconus is four times higher among Asians compared to Caucasians (48). Other studies report that ethnicity-related differences are observed in the course and severity of the disease, which provides a strong argument in favor of a genetic component (49,50). Extreme variations in the prevalence of keratoconus are observed concerning ethnicity, this component undoubtedly has an important role (46,51).

The candidate gene approach is based on the knowledge of the biochemistry and pathology of the disease, which consists of identifying mutations in the genes that encode the proteins of the affected tissue (44). The degree of genetic heterogeneity in this disease until now is unknown. Test for mutations of various family-coding genes may play a role in the development of keratoconus disease (52,53). An attempt to identify mutations in genes was made encoding interleukin-I (**ILI**) components (54), proteases (55,56), protease inhibitors (57,58), and collagens type I, III, IV, V, VI, VII, and VIII collagens are present in the cornea. The first collagen-encoding gene tested was COL6A1, but there was no significant relationship with keratoconus (59). The degree of genetic heterogeneity in this disease remains unknown, and mutations in several coding genes from families that have not yet been tested may play a role in the development of keratoconus (44). One study of

mutated gene VSX1 led to the identification of related mutations among patients affected by keratoconus. This gene codes for a legitimate transcription factor and is also elaborated in posterior polymorphous dystrophy (52), however, has only a role between 0.1–0.4 % of familial keratoconus and thus its significance in the pathogenesis of keratoconus remains low (44).

On the other hand, studies have shown that there is a strong concordance of elevated interleukin 6 (**IL**6), tumor necrosis factor α (**TNF**α), and matrix metalloproteinases (**MMP9**) found in tears of keratoconic patients (60–63). **MMP9** is one of the matrix-degrading enzymes produced by human corneal epithelium and regulated by cytokine **IL**6. **TNFα** in addition to **IL6** is considered a main pathogenic factor in systemic and corneal inflammation, it induces the expression of **MMP9**, a higher concentration of **MMP9** no statistically significant was found in keratoconic tears' eyes (60). **TNFα**, **MMP9**, and **IL**6 were strongly upregulated in the level of messenger ribonucleic acid (**mRNA**) in the epithelium of patients with keratoconus (63). However, authors could deduce that mediators of inflammation are present in keratoconic corneas. Keratoconus could be an inflammatory disorder such as many studies are indicating the presence of elevated levels of inflammatory markers but still with contradictory findings (63–65).

In general, it is thought that keratoconus is probably caused by events outside the cornea and that these events are ultimately responsible for the induction of this ectasia. Eye rubbing, atopy, CL wear, oxidative stress (61,66,67), and associated with genetic factors that cause corneal disease (68).

Also, other studies based on ribonucleic acid (**RNA**) found apoptosis of corneal keratocytes. Mace, and coworkers demonstrated that keratoconus could be related to a dysregulation of cell proliferation and differentiation pathways (69).

Therefore, the inadequate balance between cytokines (pro and anti-inflammatory, such as **IL**6/**TNFα**/**IL**12/**IL**17 and **IL**4/**IL**10, respectively) can carry to altered corneal function and structure, leading to increased apoptosis of metalloproteinases and keratocytes. The exact underlying molecular mechanisms remain to be elucidated. These studies have shown that in keratoconus there is a corneal structural imbalance, associated with metabolic stress, and an imbalance between apoptosis and proliferation. However, these studies have not yet managed to identify a clinically usable biomarker to detect keratoconus or assess its degree of severity (44).

1.1.3 EPIDEMIOLOGY OF KERATOCONUS

The incidence and prevalence of keratoconus are determined by its burden, and in turn by the provision of health care services, screening programs, and medical care. Also, genetic and environmental factors affect the incidence and prevalence of the disease. The preoperative evaluation has identified a previously undiagnosed subclinical keratoconus and thus protected them from iatrogenic worsening of ectasia. Also, cases that were previously thought to be unilateral are bilateral with modern diagnostic imaging. It is accepted that does not exist truly unilateral keratoconus, improving our understanding of the epidemiology of keratoconus has increased greatly our understanding of the pathogenesis (70).

1.1.3.1 Incidence and Prevalence.

A review of early studies between 1936 and 1966 on the prevalence of keratoconus found a range of 50 to 230 cases per 100,000 (0.05 to 0.23%) (71). A review of later studies (1959–2011) (72) found prevalence estimates that vary from 0.3 per 100,000 (0.0003 %) in Russia to 2340 per

100,000 (2.3 %) in Maharashtra, India (73). Kennedy's 1986 article, in which they used keratoscopy and keratometry to estimate the prevalence in Minnesota, USA as 54.5/100,000 (0.0545 %) (74).

Recent studies demonstrate that Middle Eastern and Central Asian ethnicity is considered a risk factor for keratoconus (75). Other recent studies using topographers provide more sensitive estimations, they provided a summary of published prevalence studies and emphasized the important methodological differences between hospital- or clinic-based reports and population-based studies (Table 2, Table 3) (76). One study performed in Lebanon by Waked N. and coworkers resulted in a prevalence of keratoconus 3.3% (77). This result was in agreement with the study of Israeli Arabs, a prevalence of 3.18 % was recorded in the population (78). Similar results were obtained in Iran in Mashhad, the prevalence of keratoconus was 2.5% (79), nevertheless, the prevalence in Shahroud population was lower, a result between 0.72%- 0.79% in men and women were found respectively (80).

The range of variation of estimates in the annual incidence of keratoconus in Saudi Arabian varies from 1.4 to 600 cases per 100,000 of the population (81). Ethnic differences influence an incidence of 25/100,000/year for Asiatic when compared with 3.3/100,000/year for Caucasians in a single catchment area (82). McMonnies' review highlighted and discussed the detection of subclinical keratoconus cases before refractive surgery. During the last decades due to modern imaging technology and diagnostic sensitivity, prevalence estimates have increased dramatically (83).

Table 2. Hospital/clinic-based epidemiological studies of keratoconus (Gordon-Shaag et al. BioMed Research International 2015—reproduced with kind permission from authors).

Author	Location	Age in years	Sample size	Incidence/ 100,000	Prevalence/ 100,000	Method
Tanabe et al. (1985)	Muroran, Japan	10–60	2601-P		9	Keratometry
Kennedy et al. (1986)	Minnesota, USA	12–77	64-P	2	54.5	Keratometry + retinoscopy
Ihalainen (1986)	Finland	15–70	294-P	1.5	30	Keratometry + retinoscopy
Gorskova and Sevost'ianov (1998)	Urals, Russia				0.2–0.4	Keratometry
Pearson et al. (2000)	Midlands, UK	10–44	382-P	4.5-W 19.6-A	57 229	Keratometry + retinoscopy
Ota et al. (2002)	Tokyo, Japan		325-P	9		Keratometry?
Georgiou et al. (2004)	Yorkshire, UK		74-P	3.3-W 25-A		Clinical examination
Assiri et al. (2005)	Asir, Saudi Arabia	8–28	125-P	20		Keratometry
Nielsen et al. (2007)	Denmark		NA	1.3	86	Clinical indices + topography
Ljubic (2009)	Skopje, Macedonia		2254		6.8	Keratometry
Ziaei et al. (2012)	Yazd, Iran	25.7 ± 9	536	22.3		Topography

An Asian (Indian, Pakistani, and Bangladeshi), *W* white, *P* patient, *NA* not available. Reproduced with permission from the Book Keratoconus: Recent Advances in Diagnosis and Treatment of Alió et al. (70).

Table 3. Population-based epidemiological studies of keratoconus (Gordon-Shaag et al. BioMed Research International2015—reproduced with kind permission from authors).

Author	Location	Age in years (mean)	Sample size	Prevalence/ 100,000 (cases)	Method	Sampling method
Hofstetter (1959)	Indianapolis, USA	1–79	13345	120	Placido disc [a]	Rural volunteers
Santiago et al. (1995)	France	18–22	670	1190	Topography	Army recruits
Jonas et al. (2009)	Maharashtra, India	>30 (49.4 ± 13.4)	4667	2300	Keratometry	Rural volunteers (8 villages)
Millodot et al. (2011)	Jerusalem, Israel	18–54 (24.4 ± 5.7)	981	2340	Topography	Urban volunteers (1 college)
Waked et al. (2012)	Beirut, Lebanon	22–26	92	3300	Topography	Urban volunteers (1 college)
Xu et al. (2012)	Beijing, China	50–93 (64.2 ± 9.8)	3166	900	Optical low coherence reflectometry	Rural + urban volunteers
Hashemi et al. (2013)	Sharud, Iran	50.83 ± 0.12	4592	760	Topography	Urban Volunteers from random cluster
Hashemi et al. (2013)	Tehran, Iran	14–81 (40.8 ± 17.1)	426	3300	Topography	Urban volunteers (stratified cluster)
Shneor et al. (2014)	Haifa, Israel	18–60 (25.05 ± 8.83)	314	3180	Topography	Urban volunteers (1 college)
Hashemi et al. (2014)	Mashhad, Iran	20–34 (26.1 ± 2.3)	1073	2500	Topography	Urban volunteers (stratified cluster in 1 university)

[a] the methods for detecting keratoconus used in these studies are now considered inadequate and the results should be interpreted with caution. Reproduced with permission from the Book Keratoconus: Recent Advances in Diagnosis and Treatment of Alió et al. (70).

1.1.3.2 Environmental and Genetic Factors.

While attributing the increase in prevalence estimates in part mainly due to technological advances in imaging, and another part due to subclinical diagnosis. Keratoconus is believed to be caused by a complex interplay between genetic and environmental factors, as well as biochemical and biomechanical disorders (46,75,84,85). A significant association with consanguinity of the genetic basis to the disease was found (86), autosomal dominant patterns of familial inheritance were noticed (87). Greater concordance was detected between monozygotic than dizygotic twins (88). In the study of Rabinowitz, 10% of the patients with keratoconus had a family history of the disease, while with the control group there was only 0.05% (89). Most cases of keratoconus are considered sporadic (90). Geographic variations in prevalence are currently thought to be related to specific environmental factors that promote the expression of genetic factors related to ethnicity (83).

1.1.3.3 Ultraviolet Light Exposure.

A higher prevalence of keratoconus has been identified in areas with high ultraviolet (**UV**) light exposure (83). The **UV** light may increase the production of reactive oxygen species within the cornea (91), and that keratoconic corneas cannot process this excess reactive oxygen species (92), leading to increased oxidative stress, cytotoxicity, and therefore corneal thinning (66). Nevertheless, there is an argument that contradicts this assumption that it is the natural **CXL** of corneal collagen is induced by ultraviolet light, which could be expected to reduce the prevalence and rate of progression of the ectasia (93).

1.1.3.4 Eye Rubbing and Allergy.

Eye rubbing and its relation to allergic or atopic disease are another environmental stressor-related to the disease of keratoconus, this association was first described in 1956 (94). Nowadays,

the association with eye rubbing and keratoconus is widely accepted (76), studies have shown that the duration of eye rubbing in patients with keratoconus appears longer than that associated with only an allergic eye disease (95), this may explain that the majority of atopic eyes do not develop keratoconus. In hot and dry climates, high levels of dust may induce frequent eye rubbing and can cause a high prevalence of keratoconus development in these areas (76). Bawazeer et al. found that keratoconus was associated with family history, atopy, and eye rubbing (96).

1.1.3.5 Gender and Age.

Results concerning gender preponderance vary between studies: some authors demonstrated female preponderance, while others proved male preponderance. Other authors demonstrated no significant gender differences. Overall keratoconus is not considered to favor one gender over the other (1).

Regarding age, keratoconus is typically a disease of adolescence and young adulthood, presenting among the ages of 20 and 30 years (97). Ihalainen reported that the mean age of keratoconic patients was 18 years, and 73 % of patients were aged 24 years or below (98). Faster progression induces a shorter time to penetrating keratoplasty. The earlier age of onset predicts a greater severity of the disease. Corneal collagen **CXL** can now arrest or slow down the progression of the disease (70).

1.1.4 HISTOPATHOLOGY OF KERATOCONUS

Keratoconus is a human disease, and the lack of an animal model has directed to the view that this disease appears only in human beings, and the access to corneal transplantation at the end stage of the disease has allowed the availability of tissue for histopathological studies. Such findings

can inform us of the underlying pathogenesis of the disease, and can also lead to a hypothesis about why keratoconus may progress (99).

Structural Changes in Keratoconus: The characteristic thinning and other biomicroscopic signs of disease progression in keratoconus would correlate with the alteration of the structural elements of the keratoconic cornea.

1.1.4.1 Epithelium.

The superficial epithelium in keratoconic corneas showed normal cellular morphology at the periphery, but highly elongated cells presented at the cone apex (100). Recent methods for the analysis of epithelial thickness included spectral-domain optical coherence tomography (**OCT**), which confirmed the presence of pronounced deviation in epithelial thickness (101,102). Confocal microscopic investigations of keratoconic patients showed that superficial epithelial cells are elongated in an oblique direction, and highly reflective with an evident area of missing cells, pathological alterations are found in principle at the fourth stage of the disease in the central area of the cornea (103–105). The new devices of the anterior segment optical coherence tomography **AS-OCT** capture instantaneously a front surface topography with pachymetry data, providing epithelial and total corneal thickness maps. In the case of keratoconus, it is known that the epithelium is thinner in the area overlying the cone (106–108). In advanced keratoconus, there could be excessive epithelial thinning that might lead to epithelial rupture and subsequent scarring (109). In keratoconus, the epithelium becomes thinner at the apex of the cone, while is surrounded by a ring of the thickened epithelium, which shows an epithelium thickness known as the "doughnut" epithelial pattern (109).

The presence of terminal deoxynucleotidyl transferase biotin-dUTP nick end labeling (**TUNEL**) staining, is an indicator of the presence of apoptotic cells, with a general pattern of

apoptosis that continues to the basal epithelium (110,111). With keratoconic corneas, the basement membrane appears irregular and contains localized tears, showing an erratic pattern of laminin 1 and 5 stainings with type VII collagen localized in basement membrane abnormalities (112). Immunohistochemical (**IHC**) studies in advanced keratoconus cases demonstrated a rupture in the cell membrane, that can lead to a significant reduction in basal epithelial cell numbers, which leads to the presence of a few layers of flattened superficial epithelium lying on an abnormal basement membrane (65,89).

1.1.4.2 Bowman's membrane (BM).

Structural abnormalities in the **BM** in the central part of the keratoconic cornea have been observed. Examination by scanning electron microscopy of the collagen organization in keratoconic tissue found edged defects and varying degrees of ruptures in Bowman's layer (113). Further studies reported discontinuities in **BM**, and with the presence of distorted stroma under these defects, including the presence of fibrotic regions with areas of direct contact of the epithelium with the corneal stroma (113,114). Confocal microscopy studies showed the presence of ruptures in **BM** with highly reflective scar tissue (104). The presence of striaes has also been described in other studies that found that there's a reflection of bright background illumination underneath **BM** due to a disarrangement of collagen fibers (103).

1.1.4.3 Stroma

- **Collagen Lamellae.**

Transmission electron microscopy (**TEM**) studies of the keratoconic stroma revealed that the thickness of collagen lamellae in keratoconus is not altered, but the number of lamellae appears to be significantly decreased than in normal corneal stroma (115). Synchrotron X-ray diffraction

studies indicated that there was no difference in interfibrillar spacing between collagens in keratoconus and control corneas, it was shown that thinning of the corneal stroma in keratoconus is not the result of a tighter packing of collagen fibers in the corneal stroma, However, it was demonstrated that there was a reduction in the volume of proteoglycan along collagen fibers in the keratoconic cornea (116). These data assume a progressive loss of collagen lamellae within the corneal stroma, but the role of keratocytes and the fate of collagen remains unknown. Low angle X-ray scattering has shown an alteration in the orientation of collagen fibrils within the lamellae in the diseased cornea (117). Suggesting that loss of structural integrity, degradation, or insufficient repair mechanisms may be important in the disease (118).

Also, confocal microscopy studies showed a presence of microstriae that is evident in the whole stroma of the cornea, which also appears as multiple dark, and thin lines in comparison with the brighter stromal reflectivity. These microstriaes could result from the degenerative process that leads to changes in the extracellular collagen lamellae of the cornea (104). These microstriaes can appear as horizontal, vertical, oblique, or as reticular lines, and they appear to extend from the most anterior stroma to Descemet's membrane (**DM**) (104). The presence of Vogt's striae in the posterior stroma's reflectivity is consistent with pathological processes of the corneal stroma (100).

- **Collagen Matrix Deposition and Scar Formation.**

The proteomic data of keratoconus shows the presence of generalized decreases in the proteoglycans that form the proteins of the extracellular matrix, and they are of the types I, III, V, VI, and XII collagen, as well as lumican and keratocan proteins (64,97,119).

The expression of **TGF-β**, **IL-1**, vimentin, and tenascin (scar-associated matrix protein) was increased in the diseased cornea (120). An increase in type IX collagen was found and there was an altered pattern in endostatin (anti-angiogenic) that induces endothelial cell apoptosis (121).

The presence of fibronectin, collagen type III, tenascin, and laminin was localized most intensively in areas of defects in keratoconic corneas. The presence of these components are signs for wound healing response and scar formation (122–124). In keratoconus-associated hydrops, deposition of few amounts of fibro-nectinin in **DM** can be observed, and punctate staining with the most intense labeling of collagen III throughout the posterior stroma adjacent to **DM** has been also noted. Also, similarly staining for laminin in hydrops keratoconic corneas was observed in stroma adjacent to Bowman's and Descemet's membranes. **ECM** deposition localized in the stroma was found uniquely in areas of the corneal hydrops involvement (123).

- **Keratocytes**

Host keratocytes of the corneal stroma show alterations in morphology and number in keratoconus patients. It has been demonstrated that keratocyte density is lower in keratoconic corneas than in normal ones (110,111,125). keratocyte apoptosis appears to be increased in keratoconic cornea and this fact leads to a general reduction in keratocyte numbers (111). In recent studies, when comparing keratocyte density across corneal stroma, the cell density appeared to be lower in the anterior-most portion of the stroma compared to the more posterior regions. These observations reinforced the suggestion that keratoconus is primarily a disease of the anterior cornea. Histochemical analysis of the keratoconic stroma reported a general reduction of keratocytes at the anterior stroma when compared to normal corneas (126). In another report, it was noticed that the most anterior stromal cells, being activated keratocytes or non-keratocyte origin, sent cellular processes (pseudopodia) within **BM**, and towards the basal epithelial lamina (127). Therefore, it was hypothesized that this cellular activity is responsible for the degradation of corneal tissue in the anterior part of the stroma and that it may contribute to the collapse of epithelial cells towards **BM** (126,128,129).

Confocal microscopy studies showed changes in the morphology of keratocytes from the anterior to the posterior stroma. They had thin and consistent nuclei in the anterior stroma and more consistent and bigger nuclei size in the mid of the stroma. The morphology of the keratocytes in the posterior stroma was similar to the one in the middle stroma, but they are smaller and less bright (104,105).

1.1.4.4 Descemet's Membrane (DM).

Ruptures and folds in **DM** are a common feature in keratoconic corneas (130). The structural changes caused by these ruptures are not very clear. Different studies of extracellular matrix proteins did not reveal differences in the detection of collagen types I, III, IV, V, VI, or VIII between keratoconic or normal corneas, neither with laminin, entactin, and perlecan (113,131).

1.1.4.5 Endothelium.

The endothelium in many keratoconic corneas sustains a normal appearance. But in some cases, a detachment from the anterior layers could be observed. Even though, it has been observed some cellular abnormalities such as elongated pleomorphic cells containing dark intracellular structures, and endothelial cell loss (132,133). With confocal microscopy findings, the endothelial cell layer might show changes such as an increase in some cell area, and a decrease in cell density, polymegathism, and pleomorphism depending on the progression of the disease (104,105). This cell loss can be associated with cell apoptosis (110), but in general, is accompanied by **DM** rupture that would appear to be responsible for significant endothelial cell degradation (132) in keratoconus corneas.

1.1.5 KERATOCONUS CLASSIFICATION

Due to the great variability among patients with keratoconus, it is very important to grade this disease to provide some general guidance for the clinician regarding the level of progression and the treatment options that can be offered.

Various keratoconus classifications are depending on which principal factors are considered:

1.1.5.1 Amsler-Krumeich Classification.

The most widely used classification is the Amsler-Krumeich (1946) scale (134). This scale is based primarily on keratometric criteria but also includes other factors, such as refraction and pachymetry.

The grade's classification as per **Amsler-Krumeich (1946) scale** is distributed into 4 grades:

Grade 1

- Eccentric steepening.
- Mean keratometric readings < 48.00 diopter (D).
- Myopia and astigmatism less than 5.00 (D).

Grade 2

- Mean keratometric readings: 48.00 to 53.00 D.
- Myopia and astigmatism between 5.00 and 8.00 D.
- Absence of scaring or striae.
- Pachymetry > 400 micron (**µm**) at the thinnest point.

Grade 3

- Mean keratometric readings: 53.00 to 55.00 D.
- Myopia and astigmatism between 8.00 and 10.00 D.
- Absence of scaring or striae.
- Pachymetry between 300 and 400 **µm** at the thinnest point.

Grade 4

- Mean keratometric readings: > 55.00 D.
- Refraction not measurable.
- Striae or scarring.
- Pachymetry between 200 and 300 µm at the thinnest point.

1.1.5.2 Morphologic Classification.

The topographic methods can provide corneal aberrometric data, the Alio-Shabayek scale (2006) was developed (135). This scale is better suited to current diagnostic methods. In addition to the factors mentioned previously, it includes aberrometry of the anterior surface of the cornea, with special emphasis on comatic aberrations. These parameters are used because coma-like aberration values (and generally higher-order aberrations) tend to increase with increasing protrusion of the cone, and hence with disease progression.

This classification of **Alio-Shabayek (2006) scale** establishes the following 4 grades:

Grade 1

- Mean central keratometric reading: less than or equal to 48.00 D.
- Root Mean Square (**RMS**) of coma-like aberrations: between 1.50 and 2.50 µm.
- Absence of scaring or striae.

Grade 2

- Mean central keratometric readings: between 48.00 and 53.00 D.
- **RMS** of coma-like aberrations: between 2.50 and 3.50 µm.
- Absence of scaring or striae.
- Pachymetry over 400 µm at the thinnest point.

Grade 3

- Mean central keratometric readings: between 53.00 and 55.00 D.
- **RMS** of coma-like aberrations: Between 3.50 and 4.50 µm.
- Absence of scaring or striae.
- Pachymetry between 300 and 400 µm at the thinnest point.

Grade 4

- Mean keratometric readings: Over 55.00 D.
- **RMS** of coma-like aberrations: over 4.50 µm.
- Striae or scarring.
- Pachymetry between 200 and 300 µm at the thinnest point.

1.1.5.3 RETICS Classification.

As a result of the multicenter cooperative work by the thematic network, a functional scale based primarily on corrected distance visual acuity (**CDVA**) was finally developed and titled the RETICS classification (8,136). So far, many classification systems have been proposed to determine the severity of the corneal ectatic disease but most have been developed taking into consideration the topographical morphology of the disease without considering other clinical variables that are closely related to the patient's visual function. For this reason, the classification system we use determines the severity of the disease, taking into account functional and not purely geometric parameters. Variables presenting a highly significant correlation, such as internal astigmatism, visual loss, comma-like **RMS**, mean central keratometry, asphericity at 8 mm of corneal diameter are considered, and which are also directly related to the degree of visual limitation.

The main features of the **RECTIS classification** are presented in 5 grades:

Grade 1

- **CDVA**: > 0.9 (decimal).
- Internal astigmatism: Between 1.59 and 2.14 D.
- **RMS** of coma-like: between 1.16 and 1.52 µm.
- Mean central keratometric readings: between 44.75 and 45.40 D.
- $Q_{8\ mm}$: between –0.22 and –0.05.
- Pachymetry: between 495 and 510 µm.

Grade 2

- 0.6 < **CDVA** ≤ 0.9.
- Internal astigmatism: between 2.18 and 2.79 D.
- **RMS** of coma-like: between 1.82 and 2.31 µm.
- Mean central keratometric readings: between 46.03 and 46.93 D.
- $Q_{8\ mm}$: between –0.48 and –0.22.
- Pachymetry: between 475 and 493 µm.

Grade 3

- 0.4 < **CDVA** ≤ 0.6.
- Internal astigmatism: between 3.04 and 4.17.
- **RMS** of coma-like: between 2.65 and 3.32 µm.
- Mean central keratometric readings: between 48.21 and 49.27 D.
- $Q_{8\ mm}$: between –0.95 and –0.58.
- Pachymetry: between 451 and 470 µm.

Grade 4

- **CDVA** ≤ 0.4.
- Internal astigmatism: between 3.68 and 4.58 D.
- **RMS** of coma-like: between 3.45 and 4.42 µm.
- Mean central keratometric readings: between 51.42 and 53.12 D.
- $Q_{8\ mm}$: between –1.21 and –0.83.
- Pachymetry between 433 and 454 µm.
- Corneal striae or scarring in 60% of cases.

Grade PLUS

- **CDVA** < 0.2.
- Internal astigmatism: over 5.50 D.
- **RMS** of coma-like: over 5.50 µm.
- Mean central keratometric readings: over 57.00 D.
- $Q_{8\ mm}$: less than –1.50.
- Pachymetry between 360 and 420 µm.
- Striae or scarring.

1.1.6 TREATMENT AND CLINICAL MANAGEMENT OF KERATOCONUS

Keratoconus in many cases is accompanied by morphological changes in the corneal tissue where a progressive and severe irregular astigmatism is originated; In the initial stages, spectacle correction is adequate in patients who can achieve no less than 20/40 (137); When vision it cannot be corrected by spectacles and leads to deterioration in visual performance and optical quality of patients (133), the favorable visual rehabilitation of keratoconus patients is the rigid gas permeable (**RGP**) contact lenses since they are adjustable to corneal shape changes and they provide a superior visual rehabilitation. The management of this ectasia includes other techniques such as thermokeratoplasty procedures (nowadays neglected), corneal collagen **CXL**, intracorneal ring segments (**ICRS**), penetrating keratoplasty (**PKP**), and lamellar keratoplasty such as deep anterior lamellar keratoplasty (**DALK**), with newly proposed transplant modalities of the Bowman's layer transplantation described by Melles (2,138–144).

1.1.6.1 Keratoconus Management in Patients with Contact Lenses.

Recalling the first modern **CL,** it was introduced by Edwin Theodor Saemisch. He was the first to insert a **CL** into the eye for protective purposes. Later, in the late 1880s, Adolph Eugen Fick, Eugene Kalt, and August Müller worked independently on the first **CL** with the idea of optically correcting the human eye myopia (145,146).

In recent years, advances in the manufacture and design of **CL** to adapt lenses more adjusted to the type of cone have been supported by the development and creation of corneal topography, and **OCT**, making the adaptation of different types of **CL** for keratoconus safer and more effective (147,148). **CL** is the main treatment option for the visual correction of keratoconus and one of the

first treatments of choice in 90% of patients suffering from an irregularity of the corneal surface (138,147–149).

In the context of nonsurgical procedures, the adaptation of **CL** will be based on the same selection criteria of any **CL** fitting, and is a favorable alternative for the management of keratoconic corneas, to restore the quality of vision, delay surgical procedures, and improve the quality of life of these patients (150). **CL**, especially **RGP**, is considered the most common and successful method of treat mild and moderate keratoconus (151), but **CL** doesn't halt the progression of the cone comparing with other invasive surgical procedures.

The fitting of **CL** depends also on the severity of the ectatic disease progression, age, visual demand, **CL** tolerance, and corneal stability. Currently, there are several compensation options, given that there is no single **CL** design suitable for all cases of keratoconus (138,150,152–154):

- Soft **CL**, and soft toric **CL**.
- Rigid gas permeable (**RGP**) **CL**.
- Piggyback system (rigid lens on the soft lens).
- Hybrid lenses (rigid center and soft peripheral hydrophilic skirt).
- Mini-sclera, scleral, and corneoscleral **CL**.

In a briefing, due to the various designs available, the **CL** management in keratoconus provides the best visual rehabilitation and improves patients' quality of life (150).

1.1.6.2 Corneal Collagen Cross-Linking.

The term **CXL**, in the biological sciences, is used to describe the formation of chemical bridges following a chemical reaction between proteins and other molecules. These chemical bridges can be formed from chemical reactions initiated by heat, pressure, or radiation, in this way the physical properties of matter are changed. This procedure can generate stiffness or causing a loss of elasticity

of corneal collagen fibers, induce corneal **CXL** was performed by a research group at the Dresden Technic (155), Riboflavin (vitamin B2) and ultraviolet radiation (**UVA**) were used to increase the formation of cross-links between collagen fibers in the corneal stroma, producing a rigid effect capable of stopping the progression of ectasia.

Following along this line of thought, over the past decade, this technique has been introduced into clinical practice to treat corneal ectatic disorders, such as keratoconus, pellucid marginal corneal degeneration, and corneal ectasia after refractive surgery. Therefore, patients diagnosed with corneal ectatic disorders now have the possibility of detaining the disease progression thus avoiding more complex and severe treatments such as corneal transplantation (156). Then, patients diagnosed with ectatic corneal disorders can hold the progression of the disease by treating with **CXL**, to reduce the risk of progression in patients with a clear central cornea, and with progressive keratoconus with thinnest corneal thickness > 400 **µm**. Patients with thinner cornea are advised to perform the Hypoosmolar **CXL** (138).

1.1.6.3 Intracorneal Ring Segments.

CL is the favorable choice in rehabilitating the vision of keratoconic corneas, but they are prone to have risks like keratitis either non-infectious or infectious. The management becomes more challenging when patients are intolerant to rigid, hybrid, or scleral lenses or because of the instability of the **CL** due to extremely steep corneas. For this reason, the controlling of this ectasia in addition to the corneal collagen **CXL**, **ICRS** is a solution before proceeding to **PKP** and lamellar keratoplasty (**LKP**) (139–143).

Along with collagen **CXL** and thermoplastic techniques, **ICRS** has also been used in patients with keratoconus (128,130,145).This technique allows surgeons to reshape the cornea for therapeutic and refractive purposes. The use of this technique was introduced by Colin et al. (141).

Theoretically, it is proposed that the collagen fibers of the corneal tissue are separated by **ICRS** (157). Hence, the cornea will be flattened by an arc shortening effect of the corneal geometry induced by **ICRS**. The traction force generated by the end of each ring segment can induce additional flattening on a reference axis, thus correcting astigmatism. Some theoretical models based on finite element analysis have demonstrated that the flattening effect of **ICRS** is inversely proportional to the corneal diameter of implantation and directly proportional to the thickness of the segment. In other words, the smaller the diameter and the thicker the segment, the higher the flattening effect will be induced (158).

To obtain the best possible outcome after **ICRS** implantation, the clinician should be aware of the following preoperative indications (159): 1) Best-corrected visual acuity < 0,9 (decimal scale), 2) Internal astigmatism is less than 3 D, 3) Corneal thickness more than 250-300 **µm** in the site of the corneal tunnel (depending on the thickness of the **ICRS** to be implanted). 4) Absence of central corneal scarring.

Considering the types of Intracorneal Segments (156)**,** there are currently four main types of intracorneal segments: 1) Keraring, 2) Intacs, 3) Ferrara, and 4) Myoring.

ICRS present an important and valuable option for the treatment of corneal ectatic diseases, especially keratoconus. However, it is crucial to discuss with the patient their limitations and the inability to precisely predict their postoperative results.

1.1.6.4 Corneal transplantation.

Most specialists would agree that a patient with advanced keratoconus is eligible for corneal transplant when spectacle correction is insufficient, continued **CL** wear is intolerable (160), stromal scars are present in the visual axis, or when other treatment modalities such **UV-CXL** (160),

topography-guided photorefractive keratectomy (**PRK**) or **ICRS** may fail to improve the **CDVA** (138), and subsequently visual acuity drops to unacceptable levels and becomes deficient for the need of the patient. Therefore, corneal transplantation is described for advanced keratoconus with extreme thinning/steepening (138,144). Approximately about 12-20% of keratoconus patients may require corneal transplantation if no treatment is applied before (137).

Ramón Castroviejo, a Spanish ophthalmologist, performed the first **PKP** for keratoconus in 1936 (161). Several years later, he concluded that keratoplasty was the only surgical procedure that met the following requirements for the treatment of the keratoconic corneas: surgery had to be limited to the cornea, and the entire corneal bulge had to be removed and replaced by normal tissue of curvature and thickness, leaving the pupillary area free of scars. Based on his experience, when a proper technique was applied, the percentage of permanent vision improvement was among 75-90% (161).

LKP was described earlier than **PKP**. Arthur von Hippel performed the first successful **LKP** in humans in 1888, decades before Edward Zinn realized the first successful human **PKP**, but this technique was abandoned in 1914 and was not reintroduced until the 1940s, However, the concept of deep lamellar keratoplasty extending to **DM** is relatively new (2). The term **DALK** is attributed to the dissection of host tissue close to **DM** and was first introduced by Archilla in 1984, who also showed the use of intrastromal air injection to opacify the cornea to facilitate removal of host tissue (162). In the last two decades, **DALK** has gained popularity based on the improvement in surgical techniques and the availability of new surgical devices and instruments. Probably the two most relevant techniques were those from Melles and Anwar (2). In 1999 Melles described a technique to visualize the corneal thickness and the dissection depth during surgery creating an optical interface at the posterior corneal surface by filling the anterior chamber with air completely (163).

In 2002 Anwar described his popular “big-bubble” technique in baring **DM** by injecting air into the deep stroma to create a large bubble between the stroma and the **DM** (164). The percentage of lamellar corneal transplantation in keratoconus in which **DALK** was used increased over years (160,165). Currently, an elective **PKP** is used for advanced keratoconus cases only if **DM** and endothelium damage is present, due to previous corneal hydrops, or when deep stromal scars involving the **DM** are observed (2).

In general, **PKP** offers good long-term visual rehabilitation for keratoconic patients. The rejection rate has been reported to be 5.8-41% with long-term follow-up (166–170). Most studies found equivalent refractive and visual outcomes between **PKP** and **DALK** as long as stromal dissection reaches the level or close to **DM** (165,171–175). However, **DALK** is preferred in patients with keratoconus because of the absence of risk of endothelial rejection, earlier tapering of steroids, decreased risk of secondary glaucoma, and increased would corneal strength.

1.2 PROGRESSING TOWARDS A NEW TYPE OF ADVANCED CORNEAL THERAPY IN KERATOCONUS

Cellular therapy of the cornea is to be considered as a promising advanced therapeutic approach for corneal diseases. However, the use of autologous human ocular keratocytes has many disadvantages, such as difficulties in its isolation, limitations in the availability of cells with high populations, and inefficient cell subculture (176)**.** Corneal stromal stem cells have the same limitation of requiring healthy corneal donor tissue. Meanwhile, stem cells from extraocular sources have demonstrated that they may be a more favorable and adequate source for the regeneration of the human corneal stroma (21,22,30,31,177–180). At present, advanced corneal therapy could be a promising approach to overcome these limitations, certainly when stem cells are combined with the use of scaffolds; here, in this project thesis, we will discuss the application of mesenchymal stem cells combined with decellularized laminas obtained from healthy donors.

1.2.1 STEM CELL SOURCES USED FOR CORNEAL STROMA REGENERATION

The cornea provides two-thirds of the refractive power of the eye and is composed of five well-defined layers (Figure. 1A), including three cellular layers separated by two acellular membranes. The phenotype of corneal diseases is seen when one or more layers of the cornea are affected. Loss of the corneal epithelial cells (**CECs**), the steering factor for many corneal diseases, is primarily due to the loss of epithelia-replenishing limbal epithelial stem cells (**LESCs**). Other factors may affect the corneal stroma (**CS**) regeneration such as corneal endothelial cells (**CEnCs**), where both **CS** and **CEnCs** derive from the neural crest cells **NCCs** which rise from the **MSCs**.

Hereafter, we will discuss briefly the main sources of **MSCs** and their involvement in corneal stroma regeneration.

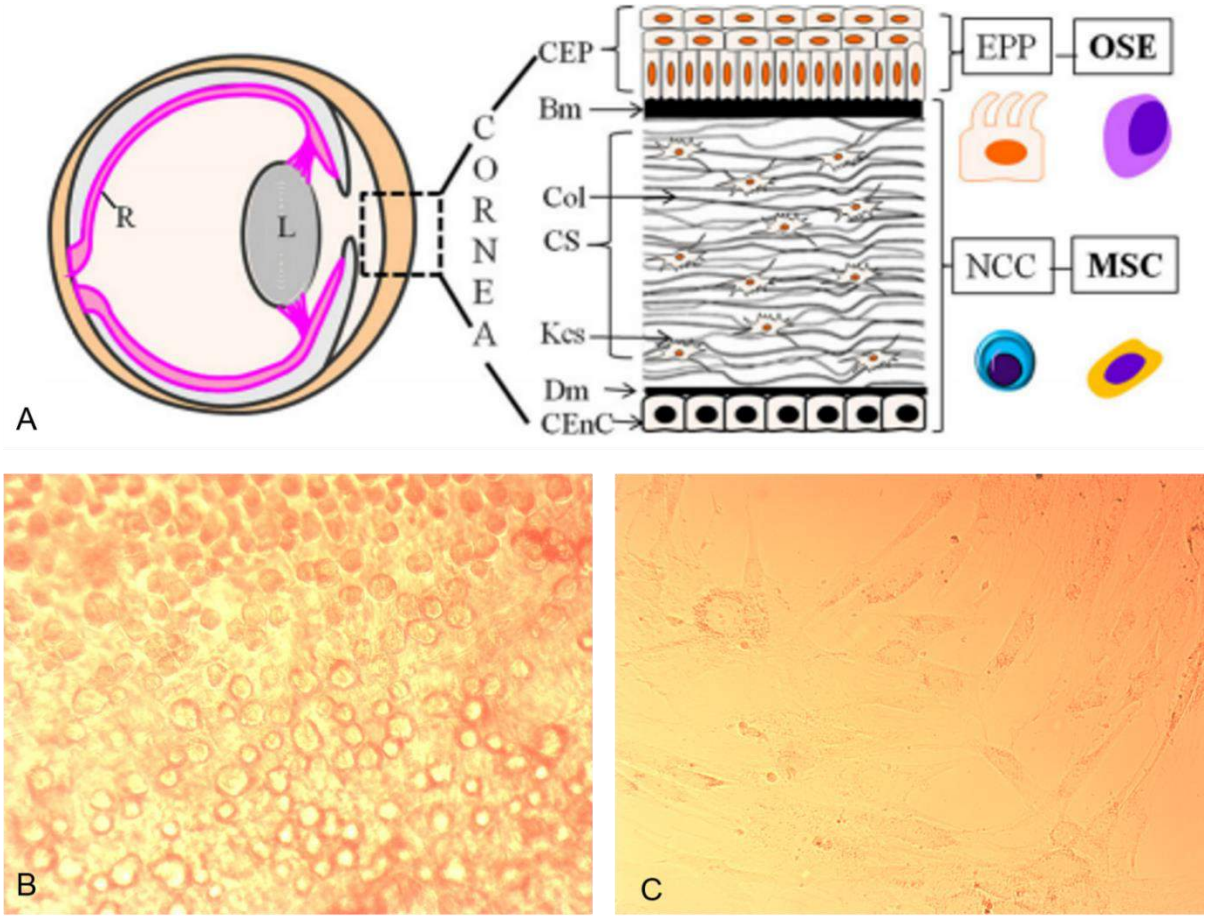

Figure 1. Microanatomy of the cornea. The appearance of human **ADASCs** in culture.
(**A**) Schema of layers in the cornea and its development. The cornea constitutes of three layers: the corneal epithelial cells: **CECs**, Corneal Stroma: **CS**, and Corneal endothelium: **CEn**, and two acellular membranes. The Bowman membrane: **BM** separating the corneal epithelium: **CEP**, and **CS**. Descemet Membrane: **DM**, sandwiched between **CS** and corneal endothelial cells: **CEnC**. The **CEP** is derived from the **EPP:** Epithelial precursors originating from the ocular surface ectoderm cells: **OSEs**. Both **CS** and **CEnCs** derive from the neural crest cells: **NCCs** which rise from **MSCs**. The figure is taken from the scientific paper with reference Chakrabarty et al. (181). **(B)** Microscopic appearance (phase-contrast photograph) of human **ADASCs** (10× magnification). **(C)** Human **ADASC** in culture. The figure is taken from the scientific chapter refered to Alió JL et al. (41).

1.2.1.1 Adipose-derived Adult Mesenchymal Stem Cells (ADASCs).

Adipose-derived adult stem cells (**ADASCs**) have raised large interest in regenerative medicine and are used widely in cell therapy. Their low immunogenicity and their ability to self-

renew, differentiate, migrate into damaged sites, and act through autocrine and paracrine pathways have been altogether stated as the main mechanisms whereby cell repair and regeneration occur. Stromal vascular fraction (**SVF**) freshly isolated from adipose tissue was considered for more suitable satisfactory tissue regeneration as it contains multipotent stem/stromal cells (called adipose-derived stem cells (**ADASCs**) widely reported for their proliferative and differentiation behavior. Moreover, in addition to stromal elements, **SVF** contained a high percentage of multiple lineages of endothelial, hematopoietic, and pericytic origin (182–185). After ***isolation and culture*** of **SVF** as described previously (186,187), adherent cells indicate the presence of homogeneity or heterogeneity of undifferentiated **ADASCs**.

Flow cytometry analysis provided evidence of the ***immunophenotyping*** of **ADASCs**; the guidelines for their characterization showed that certain markers are positively expressed contrary to others that are not expressed (187):

- **Positive markers:**
  - **Primary positive markers**: stable markers such as CD13, CD29, CD44, CD73, CD90, CD105 (>80% in **ADASCs**), and unstable markers such as CD34 (present at variable levels).
  - **Secondary positive markers**: CD10, CD26, CD36, CD49d, CD49e
- **Negative markers:**
  - **Primary negative markers**: CD31, CD45, CD235a (<2%).
  - **Secondary low or negative markers**: CD3, CD11b, CD49f, CD106, PODXL.

Without culture, freshly isolated **ADASCs** were revealed to be highly positive for CD34, and positive for CD117 and human leukocyte antigen – DR isotype (**HLA-DR)**. Meanwhile,

ADASCs when obtained by culture are mostly negative for CD34, and **HLA-DR**. This indicates clearly that primary cells are significantly more promising in case we need to maintain a certain level of CD34 in the graft (186,188); however, for a significant impact of mesenchymal cells, cultured **ADASCs** must be considered especially for differentiation.

Besides, **ADASCs** have ***immune-modulatory effects*** and ***proliferative*** characteristics: first, a recent preclinical study suggested that the **MSCs**, specially **ADASCs** downregulated numerous markers of inflammation at the **mRNA** level such as **IL-1α, IL-1β, IL-6, IL-10, TNF-α,** granulocyte colony-stimulating factor **(G-CSF),** monocyte chemoattractant protein-1 (**MCP-1**), macrophage inflammatory protein-1α (**Mip-1α**), keratinocyte chemoattractant (**KC**), leukocyte inhibitory factor **(LIF),** and upregulate the proangiogenic growth factor **VEGF** (189)**.** Implantation of **ADASCs** should be used if inflammatory cytokines have gone down to a maximum of 500 pg/ml **IL**-6 and 30 pg/ml **IL**-8 (30). **ADASCs** stimulate macrophage change immunity and inhibit T and Dendritic cells, inducing angiogenesis, a decrease in apoptosis, and fibrosis with an increase in the anti-inflammation process. Also, **ADASCs** showed higher rates of proliferation when expanded *in vitro* (190). These **ADASCs** features altogether seemed to promote them in tissue repair, where cell proliferation, angiogenesis, and anti-inflammatory processes were expected to occur rapidly in damaged sites. For transplantation uses in keratoconus applications, **ADASCs** must be in a ***quiescence*** state where proliferation is stopped and the differentiation process is initiated (21).

The **h-ADASCs** cultured *in vitro* (Figures. 1B, 1C) under keratocyte ***differentiation*** conditions express collagens and other corneal-specific matrix components. This expression is quantitatively similar to that achieved by differentiated human corneal stromal stem cells (**h-CSSCs)** (191). The differentiation of **h-ADASCs** in functional human keratocytes has also been demonstrated *in vivo*, for the first time, in a previous study by our group using the rabbit as a model

(21). Before transplantation, the multipotency of **h-ADASCs** must be established by inducing their ***differentiation*** toward mesodermal, endodermal, and ectodermal lineages (190). These cells, once implanted in the stroma, express not only collagens type I and VI (the main components of corneal extracellular matrix), but also keratocyte-specific markers such as keratocan and **ALDH.** A recent study *in vitro* reported that retinoic acid (**RA**) supplementation enhanced the differentiation of **ADASCs** towards a keratocyte phenotype. The differentiated **ADASCs** showed upregulation of keratocan, increased the amount of collagen type I, and **ECM**, and enhanced the expression of keratocan, aldehyde dehydrogenase 3A1, lumican, and decorin. Meanwhile, **RA** supplementation reduced the formation of fibrotic tissue, this newly investigated fact is interesting for our study (192).

1.2.1.2 Bone Marrow Mesenchymal Stem Cells (BM-MSCs).

Park et al. reported that human **BM-MSCs** differentiate *in vitro* into keratocyte-like cells when they are grown into specific keratocyte differentiation conditions (193). They demonstrated a strong expression of keratocyte markers such as lumican and aldehyde dehydrogenase (**ALDH**) along with the loss of expression of **MSCs** markers such as α-smooth muscle actin. However, they could not demonstrate an evident expression of keratocan on these differentiated cells (193). Trosan et al. showed that mice **BM-MSCs** cultured in corneal extracts and insulin-like growth factor-I (**IGF-I**), efficiently differentiate into corneal-like cells with expression of corneal specific markers, such as cytokeratin 12, keratocan, and lumican (194). The survival and differentiation of human **BM-MSCs** into keratocytes have also been demonstrated *in vivo* when these cells are transplanted inside the corneal stroma. Keratocan expression was observed without any sign of immune or inflammatory response (195).

1.2.1.3 Umbilical Cord Mesenchymal Stem Cells (UCMSCs).

Human **MSCs** isolated from neonatal umbilical cords have exhibited similar differentiation behavior to other types of **MSCs** when transplanted inside the corneal stroma *in vivo*, expressing keratocyte-specific markers such as keratocan without inducing immune or rejection responses (196). Liu et al. reported that the injection of these cells inside the corneal stroma of lumican null mice improved corneal transparency and increased stromal thickness with reorganized collagen lamellae, and also improved host keratocyte function through enhanced expression of keratocan and **ALDH** in these mice (26). These data are encouraging, although to date, autologous use of Umbilical Cord Mesenchymal Stem Cells (**UCMSCs**) is not possible as the umbilical cord from new births is not systematically stored with the limitations of time for long storage.

1.2.1.4 Embryonic Stem Cells (ESCs).

Current experience with these human **ESCs** for corneal stroma regeneration is much more limited. Chan et al. reported that differentiation of these cells into a keratocyte lineage can be induced *in vitro*, demonstrating an upregulation of keratocyte markers including keratocan (197).

To the best of our knowledge, no *in vivo* studies with these cells have been performed in the field of regenerative medicine for the corneal stroma. The use of these cells also raises many ethical issues, and together with the lack of *in vivo* data, discourages their current use in a clinical setting.

1.2.1.5 Induced Pluripotent Stem Cells (iPSCs).

As already discussed, the use of **ESCs** has been partially abandoned because of ethical concerns and especially since the discovery of **iPSCs** (37), which are derived from adult cells. In 2012, Shinya Yamanaka from Japan and John B. Gurdon from the UK received the Nobel Prize for Medicine for discovering that mature, specialized cells can be reprogrammed to an immature or

stem cell state and then redirected to the required cell lineage using specific factors and environmental stimuli. **iPSCs** promise to be the future of tissue and cellular engineering (37,198,199).

Regarding their application in the regeneration of the corneal stroma, human **iPSCs** have shown the capability to differentiate into neural crest cells (the embryonic precursor to keratocytes). By culturing them on the cadaveric corneal tissue, it promotes their keratocyte differentiation by acquiring a keratocyte-like morphology to express markers similar to corneal keratocytes (38,181). It has also been shown that **iPSCs**-derived **MSCs** exert immunomodulatory properties in the cornea similar to those observed with **BM-MSCs** (200). To the best of our knowledge, no studies have been published reporting the capability of **iPSCs** to differentiate into adult keratocytes *in vivo* in the animal model.

1.2.1.6 Corneal Stromal Stem Cells (CSSCs).

The limbal palisades of Vogt form a niche that contains **LESCs** and **CSSCs** (201). **CSSCs** express genes typical of descendants of the neural ectoderm such as Paired box homeotic gene 6 (**PAX6)**, adult stems cell markers such as **ABCG2**, and **MSCs** markers such as **CD73** and **CD90** (5,201). They exhibit clonal growth, self-renewal properties, and potential for differentiation into multiple distinct cell types. Unlike keratocytes, **h-CSSCs** undergo extensive expansion *in vitro* without losing their ability to adopt a keratocyte phenotype (5,201). These corneal **MSCs** have a demonstrated potential for differentiation into the corneal epithelium and adult keratocytes *in vitro* (201,202). When cultured on a substratum of parallel aligned polymeric nanofibers, **h-CSSCs** produce layers of highly parallel collagen fibers with packing and fibril diameter indistinguishable from that of the human stromal lamellae (203). The ability of **h-CSSCs** to adopt a keratocyte function has been even more striking *in vivo*. When injected into the mouse corneal stroma, **h-**

CSSCs express keratocyte **mRNA** and protein, replacing the mouse **ECM** with human matrix components. These injected cells remain viable for many months, apparently becoming quiescent keratocytes (25).

All these experimental data have raised interest in this novel cell-based therapy for corneal stromal diseases, however, before its application in clinical practice, its efficacy and safety need to be well proven in human clinical trials, while other limitations such as the high laboratory costs and potential therapeutic efficacy differences among different donors have to be given serious consideration.

1.2.2 CORNEAL STROMA REGENERATION TECHNIQUES: EARLY APPLICATION IN THE CLINICAL PRACTICE

All these types of stem cells have been used in various ways in several research projects to find the optimal procedure to regenerate the human corneal stroma. Corneal **MSCs** implantation has been assayed and studied by direct intrastromal transplantation or after implantation from the ocular surface, intravenously and the anterior chamber where cellular migration within the stroma is to be expected. Different cellular carriers have been analyzed to enhance the potential benefits of this therapy.

1.2.2.1 Ocular Surface Implantation of Stem Cells.

Surface implantation of **MSCs** would be the optimal approach for ocular surface reconstruction and **LESCs** niche regeneration. However, surface implantation of **MSCs** would still play a role in the prevention or modulation of anterior stromal scars after an ocular surface injury (like a chemical burn). As discussed previously, **MSCs** secrete paracrine factors that enhance

corneal re-epithelialization and stromal wound healing (33). Thus, the benefit of **MSCs** on the ocular surface may be more justified by these paracrine effects rather than by direct differentiation of the **MSCs** into epithelial cells, as the evidence for the latter is controversial. In this respect, Di et al. assayed *subconjunctival injections* of **BM-MSCs** in diabetic mice and reported an increased in **CECs** proliferation as well as an attenuated inflammatory response mediated by tumor necrosis factor-α-stimulated gene 6 (**TSG6)** (204).

Holan et al. suggested **MSCs** application on the ocular surface using *nanofiber scaffolds*. They reported that **BM-MSCs** grown on these scaffolds can enhance re-epithelialization, suppress neovascularization and local inflammatory reaction when applied on an alkali-injured eye in a rabbit model, and these results were comparable to those obtained with limbal epithelial stem cells, and both were better than those obtained with **ADASCs** (205). The same group suggested that these results can be improved when these nanofiber scaffolds seeded with rabbit **BM-MSCs** are covered with cyclosporine-A (**CSA**) loaded nanofiber scaffolds, observing an even greater scar suppression and healing results with the combination of both nanofibers **MSCs** and **CSA** (206).

Topical application of a suspension of autologous **ADASCs** has been reported in an isolated clinical case report where authors describe the healing of a neurotrophic ulcer that is not responsive to conventional treatment (207). The lack of further scientific evidence for this delivery method since 2012 raises questions about its real efficacy.

Finally, Basu et al. suggested the delivery of **MSCs** using *fibrin glue* (36). The resuspended **CSSCs** in a solution of human fibrinogen and this was added onto a wounded ocular surface with thrombin on the wound bed. Subsequently the fibrinogen gels. Using this application, they demonstrated the prevention of corneal scarring in the mouse model together with the generation of a new stroma with a collagen organization indistinguishable from that of native tissue. Currently,

this group is enrolled in a clinical trial to validate these findings, using autologous and heterologous **CSSCs** from limbal biopsies for cases of chemical burns, neurotrophic ulcers, and established scars. The preliminary report showed an improvement in visual parameters, corneal epithelization, corneal neovascularization, and corneal clarity (208).

1.2.2.2 Intrastromal Implantation of Stem Cells Alone.

Direct *in vivo* injection of stem cells inside the corneal stroma has been assayed in some studies, demonstrating the differentiation of stem cells into adult keratocytes without signs of immune rejection. In our study, we also demonstrated the production of human **ECM** by immunohistochemistry when **h-ADASCs** were transplanted inside the rabbit cornea (Figures. 1B, 1C, 2A, 2B) (21). As expected, collagen types I and VI were found to be expressed in the rabbits' corneal stroma as well as in the transplanted **h-ADASCs**. Collagen types III and IV, not normally expressed in the corneal stroma, were not detected either in the host corneal stroma or in the transplanted **h-ADASCs** (Figure. 2C). Du et al. (25) reported restoration of corneal transparency and thickness in lumican null mice (thin corneas, haze, and disruption of the normal stromal organization) three months after intrastromal transplant of human **CSSCs**. They also confirmed that human keratan sulfate was deposited in the mouse stroma and the host collagen lamellae were reorganized, concluding that delivery of **h-CSSCs** to the scarred human stroma may alleviate corneal scars without requiring surgery (25). Very similar findings were reported by Liu et al. who utilized **h-UMSCs** using the same animal model (26). Coulson-Thomas et al. found that, in a mouse model for mucopolysaccharidosis, transplanted **h-UMSCs** participate both in extracellular glycosaminoglycans (**GAGs**) turnover and enable host keratocytes to catabolize accumulated **GAGs** products (27).

Recently, our group has published the first clinical trial in which the preliminary safety and efficacy of the cellular therapy of the human corneal stroma is reported (30,177). In this pilot clinical trial, we implanted autologous **ADASCs** (obtained by elective liposuction) in a mid-stroma femtosecond laser-assisted lamellar pocket in patients with advanced keratoconus (Figures. 1B, 1C). No signs of inflammation or rejection were observed, confirming all previous evidence reported in the animal model (30,177).

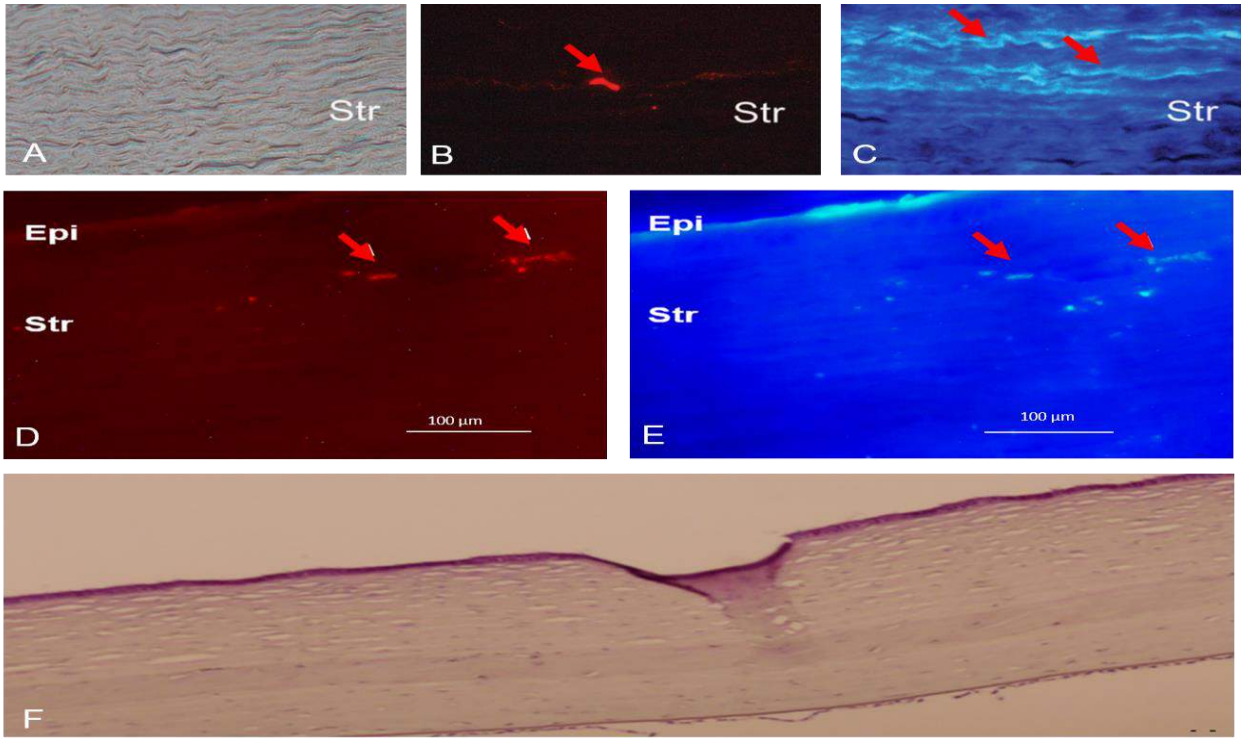

Figure 2. In vivo observation of human **ADASCs** in rabbit corneal stroma.
(A, B, C) Transplantation of human **ADASCs** into the thickness of the rabbit stroma *in vivo*. **(A)** Phase-contrast photo showing a morphologically intact stroma 3 months after transplantation. **B)** The Same section showing the survival of the implanted cells by detecting the Vybrant **CM-DiL** dye (red arrow). (**C)** The same section showing the expression of new human type I collagen inside the rabbit stroma (Str: Stroma; Magnification, 400X) (red arrows). Photo courtesy of Dr. Arnalich Montiel. Abbreviation: Str: Stroma **(D, E, F)** Corneal stroma enhancement with implantation of decellularized/recelularized human corneal stroma with **h-ADASCs** in the rabbit animal model. **(D)** Human cells (red arrows), labeled with **CM-DiI**, around and inside the implant confirming the presence of living human cells inside the rabbit corneal stroma. **(E)** Same section showing human keratocan and their eventual differentiation into human keratocytes (red arrows) (magnification 400×); Abbreviation: Epi: epithelium. **(F)** Hematoxylin-eosin staining of a rabbit cornea with an implanted graft of decellularized human corneal stroma with **h-ADASCs** colonization (magnification 200×). The figure is taken from the scientific chapter referred to Alió JL et al. (41).

1.2.2.3 Intrastromal Implantation of Stem Cells Together with a Biodegradable Scaffold.

To enhance the growth and development of the stem cells injected into the corneal stroma, transplantation together with biodegradable synthetic **ECM** has been performed. Espandar et al. injected **h-ADASCs** with a semisolid hyaluronic acid hydrogel into the rabbit corneal stroma and reported better survival and keratocyte differentiation of the **h-ADASCs** when compared with their injection alone (Figures. 3A, 3B) (22). Ma et al. used rabbit **ADASCs** with a polylactic-co-glycolic biodegradable scaffold in a rabbit model of stromal injury wherein they observed newly formed tissue with successful collagen remodeling and less stromal scarring (Figures. 3A-3C) (209). At three months a high extrusion rate of the implant was observed (Figures. 3D, 3E). Initial data show that these scaffolds could enhance stem cell effects on the corneal stroma, although further research is required and warranted.

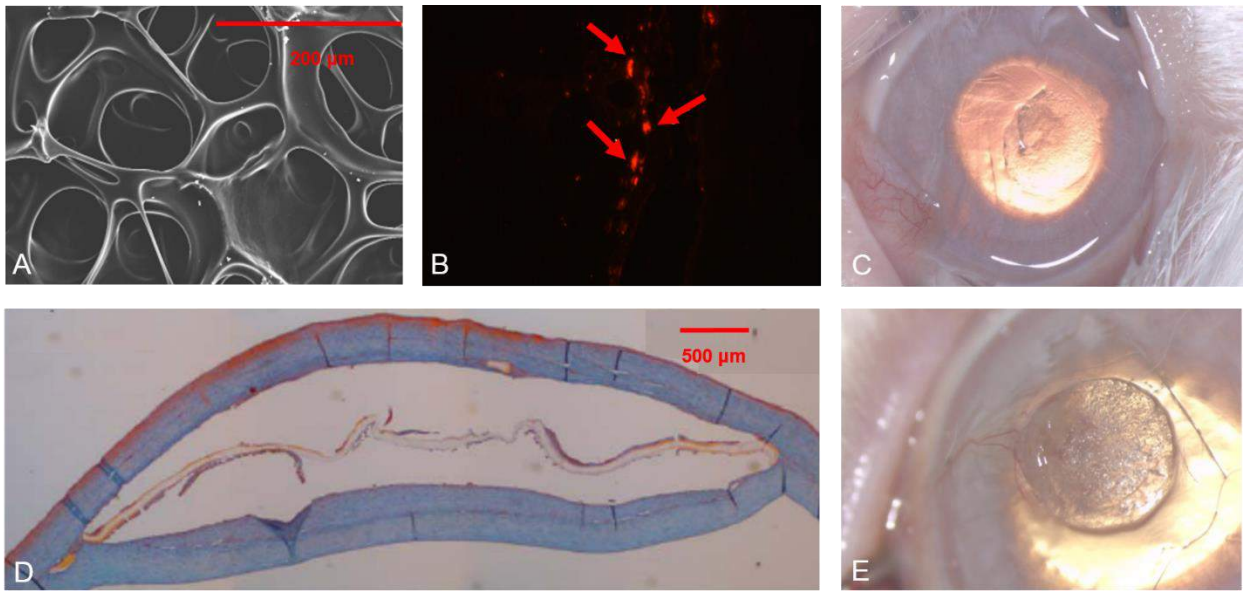

Figure 3. Transplantation of macroporous membranes of poly-ethyl-acrylate (**PEA**) membranes together with human **ADASCs** into the rabbit stroma *in vivo*.
(A) Electron microscopy image of the PEA. **(B) ADASCs** survivors after 3 months (red arrows). **(C)** Intrastromal implant *in vivo*, note its transparency. **(D)** The absence of a real biointegration leads to the detachment of the sheet of **PEA** from the surrounding stroma in the histological sections. **(E)** A high extrusion rate of the implant was observed. The figure is taken from the scientific chapter with reference Alió JL et al. (17,41).

1.2.2.4 Intrastromal Implantation of Stem Cells with a Decellularized Corneal Stroma Scaffold.

The complex structure of the corneal stroma has still not been replicated and there are well-known drawbacks to the use of synthetic scaffold-based designs: i) strong inflammatory responses induced on their biodegradation and ii) nearly all polymer materials cause a nonspecific inflammatory response (17).

Recently, several corneal decellularization techniques have been described, which provide an acellular corneal **ECM** (18). The ideal decellularization protocol must completely:

- Remove cellular content and antigen molecules from the xenograft to reduce a host immune reaction (210).
- Preserves the structural and functional proteins of the **ECM** without altering the general tissue matrix (211).
- Conserve corneal transparency (212).
- Support growth of host and corneal cells (213).

All decellularization methods can result in some disruption of the **ECM** ultrastructure, however, the decellularization process must be optimized trying to minimize these undesirable effects (214). Complete decellularization is achieved by combinations of chemical, physical, and enzymatic methods (215,216).

Recent studies performed different methods for decellularization, we summarized a brief of these methodologies:

1. **Physical treatments**: Include shaking, pressing, and freezing/thaw processes that serve to lyse cells, facilitate their rinsing, and remove of cellular content from the **ECM** (216).

2. **Chemical methods**: Consists of different methodologies among them:

- Acids or base treatments are often used in combination with other methods such as detergents and alcohols (211,217).
- Ionic and non-ionic detergents have been used in decellularization protocols with varying degrees of success. Ionic detergents, such as sodium dodecyl sulfate solution (**SDS)**, are extremely effective in the solubilization of cellular membranes but can cause denaturation of the proteins and sometimes affects the structure of the **ECM** (218). Non-ionic detergents are generally considered to be mild and relatively non-denaturing, as they break lipid-lipid and lipid-protein interactions rather than protein-protein interactions (218).
- Hypotonic and hypertonic treatments with deionized water and sodium chloride solutions can cause cells to lyse within a tissue or organ (216).
- Alcohols, such as ethanol, remove lipids from tissue and thus disrupt the cellular membrane (211). This method succeeded a complete cell removal and preserved the structure and transparency of the original corneal tissue.
- Chelating agents, such as Ethylenediaminetetraacetic acid **EDTA**, are often used in combination with other decellularizing agents including **SDS** (219).

3. **Biological methods**: Enzymatic agents, such as nun-cleases and phospholipase A2, are usually used in combination with other techniques to reach complete decellularization. Aprotinin, a competitive serine protease inhibitor, is habitually used in combination with detergent treatment to avoid enzymatic degradation of extracellular matrix proteins (215,220).

4. **Electron beam radiation (e-beam)**: Corneal tissue has been treated with electron beam radiation (e-beam), and stored in recombinant Human Serum Albumin. The use of (e-beam)

showed great success in many ophthalmic procedures because it increases the sterility of corneal tissues (221).

The decellularized tissue has gained attention in the last few years as they provide a more natural environment for the growth and differentiation of cells when compared with synthetic scaffolds. Besides, components of the **ECM** are generally conserved among species and are well tolerated by xenogeneic recipients. Moreover, keratocytes are essential for remodeling the corneal stroma and for normal epithelial physiology (222). This highlights the importance of transplanting a cellular substitute together with the structural support (acellular **ECM**) to undertake these critical functions in corneal homeostasis.

To the best of our knowledge, all attempts to repopulate decellularized corneal scaffolds have used corneal cells (213,217,223), but as already discussed, these cells have significant drawbacks that limit their autologous use in clinical practice (damage to the donor tissue, lack of cells and more difficult cell subcultures), thus redirecting efforts to find an extraocular source of autologous cells. In a previous study by our group, we showed the perfect biointegration of human decellularized corneal stromal laminas (100 **µm** thickness) with and without **h-ADASCs** colonization inside the rabbit cornea (Figures. 2D, 2F), and observed no rejection response despite the graft being xenogeneic (17). We also demonstrated the differentiation of **h-ADASCs** into functional keratocytes inside these implants *in vivo*, which then achieved their proper biofunctionalization (Figures. 2D, 2E). In our experience, decellularization of the whole (~500 µm) corneal stroma (using sodium dodecyl sulfate anionic detergent) lacks efficacy, as it not possible to completely remove the whole cellular component. However, we demonstrated that this method completely removes the cellular component and preserves the tissue integrity of the corneal stroma when thinner lenticules are treated; a method that has been later confirmed by other authors with

the use of electron microscopy (19,224,225). Others have also assayed the integration of decellularized pig articular cartilage **ECM** colonized with mice **BM-MSCs** in the rabbit corneal stroma and reported similar findings, although the transparency of these decellularized scaffolds was not clearly reported (226).

In our opinion, the implantation of **MSCs** together with decellularized corneal **ECM** would be the best technique to effectively restore the thickness of a diseased and severely weakened human cornea because the implantation of **MSCs** alone only achieves a limited new **ECM** formation and thickness restoration (21,30). Moreover, through this technique, and by using autologous **MSCs** from a given patient, it is theoretically possible to transform allogenic grafts into functional autologous grafts, thus avoiding any risk of rejection.

Decellularized tissues have the drawback of requiring specific laboratory equipment, although eye banks could potentially do it and deliver such grafts to different clinical centers. Keratophakia (intrastromal insertion of an allogeneic lenticule) was described by Barraquer in 1964 but was abandoned due to the unpredictability of the refractive outcome and the relatively high frequency of interface haze development (227). The lack of haze observed in our pilot clinical trial could be related to the absence of donor keratocytes that could potentially activate postoperatively and generate scar tissue. Moreover, rejection episodes have already been described after the implantation of allogeneic lenticules, a risk that is theoretically avoided by the use of decellularized grafts (225). We should consider that as long as human decellularized tissue is used, there will be no risk for zoonotic diseases.

1.2.2.5 Anterior Chamber Injection of Stem Cells.

Demirayak et al. reported that **BM-MSCs** and **ADASCs**, suspended in phosphate-buffered solution (**PBS**) and injected into the anterior chamber after a penetrating corneal injury in a mouse

model, can colonize the corneal stroma and increase the expression of keratocyte specific markers such as keratocan, with a demonstrated increase in keratocyte density by confocal microscopy (24). Conversely, the possible side effects of this **MSCs** injection into the anterior chamber for the lens epithelium and trabecullum is highly questionable as it may induce scarring and subsequent glaucoma. Considering this, the potential clinical use of this approach, in our opinion, is limited.

1.2.2.6 Intravenous Injection of Stem Cells.

Systemic use, by intravenous injection, of **MSCs** has also been tested. Intravenous injection of **BM-MSCs** in mice after an allograft corneal transplant was able to colonize the transplanted cornea and conjunctiva (inflamed ocular tissues) but not the contralateral ungrafted cornea, simultaneously decreasing immunity and significantly improving allograft survival rate (228). Yun et al. recently reported similar findings with the intravenous injection of **iPSCs**-derived **MSCs** and **BM-MSCs** after a surface chemical injury, where they observed that the corneal opacity, inflammatory infiltration, and inflammatory markers in the cornea were markedly decreased in the treated mice, without significant differences between both **MSCs** types (200). In contrast, our group did not observe any benefit in corneal allograft survival and rejection rates after systemic injection of rabbit **ADASCs** before surgery, during surgery, and at various times after surgery in rabbits with vascularized corneas (model more similar to human corneal transplants than those reported in mice). A shorter graft survival compared with the non-treated corneal grafts was noted (229).

1.2.3 AUTOLOGOUS VERSUS ALLOGENIC MSCs

A critical question for future clinical trials to further assess the feasibility of cellular therapy of the corneal stroma is whether the use of autologous **MSCs** is really necessary and whether

allogenic **MSCs** could achieve the same benefit without any risk of inflammation or rejection. If we consider all published evidence in the animal model where human **MSCs** were implanted in the corneal stroma, despite being a xenogeneic transplant, no signs of rejection or inflammation have ever been reported (17,19,21–28). This coincides with the strong evidence regarding the immunomodulatory and immunosuppressive properties of **MSCs**, which help them to evade host immune rejection and survive by inhibiting adhesion and invasion and inducing cell death of inflammatory cells, partially due to a rich extracellular glycocalyx that contains **TSG6** (29,230). **TSG6** has been demonstrated to play a critical role in the immunosuppressive properties exhibited by **MSCs** (28,200,204). Taken together, the use of allogenic **MSCs** would greatly simplify the clinical application of **MSCs**, as clinical application centers would not need any specific equipment because potential **MSCs** banks could store and supply stem cells for their use in patients. There are already low-cost systems available that are capable of enhancing the preservation of **MSCs** at hypothermic temperatures while maintaining their normal function, in this way widening the time frame for distribution between the manufacturing site and the clinic, and reducing the waste associated with the limited shelf life of cells stored in their liquid state (231). Funderburgh et al. recently reported that **MSCs** from different donors may have different immunosuppressive properties, and consequently, different abilities to regenerate and relieve stromal scars (232). Considering this important finding, the best donors could be selected by **MSCs** banks to expand and supply only those **MSCs** with the highest immunosuppressive and regenerative capacity, so autologous cells would not be necessary. We should also consider that adult keratocytes obtained from autologous **MSCs** may still carry the same genetic defect that led to corneal disease such as in the case of corneal dystrophy. In this scenario, the use of allogenic instead of autologous **MSCs** would be interesting. A recent study observed gene expression differences between the **iPSCs**-derived keratocytes generated from fibroblasts of both keratoconic and normal human corneal

stroma, influencing cellular growth and proliferation, confirming that, at least in keratoconus cases, adult cells obtained from **MSCs** may still not be functionally normal (233).

1.2.4 MSCs EXOSOMES

Exosomes are nano-sized extracellular vesicles that originate from the fusion of intracellular multivesicular bodies with cell membranes and are released into extracellular spaces (230). They have been implicated in the ability of **MSCs** to repair damaged tissue. Basu S. et al. recently showed that exosomes isolated from the culture media of human **CSSCs** had similar immunosuppressive properties and also significantly reduced stromal scarring in wounded corneas *in vivo* (208). This finding suggests that for some diseases, such as prevention or reduction of corneal scars, **MSCs** exosomes may provide a non-cell-based therapy (232). Zhang et al. suggested that exosomes released by transplanted **UCMSCs** in the diseased cornea can enter into host corneal keratocytes and endothelial cells, on the way to enhance their functions (230). Authors experimented *in vitro* using mucopolysaccharidosis VII mice, they discovered that **UCMSCs** -secreted exosomes assisted in the recycling process of **GAGs** in the lysosomes of diseased cells (27). These findings open an exciting new field for research as the use of exosomes may overcome some of the limitations and risks associated with intrastromal cellular injection, given that exosomes can be potentially applied topically (196).

2. JUSTIFICATION OF THE DOCTORAL THESIS

In the last decade, full-thickness penetrating keratoplasty has been partially displaced by lamellar techniques where only diseased layers are replaced, such as **DALK** for the corneal stroma (234). This technique avoids endothelial rejection, which is the most common cause of graft failure, but they still have some disadvantages such as primary immune stromal rejection or high post-operative suture-related astigmatism (235,236)**.** To avoid these drawbacks, we have developed a new model for autologous lamellar keratoplasty, which starts from allogeneic donor tissue.

Cellular therapy of the corneal stroma is a promising therapeutic approach, but the use of autologous human keratocytes has many disadvantages, such as causing damage to the donor's cornea, insufficient cells and inefficient cell subculture (176). based on previous successful animal studies performed in part by our team, it has been investigated an extraocular source of abundant and more accessible cells for this purpose (21,22)**.** It has been shown that adult human adipose tissue is an ideal source of autologous stem cells since it satisfies many requirements: it`s easy to access this tissue, it has high cell retrieval efficiency, and its stem cells known as "human adipose-derived adult stem cells" (**h-ADASCs**), can differentiate into different cell lineages such as keratinocytes, osteoblasts, chondroblasts, myoblasts, hepatocytes, neurons, among others (21,176)**.**

Moreover, these cells have shown immunomodulatory properties even in xenogeneic scenarios (17,19). We found that Human **ADASCs** transplanted into damaged rabbit corneas were able to differentiate in corneal keratocytes, and produce corneal collagens and keratocan that are characteristic of the human corneal stroma (21)**.**

In recent years, protocols have been used to obtain corneal decellularized matrices because they provide a more natural environment for the growth and differentiation of cells compared to

synthetic scaffolds. The effectiveness of **SDS** decellularization on the human cornea has also been previously demonstrated. In our study, we used **h-ADASCs** to repopulate our scaffolds, which have been shown excellent results during the follow-up, the corneal transparency has been completely preserved without any signs of scarring (19). We have been able to demonstrate that the **h-ADASCs** transplanted into a human decellularized lamina survives at least 12 weeks after transplantation *in vivo* in the animal model, and they also differentiate into human keratocytes, Therefore, with this model we could potentially be able to obtain an autologous graft using adipose tissue from the patient and an allogeneic donor cornea, theoretically avoiding the risk of stromal rejection associated with allogenic lamellar transplant options (19)**.** Also, the advantage of our protocol is the possibility of obtaining several grafts from a unique allogeneic donor, increasing the availability of donor tissue, and shortening waiting lists.

The goal of the current doctoral thesis and research line is to carry out the research done by our group and apply it to human patients suffering from keratoconus. A simple procedure of liposuction and a non-transplantable donor cornea can provide an optically transparent autologous stromal graft, with excellent demonstrated biocompatibility. With the new non-invasive surgical technique, many complications associated with the usual techniques can be avoided, improving the visual prognosis and the quality of life of patients.

These experimental studies opened the translational of this concept into the therapy of human corneal diseases, using the advanced keratoconus disease as the model for this type of advanced therapy. This study aims to build a stem cell therapy alternative to the classic corneal transplantation techniques to regenerate the corneal stroma, avoiding the complications and limitations frequently observed with current techniques.

3. HYPOTHESIS

Intrastromal implantation of adipose stem cells into keratoconic corneas, either alone or with a carrier composed by a lamina of the acellular human corneal stroma, can transform into human adult keratocytes, and improve the clinical condition of such patients by promoting the regeneration of the diseased corneal stroma *in vivo*. The evolution of these cells, as well as the evolution of the implanted acellular laminas, will be observed using confocal microscopy.

4. OBJECTIVES OF THE THESIS

4.1 PRIMARY OBJECTIVES

The main objective of the present study is to evaluate the potential of cellular therapy of the corneal stroma in patients with advanced keratoconus, by:

1. **Analyzing the safety/efficacy of the intrastromal implantation of**:

- Autologous adipose-derived adult stem cells (**ADASCs** alone).
- Decellularized human corneal stroma laminas.
- Autologous **ADASCs** recellularized human corneal stromal laminas.

2. To demonstrate that the implantation of mesenchymal **ADASCs** isolated or when they are embedded into a human acellular corneal lamina, is followed by cell proliferation and does not generate any clinical or histological response of inflammation or rejection.

3. To demonstrate that acellular corneal laminas (without cells) are well tolerated by the host cornea affected with keratoconus, with the absence of clinical complications.

4. To prove that the decellularized stromal laminas, with or without **ADASCs**, are capable of improving the thickness of the cornea as well as the corneal ectasia, and secondary irregularity.

4.2 SECONDARY OBJECTIVES

1. To explore the visual and refractive outcomes by the implantation of **ADASCs**, and the implantation of decellularized or recellularized corneal laminas.

2. To describe the biological corneal tissue response following the implantation of **ADASCs**, and the implantation of decellularized or recellularized corneal laminas by the analysis of the corneal tissue with non-invasive imaging methods such as anterior corneal segment **OCT**.

3. To prove that the implant of **ADASCs** in the corneal pocket, causes a modest enhancement in the pachymetric parameters, and the implantation of decellularized or recellularized corneal laminas causes a significant improvement in the corneal pachymetric and volumetric corneal thickness parameters, using Scheimpflug corneal topography.

4. To investigate the clinical response following the implantation of **ADASCs**, and the implantation of decellularized or recellularized corneal laminas con **ADASCs**, by slit-lamp biomicroscopy.

5. To assess the cell evolution (density, etc.) as well as the acellular laminas evolution by **confocal microscopy** development of technical approach:

- To assess the evolution of the **ADASCs** once they are implanted in the stromal pocket and monitor their evolution.
- To assess the evolution of the decellularized laminas implanted without **ADASCs**, and the biological evolution of the laminas towards recellularization.
- To assess the evolution of **ADASCs** implanted on the decellularized corneal laminas and the evolution of the decellularized tissue with the transformation and evolution of the cells.

- To define a method based on the subjective quantitative analysis of the stromal corneal cells and establish this analysis to monitor the evolution of the cell density of implanted **ADASCs** with a lamina or without a lamina during the experiment.
- To investigate both the quantitative and qualitative evolution of cell density in the anterior, mid, and posterior stroma of the patients.

5. MATERIAL AND METHODS

5.1 STUDY APPROVAL, DESIGN, AND SUBJECTS

Prospective interventional randomized, non-masked series of cases, based on the cooperation between the Research, Development, and Innovation Department of Vissum Instituto Oftalmologico de Alicante, Miguel Hernandez University, Alicante (Spain), Optica General (Saida, Lebanon), Laser Vision Center (Beirut, Lebanon) and REVIVA Research and Application Center (Middle East Hospital, Beirut, Lebanon). The Institutional Review Board (IRB) Ethical committee of Reviva Research and Application Center (Lebanese University, Beirut, Lebanon), prospectively approved this study. All patients signed informed written consent for all procedures described in this study. The study was conducted in strict adherence to the tenets of the Declaration of Helsinki, and it was officially registered in ***ClinicalTrials.gov*** (Code: NCT02932852).

Fourteen patients were enrolled in the study once selected following the inclusion criteria (see below), their mean age was 33.28 years old (range: 24–49 years of age; mean of 34.2 years of age for **G-1**, 32.2 years of age for **G-2**, and 36.25 years of age for **G-3**). The study sample was composed of 9 females and 5 males (female/male ratio of 2/3 for group 1, 4/1 for group 2, and 3/1 for group 3) as well as 10 right eyes and 4 left eyes. The patients were randomly distributed into three study groups: Group-1 (**G-1**) patients were implanted with autologous adipose-derived adult stem cells (**ADASCs** alone, 3x 10^6cells/1 mL of **PBS**) (n = 5 patients); Group-2 (**G-2**) received 120 µm thick decellularized human corneal stroma laminas implants (n = 5 patients), and Group-3 (**G-3**) received 120 µm thick recellularized human corneal stroma laminas with (**ADASCs,** 1x10^6cells/1 ml of **PBS**) (n = 4 patients). **ADASCs** were obtained by elective liposuction.

Superficial laminas with **BM** or deep laminas without **BM** were randomly distributed among the patients of **G-2** and **G-3** after the decellularization procedure.

Clinical monitoring of the study of the patients was established for safety purposes at 1 week, 1, 3, 6, 12, and 36 months postoperative, with interim reports every 6 months. Thirteen patients fully completed the three years of clinical follow-up. Only one patient from **G-1** was lost after the first postoperative month because of the inability to attend further follow-up for personal reasons unrelated to the study (30,31,177,180).

5.2 JUSTIFICATION OF THE TOTAL NUMBER OF PATIENTS

The small number of patients (a total of 14 patients), who participated in this experiment, is justifiable in the sense that this is the first clinical application of **ADASCs** in human eyes, therefore this number of patients is not guided by the rules of a generic study. Our main purpose is to ascertain the safety of this innovative surgical approach and to confirm the findings proved previously with animal study, in human patients with advanced keratoconus.

5.3 INCLUSION AND EXCLUSION CRITERIA

- **Inclusion Criteria:** Patients with advanced keratoconus defined as stage ≥ IV; according to the RETICS keratoconus classification (8), already candidates for corneal transplantation due to the advanced condition of the disease and to associated comorbidities;

Age ≥ 18 years; Negative human immunodeficiency virus (**HIV**), hepatitis B (**HBV**), hepatitis C (**HCV**) serology (30,31,177,180).

- **Exclusion Criteria:** Patients with **CDVA** < 0.1 in the contralateral eye, previous corneal hydrops or central corneal scars, active concomitant inflammatory eye disease; any other sight-threatening ocular comorbidity, previous corneal surgical procedures, including collagen **CXL**, pregnancy or breastfeeding, and history of systemic malignancy (30,31,177,180).

5.4 PATIENTS SELECTION

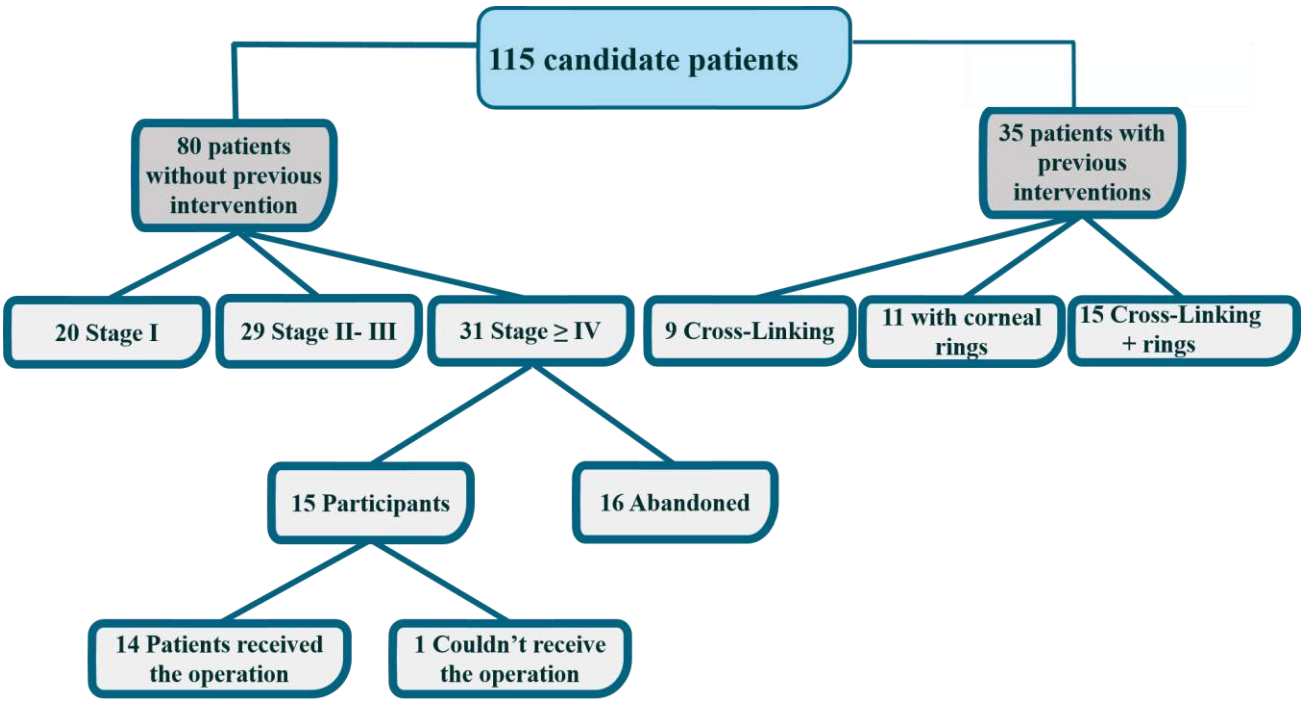

5.5 AUTOLOGOUS ADASCs ISOLATION, CHARACTERIZATION, AND CULTURE

Approximately 250 ml of fat mixed with local anesthesia was obtained by standard liposuction from each patient. The adipose tissue was processed according to the methods described in our previous reports (19,21,183,187,237). Briefly, tissue was digested in collagenase I for 40 minutes at 37ºC and then collagenase was inhibited adding autologous human serum (**AHS**). Erythrocytes were lysed in erythrocyte lysis buffer (Gibco-Life Technologies, USA). Then the pelleted cells were cultured in Dulbecco's modified eagle medium (**DMEM**) with Glutamax, and Sodium Pyruvate (Gibco), 10% **AHS**, 1% Penicillin-Streptomycin (Gibco), and 0.2% amphotericin B (Gibco). Cell characterization was performed by CD34+CD45-CD105+ labeling by flow cytometry analysis following International Federation of Adipose Therapeutics (**IFATS**) recommendations (187). 60 to 80 hours before surgery cell quiescence was induced by reducing the amount of serum to 0.5%, to transplant the **ADASCs** in a physiological status closer to the natural nonproliferative stromal keratocytes, as proliferative stem cells within the corneal stroma could potentially induce stromal scarring or haze. Quiescence, as well as the absence of apoptosis and aneuploidy, were verified by propidium iodide labeling (Invitrogen, USA), and cell cycle flow cytometry analysis, as was described in published articles by our group (19,21). Just before the intrastromal injection, the cells were collected by trypsinization (Sigma) and (3×10^6 Cells in 1 ml **PBS)** were prepared per patient (Figure. 1B). Such concentration was established based on the evidence observed in previous experimental studies and given the expected cell loss following the implantation due to the leakage of the cell solution outside the cornea (17,19,21,30,31,177,180). In **G-3**, the **ADASCs** were harvested by trypsinization (Sigma-Aldrich), 24 hours before implantation

and (0.5 × 10^6 cells per 1ml of **PBS)** were cultured for 24 and 12 hours on each surface of the decellularized corneal stroma lamina, respectively (30,31,177,180).

5.6 LAMINAS

The human corneal stroma of donor corneas with non-viable endothelium (without scars) but with negative viral serology and useful for human use were selected for this investigation. The corneas were provided by the eye bank "Banco de Ojos para el tratamiento de la Ceguera, Centro de Oftalmología Barraquer (Barcelona, Spain) following the Spanish Regulatory Directives 2004/23/EC and 206/17/EC" on standards of quality and safety for the donation, procurement, testing, processing, preservation, storage and distribution of human tissues and cells were being followed.

Donor corneas were mounted on an artificial anterior chamber (Barron, Katena Products, USA), the epithelium mechanically removed with surgical sponges, and the anterior corneal stroma cut with the 60-Khz IntraLase iFS femtosecond laser (AMO Inc, Irvine, Calif) in two consecutive laminas of 120 µm thickness and 9.0 mm diameter, that were subsequently washed in **PBS** (Sigma) supplemented with 1% antibiotic-antimicotic (Gibco). Femtosecond laser parameter settings were equivalent to the ones used for a standard **LASIK** flap dissection, except for an anterior side cut angle of 360º. With this procedure two laminas were obtained, a superficial one containing **BM**, and a deeper one without this layer. The remaining posterior cornea was discarded (31,177,180). The decellularization protocol was based on previous publications (19,31,177,180,211), briefly, the laminas were immersed in 1% (wt/vol) **SDS** (Sigma) with a protease inhibitor cocktail (P8340, Sigma), and incubated on an orbital shaker (75 rpm) for 24 hours at room temperature. Later, the

laminas were washed 8 times in **PBS** with 1% antibiotic-antimycotic in the same conditions for 15 min, each at room temperature. To remove deoxyribonucleic acid (**DNA)**, the laminas were incubated in **DNA** se (Benzonase® Nuclease 6.5 U/mL, Merck) in **PBS** with the same protease inhibitor cocktail in the same conditions at 37ºC for 72 hours. Finally, the laminas were washed 8 times for 15 min each in **PBS** with 1% antibiotic-antimicotic (Figure. 4A). 24 hours before transplant, those laminas for patients receiving recellularized tissue were then placed in tissue culture wells for recellularization with autologous **ADASC** ($0{,}5x10^6$ cells were cultured on each side of the lamina) from each patient of the **G-3** (Figure. 4B). After finishing the recellularization process, the laminas were transferred to the theatre in **PBS** at room temperature for their implantation.

Effectiveness of the decellularization and hence cell removal was monitored in one fresh lamina of each batch by three methods: Histological analysis with nuclear staining 4',6-diamidino-2-phenylindole **(DAPI),** and fluorescence microscopy staining with hematoxylin & eosin, and biochemically by digestion in proteinase K, **DNA** extraction, and **DNA** quantification by using a Picogreen Assay kit as in previous publications (Figure. 4C) (19,180,211).

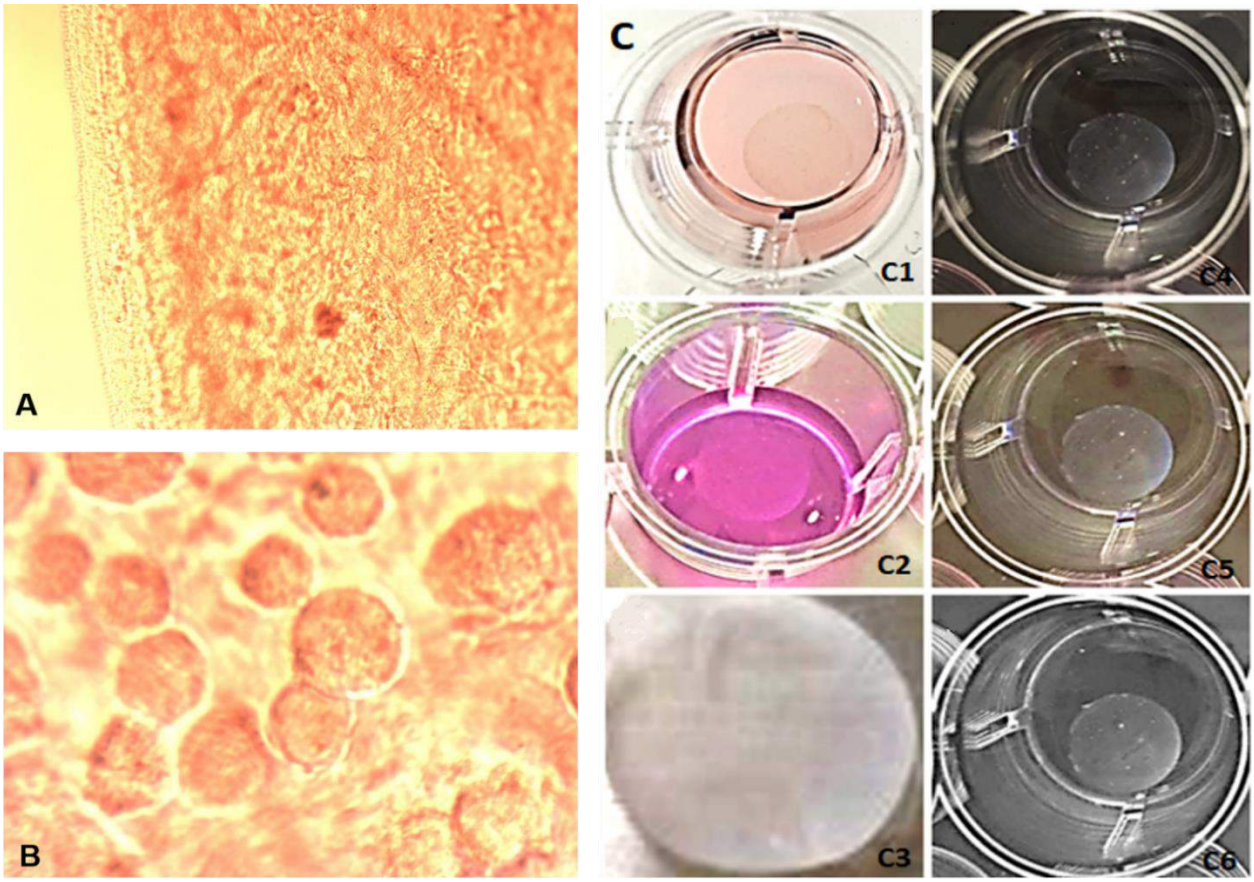

Figure 4. Observation of decellularized and recellularized laminas, and decellularization/ recellularization process.
(A) Decellularized human corneal lamina (10× magnification). **(B)** Recellularized human corneal lamina with **ADASCs** (0.5×10^6 cells were cultured on each side of the laminas) (10× magnification). Figure is taken from the scientific chapter referred to Alió JL et al. (41). **(C)** (**C1,2,3**) Lamina kept in culture medium for 2 hours then transferred to **PBS**: we observed that the color of the culture medium as expected became more red corresponding to a PH more basic, this affecting the laminas and the cells, which was more significant after 26 hours (Lamina has the aspect of gelatin and more viscous). (**C4,5,6**) lamina transferred directly into **PBS** and kept in **PBS** till the end of the procedure: the lamina remains in good condition, firm, with the maintenance of thickness and no viscous aspect was observed.

5.7 SURGICAL PROCEDURE

5.7.1 AUTOLOGOUS ADASCs IMPLANTATION

Topical anesthesia was used. A 60-kHz IntraLase iFS femtosecond laser (AMO Inc, Irvine, CA) was used in a single-pass mode for recipient corneal lamellar dissection by creating an

intrastromal laminar pocket of 9.5 mm in diameter was created at a medium depth of the thinnest preoperative pachymetry point measured by the **AS-OCT** (Carl Zeiss, Germany) (30,177,180). The femtosecond laser-assisted corneal dissection ended with a 30^0 anterior side cut as a corneal incision, the arc length incision was 3 mm and similar parameter settings of **LASIK** surgery were used in femtosecond laser. The femtosecond laser parameter settings are summarized in the publication of our group (30) (Table 4). The corneal intrastromal pocket was then opened by blunt dissection with the Morlet lamellar dissector (Duckworth & Kent, England), and subsequently, three million autologous **ADASCs** contained in 1 mL of **PBS** injected into the pocket through a 25-G cannula. Previous to the cellular injection a 1 mm corneal paracentesis was performed to reduce the intraocular pressure (**IOP**) and allow the higher volume to be injected into de stromal pocket. Topical antibiotics and steroids (Tobradex, Alcon) were applied at the end of the surgery. No patient received corneal sutures (30,177,180).

Table 4. Laser specifications for the preparation of the recipient cornea.

Lamellar Cut		**Anterior Side Cut**	
Parameter	***Value***	***Parameter***	***Value***
Diameter (mm)	9.5	Diameter (mm)	9.5
Depth (µm)	Thinnest/2	Posterior Depth (µm)	Thinnest/2 + 10
Energy (µJ)	1.50	Energy (µJ)	1.7
Tang Spot Sep (µm)	5	Cut Position (º)	90
Rad Spot Sep (µm)	5	Cut Angle (º) **G-1**	30
		Cut Angle (º) **G-2 & G-3**	50
		Arc Length Incision **G-1**	3 mm
		Arc Length Incision **G-2& G-3**	4 mm
		Spot Sep (µm)	3
		Layer Sep (µm)	3

Tang = Tangential; Sep = Separation; Rad = Radial. Tang Spot Sep: Tangential separation between points. Rad Spot Sep: Radial separation between points; Spot Sep: Separation between points; Layer Sep: Separation between layers. The table is taken in part from the scientific articles of Alió Del Barrio et al. (30,31).

5.7.2 LENTICULE IMPLANTATION

Topical anesthesia with oral sedation was used for all surgeries. The 60-Khz IntraLase iFS femtosecond laser was used in a single-pass mode for the recipient corneal lamellar dissection by creating an intrastromal lamellar cut of 9.5 mm in diameter at a half depth of the preoperative thinnest pachymetry point, measured by the Visante **AS-OCT** (Carl Zeiss, Germany). The femtosecond laser-assisted corneal dissection ended with a 50^0 anterior side cut as a corneal incision, and the arc length incision was 4 mm (Table 4). Laser parameter settings were equivalent to the ones recently reported by our group for this type of dissection (30). The corneal intrastromal pocket was then opened by blunt dissection with the Morlet lamellar dissector (Duckworth & Kent, England), and subsequently, the lamina inserted, centered, and unfolded by gentle tapping and massage from the host epithelial surface. A temporal limbal paracentesis was performed just before implantation to reduce the **IOP**. In those cases, receiving an **ADASCs -** recellularized lamina **G-3**, to compensate the expected cellular damage along the graft implantation process, the pocket was irrigated immediately before and after transplant with a solution containing 1 million autologous **ADASCs** in 1 mL of **PBS** through a 25-G cannula. The incision was closed with one interrupted 10/0 Nylon suture that was removed one week after the operation. Topical antibiotics and steroids (Tobradex, Alcon) were applied at the end of the surgery (31,177,180).

All surgeries were performed by the same surgeons at the Laser Vision Center (Beirut, Lebanon) (30,31,177–180).

5.8 IN VIVO CONFOCAL MICROSCOPE DEVICE

An HRT3 confocal microscope with a Rostock Cornea Module (RCM) (Heidelberg Engineering, Heidelberg, Germany) was used. The light source of this confocal microscope is a coherent type of diode laser, with a wavelength of 670 nm and a minimum resolution of 1024 x 768 (16 bit) (238). Coherent light was used to improve the contrast and quality of the images of the corneal stroma, particularly the cells (6).

5.8.1 USE OF THE CONFOCAL MICROSCOPE

Signed informed consent was obtained from patients for the confocal microscopy study. A drop of topical anesthetic (oxybuprocaine 0.4%) was applied to the eye to be examined. The confocal microscope was set at 12 D. A drop of a high-viscosity gel (2.0 mg/g of carbomer) was applied to the front surface of the microscope lens of the RCM. Then, an RCM TomoCap was placed on top of the RCM objective. A drop of the same viscous gel was also applied on the upper part of the outer surface of the TomoCap and in the patient's eye to be examined. The patient was placed in a stable and comfortable position, with the eye aligned with the lens of the confocal microscope, and was instructed to keep looking at the light inside the lens. The focal position was reset to 0 at the superficial epithelial cells of the examined eye. The RCM was then turned clockwise or anticlockwise 0±50 **µm**, and the focal plane was adjusted to the desired cell layer. Finally, at least four images were obtained for every 50 **µm** of depth and stored following a previously described protocol (238). The images analyzed in this study were indeed at different stromal depths but always belonged to a central diameter ≤ of 9 mm and were below the measurement of the intrastromal diameter pocket (30,31,105,177,179).

5.8.2 METHOD OF STROMAL CELL COUNTING

Images that had a better quality of contrast and illumination were selected from the images captured and stored during the experience. An area known as a region of interest (ROI) was determined, and almost the sameregion ROI (0.1000 mm^2) was used for all cell counts in all layers of the corneal stroma (6,105,179,238). The morphology criteria used in the present study to differentiate the corneal stroma cells from the inflammatory cells are described in our publication (179).

We used the 50% brightness and contrast setting (Figure. 5A) for all images. Cells that were more illuminated and more refringent (9,10,105,179) were selected and marked in blue (238), these cells were white or light gray and had clear and well-defined edges (6,105,179). Dark gray cells were not taken into consideration, as they did not belong to the chosen 50 **µm** plane (105,179). The confocal cellular brightness is attributed to the nuclear content of these cells (6,9,30,31,104,105,125,177,179,239). Because of their irregular oval-shaped bodies (9), differences in brightness among them can be attributed to different direction of incidence of the laser beam, or their different metabolic activities (9). Only the cell nuclei that were identified with the method mentioned above were defined as corneal stromal cells and included in the cell counting process. For simplification throughout the thesis, when we talk about cell density or morphology, we are referring to the density or morphology of the cell nucleus and not the cell membrane that was observed by confocal microscopy (6,9,30,31,104,105,125,177,179,239).

The highly reflective material was not considered in the cell count whenever the size of the reflective morphology exceeded the size that we considered similar to stromal keratocyte, whether

in normal or in keratoconic corneas (6,9,30,31,104,105,125,177,179,239). For this reason, we have considered that this structure corresponds to a fibrotic material (179).

After the first count was performed, the contrast was increased to the maximum and the brightness decreased to the minimum. Any stromal cell that disappeared from the chosen plane was eliminated, and only those cells that remained were used for the final cell count result, even if they were faintly identified in the observed image (Figure. 5B) (105,179).

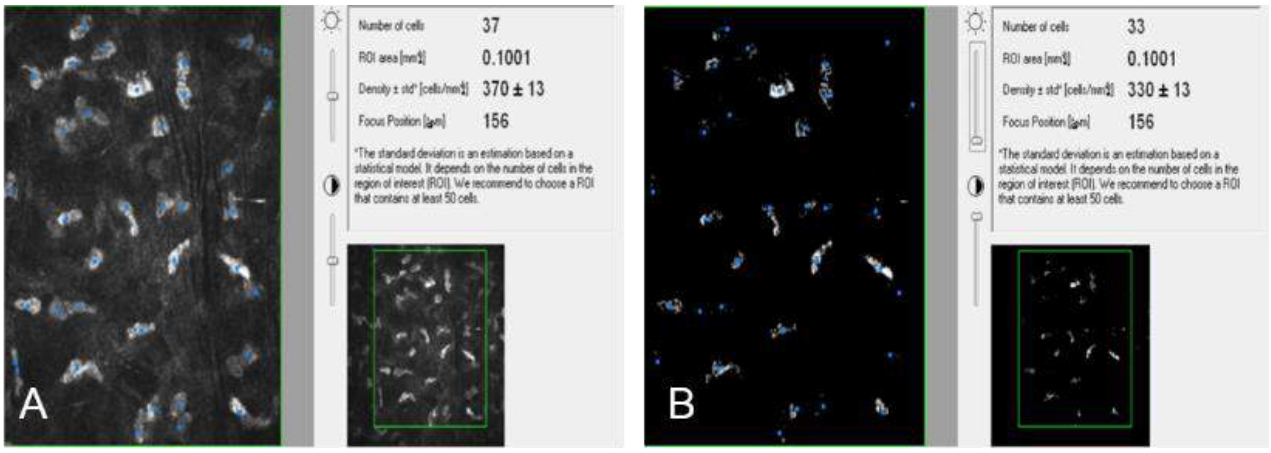

Figure 5. Cell counting method performed by confocal microscopy.
(A) Cell count performed with medium brightness and contrast. The more illuminated and more refringent cells were counted, and the keratocytes are marked in blue. (B) Elimination of keratocytes that do not belong to the plane under observation is possible using low brightness and high contrast settings. Figure is taken from the scientific paper with reference El Zarif M et al. (179) credited for this thesis.

5.8.3 ADASCs CELL COUNTING

The counting method for transplanted **ADASCs** was performed similarly. **ADASCs** appeared rounded in shape, voluminous, and refringent (Figure. 6A) (30,105,179). The morphology and evolution of the **ADASCs** over time are described later in part 6 of the results section (Figure. 6B) (179).

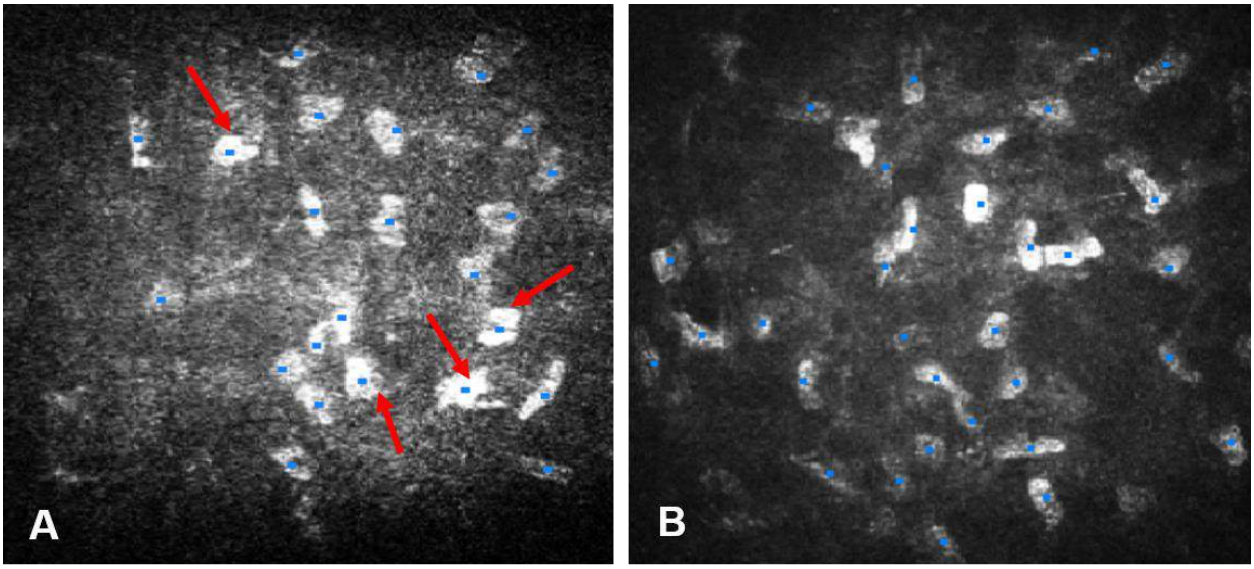

Figure 6. ADASCs counting in **G-1**.
(**A**) Count of **ADASCs** (red arrows) and keratocytes 1 month following surgery of a keratoconic patient; the cells are marked in blue. The **ADASCs** have a rounded shape and are larger, more luminous, and more refringent than the normal keratocytes. (**B**) Cell count of a keratoconic patient 1 year after implantation of **ADASCs**; all corneal stroma cells demonstrate a similar shape. The figure is taken from the scientific paper with reference El Zarif M et al. (179) credited for this thesis.

5.8.4 CELL COUNT ON DECELLULARIZED AND RECELLULARIZED LAMINAS

When the decellularized **G-2** and recellularized **G-3** laminas appeared without well-defined cell structures, they were considered totally acellular in the 0.1 mm^2 area that we delimited in our study (Figure. 7A) (31,105,177,179). All structures that appeared on the anterior surface, on the posterior surface, or in the mid-stroma of the lamina; that showed well-defined edges that were white or light gray; and that had a morphology similar to that of a keratocyte nucleus were counted as a cell (Figures. 7B, 7C, 8A-8E) (105,179).

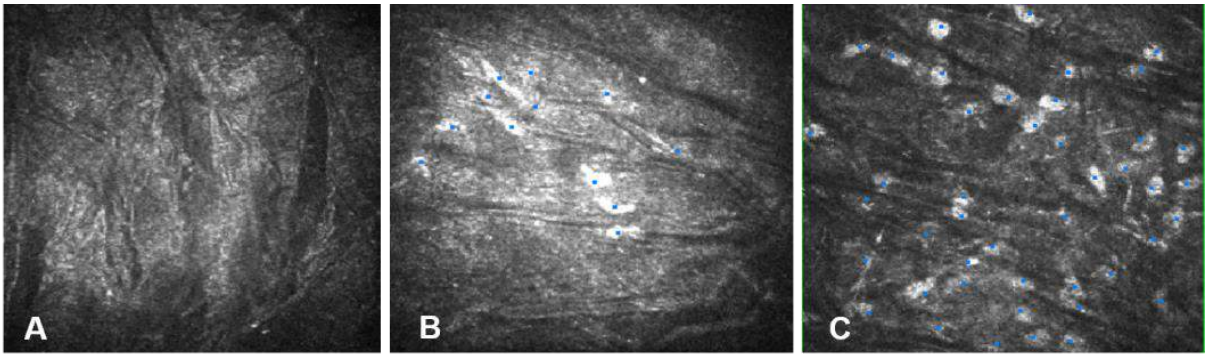

Figure 7. Cell count on decellularized laminas for case-9 in **G-2**.
(**A**) The anterior surface of a decellularized lamina appears without cells 1 month after surgery. (**B**) Cell count on the posterior surface of a lamina 3 months after surgery. Cells show different morphology from the host corneal stromal cells. These cells are smaller. (**C**) Cell count on the posterior surface of a lamina 1 year after surgery. All cells demonstrate a morphology identical to that of normal corneal stromal keratocytes. The figure is taken from the scientific paper referred to El Zarif M et al. (179) credited for this thesis.

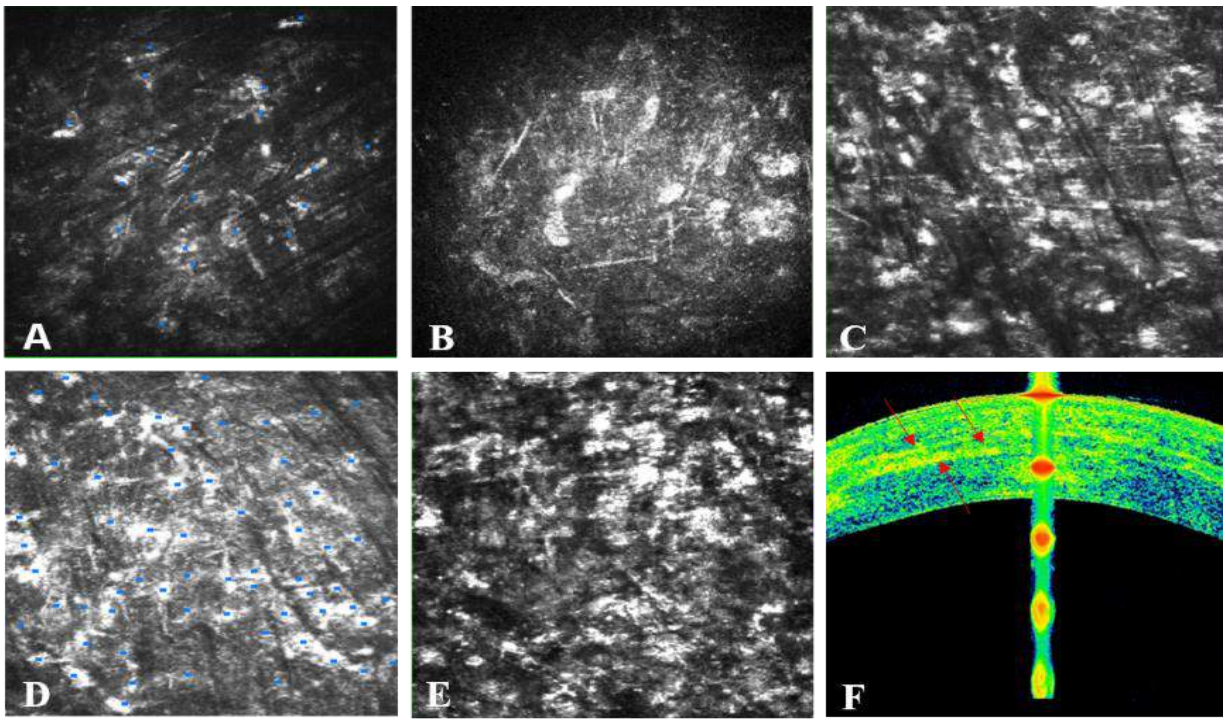

Figure 8. Cell count on recellularized lamina for case-13 in **G-3**.
(**A)** The anterior surface of a recellularized lamina 1 month after the operation; few **ADASCs** can be seen (marked in blue). (**B**) The posterior surface of the recellularized lamina 1 month after the operation; note the presence of a few **ADASCs** similar in morphology to keratocytes. (**C**) The anterior surface of the recellularized lamina 12 months after surgery showing an abundant number of stromal cells. (**D**) Mid-stroma of the lamina 12 months after surgery showing a high number of stromal cells. (**E**) The posterior surface of the recellularized lamina 12 months after surgery showing a high number of stromal

cells. (**F**) **OCT** image where the red arrows represent the anterior and posterior surfaces, as well as the mid-stroma, of the recellularized lamina 12 months after surgery. The figure is taken from the scientific paper referred to El Zarif M et al. (179) credited for this thesis.

5.8.5 CORNEAL CELL DENSITY CALCULATION

To obtain the cellular density, we first defined the region ROI (mm^2) (238) and then proceeded to count the cells with the methodology described above. The cellular density for the chosen area was calculated by the confocal microscope software as the number of cells multiplied by 10 cells/ mm^2 ± standard deviation (**SD**) (10,238).

To calculate the cell density of the corneal stroma among the three groups, we divided the measurements of the stroma into three zones: anterior, mid, and posterior stroma. The mid-stroma coincided with the surgical plane (calculated as half of the thinnest point of the cornea obtained by **OCT** ± 50 **µm**) (30,31,105,177,179). The anterior stroma is the stroma located below **BM**, and the posterior stroma is the stroma located above **DM** (30,31,105,177,179). For those measurements where a lamina was present (postoperative **G-2** and **G-3**), we divided the lamina into three areas: anterior surface, lamina posterior surface, and lamina mid-stroma (Figure. 8F) (179).

The main outcome measures of this study are the changes in and evolution of corneal stroma cellular density over a 1- year follow-up period, as analyzed using corneal confocal microscopy. Cellular density was studied before surgery and at 1, 3, 6, and 12 months after surgery. Preoperative cellular density was measured in the anterior, mid, and posterior stroma in **G-1**, as well as in **G-2** and **G-3**. Postoperative cellular density in **G-2** and **G-3** was studied in the anterior and posterior stroma and through the lamina, to explore the evolution of its cellular component during the study time (179).

5.9 POSTOPERATIVE CARE AND FOLLOW-UP SCHEDULE

Postoperatively, the patients were evaluated monthly by the study medical director and the clinical monitor of the study to ensure the correct evolution of the patients. The patients were followed at 1 day, 1 week, and at 1, 3, 6, 12 months (30,31,177). Clinical follow-up after one year was performed every 6 months till 36 months postoperatively (180). The following data were recorded preoperatively and throughout the postoperative assessment, at 1, 3, 6, 12, and 36 months: Unaided distance visual acuity (**UDVA**), **CDVA**, rigid contact lens distance visual acuity (**CLDVA**) in (decimal equivalent to the logMar scale). Refractive sphere (**Rx Sphr**) in diopters (D) and refractive cylinder (**Rx Cyl**) (D). Central corneal thickness (**CCT**) (µm) was measured by **AS-OCT** (Visante, Carl Zeiss Scheimpflug corneal topography thinnest point (**Thinnest point**) (µm), cornea volume (**CV**) (mm^3), and corneal aberrometry (Pentacam; Oculus Inc., Wetzlar, Germany), the anterior corneal surface Zernike analyses were performed at maximum 6 mm pupil diameter in all cases regardless of the patients' pupil diameter. Anterior mean keratometry (**Anterior Km**) (D), posterior mean keratometry (**Posterior Km**) (D), maximum keratometry (**Kmax**) (D), and topographic cylinder (**Topo Cyl**) (D) (Pentacam; Oculus Inc., Wetzlar, Germany). Slit-lamp biomicroscopy, fundoscopy, **IOP** (mmHg) (Goldmann applanation tonometry), and endothelial cell density (**ECD**) (cells/mm^2) by specular microscopy (Nidek, Aichi, Japan) (30,31,177,180). The confocal microscopy study was completed up to 12 months using ***the confocal microscope*** HRT3 RCM (Heidelberg) with Rostock Cornea Module (179).

5.10 ANALYSIS OF CONCORDANCE AMONG THE EXPERTS

The measures of the variables over time: Visual acuity, manifest refraction, slit lamp biomicroscopy study, corneal topography, corneal aberrometry, **AS-OCT**, and confocal microscopy have always been done with the same devices and with the same conditions. Besides, there were taught to obtain agreement on the same results that is the concordance is absolute in our study.

5.11 STATISTICAL ANALYSIS

1. The statistical analysis of the scientific paper with reference (30) published prior to this doctoral thesis: (Alió del Barrio J, **El Zarif M**, De Miguel M, Azaar A, Makdissy N, Harb W, et al. **Cellular therapy with human autologous adipose-derived adult stem cells for advanced keratoconus.** Cornea 2017; 36(8)952-60), was a descriptive analysis of the clinical outcomes.

2. The statistical analysis of the scientific paper with reference (31) published prior to this doctoral thesis: (Alió del Barrio JL, **El Zarif M**, Azaar A, Makdissy N, Khalil C, Harb W, et al. **Corneal stroma enhancement with decellularized stromal laminas with or without stem cell recellularization for advanced Keratoconus**. Am J Ophthalmol. 2018;186: 47-58), was performed with the SPSS software package version 20.0 for Windows (SPSS Inc., USA). The normality of the study data was confirmed by the Kolmogorov-Smirnov test, which determined that all variables followed a normal distribution [$P < 0.05$]. Due to the study sample (n: 9), the Wilcoxon sign test was performed to test for statistically significant differences [$P < 0.05$].

3. The statistical analysis of the scientific paper with reference (177) credited for this thesis: (Alió JL, Alió del Barrio JL, **El Zarif M**, Azaar A, Makdissy N, Khalil C et al. **Regenerative**

surgery of the corneal stroma for advanced keratoconus: 1-Year outcomes. Am J Ophthalmol. 2019;203:53-68), was performed with the SPSS software package version 20.0 for windows (SPSS Inc., USA). Due to the study sample (n:14), non-parametric statistics were used. The Wilcoxon Rank Sum test was applied to assess the significance of differences between preoperative and postoperative data. For all statistical tests, the same level of significance was used [$p < 0.05$].

4. The statistical analysis of the scientific paper with reference (180) credited for this thesis: (**El Zarif M**, Alió JL, Alió del Barrio JL, Abdul Jawad K, Palazón-Bru A, Abdul Jawad Z, et al. **Corneal stromal regeneration therapy for advanced keratoconus: long-term outcomes at 3 years**. Cornea. 2021;40(6):741–54.), was obtained by generalized linear mixed models with Poisson variables including outcomes, time, and the group as fixed effects, and individuals as random effects. A Poisson distribution is characterized by a mean rate (the **SD** is equal to this mean or lambda) and indicates the number of events for the outcome. We estimated lambda through these models, taking into account all the gathered information. The results of this statistical study did not represent at any time the outcome of one patient from the different groups, but they represented the total data collected from all the patients of each group over continuous-time and provide all of the information necessary to understand the impact of the intervention. Scatterplots were developed to help interpret the results, and the goodness-of-fit of the models was obtained through the likelihood ratio test. The type I error significance level was set when p-value [$P< 0.05$], and the statistical software we used was R 3.5.1. (180).

5. The statistical analysis of the scientific paper with reference (179) credited for this thesis: (**El Zarif M**, Abdul Jawas K, Alió del Barrio JL, Abdul Jawad Z, Palazón-Bru A, De Miguel MP, et al. **Corneal stroma cell density evolution in keratoconus corneas following the implantation**

of adipose mesenchymal stem cells and corneal laminas: an in vivo confocal microscopy study. IOVS. 2020;61(4)22), was performed by generalized linear mixed models with a Poisson variable as an outcome (fixed effects, time and group; random effects, individual). This Poisson variable corresponded to the keratocyte nuclei densities (Poisson distribution), indicating the means of cell nuclei appearing in the captured figures at different levels of the corneal stroma (anterior, intermediate, and posterior) or on the anterior surface, mid-stroma, and posterior surface of the implanted tissue for the studied time intervals. A Poisson variable, unlike one that follows a normal distribution, is expressed by a single parameter, which is the average number of events only. The **SD** of the Poisson variable (generally known as lambda) is not shown in the figures, but it is the same as the average parameter, as compared to a normal distribution which is expressed by mean and **SD**. On the other hand, this average parameter (obtained through mixed generalized linear models) takes into account all of the measurements of all of the individuals and assesses the variability between individuals and within them. Consequently, the results presented here are at the group level and provide all of the information necessary to understand the impact of the intervention. Scatterplots were developed to help interpret the results, and the goodness of fit of the models was obtained through the likelihood ratio test. The type I error significance level was set at 0.05, and the statistical software we used was R 3.5.1 (179).

The maximum number of images for each patient was collected to calculate cell density. To not alter the results, mathematical models of repeated measures were used to control the variability of each individual. We considered the average cell counts of two observers who performed them separately following the same scientific standards; when there was a discrepancy between them of more than 20%, the count was repeated or other images were taken, if possible, until achieving agreement (179).

5.12 OUTCOME MEASURES

5.12.1 THE MAIN OUTCOME MEASURES

The main outcome measures of this investigation were divided into primary and secondary:

5.12.1.1 Primary Outcome Measures.

The primary outcome measures were **UDVA**, **CDVA**, and **CLDVA** (decimal equivalent to the logMar scale). **Rx Sphr** (D), **Rx Cyl** (D). **CCT** (µm). **Thinnest point** (µm) and **CV** (mm^3). Third order aberration **RMS** (**3rd order RMS**) (µm), fourth order aberration **RMS** (**4th order RMS**) (µm), high order aberration **RMS** (**HOA RMS**) (µm), and Low order aberration **RMS** (**LOA RMS**) (µm) (30,31,177,180).

5.12.1.2 Secondary Outcome Measures.

The secondary outcome measures were **Anterior Km** (D), **Posterior Km** (D), **Kmax** (D), and **Topo Cyl** (D) (30,31,177,180).

5.12.2 CONFOCAL MICROSCOPY OUTCOMES

5.12.2.1 Morphological and Cell Densities Results.

With patients implanted with **ADASCs** Alone **G-1**, patients implanted with decellularized corneal laminas **G-2**, and patients implanted with recellularized corneal laminas **G-3**. Cell density outcomes were calculated in the anterior, mid, and posterior stroma in **G-1**. In the anterior, and

posterior stroma in **G-2**, and **G-3**, and the anterior, mid, and posterior surfaces of the implanted tissue (179).

5.12.2.2 Morphological Results of Fibrotic Tissue. (179)

6. RESULTS

THE RESULTS OF THIS STUDY ARE SHOWN IN FORM OF SCIENTIFIC REPORTS AS LISTED HEREAFTER:

6.1 In this review paper we summarized all existing evidence from preclinical experiments in the field of regenerative medicine of the corneal stroma. This evidence was the basis for the clinical trial described in the current thesis. The results demonstrated in the paper with reference (240) of the scientific publication credited for this thesis: Alió del Barrio JL, Arnalich-Montiel F, De Miguel MP, **El Zarif M**, Alió JL. **Corneal stroma regeneration: Preclinical studies**. Exp Eye Res. 2021;202:108314.

6.2 Six-month outcomes for the first application in **G-1** of autologous **ADASCs** implantation within the corneal stroma in patients with advanced keratoconus. They were published prior to this doctoral thesis in the following article with reference (30): Alió del Barrio J, **El Zarif M**, De Miguel M, Azaar A, Makdissy N, Harb W, et al. **Cellular therapy with human autologous adipose-derived adult stem cells for advanced keratoconus.** Cornea 2017; 36(8)952-60.

6.3 Six-month outcomes for the second and third applications in **G-2**, and **G-3** by the implantation of decellularized stromal laminas with or without autologous **ADASCs** for patients with advanced keratoconus**.** They were published published earlier to this doctoral thesis in the following article with reference (31): Alió del Barrio JL, **El Zarif M**, Azaar A, Makdissy N, Khalil C, Harb W, et al. **Corneal stroma enhancement with decellularized stromal laminas with or without stem cell recellularization for advanced Keratoconus**. Am J Ophthalmol. 2018;186: 47-58.

6.4 Twelve-month outcomes of the implantation of autologous **ADASCs** in **G-1**, and the implantation of decellularized stromal grafts with or without autologous **ADASCs** for patients with advanced keratoconus in **G-2**, and **G-3**. They were published in the following article with reference (177) of the scientific publication credited for this thesis: Alió JL, Alió del Barrio JL, **El Zarif M**, Azaar A, Makdissy N, Khalil C et al. **Regenerative surgery of the corneal stroma for advanced keratoconus: 1-Year outcomes**. Am J Ophthalmol. 2019;203:53-68.

6.5 Three-year outcomes of the implantation of autologous **ADASCs**, and the implantation of decellularized stromal grafts with or without autologous **ADASCs** for patients with advanced keratoconus in groups 1,2, and 3. They were published in the following article with reference (180) of the scientific publication credited for this thesis: **El Zarif M**, Alió JL, Alió del Barrio JL, Abdul Jawad K, Palazón-Bru A, Abdul Jawad Z, et al. **Corneal stromal regeneration therapy for advanced keratoconus: long-term outcomes at 3 years**. Cornea. 2021;40(6):741–54.

6.6 One-year confocal biomicroscopy outcomes following the implantation of autologous **ADASCs,** and the implantation of decellularized stromal grafts with or without autologous **ADASCs** for patients with advanced keratoconus in groups 1,2 and 3. They were published in the following article with reference (179) of the scientific publication credited for this thesis: **El Zarif M**, Abdul Jawas K, Alió del Barrio JL, Abdul Jawad Z, Palazón-Bru A, De Miguel MP, et al.**Corneal stroma cell density evolution in keratoconus corneas following the implantation of adipose mesenchymal stem cells and corneal laminas: An in vivo confocal microscopy study.** IOVS. 2020;61(4)22.

6.7 In the following publication we presented an integrated overview of the results, based on the evidence from the experimental clinical studies performed by our research group in the topic of corneal stromal regeneration for the treatment of corneal diseases, particularly in keratoconus.

This overview was published in the following paper with reference (241) of the scientific publication credited for this thesis: **El Zarif M**, Alió del Barrio JL, Arnalich-Montiel F, De Miguel MP, Makdissy N, Alió JL. **Corneal stroma regeneration: New approach for the treatment of cornea disease**. APJO. 2020;9(6):571–9.

6.8 This review summarized the results from human clinical studies reported in the peer-reviewed literature on the topic "human corneal stromal regeneration" and "corneal enhancement therapy". Also, this review offers a comparison of the results between the different recent studies carried out by other authors, and our study. The results were published in the following review with reference (242) of the scientific publication credited for this thesis: **El Zarif M**, Alió JL, Alió del Barrio JL, De Miguel MP, Abdul Jawad K, Makdissy N. **Corneal stromal regeneration: a review on human clinical studies for treatment of keratoconus.** Front Med. 2021;8:650724.

7. DISCUSSION

The topic of corneal stromal regeneration has developed over the last five years and achieved important progress based on the development of new surgical approaches such as intralamellar corneal stromal surgeries, and the use of advanced bioengineering therapies, and corneal stem cell therapy to mimic and substitute the human corneal stromal.

In this discussion, we will include comments regarding scientific publications that were published in the period prior to this doctoral thesis, directly related to it, but whose content deserves to be debated in this discussion for a better understanding of the results of this doctoral thesis (30,31).

Our research group demonstrated for the first time the feasibility of regenerative surgeries of the corneal stroma for advanced keratoconus, using autologous **ADASCs** injected into the corneal stromal pocket in cases with advanced keratoconus, confirming also the appearance of new collagen in the injected areas, that could be useful for the management of corneal dystrophies, scars and could also slightly increase the thickness of the cornea (30,177,179,180,240–242).

Also, we demonstrated for the first time that decellularized laminas of a human corneal stroma, colonized or not by autologous **ADASCs**, can be implanted for therapeutic purposes on a clinical basis (31,177,179,180,240–242).

Along the different stages of this study, we have to acknowledge the following scientific debates corresponding to each one of the stages of this investigation:

7.1 Discussion of the review with reference (240) of the scientific publication credited for this thesis**:** Alió del Barrio JL, Arnalich-Montiel F, De Miguel MP, **El Zarif M**, Alió JL. **Corneal stroma regeneration: Preclinical studies**. Exp Eye Res. 2021;202:108314.

7.2 Discussion of the article published earlier than this doctoral thesis with reference (30) : Alió del Barrio JL, **El Zarif M**, De Miguel M, Azaar A, Makdissy N, Harb W, et al. **Cellular therapy with human autologous adipose-derived adult stem cells for advanced keratoconus.** Cornea 2017; 36(8)952-60.

7.3 Discussion of the article published earlier than this doctoral thesis with reference with reference (31): Alió del Barrio JL, **El Zarif M**, Azaar A, Makdissy N, Khalil C, Harb W, et al. **Corneal stroma enhancement with decellularized stromal laminas with or without stem cell recellularization for advanced Keratoconus**. Am J Ophthalmol. 2018;186: 47-58.

7.4 Discussion of the article with reference (177) of the scientific publication credited for this thesis: Alió JL, Alió del Barrio JL, **El Zarif M**, Azaar A, Makdissy N, Khalil C et al. **Regenerative surgery of the corneal stroma for advanced keratoconus: 1-Year outcomes**. Am J Ophthalmol. 2019;203:53-68.

7.5 Discussion of the article with reference (180) of the scientific publication credited for this thesis: **El Zarif M**, Alió JL, Alió del Barrio JL, Abdul Jawad K, Palazón-Bru A, Abdul Jawad Z, et al**. Corneal stromal regeneration therapy for advanced keratoconus: long-term outcomes at 3 years**. Cornea. 2021;40(6):741–54.

7.6 Discussion of the article with reference (179) of the scientific publication credited for this thesis: **El Zarif M**, Abdul Jawas K, Alió del Barrio JL, Abdul Jawad Z, Palazón-Bru A, De Miguel MP, et al**. Corneal stroma cell density evolution in keratoconus corneas following the**

implantation of adipose mesenchymal stem cells and corneal laminas: an in vivo confocal microscopy study. IOVS. 2020;61(4)22.

7.7 Discussion of the review with reference (241) of the scientific publication credited for this thesis: **El Zarif M**, Alió del Barrio JL, Arnalich-Montiel F, De Miguel MP, Makdissy N, Alió JL. **Corneal stroma regeneration: New approach for the treatment of cornea disease**. APJO. 2020;9(6):571–9.

7.8 Discussion of the review with reference (242) of the scientific publication credited for this thesis: **El Zarif M**, Alió JL, Alió del Barrio JL, De Miguel MP, Abdul Jawad K, Makdissy N. **Corneal stromal regeneration: a review on human clinical studies for treatment of keratoconus.** Front Med. 2021;8:650724.

7.1 Alió del Barrio JL, Arnalich-Montiel F, De Miguel MP, **El Zarif M,** Alió JL. **Corneal stroma regeneration: Preclinical studies.** Exp Eye Res**.** 2021;202:108314.

This study is the fundamental basis of all the clinical studies, as far as it contains the basis of the experimental research that is the basis of this clinical project performed by our research group in the previous years. The first clinical application was accomplished based on the basic experiment performed by our research group. In this paper, we adapted the clinical experiments to the necessary fundamentals for the first clinical application of this new surgical approach, using advanced therapy techniques for the first time in the treatment of keratoconus, and how such experimental fundamentals were used transnationally to the human being (17,19,21,240).

We reviewed in this study the evidence raised in the experimental studies of our research group for its clinical application, and the use of stem cells for corneal stroma cellular therapy. The

CSSCs are a promising source for cellular therapy as the isolation technique and culture methods have been optimized and refined (36); presumably, they show greater differentiation potential into keratocytes as they are already committed to the corneal lineage (243). On the other hand, isolating **CSSCs** autologously is more technically demanding considering the small amount of tissue that they are obtained from. Furthermore, this technique still requires a contralateral healthy eye, which is not always available (bilateral disease). Therefore, these drawbacks may limit its use in clinical practice. Allogeneic **CSSCs** use requires living or cadaveric donor corneal tissue.

Human adult adipose tissue is a good source of autologous extraocular stem cells, as it satisfies many requirements: easy accessibility to the tissue, high cell retrieval efficiency, and the ability of its stem cells **h-ADASCs** to differentiate into multiple cell types (keratocytes, osteoblasts, chondroblasts, myoblasts, hepatocytes, neurons, etc.) (21). This cellular differentiation occurs due to the effect of very specific stimulating factors or environments for each cell type, avoiding the mix of multiple kinds of cells in different niches.

Bone marrow **MSCs** (**BM-MSCs**) are probably the most widely studied **MSCs**, presenting a similar profile to **ADASCs**, but their extraction requires a bone marrow puncture, which is a complicated and painful procedure requiring general anesthesia.

The **UMSCs** present an attractive alternative, but their autologous use is currently limited, as the umbilical cord is not generally stored after birth.

The **ESCs** have great potential, but also present important ethical issues. However, the use of the **iPSCs** could solve such problems (37), and their capability to generate adult keratocytes has already been proven *in vitro* (38): specialized adult cells can be reprogrammed to an immature or stem cell state and then redirected to the required cell lineage using specific factors and

environmental stimuli. It has been shown that **iPSCs**-derived **MSCs** exert immunomodulatory properties in the cornea similar to those observed with **BM-MSCs** (200). To the best of our knowledge, no studies have been published reporting the capability of **iPSCs** to differentiate into adult keratocytes *in vivo* in the animal model.

As previously discussed, it is important to highlight that the therapeutic effect of **SCs** in a damaged tissue is not always related to the potential differentiation of the **SCs** in the host tissue, as multiple mechanisms might contribute simultaneously to this therapeutic action as the already established secretion of paracrine growth factors capable of stimulating the host tissue, in which case the direct cellular differentiation of the **SCs** might not be relevant and could even be non-existent (32,39,40).

On the other hand, many physical/engineering methods have been devised to attempt to control the organization of collagen for use in engineering or for replicating tissues, including electrospinning, electrogradient transport, magnetic, shear flow, dip pen nano-lithography, wet spinning, flow-induced crystallization, and densification to a liquid crystalline state. None of them have been able to recapitulate native corneal tissue structure. In general, they can neither match the mechanical properties nor recreate local nanoscale organizations.

So far, different methods have been developed to mimic corneal stroma structure, among them: decellularized corneal sections, collagen vitrification, collagen three dimensions (**3D**) bioprinting, collagen compaction by **3D**-RAFT and plastic. The most promising approach has been previously developed by our group, using decellularized human corneal sections that were recellularized with human adipose tissue adult mesenchymal stem cells **h-ADASCs** in experimental animals (Figures. 2D, 2E) (17,19,21), and importantly also in patients suffering from corneal stromal debilitating diseases (31,177,244).

7.2 Alió del Barrio JL, **El Zarif M**, De Miguel M, Azaar A, Makdissy N, Harb W, et al. **Cellular therapy with human autologous adipose-derived adult stem cells for advanced keratoconus.** Cornea 2017; 36(8)952-60.

In this paper we reported for the first time the implantation of **ADASCs** into the corneal human stroma in cases with keratoconus, many cases are still diagnosed in an advanced state where classical corneal transplantation (either by full-thickness or lamellar techniques) is the only treatment option. Our group aimed to find an alternative therapy to classical corneal transplantation to regenerate the corneal stroma, thus avoiding the important inter and postoperative risks associated with those techniques (2). Cellular therapy of the corneal stroma by the use of stem cells has gained relevant scientific interest in the last few years. All **MSCs** seem to have similar behavior *in vivo*, being able to achieve a keratocyte differentiation and modulate the corneal stroma with also immunomodulatory properties (3). The **CSSCs** may have enhanced functions as they are already corneal cells with more directed differentiation potential. However, the number of **CSSCs** that can be obtained from human corneas is quite limited and very technically demanding, with an inefficient cell subculture and not being possible to obtain them without damaging the donor cornea. All these major drawbacks have significantly limited their use for clinical practice and preclude their autologous application, so an extraocular source of cells that could replace **CSSCs** is necessary to solve all these limitations. Human adult adipose tissue has been demonstrated to be an ideal source of autologous stem cells, as it satisfies all the requirements: easy accessibility to the tissue, high cell retrieval efficiency, and the ability of its stem cells **ADASCs**, to differentiate in multiple cell types (21). **BM-MSCs** have the same profile as **ADASCs**, but their extraction by bone marrow puncture is a more complicated and painful procedure that requires general anesthesia. Umbilical-**MSCs** present an attractive alternative, but their autologous use would be expensive and currently

impossible. The **ESCs** also present important ethical issues. A new and exciting possibility is offered by the induced pluripotent stem cells **iPSCs**, obtained from adult cells, as it has been recently demonstrated their ability to differentiate into corneal keratocytes with similar immunomodulatory properties as mesenchymal stem cells (38,200).

Up to date, many studies in animal models for different corneal abnormalities have demonstrated the possible benefits of cellular therapy to improve corneal transparency by their ability to reorganize the stromal collagen lamellas, as well as new collagen production (3,16,27–29,17,19,21–26). However, to the best of our knowledge no *in vivo* data has been published yet in humans studying the safety and efficacy of such therapies. This study was the first human application achieved with advanced keratoconus. For this purpose, we selected advanced keratoconus patients already candidates to classical corneal transplantation due to unsatisfactory visual function and contact lens intolerance as, in case of failure, a standard treatment for such patients could still be performed. Stem cell delivery to the corneal stroma was performed through a femtosecond laser-assisted lamellar pocket at half depth of the corneal stroma measured by **AS-OCT** (30). Although we are dealing with advanced keratoconic corneas with severe thinning we didn't observe intraoperative complications as corneal tears. Nevertheless, to be able to safely perform this technique, a minimal thinnest pachymetric point of 250 µm is probably required (that thickness would leave an anterior cap close to a LASIK flap). Some concerns may arise about the possible weakening effect of this corneal dissection on an already severely weakened and pathologic cornea. However, according to John Marshall's important findings, vertical side cuts through corneal lamellae rather than horizontal delamination incisions contribute to the loss of structural integrity during **LASIK** flap creation (245). In our study only a 30º anterior side cut was performed, so considering these findings the weakening effect of this dissection should be marginal.

Three million autologous **ADASCs** (contained in 1 mL) were prepared for injection into the stromal pocket. This high cellular concentration was decided, as the high cellular loss was expected during the delivery due to solution leakage outside the cornea. Before the injection, we performed a corneal paracentesis to reduce the **IOP** and allow more volume within the pocket, although no more than 10-30% of the injected volume was expected to remain within the stroma. Further studies are necessary to assess precisely the real amount of cells that remain immediately after the transplant (30).

Visual function improved in all patients for up to six months. This benefit was modest but observed in the four study patients. This early postoperative finding theoretically should be attributed to the surgical procedure itself and not to the presence of stem cells, as they have not differentiated yet into adult keratocytes (30). We couldn't observe early changes in the manifest refraction or topographic keratometry that may explain this early visual improvement (30).

Keratometric and pachymetric data obtained by corneal topography (Pentacam) showed overall stability (Figure. 9), with a possible progression of the ectasia in case-2, the keratometric outcomes have remained almost stable between 1 postoperative month, and 6 months without a true progression of ectasia, this case may have a redistribution of the anterior corneal surface as a consequence of the creation of the pocket, which led to a reduction in astigmatism, and was associated with visual gain. Therefore, it seems there was a postoperative "remodeling" effect of the corneal pocket, a future follow-up will demonstrate the possibility or not of an ectatic progression.

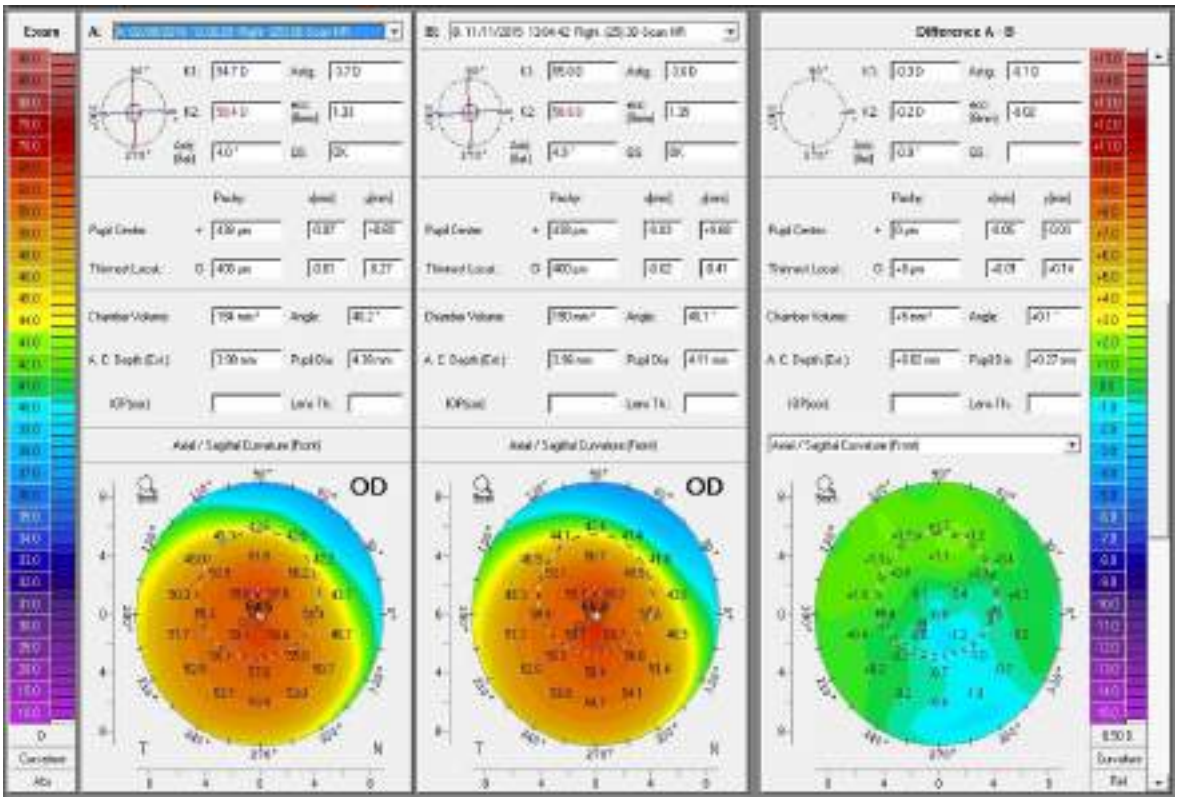

Figure 9. Corneal topography (Pentacam) comparison between preop and 6 months after in case-1. Observe the stability of the keratometric parameters. The figure is taken from the scientific paper referred to Alió del Barrio et al. (30).

Pachymetry measurement by **AS-OCT** in our study demonstrated a mild but real improvement of the **CCT** (mean value of 16.5 µm at the 6th month) (30), correlated with the presence of patched areas of new collagen production in the majority of the patients. This new collagen production appears in low amounts and not homogeneously distributed along the surgical plane, thus being this procedure not able to restore big amounts of tissue if that is the purpose as in corneal thinning diseases. As previously observed in animal models, the addition of hyaluronic acid-derived scaffolds or acellular corneal stroma may assist to achieve this goal (19,22).

We didn't observe any inter or postoperative complication up to six months (30), being the surgery well tolerated in all cases with a complete restoration of corneal transparency within 24 hours. We could also observe a significant clinical improvement of corneal opacities in case-2

(Figure. 10) (30), as has been suggested in previous studies in animal models (23). However, larger case series with corneal opacities are required to demonstrate this finding.

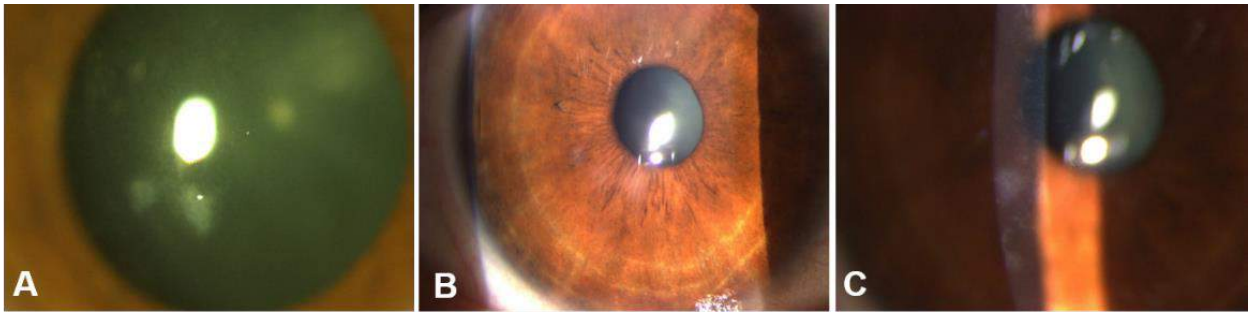

Figure 10. Slit-lamp findings from Case-2 in G-1.
(**A**) Preoperatively. (**B** and **C**) At the 6th postoperative month. Observe the postoperative improvement in the density and severity of the inferior paracentral anterior stromal scars. The figure is taken from the scientific paper referred to Alió del Barrio et al. (30).

Within experimental studies, it is easy to demonstrate, by postmortem analysis, the survival of the previously transplanted marked cells (through immunofluorescence analysis) and their differentiation into adult keratocytes (by detecting keratocan expression) (19,21). However, *in vivo*, human studies have the important drawback of being limited to confocal biomicroscopy findings (vulnerable to subjective interpretations). We could observe the presence of rounded-shape cells at the surgical plane in all patients compatible with the implanted **ADASCs**, showing later a progressive dendritic shape change until the point of being not possible to be differentiated from normal keratocytes at the end of the 6 months follow-up (30).

7.3 Alió del Barrio JL, **El Zarif M**, Azaar A, Makdissy N, Khalil C, Harb W, et al. **Corneal stroma enhancement with decellularized stromal laminas with or without stem cell recellularization for advanced Keratoconus**. Am J Ophthalmol. 2018;186: 47-58.

In this paper we described the implantation of **ADASCs** in the corneal stroma of advanced keratoconic corneas, is a novel and promising line of therapy for keratoconus and other corneal dystrophies (30), even though its effectiveness still requires to be properly established as well as the delivery technique of the stem cells improved. Nevertheless, the demonstrated production of new human **ECM**, by the transplanted mesenchymal stem cells into the corneal stroma *in vivo* in an animal models (21–27), and in humans (30) is not expected to be enough to rehabilitate a severely thinned cornea. In this scenario, we postulated that the addition of decellularized corneal stromal tissue could enhance the previously observed results with the cellular therapy alone, as it provides tectonic support and an ideal environment for the stem cells (19,224).

The implantation of decellularized or recellularized laminas presents a novel treatment line for advanced keratoconus cases, where through a straight forward and quick surgical technique that can be performed under topical anesthesia we achieve a partial functional rehabilitation of the advanced ectatic cornea and an almost complete thickness recovery, potentially allowing these corneas to be candidates again for further non-invasive surgical visual rehabilitation techniques. Each donor cornea can easily generate up to three donor laminas following this model, which could partially solve the world's shortage of donor corneas, improving patient's access to corneal transplantation in many parts of the world. Moreover, the decellularization technique by **SDS** is a non-complex and non-expensive method that allows the removal of all the allogeneic donor cellular component from the graft, avoiding any rejection risk, while the remaining extracellular matrix still preserves its normal architecture as it has been already demonstrated *in vitro* and the animal model by our group and other authors (18,19,224).

In this phase of this pilot clinical trial, we report for the first time, to the best of our knowledge, the transplantation of decellularized corneal stromal tissue into the human cornea *in*

vivo. All visual parameters moderately improved more than one line, achieving statistically significant differences on the **UDVA** despite the small study sample. This correlates well with the significant improvement of the refractive sphere and spherical aberration. All anterior keratometric parameters, coma, and total **HOA** systematically improved although. A mean improvement of the **Anterior Km** and **Kmax** of 1.5 and 3.5D respectively can be expected considering our results. All thickness parameters significantly improved over 100 µm, achieving an almost normalization of the corneal thickness (31). As initially postulated, we have not observed any clinical inflammatory signs along with the follow-up, as well as no obvious inflammatory cells at the confocal biomicroscopy (179), observing only a mild graft haze along the first postoperative month, being fully recovered by the third postoperative month in all patients.

On the other hand, within the 6 months' follow-up, we have not been able to demonstrate the potential advantages of adding mesenchymal stem cells to the decellularized stromal graft. Recellularized grafts didn't show a faster visual recovery, enhanced outcomes, or areas of new collagen production in the corneal **OCT**. Further studies with longer follow-up and larger samples are required to clarify the possible role of the cellular therapy in addition to this type of corneal graft.

Besides, in our study, some patients received randomly a decellularized or recellularized lamina with or without **BM**. Melles et al. recently described the outcomes with the transplantation of the **BM** into the mid stroma of advanced keratoconic eyes in a similar fashion as the present study (246), they obtained a maximum keratometry decreased on average from77 ± 26.2 (D) to 69.2 ± 3.7 D, the best **CDVA** improved only from 1.27 to 0.9 in LogMar, the best **CLDVA** remained stable, the mean thinnest-point pachymetry increased only from 332 ± 59 µm before surgery to 360 ± 50 µm. Meanwhile, in our study, we obtained an improvement equivalent to 1-2 lines in LogMar

scale in **CDVA,** and also **CLDVA** in all the groups, a statistically significant improvement in **CCT** and the **thinnest point** with the groups of decellularized and recellularized laminas, as well in **CV** (31,177,180). Taking into account the limitations of our small study sample, we didn't find differences between those patients receiving laminas containing or not the **BM**. If this preliminary finding is confirmed in further studies, it would suggest that we can obtain several laminas with neutral optical power from corneas not valid for a corneal graft. Our clinical results have at least the same as those reported with the **BM** transplantation as an isolated layer, we were able to demonstrate not only the feasibility of this surgery, but we could improve visual outcomes, as well corneal aberration, although the addition of stroma permits a full restoration of the thickness (a fact not achieved with **BM** only). Our results open an exciting field for research to explore how alternative and well-established visual rehabilitation techniques such as corneal collagen **CXL** and intracorneal ring segments behave in the advanced keratoconic eye with stromal thickness restoration.

An important finding shown in the current study is the fact that early recellularization signs by the host keratocytes have been observed 6 months after surgery in all patients. We couldn't demonstrate this host recellularization of the decellularized grafts in our previous animal studies with a 3 months follow-up (19). Other authors have previously reported this host keratocyte infiltration into decellularized grafts in animal models for anterior lamellar keratoplasty (247), although, to the best of our knowledge, we are reporting for the first time this finding for intrastromal decellularized grafts. This host recellularization allows a complete functionalization of the grafted tissue, which should ensure long-term transparency maintenance of the cornea.

A relevant issue not clarified in the present phase of this study is whether or not the intrastromal implantation of decellularized or recellularized stromal tissue could halt the natural progressive condition of this disease. Study patients were advanced keratoconic eyes already

candidates for corneal transplantation, and the preoperative progressive status of the disease was not well determined, so further biomechanical studies will be required to answer this issue. Nevertheless, all patients presented stability or progressive improvement of the visual and keratometric parameters.

7.4 Alió JL, Alió del Barrio JL, **El Zarif M**, Azaar A, Makdissy N, Khalil C et al. **Regenerative surgery of the corneal stroma for advanced keratoconus: 1-Year outcomes**. Am J Ophthalmol. 2019;203:53-68.

This paper reports 12 months of outcomes of the first corneal stroma cell therapy human experience up to one year. Again, what is demonstrated in this study is the lack of complications of the procedure observed in this one-year clinical study. The use of a femtosecond laser to create a stromal pocket at the mid stroma of advanced keratoconus cases is shown in the experience to be feasible and with no negative consequences, up to one-year of observation (177).

The first important issue that is demonstrated in this study is the lack of complications of the procedure observed in this one-year clinical study. The use of a femtosecond laser to create a stromal pocket at the mid stroma of advanced keratoconus cases is shown in the experience to be feasible and with no negative consequences, up to one year of observation. This finding is coherent with previous studies reported by our group, in which a large femtosecond assisted corneal lamellar dissection performed approximately at the depth of the ones followed by the implantation of an intrastromal circular ring, showed to be not affected by complications either from the visual, topographic, keratometric or anatomical perspectives (248).

The most representative data concerning the safety of the surgery is offered in this study. The only injection of cells in the pocket was followed by an immediate, even though modest, but significant improvement, that was maintained throughout the one year of the follow-up. This initial response of the cornea indicates the tolerance to this type of surgery, as no deterioration was observed in any case in the **G-1**, or the other groups. At this early level of the experience, the keratocyte differentiation and the eventual collagen production may not have any significant influence on the mechanical response of the cornea, so further studies should guarantee the feasibility of this type of surgery from the biomechanical perspective. However, femtosecond laser-assisted pockets of these dimensions were used for the implantation of intracorneal ring segments without any negative impact, either immediate or late, in the operated keratoconic corneas, even though in this experience an intracorneal foreign body was implanted for therapeutic purposes (249). Moreover, according to previous reports (245), vertical side cuts through corneal lamellae rather than horizontal delamination incisions contribute to the loss of structural integrity during **LASIK** flap creation, so a minimal impact on corneal biomechanics might be expected after the creation of a lamellar pocket such as the one performed in this clinical study. Further studies will be necessary to study the biomechanics of the corneas in patients with different stages of keratoconus after the implantation of **ADASCs**, decellularized laminas with or without **ADASCs**, and to compare the outcomes of the three types of implants.

In the current experience, the good tolerance and the possibility of increasing corneal thickness by the implantation of decellularized layers of corneal stroma created by femtosecond laser were confirmed up to one year. To induce a calculated increase in the thickness of the cornea is feasible by using these femto-dissected and decellularized laminas that can be implanted without any negative impact on the biomechanics, vision, and especially, corneal anatomy. Corneal

irregularity has been demonstrated to be improved, even though modestly, by the reduction of corneal aberrometry, as observed in this study. So, we can deduct that the calculated increase in corneal thickness induced by the use of these laminas can be used on a therapeutic basis without risk for the corneal transparency and benefits the corneal regularity and topography. The refractive sphere of these patients improved as well, which is in coherence with the flattening of the cornea which is observed in the keratometric analysis (177).

Probably, the most relevant feature is the maintenance of corneal transparency as a fact. In no case, a relevant corneal haze or corneal scarring was observed at 1 year of follow-up, and not even during the experience (except for the early haze seen along the first month after the lamina implantation in **G-2** and **G-3**) (177). This issue is extremely important because the introduction of heterologous manipulated corneal tissue could be followed by corneal scarring and eventually permanent loss of vision. The reasons for this corneal transparency are probably related to the decellularized character of the laminas as no biological interaction is happening between this foreign tissue of allogenic origin and the local host tissue cells. These findings demonstrate our previous experimental studies in which human decellularized corneal stroma laminas were well tolerated in the experimental animal model (19). Further to this, the presence of autologous **ADASCs** in the laminas of the third group could be of further relevance for the maintenance not only of the corneal transparency but also for the decrease of previous corneal scars that could be present in these cases, a fact that has been described formerly in the experimental animal model (23–28), and that we could also observe in one patient from **G-1** (30). This isolated observation of a significant biomicroscopy decrease in the scars present at the cornea preoperatively might be related to the capability of the stem cells to improve corneal transparency by their capability to reorganize previous diseased tissue

and the production of new normal collagen (177). Further studies performed on non-transparent and scarred corneas are necessary to confirm the therapeutic possibility of this new surgery.

Of particular relevance is also the observation of a positive biological response from the host keratocytes to the decellularized laminas, especially in those implanted with autologous **ADASCs.** In **G-2** (decellularized laminas with no addition of **ADASCs**) the increase in the corneal thickness maintaining the corneal transparency was parallel to the observation of an increase in the cellularity of both the anterior and posterior parts of the corneal stroma. So the decellularized corneal lamina was not only able to maintain transparent conditions increasing the corneal thickness, but there was also a positive cellular response of the host keratocytes by proliferating and even invading the implanted tissue, which indicates its biological activation (Figures. 7B, 7C). This finding was even more pronounced in those laminas implanted with **ADASCs** (Figures. 8A-8E) (177).

In **G1** (**ADASCs** alone), the confocal biomicroscopy findings are also remarkable. Initially, the **ADASCs** could be identified as rounded and regular in shape, while later during the experience these cells progressively transformed into a fusiform shape and showed an identical appearance to the normal keratocytes of the human cornea (Figure. 6) (30,177). An increase in the anterior and posterior stroma keratocyte density could be also observed in **G1** patients, so not only does the presence of the corneal lamina induce a positive biological response in the cornea but also this healing response can be enhanced by the inclusion of **ADASCs**, which might contribute not only to the biological tolerance of the decellularized corneal lamina but also to the maintenance of its transparency and integration into the host cornea.

As the first-year data on this study demonstrates, we are opening a new area of corneal surgery and corneal research. The use of parts of the cornea for a therapeutic increase in corneal

thickness in debilitated and thin keratoconic corneas is a new concept for research. Corneal clinical parameters were all maintained or improved and no deterioration was observed in any of the cases of the present study (177).

7.5 El Zarif M, Alió JL, Alió del Barrio JL, Abdul Jawad K, Palazón-Bru A, Abdul Jawad Z, et al**. Corneal stromal regeneration therapy for advanced keratoconus: long-term outcomes at 3 years**. Cornea. 2021;40(6):741–54.

In this paper, we report the 3-year outcomes of the first clinical study on corneal stromal regeneration therapy for the treatment of advanced keratoconus (30,31,177,180,241,242,250,251). We have been able to confirm in this report the absence of complications such as corneal ectasia, corneal inflammation, or any significant induction of corneal scarring or haze during the follow-up, the cornea showed transparency from the first postoperative day in **G-1** and up to three months with **G-2** and **G-3**. In a recent study with cases of mild to moderate progressive keratoconus, manual dissection of the mid-stroma was shown to be effective, there were no complications in any of the operated cases, and it was even effective in stabilizing corneal ectasia in 50% of cases, these findings are in agreement with our study in the sense that lamellar dissection is feasible in cases of progressive keratoconus (252).

Furthermore, 3 years after the surgery, we obtained an improvement of almost 1 line in the LogMar scale in **UDVA**, 2 lines in **CDVA**, and 2.3 lines in the LogMar scale in **CLDVA** in all cases (Figures. 11A-11C; Table 5). Also, **Rx Sphr** mean values showed an improvement in all groups and a change in **Rx Cyl** was observed (Figures. 11D, 11E; Table 5). In further studies, by increasing the number of patients, the patient's opinion should be taken about their satisfaction (as

the satisfaction survey NAVQ-10 questionary), and their vision quality (with the Quality of Vision questionnaire QOV of McAlinden et al.) (253). As well, to make the patients' opinion on the experience (with the MacAlinson patient satisfaction screening test).

Also, an increase in the thickness of the thinnest corneal point **CCT**, and **CV** (Figures. 11F-11H; Table 5) was obtained. There was also an improvement in all corneal aberrations, especially in the **3rd order** and **HOA RMS** (Figure. 12), and an enhancement in the secondary variables**,** in **Anterior Km,** and in **Kmax** we obtained an improvement in mean values of 2 D, and 3 D respectively up to 3-year follow-up (Figure. 13; Table 6). With the study performed by Birbal RS (252), the **CDVA** with eyeglasses remained stable in 58% of cases and improved 2 Snellen lines in 42% of patients. **CLDVA** remained stable in 44% of cases, improved ≥ 2 Snellen lines in 33%, and deteriorated in 22% of cases, however, although lamellar dissection is feasible, an improvement in corneal thickness and aberrometry cannot be achieved as it was in our study, therefore the cases with keratoconus with> 60 D showed a continuous progression.

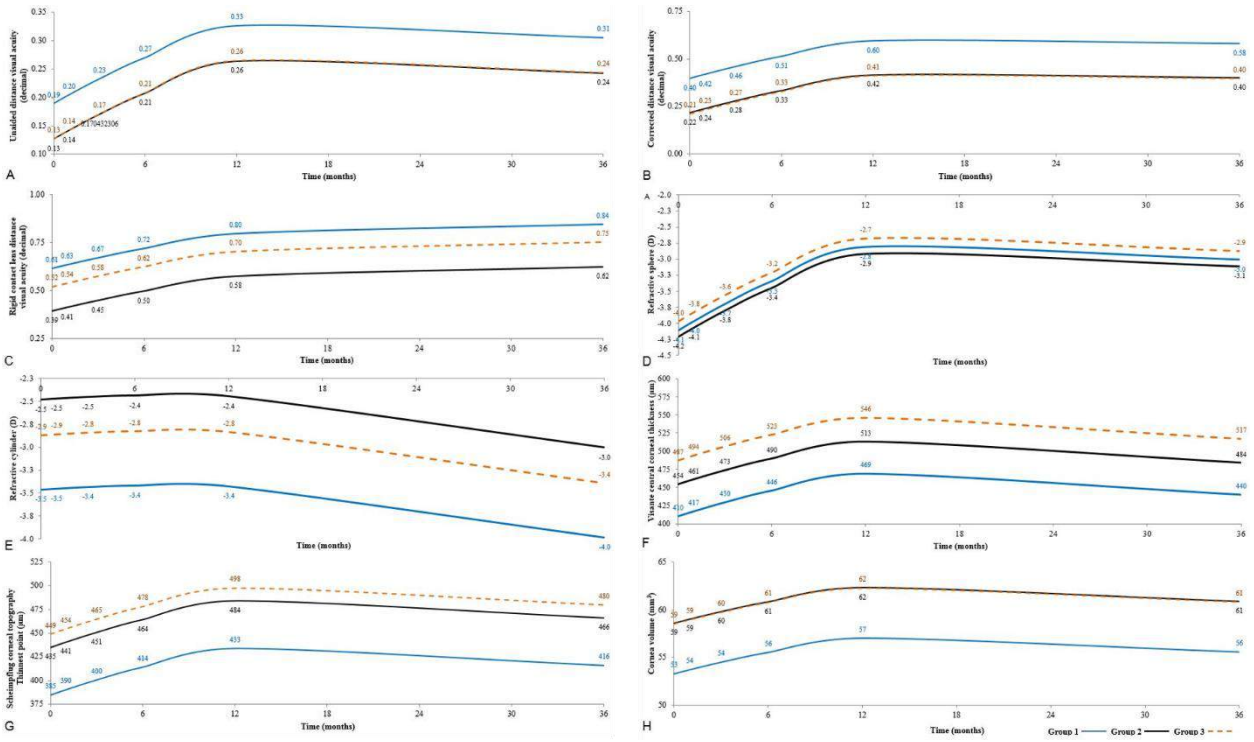

Figure 11. Satistical mean clinical results along with 3 years follow-up in **G-1**, **G-2 & G-3**. **(A, B)** Shows the upgrade in unaided visual acuity (**UDVA) &** corrected distance visual acuity (**CDVA)** (decimal) (equivalent to LogMar scale) from the pre-operative till 36 months. **(C)** Shows an enhancement in rigid contact lens visual acuity (**CLDVA)** (decimal) from the pre-operative until reach a maximum at 36 months. **(D**) Shows an improvement with refractive sphere **(Rx Sphr)** in (D) from the preoperative till 12 months, then revealed a slight decrease till 36 months. **(E)** The Refractive cylinder **(Rx Cyl)** in (D) remained almost stable from the pre-operative till 12 months, followed by an increase in mean values up to 36 months. **(F, G, H)** Presents central corneal thickness (**Visante CCT)** (µm), Pentcam Thinnest point **(Thinnest point)** (µm), Cornea Volume **(CV)** (mm^3) respectively. Observe the increase in mean values from the pre-operative, till reached a maximum at 12 months and they were established with a slow decrease at 36 months. The figure is taken from the scientific paper of El Zarif M et al. (180) credited for this thesis.

Table 5. Statistical results of the principal and secondary variables among the **G-1**, **G-2**, and **G-3** along with the three years' follow-up.

	P-value (G-2) / (G-1)	**P-value (G-3) / (G-1)**	**P-value (G-2) / (G-3)**	**σ**	**P-value (trajectories of the variables)**
UDVA	[P = 0.054]	[P = 0.069]	[P = 0.986]	0.116	[P = 0.0021]
CDVA	[P < 0.001]	[P < 0.001]	[P = 0.900]	0.151	[P < 0.001]
CLDVA	[P < 0.001]	[P = 0.090]	[P = 0.010]	0.180	[P < 0.001]
Rx Sphr (D)	[P = 0.892]	[P = 0.863]	[P = 0.747]	2.691	[P = 0.649]
Rx Cyl (D)	[P < 0.001]	[P = 0.014]	[P = 0.086]	0.824	[P = 0.015]
Visante CCT (µm)	[P = 0.012]	[P < 0.001]	[P = 0.055]	62.940	[P = 0.004]
Thinnest point (µm**)**	[P = 0.007]	[P = 0.001]	[P = 0.465]	67.966	[P = 0.021]
CV (mm^3)	[P < 0.001]	[P < 0.001]	[P = 0.948]	3.757	[P = 0.001]
3rd order RMS	[P < 0.001]	[P = 0.009]	[P = 0.376]	4.571	[P = 0.087]
4th order RMS	[P = 0.074]	[P = 0.817]	[P = 0.004]	2.515	[P = 0.117]
HOA RMS (µm**)**	[P < 0.001]	[P = 0.038]	[P = 0.091]	4.530	[P = 0.061]
LOA RMS (µm**)**	[P = 0.617]	[P = 0.870]	[P = 0.491]	27.299	[P = 0.866]
Anterior Km (D)	[P = 0.085]	[P = 0.909]	[P = 0.062]	6.436	[P = 0.351]
Posterior Km (D)	[P = 0.001]	[P = 0.636]	[P = 0.004]	1.326	[P = 0.118]
Kmax (D)	[P = 0.949]	[P = 0.387]	[P = 0. 0.391]	8.250	[P = 0.643]
Topo Cyl (D)	[P = 0.091]	[P = 0.190]	[P = 0.753]	2.383	[P = 0.525]

P-value of the (trajectories of the variables), standard deviation (**σ).** Unaided visual acuity (**UDVA)**, corrected distance visual acuity (**CDVA)**, rigid contact lens distance visual acuity (**CLDVA)** in (decimal equivalent to the logMar scale). Refractive sphere (**Rx Sphr**) in (D) and refractive cylinder **(Rx Cyl)** in (D). Anterior segment **OCT**-Visante: Central corneal thickness (**Visante CCT**) (µm) (Carl Zeiss). Scheimpflug corneal topography thinnest point **(Thinnest point)** (µm), cornea Volume (**CV**) (mm^3). Corneal aberrometry (Pentacam; Oculus Inc., Wetzlar, Germany): Third order aberration **RMS (3rd order RMS)** (µm)**,** fourth order aberration **RMS (4th order RMS)** (µm)**,**

high order aberration **RMS (HOA RMS)** (µm) and Low order aberration **RMS (LOA RMS)** (µm). Anterior mean keratometry **(Anterior Km)** in (D), posterior mean keratometry **(Posterior Km)** in (D), maximum keratometry **(Kmax)** in (D), and Topographic cylinder **(Topo Cyl)** in **(D)** (Pentacam; Oculus Inc., Wetzlar, Germany). The table is taken from the scientific paper of El Zarif M et al. (180) credited for this thesis.

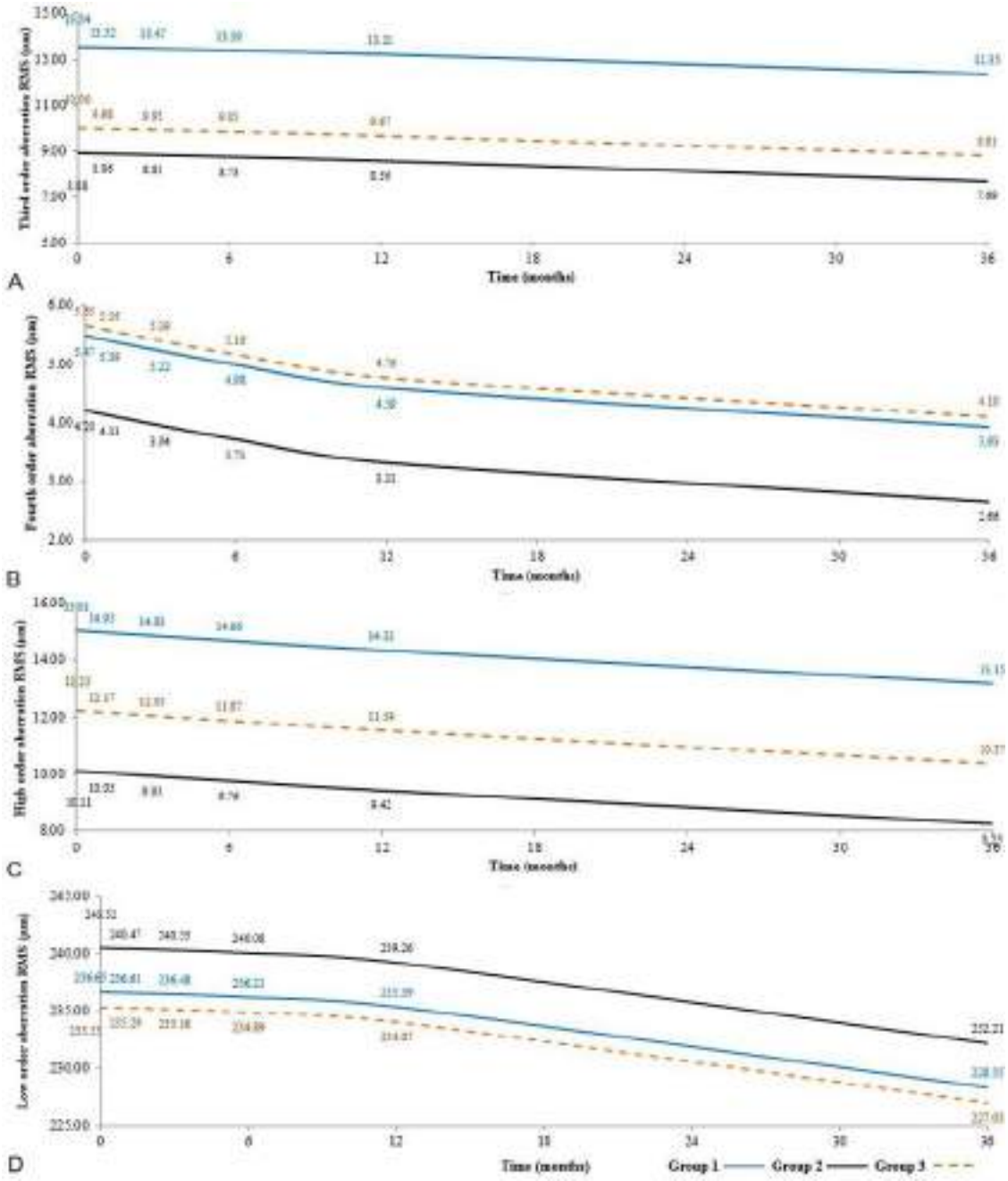

Figure 12. Statistical mean results of corneal aberrometry along with three years follow-up in **G-1**, **G-2**, and **G-3**.

Note the improvement in the statistical mean corneal aberrometry values compared to the preoperative mean values. **(A)** Shows the third order aberration **RMS (3rd order RMS)** (µm)**. (B)** Shows the fourth

order aberration **RMS (4th order RMS)** (µm). **(C)** Presents the high order aberration **RMS (HOA RMS)** (µm) **(D)** Illustrates the Low order aberration **RMS (LOA RMS)** (µm). Notice the improvement in all mean values of aberrations till 36 months' post-operative comparing with the pre-operative mean values. The figure is taken from the scientific paper of El Zarif M et al. (180) credited for this thesis.

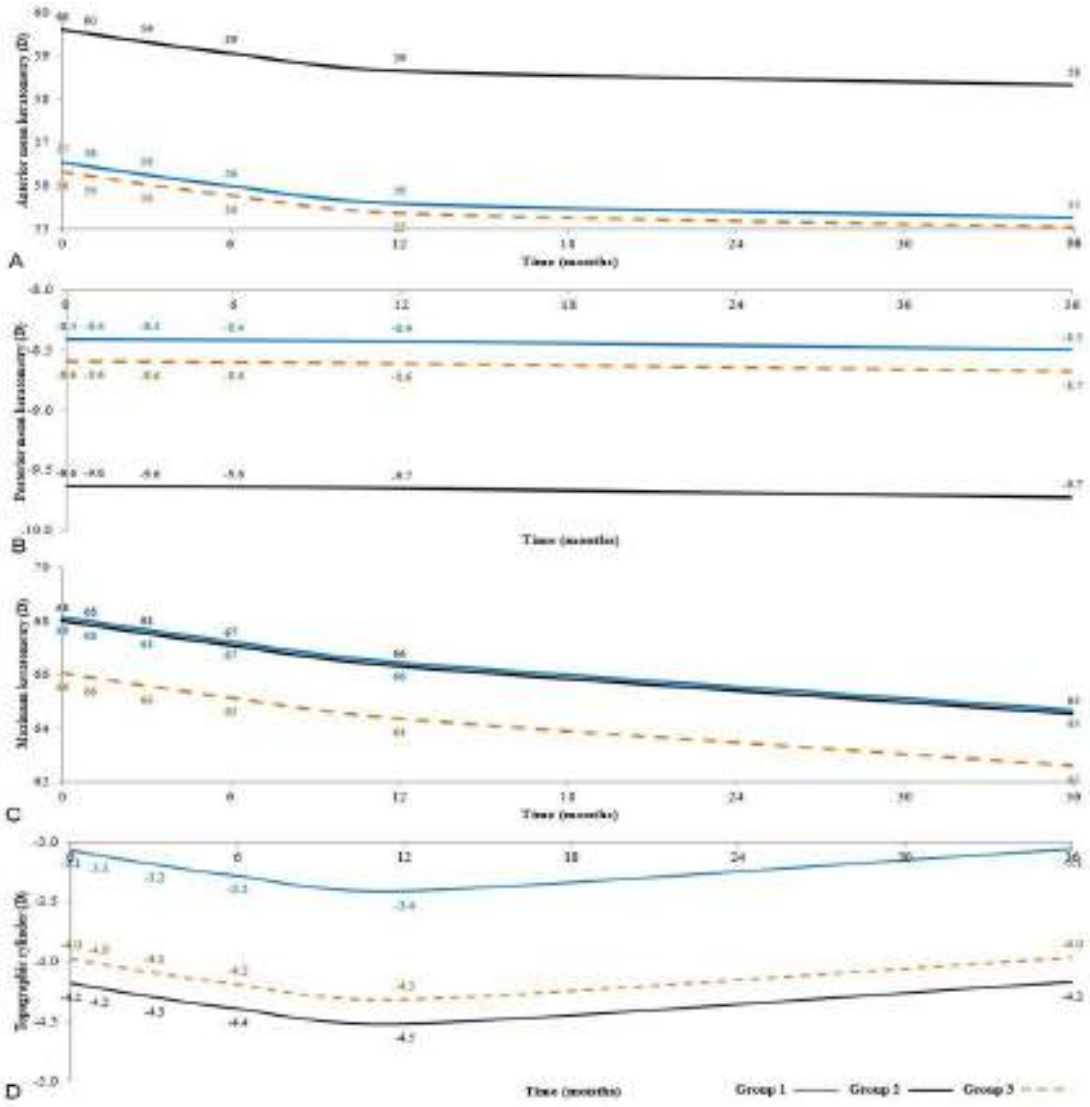

Figure 13. Statistical mean results of the secondary variables along with three years follow-up in **G-1**, **G-2**, and **G-3**/ preoperative mean values.
(A) Shows mean values of anterior mean keratometry (**Anterior Km)** in (D), notice the improvement of 1 diopter at 12 months, followed by another 1 diopter of flattening till 36 months. **(B**) Shows the posterior mean keratometry (**Posterior Km)** in (D), the mean values were nearly stable in all groups at 36 months with an only mean difference of (0.1**)** (D). **(C)** Observe the maximum keratometry (**Kmax)** in (D), there was a mean value of 2 diopters of flattening at 12 months, followed by another 1 diopter of flattening till 36 months. **(D)** Note the topographic cylinder

(Topo Cyl) in **(D),** change of -0.3 (D) at 12 months, meanwhile, at 36 months mean values rose until the same initial pre-operative results. The figure is taken from the scientific paper referred to El Zarif M et al. (180) credited for this thesis.

Table 6. Keratometric mean values of **Anterior Km** (D), and maximum keratometry **Kmax** in (D) in **G-1**, **G-2**, and **G-3**.

Group	Time/month	Anterior Km (D) Mean values	Kmax (D) Mean values
G-1	0	57.00	68.00
G-1	36	55.00	65.00
G-2	0	60.00	68.00
G-2	36	58.00	65.00
G-3	0	56.00	66.00
G-3	36	55.00	63.00
(G-1) – (G-2)	0	-3.00	0.00
(G-1) – (G-2)	36	-3.00	0.00
(G-1) – (G-3)	0	1.00	2.00
(G-1) – (G-3)	36	2.00	5.00
(G-2) – (G-3)	0	4.00	5.00
(G-2) – (G-3)	36	3.00	2.00

The difference in mean values among the groups: (**G-1**) – (**G-2**), (**G-1**) – (**G-3**) & (**G-2**) – (**G-3**). Anterior mean keratometry **(Anterior Km)** in (D), maximum keratometry **(Kmax)** in (D) (Pentacam; Oculus Inc., Wetzlar, Germany). The table is taken from the paper of El Zarif M et al. (180) credited for this thesis.

The progressive flattening of the cornea explains the improvement observed in the refractive sphere and visual parameters. The aberrometric improvement that is observed is consistent with such improvements in the visual parameters. We consider these results to be relevant for the eyes

that were selected for the investigation since they were advanced keratoconus cases with an indication for corneal graft as the only therapeutic alternative. Interestingly, the production of neo-collagen and the increase in corneal thickness were observed following the implantation of **ADASCs** and decellularized or **ADASCs** -recellularized laminas (Figure. 14). Whether this finding has any influence on the debilitated biomechanics of the cornea with advanced keratoconus, it will be warranted with further investigations (8).

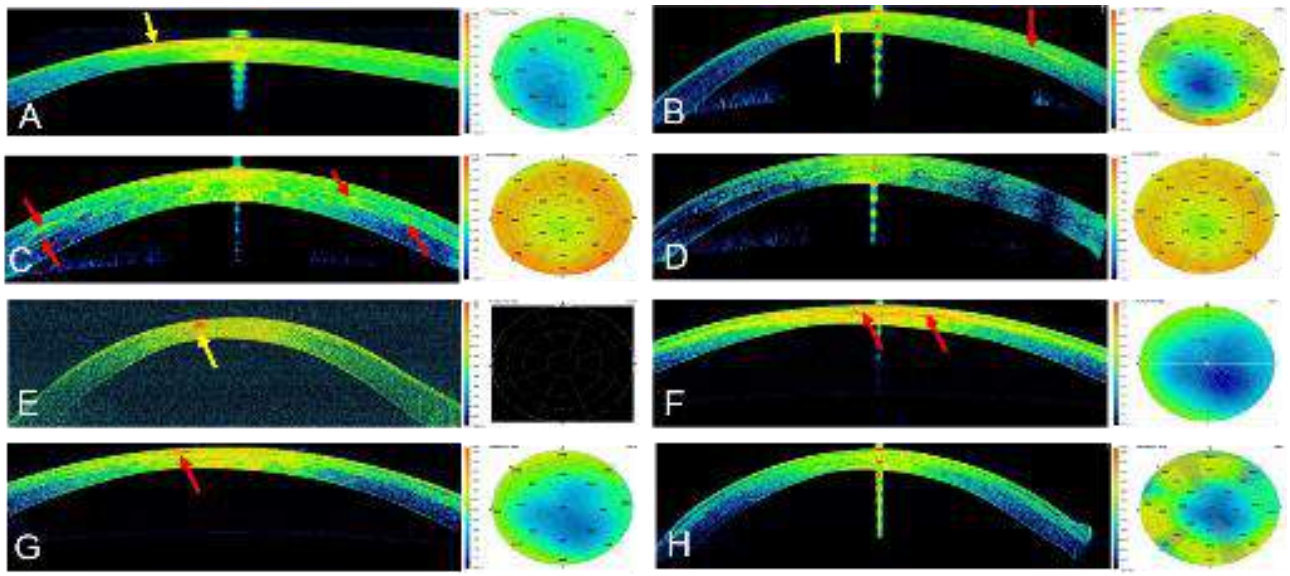

Figure 14. Cornea Visante optical coherence tomography images **(**Visante **OCT)** and pachymetric maps.
(A, B) Patient **G-1**, case-2. **(A)** At 1-month post-op, notice the reflective paracentral scar (yellow arrows). **(B)** At 3 years' post-op, shows an improvement in the reflective band of neo-collagen (red arrow). **(C, D)** Patient **G-2**, case-6. **(C)** At 6 months, observe the high reflectance of the neo-collagen band (red arrow) and the improvement in the pachymetric map (right side). **(D)** At 3 years, observe the improvement of the reflective band of neo-collagen (right side) and the stability of the pachymetric map. **(E, F, G, H)** Patient **G-3**, case-11. **(E)** At the preoperative, the reflective para-central scar can be noticed (yellow arrow). The paquimetric map was not captured due to the very thin cornea. **(F)** At 1 month, the high reflectance of the neo-collagen band can be seen (red arrow). **(G)** At 12 months, the improvement of the reflective band of neo-collagen (red arrow) and the pachymetric map can be seen. **(H)** At almost 3 years. Notice the enhancement of the integration of the lamina. The reflective paracentral scar has disappeared and the stability of the pachymetric map can be seen. The figure is taken from the scientific paper referred to El Zarif M et al. (180) credited for this thesis.

The modest increase observed in the corneal thickness in **G-1** was not significant during the 3 years' follow-up, while in **G-2** and **G-3** the increase of thickness was statistically significantly better. The implanted laminas showed evidence of biointegration of the implanted tissue in the host stroma by biomicroscopy as well as by the **AS-OCT** study. The highly reflective light observed in the results of **OCT** and the early haziness observed by the oblique light of the slit lamp, decreased gradually from the third postoperative month (31,177,254) until the end of the three years follow-up, when the lamina was well integrated into the corneal stroma. Such biointegration may be related to the slight decrease in pachymetric and volumetric parameters observed in **G-2** and **G-3**.

Biomicroscopy examination demonstrated that all corneas at 3 years had a fully transparent visual axis (Figures. 15-17). Some preoperative paracentral scars present in some cases showed a progressive improvement as in case-2, **G-1**, and case-11, **G-3**, this could be related to the implantation of **ADASCs** and the production of the neocollagen as previously demonstrated in the animal model (Figures. 15C, 15D, 15F, 17A-17E) (30,31,177–180). Also, the transparency of the implanted tissue improved over the follow-up (Figures. 16B-16E, 17B-17E). Nevertheless, the presence of mild paracentral fibrotic tissue was observed in all cases in **G-2** and **G-3** (Figures. 16D, 16F, 17C-17E, 17F right side). This fibrotic tissue was located at the paracentral lamina interface. No significant correlation was found between the recellularization of the lamina and the presence of this fibrotic tissue (179), this fact was also correlated with the corneal transparency observed from three months and up to 3-years of follow-up in the groups treated with laminas. Its formation may be avoided in the future by controlling the activation of host keratocytes as well as the keratocytes differentiated from the implanted **ADASCs**. Published studies support the hypothesis (255) that corneal wound healing is mediated by secreted extracellular vesicles (**EVs**) containing

micro ribonucleic acid (**miRNA**). These vesicles could decrease the expression of fibrotic-inducing genes and restore the normal tissue morphology transferring specific **miRNA** to the target tissue.

However, despite the limitations related to the limited number of cases included in this pilot investigation, we consider that the 3-year outcomes demonstrate the safety and therapeutic potential of our method. Nevertheless, the results must be interpreted with caution.

The results described herein show that our approach offers a new type of surgery to increase corneal thickness in advanced keratoconus cases. Visual parameters, topography, and aberrometry parameters improved in almost all the study cases. Future studies are needed with larger cohorts and selecting cases with less severe grades of keratoconus with different phenotypes to obtain more scientific evidence to support the clinical application of this new type of corneal surgery.

The potential influence of the implantation of mesenchymal stem cells and corneal laminas on the progressive nature of the disease merits further study to be confirmed. However, we consider that the 3-year outcomes give rise to a new potential for clinical application and perhaps a new horizon for the clinical use of mesenchymal **ADASC**, and a new type of corneal stroma therapy in corneal surgery.

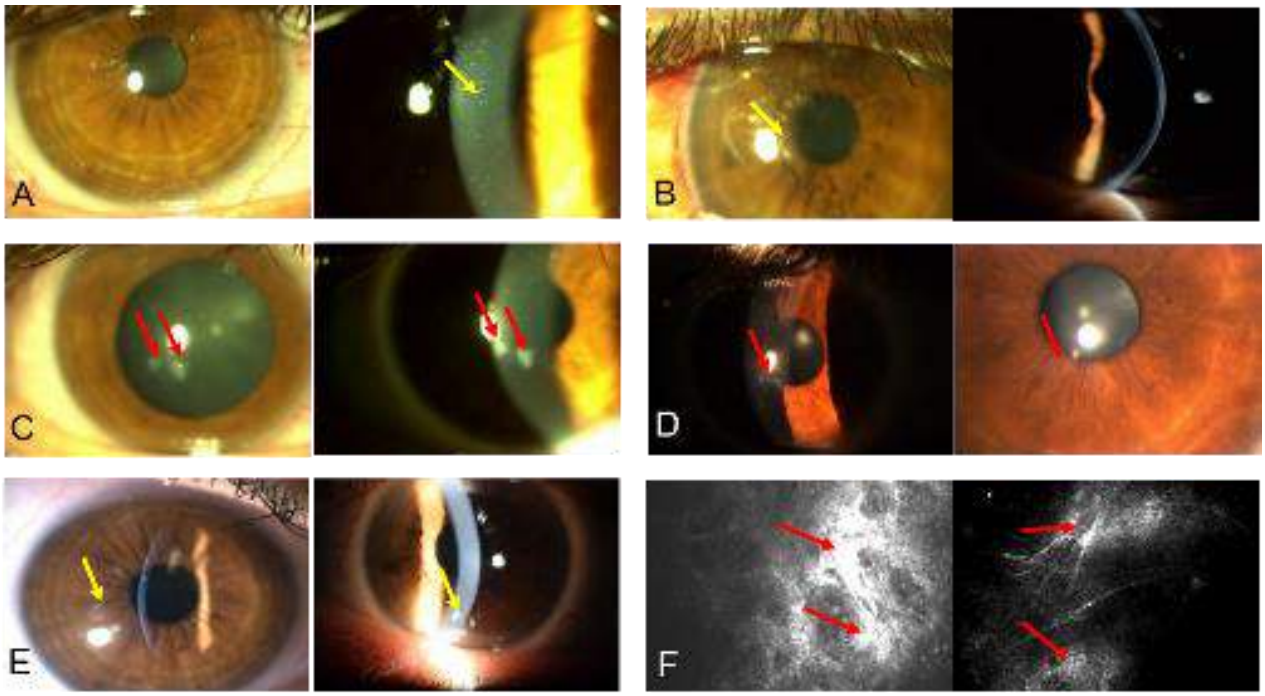

Figure 15. G-1 clinical biomicroscopic changes between the preoperative status and 36 months. (**A**) Case-1: Shows corneal transparency at 1day postoperative (left). Small grayish precipitates can be observed within the surgical plane (right) (yellow arrow) but without any impact on the visual performance. (**B**) Case-4, Observe the corneal transparency at 1 day postoperative (left) and the small grayish precipitates within the surgical plane (yellow arrow). Normal corneal transparency at 6 months (right). (**C**) Case-2: observe the presence of paracentral scars (red arrows) at the preoperative level (left) and 1 month postoperative (right). (**D**) In the same case-2, at 12 months (left) and 36 months (right): observe the marked improvement of the paracentral scars (red arrows). (**E**) Case-1 (left) and Case-4 (right) 36 months: some scattered, faint, patchy ‘‘islands’’ of haze (yellow arrows) could be observed without any impact on the visual performance. (**F**) Confocal microscopy findings in Case-2: notice the high reflective deposits and fibrotic tissue in the anterior stroma of the cornea at the preoperative level (red arrows; left), that corresponded to the paracentral scars. 12 months (right) improvement of the anterior stroma fibrotic tissue could be observed (red arrows). The figure is taken from the paper referred to El Zarif M et al. (180) credited for this thesis.

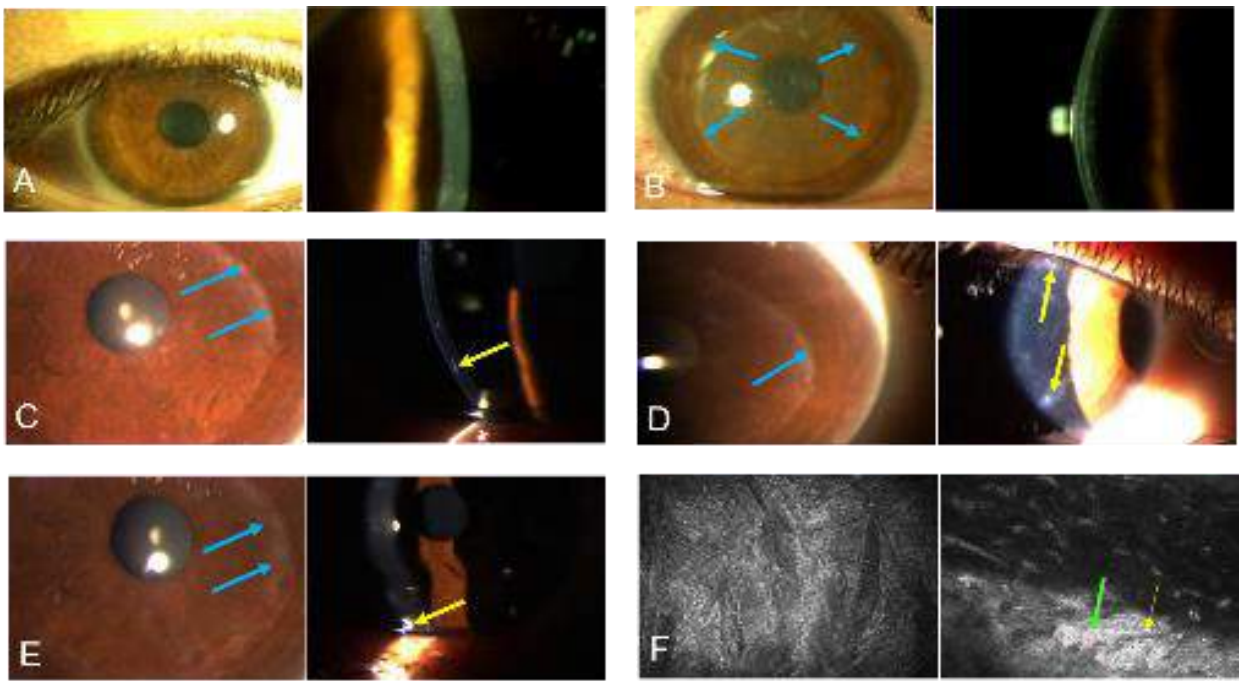

Figure 16. Biomicroscopy changes among the preoperative and 36 months in **G-2** case-5.
(A) Preoperative. (Left and right). **(B)** At 1 day postoperative (left and right): reduced transparency due to edema of the implanted lamina. (Blue arrows) show the borders of the lamina. **(C)** At 6 months: (the blue arrows; left) and the (yellow arrow; right) point to the periphery of the lamina. **(D)** At 12 months: border of the implanted lamina (blue arrow; left). Paracentral fibrotic tissue at the surgical plane (yellow arrows; right). **(E)** Improvement in the transparency of the implanted tissue at 36 months (blue arrows). Paracentral fibrotic tissue at the surgical plane (yellow arrows; right). **(F)** Confocal microscopy image in **G-2** case-5: at 1 month (left) we can observe the acellular anterior surface of the decellularized lamina. After 12 months (right), we can see the accumulation of migrating keratocytes nuclei from the host stroma toward the posterior surface of the decellularized lamina (green arrow), and the presence of some paracentral fibrotic tissue in the periphery of the lamina (yellow arrow). The figure is taken from the paper of El Zarif M et al. (180) credited for this thesis.

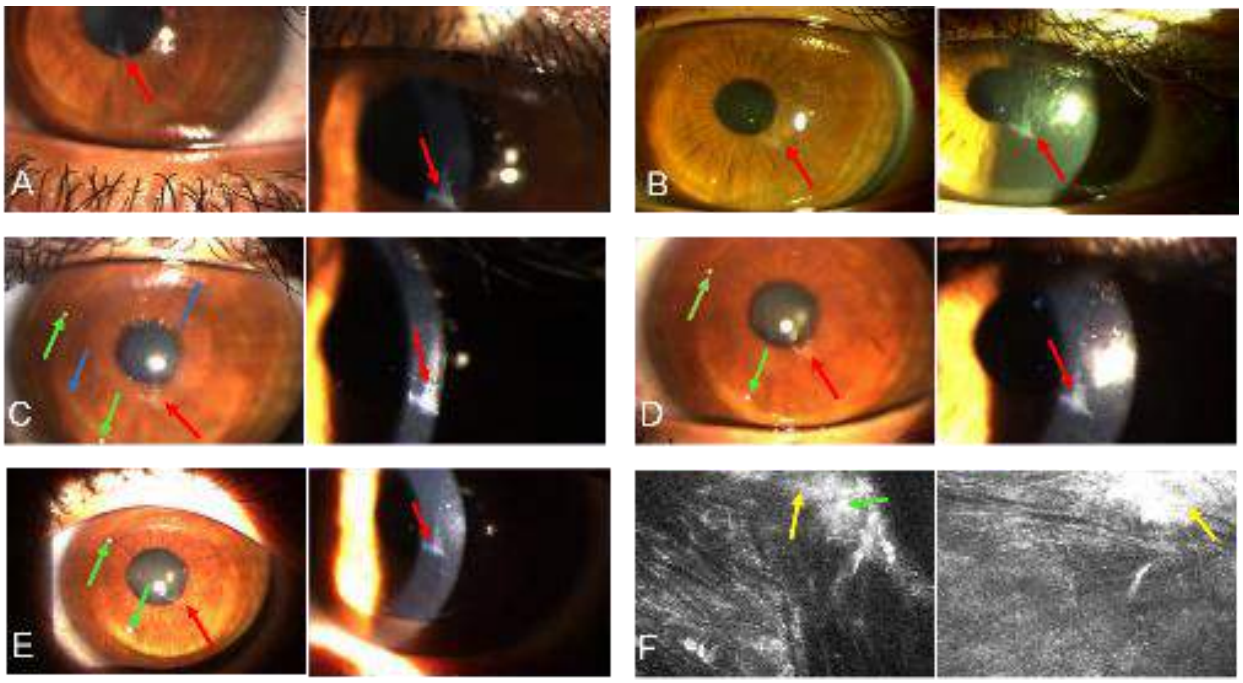

Figure 17. Biomicroscopy changes in **G-3**, case-11 from preoperative until 36 months.
(A) Preoperative. (Red arrows) shows the presence of a paracentral scar. **(B)** At 1 month. (Red arrows) shows the paracentral scar. **(C)** At 6 months. (Blue arrows) shows the periphery of the recellularized lamina, (red arrows) indicate the paracentral scar and the (green arrows) show paracentral fibrotic tissue with an accumulation of migrating keratocytes toward the border of the lamina. **(D)** 12 months: observe the slight improvement of the paracentral scar (red arrows). Note that the border of the lamina is not remarkable. (Green arrows) indicate the presence of the same paracentral fibrotic tissue. **(E)** At 36 months: observe the improvement of the paracentral opacification (red arrows). (Green arrows) shows the same fibrotic anterior tissue. (**F**) Confocal microscopy in **G-3** case-11: (green arrow) point accumulation of migrating keratocytes on the periphery of the posterior surface of the recellularized lamina (left), while the (yellow arrow) shows the presence of some fibrotic tissue. 12 months later (left), a highly reflective fibrotic tissue (yellow arrow) in the anterior surface of the recellularized lamina is present. The figure is taken from the paper referred to El Zarif M et al. (180) credited for this thesis.

7.6. **El Zarif M**, Abdul Jawad K, Alió del Barrio JL, Abdul Jawad Z, Palazón-Bru A, De Miguel MP, et al**. Corneal stroma cell density evolution in keratoconus corneas following the implantation of adipose mesenchymal stem cells and corneal laminas: An in vivo confocal microscopy study.** IOVS. 2020;61(4)22.

In this innovative clinical study, we described for the first time the evolution of the mesenchymal stem cells implanted into the human corneal stroma using *in vivo* corneal confocal microscopy. The results reported here complete the previous clinical results published elsewhere concerning this human clinical study (30,31,177,179).

According to the results of this confocal study, following the injection of only **ADASCs** into corneal pockets created using a femtosecond laser in **G-1** there was a statistically significant increase in the density of corneal keratocytes in the anterior, mid, and posterior stroma [$P < 0.001$] (Figure. 18). This correlates well with the already reported production of new collagen, which resulted in an improved corneal thickness (30). We also observed in **G-1** relevant changes in the morphology of the implanted cells from the moment of their implantation into the corneal pockets, as the morphology of the **ADASCs** was round in shape until the third month. This finding suggests survival of the implanted stem cells following their implantation. Later on, the cells showed changes ranging from forming clusters around individual cells to developing the confocal appearance of adult stromal corneal cells at 12 months after surgery (179).

In **G-2** and **G-3**, where corneal laminas were implanted with or without impregnation with **ADASCs**, we observed that implantation of such laminas, whether or not colonized by **ADASCs**, favored an increase in the number of corneal stromal cells in the anterior and posterior stroma of the cornea in a highly statistically significant level [$P < 0.001$] (Figures. 18A, 18C).

In vivo confocal microscopy offers the possibility of studying the normal morphology of the cornea and microstructural changes that can occur in keratocyte density and the morphology of keratocytes in the keratoconic cornea (6,9,104,125,238,239). Normal human keratocytes in full-thickness central corneas have been studied by various authors (125,239) using a different technology (Tandem Scanning Corporation, Reston, VA, USA) and different metrics (cells/mm^3)

with confocal microscopes. Other authors in more recent publications used a laser scanning *in vivo* confocal microscope (Heidelberg Retina Tomograph II/RCM) and found that mean keratocyte density in the control group was 786 ± 244 cells/mm^2 in the anterior stroma and 293 ± 35 cells/ mm^2 in the posterior stroma. In the keratoconus group that did not wear contact lenses, the values were 662 ± 193 cells/mm^2 and 236 ± 32.6 cells/mm^2 in the anterior and posterior stroma, respectively (6).

In our study, we increased cell densities in the anterior mid, and posterior stroma at 12 months compared to the preoperative level (Figure. 18; Table 7), but we did not detect any new formation of fibrotic structures in G-1 (Figures. 15A, 15B). The presence of fibrotic tissue seemed to be related to groups that received only laminas (with or without **ADASCs**). This was more evident in **G-3**, whereas in **G-1** fibrotic structures were absent until 12 months after surgery. We noticed an improvement of corneal scarring for case-2 from **G-1** at 12 months after surgery (Figures. 15C, 15D, 15F, 19C, 19D) (30,31,177,179). Nevertheless, in **G-2** and **G-3** fibrotic structures were present in patients almost in the periphery of the implanted laminas (Figures. 16D, 16E, 16F right side, 17C-17F, 20B, 20D, 20E, 20G; Table 8). It has been postulated that mesenchymal stem cells can either avoid or improve preexisting scars; although in the non-peripheral areas of the implanted laminas, we do not notice differences in corneal transparency between the three groups, nor the observation of corneal haze (Figures. 19C, 19D, 20A, 20C) (30,177,179).

Moreover, changes inside the acellular laminas implanted in **G-2** were also observed. This finding demonstrates that the decellularized lamina was colonized by the patient's keratocytes, a process that began in the first month. After 12 months, the lamina was found to be completely recellularized (Figures. 7B, 7C, 21).

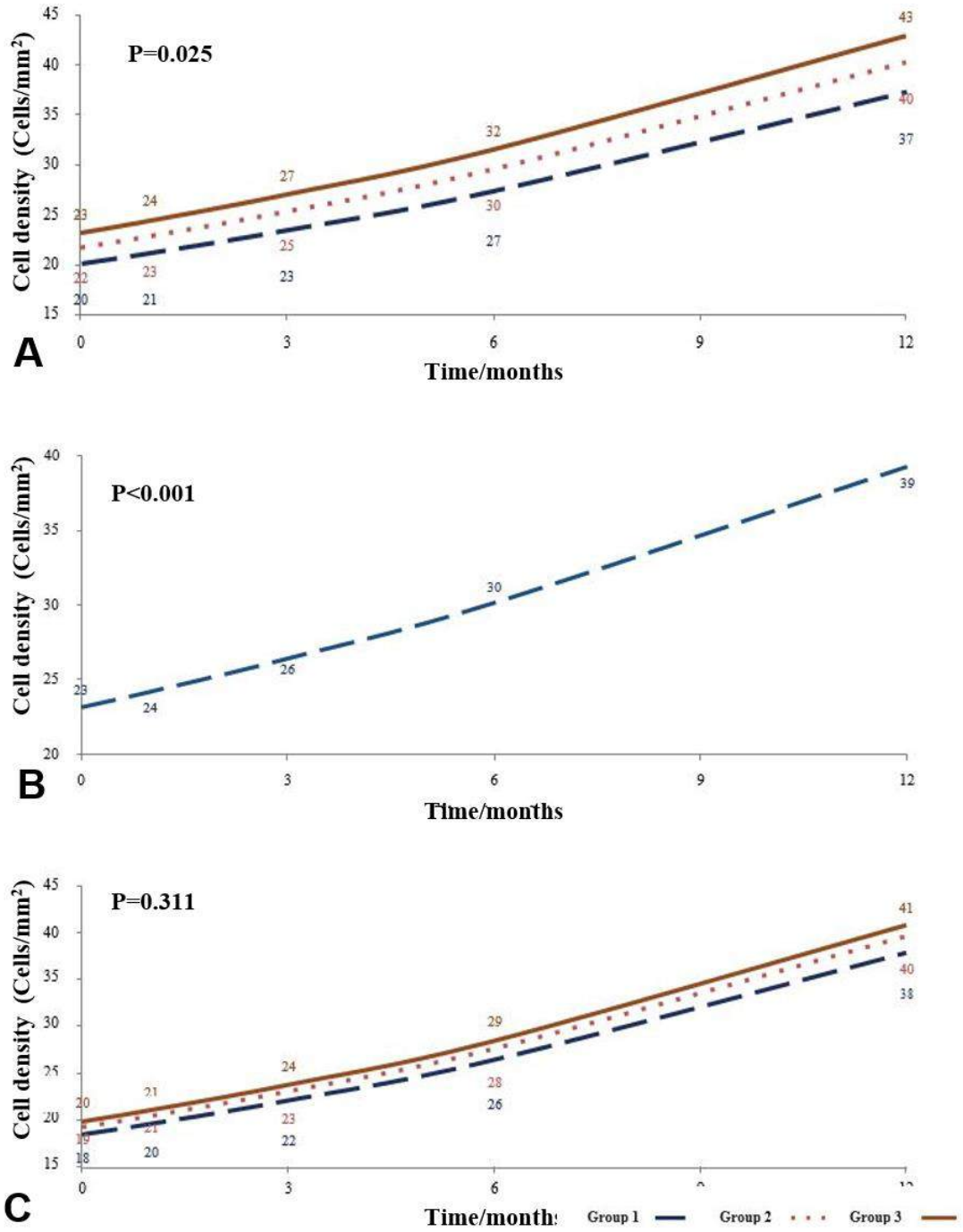

Figure 18. Statistical results of cell density changes in the corneal stroma of **G-1**, **G-2** and **G-3** along with 12 months follow-up.
(**A**) Increase in cell density over time in the anterior stroma of the cornea in **G-1**, **G-2**, and **G-3** from the preoperative period until 12 months after surgery. A significant statistical difference [P = 0.025] among the groups was detected. (**B**) Statistically significant increase in cell density [P < 0.001] over time in the mid-stroma of the cornea in **G-1** from the preoperative period until 12 months after surgery. (**C**) Increase in cell density over time in the posterior stroma of the cornea in **G-1**, **G-2**, and **G-3** from the preoperative period until 12 months after surgery. There was no significant

difference among the three groups [P = 0.311].The figure is taken from the scientific paper referred to El Zarif M et al. (179) credited for this thesis.

Table 7. Counted Nucleus Cell Ratios

	Anterior Stoma	Mid Stroma	Posterior Stroma	Ant. surface of the lamina	Within the lamina	Post. Surface of the lamina
Group-1	372/201=1.850	393/232=1.693	379/185=2.048	----	----	----
Group-2	403/217=1.857	-------	396/193=2.051	102/28=3.642	95/14=6.785	165/43=3.837
Group-3	430/232=1.853	-------	408/199=2.050	251/69=3.637	254/38=6.684	328/86=3.813

Counted nucleus cell ratios are the proportion of cell densities 12 months after surgery compared with the preoperative values in **G-1**, **G-2**, and **G-3**. The table is taken from the scientific paper of El Zarif M et al. (179) credited for this thesis.

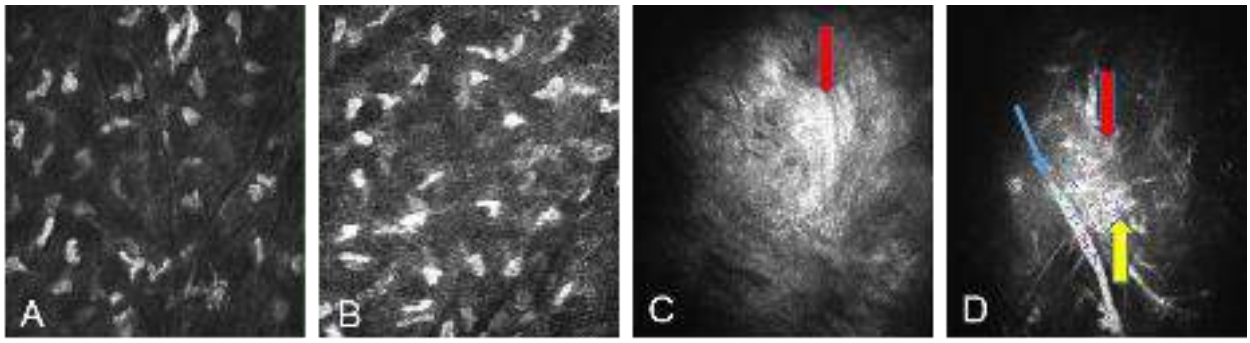

Figure 19. Findings of confocal microscopy throughout the 12 postoperative months.
(**A, B**) Cell count of the anterior and posterior corneal stroma for case-10 from **G-3,** 12 months after the operation. (**A**) Anterior corneal stroma with abundant corneal stromal cells. The number and morphology of corneal stroma cells are very similar to those of normal stroma. (**B**) Posterior corneal stroma with a high number of corneal stroma cells. The image shows that corneal stromal cells of the posterior stroma are similar in number and morphology to stromal cells of a normal cornea. (**C**) The presence of hyperreflective deposits (red arrow) corresponded with the preoperative paracentral corneal scarring observed in preoperative case-2 from **G-1**. (**D**) Improvement of the fibrotic tissue (red arrow) at the same level with the same case-2 from **G-1** is observed. Note the presence of fibroblast (yellow arrow). Part of the superficial corneal nerve can be noted (blue arrow). The figure is taken from the scientific paper of El Zarif M et al. (179) credited for this thesis.

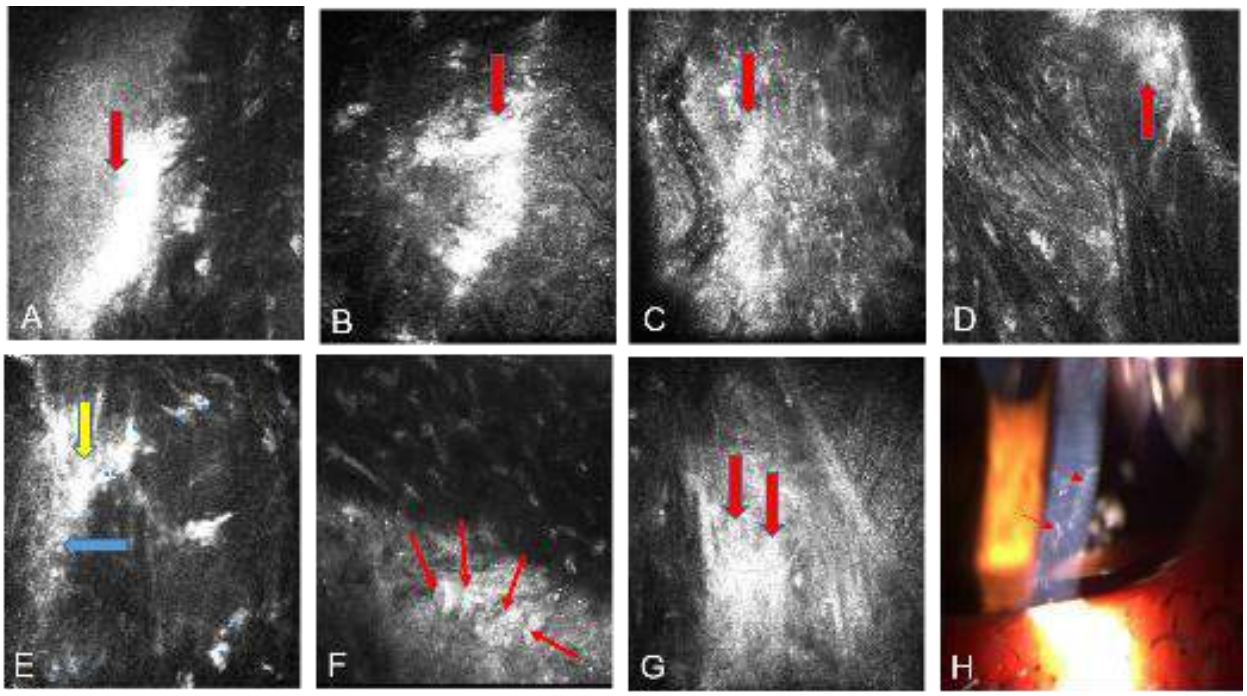

Figure 20. Findings of fibrotic tissue obtained by confocal microscopy and slit lamp. Morphological changes of corneal keratocytes.
(**A**) The presence of highly reflective fibrotic tissue (red arrow) of keratoconic in **G-3** case-11 corresponds with the preoperative paracentral anterior stroma scar observed at 3 months after surgery. (**B**) The presence of fibrotic tissue (red arrow) is highly reflective on the periphery of the posterior surface of the lamina at 3 months for the same case. (**C**) Improvement of the paracentral preoperative fibrotic tissue (red arrow) on the anterior stroma of the same case-11, 6 months after the operation. (**D**) Improvement of the fibrotic tissue (red arrow) on the periphery of the posterior surface of the recellularized lamina of the same keratoconic case, 12 months after surgery. (**E**) Presence of fibroblast or myofibroblast (yellow arrow), and fibrotic tissue (blue arrow) on the posterior surface of the decellularized lamina of a keratoconic patient 3 months after surgery. (**F**) The transition zone between the posterior surface of the decellularized lamina and the host stroma showing several migrating corneal stromal cells (possibly keratocytes?) with dendritical shapes (marked with red arrows) in a keratoconic patient 12 months after surgery. (**G**) Presence of highly reflective fibrotic tissue (red arrow) on the periphery in the mid-stroma of the decellularized lamina of a keratoconic patient 6 months after surgery. (**H**) Slit-lamp image of a keratoconic patient demonstrating peripheral scar tissue 6 months after surgery. The figure is taken from the scientific paper referred to El Zarif M (179) credited for this thesis.

Table 8. Represents Presence or Absence of Fibrotic Tissue in **G-1**, **G-2** & **G-3**.

	Group	0 month	1 month	3 months	6 months	12 months
Case-1	1	-	-	-	-	-
Case-2	1	+++ *	++ *	++ *	+ *	+ *
Case-3	1	-	-	+ †	-	-
Case-4	1	-	-	+ †	-	-
Case-5	2	-	-	+/++ †	+/+ + †	+/++
Case-6	2	-	-	-	+/++ †	+/++ †
Case-7	2	-	-	-	+/++ †	+/++/+++ †
Case-8	2	-	+ †	+/+++ †	+/++ †	-
Case-9	2	-	+ †	+/++ †	+/++ †	+/++ †
Case-10	3	-	+ †	+/++ †	+/++/+++ †	+ †
Case-11	3	+++ *	++ † +++ *	+++ † +++ *	+/++/+++ † ++ *	+/++ † + *
Case-12	3	-	-	-	+/++/+++ †	+/++/+++ †
Case-13	3	-	-	+/++ †	+/++/+++ †	+/++ †

Note: +, minor fibrotic tissue; ++, moderate fibrotic tissue; +++, high fibrotic tissue; –, absence of fibrotic tissue.

*Presence of paracentral scar with fibrotic tissue in the preoperative period; we observed an improvement of scars and a decrease of fibrosis.

†Presence of fibrotic tissue during the postoperative follow-up.

The table is taken from the scientific paper of El Zarif M (179) credited for this thesis.

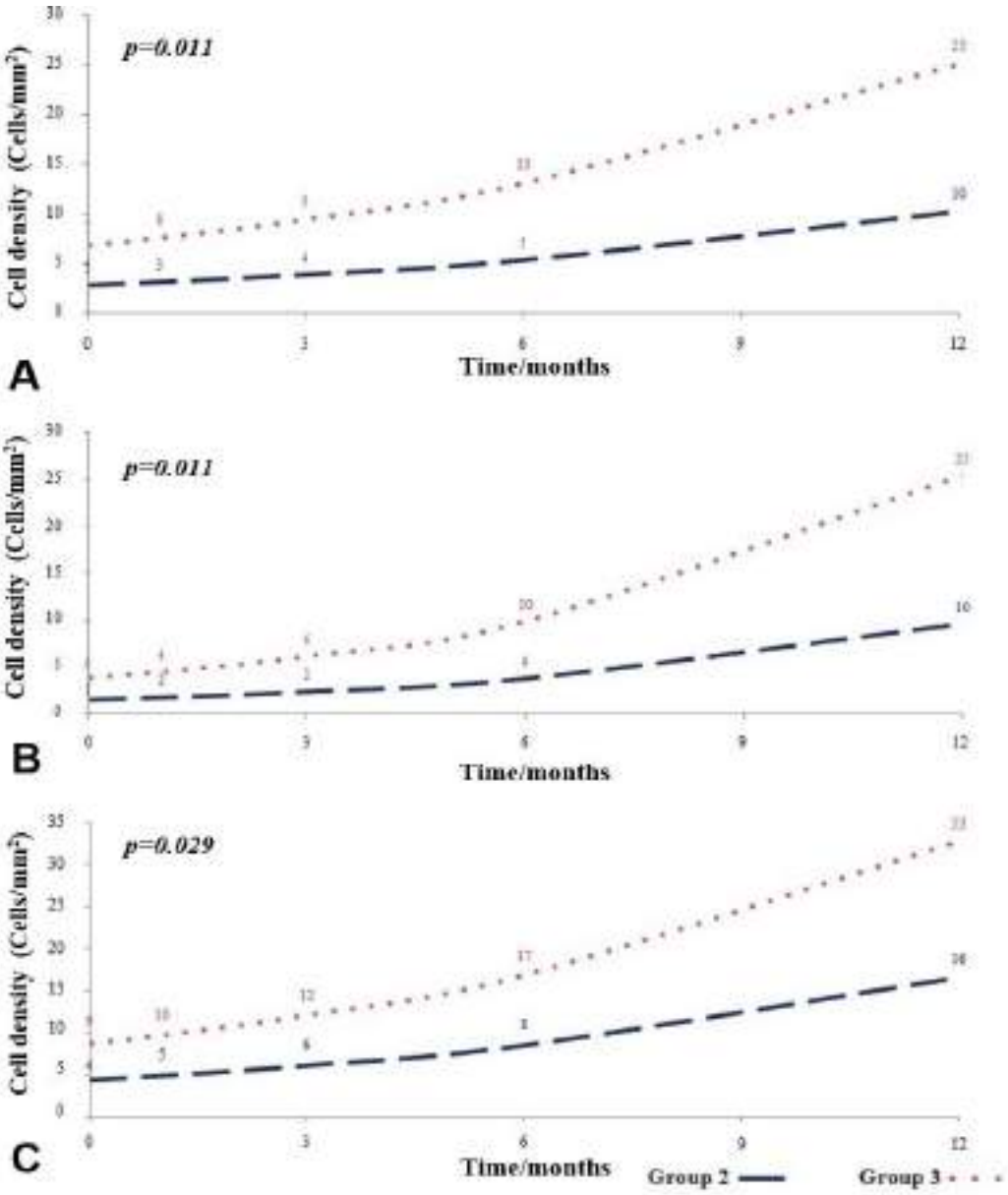

Figure 21. Statistical results of the cell density in the anterior, mid, and posterior surfaces of the laminas along with 12 months follow-up.
(**A**) Increase in cell density over time in the anterior surface of the lamina in **G-2** and **G-3** from the preoperative period until 12 months after surgery. A significant statistical difference [P = 0.011] exists between **G-2** and **G-3**. (**B**) Increase in cell density over time in the mid-stroma of the lamina in **G-2** and **G-3** from the preoperative period until 12 months after surgery. A significant statistical difference [P = 0.011] between **G-2** and **G-3** was detected. (**C**) Increase in cell density over time in the posterior surface of the lamina in **G-2** and **G-3** from the preoperative period until 12 months after surgery. A significant statistical difference [P = 0.029] between **G-2** and **G-3** was detected. The figure is taken from the scientific paper referred to El Zarif M (179) credited for this thesis.

On the other hand, we have also observed that from the first postoperative month in the recellularized laminas of **G-3** a decrease occurred in the clusters of the mesenchymal cells implanted on the laminas. Such cellular morphological changes were seen to occur first on the posterior surface followed by the anterior surface (Figures. 8A, 8B), and the number of cells statistically and significantly increased from 1 month after the surgery to 12 months after surgery (Figures. 8C-8E, 21). This finding may suggest survival and differentiation of the implanted cells toward keratocytes and/or repopulation of these laminas, with the migration of the host corneal stromal keratocytes being stimulated to proliferate toward the decellularized corneal tissue (256). As the cells could not be labeled before implantation due to possible interference with transparency and hence ethical issues, the distinction between both populations is not possible. This finding correlates well with another report (256) that demonstrated that propagation and migration of corneal fibroblasts happen in parallel with furrow ridges aligned with collagen lamellae. During the migration of these cells, tracks for propagation are established by alignment of the fibrils through the generation of a mechanical force. It is also possible that chemoattractant factors may be released by the **ADASCs** during the evolution following implantation (257).

Besides, we observed in this study that stromal cells, which are likely to be keratocytes, fibroblasts, or myofibroblasts, have migrated from the corneal stroma toward the edge of the lamina in cases where no cells were injected (Figures. 20E, 20F). Such stromal cells (keratocytes) show peripheral prolongations and morphological transformations with dendritic forms, indicating that they have differentiated into fibroblasts and myofibroblasts during their period of activity and that they are capable of sliding on the collagen fibers of the decellularized or recellularized tissue (Figures. 16F right side, 17F left side, 20E, 20F) (256). We also observed, up to 12 months after

surgery, the development of paracentral fibrotic tissue on top of the photoablated stroma of the implanted tissue (Figures. 20B, 20D, 20E, 20G) (256).

We have reported herein an evolution in the morphology of corneal stromal cells, presumed to be keratocytes. It has been reported that these cells are normally oval and irregular in shape and without a dendritic shape. It is when they migrate or are activated that they assume a dendritic shape (125,256). Because the evolution of stromal cell morphology in our study did not follow such a pattern, our observation does not support previous reports (21), which have described that in adult tissue keratocytes are mitotically quiescent and have a flat, dendritic morphology (258).

Furthermore, it would be important in future studies to establish differences among the various morphologies that are observed in stromal cells to compare the evolution of those that have a non-dendritic shape to those that have dendritic shape, and the biological implications that such morphological changes may have.

A relevant issue of the present study is the methodology used for counting stromal cells, which was a specific manual method. This may introduce a certain amount of subjectivity and interpretation bias (Figure. 5); however, this method provided us with a more accurate and discriminating cell count than the automated cell counts of the confocal microscope, which are affected by large variability, inaccuracies, and misinterpretations. The presence of highly reflective fibrotic tissue in the studied areas could make it difficult to discriminate the edges of the keratocytes nuclei that were the main focus of our study (Figures. 16F right side, 17F, 19C, 19D, 20).

We believe that it is necessary to establish a more objective cell count method based on image processing programs and specific algorithms in which the contrast and illumination can be edited, and various specialized filters are used to optimize the visualization of keratocyte cells and to better calculate their size.

7.7 El Zarif M, Alió del Barrio JL, Arnalich-Montiel F, De Miguel MP, Makdissy N, Alió JL. **Corneal stroma regeneration: New approach for the treatment of cornea disease**. APJO. 2020;9(6):571–9.

In this report, we presented an integrated overview, based on evidence, about the current stage of the experimental clinical studies performed by our research group in the topic of corneal stroma regeneration and integrated into human studies in the treatment of corneal diseases, and particularly in keratoconus.

The ideal corneal stroma constructed by bioengineering should be capable of mimicking the natural human cornea and maintaining the corneal stroma homeostasis. For these purposes, it has to contain both a cell source and a collagen scaffold (8,15,16). For the cellular component, several cell types from both ocular and extraocular sources have been investigated, being the human **MSCs** the most widely tested so far. However, further development of cheaper and standardized **iPSCs** techniques may surpass **MSCs** use (200). The use of decellularized cornea sections could be the most clinically relevant (17–19). However, it is still handicapped by the need for donated corneal tissue. The use of **MSCs** exosomes (without their cellular component) reveals an exciting field of research as their use could overcome some of the limitations and risks associated with the direct delivery of stem cells to humans *in vivo* if exosomes could be applied topically (232).

The feasibility and safety of corneal stromal cell therapy for advanced keratoconic corneas were demonstrated for the first time. The appearance of new collagen formation within the surgical plane was also observed when **MSCs** were implanted (30), though collagen was not enough to restore the thickness of the diseased corneas, play a role in the stromal remodeling of corneal dystrophies and corneal scars to enhance corneal transparency (Figures. 14A, 14B). Also, the

implantation of decellularized or recellularized human corneal stroma laminas effectively restores corneal thickness (Figures. 14C, 14D, 14F-14H), and it potentially avoids any risk of graft rejection (while this risk is still present by the use of allogenic stromal implants). So far, after three years of follow-up, no patient showed inflammation, rejection, or any evidence of scarring or haze (30,31,177,179,180).

The popularization of SMILE as a refractive surgery option is providing a large amount of corneal donor tissue that could potentially be used for human transplantation. Recent studies performed by Liu R et al. and Zhao J et al. (259,260) demonstrated after 2 years of follow-up that Small incision allogenic intrastromal lenticule implantation is feasible and safe for reshaping the cornea. The corneal healing remained stable and their results were confirmed by slit-lamp biomicroscopy and by confocal microscopy *in vivo* and corneal densitometry measurements. Additionally, the authors observed corneal reinnervation signs within the lenticule. The stromal addition of SMILE created lenticules that were proven ex vivo and *in vivo* (its feasibility, safety, and efficacy in the treatment of thinning disorders such as keratoconus) (261–263). This procedure increases corneal thickness providing additional strength to the weakened cornea as well as anterior corneal flattening when using a negative meniscus-shaped lenticule (262).

Synthetic collagen scaffolds are, by definition, a promising source of donor stromal tissue as they do not need human donor tissue and so can be potentially available all over the world. However, their difficulties that are still present today, which is to mimic the transparency and strength of the human cornea, together with the high expenses for its production in the laboratory, preclude its presence in the real clinical practice for the next few years.

7.8 El Zarif M, Alió JL, Alió del Barrio JL, De Miguel MP, Abdul Jawad K, Makdissy N. **Corneal stromal regeneration: a review on human clinical studies for treatment of keratoconus.** Front Med. 2021;8:650724.

In this review, we summarized the present status of the human clinical studies reported in the peer-reviewed literature on the topic of human corneal stromal regeneration, corneal enhancement therapy, and the immediate trends that such studies have opened new perspectives in the therapy of corneal stromal diseases, particularly in keratoconus. Besides, this review offers a comparison between the different recent studies carried out with other groups and our study, being that to our knowledge, our clinical study is the only one that has carried to regenerate the corneal stroma by the implantation of autologous **ADASCs** alone into the corneal stromal pocket, or with colonized acellular human corneal.

We discussed in our previews articles the feasibility of regenerative surgeries of the corneal stroma for advanced keratoconus. Also, we demonstrated that decellularized laminas of a human corneal stroma, colonized or not by autologous **ADASCs**, can be implanted for therapeutic purposes on a clinical basis (30,31,177,179,180).

Other reports demonstrated that allogenic refractive lenticule corneal inlay using a **SMILE** lenticule combined or not with accelerated collagen **CXL** (241,242,262,264–267), is a promising surgery, no inflammation, complication, opacification, vascularization, or infection were recorded. Jorge Alio et al. (268) performed with another group a recent prospective study in Tehran, they reported a novel method for the treatment of advanced ectasia, with customized **SMILE** lenticule implantation with 22 cases of advanced keratoconus (shape of the lenticule was compound form or necklace). Corneal thickness showed a mean enhancement of 100.4 μm at the **thinnest point** measured by **AS-OCT**. An improvement in visual parameters was obtained, best **CDVA** improved

from 0.70 (range 0.4–1) to 0.49 (range 0.3–0.7) at six months with all the patients, which was in coherence with the decrease in corneal aberration, also keratometry decreased from 54.68 ± 2.77 to 51.95 ± 2.21 (D) was obtained.

Other recent studies with stromal addition of **SMILE** lenticules have been proven ex vivo and *in vivo* its feasibility, safety, and efficacy in the treatment of thinning disorders such as keratoconus (261–263). **SILK** induced in **Kmax** a flattening of 7,34 (D) and using negative meniscus-shaped lenticule addition induced also some flattening of the cone, the improvement was (5.1 D at 6 months) in **Anterior Km** better than the ones observed with Ganesh et al. (264), and planar than the lenticules implanted by our group (180).

The comparatives surgical procedures **SFII** and **PKP** resulted in a stable corneal volume, and improved visual acuity during the 24-month study period. **SFII** was less invasive and more efficient when compared with **PKP**. Using concave lenticule implantation improved the maximum central keratometry of (-4.65 ± 2.04) (D), this outcome was more planner than the laminas implanted with our studies (180,266).

However, corneal thickness increase using planner lenticules (31,177,180) is higher than the one using allogenic **SMILE** lenticule corneal inlay implantation combined or not with collagen **CXL** (262,264,266), besides, negative meniscus-shaped lenticules achieved a larger flattening, but they are only available for pure central cones, as for eccentric cones (the ones are commonly seen in keratoconus) they would generate nonacceptable aberrations within the visual axis, unlike the planner laminas, the aberrometry parameters improved in almost all the study cases. On the other hand, the visual acuity enhancement has been slightly better with the implant of negative meniscus lenticules than with the implant of planar laminas of our group (180,262,264,266), but the goal of

the stromal implant should be to improve visual acuity and at the same time significantly increase the corneal thickness in patients with advanced keratoconus.

The studies of endokeratophakia using regular **SMILE** lenticules have shown to be a feasible option not only to correct ametropias such as hyperopia, and presbyopia, but also to increase the thickness in the keratoconic cornea (269). Nevertheless, the use of customized positive meniscus lenticules in keratoconus corneas is debatable (264,268), as theoretically could worsen myopia usually encountered in such patients, and so planar or negative meniscus lenticules are always preferable for such purpose.

The use of recombinant human collagen, synthesized in yeast and chemically cross-linked demonstrated to be feasible (14,270), improved the visual acuity, nevertheless, a large variation of corneal thickness was obtained among the cases of this study up to 24 months of follow-up, and high presence of fibrosis was observed, a fact that was not observed in our study, such all detected fibrotic tissue corresponded only with the paracentral corneal decellularized or recellularized implanted laminas (179).

All the previously described studies have the limitation that they were carried out with a very small number of patients, in our study we demonstrated that the use of acellular laminas (31,177,179,180), in which the lack of cells makes the experience out from being considered as a corneal graft, and by using autologous **MSCs** from a given patient, it was possible to transform allogenic grafts into functional autologous grafts, thus avoiding any risk of rejection. So far, the long-term follow-up did not show any complications with all the cases (180). While transplantation in the cases of allogenic corneal lenticules inlays and unstructured material in the case of the recombinant **CXL** of Collagen has shown initially to be potentially effective for the treatment of

advanced keratoconus, but still having heterologous stromal cells, and should be considered as a new form of corneal stroma transplantation. Future studies will be necessary to increase the number of cases and to increase the evidence of the effectiveness of these corneal surgeries.

Future studies will be necessary to increase the number of cases and to increase the evidence of the effectiveness of these corneal surgeries.

A GLANCE TO THE FUTURE

With this pilot investigation, our main goal was to prove the safety of the implantation of **ADASCs** and decellularized or recellularized laminas with stem cells derived from the autologous adipose human tissue. Based on the outcomes of the present investigation, we may anticipate the development of new promising areas of translational research and future applications as follows:

1. The use of autologous MSCs, particularly ADASCs for therapeutic purposes: The most relevant disease that could benefit from the results of this study is indeed keratoconus, corneal dystrophies, or even corneal scars, as these cells behave well in the corneal stroma, do not cause opacities, and do not induce any inflammatory reaction. **MSCs** can substitute the diseased corneal keratocytes, and produce collagen that could restore the corneal thickness, also the biological activation caused by **MSCs** proven in the present thesis suggests that they could be useful to improve the early stages of corneal dystrophies and scarring corneal processes.

2. The use of cell bank MSCs of genetically perfect donors for corneal treatments: Considering all published evidence in the animal model where human **MSCs** were implanted in the corneal stroma, despite being a xenogeneic transplant, no signs of rejection or inflammation have ever been reported (17,19,21–28). We should also consider that adult keratocyte obtained from autologous **MSCs** may still carry the same genetic defect that led to corneal disease such as in the case of corneal dystrophy. Also, it has been observed that a gene expression differences between the **iPSCs**-derived keratocytes generated from fibroblasts of both keratoconic and normal human corneal stroma, influencing cellular growth and proliferation, confirming that, at least in keratoconus cases, adult cells obtained from **MSCs** may still not be functionally normal (233). In this scenario, the use of allogenic instead of autologous **MSCs** would be interesting. Whether

allogenic **MSCs** could achieve the same benefit without any risk of inflammation or rejection. The use of allogenic **MSCs** would greatly simplify the clinical application of **MSCs**, as clinical application centers would not need any specific equipment because potential **MSCs** banks could store and supply stem cells for their use in patients. There are already low-cost systems available that are capable of enhancing the preservation of **MSCs** at hypothermic temperatures while maintaining their normal function, thereby widening the time frame for distribution between the manufacturing site and the clinic, and reducing the waste associated with the limited shelf life of cells stored in their liquid state (231).

3- The use of molded customized acellular corneal laminas biologically activated with normal MSCs in Keratoconus in moderate and advanced stages: In moderate stages of the diseased corneas, implantation of decellularized human corneal laminas molded with **3D** techniques (271,272), would involve collagen laminas treated conforming the optical characteristics of the eye, and seeded by allogenic **MSCs**, such implant within the corneal stroma, may produce biological, and optical solutions, and may improve topographic, pachymetric, and visual parameters of the cornea. It is a non-invasive surgery, with local anesthesia, and only one suture, the epithelium, and endothelium of the cornea are conserved intact.

4- The use of acellular corneal stroma for full corneal stroma substitution: The intralamelar implantation of autologous graft can substitute the regular corneal transplantation techniques such as **PKP** or **DALK** with patients with a terminal disease. We are planning to implant a decellularized stroma using femtosecond laser-assisted, the donated decellularized corneal stroma could be even customized using the program of **3D** according to the visual, topographic, and aberrometric needs of each patient (271,272). The proposal of such innovative, and very advanced surgery preserved intact the corneal epithelium, and endothelium, it is a much less invasive surgery

and could increase in a very significant level the thickness of the diseased cornea. Furthermore, the implanted decellularized stroma would be bioactivated with allogeneic **MSCs** that recellularized the newly implanted collagen.

CLINICAL APPLICATION PHASE II

The second clinical application shall be applied to another population, ethnicity, and race to validate these preliminary results and to increase the study sample.

This study has its next phase in the FIS study number: 2018-000523-14, it is led by the Universidad Miguel Hernandez UMH in multicenter applications in Spain, the study aims are to make a phase II clinical application, in corneas of 25 patients with different stages of keratoconus, will be implanted with adipose, autologous adults, derived stem cells **ADASCs**, decellularized laminas or recelularized ones imbibed with **ADASCs**, the study has been approved according to the protocols of the Spanish government's health research fund (Spanish protocol code: EI17-00523), it is about to start once obtained the permission from the National Drug Agency. The principal investigator is Prof. Jorge L. Alió.

LIMITATIONS OF THE STUDY

The conclusions of this pilot study should be carefully considered, since they are vulnerable to bias because the study included a small sample of patients. Clinical pilot investigations of new therapies are difficult to perform and have many limitations in terms of an administrative, approbatory and ethical basis. So, future studies with a larger sample and longer follow-up should confirm the preliminary results obtained (30,31,177,179,180,241,242).

There was no control group in which only a corneal pocket would be performed since it was considered unethical as no benefit could be offered to the patient from that procedure. As this study was performed in living human volunteers, there was no possibility to perform post-mortem analysis as none of the cases so far have required corneal transplantation, with the consequent lack of tissue sample to perform histopathology. Within the experimental studies, it is easy to demonstrate, by post-mortem analysis, the survival of the previously transplanted labeled cells (by immunofluorescence analysis) and its differentiation into adult keratocytes (by keratocan expression detection) (240). However, *in vivo*, human studies have the significant disadvantage of being limited to confocal biomicroscopy findings (vulnerable to subjective interpretations) to observe the transplant behavior of cells *in vivo* (105,179). A perfect collaboration of the patient is always needed but is not always the case with all patients, which implies reducing the accuracy of the depth measurement in the evaluated plane. Besides, the methodology used for counting stromal cells was performed with a specific manual method. This may introduce a certain amount of subjectivity and interpretation bias. However, this method currently provided us with a more accurate and discriminative cell count than the automated cell count of the microscope which is affected by large variability, inaccuracies, and misinterpretations (105,179). The presence of highly reflective fibrotic tissue in the studied areas could generate difficulties in the discrimination of the edges of keratocytes nuclei that have been the main objective of our study (Figures. 17F right side, 20B, 20G) (179). Given all these limitations, we could observe the presence of round cells in the surgical plane in all patients, compatible with transplanted **ADASCs**, showing later a progressive dendritic change until having a morphology that cannot be differentiated from normal keratocytes at 12 months postoperative follow-up.

In our reduced sample study, we have not been able to compare the results of patients who have received laminas containing or not **BM**. Future studies are necessary to show the difference in biomechanical results, sagittal curvature, aberrometry, recellularization of the implanted laminas and correlate it with the improvement of visual acuity (31,177,180).

In this present study, we have not been able to obtain a relevant difference between patients with intrastromal implantation of decellularized stromal tissue (with or without stem cells). In the future more massive studies it is expected to be able to study more results that are related to the biomechanics of the cornea. Therefore, beyond biomechanical studies will be necessary to answer this question (31,177,180).

STUDY STRENGTHS

In this study, we observed that stem cell delivery to the corneal stroma was carried out through a lamellar pocket assisted by a femtosecond laser at medium depth of the corneal stroma. Although the operated keratoconic corneas were very advanced in the disease and with severe thinning, we did not observe intraoperative complications such as corneal tears (30,31,177,179,180,241,242). Also, this study has demonstrated good tolerance and the possibility of increasing corneal thickness by implantation of decellularized/recellularized layers of corneal stroma created by the femtosecond laser was confirmed without any negative impact on the biomechanics, vision, and especially corneal anatomy and transparency (30,31,177,179,180,241,242).

Also, this is the first human clinical trial with long-term follow up available. The data from the first and three years of this study show that we are opening a new area of corneal surgery and

corneal research. The use of corneal laminas for a therapeutic increase in corneal thickness in weakened and thin keratoconic corneas is a new concept for research. All the corneal clinical parameters were conserved and even improved; no deterioration was observed in any of the cases of the present study. Besides, in case-2 of the group with **ADASCs** implantation we observe an improvement of the preexisting paracentral corneal scarring, As well, a similar improvement of the preexisting paracentral scars was observed, with case-11 from the group of implanted recellularized laminas. Based on the results of the present the corneal dystrophies or even corneal scars could be relevant, since these cells survive in the corneal stroma and they differ into keratocytes. They do not cause opacities and do not induce any inflammatory reaction or rejection, and may enhance corneal opacities (30,31,177,179,180,241,242).

8. CONCLUSIONS

THE CONCLUSIONS OF THIS WORK CAN BE SUMMARIZED IN THE FOLLOWING POINTS:

8.1 CONCLUSIONS CONCERNING THE PRIMARY OBJECTIVES

1. We could demonstrate the safety, and effectiveness of the implant in the following three groups of surgery:

- Autologous adipose-derived adult stem cells (**ADASCs** alone). Conclusion demonstrated in the scientific papers with references (30,177,179,180,240–242) of the scientific publications credited for this thesis.
- Decellularized human corneal stromal laminas. Conclusion demonstrated in the scientific papers with references (31,177,179,180,240–242) of the scientific publications credited for this thesis.
- Recellularized human corneal stromal laminas with **ADASCs**. Conclusion demonstrated in the scientific papers with references (31,177,179,180,240–242) of the scientific publications credited for this thesis.

2. We could demonstrate that the implantation of **ADASCs** isolated or when they are embedded into a human acellular corneal lamina, was followed by cell proliferation and did not generate any clinical or histological response of inflammation or rejection in none of the cases studied in our study throughout the postoperative follow-up.

3. We could demonstrate that the acellular corneal laminas were tolerated well by the keratoconic cornea, with the absence of any complications.

4. We proved that decellularized or recelularized lamina with **ADASCs** were capable of increasing (at a statistically significant level) the thickness of the diseased cornea and improving the clinical condition and visual function of these patients.

8.2 CONCLUSIONS CONCERNING THE SECONDARY OBJECTIVES

1. The study demonstrated that all the patients improved moderately (but significantly) their visual function. Besides, the study demonstrated that all patients improved significantly their refractive sphere, while the refractive cylinder remained overall stable. Conclusion demonstrated in the scientific papers with references (30,31,177,180,241,242) of the scientific publications credited for this thesis.

2. The cornea responded in a positive way to the implantation of **ADASCs**, it was observed through the **AS-OCT** formation of neocollagen in the corneal pocket in the group where only **ADASCs** were implanted, and the formation of neo-collagen in the anterior and posterior surfaces of the lamina. Over time there was noticeable integration of the lamina within the host stroma. Conclusion demonstrated in the scientific papers with references (30,31,177,180,241,242) of the scientific publications credited for this thesis.

3. The study demonstrated that all patients improved their pachymetric and volumetric corneal thickness parameters, being this improvement significantly better in those groups with decellularized or recellularized laminas. Conclusion demonstrated in the

scientific papers with references (30,31,177,180,241,242) of the scientific publications credited for this thesis.

4. The biomicroscopic slit-lamp examination demonstrated the absence of postoperative complications. No inflammation or rejection signs were recorded throughout the follow-up in all patients. Conclusion demonstrated in the scientific papers with references (30,31,177,180,241,242) of the scientific publications credited for this thesis.

5. **The confocal microscopy study** was demonstrated to be an extremely useful and necessary tool for:

- The observation of the evolution of the **ADASCs** once they are implanted into the stromal pocket and monitor their evolution.
- The observation of the evolution of the decellularized laminas implanted without **ADASCs**.
- The observation of the evolution of **ADASCs** implanted with the decellularized corneal laminas.
- The method based on the subjective quantitative analysis of the stromal corneal cells allowed us to monitor the evolution of the cell density of the implanted **ADASCs** with a lamina or without a lamina during the experiment.
- With confocal microscopy, we could investigate the quantitative and qualitative evolution of cell density in the anterior, mid, and posterior stroma of the patients.

Conclusions demonstrated in the scientific paper with reference (179) of the scientific publication credited for this thesis.

8.3 CONCLUSIONS OF THE SCIENTIFIC PUBLICATIONS

8.3.1 Conclusion of the review with reference (240) **of the scientific publication credited for this thesis:** Alió del Barrio JL, Arnalich-Montiel F, De Miguel MP, **El Zarif M**, Alió JL. **Corneal stroma regeneration: Preclinical studies**. Exp Eye Res. 2021;202:108314.

In conclusion, to achieve a proper stroma construct, mimicking the natural one, so it maintains the corneal stroma homeostasis, both a cell source and a collagen scaffold must be developed in conjunction. Regarding the cell component, several cell types, both from ocular and extraocular sources have been studied, being so far the use of **h-ADASCs** the most clinically promising one. However, in the long term, probably the development of cheaper and standardized **iPSCs** techniques will surpass **MSCs** use as well (181). Concerning collagen scaffolds, the use of decellularized cornea sections is clinically the most relevant one so far, but it still has the handicap of needing a donor cornea. In the next few years, advances in novel **3D** printing techniques at a single-cell resolution such as **LIFT** (PreciseBiohttps://www.precisebio.com), laser-assisted bioprinting (273), two-photon polymerization-based lithography (274), fused filament fabrication (275), and other methods of achieving lamellar parallel bundles of collagen, such as molecular crowding (16) will rapidly impulse the development of a biomimetic corneal stroma.

8.3.2 Conclusion of the article published earlier than this doctoral thesis with reference (30**):** Alió del Barrio JL, **El Zarif M**, De Miguel M, Azaar A, Makdissy N, Harb W, et al. **Cellular therapy with human autologous adipose-derived adult stem cells for advanced keratoconus.** Cornea 2017; 36(8)952-60.

As a conclusion of the implantation of **ADASCs** up to 6 months, with the present phase 1 study we showed preliminarily the safety of the corneal stromal transplantation of autologous adipose-derived adult stem cells in humans, their survival *in vivo*, and their ability to produce a low amount of new collagen. This study includes a small sample of patients, so future studies with larger samples are required to finally confirm the safety of the procedure, clarify the efficacy, as well as relevance of the observed findings.

8.3.3 Conclusion of the article published earlier than this doctoral thesis with reference (31**):** Alió del Barrio JL, **El Zarif M**, Azaar A, Makdissy N, Khalil C, Harb W, et al. **Corneal stroma enhancement with decellularized stromal laminas with or without stem cell recellularization for advanced Keratoconus**. Am J Ophthalmol. 2018;186: 47-58.

In conclusion, corneal stromal enhancement by decellularized corneal stromal graft transplantation is a novel technique that could raise as an alternative for advanced keratoconic eyes to classical corneal transplantation techniques. Further studies with larger follow-up and study samples are still necessary to confirm the preliminary results shown in this pilot clinical trial. The possible role of the addition of mesenchymal stem cells to such grafts remains unclear.

8.3.4 Conclusion of the article with reference (177) **of the scientific publication credited for this thesis:** Alió JL, Alió del Barrio JL, **El Zarif M**, Azaar A, Makdissy N, Khalil C et al. **Regenerative surgery of the corneal stroma for advanced keratoconus: 1-Year outcomes**. Am J Ophthalmol. 2019;203:53-68.

In conclusion, early treatment of corneal diseases with stem cells of autologous or allogenic origin could be an option even in the early stages. In advanced stages, corneal transplantation could be eliminated with the many problems involved in the availability of corneal tissue, the long recovery time, and unpredictable results. Corneal scars could have an option with the use of these mesenchymal stem cells as an alternative treatment. The most relevant disease that could benefit from the results of this study is indeed keratoconus. Keratoconus is the most frequent and important corneal dystrophy due to its sociological impact. The frequency of keratoconus is indeed relevant as well as it is the first cause of corneal transplantation in the young population (2). All these patients could benefit from this new type of surgical therapy which can be more accessible, does not depend on the viable human corneal tissue, and does not present the biological hazards related to allogenic tissue with allogenic cells.

8.3.5 Conclusion of the article with reference (180) **of the scientific publication credited for this thesis: El Zarif M**, Alió JL, Alió del Barrio JL, Abdul Jawad K, Palazón-Bru A, Abdul Jawad Z, et al**. Corneal stromal regeneration therapy for advanced keratoconus: long-term outcomes at 3 years**. Cornea. 2021;40(6):741–54.

In conclusion, in the present report, we confirmed the 3-year safety outcomes of this advanced therapy approach for the treatment of keratoconus. The cornea showed transparency for

up to 3-months with all the treated cases. The corneal thickness improvement in the corneas implanted only with cells seems to be insufficient to restore normal corneal thickness, while the intralamellar implantation showed an excellent result concerning corneal thickness restoration with better cell density in the group implanted with recellularized laminas. The modest, but significant visual and refractive improvements found in the study, with a total absence of complications, confirm the feasibility of this therapeutic approach as a potential novel technique for the treatment of keratoconus. Future studies with larger series and in less advanced cases of keratoconus will establish the therapeutic potential of this new type of surgery.

8.3.6 Conclusion of the article with reference (179) **of the scientific publication credited for this thesis: El Zarif M**, Abdul Jawas K, Alió del Barrio JL, Abdul Jawad Z, Palazón-Bru A, De Miguel MP, et al.**Corneal stroma cell density evolution in keratoconus corneas following the implantation of adipose mesenchymal stem cells and corneal laminas: an in vivo confocal microscopy study.** IOVS. 2020;61(4)22.

In conclusion, confocal corneal microscopy combined with the technology used in our investigation has shown to be a very efficient tool for *in vivo* assessment and follow-up of corneas implanted with mesenchymal stem cells for corneal regeneration purposes. We have reported the confocal microscopy outcomes after implantation of **ADASCs** in the selected surgical plane, which allowed qualitative and quantitative assessment of them during the experiment. Moreover, confocal corneal microscopy allowed monitoring of the progressive morphological changes that occurred in the decellularized and recellularized laminas throughout the observation period and assisted in determining changes in cell densities in the grafted tissue, as well as in all the corneal stroma.

Stromal cells are significantly increased at the level of implantation when they are injected into the corneal stroma. Besides, they induced a significant increase in the level of stromal cells when implanted jointly with a corneal lamina impregnated at the surface with **ADASCs**. This increase is larger than that observed when acellular corneal laminas are implanted, even when the implantation is followed by the repopulation of the acellular lamina by the resident stromal cells. Whether these findings indicate the survival of the mesenchymal **ADASCs,** and their differentiation into keratocytes or that such mesenchymal cells cause a biological stimulus for the proliferation of the resident cells, this results should be confirmed in future studies on this topic.

8.3.7 Conclusion of the review with reference (241) **of the scientific publication credited for this thesis: El Zarif M**, Alió del Barrio JL, Arnalich-Montiel F, De Miguel MP, Makdissy N, Alió JL. **Corneal stroma regeneration: New approach for the treatment of cornea disease**. APJO. 2020;9(6):571–9.

In conclusion, cellular therapy with implantation of autologous **ADASCs** decellularized human corneal stroma, and allogenic Smile Lenticule Corneal Inlay is a potentially effective therapy for keratoconus. Such promising findings open a new perspective in therapy for the corneal stroma based on corneal stromal regeneration and enhancement of corneal thickness, topographic, and visual parameters. Future studies are needed to expand on the potential application of these new therapies for the treatment of corneal stromal diseases.

8.3.8 Conclusion of the review with reference (242) **of the scientific publication credited for this thesis: El Zarif M**, Alió JL, Alió del Barrio JL, De Miguel MP, Abdul Jawad K, Makdissy

N. **Corneal stromal regeneration: a review on human clinical studies for treatment of keratoconus.** Front Med. 2021;8:650724.

In conclusion, cellular therapy with implantation of autologous **ADASCs**, decellularized human corneal stroma, allogenic **SMILE** Lenticule, Corneal Inlay, and to a lesser extent, recombinant **CXL** Collagen were discussed in this review. As this procedure indeed reported refractive and corneal topography complications, it also showed initially to be potentially effective for the treatment of advanced keratoconus. Such promising findings open a new perspective of therapy of the corneal stroma based on corneal stromal enhancement and regeneration. Future studies will expand the potential of the application of these new therapies in the treatment of corneal stromal diseases.

SUMMARY AND GENERAL CONCLUSION

Although this study involved a small study sample, and some other limitations were present, at the same time the strengths of this clinical application could open a new way for keratoconus management, as well as other corneal pathologies such as corneal dystrophies or scars. Such regenerative techniques could offer a much less aggressive treatment plan than regular penetrating or lamellar transplantation techniques, and alleviate the increasing demand for donor corneal tissue. The creation of banks for stem cells and even the storage of their exosomes could simplify further these techniques and avoid some of the limitations associated with the direct intrastromal implantation of cells.

9. BIBLIOGRAFÍA / BIBLIOGRAPHY

1. Alio J. Keratoconus: recent advances in diagnosis and treatment. Alió JL, editor. Springer; 2017.

2. Arnalich-Montiel F, Alió Del Barrio J, Alió J. Corneal surgery in keratoconus: which type, which technique, which outcomes? Eye Vis. 2016;3:2.

3. De Miguel MP, Casaroli-Marano RP, Nieto-Nicolau N, Martínez-Conesa EM, Alió del Barrio JL, Alió JL, et al. Frontiers in regenerative medicine for cornea and ocular surface. In: Rahman A, Anjum S, editors. Frontiers in Stem Cell and Regenerative Medicine Research. 1st ed. Bentham e-Books; 2015. p. 92–138.

4. Carlson EC, Liu C-Y, Chikama T, Hayashia Y, Kao CW-C, Birk DE, et al. Keratocan, a cornea-specific keratan sulfate proteoglycan, is regulated by lumican. J Biol Chem. 2005;280:25541–7.

5. Du Y, Funderburgh M, Mann M, SundarRaj N, Funderburgh J. Multipotent stem cells in human corneal stroma. Stem Cells. 2005;23(9):1266–75.

6. Ku J, Niederer R, Patel D, Sherwin T, McGhee C. Laser scanning in vivo confocal analysis of keratocyte density in keratoconus. Ophthalmology. 2008;115(5):845–50.

7. Piñero DP, Alió JL, Barraquer RI, Michael R, Jiménez R. Corneal biomechanics, refraction, and corneal aberrometry in keratoconus: An integrated study. IOVS. 2010;51:1948–55.

8. Alió J, Piñero D, Alesón A, Teus M, Barraquer R, Murta J, et al. Keratoconus-integrated characterization considering anterior corneal aberrations, internal astigmatism, and corneal biomechanics. J Cataract Refract Surg. 2011;37(3):552–68.

9. Mastropasqua L, Nubile M. Normal corneal morphology. In: Mastropasqua, L and Nubile M, editor. Confocal microscopy of the cornea. Thorofare: NJ: SLACK; 2002. p. 7–16.

10. Ali Javadi M, Kanavi M, Mahdavi M, Yaseri M, Rabiei H, Javadi A, et al. Comparison of keratocyte density between keratoconus, post-laser in situ keratomileusis keratectasia, and

uncomplicated post-laser in situ keratomileusis cases. A confocal scan study. Cornea. 2009;28(7):774–9.

11. Edmund C. Assessment of an elastic model in the pathogenesis of keratoconus. Acta Ophthalmol. 1987;65(5):545–50.

12. Gain P, Jullienne R, He Z, Aldossary M, Acquart S, Cognasse F, et al. Global survey of corneal transplantation and eye banking. JAMA Ophthalmol. 2016;134(2):167–73.

13. Griffith M, Alarcon EI, Brunette I. Regenerative approaches for the cornea. J Intern Med. 2016;280(3):276–86.

14. Fagerholm P, Lagali N, Merrett K, Jackson W, Munger R, Liu Y, et al. A biosynthetic alternative to human donor tissue for inducing corneal regeneration: 24-month follow-up of a phase 1 clinical study. Sci Transl Med. 2010;2(46):46ra61.

15. Isaacson A, Swioklo S, Connon CJ. 3D bioprinting of a corneal stroma equivalent. Exp Eye Res. 2018;173:188–93.

16. Ruberti J, Zieske J. Prelude to corneal tissue engineering - gaining control of collagen organization. Prog Retin Eye Res. 2008;27(5):549–77.

17. Alió del Barrio J, Chiesa M, Ferrer GG, Garagorri N, Briz N, Fernandez-Delgado J, et al. Biointegration of corneal macroporous membranes based on poly(ethyl acrylate) copolymers in an experimental animal model. J Biomed Mater Res A. 2015;103(3):1106–18.

18. Lynch A, Ahearne M. Strategies for developing decellularized corneal scaffolds. Exp Eye Res. 2013;108:42–7.

19. Alio del Barrio J, Chiesa M, Garagorri N, Garcia-Urquia N, Fernandez-Delgado J, Bataille L, et al. Acellular human corneal matrix sheets seeded with human adipose-derived mesenchymal stem cells integrate functionally in an experimental animal model. Exp Eye Res. 2015;132:91–100.

20. Hara H, Cooper DKC. Xenotransplantation--the future of corneal transplantation? Cornea. 2011;30(4):371–378.

21. Arnalich-Montiel F, Pastor S, Blazquez-Martinez, A Fernandez-Delgado J, Nistal M, Alio J, De Miguel M. Adipose-derived stem cells are a source for cell therapy of the corneal stroma. Stem Cells. 2008;26(2):570–9.

22. Espandar L, Bunnell B, Wang G, Gregory P, McBride C, Moshirfar M. Adipose-derived stem cells on hyaluronic acid-derived scaffold: A new horizon in bioengineered cornea. Arch Ophthalmol. 2012;130(2):202–8.

23. Mittal SK, Omoto M, Amouzegar A, Sahu A, Alexandra R, Katikireddy KR, et al. Restoration of corneal transparency by mesenchymal stem cells. Stem Cell Reports. 2016;7(4):583–590.

24. Demirayak B, Yüksel N, Çelik O, Subaşı C, Duruksu G, Unal Z, et al. Effect of bone marrow and adipose tissue-derived mesenchymal stem cells on the natural course of corneal scarring after penetrating injury. Exp Eye Res. 2016;151:227–35.

25. Du Y, Carlson E, Funderburgh M, Birk D, Pearlman E, Guo N, et al. Stem cell therapy restores transparency to defective murine corneas. Stem Cells. 2009;27(7):1635–42.

26. Liu H, Zhang J, Liu C-Y, Wang I-J, Sieber M, Chang J, et al. Cell therapy of congenital corneal diseases with umbilical mesenchymal stem cells: lumican null mice. PLoS One. 2010;5(5):e10707.

27. Coulson Thomas VJ, Caterson B, Kao W. Transplantation of human umbilical mesenchymal stem cells cures the corneal defects of Mucopolysaccharidosis VII mice. Stem Cells. 2013;31(10):2116–2126.

28. Winston W-Y K, Vivien J. CT. Cell therapy of corneal diseases. Cornea. 2016;35(Suppl 1):S9–S19.

29. De Miguel M, Fuentes-Julián S, Blázquez-Martínez A, Pascual C, Aller M, Arias J, et al. Immunosuppressive properties of mesenchymal stem cells: advances and applications. Curr Mol Med. 2012;12(5):574–91.

30. Alió Del Barrio J, El Zarif M, De Miguel M, Azaar A, Makdissy N, Harb W, et al. Cellular therapy with human autologous adipose-derived adult stem cells for advanced keratoconus. Cornea. 2017;36(8):952–60.

31. Alió Del Barrio J, El Zarif M, Azaar A, Makdissy N, Khalil C, Harb W, et al. Corneal stroma enhancement with decellularized stromal laminas with or without stem cell recellularization for advanced keratoconus. Am J Ophthalmol. 2018;186:47–58.

32. Harkin D, Foyn L, Bray L, Sutherland A, Li F, Cronin B. Concise reviews: can mesenchymal stromal cells differentiate into corneal cells? A systematic review of published data. Stem Cells. 2015;33(3):785–91.

33. Jiang Z, Liu G, Meng F, Wang W, Hao P, Xiang Y, et al. Paracrine effects of mesenchymal stem cells on the activation of keratocytes. Br J Ophthalmol. 2017;101(11):1583–90.

34. Hendijani F. Explant culture: an advantageous method for isolation of mesenchymal stem cells from human tissues. Cell Prolif. 2017;50(2):e12334.

35. Górski B. Gingiva as a new and the most accessible source of mesenchymal stem cells from the oral cavity to be used in regenerative therapies. Postepy Hig Med Dosw (Online). 2016;70(0):858–71.

36. Basu S, Hertsenberg, Andrew J Funderburgh, Martha L Burrow MK, Mann MM, Du Y, Lathrop KL, Syed-Picard, Fatima N Adams SM, et al. Human limbal biopsy-derived stromal stem cells prevent corneal scarring. Sci Transl Med. 2014;6(266):266ra172.

37. Takahashi K, Yamanaka S. Induction of pluripotent stem cells from mouse embryonic and adult fibroblast cultures by defined factors. Cell. 2006;126(4):663–76.

38. Naylor RW, Charles NJM, Cowan CA, Davidson AJ, Holm TM, Sherwin T. Derivation of corneal keratocyte-like cells from human induced pluripotent stem cells. PLoS One. 2016;11(10):e0165464.

39. Yao L, Bai H. Review: mesenchymal stem cells and corneal reconstruction. Mol Vis. 2013;19:2237–2243.

40. Caplan AI. Mesenchymal stem cells: Time to change the name! Stem Cells Transl Med. 2017;6(6):1445–51.

41. Alió JL, El Zarif M, Alió del Barrio JL. Cellular therapy of the corneal stroma: a new type of corneal surgery for keratoconus and corneal dystrophies a translational research

experience. 1st ed. Elsevier; 2020.

42. Alió JL. What is keratoconus? A new approach to a not so rare disease. In: Alió JL, editor. Keratoconus: recent advances in diagnosis and treatment. Springer; 2017. p. 3–5.

43. Zirm EK. Eine erfolgreiche totale Keratoplastik (a successful total keratoplasty). 1906. Refract Corneal Surg. 1989;5(4):258–61.

44. Fournié P, Galiacy SD, Malecaze F. Modern pathogenesis of keratoconus: genomics and proteomics. In: Alió JL, editor. Keratoconus: recent advances in diagnosis and treatment. Springer; 2017. p. 7–12.

45. Wang Y, Rabinowitz YS, Rotter JI, Yang H. Genetic epidemiological study of keratoconus: Evidence for major gene determination. Am J Med Genet. 2000;93(5):403–9.

46. Edwards M, McGhee CN, Dean S. The genetics of keratoconus. Clin Exp Ophthalmol. 2001;29(6):345–51.

47. Salabert D, Cochener B, Mage F, Colin J. Keratoconus and familial topographic corneal anomalies. J Fr Ophtalmol. 1994;17(11):646–56.

48. Pearson A, Soneji B, Sarvananthan N, Sandford-Smith J. Does ethnic origin influence the incidence or severity of keratoconus? Eye. 2000;14((Pt 4)):625–8.

49. Tay K, Chan W. Penetrating keratoplasty for keratoconus. Ann Acad Med Singapore. 1997;26(1):132–7.

50. Tuft SJ, Moodaley LC, Gregory WM, Davison CR, Buckley RJ. Prognostic factors for the progression of keratoconus. Ophthalmology. 1994;101(3):439–47.

51. Abu-Amero KK, Al-Muammar AM, Kondkar AA. Genetics of keratoconus: where do we stand? J Ophthalmol. 2014;2014:641708.

52. Héon E, Greenberg A, Kopp KK, Rootman D, Vincent AL, Billingsley G, et al. VSX1: a gene for posterior polymorphous dystrophy and keratoconus. Hum Mol Genet. 2002;11(9):1029–36.

53. Tanwar M, Kumar M, Nayak B, Pathak D, Titiyal JS, Dada R. VSX1 gene analysis in keratoconus. Mol Vis. 2010;16:2395–2401.

54. Wilson SE, He YG, Weng J, Li Q, McDowall AW, Vital M, et al. Epithelial injury induces keratocyte apoptosis: hypothesized role for the interleukin-1 system in the modulation of corneal tissue organization and wound healing. Exp Eye Res. 1996;62(4):325–7.

55. Kenney M, Chwa M, Opbroek A, Brown D. Increased gelatinolytic activity in keratoconus keratocyte cultures. A correlation to an altered matrix metalloproteinase-2/tissue inhibitor of metalloproteinase ratio. Cornea. 1994;13(2):114–24.

56. Sawaguchi S, Yue BYJT, Sugar J. Lysosomal enzyme abnormalities in keratoconus. Arch Ophthalmol. 1989;07(10):1507–10.

57. Sawaguchi S, Twining SS, Yue BYJT, Wilson P, Sugar J, Chan S-K. Alpha-1 proteinase inhibitor levels in keratoconus. Exp Eye Res. 1990;50(5):549–54.

58. Sawaguchi S, Twining SS, Yue BY, Chang SH, Zhou X, Loushin G, et al. Alpha 2-macroglobulin levels in normal human and keratoconus corneas. IOVS. 1994;35:4008–14.

59. Rabinowitz YS, Maumenee IH, Lundergan MK, Puffenberger E, Zhu D, Antonarakis S, et al. Molecular genetic analysis in autosomal dominant keratoconus. Cornea. 1992;11(4):302–8.

60. Balasubramanian SA, Mohan S, Pye DC, Willcox MDP. Proteases, proteolysis and inflammatory molecules in the tears of people with keratoconus. Acta Ophthalmol. 2012;90(4):e303-309.

61. Lema I, Durán JA. Inflammatory molecules in the tears of patients with keratoconus. Ophthalmology. 2005;112(4):654–9.

62. Lema I, Sobrino T, Durán JA, Brea D, Díez-Feijoo E. Subclinical keratoconus and inflammatory molecules from tears. Br J Ophthalmol. 2009;93(6):820–4.

63. Shetty R, Ghosh A, Lim RR, Subramani M, Mihir K, Reshma AR, et al. Elevated expression of matrix metalloproteinase-9 and inflammatory cytokines in keratoconus patients is inhibited by cyclosporine A. Randomized Control Trial. 2015;56(2):738–50.

64. Chaerkady R, Shao H, Scott S-G, Pandey A, Jun AS, Chakravarti S. The keratoconus corneal proteome: loss of epithelial integrity and stromal degeneration. J Proteomics.

2013;87:122–31.

65. Joseph R, Srivastava OP, Pfister RR. Differential epithelial and stromal protein profiles in keratoconus and normal human corneas. Exp Eye Res. 2011;92(4):282–98.

66. Kenney MC, Brown DJ. The cascade hypothesis of keratoconus. Cont Lens Anterior Eye. 2003;26(3):139–46.

67. Lema I, Ruiz C, Díez-Feijoo E, Acera A, Merayo J. Inflammatory response to contact lenses in patients with keratoconus compared with myopic subjects. Cornea. 2008;27(7):758–63.

68. Balasubramanian SA, Pye D, Willcox M. Effects of eye rubbing on the levels of protease, protease activity and cytokines in tears: relevance in keratoconus. Clin Exp Optom. 2013;96(2):214–8.

69. Macé M, Galiacy SD, Erraud A, Mejía JE, Etchevers H, Allouche M, et al. Comparative transcriptome and network biology analyses demonstrate antiproliferative and hyperapoptotic phenotypes in human keratoconus corneas. IOVS. 2011;52(9):6181–91.

70. Barbara R, Turnbull AM, Hossain P, Anderson DF, Barbara A. Epidemiology of keratoconus. In: Alió JL, editor. Keratoconus: recent advances in diagnosis and treatment. Springer; 2017. p. 13–23.

71. Krachmer JH, Feder RS, Belin MW. Keratoconus and related noninflammatory corneal thinning disorders. Surv Ophthalmol. 1984;28(4):293–322.

72. Gordon-Shaag A, Millodot M, Shneor E. The epidemiology and etiology of keratoconus. Int J Kerat Ect Cor Dis. 2012;1(1):7–15.

73. Jonas J, Nangia V, Matin A, Kulkarni M, Bhojwani K. Prevalence and associations of keratoconus in rural maharashtra in central India: the central India eye and medical study. Am J Ophthalmol. 2009;148(5):760–5.

74. Kennedy RH, Bourne WM, Dyer JA. A 48-year clinical and epidemiologic study of keratoconus. Am J Ophthalmol. 1986;101(3):267–73.

75. Gomes JAP, Tan D, Rapuano CJ, Belin MW, Jr RA, Guell JL, et al. Global consensus on

keratoconus and ectatic diseases. Cornea. 2015;34(4):359–69.

76. Gordon-Shaag A, Shneor E, Millodot M, Liu Y. The genetic and environmental factors for keratoconus. Biomed Res Int. 2015;2015:795738.

77. Waked N, Fayad AM, Fadlallah A, Rami H El. Keratoconus screening in a Lebanese students' population. J Fr Ophtalmol. 2011;35(1):23–9.

78. Shneor E, Millodot M, Gordon-shaag A, Essa M, Anton M, Barbara R, et al. Prevalence of keratoconus among young arab students in Israel. Int J Kerat Ect Cor Dis. 2014;3(1):9–14.

79. Hashemi H, Khabazkhoob M, Yazdani N, Ostadimoghaddam H, Norouzirad R, Amanzadeh K, et al. The prevalence of keratoconus in a young population in Mashhad, Iran. Ophthalmic Physiol Opt. 2014;34(5):519–27.

80. Hashemi H, Beiranvand A, Khabazkhoob M, Asgari S, Emamian MH, Shariati M, et al. Prevalence of keratoconus in a population-based study in Shahroud. Cornea. 2013;32(11):1441–5.

81. Assiri AA, Yousuf BI, Quantock AJ, Murphy PJ. Incidence and severity of keratoconus in Asir province, Saudi Arabia. Br J Ophthalmol. 2005;89(11):1403–1406.

82. Georgiou T, Funnell CL, Cassels-Brown A, O'Conor R. Influence of ethnic origin on the incidence of keratoconus and associated atopic disease in Asians and white patients. Eye. 2004;18(4):379–83.

83. McMonnies CW. Screening for keratoconus suspects among candidates for refractive surgery. Clin Exp Optom. 2014;97(6):492–8.

84. Sugar J, Macsai MS. What causes keratoconus? Cornea. 2012;31(6):716–9.

85. Francois M, Chassaing N, Calvas P. Genetics of keratoconus. In: Barbara A, editor. Textbook on Keratoconus New Insights. 1/e. NeDelhi, India: Jaypee Brothers Medical Publishers; 2012. p. 224.

86. Gordon-Shaag A, Millodot M, Essa M, Garth J, Ghara M, Shneor E. Is consanguinity a risk factor for keratoconus? Optom Vis Sci. 2013;90(5):448–54.

87. Burdon KP, Coster DJ, Charlesworth J, Mills RA, Laurie KJ, Giunta C, et al. Apparent

autosomal dominant keratoconus in a large Australian pedigree accounted for by digenic inheritance of two novel loci. Hum Genet. 2008;24(4):379–386.

88. Tuft SJ, Hassan H, George S, Frazer DG, Willoughby CE, Liskova P. Keratoconus in 18 pairs of twins. Acta Ophthalmol. 2012;90(6):e482-486.

89. Rabinowitz YS. The genetics of keratoconus. Ophthalmol Clin North Am. 2003;16(4):607–20.

90. Nowak DM, Gajecka M. The genetics of keratoconus. Middle East Afr J Ophthalmol. 2011;18(1):2–6.

91. Marchitti SA, Chen Y, Thompson DC, Vasiliou V. Ultraviolet radiation: cellular antioxidant response and the role of ocular aldehyde dehydrogenase enzymes. Eye Contact Lens. 2011;37(4):206–213.

92. Kenney MC, Brown DJ, Rajeev B. Everett Kinsey lecture. The elusive causes of keratoconus: a working hypothesis. CLAO J. 2000;26(1):10–3.

93. Chan E, Snibson GR. Current status of corneal collagen cross-linking for keratoconus: a review. Clin Exp Optom. 2013;96(2):155–64.

94. Ridley F. Contact lenses in treatment of keratocnus. Br J Ophthalmol. 1956;40(5):295–304.

95. Krachmer JH. Eye rubbing can cause keratoconus. Cornea. 2004;23(6):539–40.

96. Gasset AR, Hinson WA, Frias JL. Keratoconus and atopic diseases. Ann Ophthalmol. 1978;10(8):991–4.

97. Galvis V, Sherwin T, Tello A, Merayo J, Barrera R, Acera A. Keratoconus: an inflammatory disorder? Eye. 2015;29(7):843–59.

98. Ihalainen A. Clinical and epidemiological features of keratoconus genetic and external factors in the pathogenesis of the disease. Acta Ophthalmol Suppl. 1986;178:1–64.

99. Sherwin T, Ismail S, Loh I-P, McGhee JJ. Histopathology (from keratoconus pathology to pathogenesis). In: Alió JL, editor. Keratoconus: recent advances in diagnosis and treatment. Springer; 2017. p. 25–41.

100. Somodi S, Hahnel C, Slowik C, Richter A, Weiss DG, Guthoff R. Confocal in vivo microscopy and confocal laser-scanning fluorescence microscopy in keratoconus. Ger J Ophthalmol. 1996;5(6):518–25.

101. Yadav R, Kottaiyan R, Ahmad K, Yoon G. Epithelium and Bowman's layer thickness and light scatter in keratoconic cornea evaluated using ultrahigh resolution optical coherence tomography. J Biomed Opt. 2012;17(11):116010.

102. Zhou W, Stojanovic A. Comparison of corneal epithelial and stromal thickness distributions between eyes with keratoconus and healthy eyes with corneal astigmatism ≥ 2.0 D. PLoS One. 2014;9(1):e85994.

103. Wygledowska-Promieńska D, Rokita-Wala I, Gierek-Ciaciura S, Piatek-Koronowska G. The alterations in corneal structure at III/IV stage of keratoconus by means of confocal microscopy and ultrasound biomicroscopy before penetrating keratoplasty. Klin Ocz. 1999;101(6):427–32.

104. Mastropasqua L, Nubile M. Confocal microscopy in keratoconus. In: Confocal microscopy of the cornea. NJ: SLACK; 2002. p. 38–44.

105. El Zarif M, Abdul Jawad K, Alió JL. Confocal microscopy of the cornea in a clinical model of corneal stromal expansion using adipose stem cells and corneal decellularized laminas in patients with keratoconus. In: Alió JL, Alió del Barrio JL, Arnalich-Montiel F, editors. Corneal Regeneration therapy and surgery. 1st ed. Springer; 2019. p. 363–86.

106. Scroggs MW, Proia AD. Histopathological variation in keratoconus. Cornea. 1992;11(6):553–9.

107. Haque S, Simpson T, Jones L. Corneal and epithelial thickness in keratoconus: a comparison of ultrasonic pachymetry, Orbscan II, and optical coherence tomography. J Refract Surg. 2006;22(5):486–93.

108. Aktekin M, Sargon MF, Cakar P, Celik HH, Firat E. Ultrastructure of the cornea epithelium in keratoconus. Okajimas Folia Anat Jpn. 1998;75(1):45–53.

109. Reinstein DZ, Gobbe M, Archer TJ, Silverman RH, Coleman DJ. Epithelial, stromal, and total corneal thickness in keratoconus: three-dimensional display with artemis very-high

frequency digital ultrasound. J Refract Surg. 2010;26(4):259–71.

110. Kaldawy R, Wagner J, Ching S, Seigel G. Evidence of apoptotic cell death in keratoconus. Cornea. 2002;21(2):206–9.

111. Kim WJ, Rabinowitz YS, Meisler DM, Wilson SE. Keratocyte apoptosis associated with keratoconus. Exp Eye Res. 1999;69(5):475–81.

112. Tuori AJ, Virtanen I, Aine E, Kalluri R, Miner JH, Uusitalo HM. The immunohistochemical composition of corneal basement membrane in keratoconus. Curr Eye Res. 1997;16(8):792–801.

113. Sawaguchi S, Fukuchi T, Abe H, Kaiya T, Sugar J, Yue BY. Three-dimensional scanning electron microscopic study of keratoconus corneas. Arch Ophthalmol. 1998;116(1):62–8.

114. Kenney MC, Nesburn AB, Burgeson RE, Butkowski RJ, Ljubimov A V. Abnormalities of the extracellular matrix in keratoconus corneas. Cornea. 1997;16(3):345–51.

115. Takahashi A, Nakayasu K, Okisaka S, Kanai A. Quantitative analysis of collagen fiber in keratoconus. Nihon Ganka Gakkai Zasshi. 1990;94(11):1068–73.

116. Fullwood NJ, Tuft SJ, Malik NS, Meek KM, Ridgway AE, Harrison RJ. Synchrotron x-ray diffraction studies of keratoconus corneal stroma. Invest Ophthalmol Vis Sci. 1992;33(5):1734–41.

117. Daxer A, Fratzl P. Collagen fibril orientation in the human corneal stroma and its implication in keratoconus. Invest Ophthalmol Vis Sci. 1997;38(1):121–9.

118. Critchfield JW, Calandra AJ, Nesburn AB, Kenney MC. Keratoconus: I. Biochemical studies. Exp Eye Res. 1988;46(6):953–63.

119. Cheung IMY, McGhee CNJ, Sherwin T. A new perspective on the pathobiology of keratoconus: interplay of stromal wound healing and reactive species-associated processes. Clin Exp Optom. 2013;96(2):188–96.

120. Zhou L, Yue BY, Twining SS, Sugar J, Feder RS. Expression of wound healing and stress-related proteins in keratoconus corneas. Curr Eye Res. 1996;15(11):1124–31.

121. Määttä M, Heljasvaara R, Sormunen R, Pihlajaniemi T, Autio-Harmainen H, Tervo T.

Differential expression of collagen types XVIII/endostatin and XV in normal, keratoconus, and scarred human corneas. Cornea. 2006;25(3):341–9.

122. Zieske JD. Extracellular matrix and wound healing. Curr Opin Ophthalmol. 2001;12(4):237–41.

123. Gaskin JCF, Loh I-P, McGhee CNJ, Sherwin T. An immunohistochemical study of inflammatory cell changes and matrix remodeling with and without acute hydrops in keratoconus. Invest Ophthalmol Vis Sci. 2015;56(10):5831–7.

124. Tuori A, Virtanen I, Aine E, Uusitalo H. The expression of tenascin and fibronectin in keratoconus, scarred and normal human cornea. Graefes Arch Clin Exp Ophthalmol. 1997;235(4):222–9.

125. Erie J, Patel S, McLaren J, Nau C, Hodge D, Bourne W. Keratocyte density in keratoconus. A confocal microscopy study(a). Am J Ophthalmol. 2002;134(5):689–95.

126. Mathew JH, Goosey JD, Bergmanson JPG. Quantified histopathology of the keratoconic cornea. Optom Vis Sci. 2011;88(8):988–97.

127. Rock M, Moore M, Anderson J, Binder P. 3-D computer models of human keratocytes. Eye Contact Lens. 1995;21(1):57–60.

128. Sherwin T, Brookes NH, Loh I-P, Poole CA, Clover GM. Cellular incursion into Bowman's membrane in the peripheral cone of the keratoconic cornea. Exp Eye Res. 2002;74(4):473–82.

129. Sherwin T, Brookes NH. Morphological changes in keratoconus: pathology or pathogenesis. Clin Exp Ophthalmol. 2004;32(2):211–7.

130. Shetty R, Sathyanarayanamoorthy A, Ramachandra RA, Arora V, Ghosh A, Srivatsa PR, et al. Attenuation of lysyl oxidase and collagen gene expression in keratoconus patient corneal epithelium corresponds to disease severity. Mol Vis. 2015;21:12–25.

131. Patel D V, McGhee CNJ. Mapping the corneal sub-basal nerve plexus in keratoconus by in vivo laser scanning confocal microscopy. Invest Ophthalmol Vis Sci. 2006;47(4):1348–51.

132. Jongebloed WL, Dijk F, Worst JG. Keratoconus morphology and cell dystrophy: a SEM

study. Doc Ophthalmol. 1989;72(3–4):403–9.

133. Rabinowitz YS. Keratoconus. Surv Ophthalmol. 1998;42(4):297–319.

134. Amsler M. Keratocone classique et keratocone fruste, arguments unitaires. Oftalmologica. 1946;111:96–101.

135. Alió JL, Shabayek MH. Corneal higher order aberrations: a method to grade keratoconus. J Refract Surg. 2006;22(6):539–45.

136. Vega-Estrada A, Alio JL, Brenner LF, Javaloy J, Plaza Puche AB, Barraquer RI, et al. Outcome analysis of intracorneal ring segments for the treatment of keratoconus based on visual, refractive, and aberrometric impairment. Am J Ophthalmol. 2013;155(3):575-584.e1.

137. Jhanji V, Sharma N, Vajpayee RB. Management of keratoconus: current scenario. Br J Ophthalmol. 2011;95(8):1044–50.

138. Shetty R, Kaweri L, Pahuja N, Nagaraja H, Wadia K, Jayadev C, et al. Current review and a simplified "five-point management algorithm" for keratoconus. Indian J Ophthalmol. 2015;63(1):46–53.

139. Barnett M, Mannis MJ. Contact lenses in the management of keratoconus. Cornea. 2011;30(12):1510–6.

140. Vega-Estrada A, Alió JL, Plaza Puche AB, Marshall J. Outcomes of a new microwave procedure followed by accelerated cross-linking for the treatment of keratoconus: a pilot study. J Refract Surg. 2012;28(11):787–93.

141. Colin J, Cochener B, Savary G, Malet F. Correcting keratoconus with intracorneal rings. J Cataract Refract Surg. 2000;26(8):1117–22.

142. Snibson GR. Collagen cross-linking: a new treatment paradigm in corneal disease - A review. Clin Exp Ophthalmol. 2010;38(2):141–53.

143. Busin M, Scorcia V, Zambianchi L, Ponzin D. Outcomes from a modified microkeratome-assisted lamellar keratoplasty for keratoconus. Arch Ophthalmol. 2012;130(6):776–82.

144. van Dijk K, Parker J, Tong CM, Ham L, Lie JT, Beek EAG, et al. Midstromal isolated

Bowman layer graft for reduction of advanced keratoconus a technique to postpone penetrating or deep anterior lamellar keratoplasty. JAMA Ophthalmol. 2014;132(4):495–501.

145. Pearson RM. Kalt, keratoconus, and the contact lens. Optom Vis Sci. 1989;66(9):643–6.

146. Pearson RM, Efron N. Hundredth anniversary of August Müller's inaugural dissertation on contact lenses. Surv Ophthalmol. 1989;34(2):133–41.

147. Rabinowitz YS, Garbus C, Garbus JJ. Contact lens selection for keratoconus using a computer-assisted videophotokeratoscope. CLAO J. 1991;17(2):88–93.

148. Rosenthal P, Cotter JM. Clinical performance of a spline-based apical vaulting keratoconus corneal contact lens design. CLAO J. 1995;21(1):42–6.

149. Yeung K, Eghbali F, Weissman BA. Clinical experience with piggyback contact lens systems on keratoconic eyes. J Am Optom Assoc. 1995;66(9):539–43.

150. Rico-Del-Viejo L, Garcia-Montero M, Hernández-Verdejo JL, García-Lázaro S, Gómez-Sanz FJ, Lorente-Velázquez A. Nonsurgical procedures for keratoconus management. J Ophthalmol. 2017;2017:9707650.

151. Bilgin LK, Yilmaz S, Araz B, Yüksel SB, Sezen T. 30 years of contact lens prescribing for keratoconic patients in Turkey. Cont Lens Anterior Eye. 2009;32(1):16–21.

152. Garcia-Lledo M, Feinbaum C, Alio JL. Contact lens fitting in keratoconus. Compr Ophthalmol Updat. 2006;7(2):47–52.

153. Mandathara PS, Stapleton FJ, Willcox MDP. Outcome of keratoconus management: review of the past 20 years' contemporary treatment modalities. Eye Contact Lens. 2017;43(3):141–54.

154. Smiddy WE, Hamburg TR, Kracher GP, Stark WJ. Keratoconus. Contact lens or keratoplasty? Ophthalmology. 1988;95(4):487–92.

155. Seiler T, Spörl E, Huhle M, Kamouna A. Seiler. Annu Meet Fort Lauderdale, Florida. 1996;37(3):S1-1154.

156. Alió JL, Vega-Estrada A, Sanz-Díez P, Peña-García P, Durán-García ML, Maldonado M.

Keratoconus management guidelines. Researchgate. 2015;4(1):1–39.

157. Albertazzi R. Tratamiento del queratocono con segmentos intracorneales. In: Society BA: ECA para la K, editor. Queratocono : pautas para su diagnóstico y tratamiento / R Albertazzi (ed). 2010. p. 205–68.

158. Sakellaris D, Balidis M, Gorou O, Szentmary N, Alexoudis A, Grieshaber M, et al. Intracorneal ring segment implantation in the management of keratoconus: An evidence-based approach. Ophthalmol Ther. 2019;8((Suppl 1)):5–14.

159. Peña-García P, Alió JL, Vega-Estrada A, Barraquer RI. Internal, corneal, and refractive astigmatism as prognostic factors for intrastromal corneal ring segment implantation in mild to moderate keratoconus. J Cataract Refract Surg. 2014;40(10):1633–44.

160. Parker JS, van Dijk K, Melles GRJ. Treatment options for advanced keratoconus: a review. Surv Ophthalmol. 2015;60(5):459–80.

161. Castroviejo R. Keratoplasty for the treatment of keratoconus. Trans Am Ophthalmol Soc. 1948;46:127–53.

162. Archila EA. Deep lamellar keratoplasty dissection of host tissue with intrastromal air injection. Cornea. 1984;3(3):217–8.

163. Melles GR, Lander F, Rietveld FJ, Remeijer L, Beekhuis WH, Binder PS. A new surgical technique for deep stromal, anterior lamellar keratoplasty. Br J Ophthalmol. 1999;83(3):327–33.

164. Anwar M, Teichmann KD. Big-bubble technique to bare Descemet's membrane in anterior lamellar keratoplasty. J Cataract Refract Surg. 2002;28(3):398–403.

165. Jones MNA, Armitage WJ, Ayliffe W, Larkin DF, Kaye SB, 5) NOTAG and CO (OTAG AS. Penetrating and deep anterior lamellar keratoplasty for keratoconus: a comparison of graft outcomes in the United kingdom. Invest Ophthalmol Vis Sci. 2009;50(12):5625–9.

166. Niziol LM, Musch DC, Gillespie BW, Marcotte LM, Sugar A. Long-term outcomes in patients who received a corneal graft for keratoconus between 1980 and 1986. Am J Ophthalmol. 2013;155(2):213-219.e3.

167. Fukuoka S, Honda N, Ono K, Mimura T, Usui T, Amano S. Extended long-term results of penetrating keratoplasty for keratoconus. Cornea. 2010;29(5):528–30.

168. Choi JA, Lee MA, Kim M-S. Long-term outcomes of penetrating keratoplasty in keratoconus: analysis of the factors associated with final visual acuities. Int J Ophthalmol. 2014;7(3):517–21.

169. Buzard KA, Fundingsland BR. Corneal transplant for keratoconus: results in early and late disease. J Cataract Refract Surg. 1997;23(3):398–406.

170. Javadi MA, Motlagh BF, Jafarinasab MR, Rabbanikhah Z, Anissian A, Souri H, et al. Outcomes of penetrating keratoplasty in keratoconus. Cornea. 2005;24(8):941–6.

171. Fontana L, Parente G, Sincich A, Tassinari G. Influence of graft-host interface on the quality of vision after deep anterior lamellar keratoplasty in patients with keratoconus. Cornea. 2011;30(5):497–502.

172. Funnell CL, Ball J, Noble BA. Comparative cohort study of the outcomes of deep lamellar keratoplasty and penetrating keratoplasty for keratoconus. Eye. 2006;20(5):527–32.

173. Smadja D, Colin J, Krueger RR, Mello GR, Gallois A, Mortemousque B, et al. Outcomes of deep anterior lamellar keratoplasty for keratoconus: learning curve and advantages of the big bubble technique. Cornea. 2012;31(8):859–63.

174. Kim MH, Chung T-Y, Chung E-S. A retrospective contralateral study comparing deep anterior lamellar keratoplasty with penetrating keratoplasty. Cornea. 2013;32(4):385–9.

175. MacIntyre R, Chow S-P, Chan E, Poon A. Long-term outcomes of deep anterior lamellar keratoplasty versus penetrating keratoplasty in Australian keratoconus patients. Cornea. 2014;33(1):6–9.

176. De Miguel M, Alio J, Arnalich-Montiel F, Fuentes-Julian S, de Benito-Llopis, L Amparo F, Bataille L. Cornea and ocular surface treatment. Curr Stem Cell Res Ther. 2010;5(2):195–204.

177. Alió J, Alió Del Barrio J, El Zarif M, Azaar A, Makdissy N, Khalil C, et al. Regenerative surgery of the corneal stroma for advanced keratoconus: 1-year outcomes. Am J

Ophthalmol. 2019;203:53–68.

178. Alió J, Alió del Barrio J. Cellular therapy with human autologous adipose-derived adult stem cells for advanced keratoconus: reply to the letter to editor. Cornea. 2017;36(12):e37.

179. El Zarif M, Abdul Jawad K, Alió del Barrio J, Abdul Jawad Z, Palazón-Bru A, De Miguel M, et al. Corneal stroma cell density evolution in keratoconus corneas following the implantation of adipose mesenchymal stem cells and corneal laminas: an in vivo confocal microscopy study. IOVS. 2020;61(4):22.

180. El Zarif M, Alió J, Alió del Barrio J, Abdul Jawad K, Palazón-Bru A, Abdul Jawad Z, et al. Corneal stromal regeneration therapy for advanced keratoconus: long-term outcomes at 3 years. Cornea. 2021;40(6):741–54.

181. Chakrabarty K, Shetty R, Ghosh A. Corneal cell therapy: with iPSCs, it is no more a far-sight. Stem Cell Res Ther. 2018;9(1):287.

182. Han J, Koh YJ, Moon HR, Ryoo HG, Cho C-H, Kim I, et al. Adipose tissue is an extramedullary reservoir for functional hematopoietic stem and progenitor cells. Blood. 2010;115(5):957–64.

183. Zuk P, Zhu M, Mizuno H, Huang J, Futrell J, Katz A, et al. Multilineage cells from human adipose tissue: implications for cell-based therapies. Tissue Eng. 2001;7(2):211–28.

184. Erickson GR, Gimble JM, Franklin DM, Rice HE, Awad H, Guilak F. Chondrogenic potential of adipose tissue-derived stromal cells in vitro and in vivo. Biochem Biophys Res Commun. 2002;290(2):763–9.

185. Zimmerlin L, Donnenberg VS, Pfeifer ME, Meyer EM, Péault B, Rubin JP, et al. Stromal vascular progenitors in adult human adipose tissue. Cytom A. 2010;77(1):22–30.

186. Varma MJO, Breuls RGM, Schouten TE, Jurgens WJFM, Bontkes HJ, Schuurhuis GJ, et al. Phenotypical and functional characterization of freshly isolated adipose tissue-derived stem cells. Stem Cells Dev. 2007;16(1):91–104.

187. Bourin P, Bunnell B, Casteilla L, Dominici M, Katz A, March K, et al. Stromal cells from the adipose tissue-derived stromal vascular fraction and culture expanded adipose tissue-

derived stromal/stem cells: a joint statement of the International Federation for Adipose Therapeutics and Science (IFATS) and the International So. Cytotherapy. 2013;15(6):641–8.

188. Anderi R, Makdissy N, Azar A, Rizk F, Hamade A. Cellular therapy with human autologous adipose-derived adult cells of stromal vascular fraction for alopecia areata. Stem Cell Res Ther. 2018;9(1):141.

189. Ripoll CB, Flaat M, Klopf-Eiermann J, Fisher-Perkins JM, Trygg CB, Scruggs BA, et al. Mesenchymal lineage stem cells have pronounced anti-inflammatory effects in the twitcher mouse model of Krabbe's disease. Stem Cells. 2011;29(1):67–77.

190. Chaker D, Mouawad C, Azar A, Quilliot D, Achkar I, Fajloun Z, et al. Inhibition of the RhoGTPase Cdc42 by ML141 enhances hepatocyte differentiation from human adipose-derived mesenchymal stem cells via the Wnt5a/PI3K/miR-122 pathway: impact of the age of the donor. Stem Cell Res Ther. 2018;9(1):167.

191. Du Y, Roh DS, Funderburgh ML, Mann MM, Marra KG, Rubin JP, et al. Adipose-derived stem cells differentiate to keratocytes in vitro. Mol Vis. 2010;16:2680–9.

192. Lynch AP, Ahearne M. Retinoic acid enhances the differentiation of adipose-derived stem cells to keratocytes in vitro. Transl Vis Sci Technol. 2017;6(1):6.

193. Park SH, Kim KW, Chun YS, Kim JC. Human mesenchymal stem cells differentiate into keratocyte-like cells in keratocyte-conditioned medium. Exp Eye Res. 2012;101:16–26.

194. Trosan P, Javorkova E, Zajicova A, Hajkova M, Hermankova A, Kossl J, et al. The supportive role of insulin-like growth factor-I in the differentiation of murine mesenchymal stem cells into corneal-like cells. Stem Cells Dev. 2016;25(11):874–81.

195. Liu H, Zhang J, Liu C-Y, Hayashi Y, Kao WW-Y. Bone marrow mesenchymal stem cells can differentiate and assume corneal keratocyte phenotype. J Cell Mol Med. 2012;16(5):1114–1124.

196. Ziaei M, Zhang J, Patel D V, McGhee CNJ. Umbilical cord stem cells in the treatment of corneal disease. Surv Ophthalmol. 2017;62(6):803–15.

197. Chan AA, Hertsenberg AJ, Funderburgh ML, Mann MM, Du Y, Davoli KA, et al. Differentiation of human embryonic stem cells into cells with corneal keratocyte phenotype. PLoS One. 2013;8(2):e56831.

198. Gurdon JB. The developmental capacity of nuclei taken from intestinal epithelium cells of feeding tadpoles. J Embryol Exp Morphol. 1962;10:622–40.

199. Musunuru K. Genome editing of human pluripotent stem cells to generate human cellular disease models. Dis Model Mech. 2013;6(4):896–904.

200. Yun Y, Park S, Lee H, Ko J, Kim M, Wee W, et al. Comparison of the anti-inflammatory effects of induced pluripotent stem cell-derived and bone marrow-derived mesenchymal stromal cells in a murine model of corneal injury. Cytotherapy. 2017;19(1):28–35.

201. Pinnamaneni N, Funderburgh JL. Concise review: Stem cells in the corneal stroma. Stem Cells. 2012;30(6):1059–63.

202. Katikireddy KR, Dana R, Jurkunas U V. Differentiation potential of limbal fibroblasts and bone marrow mesenchymal stem cells to corneal epithelial cells. Stem Cells. 2014;32(3):717–29.

203. Wu J, Du Y, Watkins SC, Funderburgh JL, Wagner WR. The engineering of organized human corneal tissue through the spatial guidance of corneal stromal stem cells. Biomaterials. 2012;33(5):1343–52.

204. Di G, Du X, Qi X, Zhao X, Duan H, Li S, et al. Mesenchymal stem cells promote diabetic corneal epithelial wound healing through TSG-6–dependent stem cell activation and macrophage switch. IOVS. 2017;58(10):4344–4354.

205. Holan V, Trosan P, Cejka C, Javorkova E, Zajicova A, Hermankova B, et al. A comparative study of the therapeutic potential of mesenchymal stem cells and limbal epithelial stem cells for ocular surface reconstruction. Stem Cells Transl Med. 2015;4(9):1052–1063.

206. Cejka C, Cejkova J, Trosan P, Zajicova A, Sykova E, Holan V. Transfer of mesenchymal stem cells and cyclosporine A on alkali-injured rabbit cornea using nanofiber scaffolds strongly reduces corneal neovascularization and scar formation. Histol Histopathol.

2016;31(9):969–80.

207. Agorogiannis GI, Alexaki V-I, Castana O, Kymionis GD. Topical application of autologous adipose-derived mesenchymal stem cells (MSCs) for persistent sterile corneal epithelial defect. Graefes Arch Clin Exp Ophthalmol. 2012;250(3):455–7.

208. Basu S, Damala M, Singh V. Limbal stromal stem cell therapy for acute and chronic superficial corneal pathologies: early clinical outcomes of the funderburgh technique. Oral Present Assoc Res Vis Ophthalmol Annu Meet. 2017;58:3371.

209. Ma X-Y, Bao H-J, Cui L, Zou J. The graft of autologous adipose-derived stem cells in the corneal stromal after mechanic damage. PLoS One. 2013;8(10):e76103.

210. Sasaki S, Funamoto S, Hashimoto Y, Kimura T, Honda T, Hattori S, et al. In vivo evaluation of a novel scaffold for artificial corneas prepared by using ultrahigh hydrostatic pressure to decellularize porcine corneas. Mol Vis. 2009;15:2022–2028.

211. Ponce Márquez S, Martínez V, McIntosh Ambrose W, Wang J, Gantxegui N, Schein O, et al. Decellularization of bovine corneas for tissue engineering applications. Acta Biomater. 2009;5(6):1839–47.

212. Amano S, Shimomura N, Yokoo S, Araki-Sasaki K, Yamagami S. Decellularizing corneal stroma using N2 gas. Mol Vis. 2008;14(14):878–82.

213. Gonzalez-Andrades M, de la Cruz Cardona, J, Ionescu A, Campos A, Del Mar Perez M, Alaminos M. Generation of bioengineered corneas with decellularized xenografts and human keratocytes. Invest Ophthalmol Vis Sci. 2011;52(1):215–22.

214. Crapo PM, Gilbert TW, Badylak SF. An overview of tissue and whole organ decellularization processes. Biomaterials. 2011;32(12):3233–43.

215. Du L, Wu X. Development and characterization of a full-thickness acellular porcine cornea matrix for tissue engineering. Artif Organs. 2011;35(7):691–705.

216. Gilbert TW, Sellaro TL, Badylak SF. Decellularization of tissues and organs. Biomaterials. 2006;27(19):3675–83.

217. Choi J, Williams J, Greven M, Walter K, Laber P, Khang G, et al. Bioengineering

endothelialized neo-corneas using donor-derived corneal endothelial cells and decellularized corneal stroma. Biomaterials. 2010;31(26):6738–45.

218. Seddon AM, Curnow P, Booth PJ. Membrane proteins, lipids and detergents: not just a soap opera. Biochim Biophys Acta. 2004;1666(1–2):105–17.

219. Bayyoud T, Thaler S, Hofmann J, Maurus C, Spitzer MS, Bartz-Schmidt K-U, et al. Decellularized bovine corneal posterior lamellae as carrier matrix for cultivated human corneal endothelial cells. Curr Eye Res. 2012;37(3):179–86.

220. Du L, Wu X, Pang K, Yang Y. Histological evaluation and biomechanical characterisation of an acellular porcine cornea scaffold. Br J Ophthalmol. 2011;95(3):410–4.

221. Tran KD, Terry MA, Stoeger C. Physical properties of electron-beam irradiated corneas stored in recombinant human serum albumin. IOVS ARVO Annu Meet. 2016;57:2386.

222. Wilson SE, Liu JJ, Mohan RR. Stromal-epithelial interactions in the cornea. Prog Retin Eye Res. 1999;8(3):293–309.

223. Shafiq MA, Gemeinhart, Richard A. Yue BYJT, Djalilian AR. Decellularized human cornea for reconstructing the corneal epithelium and anterior stroma. Tissue Eng Part C Methods. 2012;18(5):340–348.

224. Yam GH-F, Yusoff NZBM, Goh T-W, Setiawan M, Lee X-W, Liu Y-C, et al. Decellularization of human stromal refractive lenticules for corneal tissue engineering. Sci Rep. 2016;6:26339.

225. Liu Y-C, Teo E, Ang M, Seah XY, Lwin NC, Yam G, et al. Biological corneal inlay for presbyopia derived from small incision lenticule extraction (SMILE). Sci Rep. 2018;8(1):1831.

226. Bai H, Wang LL, Huang YF, Huang JX. An experimental study of mesenchymal stem cells in tissue engineering scaffolds implanted in rabbit corneal lamellae to increase keratoprosthesis biointegration. Zhonghua Yan Ke Za Zhi. 2016;52(3):192–7.

227. Barraquer J. Keratophakia. Trans Ophthalmol Soc. 1972;92:499–516.

228. Omoto M, Katikireddy KR, Rezazadeh A, Dohlman TH, Chauhan SK. Mesenchymal stem

cells home to inflamed ocular surface and suppress allosensitization in corneal transplantation. Invest Ophthalmol Vis Sci. 2014;55(10):6631–8.

229. Fuentes-Julián S, Arnalich-Montiel F, Jaumandreu L, Leal M, Casado A, García-Tuñon I, et al. Adipose-derived mesenchymal stem cell administration does not improve corneal graft survival outcome. PLoS One. 2015;10(3):e0117945.

230. Zhang L, Coulson-Thomas VJ, Ferreira TG, Kao WWY. Mesenchymal stem cells for treating ocular surface diseases. BMC Ophthalmol. 2015;15(Suppl 1):155.

231. Swioklo S, Constantinescu A, Connon CJ. Alginate-encapsulation for the improved hypothermic preservation of human adipose-derived stem cells. Stem Cells Transl Med. 2016;5(3):339–49.

232. Funderburgh JL, Funderburgh ML, Mann M, Khandaker I, Shojaati G. Assessing the potential of stem cells to regenerate stromal tissue. IOral Present Assoc Res Vis Ophthalmol Annu Meet Balt. 2017;58.

233. Joseph R, Srivastava OP, Pfister RR. Modeling keratoconus using induced pluripotent stem cells. Invest Ophthalmol Vis Sci. 2016;57(8):3685–97.

234. Shimmura S, Tsubota K. Deep anterior lamellar keratoplasty. Curr Opin Ophthalmol. 2006;17(4):349–55.

235. Watson S, Tuft S, Dart J. Patterns of rejection after deep lamellar keratoplasty. Ophthalmology. 2006;113(4):556–60.

236. Krumeich J, Knülle A, Krumeich B. Deep anterior lamellar (DALK) vs. penetrating keratoplasty (PKP): a clinical and statistical analysis. Klin Monbl Augenheilkd. 2008;225(7):637–48.

237. Zuk PA, Zhu M, Ashjian P, De Ugarte D, Huang J, Mizuno H, et al. Human adipose tissue is a source of multipotent stem cells. Mol Biol Cell. 2002;13(12):4279–95.

238. Guthoff R, Klink T, Schlunck G, Grehn F. Die sickerkissenuntersuchung mittels konfokaler in-vivo mikroskopie mit dem rostocker cornea modul - erste erfahrungen. Klin Monatsbl Augenheilkd. 2005;222:R8.

239. Patel S, McLaren J, Hodge D, Bourne W. Normal human keratocyte density and corneal thickness measurement by using confocal microscopy in vivo. Invest Ophthalmol Vis Sci. 2001;42(2):333–9.

240. Alió del Barrio JL, Arnalich-Montiel F, De Miguel MP, El Zarif M, Alió JL. Corneal stroma regeneration: preclinical studies. Exp Eye Res. 2021;202:108314.

241. El Zarif M, Alió del Barrio JL, Arnalich-Montiel F, De Miguel MP, Makdissy N, Alió JL. Corneal stroma regeneration: new approach for the treatment of cornea disease. APJO. 2020;9(6):571–9.

242. El Zarif M, Alió JL, Alió del Barrio JL, De Miguel MP, Abdul Jawad K, Makdissy N. Corneal stromal regeneration: a review on human clinical studies for treatement of keratoconus. Front Med. 2021;8:650724.

243. Dos Santos A, Balayan A, Funderburgh ML, Ngo J, Funderburgh JL, Deng SX. Differentiation capacity of human mesenchymal stem cells into keratocyte lineage. Invest Ophthalmol Vis Sci. 2019;60(8):3013–23.

244. Alio Del Barrio JL, Alio J. Cellular therapy of the corneal stroma: a new type of corneal surgery for keratoconus and corneal dystrophies. Eye Vis. 2018;5:28.

245. Cartwright NEK, Tyrer JR, Jaycock PD, Marshall J. Effects of variation in depth and side cut angulations in LASIK and thin-flap LASIK using a femtosecond laser: a biomechanical study. J Refract Surg. 2012;28(6):419–25.

246. Van D, Liarakos V, Parker J, Ham L, Lie J, Groeneveld-van Beek, EA Melles G. Bowman layer transplantation to reduce and stabilize progressive, advanced keratoconus. Ophthalmology. 2015;122(5):909–17.

247. Hashimoto Y, Funamoto S, Sasaki S, Negishi J, Honda T, Hattori S, et al. Corneal regeneration by deep anterior lamellar keratoplasty (DALK) using decellularized corneal matrix. PLoS One. 2015;10(7):e0131989.

248. Alio JL, Piñero DP, Daxer A. Clinical outcomes after complete ring implantation in corneal ectasia using the femtosecond technology: a pilot study. Ophthalmology. 2011;118(7):1282–90.

249. Daxer A. Biomechanics of corneal ring implants. Cornea. 2015;34(11):1493–1498.

250. Alió JL, Alió del Barrio JL, El Zarif M. Cirugía regenerativa del estroma corneal: un nuevo futuro para el tratamiento del queratocono. Alaccsa. 2020;

251. El Zarif M, Alió JL, Alió del Barrio J. Advanced therapy of the human corneal stroma with stem cells in keratoconus. In 2021.

252. Birbal RS, Dijk K van, Parker JS, Otten H, Belmoukadim M, Ham L, et al. Manual mid-stromal dissection as a low risk procedure to stabilize mild to moderate progressive keratoconus. Eye Vis. 2018;5:26.

253. McAlinden C, Pesudovs K, Moore JE. The Development of an Instrument to Measure Quality of Vision: The Quality of Vision (QoV) Questionnaire. IOVS. 2010;51(11):5537–45.

254. Alió del Barrio JL, El Zarif M, Alió JL. Anterior segment OCT: observations in corneal stroma regeneration. In: Alió JL, Alio del Barrio J, editors. Text and Atlas of anterior segment OCT. Springer Nature; 2021. p. 207–10.

255. Shojaati G, Khandaker I, Funderburgh ML, Mann MM, Basu R, Stolz DB, et al. Mesenchymal stem cells reduce corneal fibrosis and inflammation via extracellular vesicle-mediated delivery of miRNA. Stem Cells Transl Med. 2019;8(11):1192–201.

256. Petroll WM, Kivanany PB, Hagenasr D, Graham EK. Corneal fibroblast migration patterns during intrastromal wound healing correlate with ECM structure and alignment. IOVS. 2015;56:7352–61.

257. Phinney DG, Prockop DJ. Concise review: mesenchymal stem/multipotent stromal cells: the state of transdifferentiation and modes of tissue repair--current views. Stem Cells. 2007;25(11):2896–902.

258. Jester J V, Moller-Pedersen T, Huang J, Sax CM, Kays WT, Cavangh HD, et al. The cellular basis of corneal transparency: evidence for “corneal crystallins.” J Cell Sci. 1999;112(Pt 5):613–22.

259. Liu R, Zhao J, Xu Y, Li M, Niu L, Liu H, et al. Femtosecond laser-assisted corneal small

incision allogenic intrastromal lenticule implantation in monkeys: a pilot study. IOVS. 2015;56(6):3715–20.

260. Zhao J, Liu R, Shen Y, Zhang X, Zhao Y, Xu H, et al. Two-year observation of morphologic and histopathologic changes in the monkey cornea following small incision allogenic lenticule implantation. Exp Eye Res. 2020;192:107935.

261. Pradhan K, Reinstein D, Vida R, Archer T, Dhungel S, Moptom D, et al. Femtosecond laser–assisted small incision sutureless intrastromal lamellar keratoplasty (SILK) for corneal transplantation in keratoconus. J Refract Surg. 2019;35(10):663–71.

262. Mastropasqua L, Nubile M, Salgari N, Mastropasqua R. Femtosecond laser-assisted stromal lenticule addition keratoplasty for the treatment of advanced keratoconus: a preliminary study. J Refract Surg. 2018;34(1):36–44.

263. Mastropasqua L, Nubile M. Corneal thickening and central flattening induced by femtosecond laser hyperopic-shaped intrastromal lenticule implantation. Int Ophthalmol. 2017;37(4):893–904.

264. Ganesh S, Brar S. Femtosecond intrastromal lenticular implantation combined with accelerated collagen cross-linking for the treatment of keratoconus-- initial clinical result in 6 eyes. Cornea. 2015;34(10):1331–9.

265. Ganesh S, Brar S, Rao P. Cryopreservation of extracted corneal lenticules after small incision lenticule extraction for potential use in human subjects. Cornea. 2014;33(12):1355–62.

266. Jin H, He M, Liu H, Zhong X, Wu J, Liu L, et al. Small-incision femtosecond laser–assisted intracorneal concave lenticule implantation in patients with keratoconus. Cornea. 2019;38(4):446–453.

267. Riau AK, Htoon HM, Alio del Barrio JL, Nubile M, El Zarif M, Mastropasqua L, et al. Femtosecond laser-assisted stromal keratophakia for keratoconus: a systemic review and meta-analysis. Int Ophthalmol. 2020;41(5):1965–79.

268. Doroodgar F, Jabbarvand M, Niazi S, Karimian F, Niazi F, Sanginabadi A, et al. Customized stromal lenticule implantation for keratoconus. J Refract Surg.

2020;36(12):786–94.

269. Pradhan K, Reinstein D, Carp G, Archer T, Gobbe M, Gurung R. Femtosecond laser-assisted keyhole endokeratophakia: correction of hyperopia by implantation of an allogeneic lenticule obtained by SMILE from a myopic donor. J Refract Surg. 2013;29(11):777–82.

270. Gahmberg C, Fagerholm S, Nurmi S, Chavakis T, Marchesan S, Grönholm M. Regulation of integrin activity and signalling. Biochim Biophys Acta. 2009;1790(6):431–44.

271. Velázquez JS, Cavas F, Bolarín JM, Alió JL. 3D printed personalized corneal models as a tool for improving patient's knowledge of an asymmetric disease. Symmetry (Basel). 2020;12(1):151.

272. Alifa R, Piñero D, Velázquez J, Alió Del Barrio JL, Cavas F, Alió JL. Changes in the 3D corneal structure and morphogeometric properties in keratoconus after corneal collagen crosslinking. Diagnostics (Basel). 2020;10(6):397.

273. Sorkio A, Koch L, Koivusalo L, Deiwick A, Miettinen S, Chichkov B, et al. Human stem cell based corneal tissue mimicking structures using laser-assisted 3D bioprinting and functional bioinks. Biomaterials. 2018;171:57–71.

274. Dobos A, Hoorick J Van, Steiger W, Gruber P, Markovic M, Andriotis OG, et al. Thiol-gelatin-norbornene bioink for laser-based high-definition bioprinting. Adv Heal Mater. 2020;9(15):e1900752.

275. Llewellyn-Jones T, Allen R, Trask R. Curved layer fused filament fabrication using automated toolpath generation. 3D Print Addit Manuf. 2016;3(4):236–43.

10. ANEXOS / ANNEX

El ANEXO DE ESTA TESIS DOCTORAL SE BASA EN LOS SIGUIENTES ARTÍCULOS Y CAPÍTULOS CIENTÍFICOS/

THE ANNEX OF THIS DOCTORAL THESIS IS BASED ON THE FOLLOWING SCIENTIFIC ARTICLES AND CHAPTERS:

10.1 Alió del Barrio JL, Arnalich-Montiel F, De Miguel MP, **El Zarif M**, Alió JL. **Corneal stroma regeneration: Preclinical studies**. Exp Eye Res. 2020;108314.

https://doi.org/10.1016/j.exer.2020.108314

10. 2 PUBLICACIÓN PREDOCTORAL/ PREDOCTORAL PUBLICATION:

Alió Del Barrio, J., El Zarif, M., De Miguel, M., Azaar, A., Makdissy, N., Harb, W., El Achkar, I., Arnalich-Montiel, F., Alió, J., 2017. **Cellular therapy with human autologous adipose-derived adult stem cells for advanced keratoconus**. Cornea 36, 952–960. https://doi.org/10.1097/ICO.0000000000001228

10.3 PUBLICACIÓN PREDOCTORAL/ PREDOCTORAL PUBLICATION:

Alió Del Barrio, J., El Zarif, M., Azaar, A., Makdissy, N., Khalil, C., Harb, W., El Achkar, I., Jawad, Z., de Miguel, M., Alió, J., 2018. **Corneal stroma enhancement with decellularized stromal laminas with or without stem cell recellularization for advanced keratoconus**. Am J Ophthalmol 186, 47–58. https://doi.org/10.1016/j.ajo.2017.10.026

10.4 Alió J, Alió del Barrio J, **El Zarif M**, Azaar A, Makdissy N, Khalil C et al. **Regenerative surgery of the corneal stroma for advanced keratoconus: 1-Year outcomes**. Am J Ophthalmol. 2019;203:53-68. https://doi.org/10.1016/j.ajo.2019.02.009

10.5 **El Zarif M**, Alió JL, Alió del Barrio JL, Abdul Jawad K, Palazón-Bru A, Abdul Jawad Z, et al**. Corneal stromal regeneration therapy for advanced keratoconus: long-term outcomes at 3 years**. Cornea. 2021;40(6):741–54. https://doi.org/10.1097/ICO.0000000000002646

10.6 **El Zarif M**, Abdul Jawas K, Alió del Barrio JL, Abdul Jawad Z, Palazón-Bru A, De Miguel MP, et al**. Corneal stroma cell density evolution in keratoconus corneas following the implantation of adipose mesenchymal stem cells and corneal laminas: an in vivo confocal microscopy study.** IOVS. 2020;61(4)22. https://doi.org/10.1167/iovs.61.4.22

10.7 **El Zarif M**, Alió del Barrio JL, Arnalich-Montiel F, De Miguel MP, Makdissy N, Alió JL. **Corneal stroma regeneration: new approach for the treatment of cornea disease**. APJO. 2020;9(6):571–9. https://doi.org/10.1097/APO.0000000000000337

10.8 **El Zarif M**, Alió JL, Alió del Barrio JL, De Miguel MP, Abdul Jawad K, Makdissy N. **Corneal stromal regeneration: a review on human clinical studies for treatment of keratoconus.** Front Med. 2021;8:650724. https://doi.org/10.3389/fmed.2021.650724

10.9 El Zarif, M., Abdul Jawad, K., Alió, J.L., 2019. **Confocal microscopy of the cornea in a clinical model of corneal stromal expansion using adipose stem cells and corneal decellularized laminas in patients with keratoconus.** In: Alió JL, Alió del Barrio JL, Arnalich-Montiel F, (Eds.), Corneal Regeneration therapy and surgery. 1st ed. Springer, pp. 363–386. https://doi.org/10.1007/978-3-030-01304-2_24

10.10 Alió J.L., **El Zarif M**, Alió del barrio J.L.,. **Cellular therapy of the corneal stroma: a new type of corneal surgery for keratoconus and corneal dystrophies a translational research experience.** 1st ed. Elsevier. (Accepted in 2020. Ahead of print).

10.11 Alió del barrio JL, **El Zarif M**, Alió JL., 2021**. Anterior segment OCT: observations in corneal stroma regeneration**, In: Alió J.L., Alio del Barrio J.L., (Eds.), Text and Atlas of Anterior Segment OCT. Springer Nature, pp. 207–210. https://doi.org/10.1007/978-3-030-53374-8_9

10.12 El Zarif M, Alió J.L., Alió del Barrio J.L., **Advanced therapy of the human corneal stroma in keratoconus with stem cells.** (Accepted in 2021. Ahead of print).

10.1. Alió del Barrio, J.L., Arnalich-Montiel, F., De Miguel, M.P., El Zarif, M., Alió, J.L., 2021. **Corneal stroma regeneration: preclinical studies**. Exp. Eye Res. 202, 108314. https://doi.org/10.1016/j.exer.2020.108314

Corneal stroma regeneration: Preclinical studies

Jorge L. Alio´ del Barrio [a, b], Francisco Arnalich-Montiel [c,d], María P. De Miguel [e], Mona El Zarif [f], Jorge L. Alio´ [a, b, *]

[a] *Cornea, Cataract and Refractive Surgery Unit, Vissum (Miranza Group), Alicante, Spain*
[b] *Division of Ophthalmology, Universidad Miguel Hernandez,´ Alicante, Spain*
[c] *IRYCIS. Ophthalmology Department. Ramon´ y Cajal University Hospital, Madrid, Spain*
[d] *Cornea Unit. Hospital Vissum Madrid (Miranza Group), Madrid, Spain*
[e] *Cell Engineering Laboratory, IdiPAZ, La Paz Hospital Research Institute, Madrid, Spain*
[f] *Optica General, Saida, Lebanon*

ARTICLE INFO

Keywords:
Stem cells
Regenerative medicine
Corneal transplant
Decellularized cornea
Cornea
Corneal stroma
Cellular therapy
MSC
Mesenchymal stem **cells**
ADASCs

ABSTRACT

Corneal grafting is one of the most common and successful forms of human tissue transplantation in the world, but the need for corneal grafting is growing and availability of human corneal donor tissue to fulfill this increasing demand is not assured worldwide. The stroma is responsible for many features of the cornea, including its strength, refractive power and transparency, so enormous efforts have been put into replicating the corneal stroma in the laboratory to find an alternative to classical corneal transplantation. Unfortunately this has not been yet accomplished due to the extreme difficulty in mimicking the highly complex ultrastructure of the corneal stroma, and none of the obtained substitutes that have been assayed has been able to replicate this complexity yet. In general, they can neither match the mechanical properties nor recreate the local nanoscale organization and thus the transparency and optical properties of a normal cornea. In this context, there is an increasing interest in cellular therapy of the corneal stroma using Induced Pluripotent Stem Cells (iPSCs) or mesenchymal stem cells (MSCs) from either ocular or extraocular sources, as they have proven to be capable of producing new collagen within the host stroma, modulate preexisting scars and enhance transparency by corneal stroma remodeling. Despite some early clinical data is already available, in the current article we will summary the available preclinical evidence about the topic corneal stroma regeneration. Both, in vitro and in vivo ex-periments in the animal model will be shown.

1. INTRODUCTION

Corneal grafting is one of the most common and successful forms of human tissue transplantation in the world, with more than 180,000 corneal grafts performed every year worldwide (Gain et al., 2016). Recent improvements in corneal transplantation techniques are making the incidence of corneal grafting to increase. However, corneal graft failure still represents an important concern as it increases, even more, the demand for corneal tissue (Alio´ et al., 2020). Moreover, each failure requiring re-grafting will increase the individual risk for rejection and failure of subsequent grafts (Williams et al., 2008). All these facts reflect the upcoming concern about a potential insufficient availability of human corneal donor tissue to fulfill the increasing demand. Actually, in many countries access to donor corneal tissue is already limited, with approximately 53% of the world's population not having access to corneal transplantation (Gain et al., 2016).

This global health problem has focused research interest on developing, in the laboratory, corneal substitutes that could mimic human cornea features in vivo, and sub-sequently be an alternative to human donor tissue.

The stroma constitutes more than 90% of the corneal thickness, and many features of the cornea, including its strength, morphology and transparency are attributable to the anatomy and properties of the corneal stroma (De Miguel et al., 2015). Many diseases such as corneal dystrophies, scars or ecstatic disorders induce a distortion of its anatomy or physiology leading to loss of transparency and subsequent loss of vision. As discussed before, enormous efforts have been put into replicating the corneal stroma in the laboratory to find an alternative to classical corneal transplantation, but this has still not been yet accomplished due to the extreme difficulty in mimicking the highly complex ultrastructure of the corneal stroma, obtaining substitutes that either do not achieve enough transparency

* Corresponding author. . Vissum, Calle Cabanal,˜ 1, 03016, Alicante. Spain. *E-mail address:* jlalio@vissum.com (J.L. Alio)´.

or strength (Isaacson et al., 2018; Ruberti and Zieske, 2008). Moreover, synthetic scaffold-based designs have raised some important concerns such as strong inflammatory re-sponses induced on their biodegradation, or chronic nonspecific in-flammatory responses (Alio del Barrio et al., 2015a). On the other hand, recently several corneal decellularization techniques have been described, which provide an acellular corneal ECM (Lynch and Ahearne, 2013). These scaffolds have gained attention in the last few years as, in contrast with synthetic scaffolds, they provide an ideal natural envi-ronment for the growth and differentiation of cells (either transplanted donor cells or migrating host cells) (Alio del Barrio et al., 2015a). In addition, components of the ECM are generally conserved among species and are well tolerated by xenogeneic recipients.

In the last few years, cellular therapy of the corneal stroma using mesenchymal stem cells (MSCs) from extraocular sources has also gained a lot of interest; studies show that MSCs are capable of differentiating into adult keratocytes in vitro and in vivo (De Miguel et al., 2015) Several authors, including reports from our research group (Alio del Barrio et al., 2015a; Arnalich-Montiel et al., 2008), have demon-strated that these stem cells can not only survive and differentiate into adult human keratocytes in xenogeneic scenarios without inducing any inflammatory reaction, but also I) produce new collagen within the host stroma (Arnalich-Montiel et al., 2008; Espandar et al., 2012), II) modulate preexisting scars by corneal stroma remodeling (Demirayak et al., 2016; Mittal et al., 2016), and III) improve corneal transparency in animal models for corneal dystrophies by collagen reorganization as well as in animal models for metabolopathies by the catabolism of accumulated proteins (Coulson-Thomas et al., 2013; Du et al., 2009; Kao and Coulson-Thomas, 2016; Liu et al., 2010). Mesenchymal stem cells have also shown immunomodulatory properties in syngeneic, allogeneic and even xenogeneic scenarios (De Miguel et al., 2012). Actually, the first clinical data regarding the safety and preliminary efficacy of cellular therapy of the corneal stroma from Phase 1 human clinical trials is now available (Alio Del Barrio et al., 2017, 2018, 2019), which may end up providing a real alternative treatment option for corneal diseases in the near future.

1.1. Available stem cells for corneal stroma cellular therapy

MSCs can be obtained from many human tissues, including adipose tissue, bone marrow, umbilical cord, dental pulp, gingiva, hair follicle, cornea and placenta (Hendijani, 2017). Existing scientific evidence show that all types of MSCs have probably similar behavior in vivo (Alio Del Barrio and Alio, 2018), and thus are able to achieve keratocyte differentiation and modulate the corneal stroma with immunomodula-tory properties. (Harkin et al., 2015). It has also been recently reported that MSCs secrete paracrine factors such as vascular endothelial growth factor (VEGF), platelet-derived growth factor (PDGF), hepatocyte growth factor (HGF), and transforming growth factor beta 1 (TGFβ1) (De Miguel et al., 2012). Although the precise actions of the different growth factors for cornea wound healing are not fully understood, overall, they seem to promote cell migration, keratocyte survival by apoptosis inhibition, and upregulate the expression of extracellular matrix (ECM) component genes in keratocytes, subsequently enhancing corneal re-epithelialization and stromal wound healing (Jiang et al., 2017). Actually, it has been suggested that the direct treatment of the corneal stroma with the MSC exosomes containing these growth factors could potentially achieve the same benefits of the cellular therapy, but without providing the cellular component itself (Funderburgh, 2017). Proangiogenic VEGF, HGF, and FGF2 secretion, which are known to induce neovascularization, can abrogate the corneal immune privilege and be implicated in corneal transplant rejection risk (Fuentes-Julian´ et al., 2015). Moreover, our group has demonstrated that adipose derived MSCs secrete IL-6 and IL-8 (Fuentes-Julian´ et al., 2015), which have been shown to also increase neovascularization and so increase corneal transplant rejection risk. On the other hand, cytokine production by MSCs is mediated by the environment, and hence examples of the opposite exist as well: for example, MSCs improved the renal function in a rat model of acute renal failure. RT-PCR in such renal tissue 24 h after MSC delivery demonstrated a decrease in proinflammatory cytokines IL-1β, TNF-α and IFN-γ and a promotion of anti-inflammatory cytokines such as IL-10, TGF-α or FGF2 (Togel¨ et al., 2005). Also, intravenous administration of allogenic MSCs in a mouse model of lung fibrosis alleviated the symptoms and decreased neutrophil infiltration and TNF-α production in the lungs (Ortiz et al., 2007). In a model of corneal chemical burns, MSCs engrafted in the corneal stroma decreased inflammation (mostly CD4+T-cells) allowing for epithelial regenera-tion. In this study, a drop in the production of IFN-γ and IL-2 and an increased level of TGF-β, IL-10 and IL-6 in the injured corneas were observed (Oh et al., 2008).

Corneal stroma stem cells (CSSCs) are a promising source for cellular therapy as the isolation technique and culture methods have been optimized and refined (Basu et al., 2014); presumably, they show greater differentiation potential into keratocytes as they are already committed to the corneal lineage (Dos Santos et al., 2019). On the other hand, isolating CSSCs autologously is more technically demanding considering the small amount of tissue that they are obtained from. Furthermore, this technique still requires a contralateral healthy eye, which is not always available (bilateral disease). Therefore, these drawbacks may limit its use in clinical practice. Allogeneic CSSC use requires living or cadaveric donor corneal tissue.

Human adult adipose tissue is a good source of autologous extra-ocular stem cells as it satisfies many requirements: easy accessibility to the tissue, high cell retrieval efficiency and the ability of its stem cells, *human adipose derived adult stem cells (h-ADASCs)* to differentiate into multiple cell types (keratocytes, osteoblasts, chondroblasts, myoblasts, hepatocytes, neurons, etc.) (Arnalich-Montiel et al., 2008). This cellular differentiation occurs due to the effect of very specific stimulating factors or environments for each cell type, avoiding the mix of multiple kinds of cells in different niches.

Bone marrow MSCs (BM-MSCs) are probably the most widely studied MSCs, presenting a similar profile to ADASCs, but their extraction re-quires a bone marrow puncture, which is a complicated and painful procedure requiring general anesthesia.

Umbilical Cord MSCs (UMSCs) present an attractive alternative, but their autologous use is currently limited as the umbilical cord is not generally stored after birth.

Embryonic stem cells have great potential, but also present important ethical issues. However, the use of *Induced Pluripotent Stem Cells (iPSCs)* could solve such problems (Takahashi and Yamanaka, 2006), and their capability to generate adult keratocytes has already been proven in vitro (Naylor et al., 2016): specialized adult cells can be reprogrammed to an immature or stem cell state and then redirected to the required cell lineage using specific factors and environmental stimuli. It has been shown that iPSC-derived MSCs exert immunomodulatory properties in the cornea similar to those observed with BM-MSCs (Yun et al., 2017). To the best of our knowledge, no studies have been published reporting the capability of iPSCs to differentiate into adult keratocytes in vivo in the animal model.

As previously discussed, it is important to highlight that the therapeutic effect of SCs in a damaged tissue is not always related to the potential differentiation of the SCs in the host tissue, as multiple mechanisms might contribute simultaneously to this therapeutic action as for example the already established secretion of paracrine growth factors capable of stimulating the host tissue, in which case the direct cellular differentiation of the SCs might not be relevant and could even be non-existent (Caplan, 2017; Harkin et al., 2015; Yao and Bai, 2013). Moreover, we should take into account that many preclinical studies have been performed in animals with healthy corneas, wounded or not, and the therapeutic effect from the stem cells might differ when implanted into a really diseased environment with genetically abnormal ECM. While studies in knock-out animals might reflect in a more realistic manner the potential therapeutic benefit, these studies are scantly among available all evidence

1.2. Autologous versus allogenic MSCs

A critical question for future clinical trials to further assess the feasibility of cellular therapy of the corneal stroma, is whether the use of autologous MSCs is really necessary and whether allogenic MSCs could achieve the same benefit without any risk of inflammation or rejection. If we consider all published evidence in the animal model where human MSCs were implanted in the corneal stroma, despite being a xenogeneic transplant, no signs of rejection or inflammation have ever been reported (Alio del Barrio et al., 2015a; 2015b; Arnalich-Montiel et al., 2008; Coulson-Thomas et al., 2013; Demirayak et al., 2016; Du et al., 2009; Espandar et al., 2012; Kao and Coulson-Thomas, 2016; Liu et al., 2010; Mittal et al., 2016). This coincides with the strong evidence regarding the immunomodulatory and immunosuppressive properties of MSCs, which help them to evade host immune rejection and survive by inhibiting adhesion and invasion, and inducing cell death of inflam-matory cells, partially due to a rich extracellular glycocalyx that con-tains tumor necrosis factor-α-stimulated gene 6 (TSG6). (De Miguel et al., 2012; Zhang et al., 2015). TSG6 has been demonstrated to play a critical role in the immunosuppressive properties exhibited by MSCs (Di et al., 2017a,b; Kao and Coulson-Thomas, 2016; Yun et al., 2017). Taken together, the use of allogenic MSCs would greatly simplify the clinical application of MSCs, as clinical application centers would not need any specific equipment because potential MSCs banks could store and supply stem cells for their use in patients. There are already low-cost systems available that are capable of enhancing the preservation of MSCs at hypothermic temperatures, while maintaining their normal function, thereby widening the time frame for distribution between the manufacturing site and the clinic, and reducing the waste associated with the limited shelf life of cells stored in their liquid state (Swioklo et al., 2016). Funderburgh et al. recently reported that MSCs from different donors may have different immunosuppressive properties, and consequently, different abilities to regenerate and relieve stromal scars (Funderburgh, 2017). Considering this important finding, the best donors could be selected by MSCs banks in order to expand and supply only those MSCs with the highest immunosuppressive and regenerative ca-pacity, so autologous cells would not be necessary. We should also consider that adult keratocytes obtained from autologous MSCs may still carry the same genetic defect that led to the corneal disease such as in the case of corneal dystrophy. In this scenario, the use of allogenic instead of autologous MSCs would be interesting. A recent study observed gene expression differences between the iPSC-derived keratocytes generated from fibroblasts of both keratoconic and normal human corneal stroma, influencing cellular growth and proliferation, confirming that, at least in keratoconus cases, adult cells obtained from MSCs may still not be functionally normal (Joseph et al., 2016).

2. REGENERATIVE POTENTIAL OF THE CORNEAL STROMA

Corneal stroma is a collagen-rich extracellular matrix (ECM) assembled to provide it optical properties, basically transparency and refraction of light. Tightly packed parallel collagen fibrils are stacked in multiple lamellae which is regulated by stromal extracellular matrix of a group of tissue-specific keratan sulfate proteoglycans (Chen et al., 2015). Scattered between the lamellae there is a scarce population of keratocytes which remain quiescent throughout adult life (Lagali, 2020). Thus, unlike the regenerative capability of the corneal epithe-lium, the renewal of the corneal stroma is not based on a cycle of cell apoptosis and division, but on a relatively slow collagen and ECM turnover mediated by the normal keratocytes that allows for proper lamellar alignment (Paik et al., 2018; Pinnamaneni and Funderburgh, 2012). In the need of fast corneal stromal regeneration, for instance in response to trauma or infection, keratocytes can transform to a myofibroblast phenotype, proliferate and produce aberrant collagen and therefore opaque scar tissue (Lagali, 2020).

A different population from these quiescent keratocytes, are the neural crest-derived mesenchymal stem cells that have been localized in the limbal stroma, subjacent to the epithelial basement membrane and clearly distinct from corneal epithelial stem cells. These corneal stromal stem cells (CSSCs) express genes from neural ectoderm origin such as PAX6, adult stem cell markers such as ABCG2 and MSCs markers such as CD73 and CD90 (Du et al., 2005; Pinnamaneni and Funderburgh, 2012). They exhibit clonal growth, self-renewal properties and a potential for differentiation into multiple distinct cell types, including functional keratocytes, even after multiple rounds of expansion (Pinnamaneni and Funderburgh, 2012). Although its biological significance is not yet clear, it is thought that they could be the source of keratocyte replacement when there is a need for stromal regeneration (Pinnamaneni and Fun-derburgh, 2012). Their ability to maintain the differentiation potential for corneal phenotype despite a very high number of population doublings, as well as its immunomodulation effects on the host, makes CSSCs excellent cell candidates for corneal bioengineered constructs. At the same time its ability to regenerate a normal clear stroma seen in several animal models (Du et al., 2009) may be used as anti-scarring treatment in direct cell-based therapies (Pinnamaneni and Funderburgh, 2012).

In combination with any type of corneal stromal regeneration, the therapeutic approach should also include corneal nerve regeneration. The sub-basal nerve plexus, located in the corneal stroma has a fundamental role in epithelial wound healing and thus prevents corneal stroma from ulcerating. These strategies include from epithelium-derived neurotrophic factors therapy (Di et al., 2017a,b) to corneal neurotization where a normal donor nerve is rerouted to an anesthetic cornea (Wolkow et al., 2019).

3. NEW APPROACHES FOR TISSUE ENGINEERING

3.1. Collagen based scaffolds

The arrangement of corneal collagen is the most difficult to repro-duce either by cellular remodeling or by direct manufacturing in the laboratory. Many physical/engineering methods have been devised to attempt to control the organization of collagen for use in engineering or for replicating tissues, including electrospinning, electrogradient transport, magnetic, shear flow, dip pen nano-lithography, wetspinning, flow-induced crystallization, and densification to a liquid crystalline state (for outstanding reviews see Brunette et al., 2017; Matthyssen et al., 2018, and Lagali, 2020 and Tables within).

3.1.1. Decellularized corneal sections

So far, the most promising approach has been previously developed by our group, using decellularized human corneal sections that were recellularized with human adipose tissue adult mesenchymal stem cells (h-ADASCs) in experimental animals (Arnalich-Montiel et al., 2008; Alio del Barrio et al., 2015a, 2015b) (Fig. 1) and importantly also in patients suffering from corneal stromal debilitating diseases Alio Del Barrio et al., 2018a; 2018b, 2019). In these previous highly successful studies, sur-vival of transplanted cells, differentiation into corneal keratocytes, complete integration of the implant, naturally mimicking strength, total transparency and 0% rejection rates were achieved (Fig. 1). Long term studies in these patients show stable collagen graft up to three years so far (El Zarif et al., 2020). However, although this approach can use one donor cornea for several patients, still does not supply an unlimited source of cornea prostheses for their use in patients.

In addition to the above discussed decellularized corneal sections, which basically represent naturally aligned collagen bundles (Alio del Barrio et al., 2015; 2018; Shafiq et al., 2012; Xu et al., 2008), other methods have been developed to mimic corneal stroma structure. Main difficulties linked to these approaches to the cornea are the dual requirements of optical transparency and mechanical strength. The cornea must be mechanically patent on implantation to hold the intraocular

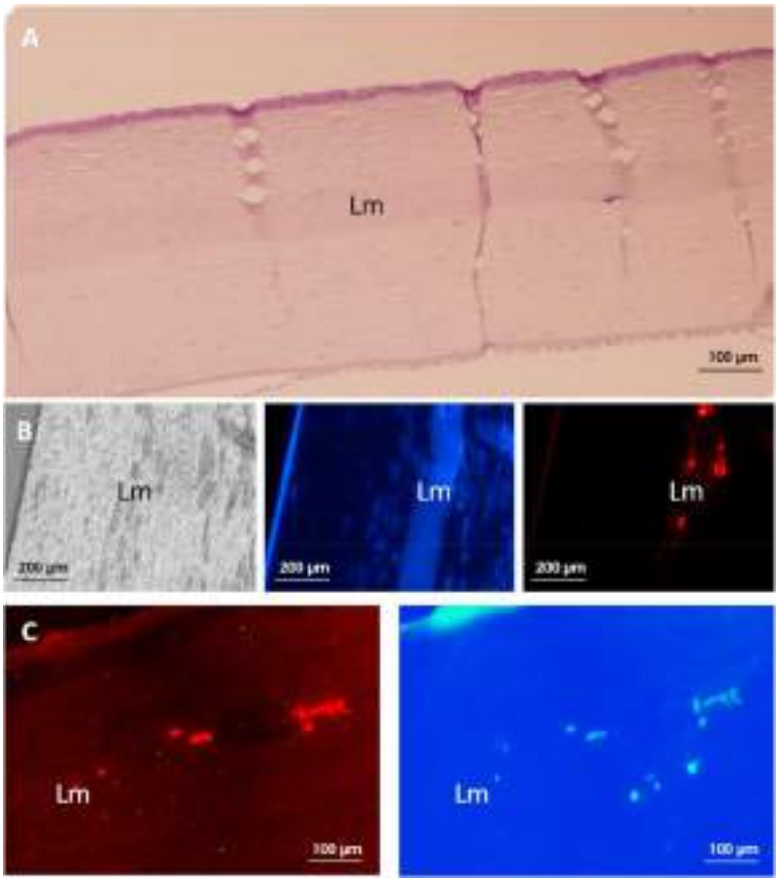

Figure. 1. Decellularized human corneal stroma section (lamina, Lm) implantation into rabbit's corneal stroma in vivo. A: Hematoxylin-eosin staining showing decellularized human lamina integrated into the rabbit's corneal stroma. B: ADASCs survival into the rabbit stroma by detecting the Vybrant CM-DiL dye in red (right), specifically into the grafted human lamina (Lm) that autofluoresces in blue (middle). Left photograph show phase contrast of the same section showing complete biointegration of the lamina. C: ADASCs in vivo differentiation towards keratocytes. Cells are detected in red by Vybrant CM-DiL (left), and keratocytes differentiation is demon-strated by anti-keratocan immunofluorescence in blue (right).

pressure and it must also be optically clear. For reconstituted laboratory collagens, these requirements are very difficult to meet simultaneously. Collagen constructs are typically quite weak mechanically and are not particularly transparent. None of them have been able to recapitulate native corneal tissue structure. In general, they can neither match the mechanical properties nor recreate local nanoscale organization:

3.1.2. Collagen vitrification

Vitrification of collagen has been studied extensively in vitro, and gelation, vitrification and rehydration steps have been optimized yielding a scaffold with light transmittance up to 85% and tensile strengths up to 12 MPa (Calderon-Colon et al., 2012). For ocular purposes, vitrified collagen has been used as carrier for conjunctival cells for conjunctival repair in animal models (Zhou et al., 2014) and corneal epithelium (Chae et al., 2015) and endothelial cells (Yoshida et al., 2017). Respect to a stromal equivalent, to our knowledge, only in vitro models have been developed so far for the purpose of chemical permeability testing (Yamaguchi and Takezawa, 2018).

Griffith and Fagerholm group performed a phase 1 clinical trial with vitrified collagen-based scaffolds into the anterior stroma of 10 patients. (Fagerholm et al., 2010). The results of the trial, which employed a vitrified and cross-linked type III reconstituted human collagen are somewhat equivocal (Fagerholm et al., 2014). While the graft incorpo-rated into the patient's eyes, the replacement of the sacrificial stromal matrix was highly inconsistent, resulting in central corneal thicknesses that varied from 211 to 568 µm in thickness after 2 years. Furthermore, performance of the replacement material after 4 years was poorer than that of donor tissue. However, while the results were not ideal, they do suggest that integration of collagen-based constructs into the corneal stroma is feasible.

3.1.3. Collagen 3D bioprinting

Recent studies have shown proof-of-concept for the use of bio-mimetic materials as corneal implants to promote corneal regeneration as an alternative to donor cornea implantation in rabbits (Liu et al., 2006). Implants were fabricated from carbodiimide cross-linked collagen. Their optical and chemical properties were similar to human corneas. When used as corneal substitutes for transplantation, implants stimulated corneal tissue regeneration in the experimental animals, without the need for immunosuppression. However, these early im-plants had tensile strengths that were significantly weaker in compari-son to the human cornea (Merrett et al., 2008). Recently, the technique for 3D bioprinting of corneal stroma equivalent has been described, and it is able to fabricate translucent corneal stromal equivalents with op-tical properties similar to native corneal stromal tissue while main-taining the keratocyte phenotype of the cells embedded in the stromal tissue (Isaacson et al., 2018; Duarte Campos et al., 2019). This technique has shown promising results in vitro, but needs to improve transparency and strength, and show in vivo functionality and durability, as long-term matrix remodeling is taking place in a continuous fashion. In the next years, a great impulse in the development of this technology is expected (see future perspectives section).

3.1.4. Self-assembling collagen peptides

Fabrication of implants comprising short peptide collagen analogs has been explored (O'Leary et al., 2011), showing in vitro good rheo-logical and morphological features in vitro and further have shown regeneration of mini-pigs corneas in vivo (Islam et al., 2016). However, addition of polyethylene glycol was needed to produce enough robust-ness of the hydrogels, which probably was responsible for a mild haze observed after 12 months (Islam et al., 2016). Similarly, short collagen-like peptides conjugated with polyethylene glycol and mixed with fibrinogen known as regeneration-stimulating liquid corneal replacement, or LiQD Cornea, has been used as a sealant/filler of full-thickness corneal perforations in rabbits and as an alternative to
lamellar corneal transplantation in Gottingen¨ mini-pigs (McTiernan et al., 2020). LiQD cornea allowed regeneration of the corneal epithe-lium, stroma and nerves restoring corneal thickness and curvature. However, in these corneal transplantation models, corneal haze and vascularization was observed in the lamellar transplant.

3.1.5. Collagen compaction by 3D-RAFT and plastic

Real Architecture for 3D Tissue (RAFT) is a simple yet efficient one-step method of collagen compaction by liquid removal using hydrophilic porous absorbers, and it has been shown to support the survival of limbal epithelial cells (Levis et al., 2013), to maintain normal limbal fibroblast phenotype in vitro (Massie et al., 2015), to deliver CSCCs in order to suppress corneal stromal scarring (Shojaati et al., 2018) and to support corneal stromal stem cell differentiation towards keratocytes in vitro (Mukhey et al., 2018), suggesting that this method could actually be useful for creating a stroma equivalent. An alternative compression method, engineered stroma with plastically comprised collagen has been tested (Mi et al., 2011). The compressed collagen, when crosslinked with UVA-riboflavin increases in breaking force while not compromising optical density or cell biocompatibility in vitro. An amalgam bio-engineered cornea made with collagen III combined with a synthetic phosphorylcholine polyethylene glycol diacrylate polymer was transplanted in the anterior cornea of three patients with high risk of corneal transplant rejection (Buznyk et al., 2015) providing relief from discomfort, restoring corneal integrity and improving vision in two pa-tients at 12 months. No data on further long-term analysis is available to our knowledge.

3.2. Non collagen-based scaffolds and tissue adhesive

The approach of using non collagen-based materials seek to achieve a higher strength than collagen-based scaffolds, but at the same time lack the theoretical higher biocompatibility that the collagen has, as these materials are not present in the normal cornea. These synthetic materials are good substrates for various kinds of corneal cells, supporting the growth and transference to the eye. However, there is a need for clinical trials of bioengineered corneal substitutes other than collagen-based materials, to establish the biocompatibility and long-term survival. Nevertheless, we review below the evidence we have on the most promising materials.

3.2.1. Silk fibroin

Silk fibroin is a protein obtained from the cocoon of the silkworm *Bombyx mori*, composed of several subunits—the heavy chain, the light chain and glycoprotein P25 (Tanaka et al., 1993). It is a promising biopolymer for fabrication of corneal scaffolds, easier to model and to prepare a porous structure, fully transparent to visible light, with controllable degradation rates, non-immunogenic, and with optimal mechanical resistance (Chen et al., 2018). In addition to this, it also successfully supports adherence and growth of stromal cells and main-tains their functional phenotype (Bray et al., 2012; Ghezzi et al., 2017). 3D functional corneal stromal tissue equivalent has been produced in vitro using corneal stromal stem cells and multi-lamellar silk film ar-chitecture (Ghezzi et al., 2017), and also has been shown to be effective for corneal stroma reconstruction in a rabbit model (Wang et al., 2015).

3.2.2. Gelatin hydrogels

Gelatin is derived through the hydrolysis of collagen. As a denatured form of collagen is more prone to biodegradation and bio-absorption than collagen itself, properties that are desired to avoid biological re-actions in vivo that can result in tissue opacities in certain scenarios. Mimura et al. established a method for three-dimensional tissue engi-neering of a corneal stroma substitute using fibroblasts and gelatin hydrogels, inducing ECM production in vivo (Mimura et al., 2008). The incorporation of crosslinked collagen to the gelatin hydrogel has shown to provide better optical properties, hydrophilicity, stiffness and Young modulus (Goodarzi et al., 2019). Gelatin hydrogels have been also successfully methacrylated (Kilic Bektas and Hasirci, 2018) or combined with chondroitin sulfate (Lai et al., 2012) or alginate (Tonsomboon et al., 2013). However, compared to silk, gelatin does not show any better overall performance in optical or physical terms.

3.2.3. Chitosan

Chitosan is a natural polymer synthesized by deacetylation of chitin, which is a long-chain polymer of N-acetylglucosamine that is a deriva-tive of glucose, and the primary component of the exoskeletons of ar-thropods (Chen et al., 2018). It is suitable for cornea regeneration due to its biocompatibility and biodegradability, and promotes corneal wound healing, and exerts antimicrobial and antifungal activity. It has been primarily used as a superior alternative to amniotic membrane as a cell carrier to reconstruct the ocular surface or the endothelium (Wang et al., 2016). Rather than pure scaffolds, it could be more useful when acting as an incorporated component in blended scaffold with other molecules such as keratin (Vazquez et al., 2015), collagen (Li et al., 2014), or silk fibroin (Guan et al., 2013). It has also a direct application for ocular drug delivery (Irimia et al., 2018).

3.2.4. Synthetic polymers

Different synthetic polymers have been used alone or blended with natural polymers for corneal tissue engineering in vitro and corneal repair in animal models due to their superb mechanical properties as well as optimal biocompatibility. These include FDA-approved polymers such as poly (lactide-*co*-glycolide) (PLGA) (Ortega et al., 2013; Kong et al., 2017), polycaprolactone (PCL) (Bakhshandeh et al., 2011; Ber-nards et al., 2013), poly-l-lactic acid (PLLA) (Aslan et al., 2018), poly (ethylene) glycol (PEG) (Tan et al., 2013), polyglycolic acid (PGA) (Hu et al., 2005), poly (acrylic acid) (PAA) (Zheng et al., 2015) or poly (ethyl acrylate) (PEA) (Alio del Barrio et al., 2015a). Most of them have only been tested in vitro with the exception of PGA (Hu et al., 2005), PEG-diacrylate or PEG-diacrylamide (Tan et al., 2013) and PEA (Alio del Barrio et al., 2015a). In PGA and PEG-diacrylate, no reconstructed stroma developed in regions where naked polymer was implanted, being the most promising ones PEG-diacrylamide and PEA.

3.3. Stromal regeneration by stem cell therapy without scaffold

Corneal MSCs implantation has been assayed and studied by direct intrastromal transplantation or after implantation from the ocular surface, intravenously and the anterior chamber where cellular migration within the stroma is to be expected. This cellular implantation without a carrier aims to remodel or generate new ECM within the corneal stroma.

3.3.1. Ocular surface implantation of stem cells

Surface implantation of MSCs would be the optimal approach for ocular surface reconstruction and corneal epithelium/limbal stem cell niche regeneration (not the aim of this review). However, surface implantation of MSCs would still play a role in the prevention or modu-lation of anterior stromal scars after an ocular surface injury (like a chemical burn).

As discussed previously, MSCs secrete paracrine factors that enhance corneal re-epithelialization and stromal wound healing (Jiang et al., 2017). Thus, the benefit of MSCs on the ocular surface may be more justified by these paracrine effects rather than by direct differentiation of the MSCs into epithelial cells, as the evidence for the latter is controversial. In this respect, Di et al. assayed *subconjunctival injections* of BM-MSCs in diabetic mice and reported an increased corneal epithelial cell proliferation as well as an attenuated inflammatory response mediated by TSG6 (Di et al., 2017a,b).

Holan et al. suggested MSCs application on the ocular surface using *nanofiber scaffolds*. They reported that BM-MSCs grown on these scaf-folds (made of a polymer of poly (L-lactic) acid) can enhance re-epithelialization, suppress neovascularization and local inflammatory reaction when applied on an alkali-injured eye in a rabbit model, and these results were comparable to those obtained with limbal epithelial stem cells, and both were better than those obtained with ADASCs (Holan et al., 2015). The same group suggested that these results can be improved when these nanofiber scaffolds seeded with rabbit BM-MSCs are covered with cyclosporine-A (CSA), observing an even greater scar suppression and healing results with the combination of both nanofibers (MSCs and CSA) (Cejka et al., 2016).

Topical application of a suspension of autologous ADASCs has been reported in an isolated clinical case report where authors describe the healing of a neurotrophic ulcer that is not responsive to conventional treatment (Agorogiannis et al., 2012). The lack of further clinical or preclinical scientific evidence for this delivery method since 2012 raises questions about its real efficacy.

Finally, Basu et al. suggested the delivery of MSCs using *fibrin glue* (Basu et al., 2014). They resuspended CSSCs in a solution of human fibrinogen, and this was added onto a wounded ocular surface with thrombin on the wound bed. Subsequently the fibrinogen gels. Using this application, they demonstrated the prevention of corneal scarring in the mouse model together with the generation of new stroma with a collagen organization indistinguishable from that of native tissue.

3.3.2. Intrastromal implantation of stem cells alone

Direct in vivo injection of stem cells inside the corneal stroma has been assayed in some studies, demonstrating the differentiation of the stem cells into adult keratocytes without signs of immune rejection (Fig. 2). The differentiation of h-ADASCs in functional human kerato-cytes was demonstrated in vivo, for the first time, in a previous study of our group using the rabbit as a model (Arnalich-Montiel et al., 2008). These cells, once implanted intrastromally, express not only collagens type I and VI (the main components of corneal extracellular matrix), but also keratocyte specific markers such as keratocan or ALDH, without inducing an immune or inflammatory response (Fig. 2). These findings were later reproduced and confirmed by other authors in several research papers (Harkin et al., 2015). Du et al. (2009) reported resto-ration of corneal transparency and thickness in lumican null mice (thin corneas, haze and disruption of normal stromal organization) three months after intrastromal transplant of human CSSCs. They also confirmed that human keratan sulfate was deposited in the mouse stroma and the host collagen lamellae were reorganized, concluding that delivery of h-CSSCs to the scarred human stroma may alleviate corneal scars without requiring surgery (Du et al., 2009). Very similar findings were reported by Liu et al. who utilized h-UMSCs using the same animal model (Liu et al., 2010). Coulson-Thomas et al. found that, in a mouse model for mucopolysaccharidosis, transplanted h-UMSCs participate both in extracellular glycosaminoglycans (GAG) turnover and enable host keratocytes to catabolize accumulated GAG products (Coulson-- Thomas et al., 2013. Recently, our group published the first clinical trial in which the preliminary safety and efficacy of the cellular therapy of the human corneal stroma is reported (Alio Del Barrio et al., 2017; Alio et al., 2019): we implanted a suspension containing quiescent autolo-gous ADASCs (obtained by elective liposuction) in a mid-stroma femtosecond laser-assisted lamellar pocket in patients with advanced (stage IV) keratoconus with poor visual function and already candidates for corneal transplantation. None of the cases had previous corneal surgeries or visually significant corneal scars. We could confirm, in humans, all previous evidence reported in the animal model (ADASCs survival in vivo, perfect biointegration without tissular or clinical inflammatory response, neocollagen production), together with a mod-erate efficacy in terms of visual improvement (Alio Del Barrio et al., 2017; Alio et al., 2019).

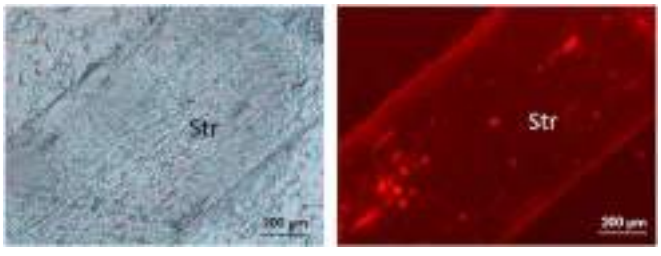

Figure 2. Human ADASCs transplantation into the rabbit's corneal stroma in vivo.
A) Phase-contrast photograph showing a morphologically intact corneal stroma 3 months after isolated h-ADASCs transplantation; B) Same section showing the survival of the implanted h-ADASCs by detecting the Vybrant CM-DiL dye; (Str: stroma; Magnification, 200x).

According to the clinical and pre-clinical available evidence, the direct intrastromal implantation of MSCs within the cornea achieves the production of new ECM, but is not expected to be quantitatively enough in order to be able to restore the thickness of a severely diseased human cornea (like in extreme keratoconic eyes). However, the direct injection of stem cells may provide a promising treatment modality for corneal dystrophies, corneal stroma progressive opacification in the context of systemic metabolic disorders, and for the modulation of corneal scars.

3.3.3. Anterior chamber injection of stem cells

Demirayak et al. reported that BM-MSCs and ADASCs, suspended in phosphate-buffered solution (PBS) and injected into the anterior chamber after a penetrating corneal injury in a mouse model, are able to colonize the corneal stroma and increase the expression of keratocyte specific markers such as keratocan, with a demonstrated increase in keratocyte density by confocal microscopy (Demirayak et al., 2016). Conversely, the possible side effects of this MSCs injection into the anterior chamber for the lens epithelium and trabecullum is highly questionable as it may induce scarring and a subsequent glaucoma. Considering this, the potential clinical use of this approach, in our opinion, is limited.

3.3.4. Intravenous injection of stem cells

Systemic use, by intravenous injection, of MSCs has also been tested. Intravenous injection of BM-MSCs in mice after an allograft corneal transplant was be able to colonize the transplanted cornea and con-junctiva (inflamed ocular tissues) but not the contralateral ungrafted cornea, simultaneously decreasing immunity and significantly improving allograft survival rate (Omoto et al., 2014). Yun et al. recently reported similar findings with the intravenous injection of iPSC-derived MSCs and BM-MSCs after a surface chemical injury, where they observed that the corneal opacity, inflammatory infiltration and inflammatory markers in the cornea were markedly decreased in the treated mice, without significant differences between both MSCs types (Yun et al., 2017). In contrast, our group did not observe any benefit in corneal allograft survival and rejection rates after systemic injection of rabbit ADASCs prior to surgery, during surgery, and at various times after surgery in rabbits with vascularized corneas (model more similar to human corneal transplants than those reported in mice). Moreover, a shorter graft survival compared with the non-treated corneal grafts was noted (Fuentes-Julian et al., 2015).

3.3.5. MSCs exosomes

Exosomes are nano-sized extracellular vesicles that originate from the fusion of intracellular multivesicular bodies with cell membranes and are released into extracellular spaces (Zhang et al., 2015). They have been implicated in the ability of MSCs to repair damaged tissue. Funderburgh et al. recently showed that exosomes isolated from the culture media of human CSSCs had similar immunosuppressive properties and also significantly reduced stromal scarring in wounded cor-neas in vivo (Shojaati et al., 2019). He suggested that the mechanism of action of these CSSCs exosomes is through the transference of microRNA to the host cells. This finding suggests that for some diseases, such as the prevention or reduction of corneal scars, MSCs exosomes may provide a non-cell based therapy (Funderburgh, 2017). Zhang et al. suggested that exosomes released by transplanted UMSCs in the diseased cornea are able to enter into host corneal keratocytes and endothelial cells and enhance their functions (Zhang et al., 2015). In their in vitro experiment using mucopolysaccharidosis VII mice, they discovered that UMSC-secreted exosomes assisted in the recycling process of accumulated glycosaminoglycans (GAGS) in the lysosomes of diseased cells (Coulson-Thomas et al., 2013). These findings open an exciting new field for research as the use of exosomes *per se* could overcome some of the limitations and risks associated to intrastromal cellular injection, given that exosomes can be potentially applied topically (Ziaei et al., 2017).

4. CONCLUSIONS & FUTURE PERSPECTIVES

In conclusion, to achieve a proper stroma construct, mimicking the natural one, so it maintains the corneal stroma homeostasis, both a cell source and a collagen scaffold must be developed in conjunction. Regarding the cell component, several cell types, both from ocular and extraocular sources have been studied, being so far the use of h-ADASCs the most clinically promising one. However, in the long term, probably the development of cheaper and standardized iPSC techniques will surpass MSCs use as well (Chakrabarty et al., 2018). Concerning collagen scaffolds, the use of decellularized cornea sections is clinically the most relevant one so far, but it still has the handicap of needing a donor cornea. In the next few years, advances in novel 3D printing techniques at single cell resolution such as LIFT (PreciseBio https://www.precis e-bio.com), laser-assisted bioprinting (Sorkio et al., 2018), two-photon polymerization-based lithography (Dobos et al., 2019), fused filament fabrication (Llewellyn-Jones et al., 2016), and other methods of achieving lamellar parallel bundles of collagen, such as molecular crowding (Ruberti and Zieske, 2008) will rapidly impulse the development of a biomimetic corneal stroma.

Declaration of competing interest

The authors, their families, their employers and their business as-sociates have no financial or proprietary interest in any product or company associated with any device, instrument or drug mentioned in this article. The authors have not received any payment as consultants, reviewers or evaluators for any of the devices, instruments or drugs mentioned in this article. The study has been carried out in the frame-

work of the Red Tematica´ de Investigacion´ Cooperativa en Salud (RETICS), reference number RD12/0034/0007 and RD16/0008/0012.

REFERENCES

Agorogiannis, G.I., Alexaki, V.I., Castana, O., Kymionis, G.D., 2012. Topical application of autologous adipose-derived mesenchymal stem cells (MSCs) for persistent sterile corneal epithelial defect. Graefes Arch. Clin. Exp. Ophthalmol. 250 (3), 455–457. https://doi.org/10.1007/s00417-011-1841-3.

Alio,´ J., Montesel, A., El Sayyad, F., Barraquer, R., Arnalich-Montiel, F., Alio´ del Barrio, J., 2020. Corneal graft failure: an update. Br. J. Ophthalmol. [Epub ahead of print].

Alio Del Barrio, J.L., Alio, J.L., 2018. Cellular therapy of the corneal stroma: a new type of corneal surgery for keratoconus and corneal dystrophies. Eye Vis (Lond) 5, 28. https://doi.org/10.1186/s40662-018-0122-1.

Alio del Barrio, J.L., Chiesa, M., Gallego Ferrer, G., Garagorri, N., Briz, N., Fernandez-Delgado, J., Sancho-Tello Valls, M., Botella, C.C., Garcia-Tunon, I., Bataille, L., Rodriguez, A., Arnalich-Montiel, F., Gomez Ribelles, J.L., Antolinos-Turpin, C.M., Gomez-Tejedor, J.A., Alio, J.L., De Miguel, M.P., 2015a. Biointegration of corneal macroporous membranes based on poly(ethyl acrylate) copolymers in an experimental animal model. J. Biomed. Mater. Res. 103 (3), 1106–1118. https://doi.org/10.1002/jbm.a.35249.

Alio del Barrio, J.L., Chiesa, M., Garagorri, N., Garcia-Urquia, N., Fernandez-Delgado, J., Bataille, L., Rodriguez, A., Arnalich-Montiel, F., Zarnowski, T., Alvarez de Toledo, J. P., Alio, J.L., De Miguel, M.P., 2015b. Acellular human corneal matrix sheets seeded with human adipose-derived mesenchymal stem cells integrate functionally in an experimental animal model. Exp. Eye Res. 132, 91–100. https://doi.org/10.1016/j. exer.2015.01.020.

Alio Del Barrio, J.L., El Zarif, M., Azaar, A., Makdissy, N., Khalil, C., Harb, W., El Achkar, I., Jawad, Z.A., de Miguel, M.P., Alio, J.L., 2018. Corneal stroma enhancement with decellularized stromal laminas with or without stem cell recellularization for advanced keratoconus. Am. J. Ophthalmol. 186, 47–58. https://doi.org/10.1016/j.ajo.2017.10.026.

Alio Del Barrio, J.L., El Zarif, M., de Miguel, M.P., Azaar, A., Makdissy, N., Harb, W., El Achkar, I., Arnalich-Montiel, F., Alio, J.L., 2017. Cellular therapy with human autologous adipose-derived adult stem cells for advanced keratoconus. Cornea 36 (8), 952–960. https://doi.org/10.1097/ICO.0000000000001228.

Alio, J.L., Alio Del Barrio, J.L., El Zarif, M., Azaar, A., Makdissy, N., Khalil, C., Harb, W., El Achkar, I., Jawad, Z.A., De Miguel, M.P., 2019. Regenerative surgery of the corneal stroma for advanced keratoconus: 1-year outcomes. Am. J. Ophthalmol. 203, 53–68. https://doi.org/10.1016/j.ajo.2019.02.009.

Arnalich-Montiel, F., Pastor, S., Blazquez-Martinez, A., Fernandez-Delgado, J., Nistal, M., Alio, J.L., De Miguel, M.P., 2008. Adipose-derived stem cells are a source for cell therapy of the corneal stroma. Stem Cell. 26 (2), 570–579. https://doi.org/10.1634/ stemcells.2007-0653.

Aslan, B., Guler, S., Tevlek, A., Aydin, H.M., 2018. Evaluation of collagen foam, poly(l-lactic acid) nanofiber mesh, and decellularized matrices for corneal regeneration. J. Biomed. Mater. Res. B Appl. Biomater. 106 (6), 2157–2168. https://doi.org/ 10.1002/jbm.b.34022.

Bakhshandeh, H., Soleimani, M., Hosseini, S.S., Hashemi, H., Shabani, I., Shafiee, A., Nejad, A.H., Erfan, M., Dinarvand, R., Atyabi, F., 2011. Poly (epsilon-caprolactone) nanofibrous ring surrounding a polyvinyl alcohol hydrogel for the development of a biocompatible two-part artificial cornea. Int. J. Nanomed. 6, 1509–1515. https://doi.org/10.2147/IJN.S19011.

Basu, S., Hertsenberg, A.J., Funderburgh, M.L., Burrow, M.K., Mann, M.M., Du, Y., Lathrop, K.L., Syed-Picard, F.N., Adams, S.M., Birk, D.E., Funderburgh, J.L., 2014. Human limbal biopsy-derived stromal stem cells prevent corneal scarring. Sci. Transl. Med. 6 (266), 266.

Bernards, D.A., Bhisitkul, R.B., Wynn, P., Steedman, M.R., Lee, O.T., Wong, F., Thoongsuwan, S., Desai, T.A., 2013. Ocular biocompatibility and structural integrity of micro- and nanostructured poly(caprolactone) films. J. Ocul. Pharmacol. Therapeut. 29 (2), 249–257. https://doi.org/10.1089/jop.2012.0152.

Bray, L.J., George, K.A., Hutmacher, D.W., Chirila, T.V., Harkin, D.G., 2012. A dual-layer silk fibroin scaffold for reconstructing the human corneal limbus. Biomaterials 33 (13), 3529–3538. https://doi.org/10.1016/j.biomaterials.2012.01.045.

Brunette, I., Roberts, C.J., Vidal, F., Harissi-Dagher, M., Lachaine, J., Sheardown, H., Durr, G.M., Proulx, S., Griffith, M., 2017. Alternatives to eye bank native tissue for corneal stromal replacement. Prog. Retin. Eye Res. J 59, 97–130. https://doi.org/10.1016/j.preteyeres.2017.04.002.

Buznyk, O., Pasyechnikova, N., Islam, M.M., Iakymenko, S., Fagerholm, P., Griffith, M., 2015. Bioengineered corneas grafted as alternatives to human donor corneas in three high-risk patients. Clin Transl Sci 8 (5), 558–562. https://doi.org/10.1111/ cts.12293.

Calderon-Colon, X., Xia, Z., Breidenich, J.L., Mulreany, D.G., Guo, Q., Uy, O.M., Tiffany, J.E., Freund, D.E., McCally, R.L., Schein, O.D., Elisseeff, J.H., Trexler, M.M., 2012. Structure and properties of collagen vitrigel membranes for ocular repair and regeneration applications. Biomaterials 33 (33), 8286–8295. https://doi.org/10.1016/j.biomaterials.2012.07.062.

Caplan, A.I., 2017. Mesenchymal stem cells: time to change the name! Stem Cells Transl Med 6 (6), 1445–1451. https://doi.org/10.1002/sctm.17-0051.

Cejka, C., Cejkova, J., Trosan, P., Zajicova, A., Sykova, E., Holan, V., 2016. Transfer of mesenchymal stem cells and cyclosporine A on alkali-injured rabbit cornea using nanofiber scaffolds strongly reduces corneal neovascularization and scar formation. Histol. Histopathol. 31 (9), 969–980. https://doi.org/10.14670/HH-11-724.

Chae, J.J., Ambrose, W.M., Espinoza, F.A., Mulreany, D.G., Ng, S., Takezawa, T., Trexler, M.M., Schein, O.D., Chuck, R.S., Elisseeff, J.H., 2015. Regeneration of corneal epithelium utilizing a collagen vitrigel membrane in rabbit models for corneal stromal wound and limbal stem cell deficiency. Acta Ophthalmol. 93 (1), e57–66. https://doi.org/10.1111/aos.12503.

Chakrabarty, K., Shetty, R., Ghosh, A., 2018. Corneal cell therapy: with iPSCs, it is no more a far-sight. Stem Cell Res. Ther. 9 (1), 287. https://doi.org/10.1186/s13287-018-1036-5.

Chen, S., Mienaltowski, M.J., Birk, D.E., 2015. Regulation of corneal stroma extracellular matrix assembly. Exp. Eye Res. 133, 69–80. https://doi.org/10.1016/j. exer.2014.08.001.

Chen, Z., You, J., Liu, X., Cooper, S., Hodge, C., Sutton, G., Crook, J.M., Wallace, G.G., 2018. Biomaterials for corneal bioengineering. Biomed. Mater. 13 (3), 032002 https://doi.org/10.1088/1748-605X/aa92d2.

Coulson-Thomas, V.J., Caterson, B., Kao, W.W., 2013. Transplantation of human umbilical mesenchymal stem cells cures the corneal defects of

mucopolysaccharidosis VII mice. Stem Cell. 31 (10), 2116–2126. https://doi.org/10.1002/stem.1481.

De Miguel, M.P., Fuentes-Julian, S., Blazquez-Martinez, A., Pascual, C.Y., Aller, M.A., Arias, J., Arnalich-Montiel, F., 2012. Immunosuppressive properties of mesenchymal stem cells: advances and applications. Curr. Mol. Med. 12 (5), 574–591. https://doi.org/10.2174/156652412800619950.

De Miguel, M.P., Casaroli-Marano, R.P., Nieto-Nicolau, N., et al., 2015. Frontiers in regenerative medicine for cornea and ocular surface. In: Rahman, A., Anjum, S. (Eds.), Frontiers in Stem Cell and Regenerative Medicine Research, first ed., vol. 1. Bentham e-Books, PA, pp. 92–138.

Demirayak, B., Yuksel, N., Celik, O.S., Subasi, C., Duruksu, G., Unal, Z.S., Yildiz, D.K., Karaoz, E., 2016. Effect of bone marrow and adipose tissue-derived mesenchymal stem cells on the natural course of corneal scarring after penetrating injury. Exp. Eye Res. 151, 227–235. https://doi.org/10.1016/j.exer.2016.08.011.

Di, G., Du, X., Qi, X., Zhao, X., Duan, H., Li, S., Xie, L., Zhou, Q., 2017a. Mesenchymal stem cells promote diabetic corneal epithelial wound healing through TSG-6-dependent stem cell activation and macrophage switch. Invest. Ophthalmol. Vis. Sci. 58 (10), 4344–4354. https://doi.org/10.1167/iovs.17-21506.

Di, G., Qi, X., Zhao, X., Zhang, S., Danielson, P., Zhou, Q., 2017b. Corneal epithelium-derived neurotrophic factors promote nerve regeneration. Invest. Ophthalmol. Vis. Sci. 58 (11), 4695–4702. https://doi.org/10.1167/iovs.16-21372.

Dobos, A., Van Hoorick, J., Steiger, W., Gruber, P., Markovic, M., Andriotis, O.G., Rohatschek, A., Dubruel, P., Thurner, P.J., Van Vlierberghe, S., Baudis, S., Ovsianikov, A., 2019. Thiol-gelatin-norbornene bioink for laser-based high-definition bioprinting. Adv Healthc Mater, e1900752. https://doi.org/10.1002/ adhm.201900752.

Dos Santos, A., Balayan, A., Funderburgh, M.L., Ngo, J., Funderburgh, J.L., Deng, S.X., 2019. Differentiation capacity of human mesenchymal stem cells into keratocyte lineage. Invest. Ophthalmol. Vis. Sci. 60 (8), 3013–3023. https://doi.org/10.1167/ iovs.19-27008.

Du, Y., Carlson, E.C., Funderburgh, M.L., Birk, D.E., Pearlman, E., Guo, N., Kao, W.W., Funderburgh, J.L., 2009. Stem cell therapy restores transparency to defective murine corneas. Stem Cell. 27 (7), 1635–1642. https://doi.org/10.1002/stem.91.

Du, Y., Funderburgh, M.L., Mann, M.M., SundarRaj, N., Funderburgh, J.L., 2005. Multipotent stem cells in human corneal stroma. Stem Cell. 23 (9), 1266–1275. https://doi.org/10.1634/stemcells.2004-0256.

Duarte Campos, D.F., Rohde, M., Ross, M., Anvari, P., Blaeser, A., Vogt, M., Panfil, C., Yam, G.H., Mehta, J.S., Fischer, H., Walter, P., Fuest, M., 2019 Sep. Corneal bioprinting utilizing collagen-based bioinks and primary human keratocytes. J. Biomed. Mater. Res. 107 (9), 1945–1953. https://doi.org/10.1002/jbm.a.36702. El Zarif, M., Alio, J.L., Alio Del Barrio, J.L., Jawad, K.A., Palazon-Bru, A., Jawad, Z.A., De Miguel, M.P., Makdissy, N., 2020. Corneal stromal regeneration therapy for advanced keratoconus: long term outcomes at 3 years. Cornea [Epub ahead of print].

Espandar, L., Bunnell, B., Wang, G.Y., Gregory, P., McBride, C., Moshirfar, M., 2012. Adipose-derived stem cells on hyaluronic acid-derived scaffold: a new horizon in bioengineered cornea. Arch. Ophthalmol. 130 (2), 202–208. https://doi.org/10.1001/archopthalmol.2011.1398.

Fagerholm, P., Lagali, N.S., Merrett, K., Jackson, W.B., Munger, R., Liu, Y., Polarek, J.W., Soderqvist, M., Griffith, M., 2010. A biosynthetic alternative to human donor tissue for inducing corneal regeneration: 24-month follow-up of a phase 1 clinical study. Sci. Transl. Med. 2 (46), 46ra61. https://doi.org/10.1126/scitranslmed.3001022.

Fagerholm, P., Lagali, N.S., Ong, J.A., Merrett, K., Jackson, W.B., Polarek, J.W., Suuronen, E.J., Liu, Y., Brunette, I., Griffith, M., 2014. Stable corneal regeneration four years after implantation of a cell-free recombinant human collagen scaffold. Biomaterials 35 (8), 2420–2427. https://doi.org/10.1016/j. biomaterials.2013.11.079.

Fuentes-Julian, S., Arnalich-Montiel, F., Jaumandreu, L., Leal, M., Casado, A., Garcia-Tunon, I., Hernandez-Jimenez, E., Lopez-Collazo, E., De Miguel, M.P., 2015. Adipose-derived mesenchymal stem cell administration does not improve corneal graft survival outcome. PLoS One 10 (3), e0117945. https://doi.org/10.1371/ journal.pone.0117945.

Funderburgh, J.L., 2017. Assessing the Potential of Stem Cells to Regenerate Stromal Tissue. Oral Presentation at the Association for Research in Vision and Ophthalmology (ARVO) Annual Meeting. Baltimore (USA).

Gain, P., Jullienne, R., He, Z., Aldossary, M., Acquart, S., Cognasse, F., Thuret, G., 2016. Global survey of corneal transplantation and eye banking. JAMA Ophthalmol 134 (2), 167–173. https://doi.org/10.1001/jamaophthalmol.2015.4776.

Ghezzi, C.E., Marelli, B., Omenetto, F.G., Funderburgh, J.L., Kaplan, D.L., 2017. 3D functional corneal stromal tissue equivalent based on corneal stromal stem cells and multi-layered silk film architecture. PLoS One 12 (1), e0169504. https://doi.org/10.1371/journal.pone.0169504.

Goodarzi, H., Jadidi, K., Pourmotabed, S., Sharifi, E., Aghamollaei, H., 2019. Preparation and in vitro characterization of cross-linked collagen-gelatin hydrogel using EDC/ NHS for corneal tissue engineering applications. Int. J. Biol. Macromol. 126, 620–632. https://doi.org/10.1016/j.ijbiomac.2018.12.125.

Guan, L., Tian, P., Ge, H., Tang, X., Zhang, H., Du, L., Liu, P., 2013. Chitosan-functionalized silk fibroin 3D scaffold for keratocyte culture. J. Mol. Histol. 44 (5), 609–618. https://doi.org/10.1007/s10735-013-9508-5.

Harkin, D.G., Foyn, L., Bray, L.J., Sutherland, A.J., Li, F.J., Cronin, B.G., 2015. Concise reviews: can mesenchymal stromal cells differentiate into corneal cells? A systematic review of published data. Stem Cell. 33 (3), 785–791. https://doi.org/10.1002/ stem.1895.

Hendijani, F., 2017. Explant culture: an advantageous method for isolation of mesenchymal stem cells from human tissues. Cell Prolif 50 (2). https://doi.org/ 10.1111/cpr.12334.

Holan, V., Trosan, P., Cejka, C., Javorkova, E., Zajicova, A., Hermankova, B., Chudickova, M., Cejkova, J., 2015. A comparative study of the therapeutic potential of mesenchymal stem cells and limbal epithelial stem cells for ocular surface reconstruction. Stem Cells Transl Med 4 (9), 1052–1063. https://doi.org/10.5966/ sctm.2015-0039.

Hu, X., Lui, W., C Lei, C., Min Wang, M., Cao, Y., 2005. Tissue engineering of nearly transparent corneal stroma. Tissue Eng. 11 (11–12), 1710–1717. https://doi.org/10.1089/ten.2005.11.1710.

Irimia, T., Dinu-Pirvu, C.E., Ghica, M.V., Lupuleasa, D., Muntean, D.L., Udeanu, D.I., Popa, L., 2018. Chitosan-based in situ gels for ocular delivery of therapeutics: a state-of-the-art review. Mar. Drugs 16 (10). https://doi.org/10.3390/md16100373.

Isaacson, A., Swioklo, S., Connon, C.J., 2018. 3D bioprinting of a corneal stroma equivalent. Exp. Eye Res. 173, 188–193. https://doi.org/10.1016/j.exer.2018.05.010.

Islam, M.M., Ravichandran, R., Olsen, D., ljunggren, M.K., Fagerholm, P., Lee, c.J., Griffith, M., Phopase, J., 2016. Self-assembled collagen-like-peptide implants as alternatives to human donor cornea transplantation. RSC Adv. 6, 55745–55749. https://doi.org/10.1039/C6RA08895C.

Jiang, Z., Liu, G., Meng, F., Wang, W., Hao, P., Xiang, Y., Wang, Y., Han, R., Li, F., Wang, L., Li, X., 2017. Paracrine effects of mesenchymal stem cells on the activation of keratocytes. Br. J. Ophthalmol. 101 (11), 1583–1590. https://doi.org/10.1136/bjophthalmol-2016-310012.

Joseph, R., Srivastava, O.P., Pfister, R.R., 2016. Modeling keratoconus using induced pluripotent stem cells. Invest. Ophthalmol. Vis. Sci. 57 (8), 3685–3697. https://doi.org/10.1167/iovs.16-19105.

Kao, W.W., Coulson-Thomas, V.J., 2016. Cell therapy of corneal diseases. Cornea 35 (Suppl. 1), S9–S19. https://doi.org/10.1097/ICO.0000000000001010.

Kilic Bektas, C., Hasirci, V., 2018. Mimicking corneal stroma using keratocyte-loaded photopolymerizable methacrylated gelatin hydrogels. J Tissue Eng Regen Med 12 (4), e1899–e1910. https://doi.org/10.1002/term.2621.

Kong, B., Sun, W., Chen, G., Tang, S., Li, M., Shao, Z., Mi, S., 2017. Tissue-engineered cornea constructed with compressed collagen and laser-perforated electrospun mat. Sci. Rep. 7 (1), 970. https://doi.org/10.1038/s41598-017-01072-0.

Lagali, N., 2020. Corneal stromal regeneration: current status and future therapeutic potential. Curr. Eye Res. 45 (3), 278–290. https://doi.org/10.1080/02713683.2019.1663874.

Lai, J.Y., Li, Y.T., Cho, C.H., Yu, T.C., 2012. Nanoscale modification of porous gelatin scaffolds with chondroitin sulfate for corneal stromal tissue engineering. Int. J. Nanomed. 7, 1101–1114. https://doi.org/10.2147/IJN.S28753.

Levis, H.J., Massie, I., Dziasko, M.A., Kaasi, A., Daniels, J.T., 2013. Rapid tissue engineering of biomimetic human corneal limbal crypts with 3D niche architecture. Biomaterials 34 (35), 8860–8868. https://doi.org/10.1016/j. biomaterials.2013.08.002.

Li, W., Long, Y., Liu, Y., Long, K., Liu, S., Wang, Z., Wang, Y., Ren, L., 2014. Fabrication and characterization of chitosan-collagen crosslinked membranes for corneal tissue engineering. J. Biomater. Sci. Polym. Ed. 25 (17), 1962–1972. https://doi.org/10.1080/09205063.2014.965996.

Liu, H., Zhang, J., Liu, C.Y., Wang, I.J., Sieber, M., Chang, J., Jester, J.V., Kao, W.W., 2010. Cell therapy of congenital corneal diseases with umbilical mesenchymal stem cells: lumican null mice. PLoS One 5 (5), e10707. https://doi.org/10.1371/journal.pone.0010707.

Liu, Y., Gan, L., Carlsson, D.J., Fagerholm, P., Lagali, N., Watsky, M.A., Munger, R., Hodge, W.G., Priest, D., Griffith, M., 2006. A simple, cross-linked collagen tissue substitute for corneal implantation. Invest. Ophthalmol. Vis. Sci. 47 (5), 1869–1875. https://doi.org/10.1167/iovs.05-1339.

Llewellyn-Jones, T., Allen, R., Trask, R., 2016. Curved layer fused filament fabrication using automated toolpath generation. 3D Print. Addit. Manuf. 3 (4), 236–243. Lynch, A.P., Ahearne, M., 2013. Strategies for developing decellularized corneal scaffolds. Exp. Eye Res. 108, 42–47. https://doi.org/10.1016/j.exer.2012.12.012.

McTiernan, C.D., Simpson, F.C., Haagdorens, M., et al., 2020. LiQD Cornea: pro-regeneration collagen mimetics as patches and alternatives to corneal transplantation. Sci Adv 6 (25), eaba2187. https://doi.org/10.1126/sciadv.aba2187. Published 2020 Jun 17.

Massie, I., Dale, S.B., Daniels, J.T., 2015. Limbal fibroblasts maintain normal phenotype in 3D RAFT tissue equivalents suggesting potential for safe clinical use in treatment of ocular surface failure. Tissue Eng. C Methods 21 (6), 576–584. https://doi.org/10.1089/ten.TEC.2014.0458.

Matthyssen, S., Van den Bogerd, B., Dhubhghaill, S.N., Koppen, C., Zakaria, N., 2018. Corneal regeneration: a review of stromal replacements. Acta Biomater. 69, 31–41. https://doi.org/10.1016/j.actbio.2018.01.023.

Merrett, K., Fagerholm, P., McLaughlin, C.R., Dravida, S., Lagali, N., Shinozaki, N., Watsky, M.A., Munger, R., Kato, Y., Li, F., Marmo, C.J., Griffith, M., 2008. Tissue-engineered recombinant human collagen-based corneal substitutes for implantation: performance of type I versus type III collagen. Invest. Ophthalmol. Vis. Sci. 49 (9), 3887–3894. https://doi.org/10.1167/iovs.07-1348.

Mi, S., Khutoryanskiy, V.V., Jones, R.R., Zhu, X., Hamley, I.W., Connon, C.J., 2011. Photochemical cross-linking of plastically compressed collagen gel produces an optimal scaffold for corneal tissue engineering. J. Biomed. Mater. Res. 99 (1), 1–8. https://doi.org/10.1002/jbm.a.33152.

Mimura, T., Amano, S., Yokoo, S., Uchida, S., Yamagami, S., Usui, T., Kimura, Y., Tabata, Y., 2008. Tissue engineering of corneal stroma with rabbit fibroblast precursors and gelatin hydrogels. Mol. Vis. 14, 1819–1828.

Mittal, S.K., Omoto, M., Amouzegar, A., Sahu, A., Rezazadeh, A., Katikireddy, K.R., Shah, D.I., Sahu, S.K., Chauhan, S.K., 2016. Restoration of corneal transparency by mesenchymal stem cells. Stem Cell Rep. 7 (4), 583–590. https://doi.org/10.1016/j.stemcr.2016.09.001.

Mukhey, D., Phillips, J.B., Daniels, J.T., Kureshi, A.K., 2018. Controlling human corneal stromal stem cell contraction to mediate rapid cell and matrix organization of real architecture for 3-dimensional tissue equivalents. Acta Biomater. 67, 229–237. https://doi.org/10.1016/j.actbio.2017.11.047.

Naylor, R.W., McGhee, C.N., Cowan, C.A., Davidson, A.J., Holm, T.M., Sherwin, T., 2016. Derivation of corneal keratocyte-like cells from human induced pluripotent stem cells. PLoS One 11 (10), e0165464. https://doi.org/10.1371/journal.pone.0165464.

Oh, J.Y., Kim, M.K., Shin, M.S., Lee, H.J., Ko, J.H., Wee, W.R., Lee, J.H., 2008. The anti-inflammatory and anti-angiogenic role of mesenchymal stem cells in corneal wound healing following chemical injury. Stem Cell. 26 (4), 1047–1055. https://doi.org/10.1634/stemcells.2007-0737.

O'Leary, L.E., Fallas, J.A., Bakota, E.L., Kang, M.K., Hartgerink, J.D., 2011. Multi-hierarchical self-assembly of a collagen mimetic peptide from triple helix to nanofibre and hydrogel. Nat. Chem. 3 (10), 821–828. https://doi.org/10.1038/ nchem.1123.

Omoto, M., Katikireddy, K.R., Rezazadeh, A., Dohlman, T.H., Chauhan, S.K., 2014. Mesenchymal stem cells home to inflamed ocular surface and suppress allosensitization in corneal transplantation. Invest. Ophthalmol. Vis. Sci. 55 (10), 6631–6638. https://doi.org/10.1167/iovs.14-15413.

Ortega, I., Ryan, A.J., Deshpande, P., MacNeil, S., Claeyssens, F., 2013. Combined microfabrication and electrospinning to produce 3-D architectures for corneal repair. Acta Biomater. 9 (3), 5511–5520. https://doi.org/10.1016/j.actbio.2012.10.039.

Ortiz, L.A., DuTreil, M., Fattman, C., Pandey, A.C., Torres, G., Go, K., Phinney, D.G., 2007. Interleukin 1 receptor antagonist mediates the antiinflammatory and antifibrotic effect of mesenchymal stem cells during lung injury. Proc. Natl. Acad. Sci. U.S.A. 104 (26), 11002–11007. https://doi.org/10.1073/pnas.0704421104.

Paik, D.C., Trokel, S.L., Suh, L.H., 2018. Just what do we know about corneal collagen turnover? Cornea 37 (11), e49–e50. https://doi.org/10.1097/ ICO.0000000000001685.

Pinnamaneni, N., Funderburgh, J.L., 2012. Concise review: stem cells in the corneal stroma. Stem Cell. 30 (6), 1059–1063. https://doi.org/10.1002/stem.1100.

Ruberti, J.W., Zieske, J.D., 2008. Prelude to corneal tissue engineering - gaining control of collagen organization. Prog. Retin. Eye Res. 27 (5), 549–577. https://doi.org/10.1016/j.preteyeres.2008.08.001.

Shafiq, M.A., Gemeinhart, R.A., Yue, B.Y., Djalilian, A.R., 2012. Decellularized human cornea for reconstructing the corneal epithelium and anterior stroma. Tissue Eng. C Methods 18 (5), 340–348. https://doi.org/10.1089/ten.TEC.2011.0072.

Shojaati, G., Khandaker, I., Sylakowski, K., Funderburgh, M.L., Du, Y., Funderburgh, J.L., 2018. Compressed collagen enhances stem cell therapy for corneal scarring. Stem Cells Transl Med 7 (6), 487–494. https://doi.org/10.1002/sctm.17-0258.

Shojaati, G., Khandaker, I., Funderburgh, M.L., Mann, M.M., Basu, R., Stolz, D.B., Geary, M.L., Dos Santos, A., Deng, S.X., Funderburgh, J.L., 2019. Mesenchymal stem cells reduce corneal fibrosis and inflammation via extracellular vesicle-mediated delivery of miRNA. Stem Cells Transl Med 8 (11), 1192–1201. https://doi.org/ 10.1002/sctm.18-0297.

Sorkio, A., Koch, L., Koivusalo, L., Deiwick, A., Miettinen, S., Chichkov, B., Skottman, H., 2018. Human stem cell based corneal tissue mimicking structures using laser-assisted 3D bioprinting and functional bioinks. Biomaterials 171, 57–71. https://doi.org/10.1016/j.biomaterials.2018.04.034.

Swioklo, S., Constantinescu, A., Connon, C.J., 2016. Alginate-encapsulation for the improved hypothermic preservation of human adipose-derived stem cells. Stem Cells Transl Med 5 (3), 339–349. https://doi.org/10.5966/sctm.2015-0131.

Takahashi, K., Yamanaka, S., 2006. Induction of pluripotent stem cells from mouse embryonic and adult fibroblast cultures by defined factors. Cell 126 (4), 663–676. https://doi.org/10.1016/j.cell.2006.07.024.

Tan, X.W., Hartman, L., Tan, K.P., Poh, R., Myung, D., Zheng, L.L., Waters, D., Noolandi, J., Beuerman, R.W., Frank, C.W., C Ta, C.N., Tan, D.T.H., Mehta, J.S., 2013. In vivo biocompatibility of two PEG/PAA interpenetrating polymer networks as corneal inlays following deep stromal pocket implantation. J. Mater. Sci. Mater. Med. 24 (4), 967–977. https://doi.org/10.1007/s10856-012-4848-3.

Tanaka, K., Mori, K., Mizuno, S., 1993. Immunological identification of the major disulfide-linked light component of silk fibroin. J. Biochem. 114 (1), 1–4. https://doi.org/10.1093/oxfordjournals.jbchem.a124122.

Togel,¨ F., Hu, Z., Weiss, K., Isaac, J., Lange, C., Westenfelder, C., 2005. Administered mesenchymal stem cells protect against ischemic acute renal failure through differentiation-independent mechanisms. Am. J. Physiol. Renal. Physiol. 2005 289, F31–F42. https://doi.org/10.1152/ajprenal.00007.2005.

Tonsomboon, K., Strange, D.G., Oyen, M.L., 2013. Gelatin nanofiber-reinforced alginate gel scaffolds for corneal tissue engineering. Conf. Proc. IEEE Eng. Med. Biol. Soc. 2013 6671–6674. https://doi.org/10.1109/EMBC.2013.6611086.

Vazquez, N., Chacon, M., Meana, A., Menendez-Menendez, Y., Ferrero-Gutierrez, A., Cereijo-Martin, D., Naveiras, M., Merayo-Lloves, J., 2015. Keratin-chitosan membranes as scaffold for tissue engineering of human cornea. Histol. Histopathol. 30 (7), 813–821.

Wang, L., Ma, R., Du, G., Guo, H., Huang, Y., 2015. Biocompatibility of helicoidal multilamellar arginine-glycine-aspartic acid-functionalized silk biomaterials in a rabbit corneal model. J. Biomed. Mater. Res. B Appl. Biomater. 103 (1), 204–211. https://doi.org/10.1002/jbm.b.33192.

Wang, T.J., Wang, I.J., Hu, F.R., Young, T.H., 2016. Applications of biomaterials in corneal endothelial tissue engineering. Cornea 35 (Suppl. 1), S25–S30. https://doi.org/10.1097/ICO.0000000000000992.

Williams, K.A., Lowe, M., Bartlett, C., Kelly, T.L., Coster, D.J., All, C., 2008. Risk factors for human corneal graft failure within the Australian corneal graft registry. Transplantation 86 (12), 1720–1724. https://doi.org/10.1097/ TP.0b013e3181903b0a.

Wolkow, N., Habib, L.A., Yoon, M.K., Freitag, S.K., 2019. Corneal neurotization: review of a new surgical approach and its developments. Semin. Ophthalmol. 34 (7–8), 473–487. https://doi.org/10.1080/08820538.2019.1648692.

Xu, Y.G., Xu, Y.S., Huang, C., Feng, Y., Li, Y., Wang, W., 2008. Development of a rabbit corneal equivalent using an acellular corneal matrix of a porcine substrate. Mol. Vis. 14, 2180–2189.

Yamaguchi, H., Takezawa, T., 2018. Fabrication of a corneal model composed of corneal epithelial and endothelial cells via a collagen vitrigel membrane functioned as an acellular stroma and its application to the corneal permeability test of chemicals. Drug Metab. Dispos. 46 (11), 1684–1691. https://doi.org/10.1124/ dmd.118.080820.

Yao, L., Bai, H., 2013. Review: mesenchymal stem cells and corneal reconstruction. Mol. Vis. 19, 2237–2243.

Yoshida, J., Yokoo, S., Oshikata-Miyazaki, A., Amano, S., Takezawa, T., Yamagami, S., 2017. Transplantation of human corneal endothelial cells cultured on bio-engineered collagen vitrigel in a rabbit model of corneal endothelial dysfunction. Curr. Eye Res. 42 (11), 1420–1425. https://doi.org/10.1080/02713683.2017.1351568.

Yun, Y.I., Park, S.Y., Lee, H.J., Ko, J.H., Kim, M.K., Wee, W.R., Reger, R.L., Gregory, C.A., Choi, H., Fulcher, S.F., Prockop, D.J., Oh, J.Y., 2017. Comparison of the anti-inflammatory effects of induced pluripotent stem cell-derived and bone marrow-derived mesenchymal stromal cells in a murine model of corneal injury. Cytotherapy 19 (1), 28–35. https://doi.org/10.1016/j.jcyt.2016.10.007.

Zhang, L., Coulson-Thomas, V.J., Ferreira, T.G., Kao, W.W., 2015. Mesenchymal stem cells for treating ocular surface diseases. BMC Ophthalmol. 15 (Suppl. 1), 155. https://doi.org/10.1186/s12886-015-0138-4.

Zheng, L.L., Vanchinathan, V., Dalal, R., Noolandi, J., Waters, D.J., Hartmann, L., Cochran, J.R., Frank, C.W., Yu, C.Q., Ta, C.N., 2015. Biocompatibility of poly (ethylene glycol) and poly(acrylic acid) interpenetrating network hydrogel by intrastromal implantation in rabbit cornea. J. Biomed. Mater. Res. 103 (10), 3157–3165. https://doi.org/10.1002/jbm.a.35453.

Zhou, H., Lu, Q., Guo, Q., Chae, J., Fan, X., Elisseeff, J.H., Grant, M.P., 2014. Vitrified collagen-based conjunctival equivalent for ocular surface reconstruction. Biomaterials 35 (26), 7398–7406. https://doi.org/10.1016/j. biomaterials.2014.05.024.

Ziaei, M., Zhang, J., Patel, D.V., McGhee, C.N.J., 2017. Umbilical cord stem cells in the treatment of corneal disease. Surv. Ophthalmol. 62 (6), 803–815. https://doi.org/10.1016/j.survophthal.2017.02.002.

10.2. Alió Del Barrio, J., El Zarif, M., De Miguel, M., Azaar, A., Makdissy, N., Harb, W., El Achkar, I., Arnalich-Montiel, F., Alió, J., 2017. **Cellular therapy with human autologous adipose-derived adult stem cells for advanced keratoconus**. Cornea 36, 952–960. https://doi.org/10.1097/ICO.0000000000001228

Cellular Therapy With Human Autologous Adipose-Derived Adult Stem Cells for Advanced Keratoconus

Jorge L. Alió del Barrio, MD, PhD,*† Mona El Zarif, OD,‡ María P. de Miguel, PhD,§ Albert Azaar, MD,¶ Norman Makdissy, PhD,¶ Walid Harb, MD,¶ Ibrahim El Achkar, MD,k Francisco Arnalich, MD, PhD,**†† and Jorge L. Alió, MD, PhD, FEBOphth*†

Purpose: The aim of this phase 1 study was to preliminarily evaluate the safety and efficacy of autologous adipose-derived adult stem cell (ADASCs) implantation within the corneal stroma of patients with advanced keratoconus.

Methods: Five consecutive patients were selected. Autologous ADASCs were obtained by elective liposuction. ADASCs (3×10^6) contained in 1 mL PBS were injected into the corneal stroma through a femtosecond-assisted 9.5-mm diameter lamellar pocket under topical anesthesia. Patients were reviewed at 1 day, 1 week, 1, 3, and 6 months postoperatively. Visual function, manifest refraction, slit-lamp biomicroscopy, intraocular pressure, endothelial cell density, corneal topography, corneal optical coherence tomography, and corneal confocal biomicroscopy were recorded.

Results: No intraoperative or postoperative complications were recorded, with full corneal transparency recovery within 24 hours. Four patients completed the full follow-up. All patients improved their visual function (mean: 1 line of unaided and spectacle-corrected distance vision and 2 lines of rigid contact lens distance vision). Manifest refraction and topographic keratometry remained stable. Corneal optical coherence tomography showed a mean improvement of 16.5 µm in the central corneal thickness, and new collagen production was observed as patchy hyperreflective areas at the level of the stromal pocket. Confocal biomicroscopy confirmed the survival of the implanted stem cells at the surgical plane. Intraocular pressure and endothelial cell density remained stable.

Conclusions: Cellular therapy of the human corneal stroma in vivo with autologous ADASCs appears to be safe. Stem cells survive in vivo with intrastromal new collagen production. Future studies with larger samples are required to confirm these preliminary results.

Received for publication January 19, 2017; revision received March 8, 2017; accepted March 16, 2017.

From the *Cornea, Cataract and Refractive Surgery Unit, Vissum Corporación, Alicante, Spain; †Division of Ophthalmology, Universidad Miguel Hernández, Alicante, Spain; ‡Optica General, Saida, Lebanon; §Cell Engineering Laboratory, IdiPAZ, La Paz Hospital Research Institute, Madrid, Spain; ¶Reviva Regenerative Medicine Center, Beirut, Lebanon; kSaint-Joseph University, Beirut, Lebanon; **IRYCIS, Ophthalmology Department, Ramón y Cajal University Hospital, Madrid, Spain; and ††Cornea Unit, Hospital Vissum Madrid, Madrid, Spain.

The authors have no funding or conflicts of interest to disclose.

Reprints: Jorge L. Alió, MD, PhD, FEBOphth, Avda de Denia s/n, Vissum, Instituto Oftalmologico de Alicante, 03016 Alicante, Spain (e-mail: jlalio@vissum.com).

KeyWords: stem cells, regenerative medicine, corneal transplant, cornea, cellular therapy, keratoconus, ADASCs.

INTRODUCTION

Stroma constitutes more than 90% of the corneal thickness. Many features of the cornea, including its strength, morphology, and transparency, are attributable to the anatomy and biomechanical properties of the corneal stroma.[1] Many diseases such as corneal dystrophies, scars, or ectatic disorders induce distortion of its anatomy or physiology, leading to loss of transparency and subsequent loss of vision. Despite the great efforts in the last decade to try to replicate the corneal stroma in the laboratory to look for an alternative to classic corneal transplantation, this has not been accomplished yet because of the extreme difficulty to mimic the highly complex ultrastructure of the corneal stroma, obtaining substitutes that do not achieve enough transparency or strength properties.[2]

In this scenario, in the last few years, cellular therapy of the corneal stroma has gained much interest by the use of mesenchymal stem cells (MSCs) from either ocular or extraocular sources, capable to differentiate in to adult keratocytes in vitro and in vivo in animal models.[1] It has already been demonstrated by several authors, including reports from our research group,[3–5] the capability of these stem cells to not only survive and differentiate into adult human keratocytes in xenogeneic scenarios without inducing any inflammatory reaction but also to produce new collagen within the host stroma,[3,6] to modulate preexisting scars by corneal stroma remodeling[7,8] and to improve corneal transparency in animal models for corneal dystrophies by collagen reorganization and in animal models for metabolopathies by the catabolism of the accumulated proteins.[9–12] MSCs have also shown immunomodulatory properties in syngeneic, allogeneic, and even xenogeneic scenarios.[12,13]

Among all MSCs, human adipose-derived adult stem cells (ADASCs) have been demonstrated to be an ideal source of autologous stem cells because they satisfy all the requirements: easy accessibility to the tissue, high cell retrieval efficiency, and the ability of these stem cells (ADASCs) to differentiate in to multiple cell types (keratocytes, osteoblasts, chondroblasts, myoblasts, hepatocytes, neurons, etc).[1]

To the best of our knowledge, no in vivo corneal stroma cellular therapy studies have been published yet in humans. The aim of this phase 1 pilot study was to preliminarily evaluate the safety and tolerance of autologous ADASCs implantation

within the corneal stroma of patients with advanced keratoconus, as well as to analyze the potential benefits of this corneal cellular therapy in such cases.

MATERIALS AND METHODS

Study Approval, Design, and Subjects

This is a prospective consecutive series of cases investigation based on the cooperation between the Research, Development, and Innovation Department of Vissum Instituto Oftalmologico de Alicante (Spain), Optica General (Saida, Lebanon), Laser Vision Center (Beirut, Lebanon), and REVIVA Research and Application Center (Middle East Hospital, Beirut, Lebanon). The Institutional Review Board Ethical committee of the Reviva Research and Application Center (Lebanese University, Beirut, Lebanon) prospectively approved this study. The study was conducted in strict adherence to the tenets of the Declaration of Helsinki, and it was registered in ClinicalTrials.gov (Identifier: NCT02932852). All patients provided written informed consent for all procedures described in this study.

All 5 consecutive patients who were included in the prospective study met the following inclusion criteria: advanced keratoconus defined as stage $\geq$ IV according to the RETICS keratoconus classification[14]; age $\geq$18 years; negative human immunodeficiency virus, hepatitis B, hepatitis C serology; and no history of malignancy.

Exclusion criteria were corrected distance visual acuity (CDVA), 0.1 in the contralateral eye; active concomitant inflammatory eye disease; other ophthalmic comorbidity such as cataract, retinal diseases, or glaucoma; previous ocular surgical interventions other than cataract; previous corneal hydrops or central corneal scars; history of cognitive impair-ments or dementia, which may affect the patient's ability to participate in the informed consent process and to appropriately complete evaluations; any immunodeficiency or immunosuppressive therapy; serologic evidence of infection with hepatitis B, hepatitis C, or HIV; and pregnancy or breast feeding. Keratoconus progressive status was not considered as an exclusion or inclusion criterion.

Isolation, Characterization, and Culture of Autologous ADASCs

Patients were subjected to standard liposuction after informed consent was obtained. All procedures were performed in good medical practice conditions. Approximately 250 mL of fat mixed with local anesthetic was obtained from each patient. Adipose tissue was processed according to methods described in previous articles.[15,16] Briefly, adipose tissue was washed in phosphate-buffered saline and digested in collagenase I for 409 at 37°C in agitation. Then, collagenase was inhibited adding autologous human serum (extracted from each patient). Erythrocytes were lysed in erythrocyte lysis buffer (Gibco-Life Technologies), and then the pelleted cells were cultured in DMEM with Glutamax and Na-Pyr (Gibco), 10% autologous human serum, 1% P/S (Penicillin-Streptomycin, Gibco) + 0.2% amphotericin B (Gibco). Cell characterization was performed by $CD34^{+}CD45^{2}CD105^{+}$ labeling and flow cytometry analy-sis as requested by the International Federation of Adipose Therapeutics (IFATS).[17] Sixty to 80 hours before transplantation, quiescence was induced by lowering the amount of serum to 0.5% (Fig. 1A) to transplant the ADASCs in a physiological status more close to the natural nonproliferative stromal keratocytes, as proliferative stem cells within the corneal stroma could potentially induce stromal scarring or haze. Quiescence and the absence of apoptosis and aneuploidy were verified by propidium iodide labeling (Invitrogen), and cell cycle analysis by flow cytometry as we have described in previous articles from our group.[3,5] Just before injection, cells were harvested by trypsinization (Sigma), and 3 x 10^{6} cells were prepared per patient in saline (Fig. 1B). This high cellular concentration was established according to evidence observed in our previous experimental studies and considering the expected high cellular loss after transplantation due to solution leakage outside the cornea.[3–5]

Surgical Intervention: Autologous ADASCs Implantation

Topical anesthesia with sedation was used for all surgeries. The 60-kHz IntraLase iFS femtosecond laser (AMO Inc, Irvine, CA) was used in the single-pass mode for recipient corneal lamellar dissection by creating an intrastromal lamellar cut of 9.5 mm in diameter at half depth of the preoperative thinnest pachymetry point measured by Visante anterior segment optical coherence tomography (OCT) (Carl Zeiss, Germany). The femtosecond laser–assisted corneal dis-section ended with a 30-degree anterior side cut as a corneal incision. The femtosecond laser parameter settings, similar to the ones used for laser in situ keratomileusis (LASIK), are summarized

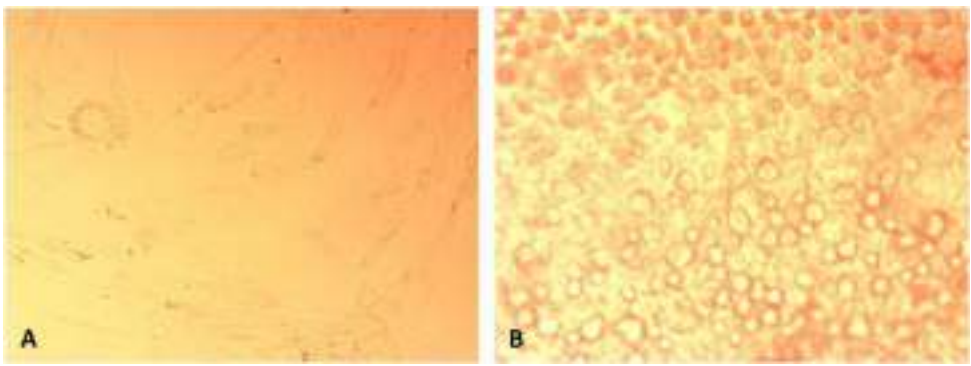

FIGURE 1. Microscopic appearance (phase-contrast photographs) of cells at 80% of confluence Before trypsinization attached to the culture flask (A; x10 magnification). Cells were then trypsinized, counted, and assessed for cell viability, and immunophenotyped before their transplantation (B; x 10 magnification).

TABLE 1. Laser Specifications for the Preparation of the Recipient Cornea

Parameter	Value	Parameter	Value
Lamellar Cut		**Anterior Side Cut**	
Diameter, mm	9.5	Diameter, mm	9.5
Depth, mm	Thinnest/2	Posterior depth, mm	Thinnest/2 + 10
Energy, mJ	1.50	Energy, mJ	1.7
Tang spot Sep, mm	5	Cut position, °	90
Rad spot Sep, mm	5	Cut angle, °	30
		Spot Sep, mm	3
		Layer Sep, mm	3

Rad, radial; Sep, separation; Tang, tangential.

in (Table 1). The corneal intrastromal pocket was then opened by blunt dissection using the Morlet lamellar dissector (Duckworth & Kent, England), and subsequently, 3 million autologous ADASCs contained in 1 ml of PBS were injected into the pocket through a 25-G cannula. Before the cellular injection, a 1-mm corneal paracentesis was performed to reduce the intraocular pressure (IOP) and allow a higher volume to be injected into the stromal pocket. Topical antibiotics and steroids (Tobradex, Alcon) were applied at the end of surgery. No patient received corneal sutures.

Postoperative Care and Follow-up Schedule

Topical antibiotics and steroids (Tobradex, Alcon) were applied every 6 hours for 1 week, followed by a descending dose of topical dexamethasone 0.1% (Maxidex, Alcon) for 3 more weeks.

Patients were reviewed at 1 day, 1 week, 1, 3, and 6 months postoperatively. All the following data were recorded at the preoperative assessment and first, third, and sixth post-operative months: unaided visual acuity (UVA), CDVA, rigid contact lens visual acuity (CLVA), manifest refraction, slit-lamp biomicroscopy, fundoscopy, IOP, endothelial cell count by specular microscopy (Nidek, Japan), corneal topography (Pentacam, Oculus Inc, Germany), anterior segment OCT-Visante (Carl Zeiss, Germany), and corneal confocal biomicroscopy with the Heidelberg Retinal Tomograph (HRT3) Rostock Cornea Module (HRT3; Heidelberg Engineering Inc, Germany).

RESULTS

The 5 consecutive patients had a mean age of 34.2 years (range: 30–42 years). The study sample comprised 3 men and 2 women as well as 3 right eyes and 2 left eyes. None of these eyes had received corneal collagen cross-linking or other ophthalmic interventions in the past. All surgeries were performed as previously described without any intraoperative complication. Four patients completed the full follow-up (6 months). One patient was lost to follow-up after the first postoperative month because of inability to attend further follow-up visits (motivations not related to the study), so this patient was excluded from the subsequent analysis. No complication had been recorded before this exclusion, and information obtained from the patient directly indicated no subjective negative findings and no complications as described by other specialized ophthalmic professionals. Results are summarized in (Table 2).

Visual Acuity

All patients improved their visual function regarding the UVA, CDVA, and CLVA (Figs. 2A–C). UVA and CDVA showed their peak at the first postoperative month (with 2 lines of mean improvement), followed by mild regression up to the sixth month, with an overall improvement of more than 1 line compared with the preoperative month. Best visual acuity with rigid contact lenses (CLVA) showed an important and progressive improvement up to the sixth month, with a total mean improvement of more than 2 lines.

Manifest Refraction

The refractive sphere improved in 2 patients (1 and 2) and remained stable in the rest (patients 3 and 4), showing an overall mean improvement of 0.5 D at the end of the

TABLE 2. Visual, Refractive, Keratometric, and Pachymetric Outcomes (Mean Parameters and Range)

	Preoperative	1 month	3 months	6 months
UVA (decimal)	0.1 (0.05 to 0.2)	0.3 (0.1 to 0.4)	0.295 (0.15 to 0.365)	0.233 (0.1 to 0.333)
CDVA (decimal)	0.325 (0.2 to 0.4)	0.525 (0.2 to 0.8)	0.487 (0.2 to 0.75)	0.481 (0.4 to 0.625)
CLVA (decimal)	0.512 (0.4 to 0.6)	0.65 (0.5 to 0.8)	0.737 (0.5 to 0.95)	0.762 (0.5 to 0.875)
Rx Sphr, D	24.06 (20.5 to 27)	23.69 (20.75 to 27)	23.812 (20.75 to 28)	23.562 (20.75 to 26.5)
Rx Cyl, D	22.937 (22.25 to 23.5)	23.562 (22.25 to 24.5)	23.19 (22.25 to 24)	23.25 (22.5 to 24)
Anterior Km, D	55.95 (47.9 to 64.9)	56.95 (50.2 to 65.6)	56.1 (49.6 to 63.4)	56.82 (50.8 to 65.4)
Posterior Km, D	28.3 (26.6 to 29.7)	28.55 (27.10 to 210.2)	28.37 (26.8 to 29.8)	28.52 (27 to 210.2)
Kmax, D	66.3 (56.7 to 79.4)	68.8 (63.2 to 81.3)	68.325 (62.1 to 82.1)	67.95 (61.8 to 81.2)
Topo Cyl, D	22.95 (20.4 to 25.8)	23.47 (21.5 to 25.8)	23.37 (21.2 to 25.3)	23.1 (20.7 to 25.7)
CCT, mm	463 (438 to 503)	456 (435 to 484)	465 (439 to 509)	460 (434 to 512)
Thinnest point, mm	405.75 (394 to 432)	407.75 (406 to 438)	411 (378 to 446)	404.5 (364 to 449)
Cornea Vol, mm^3	54.7 (52.9 to 58.1)	54.75 (42.8 to 58.9)	55.02 (53 to 57.8)	55.25 (52.2 to 59)
Visante CCT, mm	429.5 (407 to 464)	428.75 (406 to 468)	439.75 (421 to 478)	446 (419 to 481)

Cornea Vol, cornea volume; Km, mean keratometry; Kmax, maximum keratometry; Rx Cyl, refractive cylinder; Rx Sphr, refractive sphere; Topo Cyl, topographic cylinder.

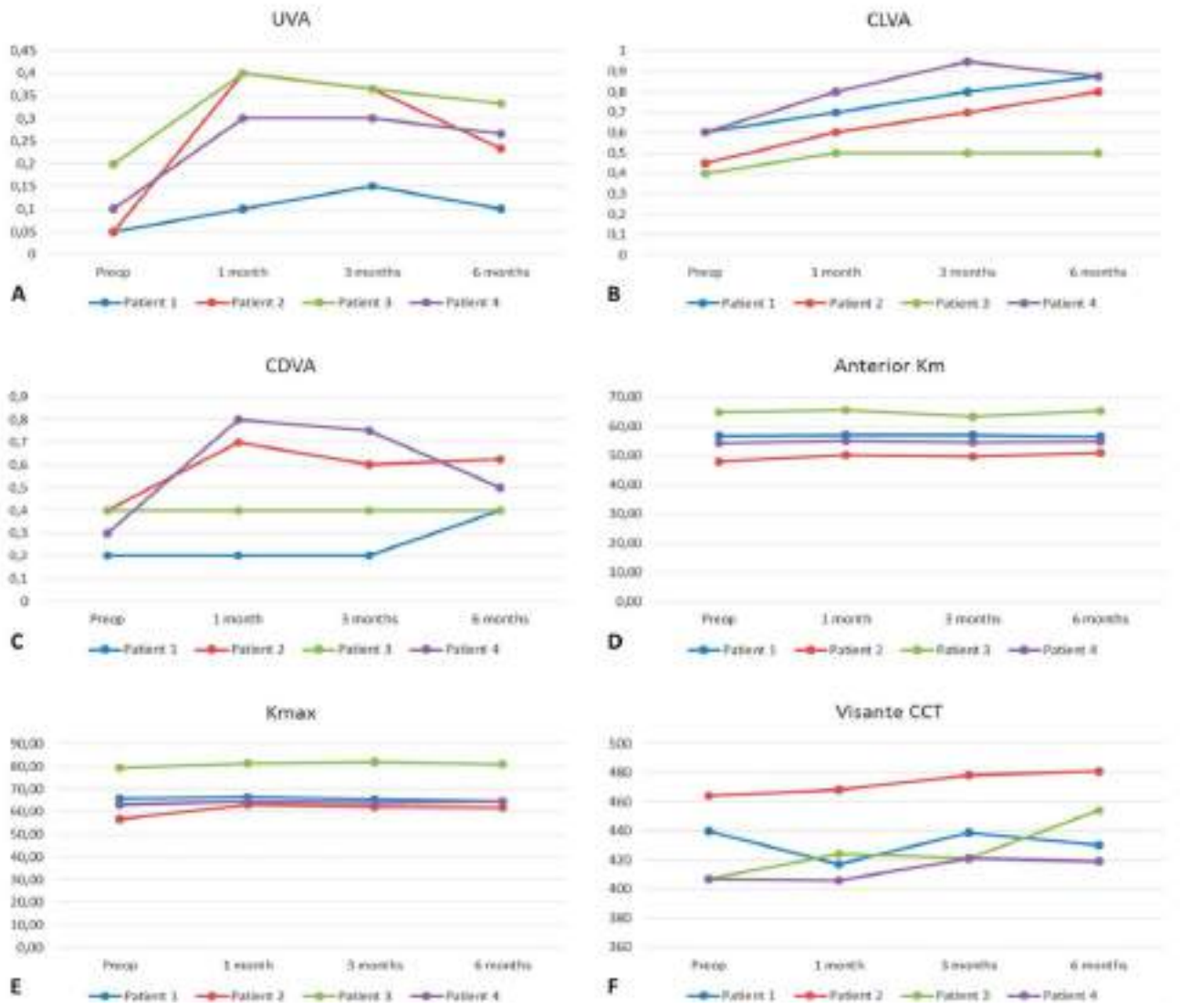

FIGURE 2. Visual (A-C), keratometric (D-E) and pachymetric (F) results along the full follow-up. Unaided visual acuity (UVA), corrected distance visual acuity (CDVA), rigid contact lens visual acuity (CLVA), mean keratometry (Km), maximum keratometry (Kmax), central corneal thickness (CCT).

follow-up (Table 2). The refractive cylinder showed mild deterioration in 3 of the 4 patients (1, 3, and 4), with an overall mean worsening of 0.3 D at the end of follow-up.

Slit-Lamp Biomicroscopy

All corneas were, preoperatively, free of posterior stromal or predescemetic scars and presented a clear visual axis. Only patient 2 presented a couple of paracentral dense anterior stromal scars (Fig. 3A). None of the patients developed any sign of inflammation or rejection during the follow-up, and corneal transparency was fully recovered within 24 hours after the surgical procedure and kept during the whole follow-up period (Fig. 3B). After the third post-operative month, we could observe progressive improvement of the preoperative corneal scars seen in patient 2, confirming this finding at the end of follow-up (Figs. 3B, C).

Corneal Topography

All keratometric parameters presented relative stability without differences over 1 D (Table 2 and Fig. 4). Anterior and posterior mean keratometry remained stable but in patient 2 who presented a deterioration of anterior mean keratometry of 2.9 D (Fig. 2D). A deterioration over 1 D in maximum keratometry was observed in 2 of the 4 patients (2 and 3), with a mean overall deterioration of 1.65 D at the sixth month (Fig. 2E). Regarding the topographic anterior cylinder, patients 1 and 4 remained stable, patient 2 showed significant improvement (from 22 D preoperatively to 20.7 D at the sixth month),

FIGURE 3. Slit-lamp images from patient 2, preoperatively (A) and at the sixth postoperative month (B and C). Observe the postoperative improvement in the density and severity of the inferior paracentral anterior stromal scars.

and patient 3, significant worsening (from 20.4 D preoperatively to 22.3 D at the sixth month).

The pachymetric values measured by the Pentacam remained stable, without detecting any obvious enhancement in the corneal thickness parameters. The central corneal thickness (CCT) remained stable in all but patient 4 (from 449 mm preoperatively to 434 mm at the sixth month) and patient 2 (from 503 mm preoperatively to 512 mm at the sixth month). The thinnest point improved or remained stable in all but patient 3 (from 394 mm preoperatively to 364 mm at the sixth month). The corneal volume improved in all but patient 4 (from 52.9 to 52.2 mm^3).

Anterior Segment OCT

Mild improvement in the CCT measured by anterior segment OCT (Visante) was observed in 3 of the 4 patients (but patient 1), with a mean increase of 16.5 µm at the sixth

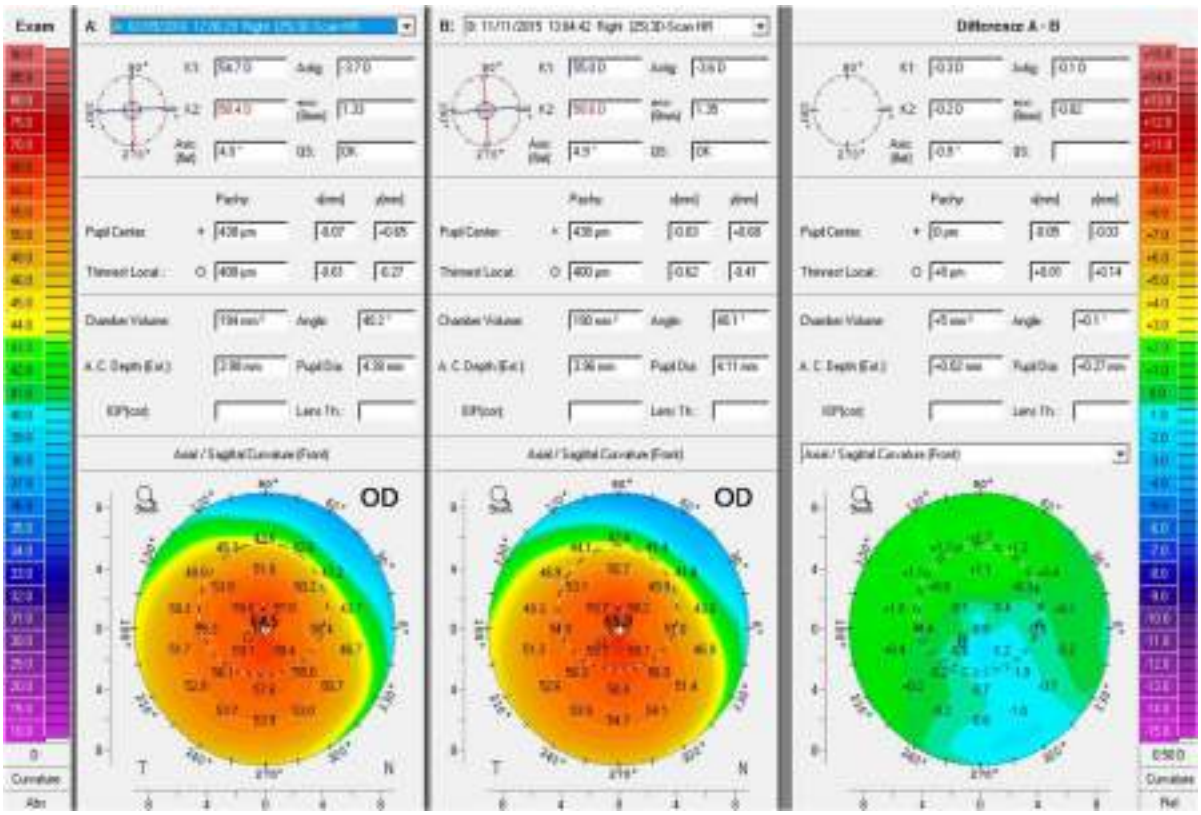

FIGURE 4. Corneal topography (Pentacam) comparison between preoperative and 6 months after surgery in patient 1. Observe the stability of the keratometric parameters.

month. This improvement in the thickness occurred after the first month (Fig. 2F).

After the third postoperative month, we also observed in 3 of the 4 patients' (1, 2, and 4) patchy hyperreflective areas at the level of the stromal pocket compatible with areas of new collagen production. These areas were not homoge-neously distributed along the stroma, appearing as isolated islands (Fig. 5).

Confocal Biomicroscopy

Up to the third postoperative month, round cells were observed in the surgical plane in all cases (Fig. 6B). These cells showed a different morphology than the usual dendritic or fusiform shape presented by the anterior and posterior stromal keratocytes (Fig. 6A). At the sixth month, these cells at the surgical level had already a fusiform shape and were not different from those observed in other stromal planes. This rounded cellular morphology was considered a landmark for cellular survival during the early postoperative period.

Other Parameters

No changes in IOP were detected. Endothelial cell density measured by specular microscopy remained stable, without evidence of endothelial cell damage (mean values of 2612 preoperatively and 2821 cells/mm^2 at the sixth month postoperatively).

DISCUSSION

Nowadays, corneal collagen cross-linking has radically changed the long-term prognosis of keratoconus, although many cases are still diagnosed in an advanced state in which classic corneal transplantation (either by full-thickness or lamellar techniques) is the only treatment option. The aim of our group was to find an alternative therapy to classic corneal transplantation to regenerate the corneal stroma, thus avoiding the important intraoperative and postoperative risks associ-ated with those techniques.[18] Cellular therapy of the corneal stroma by the use of stem cells has gained relevant scientific interest in the last few years. All MSCs seem to have similar behavior in vivo, being able to achieve keratocyte differen-tiation and modulate the corneal stroma with also immuno-modulatory properties.[1] Corneal stromal stem cells (CSSCs) may have enhanced functions, as they are already corneal cells with more directed differentiation potential. However, the number of CSSCs that can be obtained from human corneas is quite limited and technically very demanding, with an inefficient cell subculture and impossible to obtain without damaging the donor cornea. All these major drawbacks have significantly limited their use for clinical practice and pre-clude their autologous application, so an extraocular source of cells that could replace CSSCs is necessary to solve all these limitations. Human adult adipose tissue has been demon-strated to be an ideal source of autologous stem cells, as it satisfies all the requirements: easy accessibility to the tissue, high cell retrieval efficiency, and ability of its stem cells (ADASCs) to differentiate into multiple cell types.[3] Bone marrow MSCs have the same profile as ADASCs, but their extraction by bone marrow puncture is a more complicated and painful procedure that requires general anesthesia. Umbilical MSCs present an attractive alternative, but their autologous use would be expensive and currently impossible. Embryonic stem cells also present important ethical issues. A new and exciting possibility is offered by the induced pluripotent stem cells, obtained from adult cells, as recent studies[19,20] have demonstrated their ability to differentiate into corneal keratocytes with similar immunomodulatory properties as MSCs.

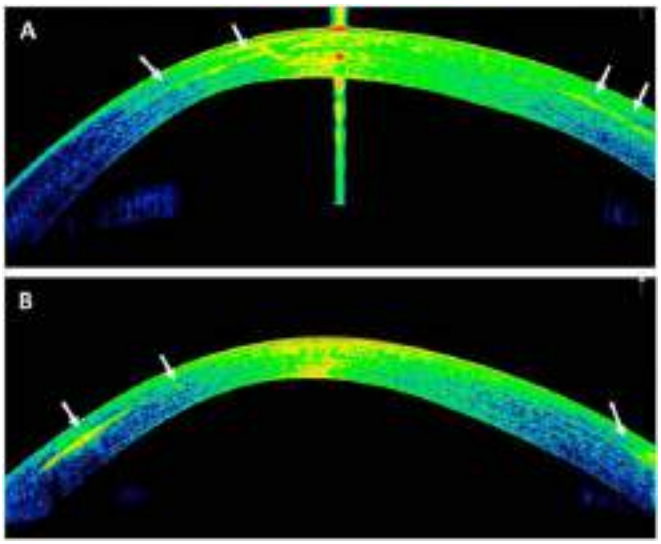

FIGURE 5. Corneal OCT images from patients 2 (A) and 4 (B) at the sixth postoperative month. Observe the patchy hyper-reflective areas (white arrows) at the level of the stromal pocket compatible with areas of new collagen production. These areas were not homogeneously distributed along the stromal surface.

To date, many studies in animal models for different corneal abnormalities have demonstrated the possible benefits of cellular therapy to improve corneal transparency by their ability to reorganize the stromal collagen lamellas and new collagen production.[1–13] However, to the best of our knowl-edge, no in vivo data have been published yet in humans studying the safety and efficacy of such therapies. With this purpose, we selected patients with advanced keratoconus as candidates for classic corneal transplantation because of unsatisfactory visual function and contact lens intolerance because, in case of failure, standard treatment for such patients could still be performed. In such cases, disease progression is hard to evaluate because of the lack of reliability from manifest refraction and corneal topography, also it loses relevance, as corneal collagen cross-linking is not an alternative and corneal transplantation is usually the only treatment option. Thus, keratoconus progression was not analyzed in our study.

Stem cell delivery to the corneal stroma was per-formed through a femtosecond laser–assisted lamellar pocket at half depth. Although we were dealing with advanced keratoconic corneas with severe thinning, we did not observe

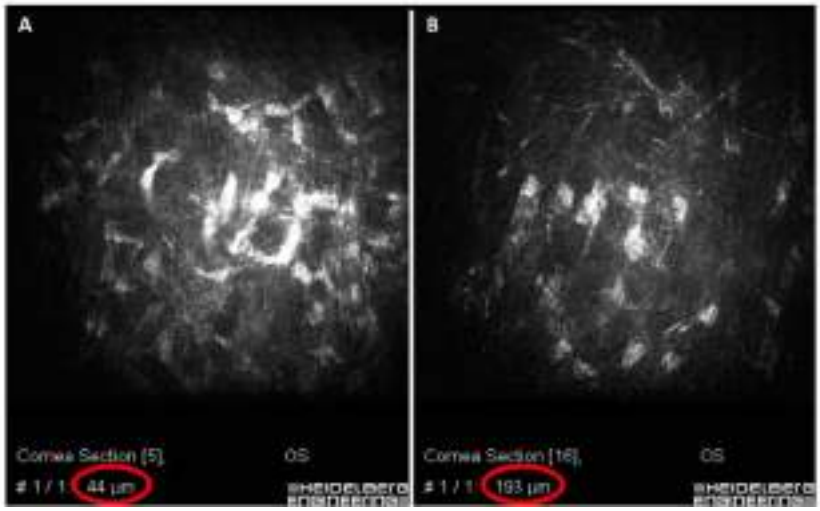

FIGURE 6. Corneal confocal biom microscopy images from patient 4 at the third postoperative month. Cellular presence is confirmed at the level of the surgical plane with cells showing a more round shape (B) compared with the usual fusiform shape presented by the corneal ker-atocytes in the stroma anterior (A) and posterior to the surgical plane.

intraoperative complications such as corneal tears. Nevertheless, to be able to safely perform this tech-nique, a minimal thinnest pachymetric point of 250 µm is probably required (that thickness would leave an anterior cap close to a LASIK flap). Some concerns may arise about the possible weakening effect of this corneal dissection on an already severely weakened and pathologic cornea. However, according to John Marshall's important findings, vertical side cuts through corneal lamellae rather than hori-zontal delamination incisions contribute to loss of structural integrity during LASIK flap creation.[21] In our study, only a 30-degree anterior side cut was performed; so considering these findings, the weakening effect of this dissection should be marginal. However, it would be interesting to demon-strate John Marshall's data again in the keratoconic cornea, but as previously discussed, progression analysis in our advanced ectatic corneas was not performed because a follow-up period of 6 months is not enough to establish conclusions in this regard, and also, this analysis would not be reliable in such corneas because of the lack of repeat-ability of topography and refraction.[22]

Three million autologous ADASCs (contained in 1 mL) were prepared for injection into the stromal pocket. This high cellular concentration was decided as high cellular loss was expected during delivery because of solution leakage outside the cornea. Before the injection, we performed a corneal paracentesis to reduce the IOP and allow more volume within the pocket, although no more than 10% to 30% of the injected volume was expected to remain within the stroma. Further studies are necessary to assess precisely the real amount of cells that remain immediately after transplantation.

Visual function improved in all patients. This benefit was modest but observed in the 4 study patients, with a pattern in which this improvement was mostly observed within the first month followed by mild subsequent regres-sion. This early postoperative finding should be theoretically attributed to the surgical procedure itself and not to the presence of stem cells, because they have not differentiated yet into adult keratocytes (considering their lack of the usual dendritic shape at confocal biomicroscopy and the absence of new collagen production on corneal OCT at the first month visit). However, we could not observe early changes in manifest refraction or topographic keratometry that may explain this early visual improvement.

Keratometric and pachymetric data obtained by corneal topography (Pentacam) showed overall stability (Fig. 4), with a possible progression of ectasia in patient 3. This patient presented the most advanced cone, so cellular therapy may not be capable to halt the progression of ectasia in such cases. Nevertheless, we should take into account the low reliability of the data measured by conventional scanning-slit corneal topographers in advanced keratoconus due to eye fixation errors and light scattering from corneal haze and opacity.[22] Some studies suggest superiority of anterior segment OCT over conventional topographers in advanced keratoconic eyes, as its scanning beam penetrates opaque tissues more deeply, providing clearer images of cloudy corneas allowing for better and more reliable preoperative assessment.[23] Pachymetry measurement by anterior segment OCT in our study demonstrated a mild but real improvement of the CCT (mean: 16.5 µm at the sixth month), correlated with the presence of patchy areas of new collagen production in the majority of the patients. This new collagen production appears in low amount and not homogeneously distributed along the surgical plane, thus this procedure is not able to restore large amounts of tissue if that is the purpose as in corneal thinning diseases. As previously observed in animal models, the addition of hyaluronic acid–derived scaffolds or acellular corneal stroma may assist to achieve this goal.[5,6]

We did not observe any intraoperative or postoperative complication, the surgery being well tolerated in all cases with complete restoration of corneal transparency within 24

hours. We could also observe significant clinical improvement of corneal opacity in patient 2 (Fig. 3), as has been suggested in previous studies in animal models.[7] However, larger case series with corneal opacity are required to demonstrate this finding.

Within experimental studies, it is easy to demonstrate, by postmortem analysis, the survival of the previously transplanted marked cells (through immunofluorescence anal-ysis) and their differentiation into adult keratocytes (by detecting keratocan expression).[3,5] However, in vivo human studies have the important drawback of being limited to confocal biomicroscopy findings (vulnerable to subjective interpretations) to observe the behavior of the transplanted cells in vivo. A perfect patient collaboration is not always possible in such a diagnostic technique, which reduces the accuracy of the depth measurement at the evaluated plane. Taking into account all these limitations, we could observe the presence of round cells at the surgical plane in all patients compatible with the transplanted ADASCs, later showing a progressive dendritic shape change until the point of being not possible to be differentiated from normal keratocytes at the end of the follow-up.

Nevertheless, the conclusions of this pilot study should be considered carefully, as they are vulnerable to bias because the study included a small sample, was not masked, and was not a controlled study. So future studies with a larger sample and longer follow-up should confirm the preliminary results observed here. Other studies should follow as well to demonstrate the role of this therapy in other nonectatic corneal dystrophies with progressive opacification of the corneal stroma due to deposit diseases, confirming the preliminary data observed in animal models.[9,11] The use of heterologous instead of autologous ADASCs would be interesting since a recent study observed gene expression differences between the induced pluripotent stem cell–derived keratocytes generated from fibroblasts of both keratoconic and normal human corneal stroma, influencing cellular growth and proliferation.[24] In this scenario, immune rejection is feasible, although the demonstrated immunomodulatory properties of these stem cells even in xenogeneic scenarios may avoid chronic steroid use and may enhance the clinical and anatomical results. Finally, it would still be interesting to evaluate the possible benefits of this therapy in mild or moderate progressive keratoconus, studying its impact on the natural course of the disease.

As a conclusion, with this phase 1 study, we show preliminarily the apparent safety of corneal stromal transplantation of autologous ADASCs in humans, their survival in vivo, and their ability to produce a low amount of new collagen. This study includes a small sample of patients, so future studies with larger samples are required to finally confirm the safety and efficacy of the procedure and to clarify the relevance of the observed findings.

ACKNOWLEDGMENTS

The authors thank Marc Assouwad and Peggy Saba from Laser Vision (Beirut, Lebanon), Ziad Abdul Jawad from Optica General (Saida, Lebanon), Charbel Khalil from Reviva Regenerative Medicine Center (Beirut, Lebanon), and Laurent Bataille from Vissum Corporación (Alicante, Spain) for their great support and assistance to the project.

REFERENCES

1. De Miguel MP, Casaroli-Marano RP, Nieto-Nicolau N, et al. Frontiers in regenerative medicine for cornea and ocular surface. In: Rahman A, Anjum S, eds. Frontiers in Stem Cell and Regenerative Medicine Research. 1st ed. Vol 1. Cambridge, PA: Bentham e-Books; 2015:92–138.
2. Ruberti JW, Zieske JD. Prelude to corneal tissue engineering—gaining control of collagen organization. Prog Retin Eye Res. 2008;27:549–577.
3. Arnalich-Montiel F, Pastor S, Blazquez-Martinez A, et al. Adipose-derived stem cells are a source for cell therapy of the corneal stroma. Stem Cells. 2008;26:570–579.
4. Alió del Barrio JL, Chiesa M, Gallego Ferrer G, et al. Biointegration of corneal macroporous membranes based on poly(ethyl acrylate) copolymers in an experimental animal model. J Biomed Mater Res A. 2015;103: 1106–1118.
5. Alio del Barrio JL, Chiesa M, Garagorri N, et al. Acellular human corneal matrix sheets seeded with human adipose-derived mesenchymal stem cells integrate functionally in an experimental animal model. Exp Eye Res. 2015;132:91–100.
6. Espandar L, Bunnell B, Wang GY, et al. Adipose-derived stem cells on hyaluronic acid-derived scaffold: a new horizon in bioengineered cornea. Arch Ophthalmol. 2012;130:202–208.
7. Mittal SK, Omoto M, Amouzegar A, et al. Restoration of corneal transparency by mesenchymal stem cells. Stem Cell Reports. 2016;7: 583–590.
8. Demirayak B, Yüksel N, Çelik OS, et al. Effect of bone marrow and adipose tissue-derived mesenchymal stem cells on the natural course of corneal scarring after penetrating injury. Exp Eye Res. 2016;151: 227–235.
9. Du Y, Carlson EC, Funderburgh ML, et al. Stem cell therapy restores transparency to defective murine corneas. Stem Cells. 2009;27: 1635–1642.
10. Liu H, Zhang J, Liu CY, et al. Cell therapy of congenital corneal diseases with umbilical mesenchymal stem cells: lumican null mice. PLoS One. 2010;5:e10707.
11. Coulson-Thomas VJ, Caterson B, Kao WW. Transplantation of human umbilical mesenchymal stem cells cures the corneal defects of mucopolysaccharidosis VII mice. Stem Cells. 2013;31:2116–2126.
12. Kao WW, Coulson-Thomas VJ. Cell therapy of corneal diseases. Cornea. 2016;1(35 suppl):S9–S19.
13. De Miguel MP, Fuentes-Julián S, Blázquez-Martínez A, et al. Immunosuppressive properties of mesenchymal stem cells: advances and applications. Curr Mol Med. 2012;12:574–591.
14. Alió JL, Piñero DP, Alesón A, et al. Keratoconus-integrated characterization considering anterior corneal aberrations, internal astigmatism, and corneal biomechanics. J Cataract Refract Surg. 2011;37:552–568.
15. Zuk PA, Zhu M, Mizuno H, et al. Multilineage cells from human adipose tissue: implications for cell-based therapies. Tissue Eng. 2001; 7:211–228.
16. Zuk PA, Zhu M, Ashjian P, et al. Human adipose tissue is a source of multipotent stem cells. Mol Biol Cell. 2002;13:4279–4295.
17. Bourin P, Bunnell BA, Casteilla L, et al. Stromal cells from the adipose tissue-derived stromal vascular fraction and culture expanded adipose tissue-derived stromal/stem cells: a joint statement of the International Federation for Adipose Therapeutics and Science (IFATS) and the International Society for Cellular Therapy (ISCT). Cytotherapy. 2013;15: 641–648.
18. Arnalich-Montiel F, Alió Del Barrio JL, Alió JL. Corneal surgery in keratoconus: which type, which technique, which outcomes? Eye Vis (Lond). 2016;18:2.
19. Naylor RW, McGhee CN, Cowan CA, et al. Derivation of corneal keratocyte-like cells from human induced pluripotent stem cells. PLoS One. 2016;11:e0165464.
20. Yun YI, Park SY, Lee HJ, et al. Comparison of the anti-inflammatory effects of induced pluripotent stem cell-derived and bone marrow-derived mesenchymal stromal cells in a murine model of corneal injury. Cytotherapy. 2017;19:28–35.

21. Knox Cartwright NE, Tyrer JR, Jaycock PD, et al. Effects of variation in depth and side cut angulations in LASIK and thin-flap LASIK using a femtosecond laser: a biomechanical study. J Refract Surg. 2012;28: 419–425.
22. Altan-Yaycioglu R, Pelit A, Akova YA. Comparison of ultrasonic pachymetry with Orbscan in corneal haze. Graefes Arch Clin Exp Ophthalmol. 2007;245:1759–1763.
23. Nakagawa T, Maeda N, Higashiura R, et al. Corneal topographic analysis in patients with keratoconus using 3-dimensional anterior segment optical coherence tomography. J Cataract Refract Surg. 2011;37: 1871–1878.
24. Joseph R, Srivastava OP, Pfister RR. Modeling keratoconus using induced pluripotent stem cells. Invest Ophthalmol Vis Sci. 2016;57: 3685–3697.

10.3. Alió Del Barrio, J., El Zarif, M., Azaar, A., Makdissy, N., Khalil, C., Harb, W., El Achkar, I., Jawad, Z., de Miguel, M., Alió, J., 2018. **Corneal stroma enhancement with decellularized stromal laminas with or without stem cell recellularization for advanced keratoconus**. Am J Ophthalmol 186, 47–58. https://doi.org/10.1016/j.ajo.2017.10.026

Corneal Stroma Enhancement With Decellularized Stromal Laminas With or Without Stem Cell Recellularization for Advanced Keratoconus

JORGE L. ALIÓ DEL BARRIO, MONA EL ZARIF, ALBERT AZAAR, NEHMAN MAKDISSY, CHARBEL KHALIL, WALID HARB, IBRAHIM EL ACHKAR, ZIAD ABDUL JAWAD, MARÍA P. DE MIGUEL, AND JORGE L. ALIÓ

• **PURPOSE:** This phase 1 study seeks to preliminarily evaluate the safety and efficacy of decellularized human corneal stromal lamina transplantation with or without autologous adipose-derived adult stem cell recellularization within the corneal stroma of patients with advanced keratoconus.

• **DESIGN:** Phase 1 clinical trial.

• **METHODS:** Femtosecond-assisted 120µm thickness and 9-mm diameter laminas were obtained from the anterior stroma of human donor corneas and decellularized with a sodium dodecyl sulfate solution. Autologous adipose-derived adult stem cells were obtained by elective liposuction and cultured onto both sides of the lamina. Five patients received the decellularized lamina alone and 4 patients the recellularized lamina into a femtosecond-assisted 9.5-mm diameter lamellar pocket under topical anesthesia. The total duration of follow-up was 6 months.

RESULTS: No case showed clinical haze or scarring by month 3. Six months after surgery, patients showed a general improvement of all visual parameters, with a mean unaided visual acuity (VA) from 0.109 to 0.232 (p=0.05) and corrected distance VA from 0.22 to 0.356 (p=0.068). Refractive sphere improved in all patients (from -4.55 [D] to -2.69 D; p=0.017), but refractive cylinder remained stable (from -2.83 to -2.61; p=0.34). An improvement tendency of all anterior keratometric values was observed. A mean improvement of 120 µm in all thickness parameters was confirmed (p=0.008), as well as an improvement in the spherical aberration (p=0.018), coma (p=0.23) and total higher order aberrations (p=0.31). No significant differences among groups were detected.

• CONCLUSIONS: Decellularized human corneal stromal laminas transplantation seems safe and moderately effective for advanced keratoconus. Potential benefits of its recellularization with autologous adipose-derived adult stem cells remains unclear.

From the Cornea, Cataract and Refractive Surgery Unit (J.L.A.B., J.L.A.), Vissum Corporación, the Division of Ophthalmology (J.L.A.B., J.L.A.), Universidad Miguel Hernández, Alicante, and the Cell Engineering Laboratory (M.P.M.), IdiPAZ, La Paz Hospital Research Institute, Madrid, Spain; Optica General, Saida (M.E., Z.A.J.), and the Reviva Regenerative Medicine Center (A.A., N.M., C.K., W.H.), Middle East Hospital, Lebanese University (N.M.), and Saint-Joseph University, Beirut, Lebanon (I.E.).

Inquiries to Jorge L. Alió, Cornea, Cataract and Refractive Surgery Unit, Vissum Corporación, Avda de Denia s/n, Alicante 03016, Spain; e-mail: jlalio@vissum.com

INTRODUCTION

CORNEAL ECTASIAS, SUCH AS KERATOCONUS, ARE characterized by a progressive thinning, bulging, and distortion of the cornea, with secondary loss of vision caused by high irregular astigmatism.[1] Visual rehabilitation of advanced corneal ectasias requires penetrating or lamellar corneal transplantation techniques, which have several drawbacks, such as graft rejection, failure, and slow visual recovery because of high levels of induced postoperative astigmatism in relation with the suture.[1] It should also be considered that in many countries access to donor corneal tissue is limited: approximately 53% of the world's population has no access to corneal transplantation.[2]

Tissue engineering of the cornea aims to solve this problem, although the highly complex structure of the corneal stroma limits the usefulness of these corneal substitutes in real clinical practice generated, to date, in the laboratory, because of a lack of either transparency or strength properties.[3] Cellular therapy of corneal stroma is gaining interest because stem cells from either ocular or extraocular sources are capable of not only surviving and differentiating in vivo into adult human keratocytes, but also of producing new collagen within the host stroma.[4,5] They improve preexisting scars or corneal transparency in animal models for corneal dystrophies by corneal stroma remodeling and host keratocyte modulation by paracrine secretion,[6–11] and also show immunomodulatory properties in syngeneic, allogeneic, and even xenogeneic scenarios.[11,12] Recently, our group reported for the first time in a pilot clinical trial the possible benefits of cellular therapy of the corneal stroma with extraocular stem cells in patients with advanced keratoconus.[13] Although additional research

studies are still necessary, cellular therapy of the corneal stroma will unlikely be able to fully rehabilitate the thickness of an already severely thinned cornea, because the collagen production by the transplanted cells has been shown to belimited.[4,13]

Several corneal decellularization techniques have been described to supply the collagen component of the corneal stroma and provide an acellular corneal extracellular matrix.[14] These scaffolds have become more popular in the last few years because they provide a natural environment for the growth and differentiation of cells and are tolerated well even by xenogeneic recipients, as components of the extracellular matrix are generally preserved among species.[15]

The aim of the present study is to preliminary evaluate the safety and efficacy of the intrastromal implantation of decellularized human corneal stromal laminas for the thickness rehabilitation of advanced keratoconic eyes in a human phase 1 pilot study, and to define the possible advantages of the addition of autologous adipose-derived adult stem cells (ADASCs) to these implants. To the best of our knowledge, this is the first report regarding the use of implants of decellularized human corneal stroma tissue, with or without mesenchymal stem cells, for human corneal transplantation.

METHODS

• **STUDY APPROVAL, DESIGN, AND SUBJECTS:** This investigation is a prospective consecutive series of cases based on the cooperation between the Research, Development and Innovation Department of Vissum Instituto Oftalmologico de Alicante, Miguel Hernandez University, Alicante (Spain), Optica General (Saida, Lebanon), Laser Vision Center (Beirut, Lebanon) and the Reviva Research and Application Center (Middle East Hospital, Beirut, Lebanon). The Institutional Review Board Ethical Committee of the Reviva Research and Application Center (Lebanese University, Beirut) prospectively approved this study. All patients gave informed written consent for all procedures described in this study. The study was conducted in strict adherence to the tenets of the Declaration of Helsinki and it was registered at ClinicalTrials.gov (NCT02932852).

Nine consecutive patients were enrolled in the study and were randomly distributed into 2 study groups. Group 1 included decellularized human corneal stroma transplanta- tion (5 patients); group 2 included autologous ADASCs recellularized human corneal stroma transplantation (4 patients).

Inclusion criteria. Inclusion criteria were as follows: advanced keratoconus defined as stage ≥IV according to the RETICS keratoconus classification[16]; age ≥18 years; negative HIV, hepatitis B virus (HBV), and hepatitis C virus (HCV) serology; and no history of malignancy.

Exclusion criteria. Exclusion criteria were as follows: corrected distance visual acuity (CDVA) <0.1 in the contralateral eye; active concomitant inflammatory eye disease; other ophthalmic comorbidity, such as cataract, retinal diseases, or glaucoma; previous ocular surgical interventions other than cataract; previous corneal hydrops or central corneal scars; history of cognitive impairments or dementia that may impact the patient's ability to participate in the informed consent process and to appropriately complete evaluations; any immunodeficiency or immunosuppressive therapy; serologic evidence of infection with HBV, HCV, or HIV; and pregnancy or breastfeeding. Keratoconus progressive status was not considered as an exclusion or inclusion criteria.

• **AUTOLOGOUS ADASCs ISOLATION, CHARACTERIZA- TION, AND CULTURE:** Patients were subjected to standard liposuction after informed consent. All procedures were performed in good medical practice conditions. Approximately 250 mL of fat mixed with local anesthesia was obtained from each patient. Adipose tissue was processed according to previous publications.[17,18] Briefly, adipose tissue was washed in phosphate-buffered saline (PBS) and digested in collagenase I for 40 minutes at 37^0C in agitation. Then, collagenase was inhibited adding autologous human serum extracted from each patient. Erythrocytes were lysed in erythrocyte lysis buffer (Gibco-Life Technologies, Waltham, MA) and then the pelleted cells were cultured in Dulbecco's modified eagle medium with Glutamax and sodium pyruvate (Gibco), 10% autologous human serum, 1% penicillin-streptomycin (Gibco) and 0.2% amphotericin B (Gibco). Cell characterization was performed by $CD34^+CD45^-CD105^+$ labeling and flow cytometry analysis as requested by the International Federation of Adipose Therapeutics.[19] Sixty to 80 hours before surgery, quiescence was induced by reducing the amount of serum to 0.5% in order to transplant the ADASCs in a physiological status more closely resembling the natural nonproliferative stromal keratocytes, because proliferative stem cells within the corneal stroma could potentially induce stromal scarring or haze. Quiescence and the absence of apoptosis and aneuploidy were verified by propidium iodide labeling (Invitrogen, Waltham, MA), and cell cycle analysis by flow cytometry as described in previous articles.[4,13,15] Twenty- four hours before implantation, ADASCs were harvested by tripsinization (Sigma, St. Louis, MO) and 0.5 x 10^6 cells were cultured on each side of the decellularized corneal stroma lamina for 24 and 12 hours, respectively (37^0C in standard CO_2 incubator).

• **DECELLULARIZATION AND RECELLULARIZATION OF HUMAN CORNEAL STROMA LAMINAS**: Corneal stroma from donor human corneas with nonviable

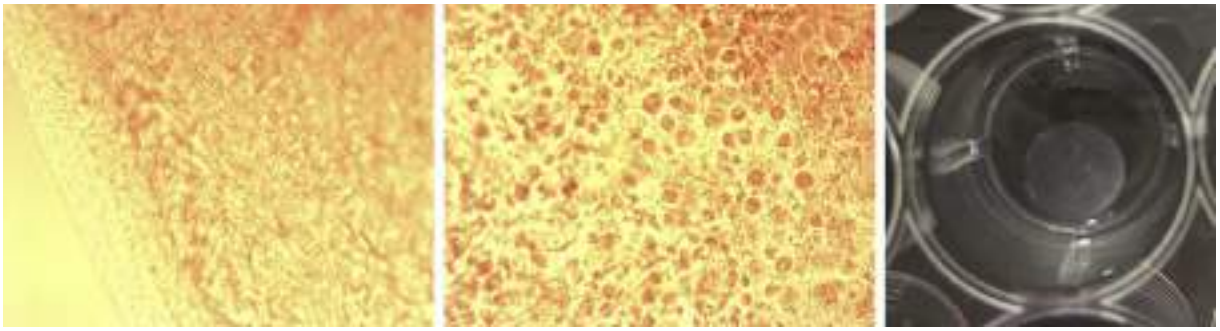

FIGURE 1. (Left) Phase-contrast photograph of a lamina after decellularization and just before recellularization (310, photograph taken at the peripheral border). (Middle) Phase-contrast photograph of a lamina 11 hours after adding adipose-derived adult stem cells to the second side of the lamina (310; total culture time 23 hours; photograph taken at the center of the lamina). (Right) Macroscopic appearance of the lamina under phosphate-buffered saline in a culture well.

endothelium but with negative viral serology were used. Corneas were provided by the eye bank Banco de Ojos para el trata- miento de la Ceguera of Centro de Oftalmolog´ıa Barraquer (Barcelona, Spain). Directive 2004/23/EC on setting stan- dards of quality and safety for the donation, procurement, testing, processing, preservation, storage, and distribution of human tissues and cells; and Directive 2006/17/EC of the Council regarding certain technical requirements for the donation, procurement, and testing of humantissues and cells were followed.

Donor corneas were mounted on an artificial anterior chamber (Barron; Katena Products, Denville, NJ). The epithelium was mechanically removed with surgical sponges, and the anterior corneal stroma cut with 60-kHz IntraLase iFS femtosecond laser (AMO, Santa Ana, CA) in 2 consecutive laminas of 120 µm thickness and 9.0 mm diameter. These were subsequently washed in PBS (Sigma) supplemented with 1% antibiotic-antimicotic (Gibco). Femtosecond laser parameter settings were equivalent to the ones used for a standard laser in situ keratomileusis flap dissection, except by an anterior side cut angle of 360^0. With this procedure, 2 laminas were obtained, a superficial one containing the Bowman membrane and a deeper one without this layer. The remaining posterior cornea was discarded. The decellularization protocol was based on previous publications.[15,20] Briefly, the laminas were immersed in 1% (wt/vol) sodium dodecyl sulfate solution (Sigma) with a protease inhibitor cocktail (P8340; Sigma), and incubated in an orbital shaker (75 rpm) for 24 hours at room temperature. Then, the laminas were washed 8 times in PBS with 1% antibiotic-antimicotic in the same conditions for 15 minutes each at room temperature. To remove DNA, the laminas were incubated in DNAse (Benzonase Nuclease 6.5 U/mL; Merck, Darmstadt, Germany) in PBS with the same prote- ase inhibitor cocktail in the same conditions at 37^0C for 72 hours. Finally, the laminas were washed 8 times for 15 minutes each in PBS with 1% antibiotic-antimicotic (Figure 1, Left). Twenty-four hours before implantation, laminas for patients receiving recellularized tissue were then placed in tissue culture wells for recellularization with autologous ADASCs (0.5×10^6 cells were cultured on each side of the lamina) (Figure 1, Middle). After finishing the recellularization process, the laminas were trans- ferred to the theatre in PBS at room temperature for their implantation (Figure 1, Right). Superficial or deep laminas were randomly used for the transplantation in both groups.

• **SURGICAL PROCEDURE: LENTICULE IMPLANTATION:** Topical anesthesia with oral sedation was used for all surgeries. The 60-kHz IntraLase iFS femtosecond laser was used in single pass mode for the recipient corneal lamellar dissection by creating an intrastromal lamellar cut 9.5 mm in diameter at half depth of the preoperative thinnest pachymetry point measured by the Visante anterior segment optical coherence tomography (OCT) (Carl Zeiss, Berlin, Germany). The femtosecond laser–assisted corneal dissection ended with a 50^o anterior side cut as a corneal incision. Laser parameter settings were equivalent to those recently reported by our group for this type of dissection.[13] The corneal intrastromal pocket was then opened by blunt dissection with a Morlet lamellar dissector (Duckworth & Kent, Hertfordshire, United Kingdom), and subsequently the lamina inserted, centered, and unfolded through gentle taping and massaging from the host epithelial surface. A temporal limbal paracentesis was performed just before implantation to reduce intraocular pressure. In patients receiving a recellularized lamina, in order to compensate the expected cellular damage by the implantation process, the pocket was irrigated immediately before and after inser- tion with a solution containing an additional 1 million autologous ADASCs in 1 mL PBS through a 25 G cannula. The incision was closed with one interrupted 10-0 nylon suture that was removed 1 week after the operation. Topical antibiotic and steroids (TobraDex; Alcon, Fort Worth, TX) were applied at the end of the surgery. All surgeries were performed by the same surgeons (J.L.A. and J.L.A.B.) at Laser Vision (Beirut).

• **POSTOPERATIVE CARE AND FOLLOW-UP SCHEDULE**: Topical antibiotic and steroids (TobraDex) were applied every 6 hours for 1 week, followed by a descending dose of topical dexamethasone 0.1% (Maxidex, Alcon) for 3 more weeks.

Patients were followed-up at 1 day, 1 week, and 1, 3, and 6 months postoperatively. The following data were recorded throughout the preoperative assessment and postoperative months 1, 3, and 6: unaided visual acuity, CDVA, rigid contact lens visual acuity, manifest refraction, slit lamp biomicroscopy, fundoscopy, intraocular pressure, endothelial cell count by specular microscopy (Nidek, Osaka, Japan), corneal topography (Pentacam, Oculus Inc., Wetzlar, Germany), corneal aberrometry (Sirius; CSO, Firenze, Italy) with 6-mm pupils, anterior segment OCT-Visante (Carl Zeiss), and corneal confocal biomicroscopy with the Heidelberg Retinal Tomograph Rostock Cornea Module (Heidelberg Engineering Inc., Heidelberg, Germany). Intrastromal in vivo keratocyte cell count was performed as previously described[21]: anterior stroma defined as the stroma immediately after the Bowman membrane up to the anterior edge of the implanted lamina. Posterior stroma is defined as the stroma in between the posterior edge of the lamina and immediately anterior to the Descemet membrane. The transplanted mid-stroma is defined as the tissue in between the anterior and posterior edges of the implanted lamina. Three clear images without motion blur or compression lines were selected from each sector (anterior, lamina, and posterior). Therefore, 9 frames per subject were selected for analysis and reviewed by an experienced observer (M.E.Z.). For all images, a standard frame size of 100 x 100 µm was selected, and keratocytes with clear cell borders within this area (using a medium image brightness and contrast) were manually counted. Subsequent keratocyte density (cells/mm^2) was recorded.

• **STATISTICAL ANALYSIS:** The statistical analysis was performed with SPSS software version 20.0 for Windows (SPSS Inc., Chicago, IL). Normality of the study data was confirmed by the Kolmogorov–Smirnov test, which determined that all variables followed a normal distribution ($P \leq 0.05$). Because of the small size of the study sample ($n = 9$), the Wilcoxon sign test was performed to test for statistically significant differences ($P \leq 0.05$).

RESULTS

THE 9 CONSECUTIVE PATIENTS HAD A MEAN AGE OF 34 years (range 24–49 years). The study sample was composed of 7 females and 2 males as well as 6 right eyes and 3 left eyes (Table 1). None of these eyes had previously received corneal collagen crosslinking or any other ophthalmic intervention. All surgeries were performed without any intraoperative complications, except for a limited anterior stromal incision tear during the implantation of the graft in 1 patient. This was managed with bandage contact lens for a week and the patient made a full recovery without further complications. All patients completed the full follow-up (6 months), and the results are summarized in (Table 2).

TABLE 1. Epidemiologic Data of the Study Groups Regarding Age and Sex

	Group 1	Group 2
Mean age, y (range)	32.2 (24–43)	36.25 (30–49)
Female:male ratio	4:1	3:1

• **VISUAL ACUITY:** A general improvement for all visual parameters was observed (Figure 2, Top left), with a mean unaided visual acuity from 0.109 (range 0.05–0.33) to 0.232 (range 0.1–0.475) 6 months after surgery ($P = 0.05$), a mean CDVA from 0.22 (range 0.1–0.4) to 0.356 (range 0.1–0.55) ($P = 0.068$), and a mean unaided visual acuity from 0.541 (range 0.2–0.875) to 0.565 (range 0.2–0.9) ($P = 0.73$). Visual acuity parameters showed, as expected, an initial worsening within the first postoperative month (in relation with a mild graft edema), with a subsequent progressive improvement over time, observing already a net improvement compared with preoperative values 3 months after surgery (for unaided visual acuity and CDVA) and 6 months postoperatively (for unaided visual acuity) (Figure 2, Left). No statistically significant differences in the improvement of visual parameters were observed between groups 1 and 2 (Table 2).

• **MANIFEST REFRACTION**: Refractive sphere improved in all patients (Figure 2 top-right), with a preoperative mean value of -4.55 D (range -12 to -0.25) and -2.69 D (range -6.5 to -0.25) six months after surgery (p=0.017). On the other hand, refractive cylinder remained stable, showing only a mild improvement tendency (Figure 2B): from preop mean value of -2.83 (range -5.5 to -1.5) to 6 months postop mean value of -2.61 (range -4 to -1.25) (p=0.34). No statistically significant differences were observed between groups (Table 2).

• **SLIT LAMP BIOMICROSCOPY:** No postoperative complications including inflammation or rejection signs were recorded throughout the follow-up period in all patients. The implanted lamina showed a mild haziness in relation with a mild lenticule edema during the first postoperative month (what correlated well with the initial loss in the visual parameters) (Figure 3, Top middle and bottom left). Corneal transparency progressively improved throughout the follow-up period, showing complete restoration 3 months postsurgery (Figure 3, Top right and bottom

TABLE 2. Visual, Refractive, Keratometric, and Pachymetric Outcomes for Groups 1 and 2[a]

	Preoperatively, Mean (Range)		Postoperatively, Mean (Range)					
			1 Month		3 Months		6 Months	
	Group 1	Group 2	Group 1	Group 2	Group 1	Group 2	Group 1	Group 2
UVA (decimal)	0.07 (0.05–0.15)	0.158 (0.05–0.33)	0.11 (0.1–0.15)	0.137 (0.1–0.2)	0.21 (0.15–0.3)	0.17 (0.1–0.233)	0.25[b] (0.15–0.475)	0.212 (0.1–0.45)
CDVA (decimal)	0.169 (0.1–0.265)	0.287 (0.1–0.4)	0.173 (0.15–0.265)	0.191 (0.1–0.266)	0.291 (0.2–0.425)	0.310 (0.15–0.5)	0.361 (0.2–0.5)	0.35 (0.1–0.55)
CLVA (decimal)	0.525 (0.2–0.85)	0.562 (0.4–0.875)	0.338 (0.2–0.475)	0.412 (0.2–0.75)	0.443 (0.266–0.65)	0.575 (0.45–0.8)	0.483 (0.2–0.7)	0.668 (0.55–0.9)
Rx Sphr (D)	—5.15 (—12 to —1)	—3.812 (—6.75 to —0.25)	—5.25 (—12 to —1)	—3.38 (—5 to —0.25)	—3 (—5.5 to —1)	—3.187 (—5.5 to —0.25)	—2.5 (—4 to —1)	—2.937 (—6.5 to —0.25)
Rx Cyl (D)	—2.65 (—5.5 to —1.5)	—3.062 (—3.25 to —3)	—2.75 (—4 to —1.5)	—2.937 (—3.25 to —2.5)	—2.30 (—3.25 to —1.25)	—2.875 (—3.50 to —2.50)	—2.4 (—4 to —1.25)	—2.875 (—3.5 to —2.5)
Anterior Km (D)	60.02 (50.5–66.5)	56.83 (47.9–65.4)	59.34 (49.4–66.3)	55.8 (47.5–64.3)	59.26 (52.9–65.1)	55.825 (46.9–65.5)	58.62 (48.4–66.4)	55.525 (46.7–62.2)
Posterior Km (D)	—9.58 (—11.3 to —7.6)	—8.7 (—10.2 to —7.1)	—9.62 (—11.3 to —7.7)	—8.6 (—10.2 to —7)	—9.64 (—11.1 to —7.8)	—8.55 (—10.2 to —6.9)	—9.66 (—11.3 to —7.5)	—8.5 (—9.9 to —6.9)
Kmax (D)	69.2 (59.3–75.5)	66.25 (55.6–81.2)	68.06 (56.3–76.9)	65.725 (54.3–83.8)	66.62 (56.1–77.1)	65.575 (53.8–82.9)	67.14 (54.8–80.3)	63.6 (54.1–74.4)
Topo Cyl (D)	—4.72 (—6.3 to —2.7)	—3.78 (—7.4 to —1.5)	—3.3 (—4.7 to —0.8)	—4.2 (—7.6 to —2.6)	—4.4 (—8.7 to —0.9)	—3.925 (—7.6 to —1.1)	—4.92 (—11.4 to —0.9)	—3.85 (—8.1 to —0.9)
CCT (mm)	389.20 (306–502)	428.25 (330–464)	509 (385–599)	523 (420–572)	510.2 (422–617)	544.75 (428–593)	517[b] (427–617)	551 (471–594)
Thinnest point (mm)	360 (255–477)	383.25 (275–451)	468.4 (320–583)	487.75 (359–561)	472.4 (367–575)	496.25 (367–553)	483.6[b] (370–595)	495.75 (410–553)
Visante CCT (mm)	376.4 (280–482)	417.5 (300–459)	497.6 (390–591)	519 (393–578)	496.4 (400–591)	556.25 (428–641)	507.4[b] (426–607)	531.75 (440–568)

CCT = central corneal thickness; CDVA = corrected distance visual acuity; CLVA = rigid contact lens visual acuity; D = diopter; Kmax = maximum keratometry; Km = mean keratometry; Rx Cyl = refractive cylinder; Rx Sphr = refractive sphere; Topo Cyl = topographic cylinder; UVA = unaided visual acuity.

[a]Group 1 underwent decellularized human corneal stroma transplantation ($n = 5$) and group 2 underwent autologous adipose-derived adult stem cell recellularized human corneal stroma transplantation ($n = 4$).

[b]Statistically sigiificant ($P \leq .05$) differences between the preoperative and 6-month postoperative values for each parameter and for each study group separately.

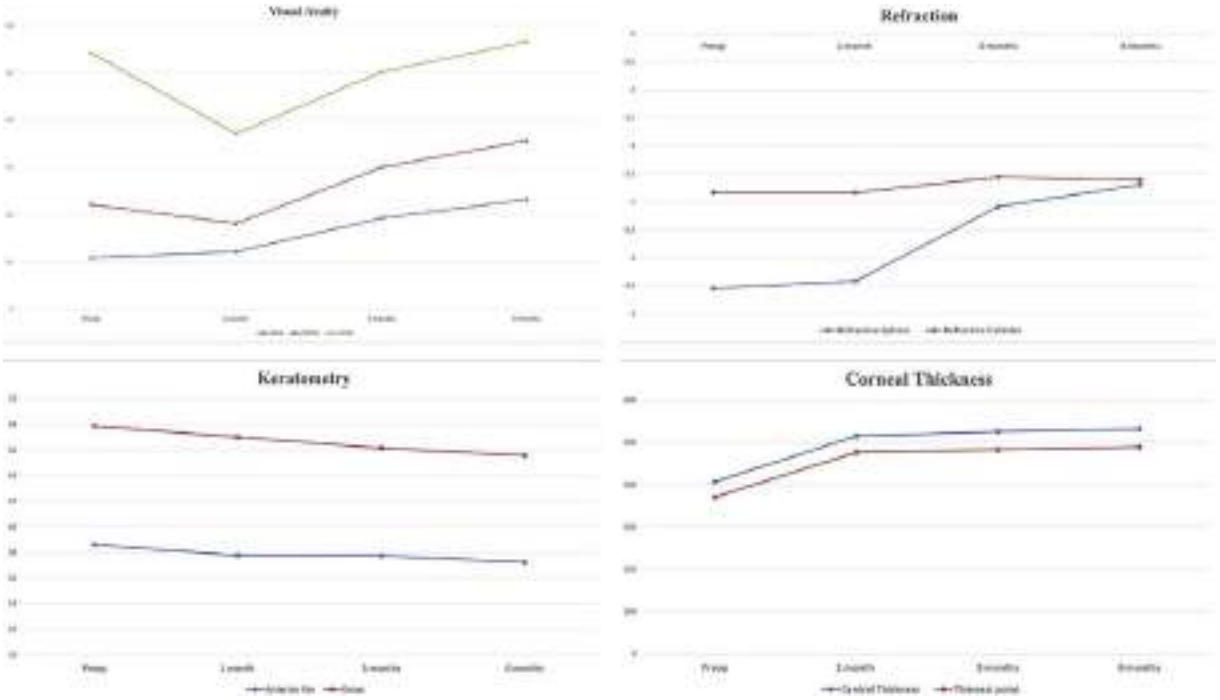

FIGURE 2. Visual (Top left), refractive (Top right), keratometric (Bottom left), and pachymetric (Bottom right) results after 6 months of follow-up. CDVA = corrected distance visual acuity; CLVA = rigid contact lens visual acuity; Kmax = maximum keratometry; Km = mean keratometry; UVA = unaided visual acuity.

right) in all cases. No case showed a residual haze or scarring at the surgical interface 6 months after surgery.

- **CORNEAL TOPOGRAPHY:** An improvement in the anterior keratometry was observed (Figures 2 bottom-left and 4 left), with a mean anterior keratometry (Km) going from 58.6D (range 47.9 to 66.5) preop to 57.24D (range 46.7 to 66.4) 6 months after surgery (p=0.06), and the maximum keratometry (Kmax) changing from 67.89D (range 55.6 to 81.2) to 65.56D (range 54.1 to 80.3) (p=0.21). Posterior keratometry remained stable, with a preoperative posterior Km of -9.19 (range -11.3 to -7.1) and -9.14 (range -11.3 to -6.9) at the 6th postoperative month (p=0.61). We could not demonstrate significant changes in the anterior topographic astigmatism: -4.30D (range -7.4 to -1.5) preop, and -4.44 (range -11.4 to -0.9) 6 months postop (p=0.72). Patient 4 (group 1) preoperatively presented the most advanced cone of the study sample, together with significant anterior stromal paracentral scars not affecting the visual axis. In this patient we could observe a significant worsening of the anterior keratometry (Kmax from 73 to 80.3D; anterior cylinder from -6.3 to -11.4D) in contrast to an improvement of the refractive sphere (from -4.5 to -3.5D) and cylinder (from -5.5 to -4D) correlated with an improvement of one line in all visual parameters (Figure 4 right). This severe keratometric progression may be justified by the presence of stromal scars and may not be real as far as the patient improved clinically. On the other hand, an inferior displacement of the apex of the cone could have induced a central corneal flattening and, subsequently, justify the observed reduction in the refractive sphere. Considering this possible bias, and excluding this case from the analysis, we observed a mean improvement of the anterior Km of 1.51D (from 57.61 to 56.1D) and a mean improvement of 3.52D in the Kmax. No statistically significant differences were observed between groups 1 and 2 (Table 2).

As expected, a mean improvement of 120 µm in all thickness parameters was observed (Figure 2 bottom right). Central corneal thickness improved from 406.56 (range 306 to 502) preoperatively to 532.11 µm (range 427 to 617) 6 months after surgery (p=0.008), and the thinnest point from 370.67 (range 255 to 477) to 489 µm (range 370 to 595) (p=0.008). No significant differences between groups 1 and 2 were detected (Table 2).

- **CORNEAL ABERROMETRY:** Corneal aberrometry with a 6-mm pupil demonstrated an important and significant improvement in the spherical aberration, coma, and total higher order aberrations in all patients except patient 4 (group 1), in which a worsening of the preoperative aberra- tions was observed. We excluded this patient from this analysis to avoid potential bias, in the same manner as discussed earlier. Spherical aberration decreased from 1.30 (range 0.3–2.65) preoperatively to 0.678 µm (range 0.08–2.39)

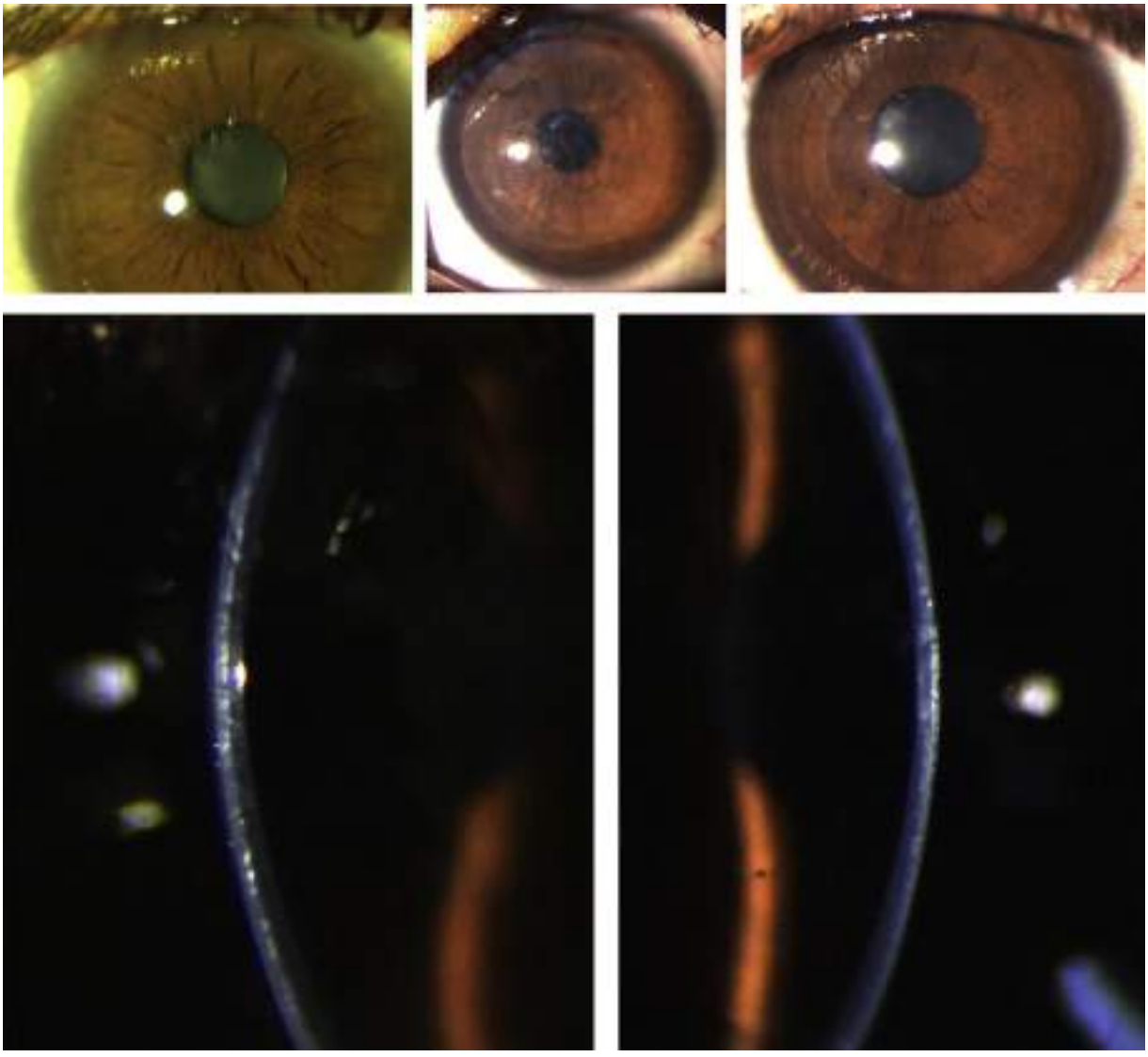

FIGURE 3. Biomicroscopic changes after corneal stroma enhancement. Slit lamp pictures from a patient from group 1 (decellularized lamina transplantation) preoperatively (Top left), 1 week postsurgery (Top middle and Bottom left), and 3 months postsurgery (Top right and Bottom right). Note the complete corneal transparency restoration 3 months postsurgery with a resolution of the initial lenticule haziness observed during the first postoperative weeks.

6 months postsurgery ($P = 0.018$). Coma decreased from 3.49 mm (range 1.20–5.82) preoperatively to 2.06 mm (range 0.8–3.71) 6 months postsurgery ($P = 0.23$). Total higher order aberrations decreased from 4.14 mm (range 1.53–6.13) preoperatively to 2.90 mm (range 1.43–4.78) 6 months postsurgery ($P = 0.31$).

- **ANTERIOR SEGMENT OCT:** Central corneal thickness measured by Visante OCT confirmed the results observed with the topography: a mean preoperative value of 394.66 µm (range 280–482) and 518.22 µm (range 426–607) 6 months after surgery ($P = 0.08$) (Figure 5, , Top right and Bottom right).

The transplanted lamina was clearly visible in the cornea OCT, showing a moderate early postoperative hyper-reflectance during the first postoperative month (Figure 5, Middle top left), in good correlation with the observed mild clinical haze in the implant in the same period of time. By the third postoperative month, the lamina already presented a normal reflectance, equivalent to the surrounding recipient stroma (Figure 5, Middle bottom left). In group 2, the findings were equivalent to those observed in group 1, only the lamina borders presented a slightly higher reflectance by the end of the follow-up (Figure 5, Bottom left). No obvious areas of new collagen production were observed.

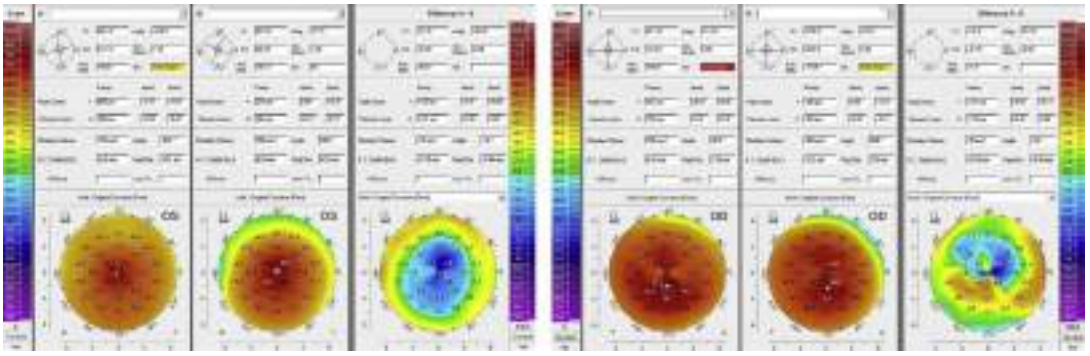

FIGURE 4. Topographic changes after corneal stroma enhancement. (Left) Keratometric change in the same patient shown in Figure 3 preoperatively and 6 months postsurgery. Note the significant flattening of the keratometry and the important improvement in all thickness parameters. (Right) Keratometric change in patient 4 from group 1. This patient had a worsening of anterior keratometry 6 months postsurgery along with refractive, pachymetric, and visual improvement.

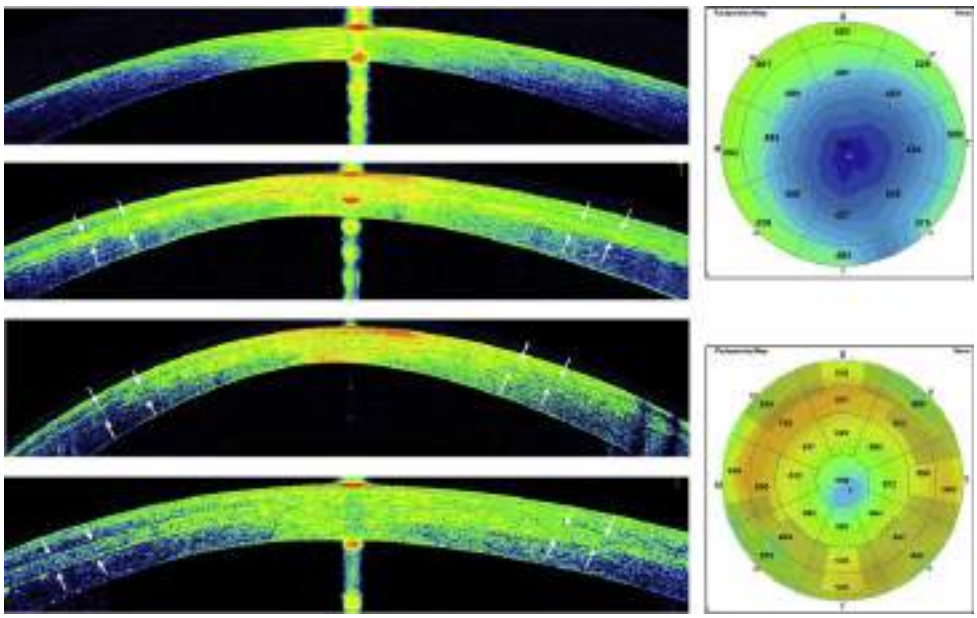

FIGURE 5. Cornea Visante optical coherence tomography images and pachymetric maps from a patient from group 1: preoperatively (Top left and Top right), 1 week postsurgery (Middle top left), and 3 months postsurgery (Middle bottom left and Bottom right). Note the normalization of the early postoperative increased reflectance of the lamina (white arrows) (Middle top left and Middle bottom left) and significant improvement in the pachymetric map (Top right and Bottom right). In patients from group 2, the lamina (white arrows) presented a similar behavior in vivo as group 1 6 months postsurgery (Bottom left), and no obvious areas of newly formed collagen were observed.

• **CONFOCAL BIOMICROSCOPY:** Throughout the first 3 postoperative months, a normal cellular pattern was observed in the anterior and posterior stroma (Figure 6, Top left). The lamina borders were easily visible as a hyperreflective linear band in the interface between the normal cellular anterior or posterior stroma and the acellular transplanted stroma (Figure 6, Top middle). The lamina showed a similar appearance in both groups without relevant differences: totally acellular stroma throughout its thickness (Figure 6, Top right and Bottom left). Six months postsurgery, all patients presented early recellularization signs with scanty isolated cells scattered throughout the lamina (Figure 6, Bottom middle). Two patients (1 from each group) showed a higher recellularization of the lamina, with more abundant cells colonizing the implanted stroma (Figure 6, Bottom right).

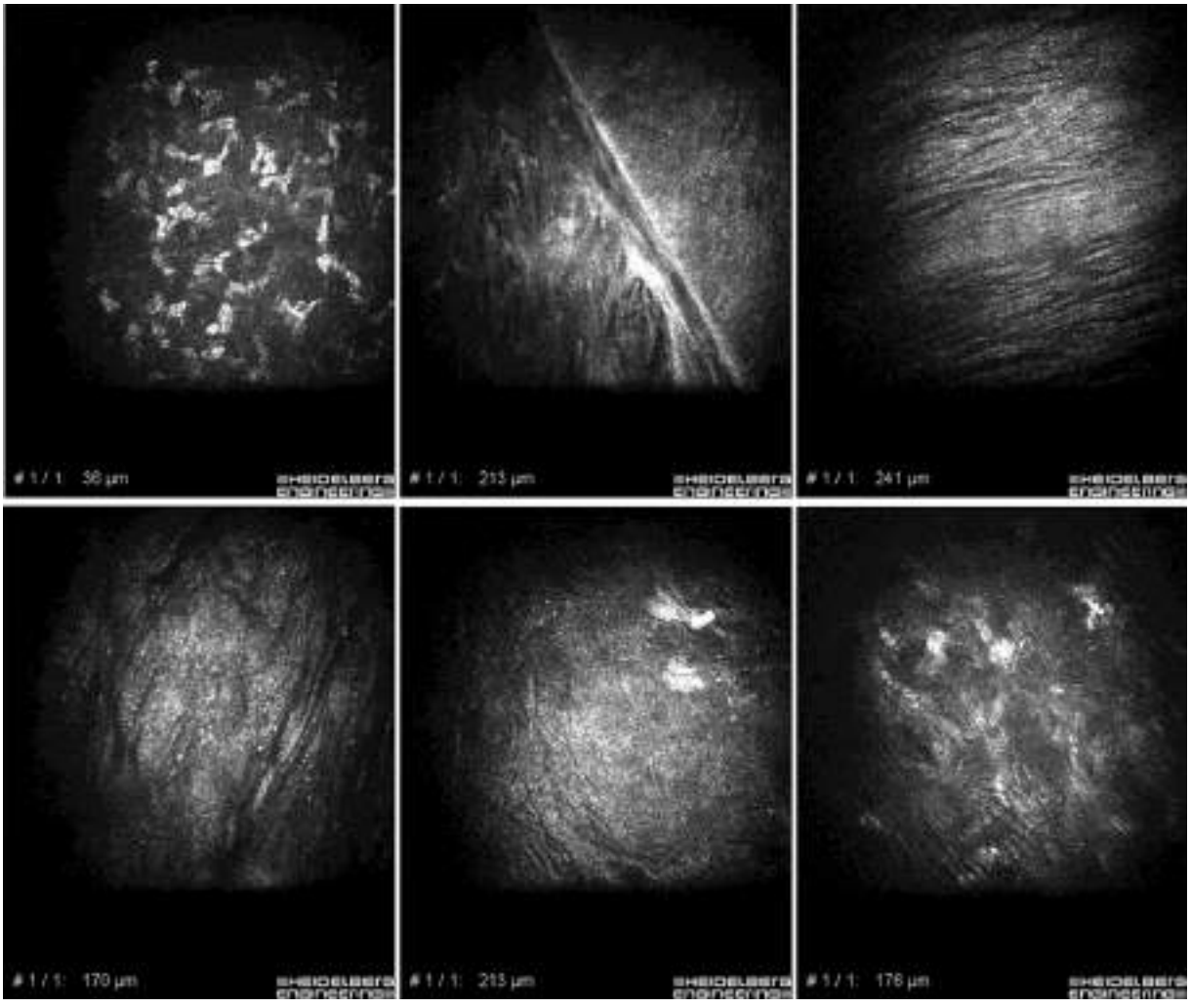

FIGURE 6. Corneal confocal biomicroscopy results from the corneal stroma anterior to the transplanted lamina (Top left), anterior edge of the lamina (Top middle), group 1 implanted lamina showing a complete acellular pattern 3 months postsurgery (Top right), group 2 implanted lamina showing a complete acellular pattern 3 months postsurgery (Bottom left), early recellularization signs in a group 1 lamina 6 months postsurgery (Bottom middle), and a more intense recellularization in a group 2 lamina 6 months postoper- atively (Bottom right).

As previously described, keratocyte cellular density (cells/mm^2) was measured preoperatively 6 months postsur- gery. Both anterior and posterior stroma keratocyte densities showed a mild increasing tendency, but this was statistically significant in the posterior stroma (anterior stroma from 207 [range 163.3–286.6] to 247 [range 190–356.6] [$P = 0.21$]; posterior stroma from 186.7 [range 136.6–216] to 238.4 [range 163.3–293.3] [$P = 0.015$]).

This observed mild increase in the keratocyte density at the anterior and posterior stroma could be in relation to an activation of the host keratocytes that are responsible for the early recellularization observed within the implanted tis- sue 6 months postsurgery, where the lamina presents a mean keratocyte density of 54.6 cells/mm^2 (range 16–156). No significant differences between groups 1 and 2 were detected (Table 3).

• OTHER CLINICAL OUTCOMES: There were no significant changes in intraocular pressure ($P = 0.213$) or endothelial cell density ($P = 0.327$).

Five patients received superficial laminas, including Bowman membrane (4 in group 1 and 1 in group 2), and 4 patients received the deeper lamina without this layer (1 in group 1 and 3 in group 2). Patients containing superficial laminas did not have better outcomes in any of the analyzed parameters of the study.

DISCUSSION

KERATOCONUS MANAGEMENT IS IN CONSTANT EVOLUtion, and in the last few years alternative and innovative

TABLE 3. Keratocyte Cellular Density for Groups 1 and 2[a]

	Preoperatively, Mean (Range)		6 Months Postoperatively, Mean (Range)	
	Group 1	Group 2	Group 1	Group 2
Anterior stroma (cells/mm^2)	222.6 (163–286.6)	187.6 (176.6–198)	215.3 (190–273.3)	286.6 (210–356.6)
Posterior stroma (cells/mm^2) Grafted	181.8 (136.6–216)	192.8 (174–203.3)	239.1[b] (213.3–265)	237.4 (163–293.3)
stroma (lamina; cells/mm^2)	N/A	N/A	54.1 (22.5–156)	55.2 (16–117.5)

N/A = not applicable.

[a]Group 1 underwent decellularized human corneal stroma transplantation (n = 5) and group 2 underwent autologous adipose-derived adult stem cell recellularized human corneal stroma transplantation (n = 4) before and 6-months postsurgery.

[b]Statistically significant ($P \leq 0.05$) differences between the preoperative and 6-month postoperative values for each parameter and for each study group separately.

approaches have been proposed to minimize the invasiveness of classical corneal transplantation techniques for the most advanced cases.[1] Regenerative medicine of the corneal stroma is a novel and promising line of therapy for keratoconus and other corneal dystrophies.[13] However, its efficacy still remains to be properly established, and an improved stem cell delivery technique is needed. Nevertheless, the demonstrated production of new human extra- cellular matrix by the transplanted mesenchymal stem cells into the corneal stroma in vivo in animal models,[4–10] and in humans,[13] is not expected to be enough to rehabilitate a severely thinned cornea. In this scenario, we postulated that the addition of decellularized corneal stromal tissue could enhance the previously observed results with cellular therapy alone,[13] because it provides a tectonic support and an ideal environment for the stem cells.[15,22]

The current study presents a novel treatment line for advanced keratoconus cases, with a straightforward and quick surgical technique that can be performed under topical anasthesia and can achieve a partial functional rehabilitation of the advanced ectatic cornea and an almost complete thickness recovery. This potentially allows these corneas to be candidates again for further noninvasive surgical visual rehabilitation techniques. Also, each donor cornea can easily generate up to 3 donor laminas following this model, which could partially solve the world's shortage of donor corneas, improving patient access to corneal trans- plantation in many parts of the world. Moreover, the decellularization technique using sodium dodecyl sulfate solution is a noncomplex and nonexpensive method that allows the removal of the entire allogeneic donor cellular component from the graft, avoiding any rejection risk, while the remaining extracellular matrix still preserves its normal architecture as has been demonstrated in vitro and in the animal model by our group and other authors.[14,15,22]

In this phase 1 pilot clinical trial, we report for first time, to the best of our knowledge, the implantation of decellularized corneal stromal tissue into the human cornea in vivo. The selected lamina thickness (120 µm) was decided upon in relation to our previous experience in the animal model.[15] We considered this thickness ideal to rehabilitate the advanced keratoconic cornea, and thicker implants may not easily fit within the intrastromal pocket. Moreover, in our previous experimental studies we observed that thin laminas were occasionally damaged during the laboratory tissue processing and, because human stromal collagen presents with a high compaction degree, decellularization was not optimal and presented heterogeneously when thick laminas were processed (unpublished data). All visual parameters moderately improved more than 1 line, achieving statistically significant differences on the unaided visual acuity despite the small study sample. This correlates well with the significant improvement of the refractive sphere and spherical aberration. All anterior keratometric parameters—coma and total higher order aberrations—systematically improved. However, we could not reach statistical significance in the current study because of the small sample size (n=9) analyzed. In fact, a mean improvement of the anterior Km and Kmax of 1.5 and 3.5 D, respectively, can be expected considering our results. All thickness parameters significantly improved over 100 µm, achieving almost normalization of the corneal thickness. As initially postulated, we did not observe any clinical inflammatory signs during the follow-up, and there were no obvious inflammatory cells during confocal biomicroscopy. We only observed a mild lenticule haze the first postoperative month in good correlation with the initial drop in the visual function; this was fully recovered by the third postoperative month in all patients. This lack of interface haze up to postoperative month 6 may be in relation with the acellular category of the implanted tissue and the lack of donor keratocytes whose activation could induce haze. In addition, recellularized laminas did not show postoperative haze because they were colonized initially by ADASCs and not by adult keratocytes. Mesenchymal stem cells have been postulated to avoid or even improve preexisting scars, although no differences in corneal transparency could be demonstrated among groups.[6–9]

On the other hand, within 6 months of follow-up, we were not able to show potential advantages of adding mesenchymal stem cells to the decellularized stromal lamina. Recellularized grafts did not show a faster visual recovery, enhanced outcomes, or areas of new collagen production using corneal OCT. However, we cannot discard the possible advantages of the transplanted ADASCs in the long-term maintenance of the collagen lenticule. In our previous study with ADASCs alone in the same type of patients, we observed a slight improvement in their visual function and in the central corneal thickness, with new collagen production.[13] Additional studies with longer follow-up and larger samples are required to clarify the possible role of the cellular therapy in addition to this type of corneal implant.

Melles and associates recently described the outcomes with the transplantation of the Bowman membrane (BM) into the mid-stroma of advanced keratoconic eyes in a similar fashion as the present study.[23] Taking into account the limitations of our small study sample, we did not find differences between patients receiving laminas containing or not containing the BM. If this preliminary finding is confirmed in additional studies, it would suggest that we could graft several laminas from each donor cornea without compromising the clinical outcome. Our clinical results are not preliminarily better than those reported with the BM transplantation as an isolated layer, although the addition of stroma permits a full restoration of the thickness (that is not achieved with BM only). Our approach opens an exciting field for research to explore how established visual rehabilitation techniques, such as corneal collagen crosslinking and intracorneal ring segments, behave in the advanced keratoconic eye with stromal thickness restoration.

An important finding shown in the current study is the fact that early recellularization signs by the host keratocytes have been observed 6 months postsurgery in all patients. We could not demonstrate this host recellularization of the decellularized laminas in our previous animal studies with 3 months of follow-up.[15] Other authors have previously reported this host keratocyte infiltration into decellularized grafts in animal models for anterior lamellar keratoplasty.[24] To the best of our knowledge, we are reporting for the first time this finding for intrastromal decellularized implants. This host recellularization would allow a complete functionalization of the implanted tissue, which should ensure long-term transparency maintenance of the cornea.

A relevant issue not clarified in the present study is whether the intrastromal implantation of decellularized stromal tissue (with or without stem cells) could halt the natural progressive condition of this disease. Study patients with advanced keratoconic eyes were already candidates for corneal transplantation, and the preoperative progressive status of the disease was not determined. Therefore, further biomechanical studies will be required to answer this question. Nevertheless, all patients but 1 (with the limitations already discussed in this case) presented with stabilization or progressive improvement of the visual and keratometric parameters.

In conclusion, corneal stroma enhancement by decellularized corneal stromal lamina transplantation is a novel technique that could be an alternative for advanced keratoconic eyes compared to classical corneal transplantation techniques. Additional studies with longer durations of follow-up and larger sample sizes are necessary to confirm the preliminary results shown in this pilot clinical trial.

FUNDING/SUPPORT: NO FUNDING OR GRANT SUPPORT. FINANCIAL DISCLOSURES: MAR´IA P. DE MIGUEL HAS RECEIVED A grant from Roche Farma SA. Jorge L. Alió has received clinical research grants from Akkolens, Carl Zeiss Meditec, CSO, Dompe, Hanita Lenses, Medi- phacos, Santen, Oculentis, and Schwind Eye-Tech-Solutions; lecturer fees from Ophthec and Schwind, and is an equity owner of Oftalcare Nutravision, Santen, VisiDome, and Blue-Green. He is a consultant for Akkolens, Carl Zeiss Meditec, Hanita Lenses, Maghrabi Hospital, Oculentis, Omeros, Presbia, Santen, Slack Inc, and Topcon Medical Systems and owns patents in Jaypee Brothers Pub. The following authors have no financial disclosures: Jorge L. Alió del Barrio, Mona El Zarif, Albert Azaar, Nehman Makdissy, Charbel Khalil, Walid Harb, Ibrahim El Achkar, and Ziad Abdul Jawad. All authors attests that the current ICMJE criteria for authorship.

Publication of this article was supported by Optica General (Saida, Lebanon), Reviva Regenerative Medicine Center (Beirut, Lebanon), and the The- matic Network OFTARED-RETICS (Spain). The authors have not received any payment as consultants, reviewers or evaluators of any of the devices, instruments or drugs mentioned in this article.

We thank Marc Assouwad and Peggy Saba from Laser Vision (Beirut, Lebanon), Laurent Bataille from Vissum Corporación (Alicante, Spain), Sandy El-Hage from Reviva Regenerative Medicine Center (Beirut, Lebanon), and Heidelberg Engineering (Heidelberg, Germany) for their great support and assistance to the project.

REFERENCES

1. Arnalich-Montiel F, Alió del Barrio JL, Alió JL. Corneal surgery in keratoconus: which type, which technique, which outcomes?. *Eye Vis (Lond)*. 2016; 3:2.
2. Gain P, Jullienne R, He Z, et al. Global Survey of Corneal Transplantation and Eye Banking. *JAMA Ophthalmol*. 2016; 134(2):167-173.
3. Ruberti JW, Zieske JD. Prelude to corneal tissue engineering—Gaining control of collagen organization. *Prog Retin Eye Res*. 2008; 27(5):549–577.
4. Arnalich-Montiel F, Pastor S, Blazquez-Martinez A, et al. Adipose-derived stem cells are a source for cell therapy of the corneal stroma. *Stem Cells*. 2008; 26(2):570–579.
5. Espandar L, Bunnell B, Wang GY, Gregory P, McBride C, Moshirfar M. Adipose-derived stem cells on hyaluronic acid-derived scaffold: a new horizon in bioengineered cornea. *Arch Ophthalmol*. 2012; 130(2):202–208.
6. Mittal SK, Omoto M, Amouzegar A, et al. Restoration of Corneal Transparency by Mesenchymal Stem Cells. *Stem Cell Reports*. 2016; 7(4):583-590.
7. Demirayak B, Yüksel N, Çelik OS, et al. Effect of bone marrow and adipose tissue-derived mesenchymal stem cells on the natural course of corneal scarring after penetrating injury. *Exp Eye Res*. 2016; 151:227-235.
8. Du Y, Carlson EC, Funderburgh ML, et al. Stem cell therapy restores transparency to defective murine corneas. *Stem Cells*. 2009; 27(7):1635–1642.
9. Liu H, Zhang J, Liu CY, et al. Cell therapy of congenital corneal diseases with umbilical mesenchymal stem cells: lumican null mice. *PLoS One*. 2010; 5(5):e10707.
10. Coulson-Thomas VJ, Caterson B, Kao WW. Transplantation of human umbilical mesenchymal stem cells cures the corneal defects of mucopolysaccharidosis VII mice. *Stem Cells*. 2013; 31(10):2116–2126.
11. Kao WW, Coulson-Thomas VJ. Cell Therapy of Corneal Diseases. *Cornea*. 2016; 35 Suppl 1:S9-S19.
12. De Miguel MP, Fuentes-Julián S, Blázquez-Martínez A, et al. Immunosuppressive properties of mesenchymal stem cells: advances and applications. *Curr Mol Med*. 2012; 12(5):574-591.
13. Alió del Barrio JL, El Zarif M, de Miguel MP, et al. Cellular Therapy with Human Autologous Adipose-derived Adult Stem Cells for Advanced Keratoconus. *Cornea*. 2017; 36(8):952-960.
14. Lynch AP, Ahearne M. Strategies for developing decellularized corneal scaffolds. *Exp Eye Res*. 2013; 108: 42-47.
15. Alió del Barrio JL, Chiesa M, Garagorri N, et al. Acellular human corneal matrix sheets seeded with human adipose-derived mesenchymal stem cells integrate functionally in an experimental animal model. *Exp Eye Res*. 2015; 132:91–100.
16. Alió JL, Piñero DP, Alesón A, et al. Keratoconus-integrated characterization considering anterior corneal aberrations, internal astigmatism, and corneal biomechanics. *J Cataract Refract Sur*g. 2011; 37(3):552-568.
17. Zuk PA, Zhu M, Mizuno H, et al. Multilineage cells from human adipose tissue: implications for cell-based therapies. *Tissue Eng*. 2001; 7(2):211-228.
18. Zuk PA, Zhu M, Ashjian P, et al. Human adipose tissue is a source of multipotent stem cells. *Mol Biol Cell*. 2002; 13(12):4279-4295.
19. Bourin P, Bunnell BA, Casteilla L, et al. Stromal cells from the adipose tissue-derived stromal vascular fraction and culture expanded adipose tissue-derived stromal/stem cells: a joint statement of the International Federation for Adipose Therapeutics and Science (IFATS) and the International Society for Cellular Therapy (ISCT). *Cytotherapy*. 2013; 15(6):641-648.
20. Ponce Márquez S, Martínez VS, McIntosh Ambrose W, et al. Decellularization of bovine corneas for tissue engineering applications. *Acta Biomater*. 2009; 5(6):1839-1847.
21. Ku JY, Niederer RL, Patel DV, Sherwin T, McGhee CN. Laser scanning in vivo confocal analysis of keratocyte density in keratoconus. *Ophthalmology*. 2008; 115(5):845-850.
22. Yam GH, Yusoff NZ, Goh TW, et al. Decellularization of human stromal refractive lenticules for corneal tissue engineering. *Sci Rep*. 2016; 6:26339.
23. van Dijk K, Liarakos VS, Parker J, et al. Bowman layer transplantation to reduce and stabilize progressive, advanced keratoconus. *Ophthalmology*. 2015; 122(5):909-917.
24. Hashimoto Y, Funamoto S, Sasaki S, et al. Corneal Regeneration by Deep Anterior Lamellar Keratoplasty (DALK) Using Decellularized Corneal Matrix. *PLoS One*. 2015; 10(7):e0131989.

10.4. Alió, J., Alió Del Barrio, J., El Zarif, M., Azaar, A., Makdissy, N., Khalil, C., Harb, W., El Achkar, I., Jawad, Z., De Miguel, M., 2019. **Regenerative surgery of the corneal stroma for advanced keratoconus: 1-year outcomes**. Am J Ophthalmol 203, 53–68. https://doi.org/10.1016/j.ajo.2019.02.009

Regenerative Surgery of the Corneal Stroma for Advanced Keratoconus: 1-Year Outcomes

JORGE L. Alió, JORGE L. Alió DEL BARRIO, MONA EL ZARIF, ALBERT AZAAR, NEHMAN MAKDISSY, CHARBEL KHALIL, WALID HARB, IBRAHIM EL ACHKAR, ZIAD ABDUL JAWAD, AND María P. DE MIGUEL

PURPOSE: This study evaluated 1-year safety and efficacy outcomes of corneal stroma cell therapy. Therapy consisted of implanting autologous adipose-derived adult stem cells (ADASCs) with or without sheets of decellularized donor human corneal stroma within the stroma of patients with advanced keratoconus.

DESIGN: This was a prospective interventional non-randomized series of cases.

METHODS: Fourteen consecutive patients were selected and divided into 3 experimental groups. Group A patients underwent implantation of autologous ADASCs alone (3 x 10^6 cells/1 mL) (n = 5). Group B patients received decellularized donor 120 µm thick corneal stroma lamina alone (n = 5). Group C patients had implantation of recellularized donor lamina with 1 X 10^6 autologous ADASCs plus another 1 x 10^6 cells/1 mL of PBS at the time of the surgery (n = 4). Autologous ADASCs were obtained by elective liposuction. Implantation was performed in the corneal stroma through a femtosecond-assisted 9.5-mm diameter lamellar dissec-tion with the patient under topical anesthesia. Twelve months of follow-up data are presented.

RESULTS: No complications were observed during the 1-year follow-up, and full corneal transparency was recovered within 3 months in all patients. No patient lost lines of visual acuity. Corrected distance visual acuity improved 0.231, 0.264, and 0.094 Snellen lines in groups 1, 2, and 3, respectively. In group 1, refractive parameters showed an overall stability, whereas in groups 2 and 3, sphere improved 2.35 diopter (D) and 0.625 D, respectively. Anterior keratometry remained stable (group 1) and improved in groups 2 and 3 (mean improvement of 2D). Corneal aberrometry improved significantly. In optical coherence tomography scans, corneal thickness showed a mean improvement of 14.5 µm (group 1) and 116.4 µm (groups 2 and 3) in the central thickness, and new collagen production was observed at the surgical plane (group 1). Confocal biomicroscopy confirmed the host recellularization of the implanted laminas.

CONCLUSIONS: Intrastromal implantation of autologous ADASCs and decellularized human corneal stroma did not show complications at 1 year of follow-up and were moderately effective for the treatment of advanced keratoconus. Am J Ophthalmol 2019;203:53–68.

Cellular therapy of the corneal stroma has been gaining interest in the last few years as a potential alternative treatment for corneal stroma diseases such as corneal scarring, dystrophies and ectasias. Along the recent years, pioneer human clinical studies have demonstrated that autologous mesenchymal adipose-derived human stem cells are able to produce corneal collagen when injected into the cornea stroma [1] and also that such cells when use together to acellular corneal laminas can increase the thickness of the keratoconic cornea in calculated amounts preserving cornea transparency and improving vision [2,3]. Such human clinical studies were supported by a background of previous experimental animal studies in which the possibilities of such therapy were confirmed as well as the potential advantages that such therapy might had in the treatment of corneal dystrophies and even corneal scarring processes. [4-12]

Corneal ectasias, such as keratoconus, are characterized by progressive thinning, bulging, and distortion of the cornea, with secondary loss of vision due to high, irregular astigmatism.[13] Visual rehabilitation of advanced corneal ectasias requires penetrating or lamellar corneal transplantation techniques, which present several drawbacks, such as graft rejection, failure and slow visual recovery due to high levels of induced postoperative astigmatism in relation to the suture.[13] Also, in many countries, access to donor corneal tissue is limited; approximately 53% of the world's population has no access to corneal transplan-tation.[14]

As an alternative, tissue engineering of the cornea aims to avoid corneal graft by replacing the diseased corneal tissue by using human stem cells and scaffolds. However, the highly complex structure of corneal stroma has, until now, limited the usefulness of these corneal substitutes in clinical practice due to a lack of either transparency or tissue strength properties.[15] On the other hand, stem cells from either ocular or extraocular

Accepted for publication Feb 6, 2019.

From the Cornea, Cataract, and Refractive Surgery Unit (J.L.A., J.L.A.DB.), Vissum Corporacio´n, Vissum, Instituto Oftalmologico de Alicante, Caban˜al, 1, 03016 Alicante, Spain; Division of Ophthalmology (J.L.A., J.L.A.DB.), Universidad Miguel Herna´ndez, Alicante, Spain; Optica General (M.E.Z., Z.A.J.), Saida, Lebanon; Reviva Regenerative Medicine Center (A.A., C.K., W.H.), Middle East Institute of Health University Hospital. Beirut, Lebanon; Lebanese University (N.M.), Beirut, Lebanon; Saint-Joseph University (I.E.A.), Beirut, Lebanon; and Cell Engineering Laboratory (M.P. DM.), IdiPAZ, La Paz Hospital Research Institute, Madrid, Spain.

Inquiries to Prof. Jorge L. Alio´, Vissum, Instituto Oftalmologico de Alicante, c/Caban˜al, 1, 03016 Alicante, Spain; e-mail: jlalio@vissum.com

https://doi.org/10.1016/j.ajo.2019.02.009

sources are capable of not only survival and in vivo differentiation into adult human keratocytes but also production of new collagen within the host stroma.[4,5] There is evidence that these cells improve corneal transparency in animal models for corneal dystrophies by corneal stroma remodeling and host keratocyte modulation by paracrine secretion.[6–11] Such cells also show immunomodulatory properties in syngeneic, allogeneic, and even xenogeneic scenarios.[11, 16]

In addition, several corneal decellularization techniques have been described that provide an acellular corneal extracellular matrix.[17] These scaffolds have become more popular in the last few years as they provide a natural environment for the growth and differentiation of cells and are well tolerated even by xenogeneic recipients, because components of the extracellular matrix are generally preserved among species.[12]

Adipose-derived adult stem cells (ADASCs) are 1 type of stem cell that has been proposed for corneal cell therapy. Our research group performed an initial animal experiment[4] in which human ADASCs were implanted into the corneal stroma of the albino rabbit and were later analyzed by immunohistochemical methods after 6 months. The outcomes demonstrated the presence of human collagen in the rabbit cornea, obviously produced by the implanted ADASCs. The corneas were transparent in all cases of the experiment, demonstrating that the newly created collagen was also transparent and not showing any evidence of scar-ring. Other experiences reported by our group in the exper-imental animal model demonstrated that decellularized laminas of corneal stroma were better suitable as carriers of the ADASCs[12] than other carrier laminas from other bio-logical or synthetic materials.[18] Other studies have confirmed the capability of mesenchymal stem cells to differentiate into keratocytes,[4–9] a finding that suggests that such stem cells could be useful in corneal surgery aiming to improve the corneal cell density in corneal cell therapy and even corneal transparency following trauma and in some corneal dystrophies.[6–11]

Considering all this evidence, our group recently reported for the first time in a phase 1 clinical trial the initial clinical outcomes of ADASCs and decellularized corneal laminas used as cellular therapy of corneal stroma in patients with advanced keratoconus, demonstrating excellent preliminary safety levels in terms of lack of com-plications at 6 month follow-up period and good clinical outcomes in terms of increased corneal thickness, regularity, and transparency.[1–3]

The present paper reports initial, preliminary 1-year out-comes to verify the hypothesis that it is possible to increase the corneal thickness in advanced keratoconus cases and to improve the optical behavior and preserve the corneal transparency of such corneas with consequent improvement in vision. For this purpose, we analyzed and report here the 1-year outcomes of a clinical study of cellular therapy of the corneal stroma in patients with advanced keratoconus following the intrastromal implantation of ADASCs alone, decellularized human corneal stromal laminas, or ADASCs recellularized human corneal stromal laminas.

METHODS

THE AUTHORS ARE REPUBLISHING THE METHODS INITIALLY

reported with the 6-month results of this study. Duplicate publication of the methods was accepted so that the full project would appear in a format suitable for a thesis of the American Ophthalmological Society.

- **STUDY APPROVAL, DESIGN, AND SUBJECTS**

This investigation was designed as an interventional, prospective, non-randomised consecutive series of cases. It was performed based on the cooperation among the following institutions: Research, Development and Innovation Department of Vissum Instituto Oftalmologico de Alicante, Miguel Hernandez University, Alicante (Spain), Optica General (Saida, Lebanon), Laser Vision Center (Beirut, Lebanon) and REVIVA Research and Application Center (Middle East Hospital, Beirut, Lebanon). The Institutional Review Board (IRB) Ethical committee of Reviva Research and Application Center approved this study. All patients gave informed written consent for every one of the procedures. The study was conducted in strict adherence to the tenets of the Declaration of Helsinki and it was registered in ClinicalTrials.gov (Code: NCT02932852).

Fourteen patients were selected and enrolled in the study during the 3-month enrollment period and were consecutively divided into 3 study groups. Group 1 patients were treated with autologous ADASCs implantation (n = 5 patients); group 2 patients received decellularized human corneal stroma transplantation (n = 5 patients); and group 3 patients received autologous ADASCs recellularized human corneal stroma transplantation (n = 4 patients).

Patient recruitment was closed after 3 months. The outcomes of the study were expected to be evaluated and reported at the end of 6 and 12 months after surgery. The study endpoint was established at 1 year after the implanta-tion. Clinical monitoring of the patients for the purpose of safety was established monthly and at 1 week and at 1, 3, 6, and 6 months for the purpose of the other clinical outcomes of the investigation. Interim analysis of the cases was planned to be performed and reported with the 6- and 12-month data. The results from the interim analysis reported by our group performed at 6 months was published previously.[1,2]

Patients were selected by the clinical staff from among patients who were followed for the treatment or eventual surgery for keratoconus by local physicians in Lebanon, as a compassionate alternative for the patients' disease. Data about the potential evolution of the disease in the selected eyes were

inconclusive in most cases due to the lack of previous historical information, especially corneal topography maps. The clinical monitor of the study and the one responsible for the assessment and recording of clinical data was M.E.Z.

Inclusion criteria: Advanced keratoconus defined as stage ≥ IV according to the RETICS keratoconus classification (19); age ≥ 18 years; negative human immunodeficiency virus (HIV), hepatitis B (HBV), hepatitis C (HCV) serology; no history of malignancy. Sex was not considered to be relevant for the purpose of patient selection.

Exclusion criteria: criteria included corrected dis-tance visual acuity (CDVA) (decimal scale) <0.1 in the contralateral eye; active concomitant inflam-matory eye disease; other ophthalmic comorbidity, such as cataract, retinal diseases or glaucoma; any pre-vious ocular surgical interventions other than cata-ract; any previous corneal intervention including collagen cross-link; previous corneal hydrops or central corneal scars; history of cognitive impairments or dementia which might have affected the patient's ability to participate in the informed consent process and to appropriately complete evaluations; any im-munodeficiency or immunosuppressive therapy; serologic evidence of infection with HBV, HCV, or HIV; and pregnancy or breast feeding. Keratoconus progression status was not considered an exclusion or in-clusion criteria.

- **AUTOLOGOUS ADASCs ISOLATION, CHARACTERIZATION AND CULTURE:** The procedure was previously described in a publication from our group.[20,21] Briefly, patients were subjected to standard liposuction under good medical practice conditions. Approximately 250 mL of fat mixed with local anesthesia was obtained, washed in phosphate-buffered saline (PBS), and digested in colla-genase I for 40 minutes at 37^{8}C. Then, collagenase was inhibited by adding autologous human serum. Erythrocytes were lysed in erythrocyte lysis buffer (Gibco-Life Technologies, Gaithersburg, Maryland). Then the pelleted cells were cultured in Dulbecco's modified eagle medium with sodium pyruvate and L-glutamine (GlutaMAX; (Gibco), 10% autologous human serum, and 1% penicillin-streptomycin (Gibco) plus 0.2% amphotericin B (Gibco).

Cell characterization was performed by CD34^{þ}CD45 CD105^{þ} labeling and flow cytometry anal-ysis as requested by International Federation of Adipose Therapeutics (IFATS).[22] Then, 60 to 80 hours before surgery, quiescence was induced, reducing the amount of serum to 0.5%. The ADASc were implanted in a physiological status more closely resembling the natural non-proliferative stromal keratocytes, as proliferative stem cells within the corneal stroma could potentially induce

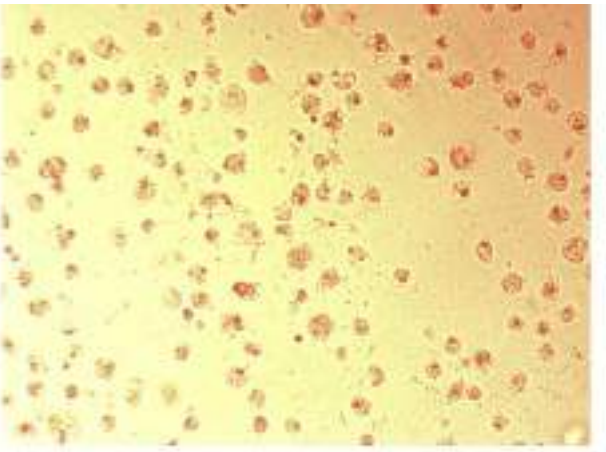

FIGURE 1. Phase-contrast view of autologous adipose-derived adult stem cells (ADASc) after trypsinization and before trans-plantation (x10 magnification).

Stromal scarring or haze. Quiescence as well as absence of apoptosis and aneuploidy were verified by propidium iodide labeling (Invitrogen, Carlsbad, California) and cell cycle analysis.[1–4,12]

In group 1, just before the injection, cells were harvested by trypsinization (Sigma-Aldrich, St. Louis, Missouri). A total of 3 3 x 10^{6} cells per patient were prepared in saline (Figure 1). This cellular concentration was established according to the observed outcomes of our previous experimental studies and aimed to compensate the expected high cellular loss happening after the implant due to the leakage of the solution.[4,12,18]

In group 3, 24 hours before implantation, the ADASCs were harvested by trypsinization (Sigma-Aldrich). An aliquot of 0.5 x 10^{6} cells were cultured on each side of the decellularized corneal stroma lamina for 24 and 12 hours, respectively.

- **DECELLULARIZATION AND RECELLULARIZATION OF HUMAN CORNEAL STROMA LAMINAS:** Corneal stroma from non-viable transplantation donor human corneas with negative viral serology were used. Corneas were supplied by the eye bank Banco de Ojos para el tratamiento de la Ceguera, Centro de Oftalmologı´a Barraquer (Barcelona, Spain) following Directives 2004/23/EC and 206/ 17/EC for standards of quality and safety for the donation, procurement, testing, processing, preservation, storage, and distribution of human tissues and cells were are followed.

Corneal laminas from the donor corneas were prepared on an artificial anterior chamber (Barron, Katena Products, Denville, New Jersey). The epithelium was mechanically removed, and the anterior corneal stroma was cut using a 60-kHz IntraLase iFS femtosecond laser (Advanced Medical Optics, Santa Anna, California) in 2 consecutive laminas of 120 µm thickness and 9.0-mm diameter. These samples were subsequently washed in PBS (Sigma-Aldrich) supplemented with a 1% antibiotic-antimycotic solution (Gibco).

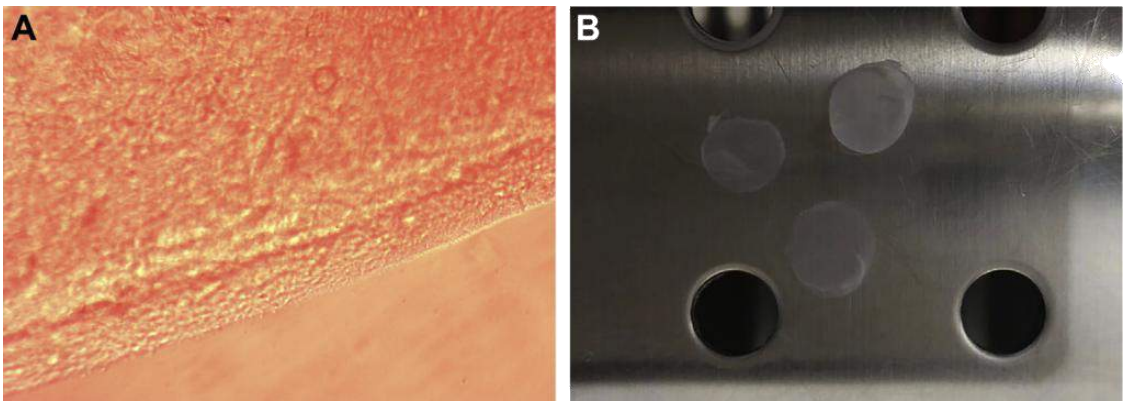

FIGURE 2. (A) Phase-contrast view of a lamina 10 hours after adding ADASCs to the first side of the lamina (310 magnification [photo was taken at the peripheral border]). (B) Macroscopic appearance of the laminas under phosphate-buffered saline in a culture well. ADASCs (autologous adipose-derived adult stem cells).

Femtosecond laser parameter settings were equiv-alent to the ones used for laser-assisted in situ keratomileusis (LASIK) flap dissection, except for an anterior side-cut angle of 360º. With this procedure, 2 laminas were obtained, a superficial one containing Bowman's membrane and a deeper one without. The remaining poste-rior cornea was discarded. The decellularization protocol was based on previous publications.[12,23] The laminas were immersed in 1% (wt/vol) solution of sodium dodecylsulfate (Sigma-Aldrich) with a protease inhibitor cocktail (P8340; Sigma-Aldrich), and incubated in an orbital shaker (at 75 rpm) for 24 hours at room temperature. Then, the laminas were washed 8 times in PBS with 1% antibiotic-antimycotic solution under the same condi-tions for 15 minutes each at room temperature. To remove DNA, the laminas were incubated in DNAse (Benzonase Nuclease, 6.5 U/mL; Merck, Darmstadt, Germany) in PBS with the same protease inhibitor cocktail under the same conditions at 37ºC for 72 hours. Then, the corneal laminas were washed 8 times for 15 mins each in PBS with a 1% antibiotic-antimycotic solution (Figure 2B). Twenty-four hours before implantation, those laminas planned for patients receiving recellularized tissue (group 3) were placed in tissue culture wells for recellularization with ADASCs (0.5 x 10^6 cells were cultured on each side of the lamina) (Figure 2A). Following the recellularization process, the laminas were transferred to the operating room for implantation in PBS. Superficial (laminas with Bowman's membrane) or deep laminas (without) were randomly used for transplantation in groups 2 and 3.

- **SURGICAL PROCEDURE:**

1. Autologous ADASCs implantation. Topical anesthesia was used. The 60-kHz IntraLase iFS femtosecond laser (Advanced Medical Optics) was used in a single-pass mode for the recipient corneal lamellar dissection. An intrastromal lamellar cut of 9.5 mm in diameter was created at half depth of the preoperative thinnest pachymetry point, as measured by the Visante anterior segment optical coherence tomography (OCT) (Carl Zeiss, Jena, Germany). A 30-degree anterior side-cut incision was made. The femtosecond laser parameter settings were similar to the ones used for LASIK. The corneal intrastromal pocket was opened with a Morlet lamellar dissector (Duckworth & Kent, reading, UK). Then, 3 million autologous ADASCs contained in 1 mL of PBs were injected into the pocket with a 25-G cannula. Previous to the cellular injection, a 1-mm corneal paracentesis was performed to reduce the intraocular pressure and allow a larger volume to be injected into the stromal pocket. A topical antibiotic and steroid (tobramycin/dexamethasone [Tobradex]; Alcon, Elkridge, Maryland) was applied at the end of the surgery. Corneal sutures were not used.

2. Lenticule implantation. Topical anesthesia with oral sedation was used for all surgeries. As described above, the 60-kHz IntraLase iFS femtosecond laser was used in single-pass mode for the recipient corneal lamellar dissection. The femtosecond laser-assisted corneal dissection ended with a 50-degree anterior side cut as a corneal incision. The corneal intrastromal pocket was then opened, and the lamina was inserted, centered, and unfolded through gentle taping and massaging from the host epithelial surface. As done in the previous group, a temporal limbal paracentesis was performed just before implantation in order to reduce the intraocular pressure. In patients who were receiving a recellularized lamina (group 3), in order to compensate for the expected cellular damage by the implantation process, the pocket was irrigated immediately before and after insertion, using a solution containing an additional 1 million autologous ADASCs in 1 mL of PBS. Cells were injected by using a 25-G cannula. The incision was then closed by using 1 interrupted 10/0 Nylon suture. The suture was removed 1 week after the operation.

Topical tobramycin/ dexamethasone (Alcon) was applied at the end of the surgery. All surgeries were performed by the same surgeons (J.L.A. and J.L.A.B.) at Laser Vision Center (Beirut, Lebanon).

- **POSTOPERATIVE CARE AND FOLLOW-UP SCHEDULE:**

Topical tobramycin/dexamethasone (Alcon) was used every 6 hours for 1 week, followed by a descending dose of topical dexamethasone 0.1% (Maxidex; Alcon) for 3 more weeks. Patients affected by allergic or vernal conjunc-tivitis were maintained on the previous antiallergic medi-cation used by the patient as necessary.

For the purpose of safety, the patients were evaluated monthly by the study clinical monitor (M.E.Z.) who recorded any evidence of ocular inflammation, subjective discomfort, or sudden unexpected visual loss. For the pur-pose of the evaluation of the other clinical parameters, the patients were followed at 1 day and 1 week and at 1, 3, 6, and 12 months postoperatively. The following data were recorded throughout the preoperative assessment, as well as at 1, 3, 6, and 12 months: unaided visual acuity (UVA), corrected distance visual acuity (CDVA), rigid contact lens visual acuity (CLVA), manifest refraction, slit lamp biomicroscopy, fundoscopy, intraocular pressure (IOP), endothelial cell count by specular microscopy (Nidek, Aichi, Japan), corneal topography (Pentacam; Oculus Inc., Wetzlar, Germany), corneal aberrometry (Sirius, CSO, Florence, Italy) with 6-mm pupils, anterior segment OCT-Visante (Carl Zeiss), and corneal confocal biomicroscopy using the Retinal Tomograph-3 (HRT3) Rostock Cornea Module (HRT3; Heidelberg Engineering Inc., Heidelberg, Germany). Intrastromal in vivo keratocyte cell counts were performed as previously described[24]: anterior stroma was defined as the stroma immediately after Bowman's membrane up to the anterior edge of the implanted lamina. Posterior stroma was defined, for the purpose of the study, as the stroma between the posterior edge of the lamina and immediately anterior to Descemet's membrane. The transplanted mid stroma was defined as the tissue between the anterior and posterior edges of the implanted lamina. Three clear images without motion blur or compression lines were selected from each sector (anterior, lamina, and posterior). Thus, 9 frames per subject were selected for analysis and reviewed by an experienced observer (M.E.Z.). For all images, a standard frame size of 100 x 100 μm was selected, and keratocytes with clear cell borders within this area (using a medium image bright-ness and contrast) were manually counted. Subsequent keratocyte density (cells per square millimeter) was recorded.

- **STATISTICAL ANALYSIS:** Statistical analysis was performed using SPSS version 20.0 software (SPSS Inc., IBM, Armonk, New York) for Windows (Microsoft, Edmond, Washington). Due to the study sample (n =14), non-parametric statistics were used. The Wilcoxon rank sum test was applied to assess the significance of differences between preoperative and postopera-tive data. For all statistical tests, the same level of significance was used [$P < 0.05$].

RESULTS

FOURTEEN PATIENTS WERE RECRUITED. THEIR MEAN AGEwas 33.28 years old (range: 24–49 years of age; mean of 34.2 years of age for group 1, 32.2 years of age for group 2, and 36.25 years of age for group 3). The study sample was composed of 9 females and 5 males (female/male ratio of 2/3 for group 1, 4/1 for group 2, and 3/1 for group 3) as well as 10 right eyes and 4 left eyes.

All surgeries were performed without any intraoperative complications, except for a limited anterior stromal incision tear during the implantation of the graft in 1 patient from group 2. This was managed with a bandage contact lens for 1 week, and a full recovery without further complications was observed. Thirteen patients completed the 12-month follow-up. One patient from group 1 was lost after the first postoperative month due to inability to attend further follow-up visits (for reasons unrelated to the study), so that patient was excluded from the subsequent analysis; however, that patient was followed by phone call interviews from the study's clinical monitor (M.E.Z.) on a monthly basis and by another physician who was recruited at the patient's new residence for biomicroscopy and clinical follow-up. No complication had been recorded before the exclusion of this patient, and no subjective negative observation or biomicroscopy or visual complications were described by the recruited ophthalmic professional. The outcomes of the study are summarized in (Tables 1 and 2).

VISUAL ACUITY: All patients moderately improved their visual function regarding the UVA, CDVA and CLVA (Figure 3), and no patient experience any loss of lines in any of these visual parameters. However, the visual improvement pattern showed different between group 1 (G1) and groups 2-3 (G2 and G3). In group 1, UVA and CDVA improvement was obtained mostly along the first postoperative month, showing an overall stabilization thereafter (mean improvement of 2.1 lines ±1.3 [$P = 0.07$] and 2.3 lines ±1.7 [$P = 0.11$] in UVA and CDVA respectively 1 year after surgery). On the other hand, best visual acuity with rigid contact lenses (CLVA) showed a progressive improvement up to the 12th month (mean total improvement of 2.6 lines ±1.0 [$P = 0.07$]), although showing already signs of stabilization after 3 months (Figure 3).

In G2 and G3, visual acuity parameters showed, as expected, an initial worsening within the first postoperative month

TABLE 1. Visual, Refractive, Keratometric, and Pachymetric Outcomes

	Preoperation mean [median] (range)			1 Month mean [median] (range)			3 Months mean [median] (range)			6 Months mean [median] (range)			12 Months mean [median] (range)		
	Group 1	Group 2	Group 3	Group 1	Group 2	Group 3	Group 1	Group 2	Group 3	Group 1	Group 2	Group 3	Group 1	Group 2	Group 3
UVA (decimal)	0.1 [0.07] (0.05–0.2)	0.07 [0.05] (0.05–0.15)	0.16 [0.12] (0.05–0.33)	0.3 [0.35] (0.1–0.4)	0.11 [0.1] (0.1–0.15)	0.137 [0.12] (0.1–0.2)	0.29 [0.33] (0.15–0.365)	0.21 [0.2] (0.15–0.3)	0.17 [0.17] (0.1–0.233)	0.233 [0.25] (0.1–0.333)	0.25 [0.2] (0.15–0.475)	0.21 [0.15] (0.1–0.45)	0.31 [0.32] (0.15–0.45)	0.24[a] [0.2] (0.1–0.5)	0.25 [0.23] (0.1–0.45)
CDVA (decimal)	0.32 [0.35] (0.2–0.4)	0.17 [0.15] (0.1–0.265)	0.29 [0.32] (0.1–0.4)	0.52 [0.55] (0.2–0.8)	0.17 [0.15] (0.15–0.265)	0.191 [0.2] (0.1–0.266)	0.49 [0.5] (0.2–0.75)	0.29 [0.3] (0.2. 0.425)	0.31 [0.29] (0.15–0.5)	0.481 [0.45] (0.4–0.625)	0.36 [0.4] (0.2–0.5)	0.35 [0.37] (0.1–0.55)	0.56 [0.56] (0.4–0.7)	0.43[a] [0.4] (0.2–0.6)	0.38 [0.44] (0.1–0.55)
CLVA (decimal)	0.51 [0.52] (0.4–0.6)	0.52 [0.57] (0.2–0.85)	0.56 [0.49] (0.4–0.875)	0.65 [0.66] (0.5–0.8)	0.34 [0.36] (0.2–0.475)	0.412 [0.35] (0.2–0.75)	0.74 [0.75] (0.5–0.95)	0.44 [0.45] (0.266–0.65)	0.57 [0.52] (0.45–0.8)	0.762 [0.84] (0.5–0.875)	0.48 [0.5] (0.2–0.7)	0.67 [0.61] (0.55–0.9)	0.77 [0.84] (0.5–0.9)	0.56 [0.52] (0.2–0.85)	0.69 [0.7] (0.5–0.875)
Rx Sphr (D)	—4.06 [—4.37] (—7 to —0.5)	—5.15 [—4.5] (—12 to —1)	—3.81 [—4.12] (—6.75 to —0.25)	—3.69 [—3.5] (—7 to —0.75)	—5.25 [—4.5] (—12 to —1)	—3.38 [—4.12] (—5 to —0.25)	—3.81 [—3.25] (—8 to —0.75)	—3 [—3.5] (—5.5 to —1)	—3.19 [—3.5] (—5.5 to —0.25)	—3.562 [—3.5] (—6.5 to —0.75)	—2.5 [—2.5] (—4 to —1)	—2.94 [—2.5] (—6.5 to —0.25)	—3.56 [—3] (—7.5 to —0.75)	—2.8 [—2] (—5 to —1)	—3.19 [—2.5] (—7.5 to —0.25)
Rx Cyl (D)	—2.94 [—3] (—3.5 to —2.25)	—2.65 [—2] (—5.5 to —1.5)	—3.06 [—3] (—3.25 to —3)	—3.56 [—3.75] (—4.5 to —2.25)	—2.75 [—3] (—4 to —1.5)	—2.937 [—3] (—3.25 to —2.5)	—3.19 [—3.25] (—4 to —2.25)	—2.30 [—2] (—3.25 to —1.25)	—2.87 [—2.75] (—3.50 to —2.50)	—3.25 [—3.25] (—4 to —2.5)	—2.4 [—2] (—4 to —1.25)	—2.87 [—2.75] (—3.5 to —2.5)	—3.5 [—3.25] (—4.5 to —3)	—2.5 [—2.5] (—4 to —1.5)	—2.87 [—3] (—3 to —2.5)
Anterior Km (D)	55.95 [55.5] (47.9–64.9)	60.02 [63.1] (50.5–66.5)	56.83 [57] (47.9–65.4)	56.95 [56] (50.2–65.6)	59.34 [61.9] (49.4–66.3)	55.8 [55.7] (47.5–64.3)	56.1 [55.7] (49.6–63.4)	59.26 [60.4] (52.9–65.1)	55.82 [55.45] (46.9–65.5)	56.82 [55.55] (50.8–65.4)	58.62 [60.6] (48.4–66.4)	55.52 [56.6] (46.7–62.2)	56.65 [55.55] (50.1–65.4)	58.02 [59.7] (48.3–66.2)	55.25 [56.35] (46.5–61.8)
Posterior Km (D)	—8.3 [—8.45] (—9.7 to —6.6)	—9.58 [—10.3] (—11.3 to —7.6)	—8.7 [—8.75] (—10.2 to —7.1)	—8.55 [—8.45] (—10.2 to —7.10)	—9.62 [—10.1] (—11.3 to —7.7)	—8.6 [—8.6] (—10.2 to —7)	—8.37 [—8.45] (—9.8 to —6.8)	—9.64 [—10] (—11.1 to —7.8)	—8.55 [—8.55] (—10.2 to —6.9)	—8.52 [—8.45] (—10.2 to —7)	—9.66 [—10.10] (—11.3 to —7.5)	—8.5 [—8.6] (—9.9 to —6.9)	—8.52 [—8.45] (—10.2 to —7)	—9.64 [—10] (—11.4 to —7.7)	—8.52 [—8.6] (—10 to —6.9)
Kmax (D)	66.3 [64.55] (56.7–79.4)	69.2 [70.4] (59.3–75.5)	66.25 [64.1] (55.6–81.2)	68.8 [65.35] (63.2–81.3)	68.06 [70.9] (56.3–76.9)	65.72 [62.4] (54.3–83.8)	68.32 [64.55] (62.1–82.1)	66.62 [68.6] (56.1–77.1)	65.57 [62.8] (53.8–82.9)	67.95 [64.4] (61.8–81.2)	67.14 [68.3] (54.8–80.3)	63.6 [62.95] (54.1–74.4)	68.32 [64.75] (62.6–81.2)	65 [66.9] (54.8–77.4)	64.67 [66.15] (53.3–73.1)
Topo Cyl (D)	—2.95 [—2.8] (—5.8 to —0.4)	—4.72 [—5.3] (—6.3 to —2.7)	—3.78 [—3.1] (—7.4 to —1.5)	—3.47 [—3.3] (—5.8 to —1.5)	—3.3 [—3.8] (—4.7 to —0.8)	—4.2 [—3.3] (—7.6 to —2.6)	—3.37 [—3.5] (—5.3 to —1.2)	—4.4 [—3.8] (—8.7 to —0.9)	—3.92 [—3.5] (—7.6 to —1.1)	—3.1 [—3] (—5.7 to —0.7)	—4.92 [—4.5] (—11.4 to —0.9)	—3.85 [—3.2] (—8.1to —0.9)	—3.02 [—3.25] (—5.4 to —0.2)	—4.78 [—3.5] (—10.7 to —1.1)	—4.3 [—3.15] (—8.9 to —2)
CCT (mm)	463 [456] (438–503)	389.20 [381] (306–502)	428.25 [459.5] (330–464)	456 [452.5] (435–484)	509 [522] (385–599)	523 [550] (420–572)	465 [456] (439–509)	510.2 [501] (422–617)	544.75 [579] (428–593)	460 [447] (434–512)	517 [509] (427–617)	551 [569.5] (471–594)	456.5 [449] (436–492)	513.6[a] [509] (425–606)	536.75 [563.5] (447–573)

Continued on next page

TABLE 1. Visual, Refractive, Keratometric, and Pachymetric Outcomes (*Continued*)

	Preoperation mean [median] (range)			1 Month mean [median] (range)			3 Months mean [median] (range)			6 Months mean [median] (range)			12 Months mean [median] (range)		
	Group 1	Group 2	Group 3	Group 1	Group 2	Group 3	Group 1	Group 2	Group 3	Group 1	Group 2	Group 3	Group 1	Group 2	Group 3
Thinnest point (mm)	405.7 [398.5] (394–432)	360 [364] (255–477)	383.25 [403.5] (275–451)	407.75 [406] (406–438)	468.4 [482] (320–583)	487.75 [515.5] (359–561)	411 [410] (378–446)	472.4 [481] (367–575)	496.25 [532.5] (367–553)	404.5 [402.5] (364–449)	483.6 [485] (370–595)	495.75 [510] (410–553)	405 [408] (364–440)	481.8[a] [481] (368–591)	474.25 [479] (384–555)
Visante CCT (mm)	429.5 [423.5] (407–464)	376.4 [370] (280–482)	417.5 [455.5] (300–459)	428.75 [420.5] (406–468)	497.6 [498] (390–591)	519 [552.5] (393–578)	439.75 [430] (421–478)	496.4 [497] (400–591)	556.25 [578] (428–641)	446 [442] (419–481)	507.4 [503] (426–607)	531.75 [559.5] (440–568)	444 [437.5] (420–481)	501.2[a] [500] (426–597)	525.5 [547.5] (438–569)

ADASC = adipose-derived adult stem cells; CCT = central corneal thickness; CDVA = corrected distance visual acuity; CLVA = contact lens visual acuity; D = diopters; Km = mean keratometry; Kmax = maximum keratometry; Rx Cyl = refractive cylinder; Rx Sphr = refractive sphere; Topo Cyl =topographic cylinder.

Decimal indicates the scale for visual parameters. Data show visual, refractive, keratometric, and pachymetric outcomes for Group 1, autologous ADASCs implantation (n = 5); Group 2, decellularized human corneal stroma implantation (n = 5); and Group 3, autologous ADASC recellularized human corneal stroma implantation (n = 4).

[a]Statistically significant ($P \leq 0.05$) differences between the preoperative and 12-month postoperative values for each parameter and for each study group separately.

TABLE 2. Mean Changes From Baseline to 12th Postoperative Month For Visual, Refractive, Keratometric, and Pachymetric Parameters

	12 Months Postoperation to Preoperation		
	Group 1 mean [median] (range)	Group 2 mean [median] (range)	Group 3 mean [median] (range)
UVA (decimal)	0.21 [0.17] (0.1–0.4)	0.17 [0.1] (0.05–0.45)	0.09 [0.05] (0.03–0.25)
CDVA (decimal)	0.23 [0.26] (0–0.4)	0.26 [0.3] (0.05–0.5)	0.09 [0.09] (0–0.2)
CLVA (decimal)	0.26 [0.29] (0.1–0.35)	0.04 [0] (0.05 to 0.17)	0.13 [0.1] (0–0.32)
Rx Sphr (D)	0.5 [0.12] (0.5 to 2.75)	2.35 [0.25] (0.5 to 10)	0.62 [0.12] (0.75 to 3)
Rx Cyl (D)	0.56 [0.62] (1.5 to 0.5)	0.15 [0] (0.5 to 1.5)	0.19 [0] (0–0.75)
Anterior Km (D)	0.70 [0.4] (0.2 to 2.2)	2 [2.2] (4.9 to 0.9)	1.58 [2.15] (3.6 to 1.6)
Posterior Km (D)	0.22 [0.2] (0.5 to 0)	0.06 [0.1] (0.5 to 0.3)	0.17 [0.1] (0.2 to 0.7)
Kmax (D)	2.02 [1.3] (0.4 to 5.9)	4.20 [4.5] (10.3 to 4.4)	1.58 [0.10] (10 to 3.5)
Topo Cyl (D)	0.08 [0.1] (1.9 to 1.8)	0.06 [0.5] (4.4 to 4.4)	0.53 [0.3] (1.5 to 0)
CCT (mm)	6.75 [9] (13 to 4)	124.40 [119] (104–157)	108.5 [108] (101–117)
Thinnest point (mm)	0.75 [7.5] (30 to 12)	121.20 [115] (113–140)	91 [102] (48–112)
Visante CCT (mm)	14.5 [15] (19 to 47)	124.8 [119] (114–146)	108 [107] (80–138)

ADASCs = adipose-derived adult stem cells; CCT = central corneal thickness; CDVA = corrected distance visual acuity; CLVA = contact lens visual acuity; D = diopters; Km = mean keratometry; Kmax = maximum keratometry; Rx Cyl = refractive cylinder; Rx Sphr = refractive sphere; Topo Cyl = topographic cylinder.

Decimal indicates the scale for visual parameters. Data show mean changes from baseline to the 12th postoperative month for visual, refractive, keratometric, and pachymetric parameters for group 1, autologous ADASCs implantation (n = 4); Group 2, decellularized human corneal stroma implantation (n = 5); and Group 3, autologous ADASCs recellularized human corneal stroma implantation (n = 4).

(in relation with a mild graft edema), with a subsequent progressive improvement over time, observing already a net improvement compared with preoperative values 3 months after surgery (for UVA and CDVA) and 6 months postop (for CLVA) (Figure 3). Mean UVA changed from 0.11 (range 0.05 to 0.33; Snellen 20/200) to 0.25 (range 0.1 to 0.5; Snellen 20/80) 12 months after surgery [P = 0.007) (mean improvement of 1.7 lines ±1.6 [P = 0.04] and 1 line ±1.0 [P = 0.06] in G2 and G3 respectively); mean CDVA changed from 0.22 (range 0.1 to 0.4; Snellen 20/100) to 0.41 (range 0.1 to 0.6; Snellen 20/50) [P = 0.01] (mean improvement of 2.6 lines ±1.7 [P = 0.04] and 0.9 lines ±0.08 [P = 0.1] in G2 and G3 respectively); and mean CLVA changed from 0.54 (range 0.2 to 0.87; Snellen 20/40) to 0.62 (range 0.2 to 0.87; Snellen 20/32) [P = 0.04] (mean improvement of 0.4 lines ±0.08 [P = 0.28] and 1.3 lines ±0.13 [P = 0.1] in G2 and G3 respectively) (Table 1 and 2).

- **MANIFEST REFRACTION:** In G1, refractive parameters showed an overall stability (Figure 3), presenting a mean sphere improvement of 0.498D ±1.5 [P = 0.90] 1 year after surgery, and a mean cylinder deterioration of -0.56D ± 0.82 [P = 0.20] (Table 1 and 2). In G2 and G3, refractive sphere improved from a preoperative mean value of -4.55D (range -12 to -0.25) to -2.97D (range -7.5 to -0.25) 12 months after surgery [P = 0.23] (mean improvement of 2.35D ±4.37 [P = 0.27] and 0.62D ± 1.63 [P = 0.59] in G2 and G3 respectively). On the other hand, refractive cylinder remained stable, showing only a mild improvement tendency (Figure 3): from preop mean value of -2.83D (range -5.5 to -1.5) to 12 months postop mean value of -2.66D (range -4 to -1.5) [P = 0.46] (mean improvement of 0.15D ± 0.78 [P = 1] and 0.19D ± 0.37 [P = 0.31] in G2 and G3 respectively) (Table 1 and 2).

- **SLIT LAMP BIOMICROSCOPY:** All corneas were, preoperatively, free of posterior stromal or predescemetic scars and presented a clear visual axis. Only three patients (one per group) presented mild paracentral non-visually significant anterior stromal scars. No postoperative complications including inflammation or rejection signs were recorded throughout the follow-up in all patients.

In G1, corneal transparency was fully recovered within 24 hours after the surgical procedure and continued throughout the whole follow-up period. As described in our previous article,[1] 1 patient from G1 presented with some anterior stromal scars, and a mild improvement of those scars was observed after the third postoperative month, although without a complete resolution up to 12 months postoperatively.

In G2 and G3, the implanted lamina showed a mild early haziness in relation to a mild lenticulare edema during the first postoperative month (which correlated well with the initial loss in the visual parameters) (Figure 4A and B).

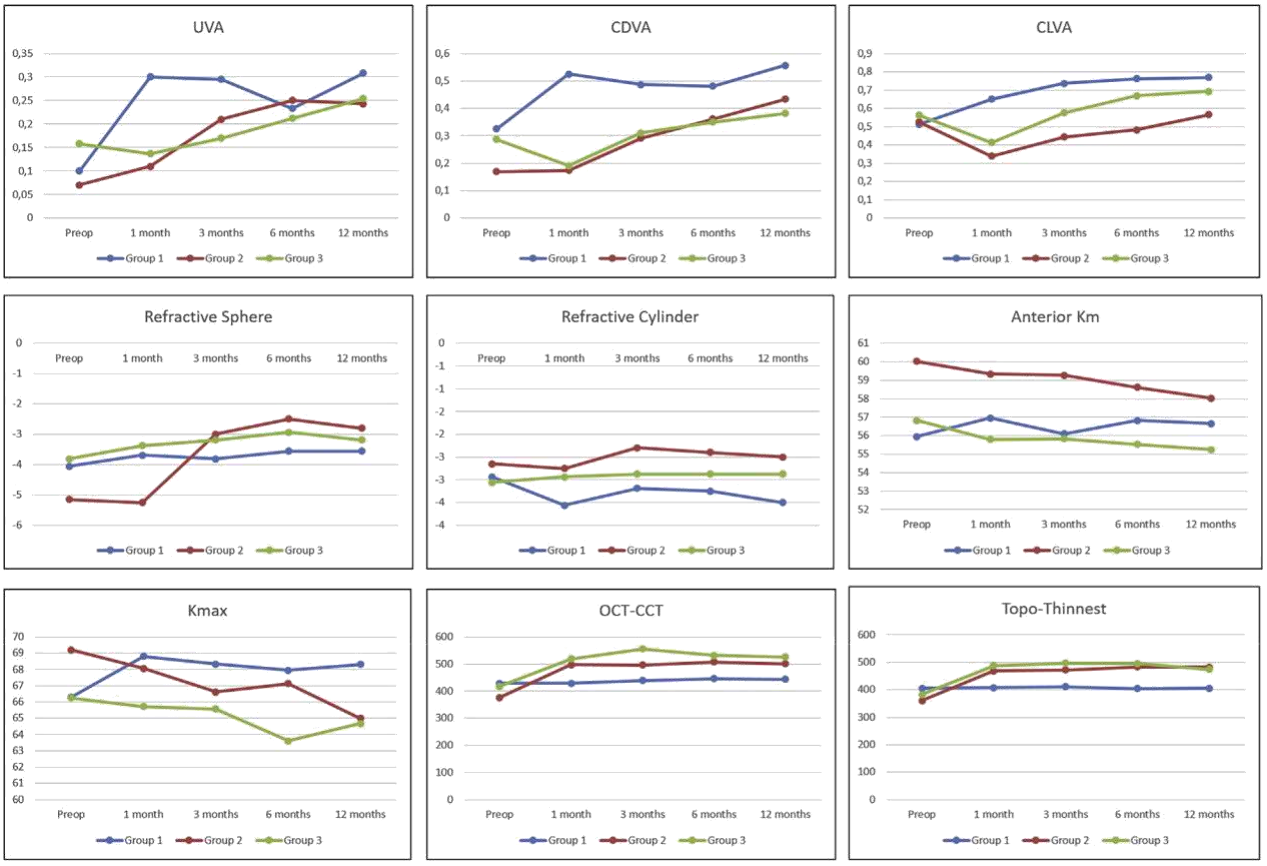

FIGURE 3. Visual, refractive, keratometric, and pachymetric outcomes 12 months after surgery. Central corneal thickness was measured by AS-OCT (OCT-CCT). The thinnest point was measured by Pentacam topographer (Topo-Thinnest). AS-OCT [ante-rior segment optical coherence tomography; CDVA = corrected distance visual acuity; CLVA = (rigid) contact lens visual acuity; Km = mean keratometry; Kmax = maximum keratometry; OCT-CCT = optical coherence tomography central corneal thickness; UVA = unaided visual acuity.

Corneal transparency improved progressively throughout the follow-up, showing complete restoration 3 months after surgery in all cases. Twelve months after surgery, no patient presented with significant interface haze or scarring (Figure 4C and D), although some scattered faint patchy ‘‘islands’’ of haze could be observed in most of the G1 and G2 patients, which resulted, however, in no impact on visual outcome (Figure 5). One patient in G1 and another in G2 presented with preoperative anterior stromal scars, but no clinical improvement was observed during the full follow-up period.

- **CORNEAL TOPOGRAPHY:** In G1, all keratometric parameters presented a relative stability (Table 1 and 2, Figure 3 and Figure 6 A). Anterior mean keratometry (Km) remained stable except in one patient who presented a deterioration of 2.2D. However, same patient’s topographic anterior cylinder significantly improved (from -2 preop to -0.2D at 12th month), explaining the visual improvement observed in this patient.

Mean anterior Km changed from 55.95D (range 47.9 to 64.9) to 56.65 (range 50.1 to 65.4) 12 months after surgery [P = 0.14] (mean deterioration of 0.7 ±1.04). Mean anterior astigmatism changed from -2.95D (range -5.8 to -0.4) to -3.02 (range -5.4 to -0.2) 12 months after surgery [P = 0.72] (mean deterioration of -0.08 ±1.56). Mean anterior maximum keratometry (Kmax) changed from 66.3D (range 56.7 to 79.4) to 68.32 (range 62.6 to 81.2) 12 months after surgery [P = 0.14] (mean deterioration of 2.02 ±2.74). Pachymetric values measured by Pentacam remained stable (Table 1 and 2, Figure 3 and 6 A), without detecting any obvious enhancement in the corneal thickness parameters.

In groups 2 and 3, an improvement in all anterior keratometric parameters was observed (Table 1 and 2, Figure 3 and Figure 6 A), with a mean anterior keratometry (Km) going from 58.6D (range 47.9 to 66.5) preop to 56.78D (range 46.5 to 66.2) 12 months after surgery [P=0.05] (mean improvement of -2D ±2.35 [P = 0.13] and -1.58D ±2.31 [P = 0.27] in G2 and G3

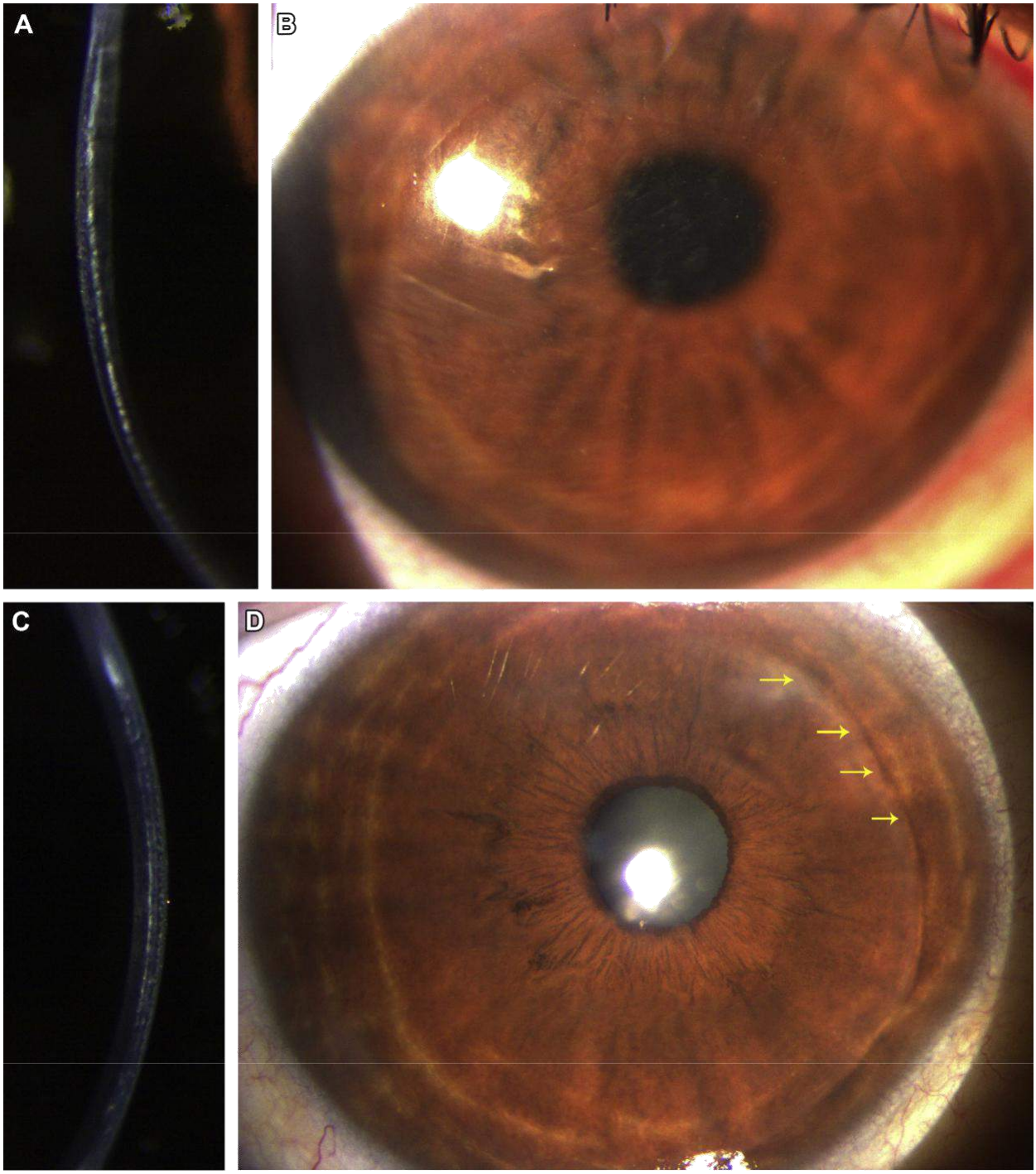

FIGURE 4. Biomicroscopic changes after corneal stroma enhancement. Slit lamp views are from group 2 patient (case 7) showing decellularized lamina transplantation, 1 week (A and B) and 12 months after surgery (C and D) yellow arrows show the lenticule edges.

respectively), and the Kmax changing from 67.89D (range 55.6 to 81.2) to 64.85D (range 53.3 to 77.4) [P = 0.21] (mean improvement of -4.20D ±5.82 [P = 0.13] and -1.58D ±6.16 [P = 0.26] in G2 and G3 respectively). We could not demonstrate significant changes in the anterior topographic astigmatism: -4.30D (range -7.4 to -1.5) preop, and -4.56 (range -10.7 to -1.1) 12 months postop [P = 0.52]. As expected, a mean improvement of 120 µm in all thickness parameters was observed in G2 and G3 (Figure 3 and 6 B and Table 1 and 2).

- **CORNEAL ABERROMETRY**: In G1, corneal aberrometry could not be analyzed due to missing preoperative data. In G2 and G3, corneal aberrometry with 6-mm pupil normalization of the reflectance demonstrated an important and significant

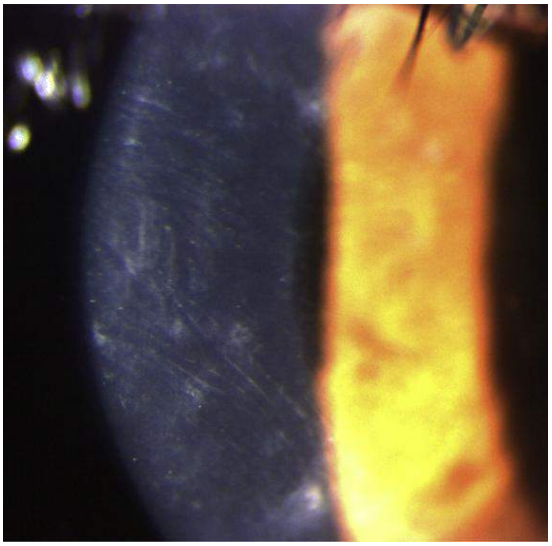

FIGURE 5. Some scattered, faint, patchy ‘‘islands’’ of haze could be observed in most of the group 1 and 2 patients. These areas of haze had no impact on the visual outcome.

improvement in the spherical aberration, coma, and total higher order aber-rations in all patients except 1 patient from G2 who presented the steepest cone of the study sample, and no reliable data could be obtained. We excluded that patient from this analysis to avoid potential bias:

- **Spherical aberration:** from 1.30 (range: 0.3–2.65) preop to 0.66 µm (range: 0.07–2.05) 12 months after surgery [P = 0.04];
- **Coma:** from 3.49 (range: 1.20–5.82) preop to 2.09 µm (range: 0.53–2.93) 12 months after surgery [P = 0.07];
- **Total higher order abberations:** from 4.14 (range: 1.53–6.13) pre op to 3.04 µm (range: 1.33–4.4) 12 months after surgery [P = 0.24].

No significant differences between the 6- and 12-month postoperative visits were observed in any of these values.

ANTERIOR SEGMENT OCT: In G1, a mild improvement in the central corneal thickness measured by anterior segment OCT (Visante) was observed in three of four patients, with a mean increase of 14.5 ±27 µm at the 12th month visit [P = 0.47]. This improvement in the thickness occurred after the 3d month, where (in all patients except in the one without thickness improvement) a hyperreflective band at the level of the stromal pocket compatible with an area of new collagen production could be observed (Figure 7 A). This area was not homogeneously distributed along the pocket. One year after surgery, two of these patients showed a partial normalization of the reflectance of the neo-collagen band (Figure 7 B), while in one patient its high reflectance was still obvious (Figure 7 C).

In G2 and G3, central corneal thickness measured by OCT Visante confirmed the results observed with the topography: mean preop value of 394.66 µm (range 280 to 482) and 512 µm (range 426 to 597) twelve months after surgery [P = 0.008] (mean improvement of 124.8 µm ±13.44 [P = 0.04] and 108 µm ±24.05 [P = 0.06] in G2 and G3 respectively). The transplanted lamina was clearly visible in the cornea OCT, showing a moderate early postoperative hyper-reflectance during the first postoperative month (Figure 8A), in good correlation with the observed mild clinical haze in the implant in the same period of time. After the third postoperative month, the lamina already presented a normal reflectance, equivalent to the surrounding recipient stroma (Figure 8B). In G2 and G3 the findings were equivalent, and no obvious areas of new collagen production were observed in G3.

- **CONFOCAL BIOMICROSCOPY:** In G1, up to Postoperative month 3, round-shaped cells were observed in the surgical plane in all cases (Figure 9A). These cells showed a different morphology than the usual dendritic or fusiform shape presented by the anterior and posterior stromal kera-tocytes (Figure 9B).[1,2] At month 6, these cells at the surgical level already had a fusiform shape and were not different from those observed in other stromal planes.[1] This rounded cellular shape could be considered a landmark for cellular survival through the early postoperative period. We were also able to demonstrate a progressive increase in the cellular density at all measured stromal levels (anterior [P = 0.07], mid [P = 0.07], and posterior stroma [P = 0.07], between preop and 12 months).

In G2 and G3, throughout the first postoperative year, a normal cellular pattern was observed in the anterior and posterior stroma (Figure 9B). The lamina borders were easily visible as a hyper-reflective linear bands in the interface between the normal cellular anterior or posterior stroma and the acellular implanted stroma.[2] The lamina showed a similar acellular appearance in both groups without relevant differences (Figure 9C). Six months after surgery, all patients presented signs of early recellulariza-tion with scant isolated cells scattered throughout the lamina. This recellularization of the lamina continued up to the first postoperative year (Figure 9D), which we could demonstrate by a statistically significant increase in the keratocyte density within the lamina, which was more marked in G3 laminas. Moreover, both anterior [P = 0.008] and posterior [P = 0.008] stroma keratocyte densities also showed a statistically significant progressive increase up to the first year.

This observed tendency for an increase in keratocyte density at the anterior and posterior stroma in all 3 groups could be related to an activation of the host keratocytes, which are

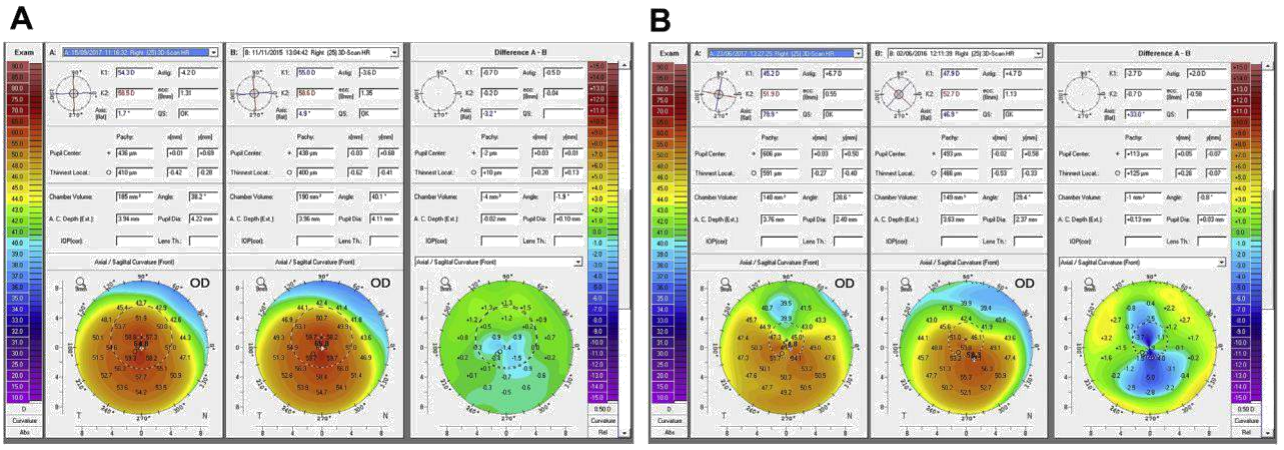

FIGURE 6. (A) Corneal topography (Pentacam) comparison before surgery and 12 months after ADASCs implantation (case 4). Note the stability of the keratometric parameters. (B) Topographic changes after corneal stroma enhancement between presurgery and 12 months after surgery (same patient as in Figure 4). Observe the significant flattening of the keratometry and the important improvement in all thickness parameters.

responsible for the recellularization observed within the implanted tissue in G2 and G3.

OTHER CLINICAL OUTCOMES: No significant changes in IOP or endothelial cell density were detected in a com-parison among preoperative and 6- and 12-month data [P > 0.05].

Five patients received superficial laminas that included Bowman's membrane (4 in G2 and 1 in G3), and 4 patients received the deeper lamina without this layer (1 in G2 and 3 in G3). Patients who received superficial laminas that included Bowman's membrane did not show better outcomes in any of the analyzed parameters of the study.

DISCUSSION

THIS PAPER REPORTS THE 1-YEAR OUTCOMES OF THE FIRST human experience with corneal stroma cell therapy. It is the first time that the behavior of autologous stem cells (ADASCs in the present study) injected into the corneal stroma demonstrated the appearance of new collagen in the area that corresponds to the injection of the cells, as well as the first time that decellularized human corneal stroma laminas, colonized or not by autologous ADASCs, were implanted in clinical cases of keratoconus for therapeutic purposes.

The first important issue that is demonstrated in this study is the lack of complications of the procedure observed in this 1-year clinical study. The use of femtosecond laser to create a stromal pocket at the mid stroma of advanced keratoconus cases is shown in the experience to be feasible and with no negative consequences, for up to 1 year of observation. This finding is consistent with our previous studies in which a large femtosecond laser-assisted corneal lamellar dissection performed approximately at the depth of the ones, followed by the implantation of an intrastromal cir-cular ring, was shown not to be affected by complications either from a visual, topographic, keratometric, or anatomical perspective.[25] The most representative data concerning the safety of the surgery is offered from G1 in which the only injection of cells in the pocket was followed by an immediate, modest but significant improvement, which was maintained throughout the first year of the follow-up. Obviously, this initial response of the cornea indicates the tolerance to this type of surgery as no deterioration was observed in any case in this or the other groups. At this early level of experience, the keratocyte differentiation and the eventual collagen production might not have had any significant influence in the mechanical response of the cornea, so further studies should guarantee the feasibility of this type of surgery from a biomechanical perspective. However, femtosecond laser-assisted pockets of these di-mensions were used for the implantation of intracorneal ring segments without any negative impact, either immedi-ate or late, in the operated keratoconic corneas, even though in this experience an intracorneal foreign body was implanted for therapeutic purposes.[26] Moreover, according to previous reports,[27] vertical side cuts through corneal lamellae, rather than horizontal delamination incisions, contributed to the loss of structural integrity during LASIK flap creation, so a minimal impact on corneal biomechanics may be expected after the creation of a lamellar pocket such as the one performed in this clinical study.

In the current experience, the good tolerance and the possibility of increasing corneal thickness by the implantation of decellularized layers of corneal stroma created by femtosecond laser were confirmed. To induce a calculated increase in the

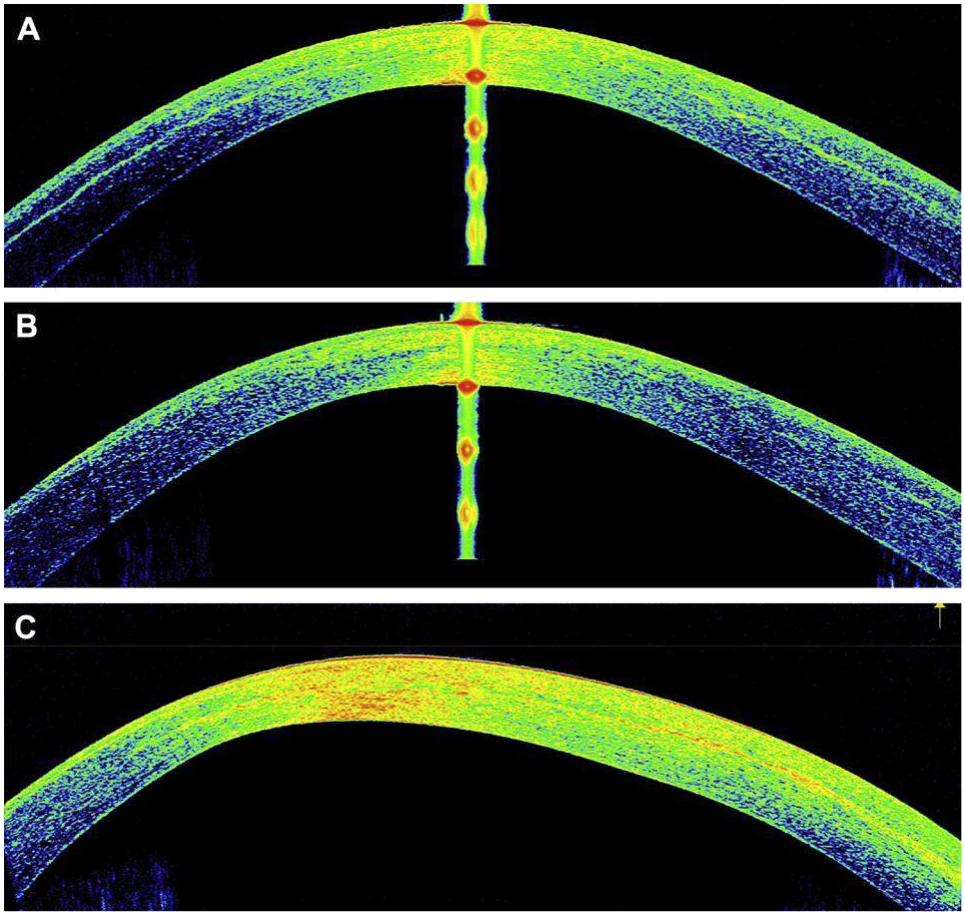

FIGURE 7. Corneal OCT views after ADASc implantation (case 3). (A) Note the hyperreflective (increased optical reflectivity) band of neo-collagen at the level of the stromal pocket 6 months after surgery (case 1). (B) Same patient one year after surgery, showing a partial normalization of the reflectance of the neo-collagen band. C: Another patient (case 4) shown 1 year after surgery, where the high reflectance of the neo-collagen band remains. OCT = optical coherence tomography.

thickness of the cornea is feasible by using these femto laser-dissected and decellularized laminas that can be implanted without any negative impact on the biomechanics, vision, and especially corneal anatomy. Corneal irregularity has been demonstrated to be improved, albeit modestly, by the reduction of corneal aberrometry, as observed in this study. Therefore, we can deduce that the calculated increase in corneal thickness induced by the use of these laminas can be used on a ther-apeutic basis without risk for the corneal transparency and benefits the corneal regularity and topography. The refractive sphere of these patients improved as well, which is in agreement with the flattening of the cornea, which is observed in the keratometric analysis.

Probably the most relevant feature is the maintenance of corneal transparency as a fact. In no case was corneal haze or corneal scarring observed at 1 year of follow-up, not even during the experience (with the exception of the early haze seen during the first month after the lamina implantation in G2 and G3). This issue is extremely important because the introduction of Heterologous manipulated corneal tis-sue could be followed by corneal scarring and eventually permanent loss of vision. The reasons for this corneal transparency are probably related to the decellularized character of the laminas as no biological interaction is happening between this foreign tissue of allogenic origin and the local host tissue cells. These findings demonstrate our previous experimental studies in which human decellularized corneal stroma laminas were well tolerated in the experimental animal model.[12] Furthermore, the presence of autologous ADASc in the laminas of G3 could be of further relevance for the maintenance not only for the corneal transparency but also for the decrease of previous corneal scars that could be present in these cases, a fact that has been described previously in the experimental animal model[6–11] and that we could also observe in 1 patient from G1.[1] This isolated observation of a significant bio-microscopy decrease in the scars present at the cornea pre-operatively might have been related to the capability of the stem cells to improve corneal transparency by their capability to reorganize previously diseased tissue, and the production of new

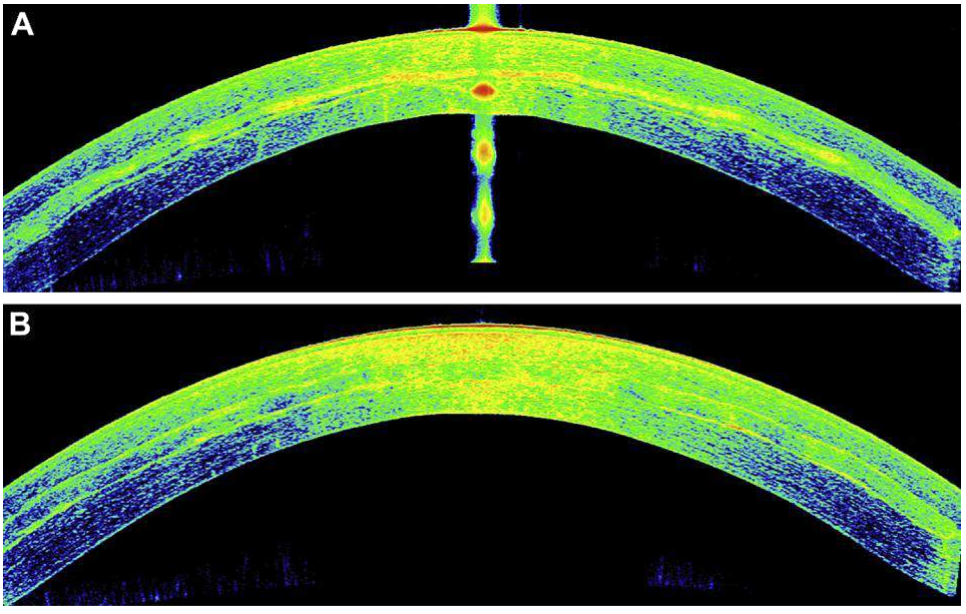

FIGURE 8. Cornea OCT Visante images after corneal stroma enhancement (same patient as in Figures 4 and 6B). (A) One month after surgery. (B) One year after surgery. Note the normalization of the early postoperative increased reflectance of the lamina. OCT = optical coherence tomography.

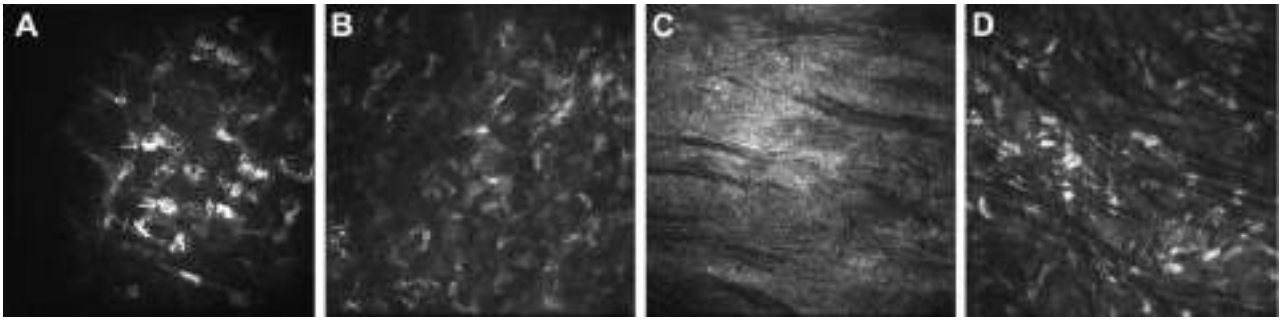

FIGURE 9. Corneal confocal biomicroscopy views. (A) Surgical plane from a group 1 patient (ADASc implantation) at 1 month after surgery (case 1). Stem cell survival is confirmed by the presence of cells showing a more rounded shape (white arrows). (B) Corneal stroma anterior to the implanted lamina; note the fusiform shape of adult keratocytes (case 8). (C) Group 2 patient with implanted lamina showing a complete acellular pattern 3 months after surgery (case 8). (D) Intense recellularization signs in a group 3 lamina 12 months after surgery (case 14).

normal collagen. Further studies performed in non-transparent and scarred corneas are necessary to confirm the therapeutic possibility of this new surgery.

Of particular relevance is the observation of a positive biological response from the host keratocytes to the decellularized laminas, especially in those implanted with autologous ADASCs. In G2 (treated with decellularized laminas with no addition of ADASCs) the increase in the corneal thickness, maintaining the corneal transparency, was parallel to the observation of an increase in the cellularity of both the anterior and the posterior parts of the corneal stroma. Therefore, the decellularized corneal lamina was not only able to maintain transparent conditions, increasing the corneal thickness, but there was also a posi-tive cellular response of the host keratocytes by prolifer-ating and even invading the implanted tissue, which indicates its biological activation (Figure 9). This finding was even more pronounced in those laminas implanted with ADASCs, although no statistically significant differences between G2 and G3 could be demonstrated, likely related to the small study sample.

In G1 (treated with ADASCs alone), the confocal biomicroscopy findings are also remarkable. Initially, the ADAS cells could be identified as rounded and regular in shape, whereas later, during the experience, these cells progressively transformed into a fusiform shape and showed an identical

appearance to the normal keratocytes of the human cornea (Figure 9).[1] An increase in the anterior and posterior stroma keratocyte densities could also be observed in G1 patients, so not only does the presence of the corneal lamina induce a positive biological response in the cornea, but also this healing response can be enhanced by the inclusion of ADASCs, which may contribute not only to the biological tolerance of the decellularized corneal lamina but also to the maintenance of its transparency and integration into the host cornea.

The presence or absence of Bowman's membrane in the implanted laminas was not relevant to the results in our study, although the small sample limited the significance of this observation.[28]

As the first-year data from this study demonstrate, we are opening a new area of corneal surgery and corneal research. The use of parts of the cornea for the purpose of a therapeutic increase in corneal thickness in debilitated and thin keratoconic corneas is a new concept for research. Corneal clinical parameters were all maintained or improved, and no deterioration was observed in any of the cases of the present study. Based on the outcomes of the present investigation, the use of autologous stem cells, particularly ADASCs, for therapeutic purposes in keratoconus or other corneal dystrophies or even corneal scars related to other causes could be relevant as these cells behave well in the corneal stroma, do not cause opacities and do not induce any inflammatory reaction.

The information in this report requires further confirmation. The limitations in this study are related to the small numbers of cases included in each group. Clinical pilot investigations of new therapies are difficult to perform and impose many limitations in terms of administration and approbation and ethics. The statistical analysis shows trends, and the outcomes should be considered within the context of the statistical limitations created by the limited number of cases of each group. However, despite these limitations, for the first time, we can offer new information which, even though it requires further confirmation, opens a new area for the clinical use of stem cells and a new type of corneal stroma therapy. The benefits of this are evident. Corneal dystrophies may have treatment alternatives that are different from those for corneal transplantation. Early treatment of these diseases with stem cells of autologous or allogenic origin could be an option even in early stages. In advanced stages, the many problems of corneal transplantation, such as corneal tissue availability, long recovery times, and unpredictable results, could be eliminated. The presence of corneal scars could have an option with the use of these mesenchymal stem cells as an alternative treatment. The most relevant disease whose treatment could benefit most from the results of this study is indeed keratoconus. Keratoconus is the most frequent and important corneal dystrophy due to its sociological impact. The frequency of keratoconus is indeed relevant because it is the primary cause of corneal transplanta-tions in the young population.[13] All these patients could benefit from this new type of surgical therapy, which can be more accessible, does not depend on viable human corneal tissue, and does not present the biological hazards related to allogenic tissue with allogenic cells.

ALL AUTHORS HAVE COMPLETED AND SUBMITTED THE ICMJE FORM FOR DISCLOSURE OF POTENTIAL CONFLICTS OF INTEREST and the following were reported.

Funding/Support: Supported By Optica General, Saida, Lebanon, and by Red Tema´tica de Investigacio´n Cooperativa en Salud Grant RD16/0008/0012; by Instituto Carlos III-General Subdirection of Networks and Cooperative Investigation Centers (R&D&I National Plan 2008–2011); by the European Regional Development Fund (Fondo Europeo de Desarrollo Regional FEDER); by the Spanish Ministry of Science and Innovation, Centro para el Desar-rollo Tecnolo´gico Industrial (CDTI); and by Customized Eye Care CeyeC grant CEN-20091021.

Financial Disclosures: Dr. Alio receives clinical research grants from Akkolens, Carl Zeiss Meditec, CSO, Dompe, Hanita Lenses, Mediphacos, Santen, Oculentis, and Schwind Eye-Tech-Solutions; and receives lecturer fees from Ophthec and Schwind; and owns equity in Oftalcare Nutravision, Santen, VisiDome, and Blue-Green; and consults for Akkolens, Carl Zeiss Meditec, Hanita Lenses, Maghrabi Hospital, Oculentis, Omeros, Presbia, Santen, Slack Inc., and Topcon Medical Systems; and holds patents in Jaypee Brothers Pub. Dr. de Miguel received a grant from Roche Farma SA.

The following authors have no financial disclosures: Jorge L. Alio del Barrio, Mona El Zarif, Albert Azaar, Nehman Makdissy, Charbel Khalil, Walid Harb, Ibrahim El Achkar, and Ziad Abdul Jawad.

The authors thank Marc Assouwad and Peggy Saba, Laser Vision, Beirut, Lebanon, for their assistance with the logistics of the study and obtaining confocal microscopy data; Sandy Al Hage, Reviva Regenerative, Beirut, Lebanon, for administrative assistance; and Eric Bangert, Heidelberg Engineering, Heidelberg, Germany, for donation of confocal microscopy and confocal software analysis software.

REFERENCES

1. Alio´ del Barrio JL, El Zarif M, de Miguel MP, Azaar A, Makdissy N, Harb W, et al. Cellular therapy with human autologous adipose-derived adult stem cells for advanced keratoconus. Cornea 2017;36:952–960.
2. Alio´ del Barrio JL, El Zarif M, Azaar A, Makdissy N, Khalil C, Harb W, et al. Corneal stroma enhancement with decellular-ized stromal laminas with or without stem cell recellulariza-tion for advanced keratoconus. Am J Ophthalmol 2018;186: 47–58.
3. Alio´ JL, Alio´ del Barrio JL. Cellular Therapy with Human Autologous Adipose-derived Adult Stem Cells for Advanced Keratoconus: Reply to the Letter to Editor. Cornea 2017;36: e37.
4. Arnalich-Montiel F, Pastor S, Blazquez-Martinez A, et al. Adipose-derived stem cells are a source for cell therapy of the corneal stroma. Stem Cells 2008;26:570–579.

5. Espandar L, Bunnell B, Wang GY, Gregory P, McBride C, Moshirfar M. Adipose-derived stem cells on hyaluronic acid-derived scaffold: a new horizon in bioengineered cornea. Arch Ophthalmol 2012;130:202–208.
6. Mittal SK, Omoto M, Amouzegar A, et al. Restoration of corneal transparency by mesenchymal stem cells. Stem Cell Reports 2016;7:583–590.
7. Demirayak B, Yu¨ksel N, C¸ elik OS, et al. Effect of bone marrow and adipose tissue-derived mesenchymal stem cells on the natural course of corneal scarring after penetrating injury. Exp Eye Res 2016;151:227–235.
8. Du Y, Carlson EC, Funderburgh ML, et al. Stem cell therapy restores transparency to defective murine corneas. Stem Cells 2009;27:1635–1642.
9. Liu H, Zhang J, Liu CY, et al. Cell therapy of congenital corneal diseases with umbilical mesenchymal stem cells: lumican null mice. PLoS One 2010;5:e10707.
10. Coulson-Thomas VJ, Caterson B, Kao WW. Transplantation of human umbilical mesenchymal stem cells cures the corneal defects of mucopolysaccharidosis VII mice. Stem Cells 2013; 31:2116–2126.
11. Kao WW, Coulson-Thomas VJ. Cell therapy of corneal diseases. Cornea 2016;35 suppl 1:S9–S19.
12. Alio´ del Barrio JL, Chiesa M, Garagorri N, et al. Acellular human corneal matrix sheets seeded with human adipose-derived mesenchymal stem cells integrate functionally in an experimental animal model. Exp Eye Res 2015;132:91–100.
13. Arnalich-Montiel F, Alio´ del Barrio JL, Alio´ JL. Corneal surgery in keratoconus: which type, which technique, which outcomes? Eye Vis (Lond) 2016;3:2.
14. Gain P, Jullienne R, He Z, et al. Global survey of corneal transplantation and eye banking. JAMA Ophthalmol 2016; 134:167–173.
15. Ruberti JW, Zieske JD. Prelude to corneal tissue engineering—gaining control of collagen organization. Prog Retin Eye Res 2008;27:549–577.
16. De Miguel MP, Fuentes-Julia´n S, Bla´zquez-Martı´nez A, et al. Immunosuppressive properties of mesenchymal stem cells: advances and applications. Curr Mol Med 2012;12:574–591.
17. Lynch AP, Ahearne M. Strategies for developing decellular-ized corneal scaffolds. Exp Eye Res 2013;108:42–47.
18. Alio´ del Barrio JL, Chiesa M, Gallego Ferrer G, et al. Biointegration of corneal macroporous membranes based on poly(ethyl acrylate) copolymers in an experimental animal model. J Biomed Mater Res A 2015;103: 1106–1118.
19. Alio´ JL, Pin˜ero DP, Aleso´n A, et al. Keratoconus-integrated characterization considering anterior corneal aberrations, internal astigmatism, and corneal biomechanics. J Cataract Refract Surg 2011;37:552–568.
20. Zuk PA, Zhu M, Mizuno H, et al. Multilineage cells from hu-man adipose tissue: implications for cell-based therapies. Tis-sue Eng 2001;7:211–228.
21. Zuk PA, Zhu M, Ashjian P, et al. Human adipose tissue is a source of multipotent Stem Cells. Mol Biol Cell 2002;13: 4279–4295.
22. Bourin P, Bunnell BA, Casteilla L, et al. Stromal cells from the adipose tissue-derived stromal vascular fraction and cul-ture expanded adipose tissue-derived stromal/stem cells: a joint statement of the International Federation for Adipose Therapeutics and Science (IFATS) and the International Society for Cellular Therapy (ISCT). Cytotherapy 2013;15: 641–648.
23. Ponce Ma´rquez S, Martı´nez VS, McIntosh Ambrose W, et al. Decellularization of bovine corneas for tissue engineering applications. Acta Biomater 2009;5:1839–1847.
24. Ku JY, Niederer RL, Patel DV, Sherwin T, McGhee CN. Laser scanning in vivo confocal analysis of keratocyte density in keratoconus. Ophthalmology 2008;115:845–850.
25. Alio JL, Pin˜ero DP, Daxer A. Clinical outcomes after complete ring implantation in corneal ectasia using the femtosecond technology: a pilot study. Ophthalmology 2011;118: 1282–1290.
26. Daxer A. Biomechanics of corneal ring implants. Cornea 2015;34:1493–1498.
27. Knox Cartwright NE, Tyrer JR, Jaycock PD, Marshall J. Effects of variation in depth and side cut angulations in LASIK and thin-flap LASIK using a femtosecond laser: a biomechanical study. J Refract Surg 2012;28:419–425.
28. van Dijk K, Liarakos VS, Parker J, et al. Bowman layer transplantation to reduce and stabilize progressive, advanced keratoconus. Ophthalmology 2015;122:909–917.

10.5. El Zarif, M, Alió, J., Alió del Barrio, J., Abdul Jawad, K., Palazón-Bru, A., Abdul Jawad, Z., De Miguel, M., Makdissy, N., 2021. Corneal stromal regeneration therapy for advanced keratoconus: long-term outcomes at 3 years. Cornea 40, 741–754. https://doi.org/10.1097/ICO.0000000000002646

Corneal Stromal Regeneration Therapy for Advanced Keratoconus: Long-term Outcomes at 3 Years

Mona El Zarif, OD, MSc,*†‡§ Jorge L. Alió, MD, PhD, FEBOphth,¶† Jorge L. Alió del Barrio, MD, PhD, FEBOS-CR,¶† Karim Abdul Jawad, BSc,* Antonio Palazón-Bru, PhD,k Ziad Abdul Jawad, OD,* María P. De Miguel, PhD,** and Nehman Makdissy, PhD§

Purpose: To report the 3-year clinical outcomes of corneal stromal cell therapy consisting of the intrastromal implantation with autologous adipose-derived adult stem cells (ADASCs), and decel-lularized or ADASC-recellularized human donor corneal laminas in advanced keratoconus.

Methods: Fourteen patients were enrolled in 3 experimental groups. Group 1 (G-1) patients underwent implantation of ADASCs alone (3 X 10^6 cells/1 mL) (n = 5). Group 2 (G-2) patients received a 120-µm decellularized corneal stroma lamina (n = 5). Group 3 (G-3) patients received a 120-µm lamina recellularized with ADASCs (1 · 10^6 cells/1 mL) (n = 4). ADASCs were obtained by elective liposuction. Implantation was performed into a femtosecond pocket under topical anesthesia.

Results: At 3 years, a significant improvement of 1 to 2 logMAR lines in uncorrected distance visual acuity was observed in all groups. A statistically significant decrease in corrected distance visual acuity was obtained in G-2 and G-3 ($P < 0.001$) when compared with that of G-1. Rigid contact lens distance visual acuity showed a statistically significant worsening in G-2 ($P < 0.001$) compared with that of G-1. A statistically significant increase in central corneal thickness was observed in G-2 ($P = 0.012$) and G-3 ($P < 0.001$); in the Scheimpflug corneal topography, the thinnest point was observed in G-2 ($P = 0.007$) and G-3 ($P = 0.001$) when compared with that of G-1.

Conclusions: Intrastromal implantation of ADASCs and decellu-larized or ADASCs-recellularized human corneal stroma laminas did not have complications at 3 years. The technique showed a moderate improvement in (uncorrected distance visual acuity) and (corrected distance visual acuity) in advanced keratoconus.

Keywords: regenerative medicine, corneal bioengineering, corneal stem cell therapy, keratoconus, adipose-derived adult stem cells, advanced corneal therapy

Received for publication May 29, 2020; revision received November 20, 2020; accepted November 20, 2020. Published online ahead of print February 22, 2021.

From the *Lebaneese university Hadath: EDST of Biotechnology, Optica General, Saida, Lebanon; †Division of Ophthalmology, Universidad Miguel Hernández University, Alicante, Spain; ‡Lebaneese university Hadath: EDST of Biotechnology, Doctoral School of Sciences and Technology, Lebanese University, Hadath, Lebanon; §GSBT Genomic Surveillance and Biotherapy Team, Faculty of Sciences, Lebanese University, Hadath, Lebanon. ¶Cornea, Cataract and Refractive Surgery Unit, Vissum Instituto Oftalmologico de Alicante, Grupo Miranza, Alicante, Spain; kDepartment of Clinical Medicine, Miguel Hernández University, Alicante, Spain; and **Cell Engineering Laboratory, IdiPAZ, La Paz Hospital Health Research Institute, Madrid, Spain.

Supported by Optica General, Saida Lebanon, and Vissum ophthalmological institute of Alicante, Spain, and, in part, by the Red Temática de Investigación Cooperativa en Salud (RETICS), reference number RD16/ 0008/0012, by the Instituto Carlos III—General Sudirection of Networks and Cooperative Investigation Centers (R&D&I National Plan 2008–2011), and by the European Regional Development Fund (Fondo Europeo de Desarrollo Regional FEDER).

The authors have no conflicts of interest to disclose.

J. L. Alió: principal investigator, principal surgeon, study concept and design, analysis and interpretation of data, writing and critical revision of the manuscript, statistical revision, and supervision. M. El Zarif: coprincipal investigator, clinical and monitor director of the study, study concept and design, data collecting, analysis and interpretation of data, writing, and critical revision of the manuscript, statistical revision, and supervision. J. L. Alió Del Barrio: second surgeon and critical correction of the manuscript. K. A. Jawad: analysis, interpretation, and editing of the data and writing the manuscript. A. Palazón-Bru: statistical analysis and the corresponding data editing. Z. A. Jawad: data collecting, processing, and administration of the study. M. P. de Miguel: biological processing. N. Makdissy: stem cell therapy processing.

Correspondence: Jorge L. Alió, MD, PhD, FEBOphth, Cornea, Cataract and Refractive Surgery Unit, Vissum Instituto Oftalmologico de Alicante, Vissum, Calle Cabañal, 1, 03016 Alicante, Spain (e-mail: jlalio@vissum.com).

INTRODUCTION

Keratoconus is the most common corneal dystrophy, with a diverse prevalence in the population, from 0.05% to 2.3%.[1] Being a relatively prevalent disease, it is more frequently detected today than ever before because of the availability of more advanced diagnostic tools that assist in its early diagnosis. Keratoconus causes progressive changes in vision, with increased myopia and myopic astigmatism, corneal irregularity, and visual loss.[2] Keratoconus is also the most frequent indication for corneal graft surgery at an age younger than 40 years in the United States and other western countries.[3] Its prevalence and progressive character have led to the proposal of different alternative therapies to corneal graft surgery. Among these, and in use today, are collagen cross-linking, intracorneal rings and segments, lamellar corneal stroma transplantation, and more recently, Bowman membrane (BM) transplantation.[3]

Recently, advanced methods of corneal therapy, which include corneal cell expansion and innovative corneal regeneration procedures using mesenchymal stem cells, have been proposed to restore the abnormal corneal stromal tissue in keratoconus, aiming

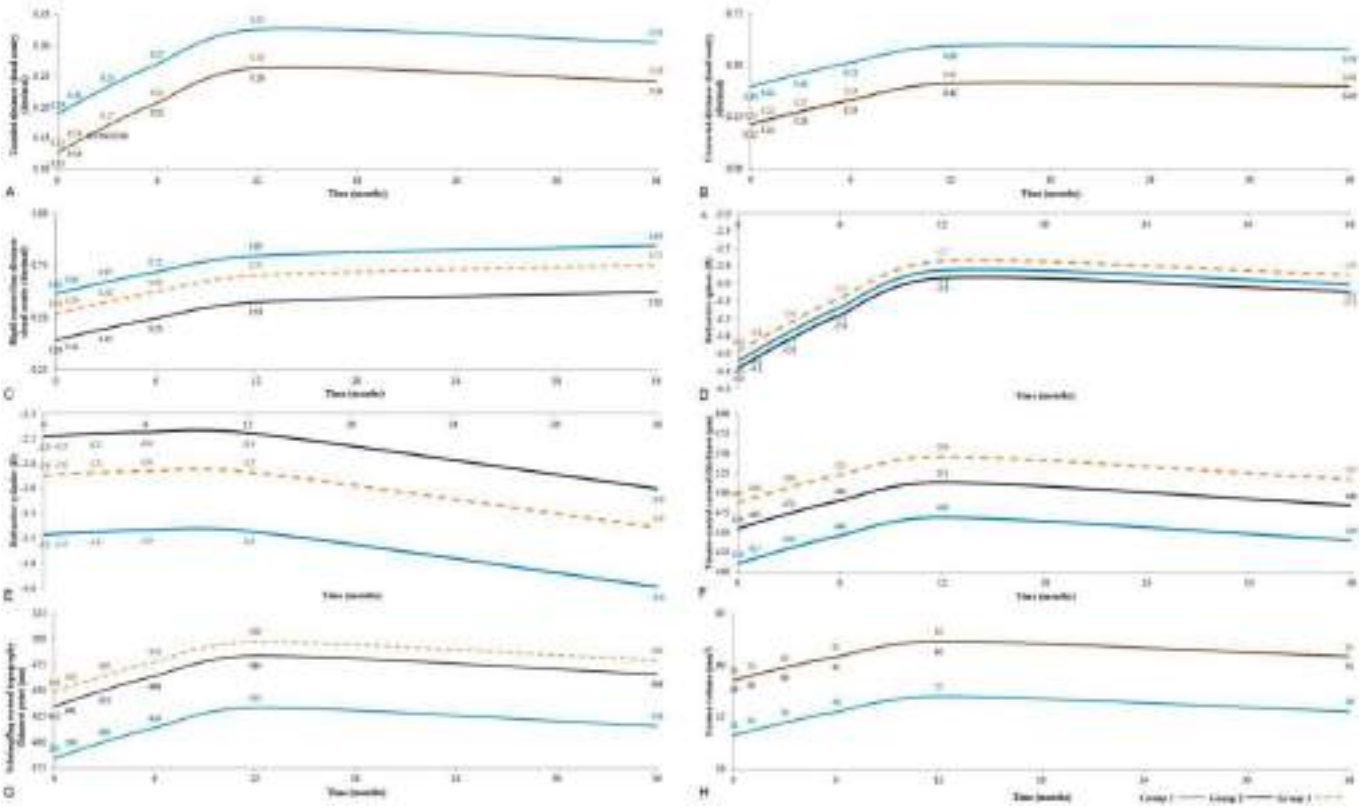

FIGURE 1. Visual, refractive, pachymetric, and volumetric outcomes in G-1, G-2, and G-3 up to 36 months after surgery. A, UDVA. B, CDVA. A statistically significant worsening was obtained in mean values in G-2 and G-3 compared with those of the G-1. C, Rigid contact lens visual acuity in decimal equivalent to logMAR scale. A statistically significant worsening was obtained in G-2 when compared with G-1 and G-3. D, Refractive sphere in diopters (D). E, Refractive cylinder (D). Mean values were statistically significantly better in G-2 and G-3 when compared with those of G-1. F, CCT was measured with AS-OCT Visante (mm). G, Scheimpflug corneal topography thinnest point (mm). H, Cornea volume was measured with Pentacam (mm^3). CCT, thinnest point, and CV showed significant improvement in the mean values in G-2 and G-3 when compared with those of G-1. (The full color version of this figure is available at www.corneajrnl.com.)

to avoid the use of corneal grafts.[4–7] Previous interim reports from our group have demonstrated that this advanced therapy seems to be safe and provides an initial modest, albeit favorable clinical outcome for up to 1 year of follow-up.[6] In this report, we present the 3-year clinical outcomes of the first clinical experience of corneal stromal regeneration using mesenchymal stem cell therapy in advanced keratoconus cases.

PATIENTS AND METHODS

Study Approval, Design, and Subjects

This is a prospective interventional randomized, non-masked series of cases, based on the cooperation between the Research, Development, and Innovation Department of Vissum Instituto Oftalmologico de Alicante, Miguel Hernandez University, Alicante (Spain), Optica General (Saida, Lebanon), Laser Vision Center (Beirut, Lebanon), and REVIVA Research and Application Center (Middle East Hospital, Beirut, Lebanon). The institutional review board ethical committee of Reviva Research and Application Center (Lebanese University, Beirut, Lebanon) prospectively approved this study. All patients signed informed written consent for all procedures described in this study. The study was conducted in strict adherence to the tenets of the Declaration of Helsinki, and it was officially registered in ClinicalTrials.gov (Code: NCT02932852).

Fourteen patients were enrolled in the study once selected following, after meeting the inclusion criteria (see further), and were randomly distributed into 3 study groups: group 1 (G-1) patients were implanted with autologous adipose-derived adult stem cells (ADASCs) (n = 5 patients); group 2 (G-2) received 120- μm thick decellularized human corneal stroma laminas implants (n = 5 patients), and group 3 (G-3) received 120- μm thick ADASCs-recellularized human corneal stroma laminas (n = 4 patients). Superficial laminas with BM or deep laminas without BM were randomly distributed among the patients of G-2 and G-3 after the decellularization procedure.

Clinical monitoring of the study of the patients was established for safety purposes at 1 week, at 1 month, at 3, 6, 12, and 36 months postoperatively, with interim reports every 6 months. Thirteen patients fully completed the 3 years of clinical follow-up. Only 1 patient from G-1 was lost after the

TABLE 1. Difference in Mean Values Between (G-1) - (G-2), (G-1) - (G-3), and (G-2) - (G-3) of All the Variables of the Study

	(G-1) - (G-2)	(G-1) - (G-3)	(G-2) - (G-3)
UDVA	0.07	0.07	0.00
CDVA	0.18*	0.19*	0.01
CLDVA	0.22*	0.10	20.12*
Rx Sphr (D)	0.10	20.10	20.20
Rx Cyl (D)	21.00*	20.60*	0.40
Visante CCT (mm)	244.00*	277.00*	233.00
Thinnest point (mm)	251.00*	265.00*	214.00
CV (mm^3)	25.00*	25.00*	0.00
Third-order RMS	4.65*	3.54*	21.11
Fourth-order RMS	1.28	20.17	21.45*
HOAs RMS	4.9	2.78	22.12
LOAs RMS	23.87*	1.32*	5.19
Anterior Km (D)	23.00	1.00	4.00
Posterior Km (D)	1.3*	0.2	21.1*
Kmax (D)	0.00	2.00	2.00
Topo Cyl (D)	1.1	0.9	20.2

*Statistically significant difference between the compared groups.

first postoperative month because of the inability to attend further follow-up for personal reasons unrelated to the study. Results of the interim analysis performed at 6 and 12 months have been already the subject of previous publications.[4,5,7,8]

Inclusion and Exclusion Criteria

Inclusion criteria: patients with advanced keratoconus defined as stage ≥IV; according to the RETICS keratoconus classification,[9] are already candidates for corneal transplantation because of the advanced condition of the disease and associated comorbidities; aged 18 years or older; and negative for human immunodeficiency virus, hepatitis B, and hepatitis C serology. Exclusion criteria: corrected distance visual acuity (CDVA) < 0.1 in the contralateral eye, previous corneal hydrops or disease; any other sight-threatening ocular comorbidity, previous corneal surgical procedures, including collagen crosslinking, pregnancy or breastfeeding, and history of systemic malignancy.

Autologous ADASCs Isolation, Characterization, and Culture

Approximately 250 mL of fat mixed with local anesthesia were obtained by standard liposuction from each patient. The adipose tissue was processed according to the methods described in our previous reports.[10–14] In brief, tissue was digested in collagenase I for 40 minutes at 37°C, and then, collagenase was inhibited adding autologous human serum. Erythrocytes were lysed in erythrocyte lysis buffer (Gibco-Life Technologies). Then, the pelleted cells were cultured in Dulbecco's modified eagle medium with Glutamax, sodium pyruvate (Gibco), 10% autologous human serum, 1% penicillin–streptomycin (Gibco), and 0.2% amphotericin B (Gibco). Cell characterization was performed by $CD34^+CD45^-CD105^+$ labeling by flow cytometry analysis following the International Federation of Adipose Therapeutics recommendations. Sixty to 80 hours before surgery, cell quiescence was induced by reducing the amount of serum to 0.5%, to more closely resemble thenatural nonproliferative state of stromal keratocytes. Quiescence and the absence of apoptosis and aneuploidy were verified by propidium iodide labeling (Invitrogen) and cell cycle flow cytometry analysis. In G-1, just before the intrastromal injection, the cells were collected by trypsinization (Sigma), and 3 X 10^6 cells in 1 mL of phosphate-buffered saline (PBS) were prepared per patient.

TABLE 2. Statistical Results of the Principal and Secondary Variables Among G-1, G-2, and G-3 Along the 3-Year Follow-up, P (Trajectories of the Variables), and s

	P (G-2)/(G-1)	P (G-3)/(G-1)	P (G-2)/(G-3)	s	P (Trajectories of the Variables)
UDVA	0.054	0.069	0.986	0.116	0.0021
CDVA	<0.001	<0.001	0.900	0.151	<0.001
CLDVA	<0.001	0.090	0.010	0.180	<0.001
Rx Sphr (D)	0.892	0.863	0.747	2.691	0.649
Rx Cyl (D)	<0.001	0.014	0.086	0.824	0.015
Visante CCT (mm)	0.012	<0.001	0.055	62.940	0.004
Thinnest point (mm)	0.007	0.001	0.465	67.966	0.021
CV (mm^3)	<0.001	<0.001	0.948	3.757	0.001
Third-order RMS	<0.001	0.009	0.376	4.571	0.087
Fourth-order RMS	0.074	0.817	0.004	2.515	0.117
HOAs RMS (mm)	<0.001	0.038	0.091	4.530	0.061
LOAs RMS (mm)	0.617	0.870	0.491	27.299	0.866
Anterior Km (D)	0.085	0.909	0.062	6.436	0.351
Posterior Km (D)	0.001	0.636	0.004	1.326	0.118
Kmax (D)	0.949	0.387	0.0.391	8.250	0.643
Topo Cyl (D)	0.091	0.190	0.753	2.383	0.525

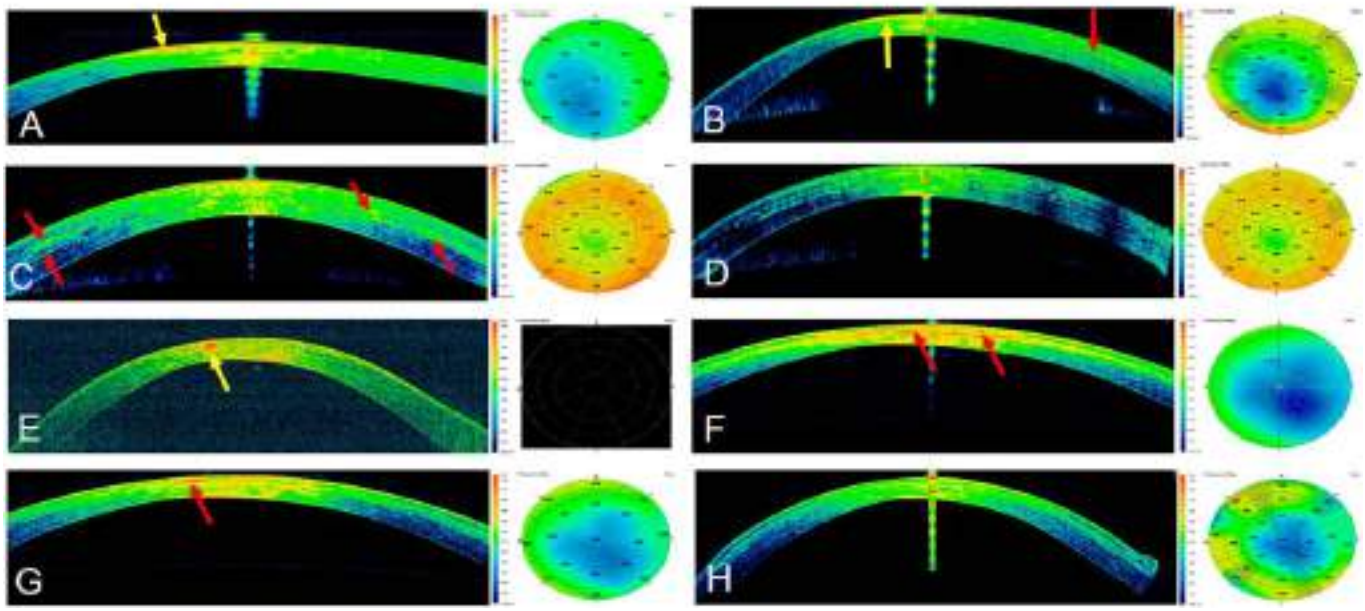

FIGURE 2. Corneal anterior segment OCT sections and pachymetric maps (Visante) in G-1, G-2, and G-3. A, A G-1 patient (case 2) at 1 month postoperatively: notice the reflective paracentral scar (yellow arrow). B, Same patient after 3 years, showing low reflectance of the band of neocollagen (red arrow), and the reflective paracentral scar has disappeared (yellow arrow). C, A G-2 patient (case 6) at 6 months: observe the high reflectance of the implanted lamina (red arrows) and the restoration of the corneal thickness (right side). D, Same patient after 3 years: observe the improvement in the integration of the implanted lamina in the host stoma and the stability of the pachymetric map. E, A G-3 patient (case 11) at the preoperative level: a reflective paracentral scar can be noticed (yellow arrow). F, Same patient 1 month after surgery: observe the high reflectance of the implanted lamina (red arrows). G, Same patient (shown in E–F) at 12 months after surgery: observe the improvement in the reflectance of the implanted lamina (red arrow). H, Same patient (shown in E–G) at 3 years after surgery: notice the integration of the implanted tissue in the host and the improvement in corneal density. (The full color version of this figure is available at www.corneajrnl.com.)

Such concentration was established based on the evidence observed in previous experimental studies and given the expected cell loss after the implantation due to the leakage of the cell solution outside the cornea.[8,14,15] In G-3, the ADASCs were harvested by trypsinization (Sigma-Aldrich), 24 hours before implantation, and 0.5 x 10^6 cells per 1 mL of PBS were cultured for 24 and 12 hours on each surface of the decellularized corneal stroma lamina, respectively.[7,8]

Laminas

Human corneal stroma of donor corneas with nonviable endothelium but with negative viral serology and useful for human use was selected for this investigation. The corneas were provided by the eye bank "Banco de Ojos para el tratamiento de la Ceguera, Centro de Oftalmología Barraquer (Barcelona, Spain), following the Spanish regulatory Direc-tives 2004/23/EC and 206/17/EC."

Donor corneas were mounted in an artificial anterior chamber (Barron; Katena Products, Denville, NJ). Then, 2 to 3 consecutive laminas were obtained, all with 120 µm thickness and 9.0 mm in diameter. Femtosecond laser parameters were similar to those used for laser-assisted in situ keratomileusis flap dissection.[7,8] The decellularization protocol was based on previous publications.[14,16,17] In brief, laminas were incubated in 1% (wt/vol) sodium dodecyl sulfate solution (Sigma-Aldrich) with a protease inhibitor cocktail (P8340; Sigma-Aldrich), on an orbital shaker (75 rpm) for 24 hours. Then, laminas were washed 8 times in PBS with 1% antibiotic–antimycotic in the same shaking conditions for 15 minutes each. As a second step to remove DNA, the laminas were incubated in DNAse (Benzonase Nuclease 6.5 U/mL; Merck) in PBS with the same protease inhibitor cocktail in the same shaking conditions at 37°C for 72 hours. Finally, the laminas were washed 8 times for 15 minutes each in PBS with a 1% antibiotic–antimycotic solution. All procedures were performed at room temperature.[14,16] Effectiveness of the decellularization and, hence, cell removal was monitored in 1 fresh lamina of each batch by 3 methods: histological analysis with nuclear 49,6-diamidino-2-phenylindole staining and fluorescence microscopy staining with hematoxylin and eosin, and biochemically by digestion in proteinase K, DNA extraction, and DNA quantification by using a Picogreen Assay kit as in previous publications.[14,16]

Surgical Procedure

Autologous ADASCs Implantation

The method for the implantation of the mesenchymal stem cells has been previously described by our group.[4,5] Topical anesthesia was used. A 60-kHz IntraLase iFS femtosecond laser (AMO Inc, Irvine, CA) was used in single-pass mode for recipient corneal lamellar dissection by creating an intrastromal laminar pocket of 9.5 mm in diameter at a medium depth of the thinnest preoperative pachymetry point measured by the anterior segment optical coherence tomography (AS-OCT) (Carl Zeiss, Germany). The anterior side-cut incision

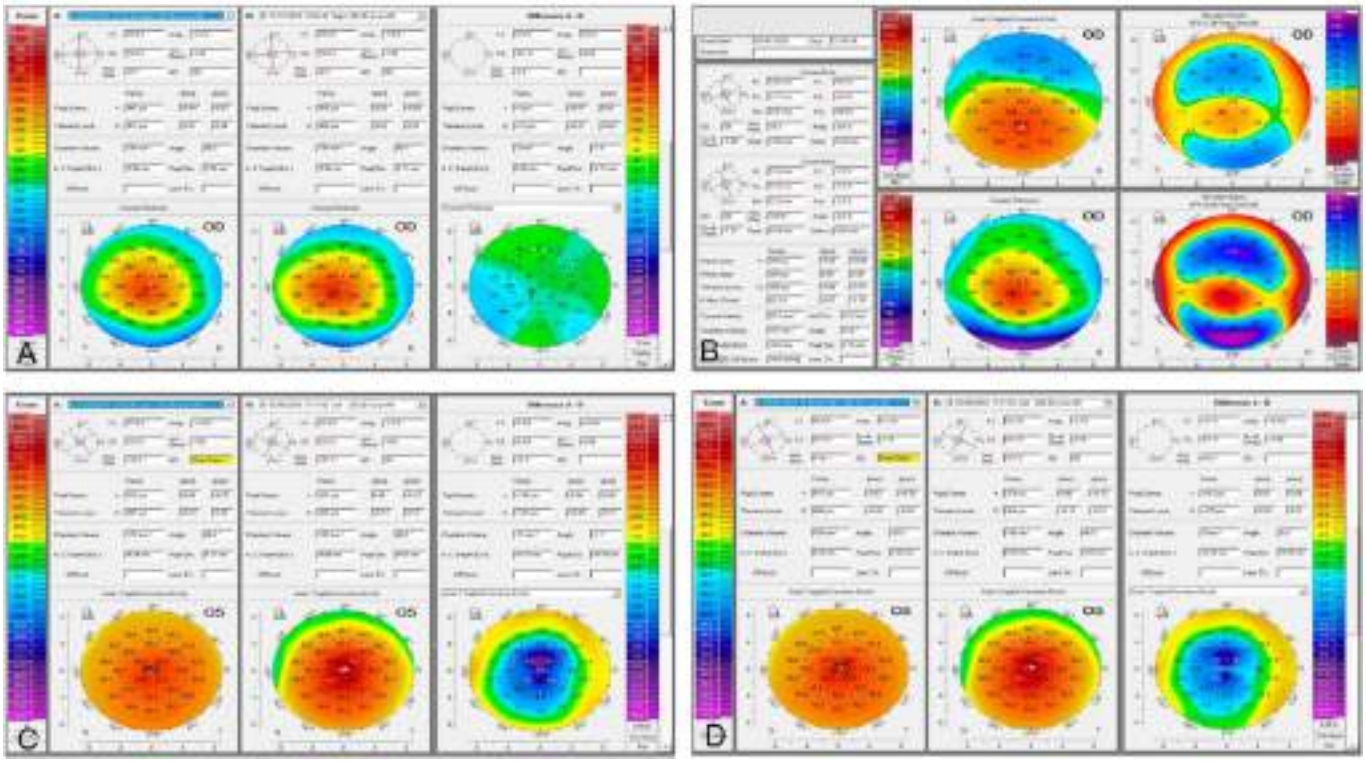

FIGURE 3. Topography changes preoperatively and at 12 and 36 months postoperatively in G-1 and G-2. A, Preoperative versus 12 months postoperative in G-1 case 1: observe the minimal enhancement of the pachymetric parameters. B, Four maps of corneal topography in G-1 case 2 at 3 years postoperative: no significant increase of the pachymetric or keratometric parameters was observed. C and D, Preoperative versus 12 months postoperative (C) and preoperative versus 3 years postoperative (D), in G-2 case 7: notice the keratometric improvement. (The full color version of this figure is available at www.corneajrnl.com.)

was made at 30 degrees, the arc length incision was 3 mm, and similar parameter settings of laser in situ keratomileusis surgery were used in femtosecond laser. The corneal intrastromal pocket was then opened by blunt dissection using the Morlet lamellar dissector (Duckworth & Kent, Baldock, United Kingdom), and consequently, 3 million autologous ADASCs contained in 1 mL of PBS were injected into the pocket with a 25-G cannula. To reduce intraocular pressure (IOP) and allow a larger volume of cells to be injected into the stroma pocket, a 1 mm corneal paracentesis was performed. Topical antibiotics and steroids (Tobradex; Alcon) were applied at the end of surgery. No patient received corneal sutures.[4,8]

Lenticule Implantation

Topical anesthesia was applied with oral sedation for all surgeries, and the 60-kHz IntraLase iFS femtosecond laser was used in single-pass mode. Assisted corneal dissection was performed with a 50-degreeanterior cut, and the arc length incision was 4 mm.

Then, the corneal intrastromal pocket was opened by blunt dissection with the Morlet lamellar dissector (Duckworth & Kent); the lamina was inserted, centered, and unfolded through gentle tapping and massaging from the epithelial surface of the host. In addition, before implantation and to facilitate the implantation technique, a limbal paracentesis was performed to reduce IOP. In those cases who received an ADASCs- recellularized lamina (G-3), the pocket was irrigated immediately before and after insertion with a solution containing an additional 1 million autologous ADASCs in 1 mL of PBS with a 25-G cannula. The incision was then closed with an interrupted 10-0 nylon suture that was removed 1 week after the operation.[7,8] All surgeries were performed by the same surgeons (J.L.A. and J.L.A.d.B.) at the Laser Vision Center (Beirut, Lebanon).[4–8]

Postoperative Care and Follow-up Schedule

Postoperatively, the patients were evaluated monthly by the study medical director and the clinical monitor of the study (M.E.Z.) to ensure the correct evolution of the patients. The patients were followed up at 1 day, 1 week, 1 month, and 3, 6, and 12 months.[4,7,8] Clinical follow-up after 1 year was performed every 6 months till 36 months postoperatively. The following data were recorded preoperatively and throughout the postoperative assessment, at 1 month and 3, 6, 12, and 36 months: uncorrected distance visual acuity (UDVA), CDVA, and rigid contact lens distance visual acuity (CLDVA) (in decimal equivalent to the logMAR scale); refractive sphere (Rx Sphr) in diopters (D) and refractive cylinder (Rx Cyl) (D); central corneal thickness (CCT) (mm) measured by AS-OCT (Visante; Carl Zeiss); Scheimpflug corneal topography thinnest point (thinnest point) (mm), cornea volume (CV) (mm^3) and corneal aberrometry (Pentacam; Oculus Inc, Wetzlar, Germany), and the anterior corneal surface Zernike analyses performed at maximum 6 mm pupil diameter in all cases

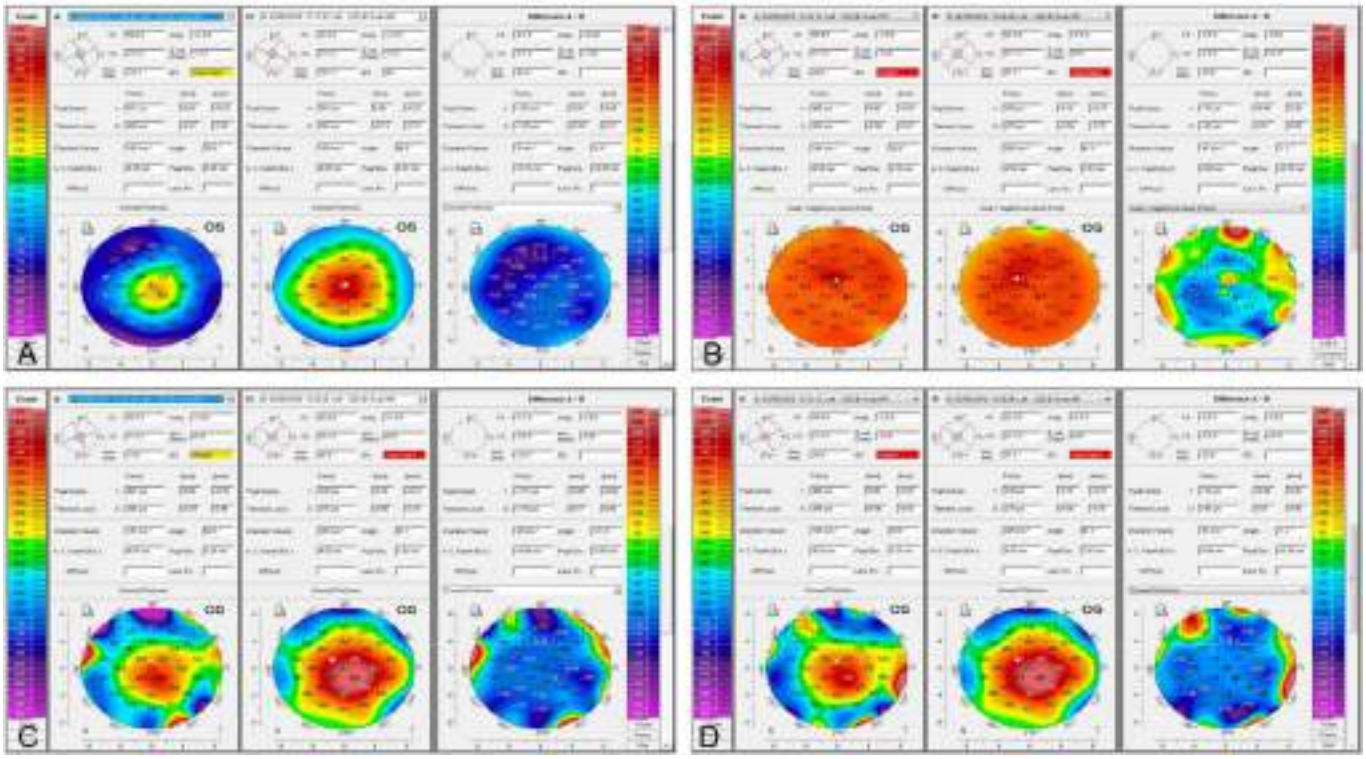

FIGURE 4. Topographic changes between preoperative and 12- and 36-month postoperative values in G-2 and G-3. A, Preoperative versus 3 years postoperative in G-2 case 7: observe the enhancement of all pachymetric parameters. B, Preoperative versus 3 years postoperative in G-3 case 11: notice the improvement of the keratometric parameters. C and D, Preoperative versus 12 months postoperative and preoperative versus 3 years postoperative respectively in G-3 case 11: notice the keratometric improvement and a major increase of the pachymetric parameters. (The full color version of this figure is available at www.corneajrnl.com.)

regardless of the patients' pupil diameter; anterior mean keratometry (anterior Km) (D), posterior mean keratometry (posterior Km) (D), maximum keratometry (Kmax) (D), and topographic cylinder (Topo Cyl) (D) (Pentacam; Oculus Inc); and slit lamp biomicroscopy, fundoscopy, IOP (Goldmann applanation tonometry IOP) (mm Hg), and endothelial cell density (cells/mm^2) by specular microscopy (Nidek, Aichi, Japan). The confocal microscopy study was completed up to 12 months using the confocal microscope HRT3 RCM (Heidelberg) with Rostock Cornea Module.

Statistical Analysis

We obtained generalized linear mixed models with Poisson variables including outcomes, time, and the group as fixed effects and individuals as random effects. A Poisson distribution is characterized by a mean rate (the standard deviation is equal to this mean or l) and indicates the number of events for the outcome. We estimated l through these models, taking into account all the gathered information. The results of this statistical study did not represent at any time the outcome of 1 patient from the different groups, but they represented the total data collected from all the patients of each group over continuous-time and provide all information necessary to understand the impact of the intervention. Scatterplots were developed to help interpret the results, and the goodness-of-fit of the models was obtained through the likelihood ratio test. The type I error significance level was set at P value <0.05, and the statistical software we used was R 3.5.1.

Main Outcome Measures

The main outcome measures of this investigation were divided into primary and secondary measures, as described further.

Primary Outcomes Measures

These included the following: UDVA, CDVA, and CLDVA (decimal equivalent to the logMAR scale); Rx Sphr (D) and Rx Cyl (D); CCT (mm), thinnest point (mm), and CV (mm^3); and third-order aberration root mean square (RMS) (mm), fourth-order aberration RMS (mm), higher-order aber-rations RMS (HOAs RMS) (mm), and lower-order aberrations RMS (LOAs RMS) (mm).

Secondary Outcome Measures

These included anterior Km (D), posterior Km (D), Kmax (D), and Topo Cyl (D).

RESULTS

Primary Outcome Measures

Visual Outcomes

At 3 years, all cases showed a significant improvement in their UDVA, CDVA, and CLDVA (decimal equivalent to the logMAR scale). We also observed an increase in mean values in all the patients of each group with UDVA (0.31, 0.24, and 0.24) and CDVA (0.58, 0.40, and 0.40), regarding the preoperative

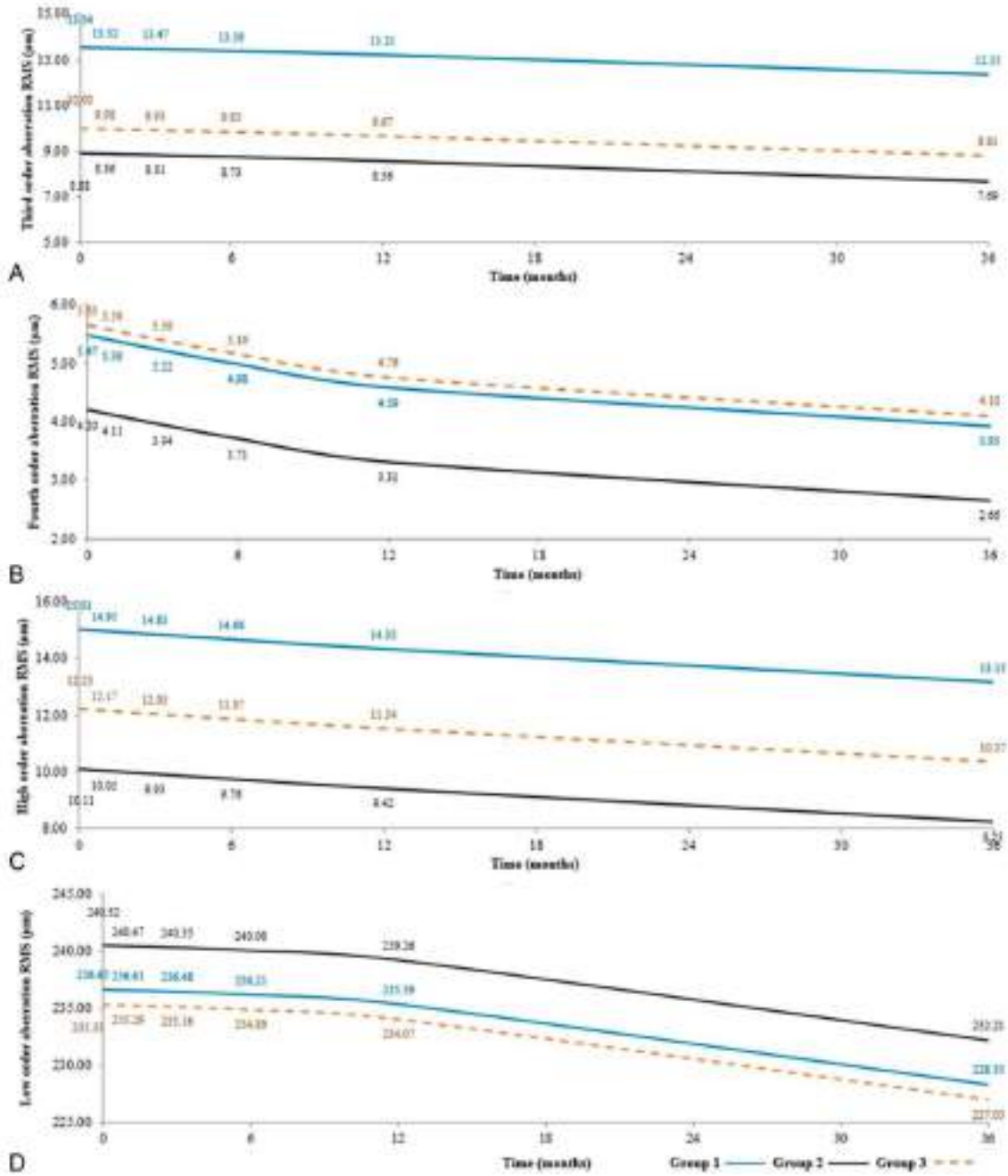

FIGURE 5. Aberrometry outcomes after 3 years in G-1, G-2, and G-3. A, Third-order aberration RMS (mm). B, Fourth-order aberration RMS (mm). C, Higher-order aberrations RMS (mm). D, Lower-order aberrations RMS (mm). Notice the progressive improvement of all mean aberrometric values along the study period. (The full color version of this figure is available at www. corneajrnl.com.)

means values of UDVA (0.19, 0.13, and 0.13) and CDVA (0.40, 0.22, and 0.21) in G-1, G-2, and G-3, respectively. The improvement in mean values was 0.12 in G-1 and 0.11 in G-2 and G-3 in decimal scale, equivalent to 1.2 and 1.1 lines in logMAR scale with UDVA, respectively. Concerning CDVA, the improvement in mean values was 0.18 in G-1 and G-2 and 0.19 in G-3 in decimal scale, equivalent to 1.8 and 1.9 lines in the logMAR scale, respectively (Figs. 1A, B; Table 1).

Moreover, at 3 years, all cases showed an improvement in CLDVA, reaching maximum mean values at 36 months (0.84, 0.62, and 0.75) when compared with the preoperative mean values (0.61, 0.39, and 0.52) in G-1, G-2, and G-3, respectively. The total improvement detected in mean values at 3 years was 0.23 in G-1, G-2, and G-3 in decimal scale, equivalent to 2.3 lines in logMAR scale regarding the preoperative mean values (Fig. 1C; Table 1).

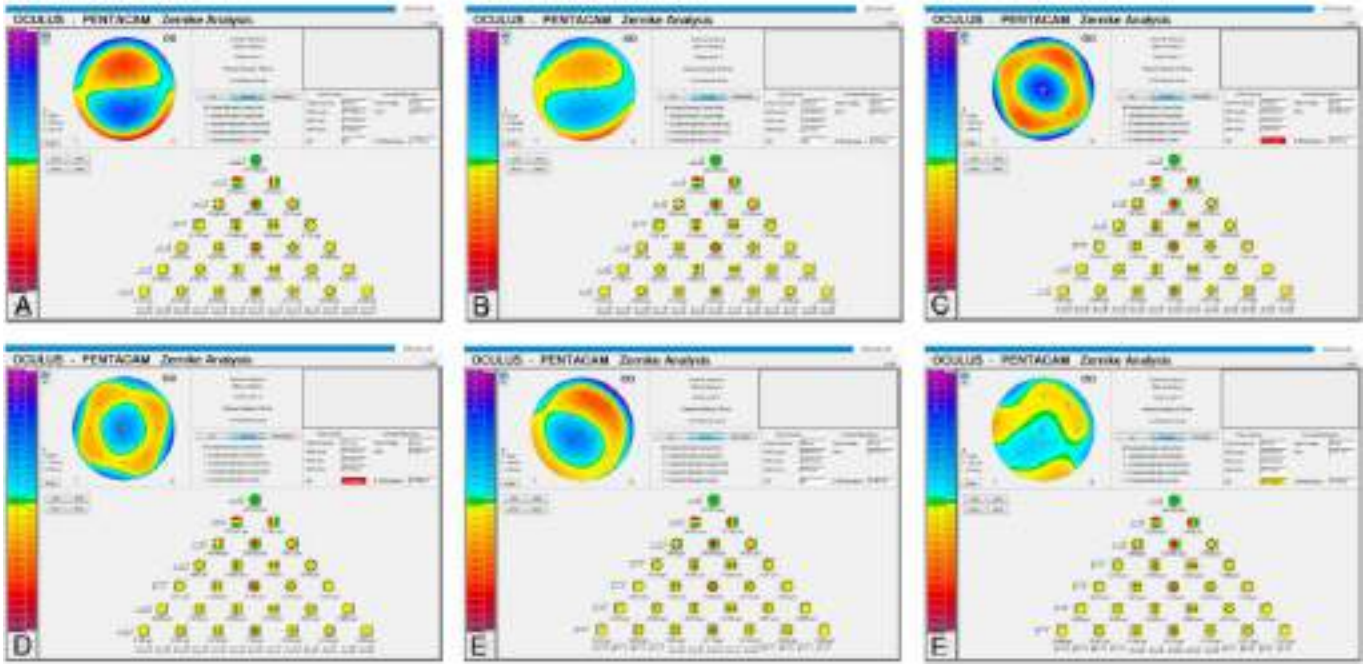

FIGURE 6. Corneal aberrometry (Pentacam) comparison between the preoperative and 36-month postoperative values in G-2 and G-3. A and B, Third-order aberration RMS (mm) in G-2 case 6 at 36 months. C and D, Fourth-order aberration RMS (mm) comparison between the preoperative and 36-month postoperative values in G-3 case 12. E and F, HOAs RMS (mm) comparison between the preoperative and 36-month values in G-2 case 9. (The full color version of this figure is available at www.corneajrnl. com.)

Comparing the results of mean visual values among the 3 groups during the follow-up, no statistically significant differences were found in UDVA in G-2 (P = 0.054) and G-3 (P = 0.069), respectively, compared with that of G-1, nor in G-2 compared with that of G-3 (P = 0.986) (Fig. 1A; Table 2). A statistically significant worsening with CDVA in mean values were observed in G-2 and G-3 (P < 0.001) when compared with those of G-1. No significant improvement in mean visual values was observed comparing G-2 with G-3 (P = 0.9) (Fig. 1B; Table 2). CLDVA mean values were statistically significantly worse in G-2 (P < 0.001) compared with those of G-1. We did not obtain significant statistical differences in G-3 (P = 0.090) compared with G-1. However, we obtained a statistically significant worsening in G-2 (P = 0.01) when compared with G-3 (Fig. 1C; Table 2). We detected a statistically significant trend during the 3-year follow-up concerning the following visual results: UDVA (P = 0.015); CDVA (P < 0.001), and CLDVA (P < 0.001) (Table 2).

Manifest Refraction

Rx Sphr (D) mean values in all the patients of each group showed a significant improvement from the preoperative (-4.1, -4.2, and -4.0) till 36 months (-3.0, -3.1, and -2.9) in G-1, G-2, and G-3, respectively. Significant statistical differences were not found in G-2 (P = 0.0892) or in G-3 (P = 0.0863) compared with G-1 or between G-2 and G-3 (P = 0.747) (Fig. 1D; Tables 1 and 2).

Rx Cyl (D) remained almost stable, showing only a mean change of 0.1 (D), from the preoperative (-3.5, -2.5, and -2.9) until 12 months postoperatively (-3.4, -2.4, and -2.8) in G-1, G-2, and G-3, respectively. This was followed by a slight deterioration of the mean difference in all patients of each group until 36 months postoperatively (-4.0, -3.0, and -3.4, respectively). Comparing the results of the 3 groups during the 3-year follow-up, there was a statistically significant improvement in G-2 (P < 0.001) and G-3 (P = 0.014) when compared with G-1. No significant differences were observed between G-2 and G-3 (P = 0.086) (Fig. 1E; Tables 1 and 2). A statistically significant trend (P = 0.015) in Rx Cyl was found during the 3-year follow-up (Table 2).

Cornea Thickness and Volume Parameters

AS-OCT Visante CCT (mm), thinnest point (mm), and CV (mm^3) mean values were at the preoperative time (410, 454, and 487 µm), (385, 435, and 449 µm), and (53, 59, and 59 mm^3), respectively. These values reached a maximum average increase at 12 months postoperatively in G-1, G-2, and G-3: CCT (469, 513, and 546 µm), thinnest point (433, 484, and 498 µm), and CV (57, 62, and 62 mm^3), respectively. At 36 months postoperatively, the mean values changed to 440, 484, and 517 µm in CCT, 416, 466, and 480 µm in thinnest point, and 56, 61, and 61 mm^3 in CV in G-1, G-2, and G-3, respectively. An increase in the pachymetric and volumetric parameters was observed in all patients of each group when comparing the results during the 3-year follow-up (Figs. 1F–H, 2–4; Table 1). CCT mean values showed a significant improvement in G-2 (P = 0.012) and G-3 (P < 0.001), when compared with that of the G-1 (Fig. 1F; Table 2). The thinnest point mean values also significantly improved in G-2 (P = 0.007) and G-3 (P = 0.001) when compared with that of G-1 (Fig. 1G; Table 2). Similarly, CV showed significant improvement in the mean values in

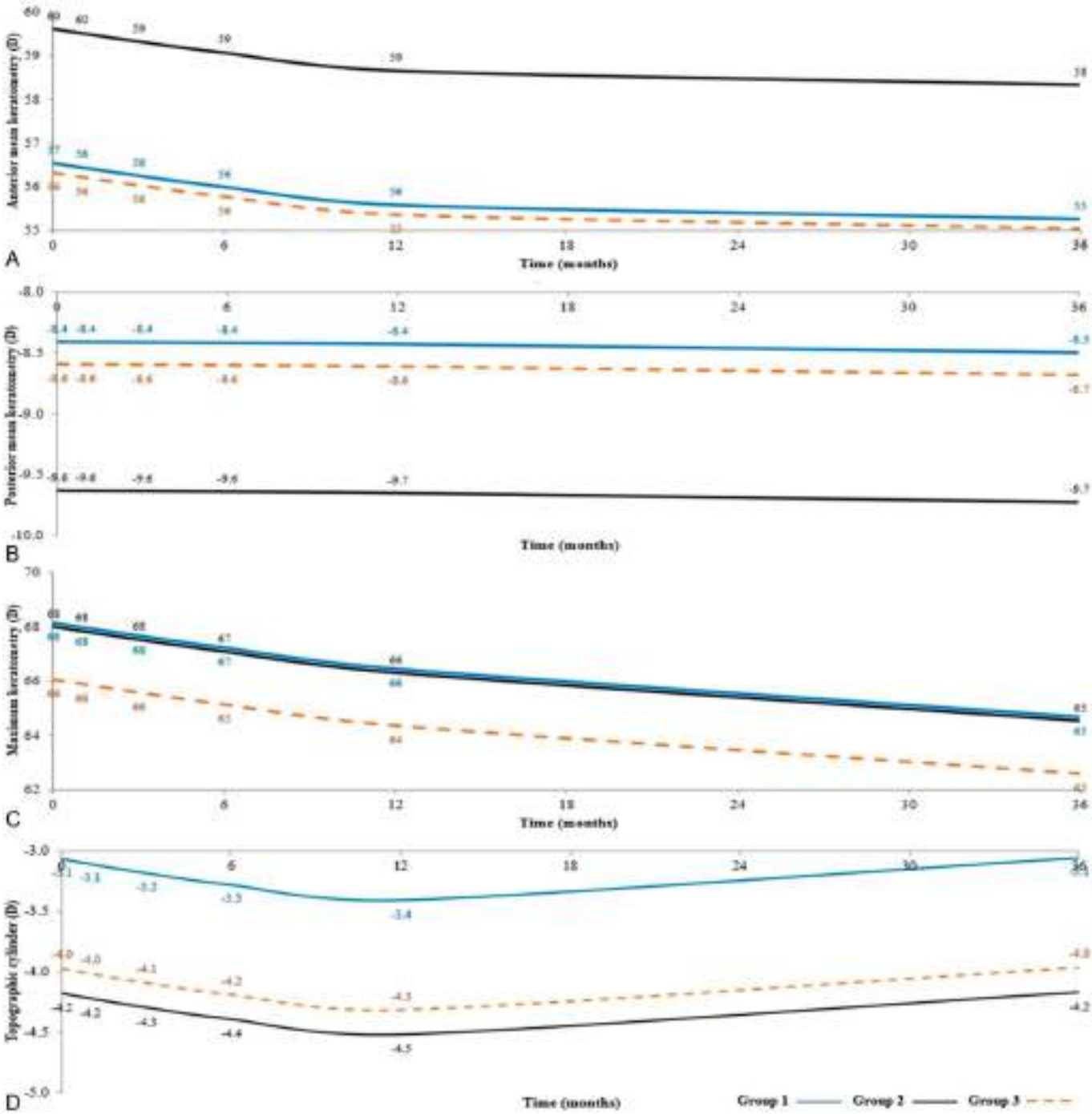

FIGURE 7. Keratometric outcomes after 3 years of follow-up in G-1, G-2 and G-3. A, Anterior mean keratometry (D): notice the mean improvement of 1 D at 12 months, followed by another 1 D of flattening at 36 months. B, Posterior mean keratometry (D): mean values remained stable along the study period in all groups. C, Maximum keratometry (D): there was a mean flattening of 2 D at 12 months, followed by another 1 D of flattening at 36 months. D, Note the topographic cylinder change of 20.3 D at 12 months, whereas, at 36 months, mean values rose until the same preoperative level. (The full color version of this figure is available at www.corneajrnl.com.)

G-2 and G-3 ($P < 0.001$) compared with that of G-1 (Fig. 1H; Table 2). There was no significant difference in mean values between G-2 and G-3 ($P = 0.055$, $P = 0.465$, and $P = 0.948$) in the CCT, thinnest point, and CV values, respectively (Figs. 1F–H; Table 2). A statistically significant trend during the follow-up was obtained in the following variables: Visante CCT ($P = 0.004$); thinnest point ($P = 0.021$); and CV ($P = 0.001$) (Table 2).

TABLE 3. Anterior Km (D) and Kmax (D) Mean Values in G-1, G-2, and G-3, and Difference in Mean Values Between (G-1) 2 (G-2), (G-1) 2 (G-3), and (G-2) 2 (G-3).

Group	Time (mo)	Anterior Km (D), Mean Values	Kmax (D), Mean Values
G-1	0	57.00	68.00
G-1	36	55.00	65.00
G-2	0	60.00	68.00
G-2	36	58.00	65.00
G-3	0	56.00	66.00
G-3	36	55.00	63.00
(G-1) 2 (G-2)	0	23.00	0.00
(G-1) 2 (G-2)	36	23.00	0.00
(G-1) 2 (G-3)	0	1.00	2.00
(G-1) 2 (G-3)	36	2.00	5.00
(G-2) 2 (G-3)	0	4.00	5.00
(G-2) 2 (G-3)	36	3.00	2.00

Evolution of the Aberrometry Variables

Third-order RMS, fourth-order RMS, HOAs RMS, and LOAs RMS were measured at a maximum of 6 mm of pupil diameter. The results of the mean values showed an improvement in all patients at 36 months postoperatively in G-1, G-2, and G-3 (12.35, 7.69, and 8.81 µm), (3.93, 2.66, and 4.10 µm), (13.15, 8.25, and 10.37 µm), and (228.35, 232.21, and 227.03 µm), regarding the preoperative mean values (13.54, 8.88, and 10.00 µm), (5.47, 4.20, and 5.65 µm), (15.01, 10.11, and 12.23 µm), and (236.65, 240.52, and 235.33 µm), respectively (Figs. 5 and 6; Table 1). During the 3-year follow-up, we observed only that third-order RMS values were statistically significantly better in G-2 ($P < 0.001$) and G-3 ($P = 0.009$) when compared with those of the G-1 (Fig. 5A; Table 2), and moreover, a statistically significant improvement was observed in mean values of HOAs RMS with G-2 ($P < 0.001$) and G-3 ($P = 0.038$) when compared with those of G-1 (Fig. 5C; Table 2). Concerning G-2 and G-3, there were only statistically significant differences in the mean values of fourth-order RMS ($P = 0.004$), with G-2 being better than G-3 (Table 2).

Secondary Outcome Measures

Corneal Topography

Anterior Km (D): We observed in all groups a mean improvement of 1 D until 12 months postoperatively (56, 59, and 55 D) when compared with the preoperative mean values (57, 60, and 56 D) in G-1, G-2, and G-3, respectively. This was followed by another 1 D of mean flattening until 36 months postoperatively (55, 58, and 54 D, respectively). Hence, a total improvement of 2 D regarding the preoperative mean values was observed after 3 years of postoperative evolution. No significant differences were found among the 3 groups (Figs. 3, 4, 7A; Tables 1–3).

Posterior Km (D): Mean values remained stable in all groups at 36 months postoperatively compared with the preoperative mean values, with only a slight nonsignifi-cant mean difference of 0.1 D. During the 3-year follow-up, we found a significant worsening only in G-2 ($P = 0.001$) but not in G-3 ($P = 0.636$) when compared with that in G-1. A significant worsening was observed in G-2 when compared with that in G-3 ($P = 0.004$) (Figs. 3, 4, 7B; Table 2).

Kmax (D): We found in all groups a mean flattening of 2 D at 12 months postoperatively (66, 66, and 64 D) compared with the preoperative mean values (68, 68, and 66 D) in G-1, G-2, and G-3, respectively. This was followed by another 1 D of mean flattening till 36 months postoperatively (65, 65, and 63 D, respectively). We did not find any significant differences among G-1, G-2, and G-3 during the 3-year follow-up (Figs. 3, 4, 7C; Tables 1–3).

Topo Cyl (D): G-1, G-2, and G-3 showed at 12 months postoperatively the following mean values (23.4, 24.5, and 24.3 D) compared with the mean preoperative values (23.1, 24.2, and 24.0 D), respectively, and then, a change of (20.3 D) was obtained. Meanwhile, at 36 months postoperatively, mean values (23.1, 24.2, and 24.0 D respectively) increased again, reaching a similar value to the preoperative measurement. Comparing the results during the 3-year follow-up of the study, the mean values were not statistically significant among the 3 groups (Figs. 3, 4, 7D; Table 1 and 2).

Slit Lamp Biomicroscopy

Before surgery and during the 36-month follow-up, all corneas presented a fully transparent central area and visual axis and remained the same, with no traces of scars at any level (Figs. 8–10). Only 1 patient in each group showed mild preoperative paracentral anterior stromal scars (cases 2, 9, and 11) (Figs. 8C, 10A). Inflammatory complications were not observed in any of the cases during the 3-year follow-up period (Figs. 8–10). Corneal transparency in G-1 was completely recovered within 24 hours after surgery, and it was maintained throughout the 36-month follow-up period (Fig. 8). As described in our previous interim reports,[4,6,8] case 2 from G-1 presented with preoperative paracentral anterior stromal scars, but after the third postoperative month, we observed an evident improvement of those scars, which continued to improve over the 36-month study period (Figs. 1C, D). This improvement was demonstrated also in the confocal microscopy study (Fig. 8F). In G-2 and G-3, during the first postoperative month, the implanted lamina showed a clinical mild early haziness that was related to mild lenticular edema (Figs. 9B, 10B). Then, corneal transparency improved progressively showing a complete restoration before the third month of follow-up in all cases. No patient showed any trace of corneal haze or scarring (Figs. 8–10).[6–8] An improvement in paracentral scarring was also noticed in case 11 of G-3 when the preoperative findings were compared with those at 36 months (Figs. 10A–E). This observation correlated well with the findings of the confocal microscopy study because we could observe hyperreflective deposits that corresponded to paracentral corneal scarring in the preoperative period in case-2 of G-1 and case 11 of G-3. These scars improved during the following 12 postoperative months (Fig. 8F),[6] a finding that was already described in our previous interim publications.[4,6–8] In

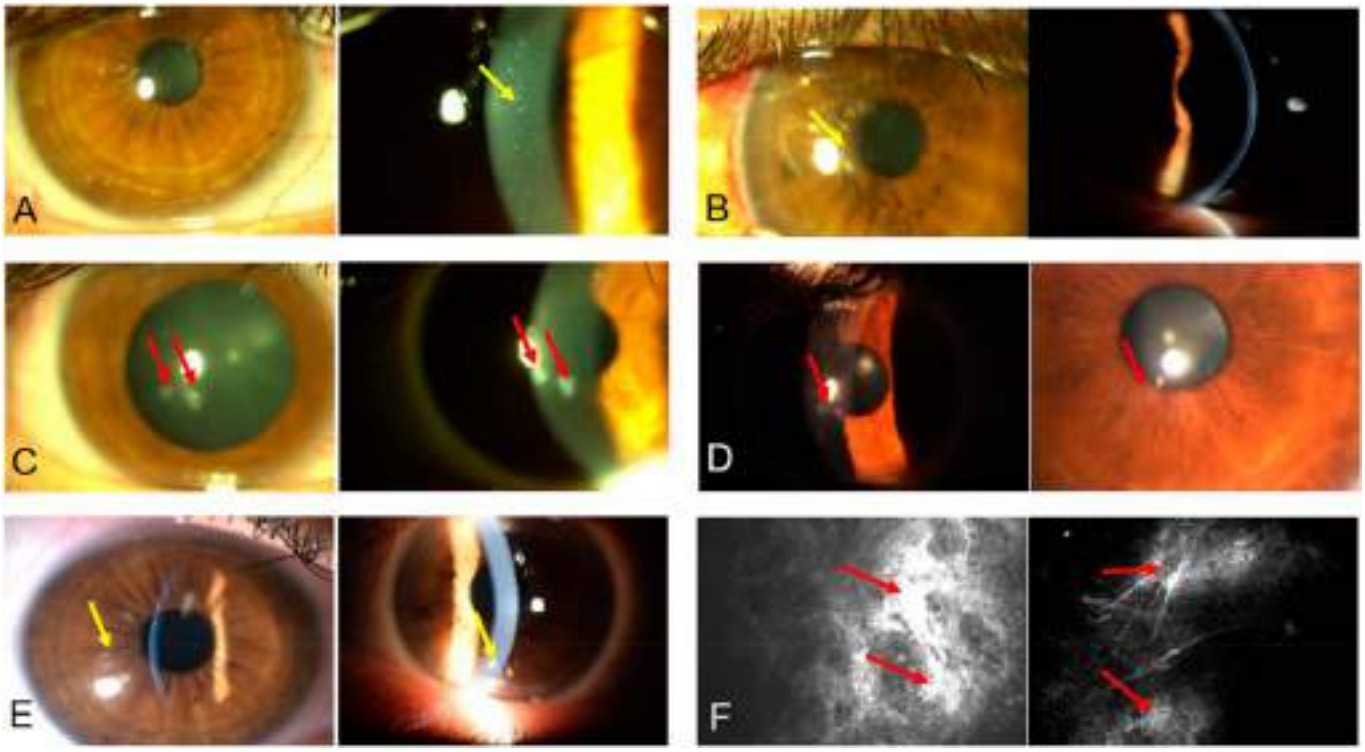

FIGURE 8. G-1 clinical biomicroscopic changes between the preoperative status and 36 months after surgery. A, Case 1: corneal transparency at 1 day postoperative (left). Small grayish precipitates can be observed within the surgical plane (right) (yellow arrow) but without any impact on the visual performance. B, Case 4: observe the corneal transparency at 1 day postoperatively (left) and the small grayish precipitates within the surgical plane (yellow arrow). Normal corneal transparency at 6 months (right). C, Case 2: observe the presence of paracentral scars (red arrows) at the preoperative level (left) and 1 month postoperatively (right). D, The same case 2 at 12 months (left) and at 36 months (right): observe the marked improvement of the paracentral scars (red arrows). E, Case 1 (left) and case 4 (right) at 36 months: some scattered, faint, patchy islands of haze (yellow arrows) could be observed without any impact on the visual performance. F, Confocal microscopy findings in case 2: notice the high reflective deposits and fibrotic tissue in the anterior stroma of the cornea at the preoperative level (red arrows; left), which corresponded to the paracentral scars. At 12 months (right), improvement of the anterior stroma fibrotic tissue could be observed (red arrows). (The full color version of this figure is available at www.corneajrnl.com.)

addition, in most patients of G-1, G-2, and G-3, some dispersed fog "islands" were observed (Figs. 8E, 9D), which did not have any negative impact on visual acuity.[7,8] Such fog islands in G-2 and G-3, when studied with confocal microscopy, showed to be clusters of migrated keratocytes from the host stroma toward the border of the implanted laminas (Figs. 9F, 10F). Moreover, we observed the presence of hyperreflective structures related to the formation of paracentral fibrotic tissue. These hazy areas did not have any impact on the visual outcomes in any of the patients in whom such findings were observed (Figs. 9F, 10F).[4–8]

Other Clinical Outcomes

During the 3 years of observation, no significant changes were detected in IOP (mm Hg) or endothelial cell density (cells/mm^2).

DISCUSSION

This study reported the 3-year outcomes of the first clinical study on corneal stromal regeneration therapy for the treatment of advanced keratoconus.[4,5,7] It is the first time that ADASCs have been implanted in the human corneal stroma[4–8] and the first time that decellularized human cornea stroma laminas, colonized or not by autologous ADASCs, have been implanted in clinical cases of keratoconus for therapeutic purposes (Figs. 2–4, 6, 8–10).[6–8] We have been able to confirm in this report the absence of complications such as corneal inflammation or any significant induction of corneal scarring or haze during the postoperative period.

Furthermore, 3 years after surgery, we obtained an improvement of almost 1 line in the logMAR scale in UDVA, 2 lines in CDVA, and 2.3 lines in CLDVA in all cases (Figs. 1A–C; Table 2). In addition, Rx Sphr mean values showed an improvement in all groups, and a change in Rx Cyl was observed (Figs. 1D, E; Table 2). An increase in the thickness of the thinnest corneal point, CCT, and CV (Figs. 1F–H; Table 2) was obtained. There was also an improvement in all corneal aberrations, especially in the third-order and HOAs RMS (Figs. 5A, C) and an improvement in anterior Km and Kmax mean values (Figs. 7A, C; Table 3).

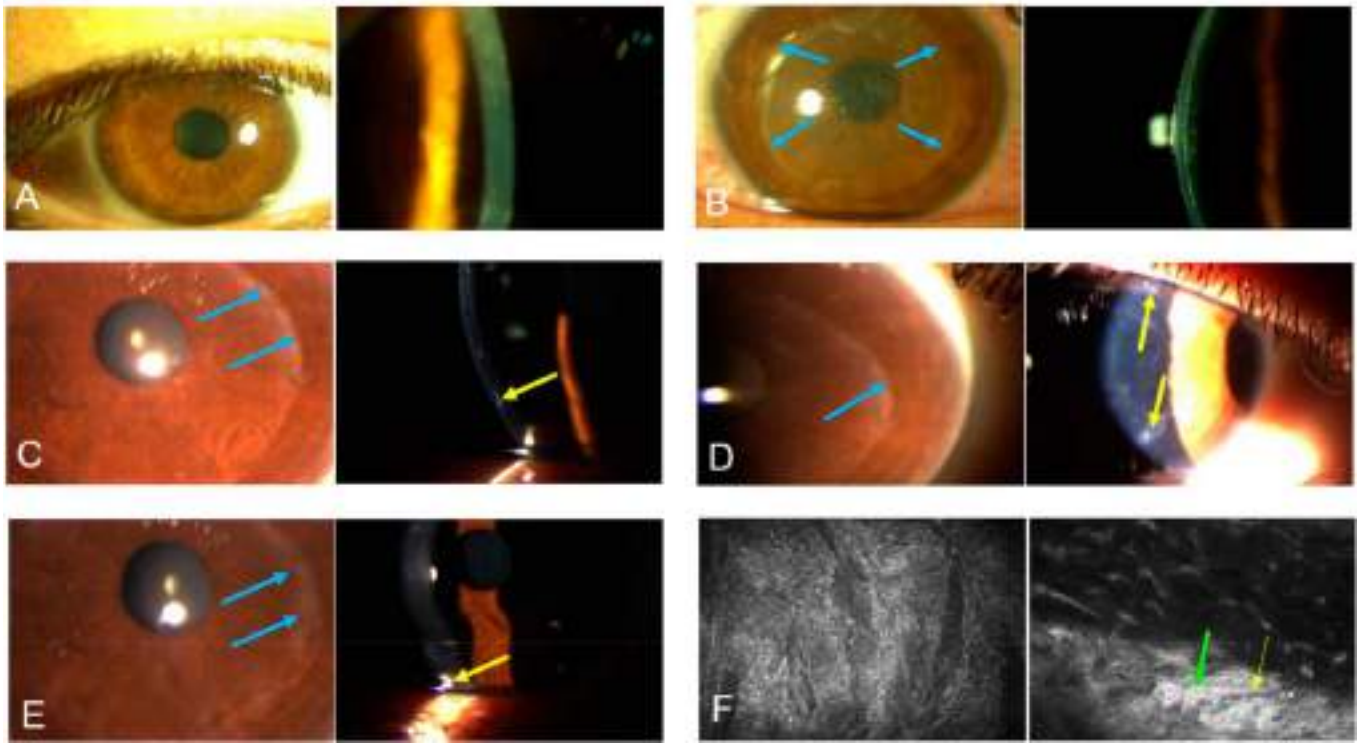

FIGURE 9. Biomicroscopy changes among the preoperative and 36 months after surgery in G-2 case-5. A, Preoperative (left and right). B, At 1 day postoperative (left and right): reduced transparency due to edema of the implanted lamina. Blue arrows show the borders of the lamina. C, At 6 months (the blue arrows; left) and the (yellow arrow; right) point to the periphery of the lamina. D, At 12 months: border of the implanted lamina (blue arrow; left). Paracentral fibrotic tissue at the surgical plane (yellow arrows; right). E, Improvement in the transparency of the implanted tissue at 36 months (blue arrows). Paracentral fibrotic tissue at the surgical plane (yellow arrows; right). F, Confocal microscopy image in G-2 case-5: at 1 month (left) we can observe the acellular anterior surface of the decellularized lamina. After 12 months (right), we can see the accumulation of migrating keratocytes nuclei from the host stroma toward the posterior surface of the decellularized lamina (green arrow), and the presence of some para-central fibrotic tissue in the periphery of the lamina (yellow arrow). (The full color version of this figure is available at www. corneajrnl.com.)

The progressive flattening of the cornea explains the improvement observed in the refractive sphere and visual parameters. The aberrometric improvement that is observed is consistent with such improvements in the visual parameters. We consider these results to be relevant for the eyes that were selected for the investigation because they were advanced keratoconus cases with an indication for corneal graft as the only therapeutic alternative. Interestingly, the production of neocollagen and the increase in corneal thickness was observed after the implantation of ADASCs and decellularized or ADASC-recellularized laminas (Fig. 2). Whether this finding has any influence on the debilitated biomechanics of the cornea with advanced keratoconus warrants further investigations.[9]

The modest increase observed in the corneal thickness in G-1 was not significant during the 3-year follow-up, whereas in G-2 and G-3, the increase of thickness was statistically significantly better. The implanted laminas showed evidence of biointegration of the implanted tissue in the host stroma by biomicroscopy and by the AS-OCT study. The highly reflective light observed in the results of OCT and the early haziness observed by the oblique light of the slit lamp decreased gradually from the third postoperative month[7,8] until the end of the 3-year follow-up, when the lamina was well integrated into the corneal stroma. Such biointegration may be related to the slight decrease in pachymetric and volumetric parameters observed in G-2 and G-3.

Biomicroscopy examination demonstrated that all corneas at 3 years had a fully transparent visual axis (Figs. 8–10). Some preoperative paracentral scars present in some cases showed a progressive improvement as in case 2 in G-1 and case 11 in G-3; this could be related to the implantation of ADASCs and the production of the neo-collagen as previously demonstrated in the animal model (Figs. 8C, D, F, 10–E).[4–8] In addition, the transparency of the implanted tissue improved over the follow-up (Figs. 9B–E, 10–E). Nevertheless, the presence of mild para-central fibrotic tissue was observed in all cases in G-2 and G-3 (Figs. 9D, F, 10C–E). This fibrotic tissue was located at the paracentral lamina interface. No significant correla-tion was found between the recellularization of the lamina and the presence of this fibrotic tissue.[6] Its formation may be avoided in the future by controlling the activation of host keratocytes and the keratocytes differentiated from the implanted ADASCs. Published studies support the

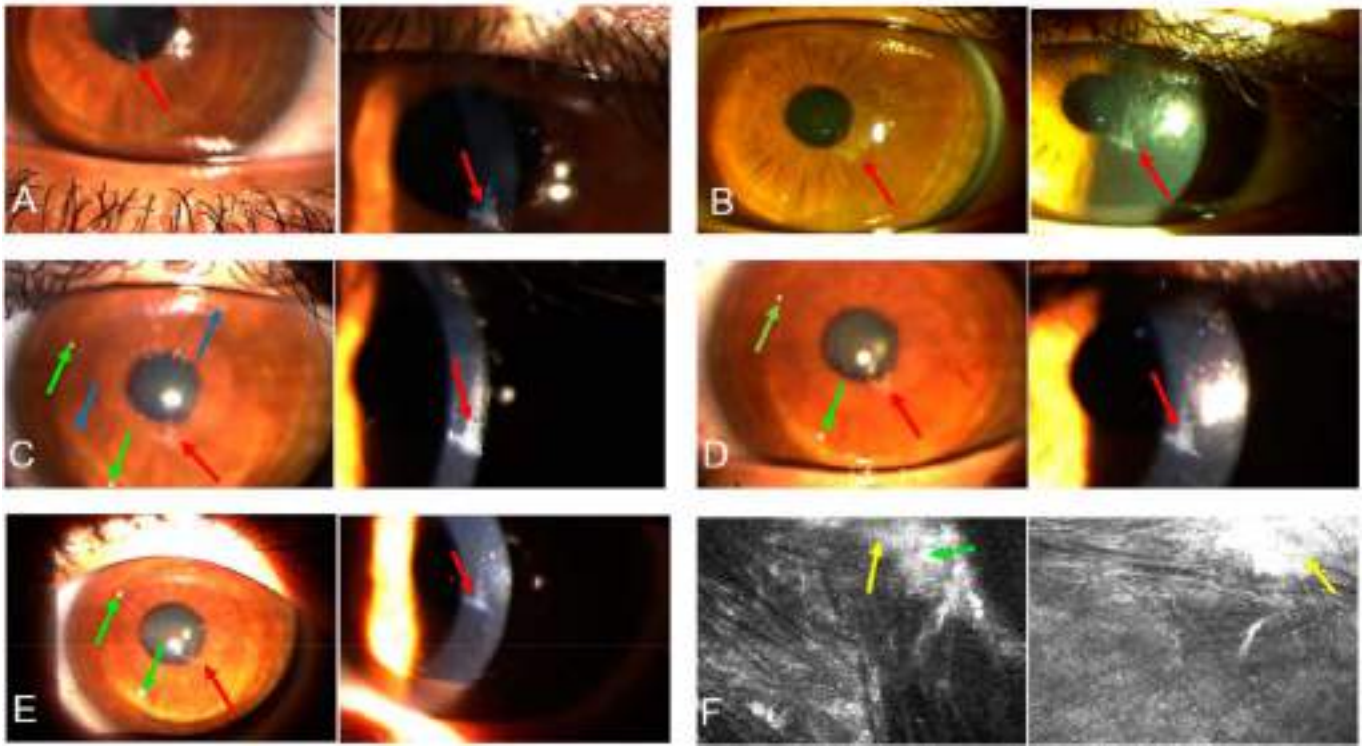

FIGURE 10. G-3 biomicroscopy changes in case 11 from preoperative until 36 months after surgery. A, Preoperative: red arrows show the presence of a paracentral scar. B, At 1 month: red arrows show the paracentral scar. C, At 6 months: blue arrows show the periphery of the recellularized lamina, red arrows indicate the paracentral scar, and the green arrows show paracentral fibrotic tissue with an accumulation of migrating keratocytes toward the border of the lamina. D, At 12 months: observe the slight improvement of the paracentral scar (red arrows). Note that the border of the lamina is not remarkable. Green arrows indicate the presence of the same paracentral fibrotic tissue. E, At 36 months: observe the improvement of the paracentral opacification (red arrows). Green arrows show the same fibrotic anterior tissue. F, Confocal microscopy in G-3 case 11: green arrow points accu-mulation of migrating keratocytes on the periphery of the posterior surface of the recellularized lamina (left), whereas the yellow arrow shows the presence of some fibrotic tissue. At 12 months postoperatively (left), a highly reflective fibrotic tissue (yellow arrow) in the anterior surface of the recellularized lamina is present. (The full color version of this figure is available at www. corneajrnl.com.)

hypothesis[18] that corneal wound healing is mediated by secreted extracellular vesicles containing microRNAs. These vesicles could decrease the expression of fibrotic-inducing genes and restore the normal tissue morphology transferring specific microRNA to the target tissue.

Other authors' parallel studies[19 –25] using allogenic lenticule obtained using small-incision lenticule extraction as corneal inlay implants have shown that laminas implants from small-incision lenticule extraction are a feasible option for refractive correction of aphakia and other refractive errors. Such studies have shown an improvement in visual acuity in all cases correlated with an improvement in the refractive parameters, even when the follow-up of the patients was limited to 6 to 12 months. However, such an approach has relevant limitations to be considered as a surgical alternative to keratoconus treatment. In our method,[7,8] we have used neutral optical power stromal laminas obtained from corneas not valid for a corneal graft. According to our results, each cornea from the eye bank can provide 2 to 3 valid sheets for transplantation and, thus, are conveniently cost-effective.

However, despite the limitations related to the limited number of cases included in this pilot investigation, we consider that the 3-year outcomes demonstrate the safety and therapeutic potential of our method. Nevertheless, the results must be interpreted with caution. There was no control group in which only a corneal pocket would be performed because it was considered unethical as no benefit could be offered to the patient from that procedure. Because this study was per-formed in living human volunteers, there was no possibility to perform postmortem analysis because none of the cases so far have required corneal transplantation, with the consequent lack of tissue sample to perform histopathology.[4,7,8]

The results described in this study show that our approach offers a new type of surgery to increase corneal thickness in advanced keratoconus cases. Visual parameters, topography, and aberrometry parameters improved in almost all the study cases. Future studies are needed with larger cohorts and by selecting cases with less severe grades of keratoconus with different phenotypes to obtain more scientific evidence to support the clinical application of this new type of corneal surgery.

Moreover, the potential influence of the implantation of mesenchymal stem cells and corneal laminas on the progressive nature of the disease merits further study to be confirmed. However, despite these limitations, we consider that the outcomes of this study give rise to a new potential for clinical application, and perhaps a new horizon for the clinical use of mesenchymal ADASCs, and a new type of corneal stroma therapy in corneal surgery.

In conclusion, in this report, we confirmed the 3-year safety outcomes of this advanced therapy approach for the treatment of keratoconus. Corneal thickness improvement in the corneas implanted only with cells seems to be insufficient to restore normal corneal thickness, whereas the intralamellar implantation showed an excellent result concerning corneal thickness restoration with better cell density in the group implanted with recellularized laminas. The modest but significant visual and refractive improvements found in the study, with a total absence of complications, confirm the feasibility of this therapeutic approach as a potential novel technique for the treatment of keratoconus. Future studies with larger series and in less advanced cases of keratoconus will establish the therapeutic potential of this new type of surgery.

ACKNOWLEDGMENTS

The authors thank Eric Bangert and Heidelberg Engineering Co. (Heidelberg, Germany) for the generous temporary donation of the confocal microscopy and confocal software analysis software used for this investigation; Marc Assouwad from Laser Vision (Beirut, Lebanon) for her assistance in the logistics of the study and Peggy Saba for the data collecting; Albert Aazar and Reviva Regenerative, Beirut, Lebanon, for the administrative management of the Laboratory; and Ibrahim Achkar who was responsible for the liposuction and adipose tissue management until the moment of the laboratory study.

REFERENCES

1. Barbara R, Turnbull AM, Hossain P, et al. Epidemiology of keratoconus. In: Alió JL, ed. Keratoconus: Recent Advances in Diagnosis and Treatment. Cham, Switzerland: Springer; 2017:13–23.
2. Alio J. Keratoconus: Recent Advances in Diagnosis and Treatment. Cham, Switzerland: Springer; 2017.
3. Arnalich-Montiel F, Alió Del Barrio J, Alió J. Corneal surgery in keratoconus: which type, which technique, which outcomes? Eye Vis. 2016;3:2.
4. Alió Del Barrio J, El Zarif M, de Miguel M, et al. Cellular therapy with human autologous adipose-derived adult stem cells for advanced keratoconus. Cornea. 2017;36:952–960.
5. Alió JL, Alió del Barrio JL. Cellular therapy with human autologous adipose-derived adult stem cells for advanced keratoconus: reply to the letter to editor. Cornea. 2017;36:e37.
6. El Zarif M, Abdul Jawad K, Alió del Barrio JL, et al. Corneal stroma cell density evolution in keratoconus corneas following the implantation of adipose mesenchymal stem cells and corneal laminas: an in vivo confocal microscopy study. Invest Ophthalmol Vis Sci. 2020;61:22.
7. Alió Del Barrio J, El Zarif M, Azaar A, et al. Corneal stroma enhancement with decellularized stromal laminas with or without stem cell recellularization for advanced keratoconus. Am J Ophthalmol. 2018; 186:47–58.
8. Alió JL, Alió Del Barrio JL, El Zarif M, et al. Regenerative surgery of the corneal stroma for advanced keratoconus: 1-Year outcomes. Am J Ophthalmol. 2019;203:53–68.
9. Alió JL, Piñero DP, Alesón A, et al. Keratoconus-integrated characterization considering anterior corneal aberrations, internal astigmatism, and corneal biomechanics. J Cataract Refract Surg. 2011;37:552–568.
10. Zuk PA, Zhu M, Mizuno H, et al. Multilineage cells from human adipose tissue: implications for cell-based therapies. Tissue Eng. 2001;7: 211–228.
11. Zuk PA, Zhu M, Ashjian P, et al. Human adipose tissue is a source of multipotent stem cells. Mol Biol Cell. 2002;13:4279–4295.
12. Bourin P, Bunnell B, Casteilla L, et al. Stromal cells from the adipose tissue-derived stromal vascular fraction and culture expanded adipose tissue-derived stromal/stem cells: a joint statement of the International Federation for Adipose Therapeutics and Science (IFATS) and the International Society for Cellular Therapy (ISCT). Cytotherapy. 2013;15: 641–648.
13. Arnalich-Montiel F, Pastor S, Blazquez-MartinezA, et al. Adipose-derived stem cells are a source for cell therapy of the corneal stroma. Stem Cells. 2008;26:570–579.
14. Alio del Barrio J, Chiesa M, Garagorri N, et al. Acellular human corneal matrix sheets seeded with human adipose-derived mesenchymal stem cells integrate functionally in an experimental animal model. Exp Eye Res. 2015;132:91–100.
15. Alió del Barrio JL, Chiesa M, Ferrer GG, et al. Biointegration of corneal macroporous membranes based on poly(ethyl acrylate) copolymers in an experimental animal model. Adv Sci. 2015;103:1106–1118.
16. Ponce Márquez S, Martínez V, McIntosh Ambrose W, et al. Decellularization of bovine corneas for tissue engineering applications. Acta Biomater. 2009;5:1839–1847.
17. Lynch AP, Ahearne M. Strategies for developing decellularized corneal scaffolds. Exp Eye Res. 2013;108:42–47.
18. Shojaati G, Khandaker I, Funderburgh ML, et al. Mesenchymal stem cells reduce corneal fibrosis and inflammation via extracellular vesicle-mediated delivery of miRNA. Stem Cells Transl Med. 2019;8: 1192–1201.
19. Ganesh S, Brar S. Femtosecond intrastromal lenticular implantation combined with accelerated collagen cross-linking for the treatment of keratoconus: initial clinical result in 6 eyes. Cornea. 2015;34: 1331–1339.
20. Ganesh S, Brar S, Rao PA. Cryopreservation of extracted corneal lenticules after small incision lenticule extraction for potential use in human subjects. Cornea. 2014;33:1355–1362.
21. Jacob S, Kumar DA, Agarwal A, et al. Preliminary evidence of successful near vision enhancement with a new technique: PrEsbyopic allogenic refractive lenticule (PEARL) corneal inlay using a SMILE lenticule. J Refract Surg. 2017;33:224–229.
22. Pradhan KR, Reinstein DZ, Carp GI, et al. Femtosecond laser-assisted keyhole endokeratophakia: correction of hyperopia by implantation of an allogeneic lenticule obtained by SMILE from a myopic donor. J Refract Surg. 2013;29:777–782.
23. Sun L, Yao P, Li M, et al. The safety and predictability of implanting autologous lenticule obtained by SMILE for hyperopia. J Refract Surg. 2015;31:374–379.
24. Mastropasqua L, Nubile M, Salgari N, et al. Femtosecond laser-assisted stromal lenticule addition keratoplasty for the treatment of advanced keratoconus: a preliminary study. J Refract Surg. 2018;34:36–44.
25. Sekundo W, Kunert KS, Blum M. Small incision corneal refractive surgery using the small incision lenticule extraction (SMILE) procedure for the correction of myopia and myopic astigmatism: results of a 6 month prospective study. Br J Ophthalmol. 2011;95: 335–339.

10.6. El Zarif, M, Abdul Jawad, K., Alió del Barrio, J., Abdul Jawad, Z., Palazón-Bru, A., De Miguel, M., Saba, P., Makdissy, N., Alió, J., 2020. Corneal stroma cell density evolution in keratoconus corneas following the implantation of adipose mesenchymal stem cells and corneal laminas: an in vivo confocal microscopy study. IOVS 61, 22. https://doi.org/10.1167/iovs.61.4.22

Corneal Stroma Cell Density Evolution in Keratoconus Corneas Following the Implantation of Adipose Mesenchymal Stem Cells and Corneal Laminas: An In Vivo Confocal Microscopy Study

Mona El Zarif,[1,3,7,8] Karim A. Jawad,[1] Jorge L. Alió Del Barrio,[2,3] Ziad A. Jawad,[1] Antonio Palazón-Bru,[4] María P. de Miguel,[5] Peggy Saba,[6] Nehman Makdissy,[7] and Jorge L. Alió[2,3]

[1]Optica General, Saida, Lebanon
[2]Cornea, Cataract and Refractive Surgery Unit, Vissum Corporación, Alicante, Spain
[3]Division of Ophthalmology, Miguel Hernández University, Alicante, Spain
[4]Department of Clinical Medicine, Miguel Hernández University, Alicante, Spain
[5]Cell Engineering Laboratory, IdiPAZ, La Paz Hospital Research Institute, Madrid, Spain
[6]Institut Technique Industriel Superieur Dekwaneh, Beirut, Lebanon
[7]Genomic Surveillance and Biotherapy Laboratory, Faculty of Sciences, Lebanese University, Tripoli, Lebanon
[8]Doctoral School of Sciences and Technology, Lebanese University, Hadath, Lebanon

Correspondence: Jorge L. Alió, Vissum, Calle Cabañal, 1. 03016 Alicante, Spain; jlalio@vissum.com.

Received: November 15, 2019
Accepted: February 26, 2020
Published: April 17, 2020

Citation: El Zarif M, A. Jawad K, Alió Del Barrio JL, et al. Corneal stroma cell density evolution in keratoconus corneas following the implantation of adipose mesenchymal stem cells and corneal laminas: an in vivo confocal microscopy study. https://doi.org/10.1167/iovs.61.4.22

Purpose. To report the corneal stroma cell density evolution identified by in vivo corneal confocal microscopy in humans using injected autologous adipose-derived adult stem cells (ADASCs) and corneal decellularized laminas in corneas with advanced keratoconus.

Methods. Interventional prospective, consecutive, randomized, comparative series of cases. A total of 14 keratoconic patients were randomly distributed into three groups for three types of surgical interventions: group 1 (G-1), autologous ADASC implantation (n = 5); group 2 (G-2), decellularized human corneal stroma (n = 5); and group 3 (G-3), autologous ADASCs + decellularized human corneal stroma (n = 4).

Results. A gradual and significant increase ($P < 0.001$) was observed in the cellularity in the anterior and posterior stroma of patients in G-1, G-2, and G-3 a year after the surgery in comparison with the preoperative density level. The same result was observed at the mid-corneal stroma in G-1 and at the anterior and posterior surfaces and within the laminas in G-2 and G-3. The cell density of patients receiving ADASC recellularized laminas (G-3) was statistically significantly higher ($P = 0.011$) at the anterior surface and within the lamina ($P = 0.029$) and at the posterior surface than in those implanted only with decellularized laminas (G-2).

Conclusions. A significant increase in cell density occurred up to 1 postoperative year at the corneal stroma following the implantation of ADASCs alone, as well as in those cases implanted with decellularized and recellularized laminas at the different levels of the analysis. However, this increase was significantly higher in the ADASC recellularized laminas.

Keywords: corneal confocal microscopy, keratocytes, keratoconus, autologous adipose-derived adult stem cells, corneal stem cell therapy

INTRODUCTION

Keratoconus is the most frequent and prevalent type of corneal dystrophy.[1,2] It consists of a progressive loss of corneal strength,[3] associated with a gradual loss of the stromal keratocytes. The number of keratocytes decreases from the anterior to posterior stroma,[4] and there is a progressive thinning of the corneal stroma,[4,5] even though some phenotypic differences in the expression of the disease are present.[6] However, in all cases, a loss of keratocyte density, apoptosis, and a loss of corneal stroma occur over time,[4,7–8] with corneal deformation and a shift in the location of the corneal apex[9] leading to progressive visual loss.[6]

The disease still has an unclear genomic profile.[10] In keratoconus, the use of noninvasive diagnostic methods, such as confocal microscopy, has recently provided relevant information about the microanatomical changes that happen during the evolution of the disease.[4,11]

The visual loss that keratoconus patients suffer is treated in different ways, ranging from contact lenses that reduce the higher order aberrations and mask the irregular astigmatism[12] to surgical options, with variable success[13]; however, none of these procedures has yet addressed regeneration of the diseased corneal tissue. Recently, we proposed the

clinical use of acellular corneal tissue, with or without autologous stem cell repopulation, to increase the corneal thickness and to promote the production of new collagen, aiming to improve the biological and clinical condition of the keratoconic cornea and halting the progression of the disease.[14–19] Based on these reports, the use of mesenchymal stem cells such as autologous adipose-derived adult stem cells (ADASCs) or corneal stroma decellularized lami-nas with or without ADASC recellularization implanted in the corneal stroma has become a promising therapeutic option for keratoconus treatment.

We report herein the results of our evaluation of the evolution of corneal stroma cellularity, studied with corneal confocal microscopy, in eyes that have been the subject of corneal regeneration experiences.[14–16] The visual and refractive results from the interim analyses of this cohort performed by our group at 6 and 12 months have been reported in previous publications.[14–16] Here, we report the changes induced in the cellularity and distribution of corneal cells following implantation of ADASCs, alone or via decel-lularized laminas as carriers, after 1 year of follow-up.

Methods

Study Design and Patients

This study was an interventional, prospective, randomized clinical investigation of 14 consecutive advanced keratoconus patients. The study was conducted in strict adherence to the tenets of the Declaration of Helsinki. The ethical committee of the institutional review board of the Reviva Research and Application Center approved this study (ClinicalTrials.gov number NCT02932852). All study patients signed an adequate consent form prior to the surgical proce-dure. All patients were randomly distributed into three study groups:

Group 1 (G-1)—Autologous ADASC implantation (five patients, two females and three males; ages ranging from 23 to 43 years with an average age of 32.2).

Group 2 (G-2)—Decellularized human corneal stroma trans-plantation (five patients, four females and one male; ages ranging from 25 to 43 years with an average age of 32.4).

Group 3 (G-3)—Autologous ADASC + decellularized human corneal stroma transplantation (four patients, three females and one male; ages ranging from 30 to 49 years with an average age of 36.25).

The inclusion and exclusion criteria of the study have been defined in our previous publications on this clinical study.[14–16]

Surgical Procedure

Autologous ADASC Implantation. Topical anesthe-sia was used, and a 60-kHz IntraLase iFS femtosecond laser (Abbott Medical Optics, Inc., Irvine, CA, USA) was utilized in single-pass mode for the recipient corneal lamellar dissection. An intrastromal laminar cut 9.5 mm in diameter was created mid-depth in the thinnest preoperative pachymetry point measured by anterior segment optical coherence tomography (OCT) (Visante OCT; Carl Zeiss Meditec, Jena, Germany). A 30° anterior side-cut incision was made. The corneal intrastromal pocket was opened with a Morlet lamellar dissector (Duckworth & Kent, Baldock, UK). Then, with a 25-gauge cannula, 3 million autologous ADASCs contained in 1 ml of PBS were injected into the pocket (Fig. 1). To reduce intraocular pressure and allow a larger volume of cells to be injected into the stroma pocket, a 1-mm corneal paracentesis was performed. Topical antibiotics and steroids (Tobradex; Alcon, Geneva, Switzerland) were applied at the end of the surgery. No corneal sutures were used.[14,16]

Lenticule Implantation. Topical anesthesia was applied with oral sedation for all surgeries. The IntraLase iFS femtosecond laser was used to perform the same stromal dissection but with a 50° anterior side cut. After opening the corneal intrastromal pocket, the lamina was inserted, centered, and unfolded through gentle tapping and massage from the epithelial surface of the host (Fig. 2). As before, a temporary limbal paracentesis was performed to reduce the intraocular pressure. In those cases that received recellularized laminas (G-3), to compensate for the cellular damage expected by the implantation process, the pocket was irrigated, immediately before and after the lamina insertion, with a solution containing an additional 1 million autologous ADASCs in 1 ml of PBS with a 25-gauge cannula (Figs. 2E–2H). The incision was then closed with an interrupted 10/0 nylon suture that was removed 1 week after the operation. Topical antibiotics and steroids (Alcon Tobradex) were applied at the end of the surgery.[15,16]

All surgeries were performed by the same surgeons (J.L.A. and J.L.A.B.) at the Laser Vision Center (Beirut, Lebanon).

In Vivo Confocal Microscope Device

A HRT3 confocal microscope with a Rostock Cornea Module (RCM) (Heidelberg Engineering, Heidelberg, Germany) was used. The light source of this confocal microscope is a coher-ent type of diode laser, with a wavelength of 670 nm and a minimum resolution of 1024 × 768 (16 bit).[20] Coherent light was used to improve the contrast and quality of the images of the corneal stroma, particularly the cells.[4]

Use of the Corneal Microscope. A signed informed consent was obtained from patients for the confocal microscopy study. A drop of topical anesthetic (oxybupro-caine 0.4%) was applied in the eye to be examined. The confocal microscope was set at +12 D. A drop of a high-viscosity gel (2.0 mg/g of carbomer) was applied to the front surface of the microscope lens of the RCM. Then, a RCM TomoCap was placed on top of the RCM objective. A drop of the same viscous gel was also applied on the upper part of the outer surface of the TomoCap and in the patient's eye to be examined. The patient was placed in a stable and comfortable position, with the eye aligned with the lens of the confocal microscope, and was instructed to keep look-ing at the light inside the lens. The focal position was reset to 0 at the superficial epithelial cells of the examined eye. The RCM was then turned clockwise or anticlockwise 0 ± 50 μm, and the focal plane was adjusted to the desired cell layer. Finally, at least four images were obtained for every 50 μm of depth and stored following a previously described protocol.[20] The images analyzed in this study were indeed at different stromal depths but always belonged to a central diameter ≤ 9 mm and were below the measurement of the intrastromal diameter pocket.[14–16]

Method of Stromal Cell Counting. Images that had a better quality of contrast and illumination were selected from the images captured and stored during the experience.

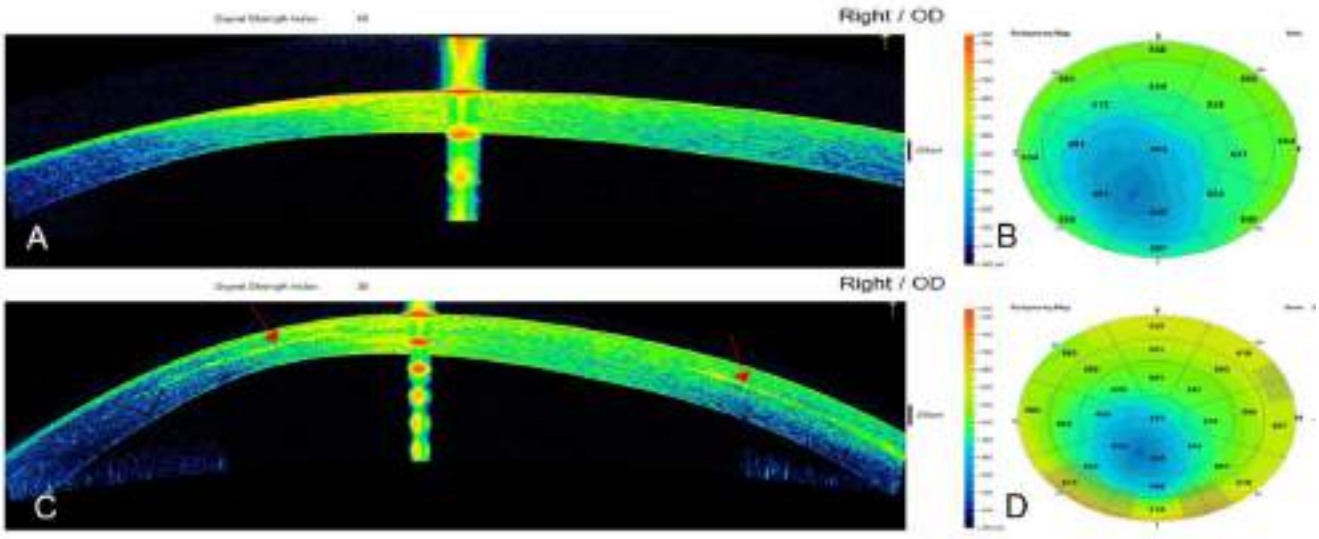

Figure 1. Cornea Visante OCT images and pachymetric maps for case 2 from G-1. (**A**, **B**) Preoperative examination, and (**C**, **D**) 12 months after surgery. Observe the patchy hyperreflective areas (red arrows) at the level of the stromal pocket compatible with areas of new collagen production. The distribution of these areas was not homogeneous along the surgical plane.

An area known as a region of interest (ROI) was determined, and the same ROI (0.1000 mm^2) was used for all cell counts in all layers of the corneal stroma.[4,20] The morphology criteria used in the present study to differentiate the corneal stroma cells from the inflammatory cells are described below.

We used 50% brightness and contrast (Fig. 3A) for all images. Cells that were more illuminated and more refringent[7, 8] were selected and marked in blue.[20] These cells were white or light gray in color and had clear and well-defined edges.[4] Dark gray cells were not taken into consideration, as they did not belong to the chosen 50-µm plane. The confocal cellular brightness is attributed to the nuclear content of these cells.[4,7,11,14–16,21,22] Because of their irregular oval-shaped bodies,[7] differences in brightness among them can be attributed to different metabolic activation and direction of incidence of the laser beam.[7] Only the cell nuclei that were identified with the method mentioned above were defined as corneal stromal cells and included in the cell counting process. For simplification throughout the paper, when we talk about cell density or morphology, we are referring to the density or morphology of the cell nucleus and not the cell membrane that was observed by confocal microscopy.[4,7,11,14–16,21,22]

The highly reflective material was not considered in the cell count whenever the size of the reflective morphology exceeded the size that we considered similar to stromal keratocyte, whether in normal or in keratoconic corneas.[4,7,11,14–16, 21,22] For this reason, we have considered that this structure corresponds to a fibrotic material.

After the first count was performed, the contrast was increased to the maximum and the brightness decreased to the minimum. Any stromal cell that disappeared from the chosen plane was eliminated, and only those cells that remained were used for the final cell count, even if they were faintly identified in the image (Fig. 3B).

ADASC Cell Counting. The counting method for transplanted ADASCs was performed in a similar way. ADASCs appear rounded in shape, voluminous, and refringent (Fig. 4A).[14]

The morphology and evolution of the ADASCs over time are described later in the Results section (Fig. 4B).

Cell Count on Decellularized and Recellularized Laminas. When the decellularized (G-2) and recellular-ized (G-3) laminas appeared without well-defined cell structures, they were considered totally acellular in the 0.1-mm^2 area that we delimited in our study (Fig. 5A).[15,16] All structures that appeared on the anterior surface, on the posterior surface, or in the mid-stroma of the lamina; that showed well-defined edges that were white or light gray in color; and that had a morphology similar to that of a keratocyte nucleus were counted as a cell (Figs. 5B, 5C, 6).

Corneal Cell Density Calculation. To obtain the cellular density, we first defined the ROI (mm^2)[20] and then proceeded to count the cells with the methodology described above. The cellular density for the chosen area was calculated by the confocal microscope software as the number of cells multiplied by 10 cells/mm^2 ± SD.[8,20]

To calculate the cell density of the corneal stroma among the three groups, we divided the measurements of the stroma into three zones: anterior, mid-, and posterior stroma. The mid-stroma coincided with the surgical plane (calculated as half of the thinnest point of the cornea obtained by OCT ± 50 µm).[14– 16] The anterior stroma is the stroma located below Bowman's membrane, and the posterior stroma is the stroma located above Descemet's membrane.[14–16] For those measurements where a lamina was present (postoperative G-2 and G-3), we divided the lamina into three areas: anterior surface, lamina posterior surface, and lamina mid-stroma (Fig. 6F).

The main outcome measures of this study are the changes in and evolution of corneal stroma cellular density over a 1-year follow-up period, as analyzed using corneal confocal microscopy. Cellular density was studied before surgery and at 1, 3, 6, and 12 months after surgery. Preoperative cellular density was measured in the anterior, mid-, and posterior stroma in G-1, as well as in G-2 and G-3. Postoperative cellular density in G-2 and G-3 was studied in the anterior and posterior stroma and through

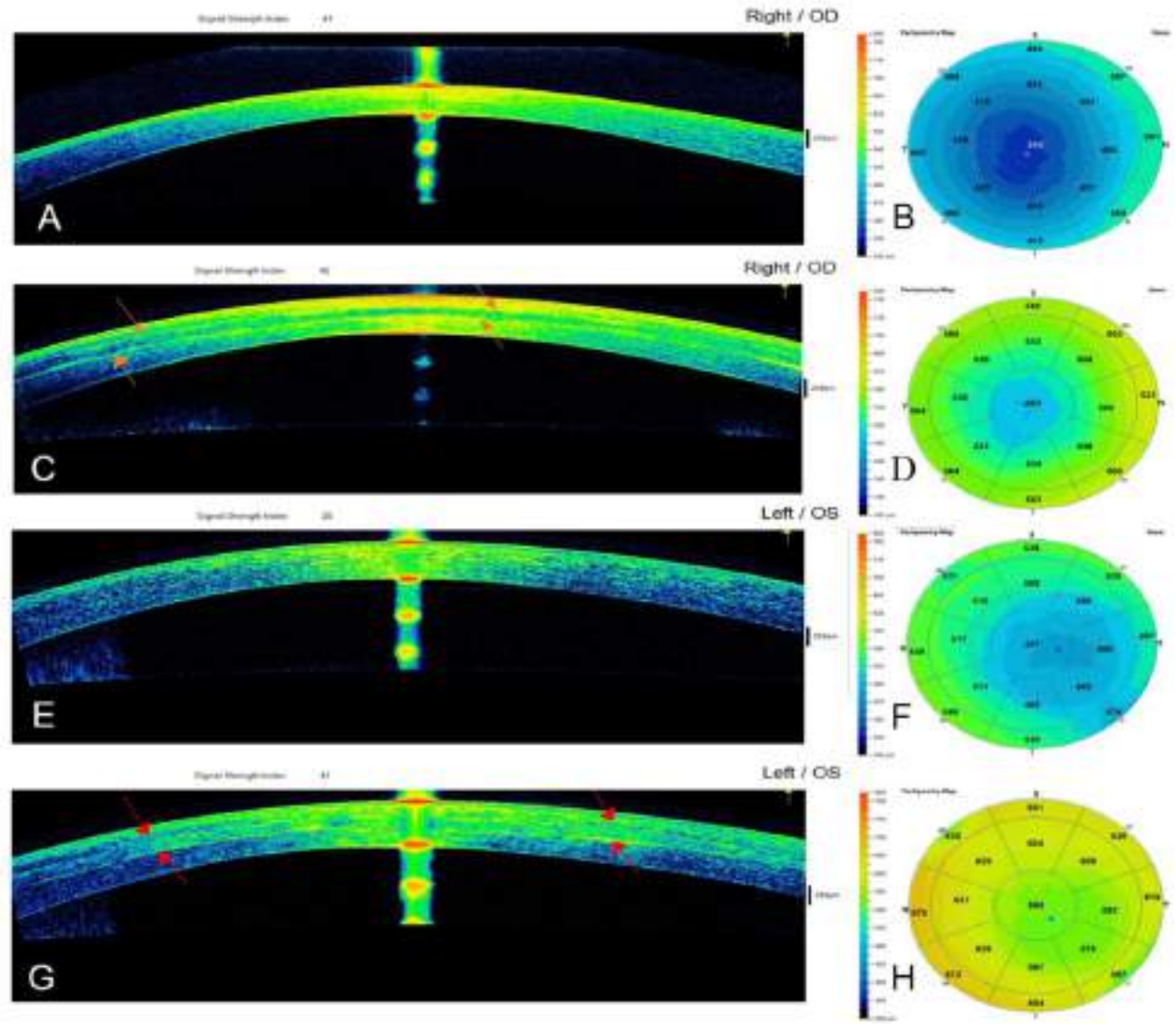

Figure 2. Cornea OCT images and pachymetric maps for case 5 from G-2: (**A**) Preoperative OCT examination, (**B**) preoperative pachymetric map, (**C**) 12-month postoperative OCT (red arrows represent the graft edges), and (**D**) significant improvement in the pachymetric map 12 months after surgery. Cornea OCT images and pachymetric maps for case 10 from G-3: (**E**) preoperative OCT examination, (**F**) preoper-ative pachymetric map, (**G**) 12-month postoperative OCT (red arrows represent the graft edges), and (**H**) significant improvement in the pachymetric map 12 months after surgery.

the lamina, with the purpose of exploring the evolution of its cellular component during the study time.

Statistical Analysis

Statistical analysis was performed by generalized linear mixed models with a Poisson variable as an outcome (fixed effects, time and group; random effects, individual). This Poisson variable corresponded to the keratocyte nuclei densities (Poisson distribution), indicating the means of cell nuclei appearing in the captured figures at different levels of the corneal stroma (anterior, intermediate, and posterior) or on the anterior surface, mid-stroma, and posterior surface of the implanted tissue for the studied time intervals. A Poisson variable, unlike one that follows in a normal distribution, is expressed by a single parameter, which is the average number of events only (Figs. 7, 8). The standard deviation of the Poisson variable (generally known as lambda) is not shown in the figures, but it is the same as the average parameter, as compared to a normal distribution which is expressed by mean and standard deviation. On the other hand, this average parameter (obtained through mixed generalized linear models) takes into account all of the measurements of all of the individuals and assesses the variability between individuals and within them. Consequently, the results presented here are at the group level and provide all of the information necessary to understand the impact of the intervention. Scatterplots were developed to help interpret the results, and the goodness of fit of the models was obtained through the likelihood ratio test. The type I error significance level was set at 0.05, and the statistical

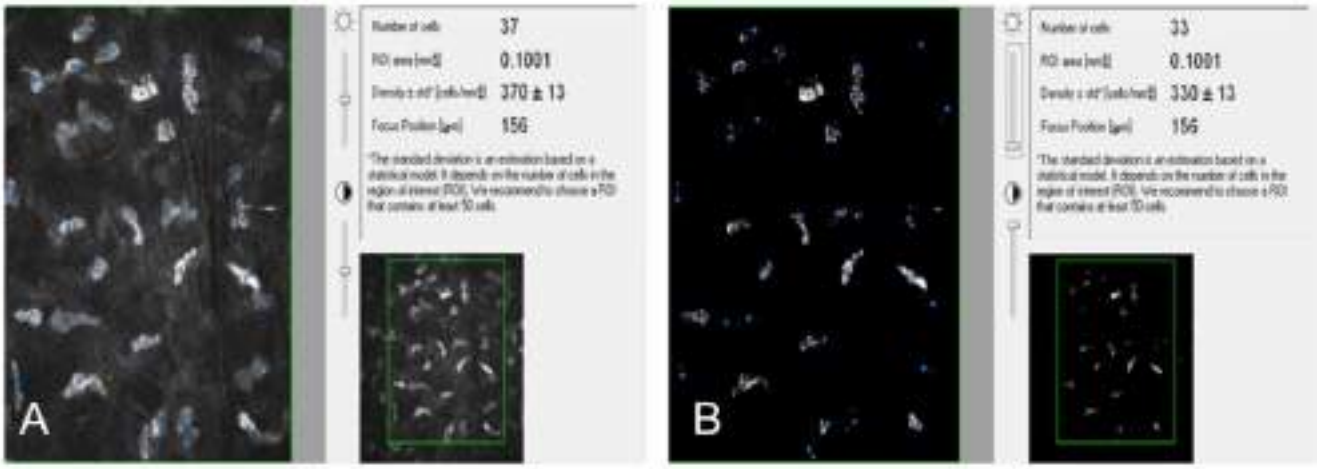

Figure 3. (**A**) Cell count performed with medium brightness and contrast. The more illuminated and more refringent cells were counted, and the keratocytes are marked in blue. (**B**) Elimination of keratocytes that do not belong to the plane under observation is possible using low brightness and high contrast settings.

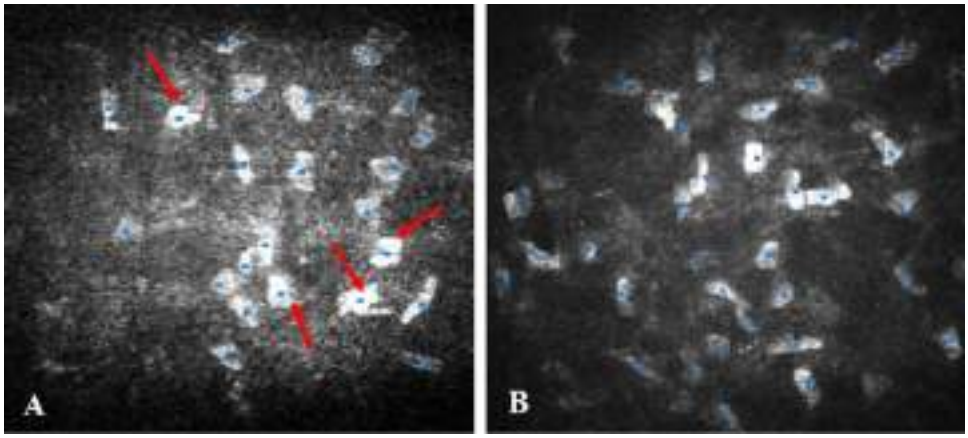

Figure 4. ADASC counting in G-1. (A) Count of ADASCs (red arrows) and keratocytes 1 month following surgery of a keratoconic patient; the cells are marked in blue. The ADASCs have a rounded shape and are larger, more luminous, and more refringent than the normal keratocytes. (**B**) Cell count of a keratoconic patient 1 year after implantation of ADASCs; all corneal stroma cells demonstrate a similar shape.

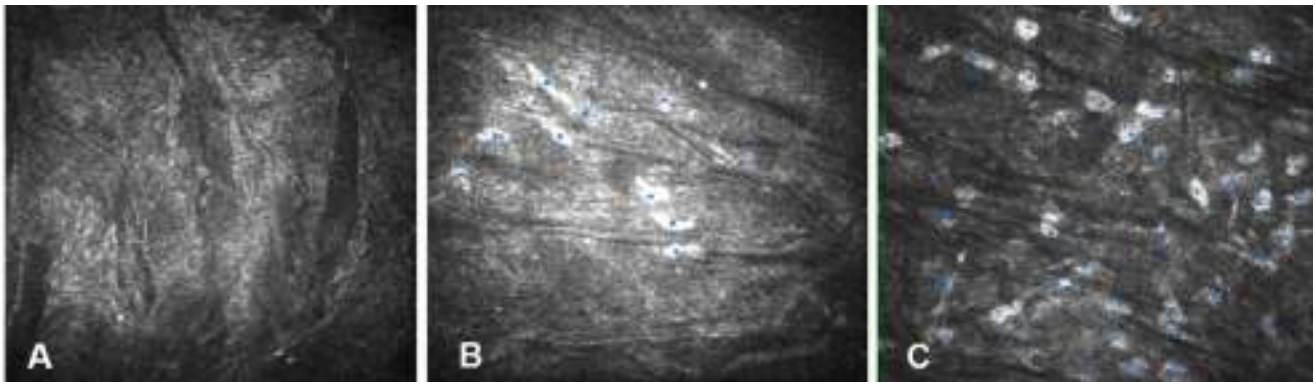

Figure 5. Cell count on decellularized laminas for case 9 from G-2. (**A**) Anterior surface of a decellularized lamina that appears without cells 1 month after surgery. (**B**) Cell count on the posterior surface of a lamina 3 months after surgery. Cells show different morphology from the host corneal stromal cells. These cells are smaller. (**C**) Cell count on the posterior surface of a lamina 1 year after surgery. All cells demonstrate a morphology identical to that of normal corneal stromal keratocytes.

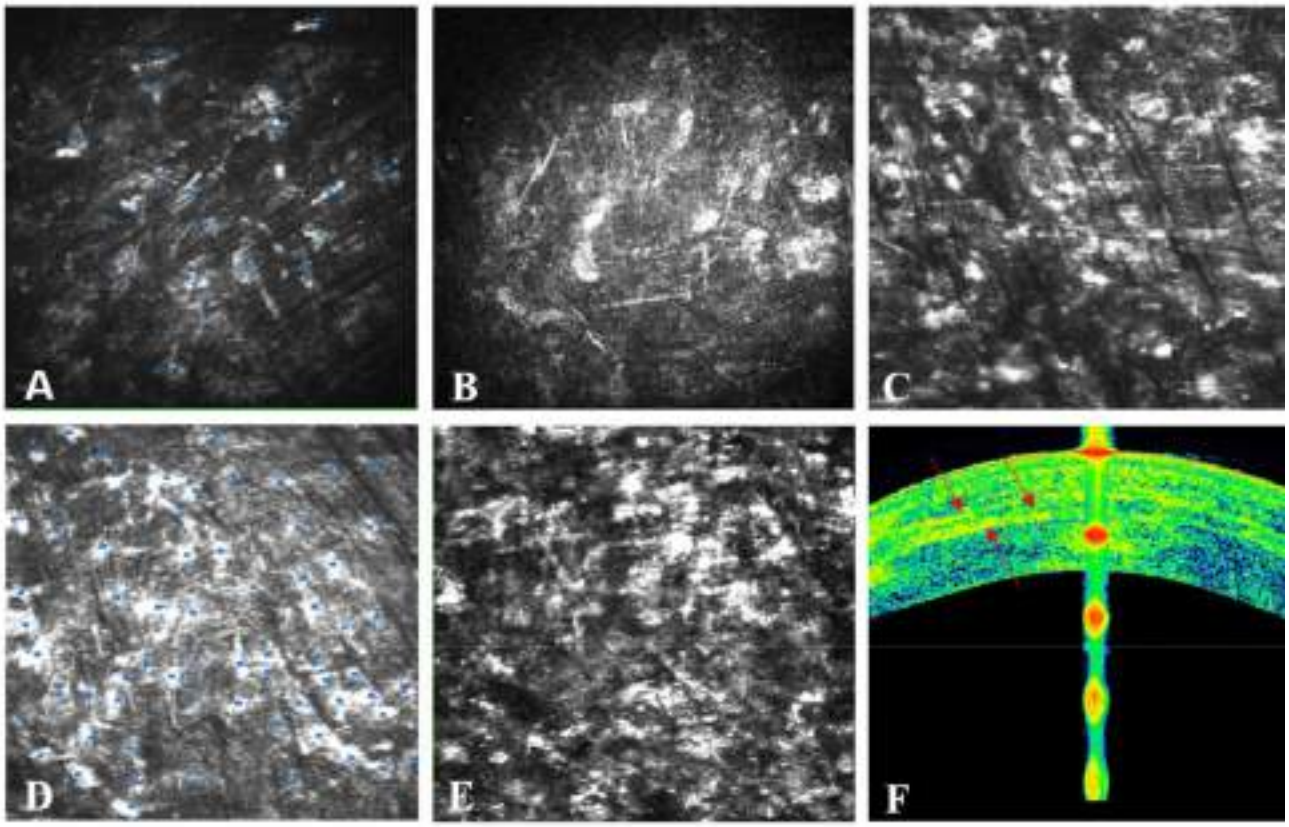

Figure 6. Cell count on recellularized lamina for case 13 from G-3. (**A**) Anterior surface of a recellularized lamina 1 month after the operation; few ADASCs can be seen (marked in blue). (**B**) Posterior surface of the recellularized lamina 1 month after the operation; note the presence of a few ADASCs similar in morphology to keratocytes. (**C**) Anterior surface of the recellularized lamina 12 months after surgery showing an abundant number of stromal cells. (**D**) Mid-stroma of the lamina 12 months after surgery showing a high number of stromal cells. (**E**) Posterior surface of the recellularized lamina 12 months after surgery showing a high number of stromal cells. (**F**) OCT image where the red arrows represent the anterior and posterior surfaces, as well as the mid-stroma, of the recellularized lamina 12 months after surgery.

software we used was R 3.5.1.

The maximum number of images for each patient was collected to calculate cell density. To not alter the results, mathematical models of repeated measures were used to control the variability of each individual.

We considered the average cell counts of two observers who performed them separately following the same scientific standards; when there was a discrepancy between them of more than 20%, the count was repeated or other images were taken, if possible, until achieving agreement.

Results

Patients Implanted with ADASCs Alone (G-1)

Morphological Results. Implanted ADASCs could be seen in clusters 1 to 3 months following the implantation surgery. The ADASCs appeared to be rounded in shape, more luminous, more refringent, compared with the host keratocytes (Fig. 2A).[14, 16] However, the shape of the ADASCs changed from round to fusiform 6 months after the implantation.[14,16] The morphological differences between the ADASCs and host keratocytes disappeared over time (Fig. 4B).

Cell Density Results. Twelve months after implanta-tion, we observed a gradual, statistically significant increase ($P < 0.001$) in the cellular density at the anterior, mid-, and posterior stroma (Fig. 7).

Patients Implanted with Decellularized Corneal Laminas (G-2)

Morphological Results. One month after surgery, the decellularized lamina appeared acellular (Fig. 5A). Three months after surgery, the patient's host cells began to colonize the lamina, progressively increasing in number over time (Figs. 5B, 8). These cells differed in morphology from the native keratocytes of the cornea, as they appeared smaller and less voluminous (Fig. 5B). The shape of these cells at 6 months became more similar to the usual keratocytes of the corneal stroma,[15] before fully developing into cells that had an identical morphology to the normal keratocytes 1 year after surgery (Fig. 5C).[16]

Cell Density Results. One month after surgery, the transplanted laminas generally remained acellular in most of the patients (Fig. 5A).[15, 16] We observed means of 31 cells/mm^2 in the anterior surface of the lamina, 17 cells/mm^2 within the lamina, and 48 cells/mm^2 in the posterior surface of the lamina (Fig. 8). Cell density increased over time (Figs. 5B, 8). We observed that recellularization began on the posterior surface of the lamina,

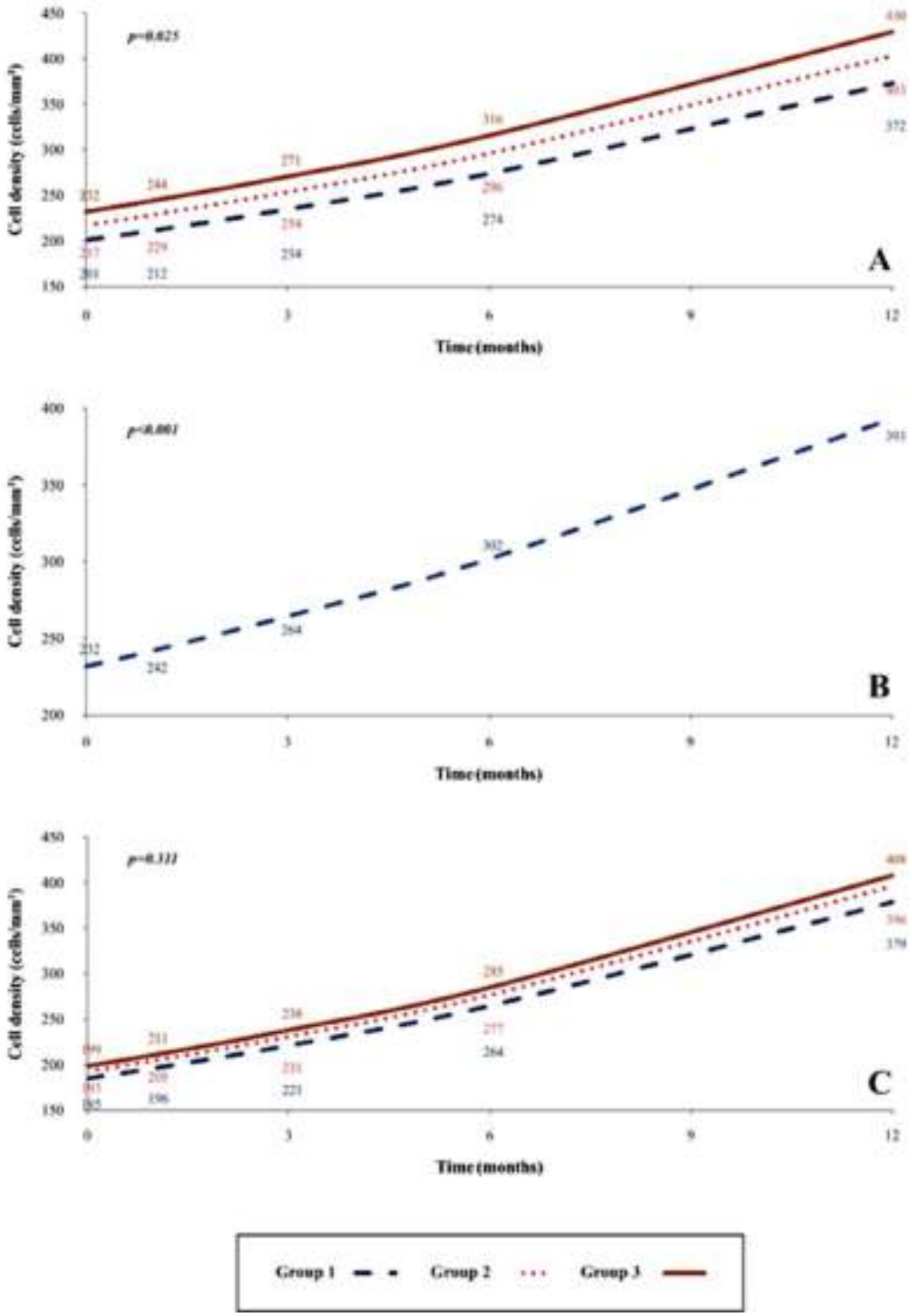

Figure 7. Cellular density change in the corneal stroma of G-1, G-2, and G-3. (A) Increase in cell density over time in the anterior stroma of the cornea in G-1, G-2, and G-3 from the preoperative period until 12 months after surgery. A significant statistical difference ($P = 0.025$) among the groups was detected. (B) Statistically significant increase in cell density ($P < 0.001$) over time in the mid-stroma of the cornea in G-1 from the preoperative period until 12 months after surgery. (C) Increase in cell density over time in the posterior stroma of the cornea in G-1, G-2, and G-3 from the preoperative period until 12 months after surgery. There was no significant difference among the three groups ($P = 0.311$).

followed by on the anterior surface and within the lamina (Fig. 8). Moreover, 1 year after implantation, the anterior, mid-, and posterior surfaces of the laminas were more colonized by keratocyte-type cells (Fig. 5C),[16] until reaching statistically significant values ($P < 0.001$) 12 months after surgery in comparison to the first postoperative

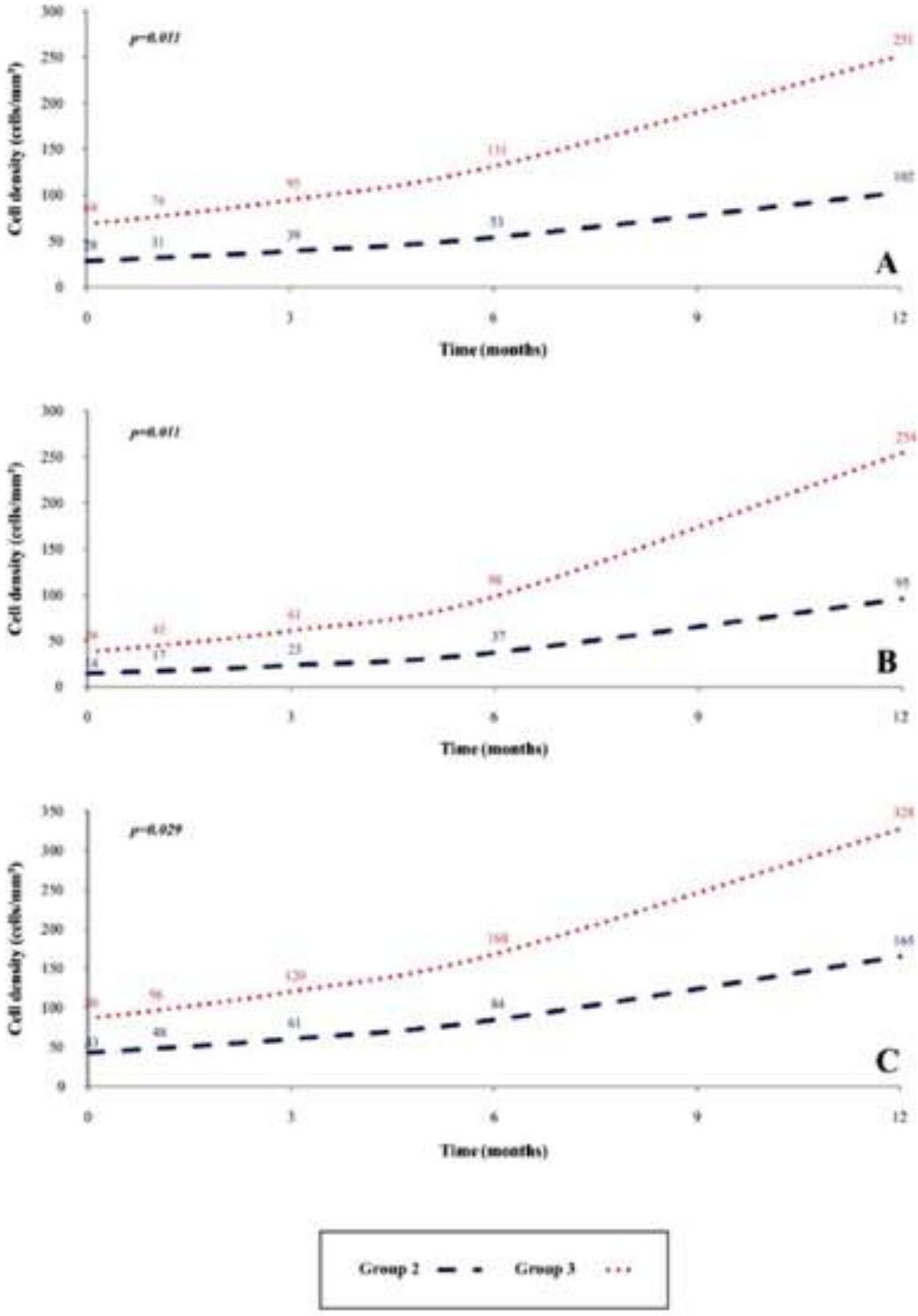

Figure 8. Cellular density change in the anterior and posterior surfaces of the lamina, as well as the mid-stroma of the lamina. (A) Increase in cell density over time in the anterior surface of the lamina in G-2 and G-3 from the preoperative period until 12 months after surgery. A significant statistical difference (P = 0.011) exists between G-2 and G-3. (B) Increase in cell density over time in the mid-stroma of the lamina in G-2 and G-3 from the preoperative period until 12 months after surgery. A significant statistical difference (P = 0.011) between G-2 and G-3 was detected. (C) Increase in cell density over time in the posterior surface of the lamina in G-2 and G-3 from the preoperative period until 12 months after surgery. A significant statistical difference (P = 0.029) between G-2 and G-3 was detected.

month (Fig. 8). The keratocyte density 12 months after surgery in the anterior and posterior stroma increased, as well, in a statistically significant manner compared with preoperative values (P < 0.001) (Figs. 7A, 7C).

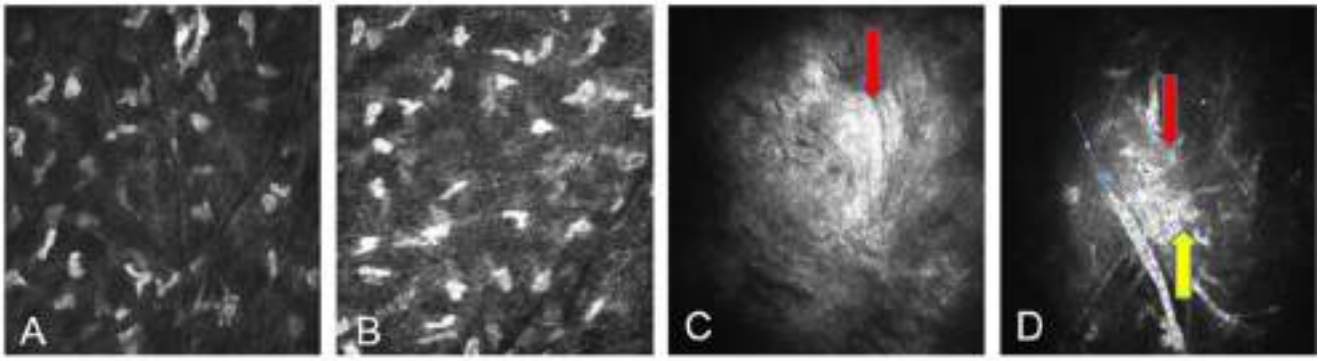

Figure 9. Cell count of the anterior and posterior corneal stroma for case 10 from G-3 12 months after the operation. (**A**) Anterior corneal stroma with abundant corneal stroma cells in a female patient 12 months after surgery. The number and morphology of corneal stroma cells are very similar to those of a normal stroma. (**B**) Posterior corneal stroma with a high number of corneal stroma cells for the same patient 12 months after surgery. The image shows that corneal stroma cells of the posterior stroma are similar in number and morphology to stromal cells of a normal cornea. (**C**) Presence of hyperreflective deposits (red arrow) corresponded with the preoperative paracentral corneal scarring observed in preoperative case 2 from G-1. (**D**) Improvement of the fibrotic tissue (red arrow) at the same level with the same case 2 from G-1 is observed. Note the presence of fibroblast (yellow arrow). Part of the superficial corneal nerve can be noted (blue arrow).

Patients Implanted with Recellularized Corneal Laminas (G-3)

Morphological Results. Unlike the decellularized laminas (G-2), which were mainly acellular (Fig. 5A), few ADASCs were seen in G-3 at 1 month after surgery. They were smaller than normal keratocytes on the anterior lamina surface (Fig. 6A), but they were more evident and similar to those on the posterior surface (Fig. 6B). At the same time, we also noticed that these cells were distributed in clusters (Figs. 6A, 6B). These clusters of mesenchymal cells dispersed over time until obtaining a geometrical distribution similar to that of normal corneal stroma (Figs. 6C–6E). In addition, the recellularized laminas consistently contained a higher number of keratocytes than the decellularized ones when observed 1 to 12 months after surgery (Fig. 8),[16] with some of them presenting dendritic shapes (Figs. 6C–6E).

Cell Density Results. One month after surgery, we observed only a few cells: a mean of 76 cells/mm^2 on the anterior surface of the lamina, 45 cells/mm^2 within the lamina, and 96 cells/mm^2 on the posterior surface of the lamina (Fig. 8). At 3 and 6 months, the cell density increased gradually over time (Fig. 8). Twelve months after implantation, the increase in cellular density on the recellularized anterior surface, posterior surface, and mid-lamina was statistically significant ($P < 0.001$) with respect to the first month after surgery (Figs. 6C, 6D, 8).

One year after surgery, the cellularity of the anterior and posterior corneal stroma showed a significantly higher number of keratocytes,[16] similar to that found in a normal cornea (Figs. 9A, 9B). Cell density on the anterior stroma ($P < 0.001$) and posterior stroma ($P < 0.001$) showed a statistically significant increase in the number of keratocytes with respect to the preoperative values (Figs. 7A, 7C).

Morphological Result of Fibrotic Tissue

We observed an absence of fibrotic tissue for cases 1 and 4 from G-1. We detected the presence of a few fibrotic tissues at 3 months after surgery in cases 2 and 3 and then observed full recovery of the corneal stroma during follow-up. Hyper-reflective deposits that were observed corresponded with paracentral corneal scarring in preoperative case 2. Nevertheless, this scarring improved over the following months (Figs. 9C, 9D; Table 1).[14–16]

Table 1. Presence or Absence of Fibrotic Tissue in Groups 1, 2, and 3

Case	Group	Months 0	1	3	6	12
1	1	–	–	–	–	–
2	1	+++*	++*	++*†	+*	+*
3	1	–	–	+†	–	–
4	1	–	–	+ †	– †	–
5	2	–	–	+/++	+/++ †	+/++†
6	2	–	–	–	+/++ †	+/++ †
7	2	–	–†	– †	+/++ †	+/++/+++
8	2	–	+†	+/+++†	+/++ †	– †
9	2	–	+†	+/++ †	+/++ †	+/++†
10	3	–	+	+/++	+/++/+++	+
11	3	+++*	++†+++†+/++/+++†+/++†			
			+++*	+++*	++* †	+* †
12	3	–	–	– †	+/++/+++†	+/++/+++†
13	3	–	–	+/++	+/++/+++	+/++

Note: +, minor fibrotic tissue; ++, moderate fibrotic tissue; +++, high fibrotic tissue; –, absence of fibrotic tissue.

* Presence of paracentral scar with fibrotic tissue in the preop-erative period; we observed an improvement of scars and decrease of fibrosis.

† Presence of fibrotic tissue during the postoperative follow-up.

The presence of fibrotic tissue in G-2 was observed begin-ning with the first postoperative month in cases 8 and 9, in the third month in case 5, and in the sixth month in cases 6 and 7. All detected fibrotic tissue corresponded to the paracentral corneal decellularized implanted laminas. However, at 12 months after surgery, we noted an absence of fibrotic tissue in case 8 (Table 1).

In G-3, we detected the presence of preoperative fibrotic tissue corresponding with the paracentral cornea scar in the anterior stroma in case 11. We observed the presence of postoperative fibrotic tissue at the first month in cases 10 and 11, as well as in case 13 beginning at the third month and in case 12 beginning at the sixth month. From 6 to 12 months, a decrease in fibrosis

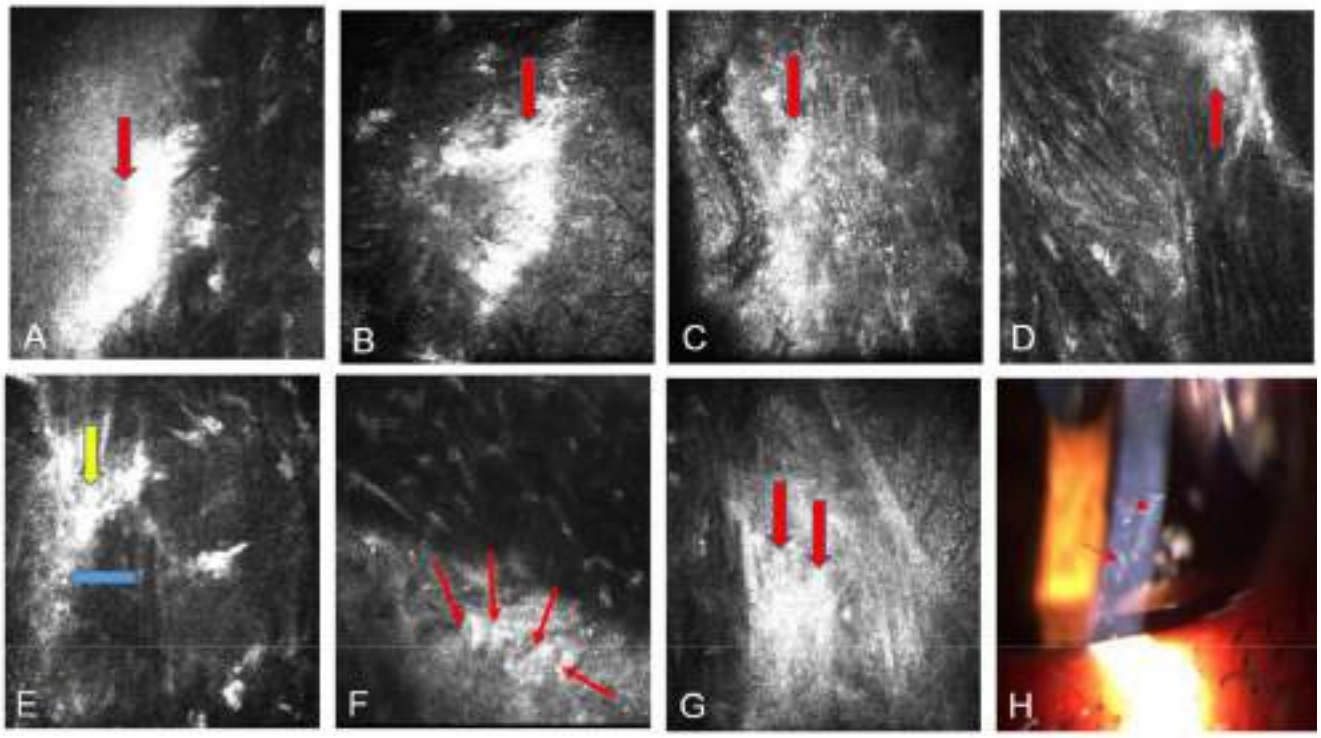

Figure 10. (**A**) The presence of highly reflective fibrotic tissue (red arrow) of keratoconic case 11 corresponds with the preoperative paracentral anterior stroma scar observed at 3 months after surgery. (**B**) The presence of fibrotic tissue (red arrow) is highly reflective on the periphery of the posterior surface of the lamina at 3 months for the same case. (**C**) Improvement of the paracentral preoperative fibrotic tissue (red arrow) on the anterior stroma of the same keratoconic case 6 months after the operation. (**D**) Improvement of the fibrotic tissue (red arrow) on the periphery of the posterior surface of the recellularized lamina of the same keratoconic case 12 months after surgery. (**E**) Presence of fibroblast or myofibroblast (yellow arrow) and fibrotic tissue (blue arrow) on the posterior surface of the decellularized lamina of a keratoconic patient 3 months after surgery. (**F**) Transition zone between the posterior surface of the decellularized lamina and the host stroma showing a number of migrating corneal stroma cells (possibly keratocytes?) with dendritical shapes (marked with red arrows) in a keratoconic patient 12 months after surgery. (**G**) Presence of highly reflective fibrotic tissue (red arrow) on the periphery in the mid-stroma of the decellularized lamina of a keratoconic patient 6 months after surgery. (**H**) Slit-lamp image of a keratoconic patient demonstrating peripheral scar tissue 6 months after surgery.

was noted in case 11 in the paracentral preoperative scar. In addition, we detected an improvement in postoperative fibrosis in most of the cases of this group (Figs. 10A–10D; Table 1).

In our study, the association between the degree of fibrosis and recellularization was evaluated through cumulative linked ordinal models to determine whether the coefficient associated with the independent variable (number of keratocytes densities) was statistically significant. However, we did not find a direct and significant association between recellularization and the presence of fibrotic tissue on the periphery of the decellularized or recellularized laminas. In G-2, *P* values obtained in the periphery of the anterior, middle, and posterior surfaces of the laminas were 0.823, 0.218, and 0.567, respectively. In G-3, *P* values obtained in the middle and posterior surfaces of the laminas were 0.505 and 0.123, respectively. On the periphery of the anterior surface of the laminas, we observed few occurrences of fibrotic tissue; thus, we have not obtained convergent results.

Comparison of Results Among the Three Groups

In our study, density was expressed as the number of cells/mm^2. Comparing the results obtained 12 months after surgery with preoperative conditions, the number of keratocytes increased (1) in the anterior stroma (ratios values 1.850, 1.857, and 1.853 in G-1, G-2, and G-3, respec-tively); (2) in the mid-stroma (ratio value 1.693 in G-1); and (3) in the posterior stroma (ratio values 2.048, 2.051, and 2.050 in G-1, G-2, and G-3, respectively) (Fig. 7; Table 2). We showed that the cell keratocyte densities in posterior stroma were higher in all of our groups than the normal kerato-cytes densities obtained in previous studies (408, 396, and 379 cells/mm^2) but lower than those found for the anterior stroma (430, 403, and 372 cells/mm^2) in all the cases, as well as in in the mid-stroma in G-1 (393 cells/mm^2) (Fig. 7).[4,14–16]

Twelve months after surgery, we observed in the anterior stroma a statistically significant difference (P = 0.025) in cell density among the three groups, with G3 having the highest cell density followed by G2 and then G1. However, in the posterior stroma, this difference in cell density among the groups was not statistically significant (P = 0.311) (Figs. 7A, 7C).

In addition, the anterior surface cell densities of the recellularized laminas in G-3 were statistically significant higher than in G-2 12 months after surgery (P = 0.011). Equivalent results in cellular densities were found in the mid-stroma of the laminas (P = 0.011), and a similar result was found for the posterior surface cellular density of the laminas (P = 0.029) (Fig. 8).

Table 2. Counted Nucleus Cell Ratios

Group	Anterior Stroma	Mid-Stroma	Posterior Stroma	Anterior Surface of the Lamina	Within the Lamina	Posterior Surface of the Lamina
1	372/201 = 1.850	393/232 = 1.693	379/185 = 2.048	—	—	—
2	403/217 = 1.857	—	396/193 = 2.051	102/28 = 3.642	95/14 = 6.785	165/43 = 3.837
3	430/232 = 1.853	—	408/199 = 2.050	251/69 = 3.637	254/38 = 6.684	328/86 = 3.813

Counted nucleus cell ratios are the proportion of cell densities 12 months after surgery compared with the preoperative values in groups 1, 2, and 3.

Discussion

In this innovative clinical study, we used confocal microscopy to observe the evolution of implanted mesenchymal stem cells with the aim of applying corneal regeneration as a new keratoconus therapy utilizing ADASCs. The results reported here complete the previous clinical results published elsewhere concerning this human clinical study.[14–16]

According to the results of this confocal study, following the injection of only ADASCs into corneal pockets created using a femtosecond laser in G-1 there was a statistically significant increase in the density of corneal keratocytes in the anterior, mid-, and posterior stroma ($P < 0.001$). This correlates well with the already reported production of new collagen, which resulted in an improved corneal thickness.[14] We also observed in G-1 relevant changes in the morphology of the implanted cells from the moment of their implantation into the corneal pockets, as the morphology of the ADASCs was round in shape until the third month. This finding suggests survival of the implanted stem cells following their implantation. Later on, the cells showed changes rang-ing from forming clusters around individual cells to devel-oping the confocal appearance of adult stromal corneal cells at the 12 months after surgery.

In G-2 and G-3, where corneal laminas were implanted with or without impregnation with ADASCs, we observed that implantation of such laminas, whether or not colonized by ADASCs, favored an increase in the number of corneal stromal cells in the anterior and posterior stroma of the cornea in a highly statistically significant level ($P < 0.001$) (Figs. 7A, 7C).

In vivo confocal microscopy offers the possibility of studying the normal morphology of the cornea and microstructural changes that can occur in keratocyte density and in the morphology of keratocytes in keratoconic cornea.[4,7,11,20,21,22] Normal human keratocytes in full-thickness central corneas have been studied by various authors[21,22] using a different technology (Tandem Scanning Corporation, Reston, VA, USA) and different metrics (cells/mm^3) with confocal microscopes. Other authors in more recent publications used a laser scanning in vivo confo-cal microscope (Heidelberg Retina Tomograph II/RCM) and found that mean keratocyte density in the control group was 786 ± 244 cells/mm^2 in the anterior stroma and 293 ± 35 cells/mm^2 in the posterior stroma. In the keratoconus group that did not wear contact lenses, the values were 662 ± 193 cells/mm^2 and 236 ± 32.6 cells/mm^2 in the anterior and posterior stroma, respectively.[4]

In our study, we increased cell densities in the anterior mid- and posterior stroma at 12 months compared to the preoperative level (Figs. 7A–7C; Table 2), but we did not detect any new formation of fibrotic structures (Figs. 9A, 9B).

The presence of fibrotic tissue seemed to be related to groups that received only laminas (with or with-out ADASCs). This was more evident in G-3, whereas in G-1 there was an absence of fibrotic structures until 12 months after surgery. We noticed an improvement of corneal scarring for case 2 from G-1 at 12 months after surgery (Figs. 9C, 9D; Table 1).[14–16] Nevertheless, in G-2 and G-3 fibrotic structures were present in patients almost in the periphery of the implanted laminas (Table 1). It has been postulated that mesenchymal stem cells can either avoid or improve preexisting scars (Figs. 9C, 9D, 10A, 10C), although, in the non-peripheral areas of the implanted laminas, we did not observe differences in corneal transparency among the three groups, nor did we observe cornea haze.[14–16]

Moreover, changes inside the acellular laminas implanted in G-2 were also observed. This finding demonstrates that the decellularized lamina was colonized by the patient's own keratocytes, a process that began in the first month. After 12 months, the lamina was found to be completely recellularized (Fig. 8).

On the other hand, we have also observed that, from the first postoperative month in the recellularized laminas of G-3, a decrease occurred in the clusters of the mesenchymal cells implanted on the laminas. Such cellular morphological changes were clearly seen to occur first on the posterior surface followed by the anterior surface, and the number of cells statistically and significantly increased from 1 month after the surgery to 12 months after surgery. This finding may suggest survival and differentiation of the implanted cells toward keratocytes and/or repopulation of these laminas, with migration of the host corneal stromal keratocytes being stimulated to proliferate toward the decellularized corneal tissue.[23] Obviously, as the cells could not be labeled before implantation due to possible interference with transparency and hence ethical issues, the distinction between both populations is not possible. This finding correlates well with another report[23] that demonstrated that propagation and migration of corneal fibroblasts happens in parallel with furrow ridges aligned with collagen lamellae. During the migration of these cells, tracks for propagation are established by alignment of the fibrils through the generation of a mechanical force. It is also possible that chemoattractant factors may be released by the ADASCs during the evolution following implantation.[24]

In addition, we observed in this study that stromal cells, which are likely to be keratocytes, fibroblasts, or myofibroblasts, have migrated from the corneal stroma toward the edge of the lamina in cases where no cells were injected (Figs. 10E, 10F). Such stromal cells (keratocytes) show peripheral prolongations and morphological transformations with dendritic forms, indicating that they have differentiated into fibroblasts and myofibroblasts during their period of activity and that they are capable of sliding

on the collagen fibers of the decellularized tissue (Figs. 10E, 10F).[23] We also observed, up to 12 months after surgery, the development of paracentral fibrotic tissue on top of the photoablated stroma of the implanted tissue (Figs. 10B, 10D, 10E, 10G, 10H).[23]

We have reported herein an evolution in morphology of corneal stromal cells, presumed to be keratocytes. It has been reported that these cells are normally oval and irregular in shape and without a dendritic shape. It is when they migrate or are activated that they assume a dendritic shape.[22,23] Because the evolution of stromal cell morphology in our study did not follow such a pattern, our observation does not support previous reports,[17] which have described that in adult tissue keratocytes are mitotically quiescent and have a flat, dendritic morphology.[25] Furthermore, it would be important in future studies to establish differences among the various morphologies that are observed in stromal cells to compare the evolution of those that have a non-dendritic shape to those that have dendritic shape and the biological implications that such morphological changes may have.

A relevant issue of the present study is the methodology used for counting stromal cells, which was a specific manual method. This may introduce a certain amount of subjectivity and interpretation bias; however, this method provided us with a more accurate and discriminating cell count than the automated cell counts of the microscope, which are affected by large variability, inaccuracies, and misinterpretations (Fig. 3). The presence of highly reflective fibrotic tissue in the studied areas could make it difficult to discriminate the edges of the keratocytes nuclei that were the main focus of our study (Figs. 9C, 9D, 10).

We believe that it is necessary to establish a more objective cell count method based on image processing programs and specific algorithms in which the contrast and illumination can be edited and various specialized filters used to optimize visualization of keratocytes cells and to better calculate their size.

In conclusion, confocal corneal microscopy combined with the technology used in our investigation has shown to be a very efficient tool for in vivo assessment and follow-up of corneas implanted with mesenchymal stem cells for corneal regeneration purposes. We have reported the confocal microscopy outcomes after implantation of ADASCs in the selected surgical plane, which allowed qualitative and quantitative assessment of them during the experiment. Moreover, confocal corneal microscopy allowed monitoring of the progressive morphological changes that occurred in the decellularized and recellularized laminas throughout the observation period and assisted in determining changes in cell densities in the grafted tissue, as well as in all the corneal stroma.

Stromal cells are significantly increased at the level of implantation when they are injected into the corneal stroma (Fig. 7B). In addition, they induce a significant increase in the level of stromal cells when implanted jointly with a corneal lamina impregnated at the surface with ADASCs. This increase is larger than that observed when acellular corneal laminas are implanted (Figs. 7A, 7C), even when the implantation is followed by repopulation of the acellular lamina by the resident stromal cells (Fig. 8). Whether these findings indicate survival of the mesenchymal ADASCs and their differentiation into keratocytes or that such mesenchymal cells cause a biological stimulus for the proliferation of the resident cells has yet to be confirmed in future studies.

Acknowledgments

The authors thank Eric Bangert and Heidelberg Engineering for the generous temporary donation of the confocal microscopy and confocal software analysis software used for this investigation; Marc Assouwad from Laser Vision for her assistance in the logistics of the study; Albert Aazar and Reviva Regenerative for administrative management of the laboratory; and Ibrahim Achkar, who was responsible for the liposuction and adipose tissue management until the moment of the laboratory study.

Supported by Optica General, Saida Lebanon, and the Vissum Ophthalmological Institute of Alicante, Spain; by the Red Temática de Investigación Cooperativa en Salud (RD16/0008/0012); by the Instituto Carlos III–General Subdirec-tion of Networks and Cooperative Investigation Centers (R&D&I National Plan 2008-2011); by the European Regional Develop-ment Fund; and by a Roche Farma SA grant (MPdM).

Disclosure: **M. El Zarif**, None; **K.A. Jawad**, None; **J.L. Alió Del Barrio**, CSO (C); **Z.A. Jawad**, None; **A. Palazón-Bru**, None; **M.P. de Miguel**, Roche Farma SA (F); **P. Saba**, None; **N. Makdissy**, None; **J.L. Alió**, AkkoLens (C, R), Blue Green Company (F), Carl Zeiss Meditec (C, R), CSO (R), Dompé (R), Hanita Lenses (C, R), Jaypee Brothers (P), Maghrabi Hospital (C), Mediphacos (R), Oftalcare Nutravision (F), Omeros (C), Ophtec (F), Santen Phar-maceutical (C, F, R), Oculentis (C, R), Presbia (C), Schwind eye-tech-solutions (F, R), Slack Incorporated (C), Topcon Medical Systems (C), VisiDome (F)

References

1. Sekundo W, Stevens JD. Surgical treatment of keratoconus at the turn of the 20th century. *J Refract Surg*. 2001;17: 69–73.
2. Bechrakis N, Blom ML, Stark WJ, Green WR. Recurrent kera-toconus. *Cornea*. 1994;13:73–77.
3. Pinero DP, Alió JL, Barraquer RI, et al. Corneal biome-chanics, refraction, and corneal aberrometry in keratoconus: an integrated study. *Invest Ophthalmol Vis Sci*. 2010;51: 1948–1955.
4. Ku JY, Niederer RL, Patel DV, et al. Laser scanning in vivo confocal analysis of keratocyte density in keratoconus. *Ophthalmology*. 2008;115:845–850.
5. Sherwin T, Ismail S, Loh I, McGhee JJ. Histopathology (from keratoconus pathology to pathogenesis). In: Alió J , ed. *Keratoconus: Recent Advances in Diagnosis and Treatment (Essentials in Ophthalmology)*. Cham, Switzerland: Springer; 2017:25–41.
6. Alió JL, Pinero DP, Aleson A, et al. Keratoconus-integrated characterization considering anterior corneal aberrations, internal astigmatism, and corneal biomechanics. *J Cataract Refract Surg*. 2011;37:552–568.
7. Mastropasqua L, Nubile M. *Confocal Microscopy of the Cornea*. Thorofare, NJ: Slack; 2002;7–16.
8. Ali Javadi M, Kanavi MR, Mahdavi M, et al. Comparison of keratocyte density between keratoconus, post-laser in situ keratomileusis keratectasia, and uncomplicated post-laser in situ keratomileusis cases. A confocal scan study. *Cornea*. 2009;28:774–779.
9. Edmund C. Assessment of an elastic model in the pathogenesis of keratoconus. *Acta Ophthalmol (Copenh)*. 1987;65:545–550.
10. Fournié P, Galiacy SD, Malecaze F. Modern pathogenesis of keratoconus: genomics and proteomics. In: Alió JL, ed. *Keratoconus: Recent Advances in Diagnosis and Treatment (Essentials in Ophthalmology)*. Cham, Switzerland: Springer; 2017;7–12.

11. Mastropasqua L, Nubile M. *Confocal Microscopy of the Cornea*. Thorofare, NJ: Slack; 2002;38–44.
12. Watts A, Colby K. Contact lenses for keratoconus. In: Alió J , ed. *Keratoconus: Recent Advances in Diagnosis and Treatment (Essentials in Ophthalmology)*. Cham, Switzer-land: Springer; 2017:187–194.
13. Arnalich-Montiel F, Alio Del Barrio JL, Alio JL. Corneal surgery in keratoconus: which type, which technique, which outcomes? *Eye Vis (Lond)*. 2016;3:2.
14. Alió Del Barrio JL, El Zarif M, de Miguel MP, et al. Cellular therapy with human autologous adipose-derived adult stem cells for advanced keratoconus. *Cornea*. 2017;36:952–960.
15. Alió Del Barrio JL, El Zarif M, Azaar A, et al. Corneal stroma enhancement with decellularized stromal laminas with or without stem cell recellularization for advanced kerato-conus. *Am J Ophthalmol*. 2018;186:47–58.
16. Alió JL, Alió Del Barrio JL, El Zarif M, et al. Regenerative surgery of the corneal stroma for advanced keratoconus: one year outcomes. *Am J Ophthalmol*. 2019;203:53–68.
17. Arnalich-Montiel F, Pastor S, Blazquez-Martinez A, et al. Adipose-derived stem cells are a source for cell therapy of the corneal stroma. *Stem Cells*. 2008;26:570–579.
18. Du Y, Carlson EC, Funderburgh ML, et al. Stem cell ther-apy restores transparency to defective murine corneas. *Stem Cells*. 2009;27:1635–1642.
19. Liu H, Zhang J, Liu CY, et al. Cell therapy of congenital corneal diseases with umbilical mesenchymal stem cells: lumican null mice. *PLoS One*. 2010;5:e10707.
20. Guthoff R, Klink T, Schlunck G, Grehn F. Die sickerkisse-nuntersuchung mittels konfokaler in-vivo mikroskopie mit dem rostocker cornea modul - erste erfahrungen. *Klin Monatsbl Augenheilkd*. 2005;222:R8.
21. Patel S, McLaren J, Hodge D, Bourne W. Normal human keratocyte density and corneal thickness measurement by using confocal microscopy in vivo. *Invest Ophthalmol Vis Sci*. 2001;42:333–339.
22. Erie JC, Patel SV, McLaren JW, et al. Keratocyte density in keratoconus. A confocal microscopy study(a). *Am J Ophthal-mol*. 2002;134:689–695.
23. Petroll WM, Kivanany PB, Hagenasr D, Graham EK. Corneal fibroblast migration patterns during intrastromal wound healing correlate with ECM structure and alignment. *Invest Ophthalmol Vis Sci*. 2015;56:7352–7361.
24. Phinney DG, Prockop DJ. Concise review: mesenchymal stem/multipotent stromal cells: the state of transdifferenti-ation and modes of tissue repair–current views. *Stem Cells*. 2007;25:2896–2902.
25. Jester JV, Moller-Pedersen T, Huang J, et al. The cellular basis of corneal transparency: evidence for ‘corneal crys-tallins’. *J Cell Sci*. 1999;112:613–622.

10.7. El Zarif, Mona, Alió del Barrio, J.L., Arnalich-Montiel, F., De Miguel, M.P., Makdissy, N., Alió, J.L., 2020. Corneal stroma regeneration: new approach for the treatment of cornea disease. APJO 9, 571–579. https://doi.org/10.1097/APO.0000000000000337

Corneal Stroma Regeneration: New Approach for the Treatment of Cornea Disease

Mona El Zarif, OD, MSc z§{, Jorge L. Alio´ del Barrio, MD, PhD, FEBOS-CRyz, Francisco Arnalich-Montiel, MD, PhD, FEBOS-CRyjj, Marı´a P. De Miguel, PhD , Nehman Makdissy, PhD§, and Jorge L. Alio´, MD, PhD, FEBOphthyz

Abstract: Corneal grafting is one of the most common forms of human tissue transplantation. The corneal stroma is responsible for many characteristics of the cornea. For these reasons, an important volume of research has been made to replicate the corneal stroma in the laboratory to find an alternative to classical corneal transplantation techniques.

There is an increasing interest today in cell therapy of the corneal stroma using induced pluripotent stem cells or mesenchymal stem cells since these cells have shown to be capable of producing new collagen within the host stroma and even to improve its transparency.

The first clinical experiment on corneal stroma regeneration in advanced keratoconus cases has been reported and included. Fourteen patients were randomized and enrolled into 3 experimental groups: (1) patients under-went implantation of autologous adipose-derived adult stem cells alone,

(2) patients received decellularized donor corneal stroma laminas, and (3) patients received implantation of recellularized donor laminas with adipose-derived adult stem cells. Clinical improvement was detected with all cases in their visual, pachymetric, and topographic parameters of the operated corneas.

Other recent studies have used allogenic SMILE implantation lenticule corneal inlays, showing also an improvement in different visual, topographic, and keratometric parameters.

In the present report, we try to summarize the available preclinical and clinical evidence about the emerging topic of corneal stroma regeneration.

Keywords: adipose-derived adult stem cells, cornea surgery, corneal bioengineering, corneal stem cell therapy, corneal transplant, keratoconus, stem cells

INTRODUCTION

Human corneal transplantation with donor corneas has been the only option for treating corneal blindness for decades.
Despite recent improvements in surgical techniques, donor corneal transplantation continues to be plagued by risks of suboptimal optical outcomes, visual loss, immune rejection, and the consequent graft failure. The demand for adequate donor corneas is increasing faster than the number of donors, leaving thousands of patients around the world waiting for possible treatment.[1–3]

Due to these facts, the development of alternative approaches such as corneal bioengineering to obtain corneal substitutes that could have similar characteristics to the human donor cornea becomes important today. Efforts have been made to replicate the corneal stroma in the laboratory to find an alternative to classical corneal transplantation, but due to the highly complex ultrastruc-ture of the corneal stroma, the laboratory construction of the corneal stroma with enough transparency or strength for clinical use has not yet been achieved.[4–6]

Synthetic scaffold-based designs have raised some concerns about their potential to induce inflammatory responses caused by the involved biomaterials.[7] As an alternative, in the last decade the acellular corneal stroma has been proposed as a scaffold and several corneal decellularization techniques have been described, which provide an acellular corneal extracellular matrix (ECM).[8] These scaffolds have gained increasing interest as they provide an ideal natural environment for the growth and differentiation of cells (either transplanted donor cells or migrating host cells).[7] Besides this, the removal of all immunogenic cellular component could open the field of xenotransplantation by using donor tissue from other animals such as the pig, that shares important similarities with the human cornea.[9]

From the Optica General, Saida, Lebanon; yCornea, Cataract, and Refractive Surgery Unit, Vissum Corporacio´n, Alicante, Spain; zDivision of Ophthalmol-ogy, Universidad Miguel Herna´ndez University, Alicante, Spain; §Lebanese University, Faculty of Sciences, Genomic Surveillance and Biotherapy Team, Mont Michel Campus, Lebanon; {Lebanese University, Doctoral School of Sciences and Technology, Hadath, Lebanon; jjIRYCIS, Ophthalmology Department, Ramo´n y Cajal University Hospital, Madrid, Spain; and Cell Engineering Laboratory, IdiPAZ, La Paz Hospital Research Institute, Madrid, Spain.

Submitted August 28, 2020; accepted September 28, 2020.

Author contributions: M.E.Z.: co-principal investigator, clinical and monitor director of the study, study concept and design, data collecting, analysis and interpretation of data, writing and critical revision of the manuscript, statistical revision, and supervision; J.L.A.dB.: second surgeon, corresponding data editing, and critical correction of the manuscript; F.A.: Wrote part of the manuscript and collected data; M.P.dM.: biological and stem cell therapy processing; N.M.: biological and stem cell therapy processing; J.L.A.: principal investigator, principal surgeon, study concept and design, analysis and inter-pretation of data, writing and critical revision of the manuscript, statistical revision, and supervision in all the stages of this original.

This study has been financed by Optica General, Saida, Lebanon and Vissum Ophthalmological Institute of Alicante, Spain. It was also supported in part by the Red Tema´tica de Investigacio´n Cooperativa en Salud (RETICS), reference number RD16/0008/0012, financed by the Instituto Carlos III – General Subdirection of Networks and Cooperative Investigation Centers (R&D&I National Plan 2008–2011) and the European Regional Development Fund (Fondo Europeo de Desarrollo Regional, FEDER).

No specific financial disclosures for the purpose of this report.

The authors, their families, their employers, and their business associates have no financial or proprietary interest in any product or company associated with any devices, instruments, or drugs mentioned in this study. The authors have not received any payment as reviewers, consultants, or evaluators of any of the instruments, devices, or drugs mentioned in this study.

The authors report no conflicts of interest.

Address correspondence and reprint requests to: Jorge L. Alio, Vissum, Calle Caban˜al, 1, 03016 Alicante, Spain. E-mail: jlalio@vissum.com.

ISSN: 2162-0989
DOI: 10.1097/APO.0000000000000337

In recent years, corneal stromal cell therapy has attracted much interest. Looking for extraocular sources of mesenchymal stem cells (MSCs), studies have shown that MSCs are capable of surviving and differentiating into adult human keratocytes in vitro and in vivo,[10,11] even in xenogeneic scenarios in vivo, they do not induce any inflammatory reaction.[7,12] MSCs have also shown immunomodulatory properties in syngeneic, allogenic, and even xenogeneic scenarios.[13] Bone marrow MSC, umbilical cord MSC, and corneal stromal stem cells (CSSCs) form an alternative source to differentiate MSCs.[11,14,15] Adipose-derived adult stem cells (ADASCs) form a wide source of MSCs (Fig. 1) and satisfy many requirements for their application to human corneal therapy.[11,12] Embryonic stem cells have great potential to differentiate MSCs, but their use also involves important ethical issues. The use of induced pluripotent stem cell technology has opened a new and very promising field for future research; it has shown to exert immunomodulatory properties in the cornea similar to those observed with MSC,[16] since theoretically they are cells with the ability to generate adult keratocytes in vitro.[17]

Pioneering human clinical studies demonstrated published evidence that human ADASCs form an abundant extraocular source, are capable of surviving and differentiating in vivo into adult human keratocytes, and have demonstrated their ability to produce new collagen within the host stroma,[18] as it was previ-ously demonstrated in experimental animal models.[12,19]

This report aims to offer an integrated overview, based on evidence, about the current stage of human studies on the subject of regenerative advanced corneal stromal therapies in the treat-ment of corneal disease and, particularly, in keratoconus.

PRECLINICAL STUDIES

Collagen-Based Scaffolds

The arrangement of corneal collagen is the most difficult structure to reproduce either by cellular remodeling or by direct manufacturing in the laboratory. Many physical/engineering methods have been devised to attempt to control the organization of collagen, but none of them have been able to duplicate native corneal tissue structure. In general, they can neither match the mechanical properties nor recreate the local nanoscale organiza-tion. Although non–collagen-based materials (such as silk fibroin, gelatin hydrogels, chitosan, or synthetic polymers) seek to achieve higher strength than collagen-based scaffolds,[11] at the same time they lack the theoretical higher biocompatibility that the collagen has, as these synthetic materials are not present in the normal cornea. For this reason, collagen-based scaffolds have gained more attention due to their excellent biocompatibility with the recipient corneal stroma, and because they provide an optimal scaffold to support cellular growth (either from donor implanted or host migrated cells).

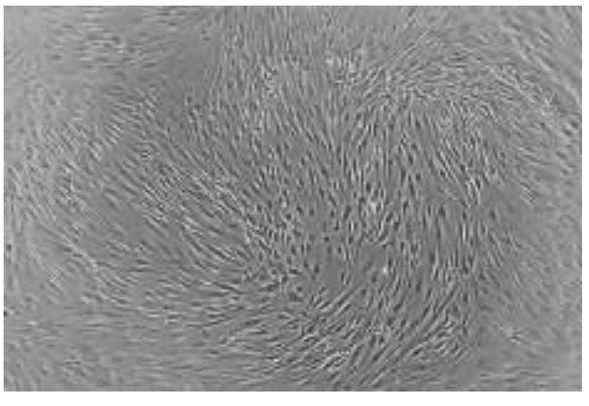

FIGURE 1. Microscopic appearance (phase-contrast photograph) of human adipose-derived adult stem cell in culture (100 magnification).

Currently, the most promising approach that is reaching clinical practice is the use of decellularized corneal stroma. Multiple decellularized corneal sections can be obtained from a single donor cornea, and even xenogeneic donors (such as pigs) have been suggested for human transplantation through the application of these decellularization methods.[7,9] Decellularized human corneal sections (Fig. 2A, B) that were recellularized with human ADASC have been assayed, in experimental animals (Fig. 2C)[7,20] and most importantly, in patients suffering from corneal stromal debilitating diseases.[18,21–23] Survival of the trans-planted cells with differentiation into corneal keratocytes and complete integration of the implant with naturally mimicking strength and total transparency with no rejection episodes was achieved in both preclinical and clinical studies (Fig. 2). Nevertheless, this approach still requires donor tissue and does not supply an unlimited source of cornea prostheses for their use in clinical patients.

In addition to the above-discussed decellularized corneal laminas (which represent naturally aligned collagen bundles), other methods have been proposed to mimic the corneal stroma structure, such as collagen vitrification.[24] In this regard, a phase 1 clinical trial with vitrified collagen-based scaffolds grafted onto the anterior stroma was performed and demonstrated a suboptimal performance when compared with regular corneal donor tissue.[2] Collagen 3D bioprinting[25] has accomplished outcomes showing material with optical and chemical properties similar to human cornea but weaker tensile strength,[26] among other limitations. Also, allogenic small incision lenticule extraction (SMILE) lenticule implantation has been assayed in both animals and humans, demonstrating to be a feasible approach, which can offer also possibilities for the correction of refractive errors and the improvement of corneal thickness, with potential applications in debilitating diseases such as corneal ectasias.[27–29]

Stem Cell Therapy Without Scaffold

Corneal MSC implantation has been assayed by different approaches: direct intrastromal transplantation, implantation at the ocular surface, intravenous, or at the anterior chamber, where cellular migration toward the inner stroma is expected.[11] This cellular implantation without a carrier aims to remodel or generate new ECM within the corneal stroma.

Direct in vivo injection of stem cells inside the corneal stroma has been assayed in some studies, demonstrating the differentiation of the stem cells into adult keratocytes without evidence of immune rejection. The differentiation of human ADASC in functional human keratocytes (Fig. 3) was demonstrated in vivo using the rabbit as a model,[12] and such cells, once implanted in the corneal stroma, express not only collagens type I and VI (the main components of corneal ECM), but also keratocyte-specific markers such as keratocan or ALDH, without inducing an immune or inflammatory response.[30] Du et al[31]

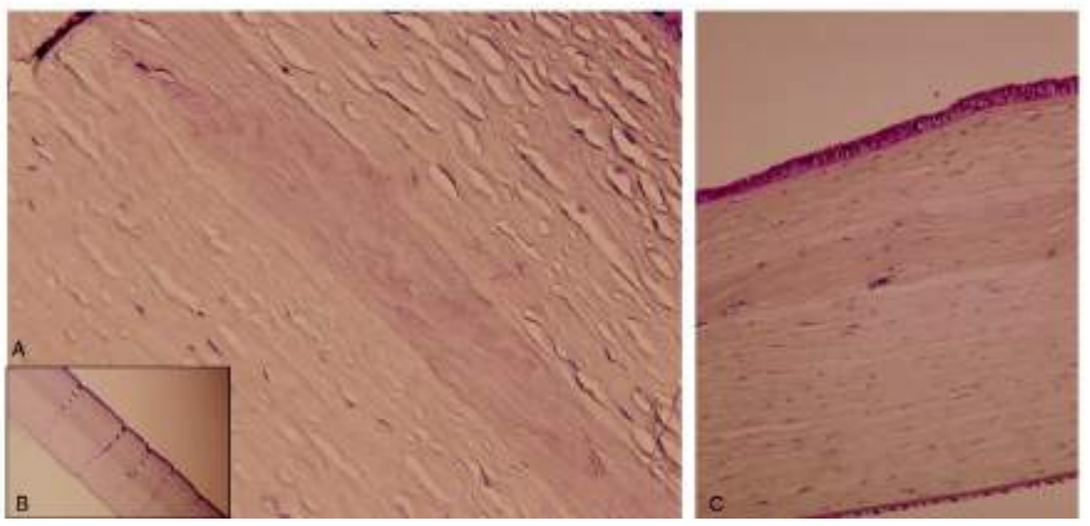

FIGURE 2. Decellularized human corneal stroma lamina implantation into a rabbit's corneal stroma in vivo. Hematoxylin-eosin staining showing decellularized (A and B) and human adipose-derived adult stem cell recellularized (C) lamina perfectly integrated into the rabbit's corneal stroma 3 months after implantation.

reported restoration of corneal transparency and thickness in lumican-null mice 3 months after intrastromal transplant of human CSSC. They also confirmed that human keratan sulfate was deposited in the mouse stroma and the host collagen lamellae were reorganized, concluding that delivery of human CSSCs to the scarred human stroma may alleviate corneal scars without requiring invasive surgery.[31] Very similar findings were reported by Liu et al who utilized human umbilical cord MSCs using the same animal model.[32] Coulson-Thomas et al found that in a mouse model for mucopolysaccharidosis, transplanted human umbilical cord MSCs participate both in extracellular glycosa-minoglycans turnover and enable host keratocytes to catabolize accumulated glycosaminoglycan products.[33]

The first clinical trial in clinical cases of keratoconus with implantation of autologous ADASCs decellularized and/or recel-lularized corneal stromal laminas, and confirmed preliminary the safety and efficacy of the cellular therapy of the human corneal stroma.[18,22,23,34] According to the clinical and preclinical available evidence, the direct intrastromal implantation of MSC within the cornea achieves the production of new ECM but is not expected to be quantitatively enough to be able to restore the thickness of a severely diseased human cornea, like in advanced keratoconus cases. However, the direct injection of stem cells may provide a promising treatment modality for the early treatment of corneal dystrophies, including keratoconus, in cases of corneal stroma progressive opacification in the context of systemic metabolic disorders, and for the modulation of corneal scars.

MSC Exosomes

It is important to highlight that the therapeutic effect of SCs in a damaged tissue is not always directly related to the potential differentiation of the SCs since multiple mechanisms might simul-taneously contribute to this therapeutic action, for example, the secretion of paracrine growth factors capable of stimulating the host tissue (in which case the direct cellular differentiation of the SCs might not be relevant and could even be nonexistent).[30,35,36] It has been demonstrated that MSCs secrete paracrine factors such as vascular endothelial growth factor, platelet-derived growth factor, hepatocyte growth factor, among others[13] that seem to promote cell migration and keratocyte survival by apoptosis inhibition, and upregulate the expression of ECM component genes in keratocytes, subsequently enhancing corneal re-epithelialization and stromal wound healing.[37] Because of this, it has been suggested that the direct treatment of the corneal stroma with the MSC exosomes containing these growth factors could potentially achieve the same benefits of the cellular therapy, but without providing the cellular component itself.[38] Funderburgh et al showed that

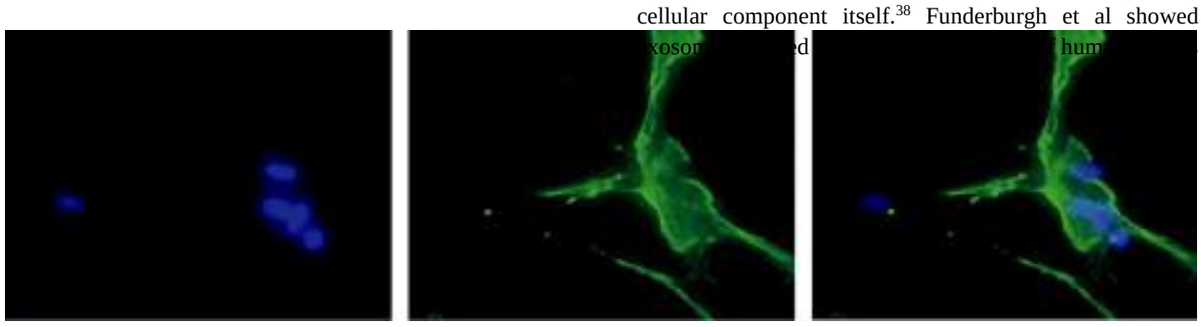

FIGURE 3. Confocal microscopy image of keratocan production by human adipose-derived adult stem cell in culture. Cellular nuclei appear with blue fluorescence due to 4^0,6-diamidino-2-phenylindole staining.

offer similar immunosuppressive properties and significantly reduced stromal scarring in wounded corneas in vivo.[39]

HUMAN CLINICAL STUDIES

Femtosecond Laser–Assisted Refractive Stromal Lenticule Addition

Donor stomal lenticules can be obtained from corneo-scleral eye bank buttons using a refractive lenticule extraction procedure with a 500-kHz VisuMax femtosecond laser (Carl Zeiss Meditec, Jena, Germany) and cryopreserved or stored in organ culture to be subsequently used for implantation. The implantation of these stromal lenticules has been proposed as a way to reverse the effect of previous laser refractive surgery,[40,41] to treat different types of ametropia,[42] and as a therapy for cornea ectatic disorders such as keratoconus, where progressive stromal thinning causes irregular astigmatism and refractive instability.

The myopic correction algorithm for SMILE produces positive meniscus lenticules, thicker in the center and gradually becoming thinner toward the periphery. The implantation of these lenticules induces an increase in anterior corneal curvature and has been used to correct hyperopia in humans. An inverted thickness profile that gradually becomes thicker from the center toward the periphery can also be produced using a hyperopic algorithm for SMILE. The implantation of these negative meniscus-shaped lenticules in an ex vivo study on human corneas causes a reproducible flattening of the central cornea and an increase of the stromal thickness, both desirable effects of any procedure for treating keratoconus eyes.[43]

Mastropasqua et al[44] were able to replicate these results in 10 advanced keratoconus eyes. They coined this procedure "stromal lenticule addition keratoplasty" as a feasible and effective tech-nique for stromal remodeling in advanced central keratoconus. The lenticules programmed for 8.00 diopter (D) of hyperopic correction with a 6-mm optical zone was introduced in a femtosecond intrastromal pocket at 120 μm from the corneal surface. No intraoperative or relevant postoperative complications were reported, and 9 of 10 showed improvement in corrected distance visual acuity 6 months after implantation, ranging from 1 to 3 lines. Mean central keratometry significantly decreased by a mean of 5 D, corneal thickness increased by 50 μm, and there was a significant improvement of corneal asphericity. The lenticule-host inferfaces could be identified using in vivo confocal microscopy, but keratocyte morphology appeared normal and extracellular tissue presented normal transparency.[44]

Using a different approach, Pradhan et al[45] proposed femto-second laser–assisted small incision sutureless intrastromal lamel-lar keratoplasty as an alternative to corneal transplantation in keratoconus and presented the 1-year follow-up result in a single patient. As in the stromal lenticule addition keratoplasty procedure, sutureless intrastromal lamellar keratoplasty showed an improve-ment of the uncorrected and best-corrected visual acuity and a reduction of 7 D in the maximum keratometry with a considerable thicker lenticule (up to 332 μm in the central cornea).

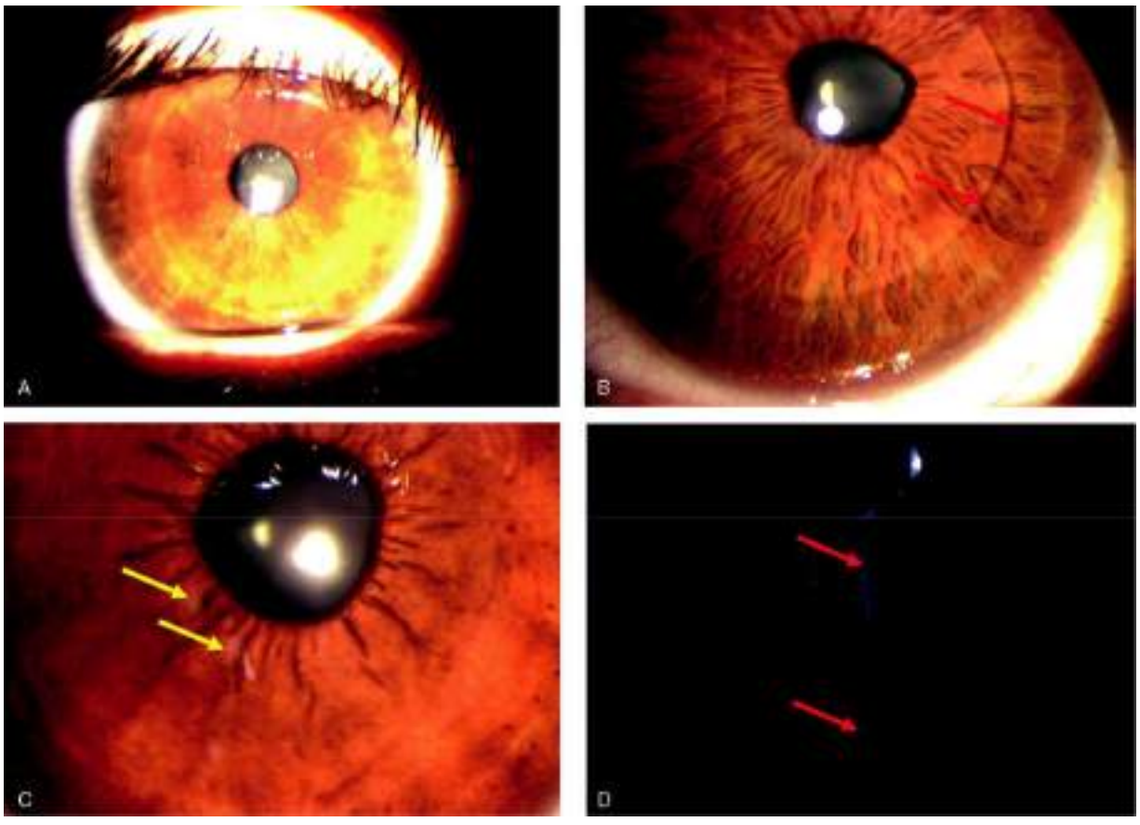

FIGURE 4. Biomicroscopic findings at 36 months after operation. A, Group 1, case 2 shows the transparency of the cornea. B, Group 2, case 9 notices the transparency of the implanted decellularized lamina. Red arrows present the periphery of the lamina. C, Group 2, case 7, shows some scattered, faint, patchy ''islands'' of haze (yellow arrows). These paracentral areas of haze did not have any impact on the visual outcomes. D, Group 3, case 10 indicates the periphery of the recellularized lamina (red arrows). Notice the transparency of the implanted tissue.

Stem Cell Therapy of the Corneal Stroma for Advanced Keratoconus

Surgical Procedure

The results of the implantation of autologous ADASCs in the corneas of 5 patients from group 1 (G1) with advanced kerato-conus have been reported.[12,18,46,47] From simple liposuction performed with local anesthesia, 250 mL of human autologous adipose tissue was obtained, followed by the identification, isolation, characterization, and culture of adipose tissue mesen-chymal-derived stem cells. A femtosecond laser was used in single-pass mode to dissect the corneas in the mid-stroma of 5 eyes with advanced keratoconus. Each of these eyes received an injection of 3 x 10^6 cells of autologous ADASCs in 1 mL of the phosphate-buffered solution into the stromal pocket, using a 25-G cannula. The surgical procedure and its outcomes were described in a previous publication.[18]

Five patients' eyes of group 2 (G2) with advanced keratoconus received 120 µm decellularized human corneal stroma laminas only, and another 4 eyes from group 3 (G3) received the implan-tation of 120 µm human corneal stroma recellularized with autologous ADASCs (1 x 10^6cells/1 mL of phosphate-buffered solution, half million on each side).[23,34] The corneal laminas were obtained from human corneas that were not suitable for corneal transplantation. The corneas of patients from G2 and G3 were dissected by femtosecond laser in the mid-stroma of the thinnest point measured by anterior segment optical coherence tomogra-phy. The protocol of decellularization and the surgical procedures were described in previous publications.[7,23,34]

The confocal microscope, the Rostock Cornea Module of the Heidelberg Retina Tomograph 3, was used to observe the evo-lution and the morphological change of implanted ADASCs and the decellularized/ADASCs recellularized human corneal stromal laminas.[48,49]

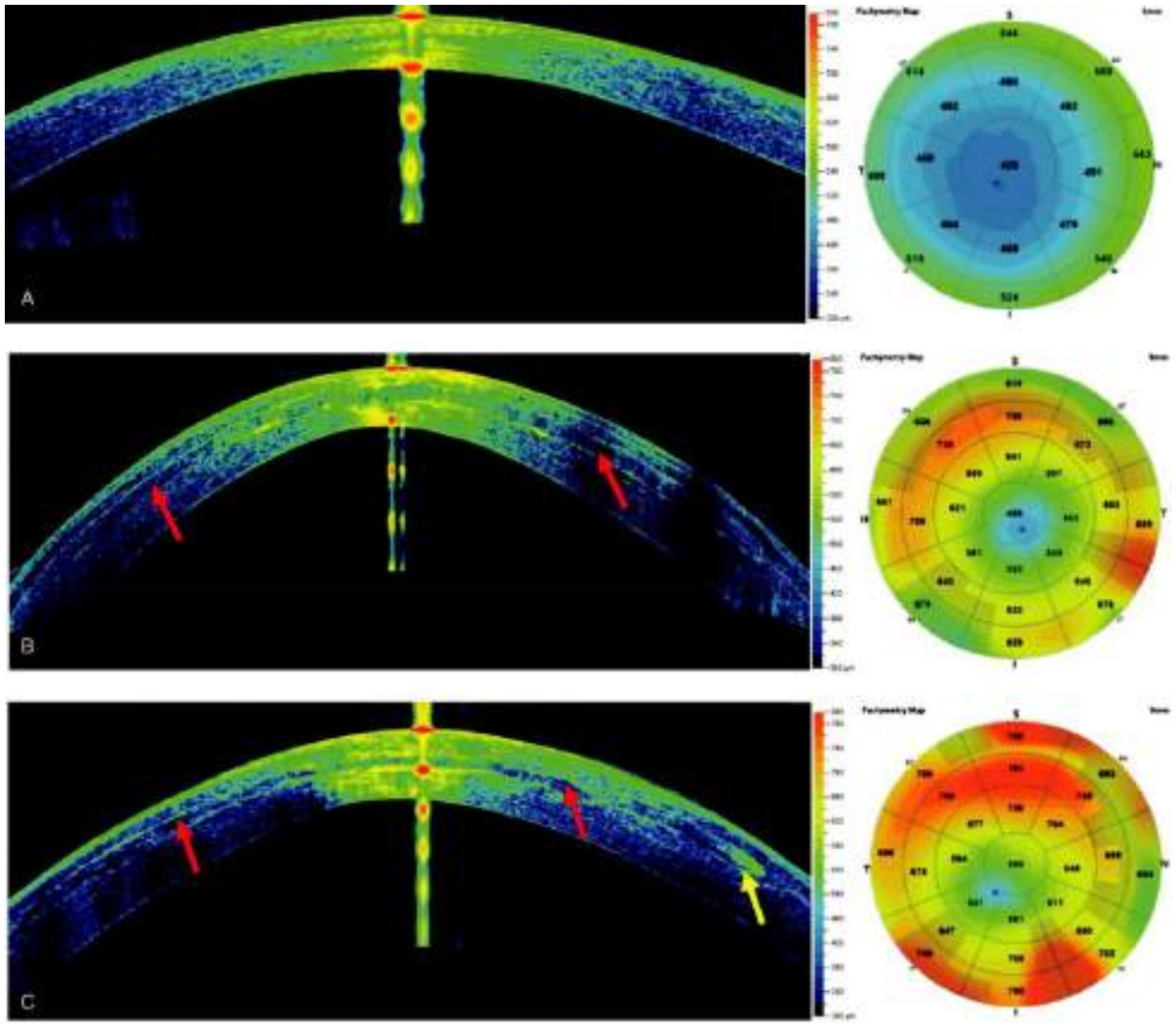

FIGURE 5. Corneal AS-OCT sections and pachymetric maps (Visante) in group 1, group 2, and group 3. A, Group 1, case 1, OCT at 12 months. Notice the perfect transparency of the cornea (left side). Observe the pachymetry map (right). B, Group 2, case 7, OCT at 36 months. Observe the integration of the implanted decellularized lamina in the host stoma and the improvement in corneal density (left). The paquimetry map (right) shows the enhancement in the thickness of the cornea. C, Group 3, case 12, OCT at 36 months. The enhancement in the integration of the implanted lamina in the host stroma (red arrows), and an improvement in corneal density can be noticed. Yellow arrow indicates the border of the lamina. Observe the enhancement in the pachymetry map (right). AS-OCT indicates Anterior segment optical coherence tomography; OCT, optical coherence tomography.

RESULTS

No complications such as haze or infection were observed during the 3-year follow-up. Full corneal transparency was recov-ered within the first postoperative day in all patients of the G1 (Fig. 4A). Meanwhile, in G2 and G3, the implanted laminas showed mild early haziness during the first postoperative month. Corneal recovery and full transparency were observed within the third postoperative month in all patients (Fig. 4B, C). All patients were followed at 1 day, 1 week, and at 1, 3, 6, 12, and 36 months after operation.[34]

All cases improved at 36 months: 1 to 2 lines in LogMAR scale in their unaided distance visual acuity, corrected distance visual acuity, and rigid contact lens distance visual acuity in comparison with the preoperative values.[34]

A significant improvement in the refractive sphere was observed at 36 months. However, refractive cylinder presented minor changes in the 3 groups.

Results of AS-OCT: central corneal thickness (Fig. 5), thinnest point measured by Pentacam Scheimpflug corneal topography (Oculus Inc., Wetzlar, Germany) (Fig. 6), and cornea volume showed a significant increase in all groups. The mean value results were better in G2 and G3 compared with G1.[34] Also, significant improvement was obtained in mean values in third-order aberration root mean square and high-order aberration root mean square, where the results were better when comparing G2 and G3 with G1.[34]

Moreover, an improvement of 2D in the mean values with the results of the anterior mean keratometry was obtained (Fig. 6). In maximum keratometry, a flattening of 3D was obtained at 36 months. More results were recorded in previous publications.[15,23,34]

Confocal microscopy showed a morphological change with G1, where ADASCs appeared rounded in shape, more voluminous, and refringent up to 6 months regarding host keratocytes (Fig. 7A). Then, implanted cells changed from round to a fusiform shape similar to normal keratocytes (Fig. 7B). The cellular density showed a gradual statistically significant increase at the anterior, mid, and posterior host stroma when compared with preoperative values. In G2, decellularized laminas appeared acellular during the first month (Fig. 7C). Unlike the recellularized ones in G3, cell structures similar to corneal keratocytes were observed within the laminas (Fig. 7D). The cell density increased during the 12 months' follow-up until reaching a statistically significant increase in the anterior, mid, and posterior surfaces of the decellularized and recellularized laminas (Fig. 7E–G), and in the anterior and posterior host stroma with all the cases (Fig. 7H).

DISCUSSION

The ideal corneal stroma constructed by bioengineering should be capable of mimicking the natural human cornea and maintaining the corneal stroma homeostasis. For these purposes,

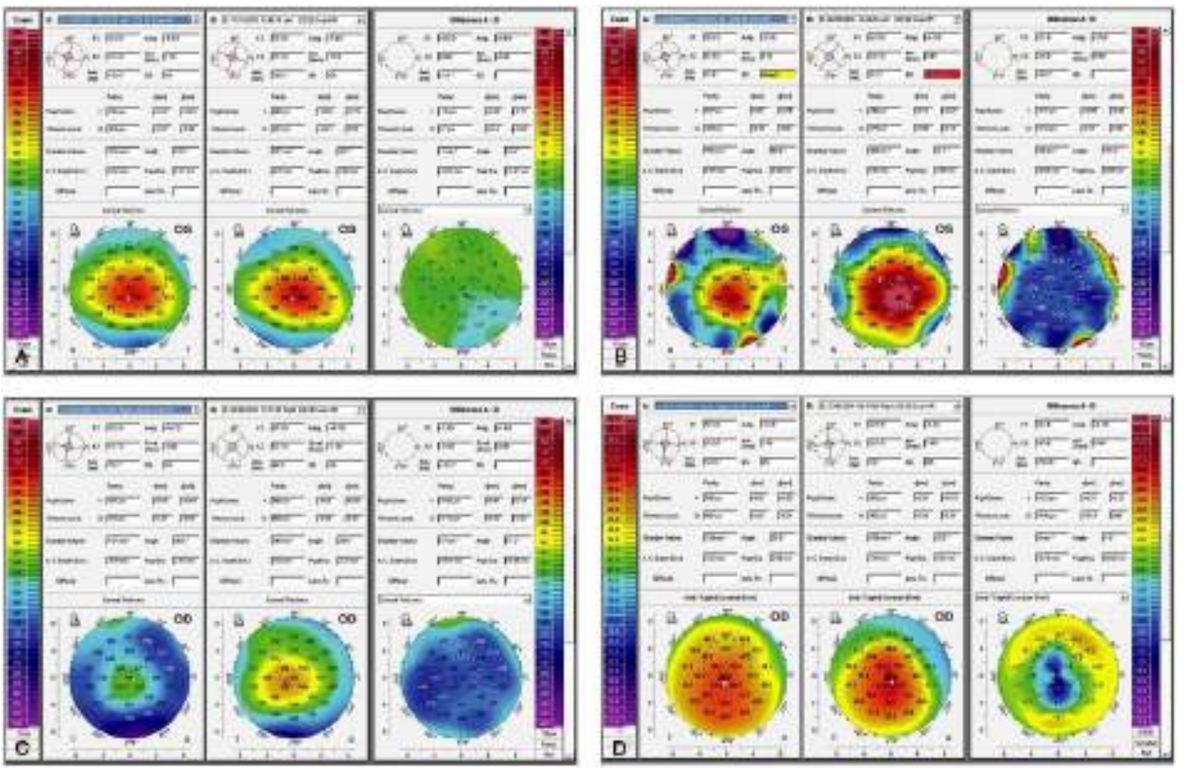

FIGURE 6. Corneal topography changes (Pentacam) among preoperation, 12 months, and 36 months in groups 1, 2, and 3. A, Comparative pachymetry examinations (right) among preoperation (middle) and 12 months (left) in case 4, group 1. Observe the modest enhancement in the pachymetry parameters in the inferior part of the cornea. B, Comparative pachymetry examinations (right) among preoperation (middle) and 12 months (left) in case 12, group 3. Observe the improvement of the corneal thickness. C, Comparative pachymetry examinations (right) among preoperation (middle) and 36 months (left) in case 6, group 2. Observe the improvement of the corneal thickness. D, Corneal topography (Pentacam) comparison (right side) between preoperation (middle) and nearly 3 years (left side) in case 5, group 2. The enhancement of the keratometric parameters can be seen.

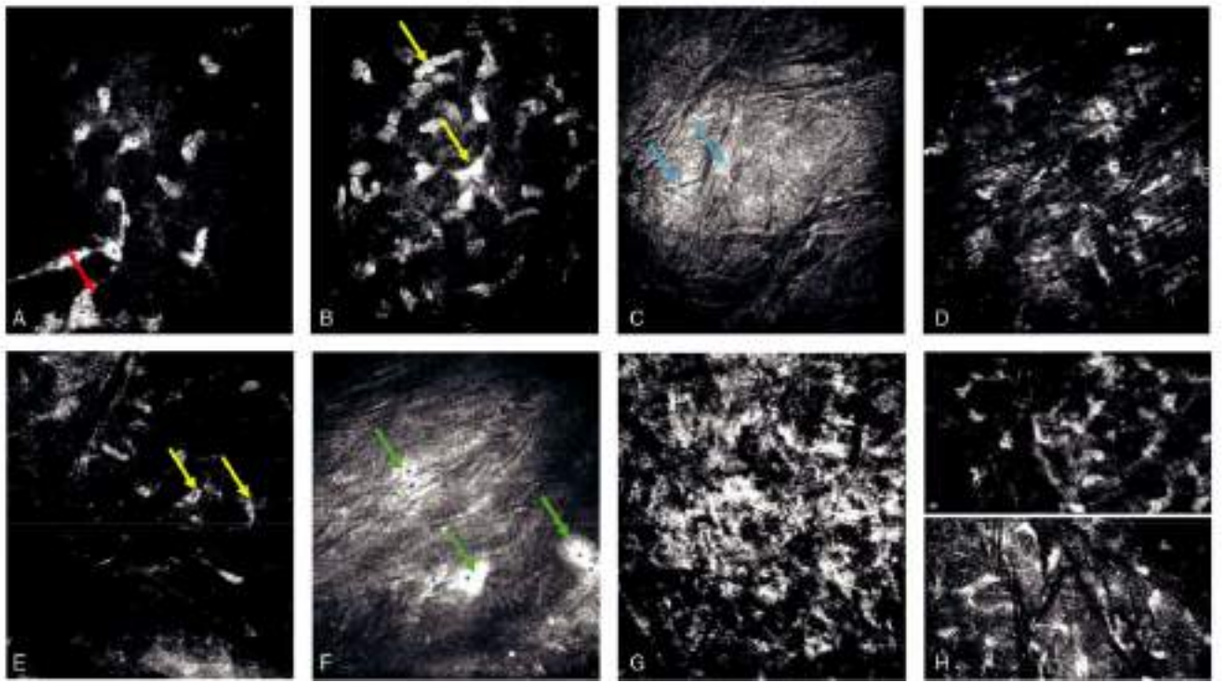

FIGURE 7. Confocal microscopy findings up to 12 months. A, Group 1, case 1, count of keratocytes and adipose-derived adult stem cells (ADASCs) (red arrow) in the surgical plane at 3 months after surgery. ADASCs appear rounded, larger, and more refringent than the normal keratocytes. B, Group 1, case 2, 1 year, all corneal stromal cells in the surgical plane assimilate a similar shape (yellow arrows). C, Group 2, case 7, anterior surface of a decellularized lamina appears without cells at 1 month. Observe the presence of reflective dots' structures (blue arrows). D, Group 3, case 13, anterior surface of a recellularized lamina at 1 month. Few ADASCs can be seen (marked in blue). E, Group 2, case 9, posterior surface of the decellularized lamina at 1 year. The cells assimilate a morphology identical to that of normal corneal stromal keratocytes (yellow arrows). F, Group 3, case 10, posterior surface of a recellularized lamina at 3 months. Observe ADASCs round in shape more luminous and refringent (green arrows). G, Group 3, case 13, anterior surface of a recellularized lamina at 12 months. High number of stromal cells can be seen. H, Anterior corneal stroma (up) in group 2, case 9, and posterior corneal stroma (down) in group 3, case 13, with abundant corneal stromal cells at 12 months.

It has to contain both a cell source and a collagen scaffold.[4–6] For the cellular component, several cell types from both ocular and extraocular sources have been investigated, being the human MSC the most widely tested so far. However, further development of cheaper and standardized induced pluripotent stem cell tech-niques may surpass MSC use.[16] The use of decellularized cornea sections could be the most clinically relevant.[7,8,20] However, it is still handicapped by the need for donor corneal tissue. The use of MSC exosomes (without their cellular component) reveals an exciting field of research as their use could overcome some of the limitations and risks associated with the direct delivery of stem cells to humans in vivo if exosomes could be applied topically.[38]

The popularization of SMILE as a refractive surgery option is providing a large amount of donor corneal tissue that could potentially be used for human transplantation. Liu et al and Zhao et al[27,28] demonstrated after 2 years' follow-up that small incision allogenic intrastromal lenticule implantation is feasible and safe for reshaping the cornea. The corneal healing remained stable and their results were confirmed by slit-lamp biomicroscopy and by confocal microscopy in vivo and corneal densitometry measure-ments. Additionally, the authors observed corneal reinnervation signs within the lenticule. The stromal addition of SMILE created lenticules that were proven ex vivo and in vivo (its feasibility, safety, and efficacy in the treatment of thinning disorders such as keratoconus).[43–45] This procedure increases corneal thickness providing additional strength to the weakened cornea and anterior corneal flattening when using a negative meniscus-shaped lenticule.[44] The transplantation of negative meniscus lenticules induced more flattening than the one observed with planar lenticules. However, the latter can be implanted in eccentric cones, whereas the former only in central cones (a much less common situation in keratoconus patients).[34,44] The feasibility and safety of corneal stromal cell therapy for advanced kerato-conic corneas were demonstrated for the first time. The appear-ance of new collagen formation within the surgical plane was also observed when MSCs were implanted. Although it was not enough to restore the thickness of the diseased corneas, this neo-collagen may play a role in the stromal remodeling of corneal dystrophies and corneal scars to enhance corneal transparency (Figs. 5A, 6A).[18] The implantation of decellularized or recellu-larized human corneal stroma laminas effectively restores corneal thickness, and it potentially avoids any risk of graft rejection (while this risk is still present by the use of allogenic stromal implants). The increase in corneal thickness is lower when negative meniscus laminas are used compared with planar len-ticules as they are thinner in the center.[44] However, they achieve a larger flattening effect in central cones. It has also to be consid-ered that negative meniscus-shaped lenticules may generate unacceptable aberrations within the visual axis in eccentric cones. Therefore, they might not be indicated in many cases of kerato-conus.[34,44]

Synthetic collagen scaffolds are, by definition, a promising source of donor stromal tissue as they do not need human donor tissue and can be potentially available all over the world.

However, their difficulties that are still present today, which are to mimic the transparency and strength of the human cornea, together with the high expenses for their production in the laboratory, preclude their presence in the real clinical practice for the next few years.

CONCLUSIONS

Cellular therapy with implantation of autologous ADASCs decellularized human corneal stroma, and allogenic SMILE lenticule corneal inlays have been shown to be a potentially effective therapy for keratoconus. Such promising findings open a new perspective in therapy for the corneal stroma based on corneal stromal regeneration and enhancement of corneal thickness, and topographic and visual parameters. Future studies are needed to expand on the potential application of these new therapies for the treatment of corneal stromal diseases.

REFERENCES

1. Griffith M, Alarcon EI, Brunette I. Regenerative approaches for the cornea. J Intern Med. 2016;280:276 –286.
2. Fagerholm P, Lagali N, Merrett K, et al. A biosynthetic alternative to human donor tissue for inducing corneal regeneration: 24-month follow-up of a phase 1 clinical study. Sci Transl Med. 2010;2:46ra61. doi:10.1126/scitranslmed.3001022.
3. Gain P, Jullienne R, He Z, et al. Global survey of corneal transplantation and eye banking. JAMA Ophthalmol. 2016;134:167 –173.
4. Isaacson A, Swioklo S, Connon CJ. 3D bioprinting of a corneal stroma equivalent. Exp Eye Res. 2018;173:188 –193.
5. Ruberti J, Zieske J. Prelude to corneal tissue engineering—gaining control of collagen organization. Prog Retin Eye Res. 2008;27:549–577.
6. Alio´ JL, Pin˜ero DP, Aleso´n A, et al. Keratoconus-integrated characterization considering anterior corneal aberrations, internal astigmatism, and corneal biomechanics. J Cataract Refract Surg. 2011;37:552 –568.
7. Alio´ del Barrio JL, Chiesa M, Garagorri N, et al. Acellular human corneal matrix sheets seeded with human adipose-derived mesenchymal stem cells integrate functionally in an experimental animal model. Exp Eye Res. 2015;132:91 –100.
8. Lynch A, Ahearne M. Strategies for developing decellularized corneal scaffolds. Exp Eye Res. 2013;108:42 –47.
9. Hara H, Cooper DKC. Xenotransplantation—the future of corneal transplantation? Cornea. 2011;30:371 –378.
10. De Miguel MP, Casaroli-Marano RP, Nieto-Nicolau N, et al. Frontiers in regenerative medicine for cornea and ocular surface. Rahman AU, editor. Bentham ebooks; 2015. 92–138 p.
11. Alio´ del Barrio JL, Arnalich-Montiel F, De Miguel MP, Alio´ JL. Corneal stroma regeneration (part A): preclinical studies. Exp Eye Res. 2020.
12. Arnalich-Montiel F, Pastor S, Bla´zquez-Martı´nez A, et al. Adipose-derived stem cells are a source for cell therapy of the corneal stroma. Stem Cells. 2008;26:570 –579.
13. De Miguel MP, Fuentes-Julia´n S, Bla´zquez-Martı´nez A, et al. Immunosuppressive properties of mesenchymal stem cells: advances and applications. Curr Mol Med. 2012;12:574–591.
14. Hendijani F. Explant culture: an advantageous method for isolation of mesenchymal stem cells from human tissues. Cell Prolif. 2017;50:e12334. doi:10.1111/cpr.12334.
15. Alio´ JL, El Zarif M, Alio´ del Barrio JL. Cellular therapy of the corneal stroma: a new type of corneal surgery for keratoconus and corneal dystrophies a translational research experience. 1st ed. Amsterdam, The Netherlands: Elsevier; 2020.
16. Yun Y, Park S, Lee H, et al. Comparison of the anti-inflammatory effects of induced pluripotent stem cell–derived and bone marrow –derived mesenchymal stromal cells in a murine model of corneal injury. Cytotherapy. 2017;19:28 –35.
17. Naylor RW, Charles NJM, Cowan CA, Davidson AJ, Holm TM, Sherwin T. Derivation of corneal keratocyte –like cells from human induced pluripotent stem cells. PLoS One. 2016;11:e0165464. doi:10.1371/journal.pone.0165464.
18. Alio´ del Barrio JL, El Zarif M, De Miguel MP, et al. Cellular therapy with human autologous adipose-derived adult stem cells for advanced keratoconus. Cornea. 2017;36:952 –960.
19. Espandar L, Bunnell B, Wang G, Gregory P, McBride C, Moshirfar M. Adipose-derived stem cells on hyaluronic acid –derived scaffold: a new horizon in bioengineered cornea. Arch Ophthalmol. 2012;130:202 –208.
20. Alio´ del Barrio JL, Chiesa M, Ferrer GG, et al. Biointegration of corneal macroporous membranes based on poly(ethyl acrylate) copolymers in an experimental animal model. Adv Sci. 2015;103:1106–1118.
21. Alio´ del Barrio JL, Alio´ JL. Cellular therapy of the corneal stroma: a new type of corneal surgery for keratoconus and corneal dystrophies. Eye Vis. 2018;5:28. doi:10.1186/s40662-018-0122-1.
22. Alio´ del Barrio JL, El Zarif M, Azaar A, et al. Corneal stroma enhancement with decellularized stromal laminas with or without stem cell recellularization for advanced keratoconus. Am J Ophthalmol. 2018;186:47 –58.
23. Alio´ JL, Alio´ del Barrio JL, El Zarif M, et al. Regenerative surgery of the corneal stroma for advanced keratoconus: 1-year outcomes. Am J Ophthalmol. 2019;203:53 –68.
24. Caldero´n-Colo´n X, Zhiyong X, Breidenich JL, et al. Structure and properties of collagen vitrigel membranes for ocular repair and regeneration applications. Biomaterials. 2012;33:8286–8295.
25. Liu Y, Gan L, Carlsson DJ, et al. A simple, cross-linked collagen tissue substitute for corneal implantation. Invest Ophthalmol Vis Sci. 2006;47:1869 –1875.
26. Merrett K, Fagerholm P, McLaughlin CR, et al. Tissue-engineered recombinant human collagen-based corneal substitutes for implantation: performance of type I versus type III collagen. Cornea. 2008;49:3887–3894.
27. Liu R, Zhao J, Xu Y, et al. Femtosecond laser–assisted corneal small incision allogenic intrastromal lenticule implantation in monkeys: a pilot study. Invest Opthalmol Vis Sci. 2015;56:3715 –3720.
28. Zhao J, Liu R, Shen Y, et al. Two-year observation of morphologic and histopathologic changes in the monkey cornea following small incision allogenic lenticule implantation. Exp Eye Res. 2020;192:107935.
29. Zhao J, Shen Y, Tian M, et al. Corneal lenticule allotransplantation after femtosecond laser small incision lenticule extraction in rabbits. Cornea. 2017;36:222 –228.
30. Harkin D, Foyn L, Bray L, Sutherland A, Li F, Cronin B. Concise reviews: can mesenchymal stromal cells differentiate into corneal cells? A systematic review of published data. Stem Cells. 2015;33:785–791.
31. Du Y, Carlson E, Funderburgh M, et al. Stem cell therapy restores transparency to defective murine corneas. Stem Cells. 2009;27:1635 –1642.
32. Liu H, Zhang J, Liu C-Y, et al. Cell therapy of congenital corneal diseases with umbilical mesenchymal stem cells: lumican null mice. PLoS One. 2010;5:e10707. doi:10.1371/journal.pone.0010707.

33. Coulson-Thomas VJ, Caterson B, Kao W. Transplantation of human umbilical mesenchymal stem cells cures the corneal defects of mucopolysaccharidosis VII mice. Stem Cells. 2013;31:2116 –2126.

34. El Zarif M, Alio´ JL, Alio´ del Barrio JL, et al. Corneal stromal regeneration therapy for advanced keratoconus: long-term outcomes at 3 years. Cornea. 2020.

35. Caplan AI. Mesenchymal stem cells: time to change the name! Stem Cells Transl Med. 2017;6:1445 –1451.

36. Yao L, Bai H. Review: mesenchymal stem cells and corneal reconstruction. Mol Vis. 2013;19:2237 –2243.

37. Jiang Z, Liu G, Meng F, et al. Paracrine effects of mesenchymal stem cells on the activation of keratocytes. Br J Ophthalmol. 2017;101:1583 –1590.

38. Funderburgh JL, Funderburgh ML, Mann M, Khandaker I, Shojaati G. Assessing the potential of stem cells to regenerate stromal tissue. Investig Ophthalmol Vis Sci. 2017;58:1425.

39. Shojaati G, Khandaker I, Funderburgh ML, et al. Mesenchymal stem cells reduce corneal fibrosis and inflammation via extracellular vesicle –mediated delivery of miRNA. Stem Cells Transl Med. 2019;8:1192 –1201.

40. Riau AK, Angunawela RI, Chaurasia SS, Lee WS, Tan DT, Mehta JS. Reversible femtosecond laser–assisted myopia correction: a nonhuman primate study of lenticule reimplantation after refractive lenticule extraction. PLoS One. 2013;8:e67058. doi:10.1371/journal.pone.0067058.

41. Angunawela RI, Riau AK, Chaurasia SS, Tan DT, Mehta JS. Refractive lenticule reimplantation after myopic ReLEx: a feasibility study of stromal restoration after refractive surgery in a rabbit model. Investig Ophthalmol Vis Sci. 2012;53:4975 –4985.

42. Jacob S, Kumar DA, Agarwal A, Agarwal A, Aravind R, Saijimol AI. Preliminary evidence of successful near vision enhancement with a new technique: PrEsbyopic allogenic refractive lenticule (PEARL) corneal inlay using a SMILE lenticule. J Refract Surg. 2017;33:224 –229.

43. Mastropasqua L, Nubile M. Corneal thickening and central flattening induced by femtosecond laser hyperopic-shaped intrastromal lenticule implantation. Int Ophthalmol. 2017;37:893–904.

44. Mastropasqua L, Nubile M, Salgari N, Mastropasqua R. Femtosecond laser–assisted stromal lenticule addition keratoplasty for the treatment of advanced keratoconus: a preliminary study. J Refract Surg. 2018;34:36 –44.

45. Pradhan KR, Reinstein DZ, Vida RS, et al. Femtosecond laser–assisted small incision sutureless intrastromal lamellar keratoplasty (SILK) for corneal transplantation in keratoconus. J Refract Surg. 2019;35:663 –671.

46. Zuk PA, Zhu M, Mizuno H, et al. Multilineage cells from human adipose tissue: implications for cell-based therapies. Tissue Eng. 2001;7:211 –228.

47. Zuk PA, Zhu M, Ashjian P, et al. Human adipose tissue is a source of multipotent stem cells. Mol Biol Cell. 2002;13:4279 –4295.

48. Guthoff R, Klink T, Schlunck G, Grehn F. Die sickerkissenuntersuchung mittels konfokaler in-vivo mikroskopie mit dem rostocker cornea modul—erste erfahrungen. Klin Monatsbl Augenheilkd. 2005;222:R8. doi:10.1055/s-2005-922279.

49. El Zarif M, Abdul Jawad K, Alio´ del Barrio JL, et al. Corneal stroma cell density evolution in keratoconus corneas following the implantation of adipose mesenchymal stem cells and corneal laminas: an in vivo confocal microscopy study. Invest Opthalmol Vis Sci. 2020;61:22. doi:10.1167/iovs.61.4.22.

10.8. El Zarif, Mona, Alió, J.L., Alió del Barrio, J.L., De Miguel, M.P., Abdul Jawad, K., Makdissy, N., 2021. Corneal stromal regeneration: a review on human clinical studies for treatement of keratoconus. Front Med 8, 650724. https://doi.org/10.3389/fmed.2021.650724

Corneal Stromal Regeneration: A Review of Human Clinical Studies in Keratoconus Treatment

Mona El Zarif [1,2,3,4], Jorge L. Alió [2,5]*, Jorge L. Alió del Barrio [2,5], Maria P. De Miguel [6], Karim Abdul Jawad [1] and Nehman Makdissy [3]

[1] Optica General, Saida, Lebanon, [2] Division of Ophthalmology, Universidad Miguel Hernández, Alicante, Spain, [3] Faculty of Sciences, GSBT Genomic Surveillance and Biotherapy Team, Mont Michel Campus, Lebanese University, Beirut, Lebanon,

[4] Doctoral School of Sciences and Technology, Lebanese University, Hadath, Lebanon, [5] Cornea, Cataract and Refractive Surgery Unit, Vissum (Miranza Group), Alicante, Spain, [6] Cell Engineering Laboratory, IdiPAZ, La Paz Hospital Research Institute, Madrid, Spain

The use of advanced therapies with stem cells to reconstruct the complex tissue of corneal stroma has gained interest in recent years. Besides, collagen-based scaffolds bioengineering has been offered as another alternative over the last decade. The outcomes of the first clinical experience with stem cells therapy on corneal stroma regeneration in patients with advanced keratoconus were recently reported. Patients were distributed into three experimental groups: Group 1 (G-1) patients underwent implantation of autologous adipose-derived adult stem cells (**ADASCs)** alone, Group 2 (G-2) received a 120 µm decellularized donor corneal stromal laminas, and Group 3 (G-3) received a 120 µm recellularized donor laminas with **ADASCs.** A follow up of 36 months of clinical data, and 12 months of confocal microscopy study was performed, the authors found significant clinical improvement in almost all studied mean values of primary and secondary outcomes. Corneal confocal microscopy demonstrated an increase in cell density in the host stroma, as well as in the implanted tissue. Using different approaches, allogenic small incision lenticule extraction **(SMILE)** implantation was applied in cases with advanced keratoconus. Some authors reported the implantation of **SMILE** intrastromal lenticules combined with accelerated collagen cross-linking. Others performed intrastromal implantation of negative meniscus-shaped corneal stroma lenticules. Others have compared the outcomes of penetrating keratoplasty (**PKP**) vs. small-incision Intralase femtosecond (IFS) intracorneal concave lenticule implantation (**SFII**). Femtosecond laser-assisted small incision sutureless intrasotromal lamellar keratoplasty (**SILK)** has been also investigated. The published evidence shows that the implantation of autologous **ADASCs**, decellularized or recellularized human corneal stroma, allogenic **SMILE** lenticules corneal inlay, and recombinant cross-linked collagen have shown initially to be potentially effective for the treatment of advanced keratoconus. In light of the present evidence available, it can be said that the era of corneal stromal regeneration therapy has been already started.

Keywords: stem cells, regenerative medicine, corneal bioengineering, corneal stem cell therapy, keratoconus, autologous adipose-derived adult stem cells, cross-linked collagen, corneal surgery

Edited by:
Claudia Fabiani,
University of Siena, Italy

Reviewed by:
Luigi Fontana,
Local Health Authority of Reggio Emilia, Italy
Juan Alvarez De Toledo Elizalde,
Clínica Oftalmológica Barraquer, Spain

***Correspondence:**
Jorge L. Alió
jlalio@vissum.com

Specialty section:
This article was submitted to Ophthalmology, a section of the journal Frontiers in Medicine

Received: 07 January 2021
Accepted: 28 January 2021
Published: 23 February 2021

Citation:
El Zarif M, Alió JL, Alió del Barrio JL, De Miguel MP, Abdul Jawad K and Makdissy N (2021) Corneal Stromal Regeneration: A Review of Human Clinical Studies in Keratoconus Treatment. Front. Med. 8:650724. doi: 10.3389/fmed.2021.650724

INTRODUCTION

Cellular therapy and tissue engineering of the corneal stroma has gained interest over the last decade as a potential alternative treatment for corneal stroma diseases, such as corneal scarring, dystrophies, and ectasias, such as keratoconus (1).

However, the highly complex structure of the corneal stroma, which involves very specific considerations concerning transparency, biomechanics, and optical behavior related to its very particular anatomical features (2), limits the usefulness of many of these corneal substitutes generated in preclinical experimental studies in the real clinical practice (3). On the other hand, published evidence has already demonstrated in pioneer human clinical studies that autologous stem cells from extraocular sources are capable not only to survive and differentiate *in vivo* into adult human keratocytes but also to produce new collagen within the host stroma (1). Mesenchymal stem cells (**MSCs**) may improve preexisting scars or defects in corneal transparency as it has been demonstrated in animal models (4, 5). Such **MSCs** have also shown immunomodulatory properties in syngeneic, allogeneic, and even xenogeneic scenarios, findings that make even more attractive their use in corneal stromal regeneration experiences (6, 7). Additionally, acellular corneal extracellular matrix (**ECM**) has been demonstrated to be an excellent scaffold for mesenchymal cells, acting as a carrier when implanted into the human cornea (8).

For all these reasons, cellular therapy of the cornea is to be considered as a promising advanced therapeutic approach for corneal diseases. However, the use of autologous human ocular keratocytes has many disadvantages, such as difficulties in its isolation, limitations in the availability of cells in high populations, and inefficient cell subculture (9). Corneal stromal stem cells have the same limitation of requiring healthy corneal donor tissue. Meanwhile, stem cells from extraocular sources have demonstrated that they may be a more favorable and adequate source for the regeneration of the human corneal stroma (1, 4, 5, 10–14).

This review aims to summarize the present status of the human clinical studies reported in the peer-reviewed literature on the topic of human corneal stromal regeneration, corneal enhancement therapy, and the immediate trends that such studies have opened new perspectives in the therapy of corneal stromal diseases, particularly in keratoconus.

BACKGROUND

The first human clinical trials using an extraocular source of **MSCs** for corneal stem cell therapy in advanced keratoconus cases were performed and reported recently by our group (1, 10– 14), based on previous successful animal studies performed in part by the same research group (4, 5). In such preclinical studies, it has been shown that adult **MSCs** from human adipose tissue is an ideal source since they satisfy many requirements, such as easy access, high cell retrieval efficiency, and high differentiation capacity. They are known as "Human Adipose-Derived Adult Stem Cells" (**h-ADASCs**), these cells can be differentiated into different cell types, such as keratinocytes, osteoblasts, chondroblasts, myoblasts, hepatocytes, neurons, among others (4, 9).

Also, these cells have shown immunomodulatory properties in autologous, allogenic, and xenogeneic scenarios (6, 7). More than a decade ago, we found that **h-ADASCs** transplanted into damaged rabbit corneas were able to differentiate into corneal keratocytes and produced collagen and keratocan which are characteristics of the corneal stroma (4). To provide such collagen in an adequate volume to restore corneal thickness, protocols have been used to obtain corneal decellularized matrices as they provide a more natural environment for the growth and differentiation of **MSCs** compared to synthetic scaffolds (8, 15, 16). The effectiveness in this regard of sodium dodecyl sulfate decellularization on the human donor cornea has also been demonstrated in previous studies (8, 10, 11, 16). Such findings demonstrated that human cornea scaffolds provide a more adequate and natural environment for the growth and differentiation of cells, compared to synthetic scaffolds (8, 16). The use of **h-ADASCs** to repopulate scaffolds was also attempted (4, 5, 8, 16). We were able to demonstrate that the implanted cells survive at least 12 weeks after transplantation and they also differentiate into human keratocytes in the experimental animal model (16).

These experimental studies opened the translational of this concept from the animal into the human as a new therapy for human corneal disease, using the advanced keratoconus disease as the model for this type of advanced therapy.

CELLULAR THERAPY OF THE CORNEAL STROMA IN KERATOCONUS

MSCs obtained from a simple procedure of liposuction followed by the isolation, characterization, and culture of autologous adipose tissue stem cells (4, 17, 18) were used. Corneal laminas obtained from human corneas IntraLase femtosecond (**IFS)** not suitable for corneal transplantation, duly decellularized and

Abbreviations: ADASCs, Adipose-derived adult stem cells; SMILE, Small incision lenticule extraction; PKP, Penetrating keratoplasty; SFII, Femtosecond laser-assisted intracorneal concave lenticule implantation; SILK, Small incision sutureless intrasotromal lamellar keratoplasty; UDVA, Unaided distance visual acuity; CDVA, Corrected distance visual acuity; MSCs, Mesenchymal stem cells; ECM, Extracellular matrix; h-ADASCs, Human Adipose-Derived Adult Stem Cells; PBS, Phosphate-buffered saline; IFS, IntraLase femtosecond laser; AS-OCT, Anterior segment optical coherence tomography; CLDVA, Contact lens visual acuity; CCT, Central corneal thickness; Thinnest point, Scheimpflug corneal topography Thinnest point; CV, Cornea Volume; Rx Sphr, Refractive sphere; Rx Cyl, Refractive cylinder; 3rd order RMS, Third-order aberration RMS; 4th order RMS, Fourth-order aberration RMS; HOA RMS, High order aberration RMS; LOA RMS, Low order aberration RMS; Anterior Km, Anterior mean keratometry; Posterior Km, Posterior mean keratometry; Kmax, Maximum keratometry; Topo Cyl, Topographic cylinder; FILI, Femtosecond intrastromal lenticular implantation; UV, Ultra-violet; CXL, Cross-linking; SLAK, Stromal lenticule addition keratoplasty; IOP, Intraocular pressure; DALK, Deep anterior lamellar keratoplasty; RHC, Recombinant human collagen; EDC, 1-ethyl-3-(3-dimethylaminopropyl) carbodiimide; NHS, N-hydroxysuccinimide; ALK, Anterior lamellar keratoplasty.

recellularized following an adequate corneal lamina protocol were also used (10, 11, 13, 14, 16, 19). The implants were performed into a mid-corneal stroma pocket created also with a femtosecond laser in corneas with advanced keratoconus. Patients were implanted with either adipose-derived adult stem cells (**ADASCs)** alone or with decellularized or recellularized laminas. The outcome at 1 month in all cases was an optically transparent autologous stromal graft, remaining transparent at 1 and 3 years (11, 14). The use of *in vivo* corneal confocal microscopy was very useful throughout the experience to observe the evolution of implanted **ADASCs** as well as the evolution of implanted tissue (13).

Intrastromal Implantation of Autologous ADASCs Alone

Autologous ADASCs Isolation, Characterization, and Culture The group of Jorge Alió performed a clinical trial phase 1 in five patients with advanced keratoconus. Standard liposuction under local anesthesia was performed and ∼250 ml of adipose tissue was obtained from each patient. Processing of adipose tissue was performed according to the methods described in previous reports (1, 10–14, 17, 18). From 60 to 80 h before transplantation, quiescence of the **ADASCs** was induced by reducing the amount of serum in the culture media to 0, 5% to transplant them in a physiological state closer to non-proliferative natural stromal keratocytes. Quiescence and the absence of apoptosis and aneuploidy as well as blocking the pro-inflammatory and inducing the anti-inflammatory **ADASCs** properties, and the absence of infection as quality controls were verified as the authors described in the previous article. 3×10^6 cells per patient were prepared in phosphate-buffered saline (**PBS**), the cell dose was based on the evidence observed in previous studies (1, 10–16), and the cells were transplanted directly *in situ*.

Surgical Procedure

Topical anesthesia was administered. **IFS** femtosecond laser (AMO Inc, Irvine, CA) 60 Khz. IntraLase was used in a single-pass mode for the recipient corneal lamellar dissection. At the medium depth of the thinnest preoperative pachymetry point measured by an anterior segment optical coherence tomography (**AS-OCT)** (Visante, Carl Zeiss, Germany), an intrastromal laminar cut of 9.5 mm of diameter was created and dissected. An injection of 3 million autologous **ADASCs** in 1 ml **PBS** in the stroma pocket using a 25-G cannula was performed. No corneal sutures were used (**Figures 1A–C**, **2A–D**) (1).

Clinical Results

No complications were observed during the 3 year follow-up. No adverse events, such as haze or infection were encountered. Full corneal transparency was recovered within the first postoperative day in all patients (**Figures 2A–D**). New collagen production was observed as patchy hyperreflective areas at the level of the stromal pocket (1, 11). No patient lost lines of visual acuity. All cases presented an improvement in their Unaided distance visual acuity (**UDVA**) of (0.08, 0.14, 0.12), also in their corrected distance visual acuity (**CDVA**) of (0.11, 0.2, 0.18) (**Figure 3A**), and rigid contact lens distance visual acuity (**CLDVA**) of (0.11, 0.19, 0.23) (**Figure 3B**), in decimal lines mean value equivalents in LogMar scale at 6, 12, and 36 months of follow up (14).

Results of Central corneal thickness (**CCT**) (μm) was measured by **AS-OCT** (Visante, Carl Zeiss) (**Figures 1**, **3C**)**,** Scheimpflug corneal topography Thinnest point (**Thinnest point**) (μm) (**Figures 3D**, **4A**) and Cornea Volume **(CV**) (mm^3) showed an increase in mean values in all patients of this group (36, 59, 30) (μm), (29, 48, 31) (μm), and (3, 3, 4) (mm^3) during the 6, 12, and 36 months of follow-up (14).

On the other hand, the Refractive sphere (**Rx Sphr**) (D) presented an improvement of (0.8, 1.3, 1.1) myopic diopters at 6, 12, and 36 months. Meanwhile, the refractive cylinder (**Rx Cyl**) (D) remained almost stable 12 months post-operative followed by a deterioration of 0.5 (D) until 36 months post-operative regarding the pre-operative mean values (14).

Also, an improvement in mean values was observed during the 3 year follow up in third-order aberration RMS **(3rd order RMS)** (μm)**,** fourth-order aberration RMS **(4th order RMS)** (μm)**,** high order aberration RMS **(HOA RMS)** (μm) (**Figure 3E**) and Low order aberration RMS **(LOA RMS)** (14).

Additionally, results of Anterior mean keratometry (**Anterior Km**) (D) (**Figure 4B**) presented a modest improvement of mean values of 1 (D) to 12 months post-operative and another 1 (D) at 36 months post-operative regarding the pre-operative mean values. The authors detected stability in mean values of Posterior mean keratometry (**Posterior Km**) (D) up to 36 months post-operative. Nevertheless, they found a flattening in mean values of 2 (D) in maximum keratometry (**Kmax**) (D) (**Figure 3F**) up to 12 months post-operative, followed by 1 (D) up to 36 months post-operative regarding the pre-operative mean values. Finally, a deterioration of −0.3 (D) was obtain**ed** at 12 months post-operative in the topographic cylinder **(Topo Cyl)** (D)**,** at 36 months post-operative they found the same pre-operative mean values (14).

Collagen-Based Scaffolds

Decellularization and Recellularization of Human Corneal Stroma Laminas In this phase 1 of our clinical trial in advanced keratoconus, five patients received decellularized human corneal stroma laminas only, and four patients received human corneal stroma recellularized with autologous **ADASCs**. Laminas were obtained from donor corneas from an eye bank. The epithelium was removed mechanically, the anterior corneal stroma was cut by 60 kHz IntraLase **IFS** femtosecond laser (AMO, Santa Ana, CA), 2–3 consecutive laminas 120 μm thick and 9.0 mm in diameter were obtained, a surface that contains the Bowman membrane and a deeper one without this layer. The decellularization protocol was based on previous publications (8, 10, 20). The laminas for patients who received recellularized tissues [(1, 10– 14), del Barrio et al., 2015], were placed in tissue culture medium for recellularization 24 h before implantation with autologous **ADASCs** (0.5×10^6

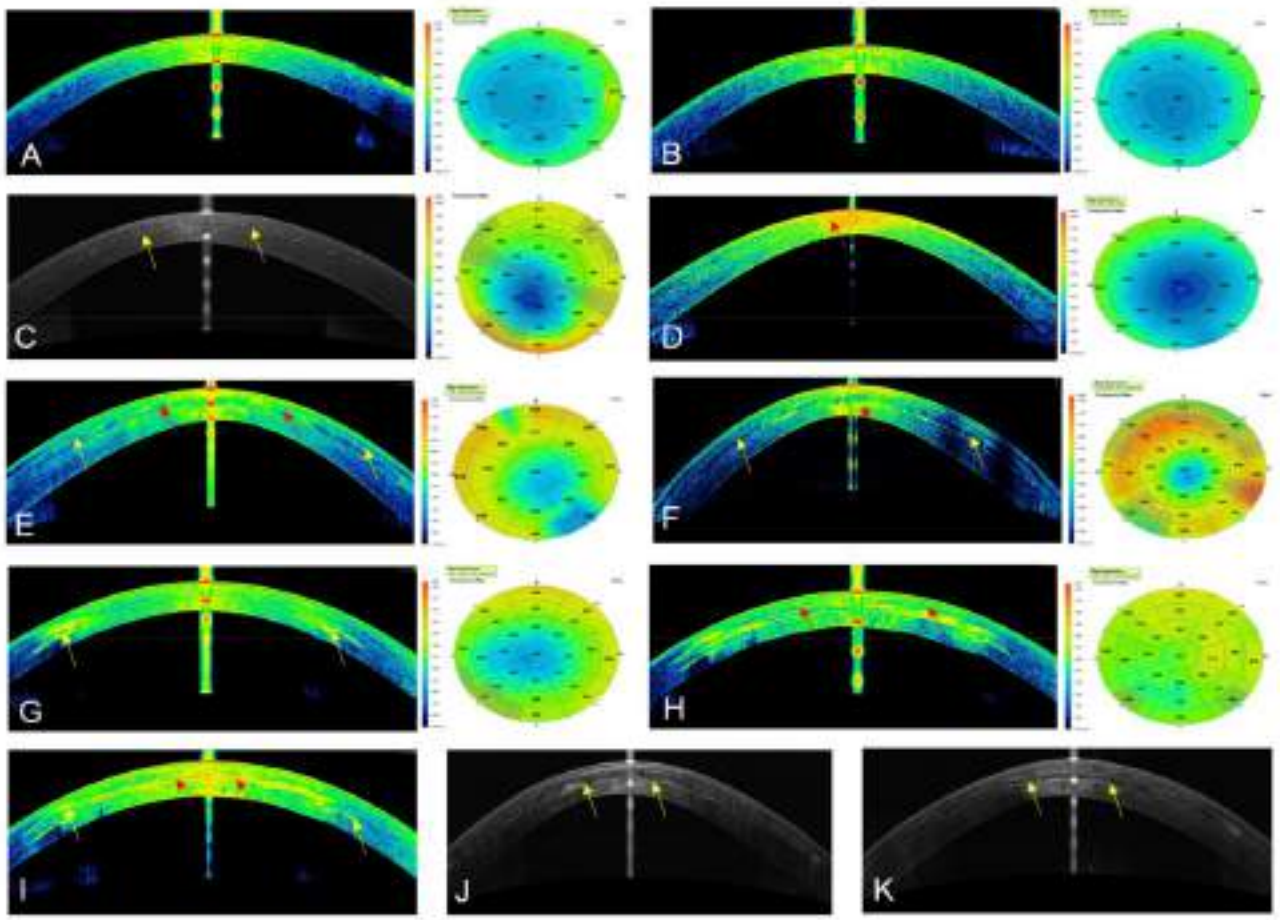

FIGURE 1 | Cornea Visante optical coherence tomography images and pachymetric maps. **(A)** Preoperative **OCT** in case 1, G-1. **(B) OCT** at 12 months post-op of the same patient, notice the transparency of the cornea. **(C) OCT** at 36 months post-op with case 2, G-1. Observe the transparency of the cornea, the (yellow arrows) demonstrate the limit of the flap. **(D)** Preoperative **OCT** in case 7, G-2, Notice the highly reflective area in the corneal stroma (red arrow). **(E,F) OCT** at 12 months and 36 postoperative in case 7. The improvement of the reflective band of neo-collagen in the periphery of the implanted lamina (yellow arrows) can be seen. The reflectance of the neo-collagen band (red arrow) is higher at 12 months in the center of the implanted lamina. **(G)** Preoperative **OCT** in case 13, G-3. The reflective paracentral scars can be noticed (yellow arrow). **(H,I) OCT** at 12 and 36 months post-op. The high reflectance of the neo-collagen band (red arrow) can be seen more evident at 36 months with this patient in the center of the lamina. Notice the improvement of the preoperative paracentral scars at 36 months post-op (yellow arrows). **OCT** in Case9, G-2, and **(K)** in Case 12, G-3 at 36 months post-op. (yellow arrows) shows the limits of the laminas.

cells were cultured on each side of the laminas). After finishing the recellularization process, the laminas were washed with **PBS** at room temperature before implantation (10).

Surgical Procedure: Lenticule Implantation

Topical anesthesia was applied with oral sedation for all surgeries. The 60-kHz IntraLase **IFS** femtosecond laser was used in single-pass mode. Assisted corneal dissection was done with a 50° anterior cut, the lamina was inserted through the corneal intrastromal pocket, then centered and unfolded through gentle tapping and massaging from the epithelial surface of the cornea. In those cases that received a recellularized lamina, the pocket was irrigated immediately before and after insertion with a solution containing an additional 1 million autologous **ADASCs** in 1 ml of **PBS** with a 25G cannula. One interrupted 10/0 nylon suture was performed and was then removed 1 week after the operation (**Figures 1D–K**, **2E–J**) (10).

Clinical Results

The authors did not observe any complications during the 3 year follow-up, with the exception that the implanted lamina showed a mild early haziness during the first postoperative month. This issue was related to mild lenticular edema. Corneal recovery and full transparency were observed within the third post-operative month in all patients. No adverse events of any type were observed over the 3 years (**Figures 2E–J**) (14).

All patients with decellularized or recellularized laminas gained an improvement during 6, 12, and 36 months of follow up, the enhancement in **UDVA** was (0.08, 0.13, 0.11) in decimal values nearly equivalent to one line in logMar scale with decellularized and recellularized laminas, **CDVA** was (0.11, 0.2, 0.18) with decellularized lamina and (0.12, 0.2, 0.19) with recellularized ones, equivalent to 1–2 lines in LogMar scale (**Figure 3A**), as well **CLDVA** means improvement was (0.11,

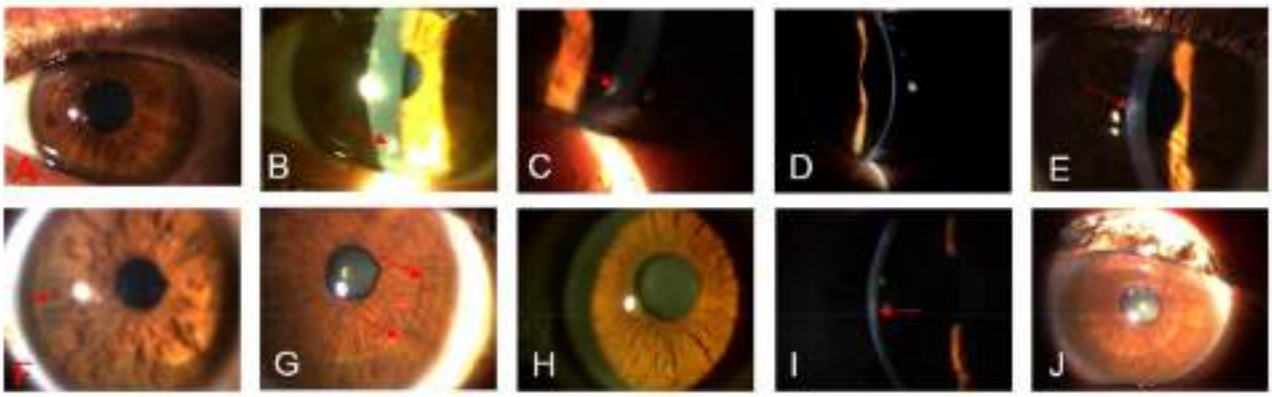

FIGURE 2 | Biomicroscopic changes between the preoperative up to 36 months post-operative. **(A)** G-1, case 4, OS, shows the transparency of the cornea in the preoperative. **(B)** G-1, case 4, shows the transparency of the cornea. The presence of a peripheral surgical scar (red arrow) at 1month post-op can be noticed. **(C)** G-1, case 4, shows the stability of the peripheral scaring (red arrow) in the cornea at 12 months post-op. **(D)** G-1, case 4, shows the transparency of the cornea at 36 months post-op. **(E)** G-2, case 9, OD, shows the presence of a slight paracentral scar(red arrows) at the pre-operative. **(F)** G-2, case 9, 12 months post-op, observe the improvement in the transparency of the implanted lamina, (red arrow) represent the periphery of the lamina. **(G)** G-2, case 9, 36 months post-op, notice the marked improvement in the transparency of the lamina, the periphery of the sheet becomes not very marked (red arrow). **(H)** G-3, case 12, OD, shows the transparency of the cornea in the preoperative. **(I)** G-3, case 12, 12 months post-op. The (red arrow) indicates the implanted recellularized lamina. **(J)** G-3, case 12, 36 months post-op. The (red arrow) indicates the periphery of the recellularized lamina. Notice the improvement of the transparency of the implanted tissue.

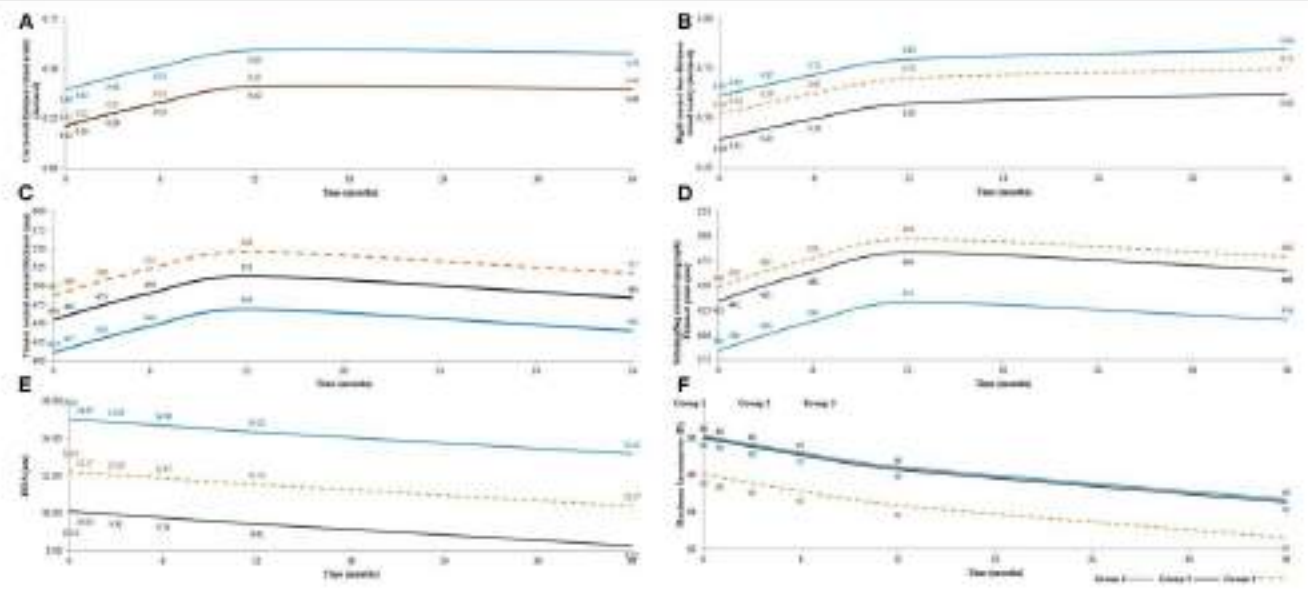

FIGURE 3 | Shows statistical mean results after 3 years follow-up in G-1, G-2, and G-3, respectively **(A)** Shows an amelioration in **CDVA** (corrected distance visual acuity) (decimal), mean values in the pre-operatives were (0.40, 0.22, 0.21), at 12 months post-operatives mean values were (0.60, 0.42, 041) and (0.58, 0.40, 0.40) at 36 months post-operative. Desviation Standard = 0.151. **(B)** Shows an upgraded in **CLDVA** (decimal equivalent to logMar scale) from the pre-operative (0.61, 0.39, 0.52) until reach a maximum mean values at 36 months post-operative (0.84, 0.62, 0.75). Desviation Standard = 0.180. **(C)** Presents Visante **CCT** (central corneal thickness) (µm) mean values in the pre-operative (410, 454, 487) (µm), at 12 months post-operative, these values reached a maximum average (469, 513, (µm), then at 36 months post-operative, they were established with the following average values (440, 484, 517) (µm). Desviation Standard = 62.940. **(D)** Presents the Scheimpflug corneal topography thinnest point (µm) mean values in the preop (385, 435, 449) (µm), there were an increase in the topographic mean values till 12 months post-operative (433, 484, 498) (µm), than at 36 months post-operative, a small decrease was obtained with this mean values (416, 466, 480) (µm). Desviation Standard = 67.966. **(E)** Observe the amelioration in RMS HOA (high order aberration in µm) in mean values at the pre-operative values (15.01,10.11, 12.23), at 36 months post-operative (13.15, 8.25, 10.37). Desviation Standard = 4.530. **(F)** Observe **Kmax** , the pre-operative mean values (68, 68, 66), there was a mean values of 2 diopters more flatter at 12 months post-operative (66, 66, 64) regarding the preoperative, followed by another mean value of 1 diopter of flattening till 36 months post-operative (65, 65, 63). Desviation Standard = 8.250.

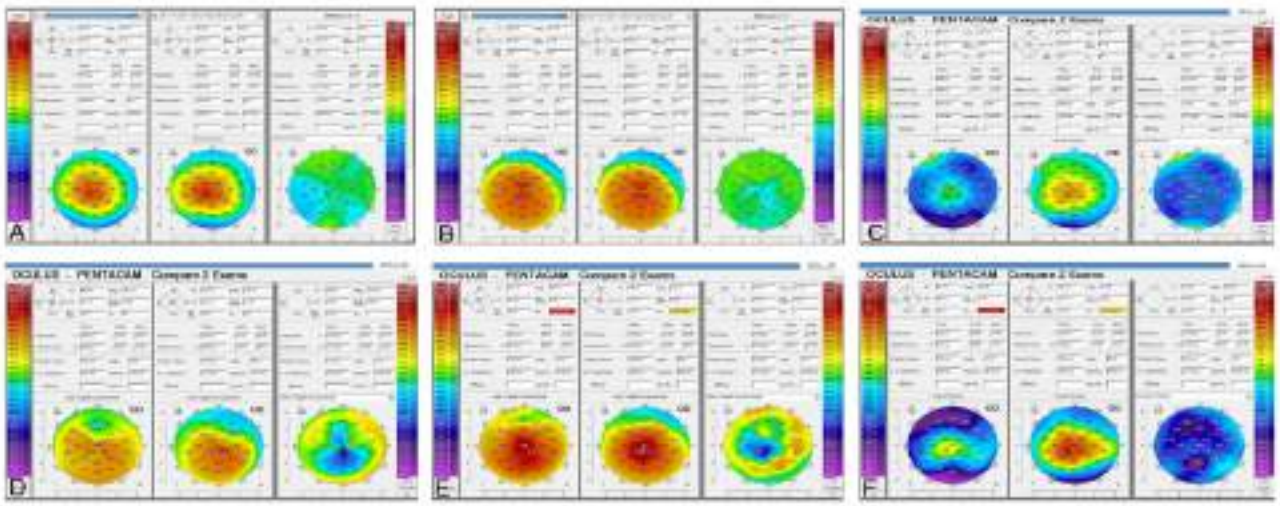

FIGURE 4 | Corneal topography (Pentacam) comparison between preoperative, 12 and 36 months post-op. **(A)** Comparative paquimetric examinations (right side) among the preoperative (middle) and 12 months post-op (left side) in case 1, G-1. Observe the modest improvement of the corneal thickness **(B)** Preoperative (middle) and 12 months post-op (left side) sagittal curvature comparative exams (right side), in case 1, G-1. Notice the modest improvement in the keratometric parameters of the cornea. **(C)** Comparative paquimetric examinations (right side) among the preoperative (middle) and 12 months post-op (left side) in case 6, G-2. Observe the improvement of the corneal thickness. **(D)** Preoperative (middle) and 36 months post-op (left side) sagittal curvature comparative exam (right side), in case 6, G-2. Notice the improvement in the keratometric parameters of the cornea. **(E)** Sagittal curvature comparative exam (right side) among the preoperative (middle) and almost 3 years post-op (left side) in case 12, G-3. Enhancement of the keratometric parameters can be observed. **(F)** Comparison pachymetric exam (right side) among the preoperative (middle) and 3 years post-op (left side) in case 12, G-3. The markable enhancement of the paquimetric parameters can be noticed.

TABLE 1 | Shows the difference in mean values among (G-1)–(G-2), (G-1)–(G-3), and (G-2)–(G-3) of the variables of the study.

	(G-1)–(G-2)	(G-1)–(G-3)	(G-2)–(G-3)
UDVA (LgogMar)	0.07	0.07	0.00
CDVA (LgogMar)	0.18*	0.19*	0.01
CLDVA (LgogMar)	0.22*	0.10	−0.12*
3rd order RMS	4.65*	3.54*	−1.11
4th order RMS	1.28	−0.17	−1.45*
HOA RMS	4.9	2.78	−2.12
LOA RMS	-3.87*	1.32*	5.19
Visante CCT (μm)	−44.00*	−77.00*	−33.00
Thinnest point (μm)	−51.00*	−65.00*	−14.00
CV (mm^3)	−5.00*	−5.00*	0.00
Rx Sphr (D)	0.10	−0.10	−0.20
Rx Cyl (D)	−1.00*	−0.60*	0.40
Kmax (D)	0.00	2.00	2.00
Topo Cyl (D)	1.1	0.9	−0.2
Anterior Km (D)	−3.00	1.00	4.00
Posterior Km (D)	1.3*	0.2	−1.1*

*Indicates a statistically significant difference between the compared groups.

0.19, 0.23) with decellularized laminas and (0.1, 0.18, 0,23) with recellularized laminas (**Figure 3B**), equivalent to 1-2 lines in LogMar scale. Differences among the groups were summarized in **Table 1**.

Results of **CCT** (μm) (**Figure 3C**)**, Thinnest point** (μm) (**Figure 3D**) showed an improvement of (36, 59, 30) (μm)**,** and (29, 49, 31) (μm), respectively, also, mean value results **of CV** (mm^3) demonstrated an improvement of (2, 2, 3) (mm^3) in both laminas' groups at 6, 12, and 36 months of follow up (14). The results were statistically significantly better in G-2 and G-3 comparing with G-1 (**Table 1**).

Besides the **Rx Sphr** (D), **Rx Cyl** (D), Results of **3rd order RMS** (μm) (**Figures 5A,B**), **4th order RMS** (μm), **HOA RMS** (μm) (**Figures 3E**, **5C,D**), and **LOA RMS** (μm). **Anterior Km** (D), **Posterior Km** (D), **Kmax** (D) (**Figure 3F**), and **Topo Cyl** (D) with decellularized and recellularized laminas showed results close to patients' results with implantation of **ADASCs** (14) (**Table 1**).

More information about the comparative results among the three groups was summarized in **Table 1**.

Confocal Microscopy Study

Methodology

The confocal microscope HRT3 RCM (Heidelberg) with Rostock Cornea Module was used. An area is known as the "region of interest" was determined (13, 21). The same area was taken in all the studied pictures (0.1 mm^2). Nuclei cell count was performed with 50% brightness and contrast, and the nucleus of cells that were more illuminated, more refringent was selected (13, 22, 23), the selected nucleus had well-defined edges (**Figures 6A,B**) (13, 24).

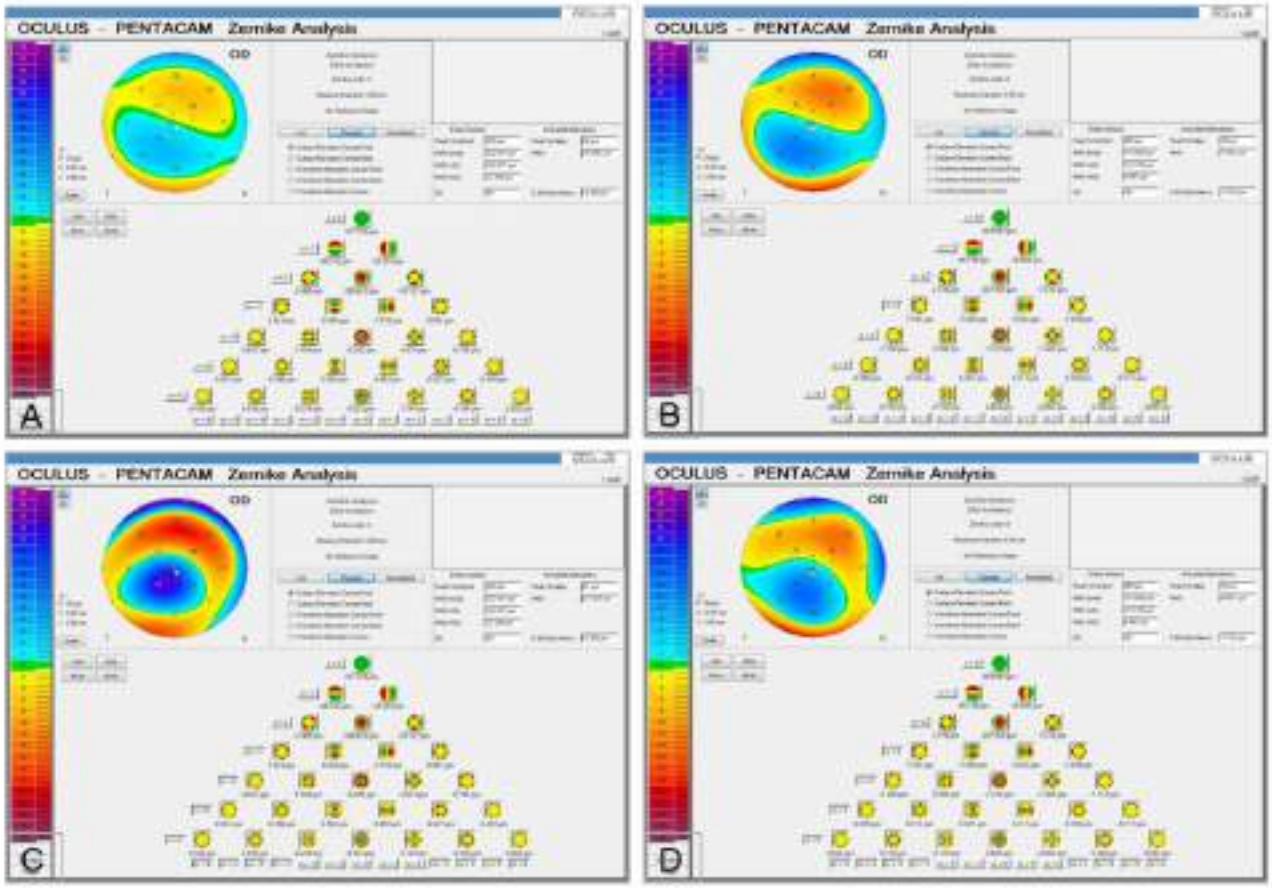

FIGURE 5 | Corneal Aberrometry with case 5, G-2. **(A,B)** (Pentacam) Third-order aberration RMS **3rd order RMS** (μm). Observe the improvement in mean values from the preoperative (10.356) (μm) till (7.924) (μm) at 36 months post-op. **(C,D)** (Pentacam) high order aberration RMS **HOA RMS** (μm). Notice the amelioration between the preoperative mean values (12.339) (μm) and 36 months post-op (8.451) (μm).

ADASCs Counting

The counting method for transplanted **ADASCs** was performed similarly 1 month after the surgery. **ADASCs** appeared rounded in shape, more voluminous, and refringent (13).

Cell Count on Decellularized and Recellularized Laminas

One month after surgery, the decellularized laminas appeared without well-defined cell structures, then they were considered acellular. With the recellularized ones, the presence of a few **ADASCs** was observed, and they had a similar morphology to normal keratocytes nucleus and these structures were counted as cell nuclei (**Figures 6C–F**) (13).

Results

Autologous ADASCs Implantation

Morphological results demonstrated that **ADASCs** appeared rounded in shape, more voluminous, and refringent than the host corneal keratocytes up to 6 months post-operative. Also, statistical results at 12 months after the operation showed a gradual statistically significant increase in the cellular density at the anterior, mid, and posterior host stroma when comparing the preoperative values (**Figures 6A,B**) (13). Moreover, the authors detected the presence of a small fibrotic tissue at 3 months postoperative in 2 out of the 4 patients, but a full recovery of the corneal stroma was observed at 12 months follow-up (13).

Decellularized and Recellularized Corneal Laminas Implantation

Decellularized laminas appeared acellular during the first months unlike the recellularized ones, which showed similar structures to corneal keratocytes, where the number of cells increased during the 12 months follow-up. The anterior, mid, and posterior surfaces of the decellularized and recellularized laminas became more colonized by keratocyte-type cells until they showed similar morphology of normal corneal keratocytes (**Figures 6C–F**) and reached statistically significant increased cell density values in comparison to the first postoperative month. 12 months after surgery, the cell density of the anterior, and posterior corneal stroma showed a statistically significant increase in

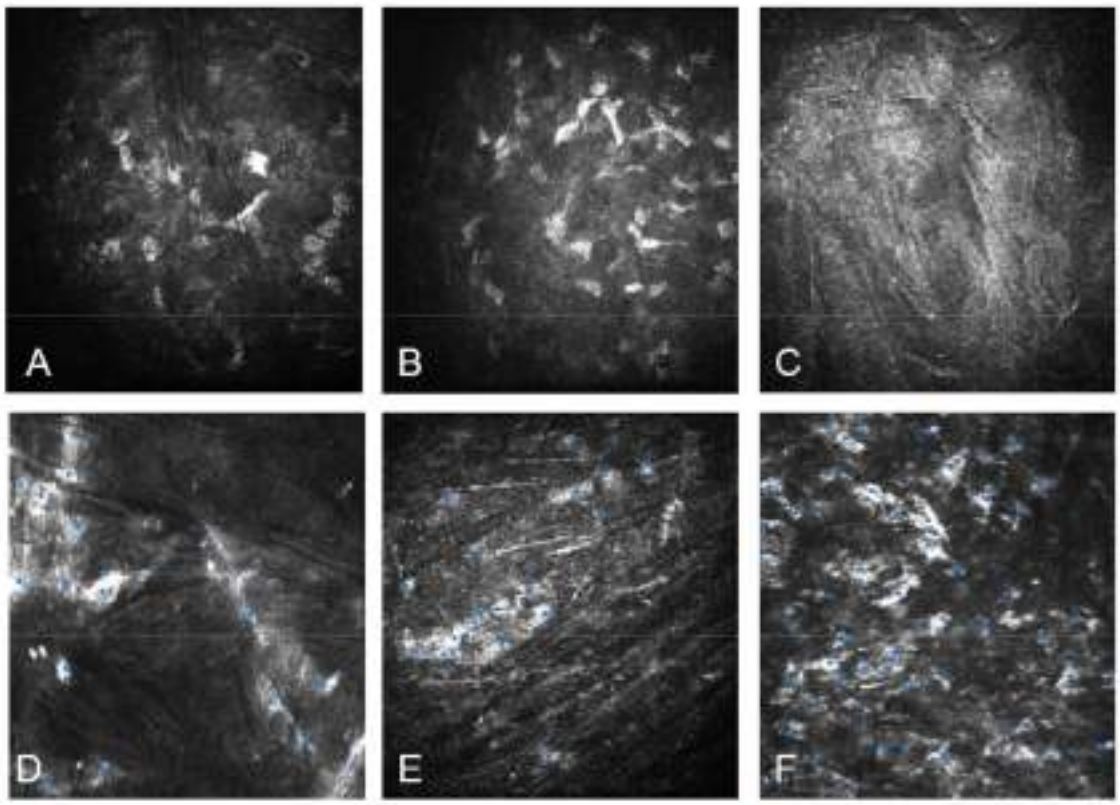

FIGURE 6 | Confocal microscopy study with HRT3 RCM (Heidelberg). **(A)** Confocal microscopy of the anterior corneal stroma with case 1, G-1. Notice the few nuclear corneal cell density. **(B)** Nuclear cell density in the anterior stroma with case 1 at 12 months post-operative. Notice the increment of the cell density. **(C)** Acellular implanted lamina with case 5, G-2 at 1 month post-operative. **(D)** Recellularization of the anterior surface of the implanted decellularized lamina in the same case 5 at 12 months postoperative. **(E)** The posterior surface of the recellularized lamina with case 13, G-3 at 1 month after the operation: the presence of few **ADASCs** with similar morphology of keratocytes. **(F)** The posterior surface of the recellularized lamina with case 13 at 12 months after surgery: Observe the abundant number of stromal cells.

the number of keratocytes close to that found in a normal cornea (13). The confocal microscopy study also showed the formation of fibrotic tissue in non-central corneal areas in almost all of the cases implanted with decellularized lamina's and recellularized ones, but no significant association was found between recellularization and cell density and the presence of such fibrotic tissue (13).

ALLOGENIC SMILE LENTICULE CORNEAL INLAY IMPLANTATION

The implantation of these stromal lenticules has been proposed as a way to reverse the effect of previous laser refractive surgery (25, 26), to treat different types of ametropia (27), and also as a therapy for cornea ectatic disorders such as keratoconus (28–33).

The hyperopic algorithm for small incision lenticule extraction **(SMILE)** produces negative meniscus lenticules thicker from the center toward the periphery, the implantation of these negative meniscus shaped lenticules in an *ex vivo* study on human corneas caused a reproducible flattening of the central cornea and increase of the stromal thickness, both desirable effects of any procedure for treating keratoconus eyes (28–33). The myopic correction algorithm for **SMILE** produces positive meniscus lenticules, thicker in the center and gradually becoming thinner toward the periphery. Conversely, positive meniscus lenticules have been used to correct hyperopia in humans (28–33).

Lenticular Implantation Combined With Collagen Cross-Linking

Methodology

Ganesh et al. in one pilot clinical study were reported including 6 patients with advanced keratoconus, to evaluate the outcomes of femtosecond intrastromal lenticular implantation (**FILI**) from corneal stroma donor tissue, combined with accelerated collagen cross-linking (28, 29). Only lenticules with spherical myopic refractive errors were chosen for cryopreservation, the details of the methods have been described in previews publication (28, 29). The tissue was soaked in 0.25% riboflavin dye and kept aside and a 3-mm corneal trephine was used to punch the center of the lenticule to obtain a donut-shaped tissue. After that, topical anesthesia was applied. A pocket was created with Visumax femtosecond laser

(Carl Zeiss Meditec AG), with 7.0–8.0 mm diameter at 100 μm depth, then the donut-shaped lenticule was inserted gently into the pocket through the 4 mm superior incision and finally, the eye was exposed to ultra-violet radiation (**UV**-A) using the Avedro Cross-linking (**CXL)** system. Follow-up of patients was performed for a mean period of 190 days.

Results

The authors did not observe any adverse reaction, such as haze, infection, or allogeneic graft rejection during the 3 years postoperative follow up. Clinical improvement was observed in all patients, no eye lost lines of corrected distance visual acuity, and amelioration was detected in **UDVA** from 1.06 to 0.38 (logMar scale), **CDVA** from 0.51 to 0.2 (logMar scale), and manifest spherical equivalent from −3.47 to −1.77 D. There was flattening of **Km** in 3- and 5-mm zones by 3.42 and 1.70 (D), respectively. Also mean pachymetry in the central and mid-peripheral zones increased by 18.3 and 33.0 (μm), respectively. All patients had improvement in high-order aberrations, especially in coma (29).

Femtosecond Laser-Assisted Stromal Lenticule Addition Keratoplasty (SLAK)

Surgical Technique

Mastropasqua et al. (30, 31) reported the visual and refractive outcomes after the intrastromal implantation of negative meniscus-shaped corneal stroma lenticules (thicker in the periphery than in the center) for advanced keratoconus patients (n = 10) as an alternative approach to classical corneal transplantation techniques. They termed this technique as stromal lenticule addition keratoplasty (**SLAK**). These allogeneic lenticules (6.7 mm in diameter) were dissected with a Femtosecond laser (Visumax, Zeiss, Germany) from donor corneas, and implanted into a Femto dissected pocket within the patient's recipient cornea.

Results

At 6 months, **UDVA** and **CDVA** showed statistically significant improvements from 1.58 ± 0.36 to 1.22 ± 0.37 and from 1.07 ± 0.17 to 0.70 ± 0.23 (logMAR), respectively. 8/10 eyes showed an improvement in **UDVA** that ranged between 1 and 3 lines. All except one eye presented improved **CDVA**. These allogeneic negative in refraction, meniscus-shaped lenticules induced a generalized flattening of the cone, with a reduction of **Anterior Km** from 58.69 ± 3.59 to 53.59 ± 3.50 (D) at 6 months after surgery. Postoperative **AS-OCT** showed a significant increase in the thickness of the central and mid-peripheral corneal mean **CCT** values increased from 406 ± 43 to 453 ± 39 (μm) at the end of the follow-up (30, 31). Confocal microscopy (HRT II Rostock Cornea Module, Heidelberg Engineering GmbH, Germany) showed identification of the lenticule–host interfaces in all cases. Both anterior and posterior lenticule interfaces were characterized by dishomogeneous hyperreflectivity and acellular aspect, this reflectivity decreased over time with all the cases. At 1 week an activated and lower reflective elongated keratocytes within the lenticule lamellae were observed. At 6 months, keratocyte morphology appeared similar to normal, keratocytes structures were observed within the implanted lenticules with regular shape and reflectivity, whereas the extracellular tissue presented normal transparency (30, 31).

Intracorneal Concave Lenticule Implantation With PKP and SFII

Surgical Technique

Xingwu et al. realized a comparative study with a total of 31 consecutive patients (31 eyes) with progressive keratoconus, 11 patients underwent small-incision femtosecond laser-assisted intracorneal concave lenticule implantation **SFII** (SFII group), and 20 of them underwent penetrating keratoplasty (**PKP**) (PKP group).

SFII group: The donor cornea was placed into an artificial anterior chamber, and a lamellar incision was made with a femtosecond laser (32, 33). An anterior incision was made with a diameter of 7.5 (mm) and was located with a depth of 320 (μm), then a myopia correction of −4.00 diopters was executed (69.59 μm thickness) with an excimer laser (WaveLight GmbH, Erlangen, Germany). The lenticule was then separated from the stromal bed and used as a graft. Then, **SMILE** treatment with a myopic correction of −0.75 (D) (28 μm thickness) was effectuated in the recipient cornea with 160 (μm) cap thickness, 7.8 (mm) cap diameter, and 7.8 (mm) lamellar cornea diameter (32, 33). Finally, the graft was implanted into the stromal pocket.

PKP group: PKP was performed under general anesthesia, the donor corneas were cut using a punch trephine on a Troutman guide. All the grafts had diameters between (7.0–8.0 mm). All grafts were closed with a running 24-bite 10-0 nylon suture.

Results

At 3 months postoperative in the **SFII** group, all patients improved their **UDVA** and **CDVA**, then they remained stable, at 24 months 82% of the operated patients from this group improved 3 lines, 9% gained 2 lines, and other 9% gained 1 line in Snellen scale. In the **PKP** group, all patients did not improve their **UDVA** during the 24 months follow-up, nevertheless, they improved their **CDVA**, only 60% improved 3 lines on the Snellen scale (33). Minimum central keratometry and maximum central keratometry improved (−3.9 ± 0.95) (D) and (−4.65 ± 2.04) (D) respectively, but less than with **PKP** results (33). Changes of the anterior corneal depth were (−0.12 ± 0.09) (mm) with **SFII** group, and (−0.46 ± 0.29) (mm) with **PKP** at 24 months (33).

The intraocular pressure (**IOP**) with the group **PKP** increased during the first-month follow-up and it declined up to the third month. In the **SFII** group, the **IOP** maintained stability during the first month. An increased in the corneal thickness was better in the **SFII** group than in the **PKP** group at 3 months after the surgery. Confocal microscopy study revealed the presence of dendritic cells in the subepithelial region, also, dendritic and inflammatory cells could be observed among graft and the host cornea up to 1 month with the group **SFII**, and up to 3 months with the **PKP** group (32, 33).

IFS Assisted Small Incision Sutureless Intrastromal Lamellar Keratoplasty (SILK)

Surgical Technique

Pradhan et al. (34), using a different approach, proposed femtosecond laser-assisted small incision sutureless intrastromal lamellar keratoplasty (**SILK**) as an alternative to corneal traditional anterior lamellar or full-thickness corneal transplantation in keratoconus with one single patient, and 1 year follow up was presented. Intrastromal addition of a corneal lenticule was preceded by intrastromal extraction of stroma from the recipient cornea. The donor cornea was prepared using the VisuMax deep anterior lamellar keratoplasty (**DALK**) software module, and 50 microns myopic ablation was performed using a MEL-80 excimer laser (Carl Zeiss Meditec), to obtain a negative meniscus in the anterior surface. The recipient intrastromal pocket was created using a combination of the **DALK** and laser *in situ* keratomileusis (**LASIK**) flap software modules. The donor stromal lenticule was then implanted into the recipient through 3-mm small incision.No sutures were applied.

Results

With the **SILK** technique, an improvement in visual parameters was obtained, the preoperative **UDVA** was counting fingers, and the **CDVA** was (20/80, Snellen), One year postoperatively, **UDVA** changed to (20/80), and with the manifest refraction **CDVA** improved to (20/40). As well a reduction of 7,34 (D) in **Kmax** was obtained and resulting from a considerable thicker lenticule of 332 (μm) in the central cornea (34).

RECOMBINANT CROSS-LINKED COLLAGEN FOR CORNEAL ENHANCEMENT

Surgical Technique

Recent studies (35, 36) performed a phase 1 clinical trial in 10 patients with vision loss because of keratoconus or scarring, 9 eyes with keratoconus, and 1 eye with a scar. The cohort comprised eight men and two women (age range: 18–75 years), at the time of surgery. They used recombinant human collagen III-based (13.7% wt/wt) (**RHCIII**), scaffolds cross-linked with 1-ethyl-3-(3-dimethylaminopropyl) carbodiimide (**EDC**) and N-hydroxysuccinimide (**NHS**) (**EDC-NHS**) and fabricated into substitutes with the dimensions of a human cornea and transplanted into the anterior stroma. They performed anterior lamellar keratoplasty (**ALK**) under general or local anesthesia. Patients received these biomimetic substitutes (6.25–6.75 mm diameter, 500 μm thick) anchored with three to four overlying 10–0 nylon sutures and covered with a bandage lens. Bandage lenses and sutures were removed 5 weeks after surgery (35, 36).

RESULTS

After 6–7 months, the corneal substitutes were well-integrated into all 10 recipients, without adverse effects or complications, such as neovascularization, inflammation, or rejection. Remodeling of the thick substitutes was reported, resulting in the restoration of a seamless host–graft interface and a corneal surface becoming progressively smoother over time. At 24 months, they showed stable biointegration and corneal reepithelialization, but localized implant thinning that varied from 211 to 568 microns in thickness after 2 years and fibrosis in several patients. Vision improved in 6 out the 10 patients. Four years after the grafting (37), patient **CDVA** was 20/54 on average and a gain of more than the 5 Snellen lines of vision on an eye chart. At four years, the biosynthetic corneas showed steeper surface curvatures and were more irregular than that of donor tissue showing increased astigmatism (38).

DISCUSSION

Our research group demonstrated for the first time the feasibility of regenerative surgeries of the corneal stroma for advanced keratoconus, using autologous **ADASCs** injected into the corneal stromal pocket in cases with advanced keratoconus, confirming also the appearance of new collagen in the injected areas, that could be useful for repairing the corneal dystrophies, scars and could also slightly increase the thickness of the cornea (1, 11, 14).

Also, we demonstrated for the first time that decellularized laminas of a human corneal stroma, colonized or not by autologous **ADASCs**, can be implanted for therapeutic purposes on a clinical basis (**Figures 1E–K**, **4C–F**). After 3 years of follow-up, no patient showed inflammation, rejection, or any evidence of scarring or haze (**Figures 1**, **2**) (10, 11, 13, 14). Furthermore, there was an improvement in all the visual parameters with 1-2 lines in LogMar (**Figures 3A,B**). The results of the G-1 showed an increase of 30 (μm), 31 (μm), and 3 (mm^3)in **CCT**, **thinnest point** and **CV,** respectively, statistical differences were significantly better obtained at 36 months in patients with implanted laminas, the **CCT** mean difference among G-1/G-2 was 44 (μm), nevertheless, this mean difference was 77 (μm) when comparing G-1/G-3 (**Figure 3C**; **Table 1**). The mean difference in the **thinnest point** was 51 (μm) among G-1/G-2 and 65 (μm) among G-1/G-3 (**Figure 3D**; **Table 1**). Also mean differences in **CV** were 5 (mm^3) when comparing G-1/G-2, and G-1/G-3 (**Table 1**) (14). There was also an improvement in all the corneal aberrations (**Figures 3E**, **5**), and corneal topographic parameters (**Figure 4**) (14).

The 12 months follow up of the confocal microscopy study showed the evolution of **ADASCs** nuclei and their morphological changes from being rounded shape and highly refringent cells at 6 months to fusiform structures and less nucleus refringent. These findings demonstrate in the human clinical model that the **ADASCs** implanted in the corneal human pocket have survived and have been able to differentiate into keratocytes (**Figures 6A,B**) (13). One year after the surgery, a gradual and significant increase ($P < 0.001$) was observed in the cellularity in the anterior, mid, and posterior stroma in G-1, as well in the anterior, and posterior stroma, and among the implanted decellularized/recellularized laminas in G-2 and G-3, in comparison with the preoperative density level (13). Such findings confirm the previous animal studies in which the post-mortem analysis demonstrated the presence and survival of these

human cells and the human collagen produced by them in the rabbit cornea (4, 15).

Allogenic refractive lenticule corneal inlay using a **SMILE** lenticule combined or not with accelerated collagen cross-linking (28, 29, 31, 33), is a promising surgery, no inflammation, complication, opacification, vascularization, or infection were recorded. Another group performed a recent prospective study in Tehran (39), they reported a novel method for the treatment of advanced ectasia, with customized SMILE lenticule implantation with 22 cases of advanced keratoconus (shape of the lenticule was compound form or necklace). Corneal thickness showed a mean enhancement of 100.4 μm at the thinnest point measured by **AS-OCT**. An improvement in visual parameters was obtained, best **CDVA** improved from 0.70 (range 0.4–1) to 0.49 (range 0.3–0.7) at 6 months with all the patients, which was in coherence with the decrease in corneal aberration, also keratometry decreased from 54.68 ± 2.77 to 51.95 ± 2.21 (D) was obtained.

Stromal addition of **SMILE** created lenticules have been proven *ex vivo* and *in vivo* its feasibility, safety, and efficacy in the treatment of thinning disorders such as keratoconus (30, 31, 34). **SILK** induced in **Kmax** a flattening of 7,34 (D) and using negative meniscus-shaped lenticule addition induced also some flattening of the cone, the improvement was (5.1 D at 6 months) in **Anterior Km** better than the ones observed with Ganesh et al. (29), and planar than the lenticules implanted by El Zarif et al. (14).

The comparatives surgical procedures **SFII** and **PKP** resulted in a stable corneal volume, and improved visual acuity during the 24 month study period. **SFII** was less invasive and more efficient when compared with **PKP**. Using concave lenticule implantation improved the maximum central keratometry of (−4.65 ± 2.04) (D), this outcome was more planner than the laminas implanted with El Zarif et al. (14) and Jin et al. (33).

However, corneal thickness increase using planner lenticules (1, 10, 11, 14) is higher than the one using allogenic **SMILE** lenticule corneal inlay implantation combined or not with collagen Cross-Linking (29, 31, 33), besides, negative meniscus-shaped lenticules or donut-shaped lenticules are only available for pure central cones, as for eccentric cones (the ones are commonly seen in keratoconus) they would generate non-acceptable aberrations within the visual axis, unlike the planner laminas, the aberrometry parameters improved in almost all the study cases.

Visual acuity enhancement has been slightly better with the implant of negative meniscus lenticules than with the implant of planar laminas (14, 29, 31, 33), but the goal of the stromal implant should be to improve visual acuity and at the same time significantly increase the corneal thickness in patients with advanced keratoconus. Future studies are needed to improve the results in all these studies cited above.

Currently, a multicenter **SLAK** research group is working on the generation of customized lenticules that could combine the advantages of both planar (higher thickness increase and availability for eccentric cones) and negative meniscus-shaped lenticules (higher flattening effect).

The use of recombinant human collagen, synthesized in yeast and chemically cross-linked demonstrated to be feasible (35, 36), improved the visual acuity, nevertheless, a large variation of corneal thickness was obtained among the cases of this study up to 24 months of follow-up, and high presence of fibrosis was observed.

The use of acellular laminas (10, 11, 13, 14), in which the lack of cells makes the experience out from being considered as a corneal graft, and by using autologous **MSCs** from a given patient, it was possible to transform allogenic grafts into functional autologous grafts, thus avoiding any risk of rejection. So far, the long-term follow-up did not show any complications with all the cases (14).

Other recent studies of endokeratophakia using regular **SMILE** lenticules have shown to be a feasible option to correct ametropias such as hyperopia, presbyopia or to increase the thickness in the keratoconic cornea (40). Nevertheless, the use of customized positive meniscus lenticules in keratoconus corneas is debatable (29, 39), as theoretically could worsen myopia usually encountered in such patients, and so planar or negative meniscus lenticules are always preferable for such purpose. Implantation of autologous fresh lenticules from **SMILE** for hyperopia was well-integrated into the host stroma (41, 42). The fact that refractive lenticules can be stored, and be later re-implanted, opens up the possibility of using lenticules for other purposes to restore ectatic corneas or providing an opportunity for reversing refractive surgeries (40).

All the conclusions of these described studies should be carefully considered since they are vulnerable to bias because all the studies included a small sample of patients. However, all the surgeries reported in this review showed initially to be potentially effective for the treatment of advanced keratoconus. In none of the reviewed studies, there was obtain any rejection or inflammation in the treated corneas. Further studies will be necessary to increase the number of cases, and to increase the evidence of the effectiveness of these corneal surgeries with keratoconus or with other corneal stromal dystrophies.

CONCLUSION

Cellular therapy with implantation of autologous **ADASCs**, decellularized human corneal stroma, allogenic **SMILE** Lenticule, Corneal Inlay, and to a lesser extent recombinant Cross-linked Collagen were discussed in this review. As this procedure indeed reported refractive and corneal topography complications it also showed initially to be potentially effective for the treatment of advanced keratoconus. Such promising findings open a new perspective of therapy of the corneal stroma based on corneal stromal enhancement and regeneration. Future studies will expand the potential of the application of these new therapies in the treatment of corneal stromal diseases.

AUTHOR CONTRIBUTIONS

JLA: principal investigator, principal surgeon, study concept and design, analysis and interpretation of data, writing and critical revision of the manuscript, statistical revision, and supervision. MEZ: co-principal investigator, clinical and monitor director of the study, study concept and design, data collecting, analysis and interpretation

of data, writing and critical revision of the manuscript, statistical revision, and supervision. MPdM: biological processing, corresponding data editing, and critical correction of the manuscript. JLAdB: second surgeon, corresponding data editing, and critical correction of the manuscript. KAJ: analysis, interpretation, editing of the data, and writing the manuscript. NM: stem cells therapy processing. All authors contributed to the article and approved the submitted version.

FUNDING

This study has been financed by Optica General, Saida Lebanon, and Vissum ophthalmological institute of Alicante, Spain. It was also supported in part by the Red Temática de Investigación Cooperativa en Salud (RETICS), reference number RD16/0008/0012, financed by the Instituto Carlos III – General Subdirection of Networks and Cooperative Investigation Centers (R&D&I National Plan 2008-2011) and the European Regional Development Fund (Fondo Europeo de Desarrollo Regional FEDER).

ACKNOWLEDGMENTS

The authors acknowledged Eric Bangert and Heidelberg Engineering (Heidelberg-Germany) Co. for the generous temporary donation of the confocal microscopy and confocal software analysis software used for this investigation. Ziad Abdul Jawad who was responsible for data collecting, processing, and administration of the study. Antonio Palazón-Bru who did the statistical analysis. Albert Azaar and Reviva Regenerative, Beirut- Lebanon, for the administrative management of the Laboratory. Marc Assouwad from Laser Vision (Beirut, Lebanon) for his assistance in the logistics of the study. Peggy Saba who was responsible for data collecting. Ibrahim Achkar who was responsible for the liposuction and adipose tissue management up to the moment of the laboratory study.

REFERENCES

1. Alió Del Barrio JL, El Zarif M, de Miguel MP, Azaar A, Makdissy N, Harb W, et al. Cellular therapy with human autologous adipose-derived adult stem cells for advanced keratoconus. *Cornea*. (2017) 36:952–60. doi: 10.1097/ICO.0000000000001228
2. Alió JL, Piñero DP, Alesón A, Teus MA, Barraquer RI, Murta J, et al. Keratoconus-integrated characterization considering anterior corneal aberrations, internal astigmatism, corneal biomechanics. *J Cataract Refract Surg*. (2011) 37:552–68. doi: 10.1016/j.jcrs.2010.10.046
3. Ruberti JW, Zieske JD. Prelude to corneal tissue engineering - gaining control of collagen organization. *Prog Retin Eye Res*. (2008) 27:549–77. doi: 10.1016/j.preteyeres.2008.08.001
4. Arnalich-Montiel F, Pastor S, Blazquez-Martinez J, Fernandez-Delgado A, Nistal M, Alio JL, et al. Adipose-derived stem cells are a source for cell therapy of the corneal stroma. *Stem Cells*. (2008) 26:570–9. doi: 10.1634/stemcells.2007-0653
5. Espandar L, Bunnell B, Wang GY, Gregory P, McBride C, Moshirfar M. Adipose-derived stem cells on hyaluronic acid-derived scaffold: a new horizon in bioengineered cornea. *Arch Ophthalmol*. (2012) 130:202–8. doi: 10.1001/archopthalmol.2011.1398
6. Kao WWY, Coulson Thomas VJ. Cell therapy of corneal diseases. *Cornea*. (2016) 35(Suppl. 1):S9–19. doi: 10.1097/ICO.0000000000001010
7. De Miguel MP, Fuentes-Julián S, Blázquez-Martínez A, Pascual CY, Aller MA, Arias J, et al. Immunosuppressive properties of mesenchymal stem cells: advances and applications. *Curr Mol Med*. (2012) 12:574–91. doi: 10.2174/1566524128006199 50
8. Lynch AP, Ahearne M. Strategies for developing decellularized corneal scaffolds. *Exp Eye Res*. (2013) 108:42–7. doi: 10.1016/j.exer.2012.12.012
9. De Miguel MP, Alio JL, Arnalich-Montiel F, Fuentes-Julian S, de Benito-Llopis F, Amparo L, et al. Cornea and ocular surface treatment. *Curr Stem Cell Res Ther*. (2010) 5:195–204. doi: 10.2174/157488810791268663
10. Alió Del Barrio JL, El Zarif M, Azaar A, Makdissy N, Khalil C, Harb W, et al. Corneal stroma enhancement with decellularized stromal laminas with or without stem cell recellularization for advanced keratoconus. *Am J Ophthalmol*. (2018) 186:47–58. doi: 10.1016/j.ajo.2017.10.026
11. Alió JL, Alió Del Barrio JL, El Zarif M, Azaar A, Makdissy N, Khalil C, et al. Regenerative surgery of the corneal stroma for advanced keratoconus: 1-year outcomes. *Am J Ophthalmol*. (2019) 203:53–68. doi: 10.1016/j.ajo.2019.02.009
12. Alió JL, Alió del Barrio LJ. Cellular therapy with human autologous adipose-derived adult stem cells for advanced keratoconus: reply to the letter to editor. *Cornea*. (2017) 36:e37. doi: 10.1097/ICO.0000000000001347
13. El Zarif M, Abdul Jawad K, Alió del Barrio JL, Abdul Jawad Z, Palazón-Bru A, De Miguel MP, et al. Corneal stroma cell density evolution in keratoconus corneas following the implantation of adipose mesenchymal stem cells and corneal laminas: an *in vivo* confocal microscopy study. *IOVS*. (2020) 61:22. doi: 10.1167/iovs.61.4.22
14. El Zarif M, Alió JL, Alió del Barrio JL, Abdul Jawad K, Palazón-Bru A, Abdul Jawad Z, et al. Corneal stromal regeneration therapy for advanced keratoconus: long-term outcomes at 3 years. *Cornea*. (2020).
15. Alió del Barrio J, Chiesa M, Ferrer GG, Garagorri N, Briz N, Fernandez-Delgado J, et al. Biointegration of corneal macroporous membranes based on poly(ethyl acrylate) copolymers in an experimental animal model. *J Biomed Mater Res A*. (2015) 103:1106–18. doi: 10.1002/jbm.a.35249
16. Alió del Barrio J, Chiesa M, Garagorri N, Garcia-Urquia N, Fernandez-Delgado J, Bataille L, et al. Acellular human corneal matrix sheets seeded with human adipose-derived mesenchymal stem cells integrate functionally in an experimental animal model. *Exp Eye Res*. (2015) 132:91–100.
17. Zuk PA, Zhu M, Mizuno H, Huang J, Futrell JW, Katz AJ, et al. Multilineage cells from human adipose tissue: implications for cell-based therapies. *Tissue Eng*. (2001) 7:211–28. doi: 10.1089/1076327013000 62859
18. Zuk PA, Zhu M, Ashjian P, De Ugarte DA, Huang JI, Mizuno H, et al. Human adipose tissue is a source of multipotent stem cells. *Mol Biol Cell*. (2002) 13:4279–95. doi: 10.1091/mbc.e02-02-0105
19. Arnalich-Montiel F, Alió Del Barrio JL, Alió JL. Corneal surgery in keratoconus: which type, which technique, which outcomes?" *Eye Vis*. (2016) 3:2. doi: 10.1186/s40662-016-0033-y
20. Ponce Márquez S, Martínez VS, McIntosh Ambrose W, Wang J, Gantxegui NG, Schein O, et al. Decellularization of bovine corneas for tissue engineering applications. *Acta Biomater*. (2009) 5:1839–47. doi: 10.1016/j.actbio.2009.02.011
21. Guthoff R, Klink T, Schlunck G, Grehn F. Die sickerkissenuntersuchung mittels konfokaler *in-vivo* mikroskopie mit dem rostocker cornea modul - erste erfahrungen. *Klin Monatsbl Augenheilkd*. (2005) 222:R8. doi: 10.1055/s-2005-922279
22. Mastropasqua L, Nubile M. Normal corneal morphology. In: Mastropasqua L, Nubile M, editors. *Confocal Microscopy of the Cornea*. Thorofare, NJ: SLACK (2002). p. 7–16.
23. Ali Javadi M, Kanavi MR, Mahdavi M, Yaseri M, Rabiei HM, Javadi A, et al. Comparison of keratocyte density between keratoconus, post-laser *in situ* keratomileusis keratectasia, and uncomplicated post-laser *in situ* keratomileusis cases. A Confocal Scan Study. *Cornea*. (2009) 28:774–9. doi: 10.1097/ICO.0b013e3181aa265b

24. Ku JYF, Niederer RL, Patel DV, Sherwin T, McGhee CN. Laser scanning *in vivo* confocal analysis of keratocyte density in keratoconus. *Ophthalmology*. (2008) 115:845–50. doi: 10.1016/j.ophtha.2007.04.067

25. Riau AK, Angunawela RI, Chaurasia SS, Lee WS, Tan DT, Mehta JS. Reversible femtosecond laser-assisted myopia correction: a non-human primate study of lenticule re-implantation after refractive lenticule extraction. *PloS ONE. (*2013) 8:e67058. doi: 10.1371/journal.pone.0067058

26. Angunawela RI, Riau AK, Chaurasia SS, Tan DT, Mehta JS. Refractive lenticule re-implantation after myopic relex: a feasibility study of stromal restoration after refractive surgery in a rabbit model. *Investig Ophthalmol Vis Sci*. (2012) 53:4975–85. doi: 10.1167/iovs.12-10170

27. Jacob S, Kumar DA, Agarwal A, Agarwal A, Boptom AR, Saijimol AI. Preliminary evidence of successful near vision enhancement with a new technique: PrEsbyopic Allogenic Refractive Lenticule. (PEARL) corneal inlay using a SMILE lenticule. *J Refract Surg*. (2017) 33:224–9. doi: 10.3928/1081597X-20170111-03

28. Ganesh S, Brar S, Rao PA. Cryopreservation of extracted corneal lenticules after small incision lenticule extraction for potential use in human subjects. *Cornea*. (2014) 33:1355–62. doi: 10.1097/ICO.0000000000000276

29. Ganesh S, Brar S. Femtosecond intrastromal lenticular implantation combined with accelerated collagen cross-linking for the treatment of keratoconus– initial clinical result in 6 eyes. *Cornea*. (2015) 34:1331–9. doi: 10.1097/ICO.0000000000000539

30. Mastropasqua L, Nubile M. Corneal thickening and central flattening induced by femtosecond laser hyperopic-shaped intrastromal lenticule implantation. *Int Ophthalmol*. (2017) 37:893–904. doi: 10.1007/s10792-016-0349-6

31. Mastropasqua L, Nubile M, Salgari N, Mastropasqua R. Femtosecond laser-assisted stromal lenticule addition keratoplasty for the treatment of advanced keratoconus: a preliminary study. *J Refract Surg*. (2018) 34:36–44. doi: 10.3928/1081597X-20171004-04

32. Jin H, Liu L, Ding H, He M, Zhang C, Zhong X. Comparison of femtosecond laser-assisted corneal intrastromal xenotransplantation and the allotransplantation in rhesus monkeys. *BMC Ophthalmol*. (2017) 17:202. doi: 10.1186/s12886-017-0595-z

33. Jin H, He M, Liu H, Zhong X, Wu J, Liu L, et al. Small-incision femtosecond laser–assisted intracorneal concave lenticule implantation in patients with keratoconus. *Cornea*. (2019) 38:446–53. doi: 10.1097/ICO.0000000000 001877

34. Pradhan KR, Reinstein DZ, Vida RS, Archer TJ, Dhungel S, Moptom D, et al. Femtosecond laser–assisted small incision Sutureless Intrastromal Lamellar Keratoplasty (SILK) for corneal transplantation in keratoconus. *J Refract Surg*. (2019) 35:663–71. doi: 10.3928/1081597X-20190826-01

35. Gahmberg CG, Fagerholm SC, Nurmi SM, Chavakis T, Marchesan SI, Grönholm M. Regulation of integrin activity and signalling. *Biochim Biophys Acta*. (2009) 1790:431–44. doi: 10.1016/j.bbagen.2009.03.007

36. Fagerholm P, Lagali NS, Merrett K, Jackson WB, Munger R, Liu Y, et al. A biosynthetic alternative to human donor tissue for inducing corneal regeneration: 24-month follow-up of a phase 1 clinical study. *Sci Transl Med*. (2010) 2:46ra61. doi: 10.1126/scitranslmed.3001022

37. Fagerholm P, Lagali NS, Ong J, Merrett K, Jackson WB, Polarek JW, et al. Stable corneal regeneration four years after implantation of a cell-free recombinant human collagen scaffold. *Biomaterials*. (2014) 35:2420–7. doi: 10.1016/j.biomaterials.2013.11.079

38. Ong JA, Auvinet E, Forget KJ, Lagali N, Fagerholm P, Griffith M, et al. 3D Corneal shape after implantation of a biosynthetic corneal stromal substitute. *Invest Ophthalmol Vis Sci*. (2016) 57:2355–65. doi: 10.1167/iovs.15-18271

39. Doroodgar F, Jabbarvand M, Niazi S, Karimian F, Niazi F, Sanginabadi A, et al. Customized stromal lenticule implantation for keratoconus. *J Refract Surg*. (2020) 36:786–94. doi: 10.3928/1081597X-20201005-01

40. Pradhan KR, Reinstein DZ, Carp GI, Archer TJ, Gobbe M, Gurung R. Femtosecond laser-assisted keyhole endokeratophakia: correction of hyperopia by implantation of an allogeneic lenticule obtained by SMILE from a myopic donor. *J Refract Surg.* (2013) 29:777–82. doi: 10.3928/1081597X-20131021-07

41. Sekundo W, Kunert KS, Blum M. Small incision corneal refractive surgery using the Small Incision Lenticule Extraction. (SMILE) procedure for the correction of myopia and myopic astigmatism: results of a 6 month prospective study. *Br J Ophthalmol*. (2011) 95:335–9. doi: 10.1136/bjo.2009.174284

42. Sun L, Yao P, Li M, Shen Y, Zhao J, Zhou X. The safety and predictability of implanting autologous lenticule obtained by SMILE for hyperopia. *J Refract Surg*. (2015) 31:374–9. doi: 10.3928/1081597X-20150521-03

Conflict of Interest: The authors declare that the research was conducted in the absence of any commercial or financial relationships that could be construed as a potential conflict of interest.

10. 9 El Zarif M., Jawad K.A., Alió J.L. (2019) Confocal microscopy of the cornea in a clinical model of corneal stromal expansion using adipose stem cells and corneal decellularized laminas in patients with keratoconus. In: Alió J., Alió del Barrio J., Arnalich-Montiel F. (eds) Corneal regeneration therapy and surgery. pp 363-386. Essentials in Ophthalmology. Springer, Nature. Cham, Switzerland https://doi.org/10.1007/978-3-030-01304-2_24

Confocal Microscopy of the Cornea in a Clinical Model of Corneal Stromal Expansion Using Adipose Stem Cells and Corneal Decellularized Laminas in Patients with Keratoconus

Mona El Zarif, Karim Abdul Jawad,and Jorge L. Alió

24.1 Introduction

Keratoconus is characterized by a progressive decrease in corneal strength [1], related to a progressive loss of keratocytes of the human eye, the number of keratocytes decrease from anterior to posterior stroma [2], and the progressive thinning of the corneal stroma [2, 3]. This definition is valid for most patients with keratoconus, although some variations in the phenotypic expression of the disease might be present [4]. Most of keratoconus cases have thin corneas and a weak mechanical resistance related to the progressive loss of keratocyte density [5]. Apoptosis of keratocytes [2, 6] or release of enzymes is thought to be the cause of keratocyte loss and consequently loss of corneal stroma over time [2, 6]. The proportion of keratocytes in the corneal stroma is decreased with the progression of the disease [2].

In the end stages of keratoconus, the clinical aspects of the thin and debilitated cornea are associated with a sharp decrease in the amount of keratocytes. There is severe corneal deformation [2], and alteration in the location of the corneal apex [7] consequently causes severe visual loss.

The treatment of keratoconus should be directed towards the recovery of the normal characteristics of the corneal stroma. This can be achieved by substituting the diseased cornea with a healthy cornea, by inserting into the cornea different materials to increase resistance such as intracorneal rings, or biological tissues, or by stimulating cells present in the corneal stroma to produce collagen. Such recovery of the corneal stroma could be induced by either stimulating the cells that produce collagen or by increasing the thickness with the use of corneal stroma or any other tissue that could increase the corneal thickness and optical performances while improving the corneal thickness with the production of new collagen, substituting the one lost due to the progression of the disease.

M. El Zarif (✉)
Optica General Sarl, Department of Optometry and contactology, Saida, Lebanon

Vissum Instituto Oftalmologico de Alicante, Alicante, Spain

K. A. Jawad
Optica General Sarl, Department of Optometry and Contactology, Saida, Lebanon

University of Nicosia, Department of Life and Health Sciences, Nicosia, Cyprus

J. L. Alió
Professor and Chairman of Ophthalmology, University Miguel Hernandez, Vissum-Instituto Oftalmologico de Alicante, Alicante, Spain

https://doi.org/10.1007/978-3-030-01304-2_24

Based on the authors' experience in corneal regeneration [8–10], we proposed the use of corneal decellularized lamina with or without ADASCs for the treatment of severe thin corneas suf- fering from keratoconus [8]. The extremely thin cornea that exists in severe cases could at the same time further increase in thickness with the use of a corneal lamina [9], cut by a femtosecond laser from corneas of eye bank donors, that could be implemented in its biological value with the associated use of the above-described stem cells with the purpose of increasing the corneal thick- ness even further [8]. Along this chapter, we are going to describe the evolution of confocal microscopy following a clinical experiment, in which autologous stem cells have been injected in the corneal stroma [8]. Corneal human donorsunsuitable for corneal graft with or without the impregnation of autologous stem cells, for the purpose of treating of patients with advanced stages of keratoconus [9, 10].

We are going to report herein the results of this experiment with the use of confocal microscopy as an investigational tool to ascertain the fate of the stem cells used along the experiment and the impact that this cellular therapy might have in the future treatment of keratoconus [8].

24.2 Patients and Methods

24.2.1 Patients

Fourteen consecutive keratoconus patients were enrolled in the study and randomly distributed into three study groups:

Group 1: Autologous ADASCs implantation (5 patients)
Group 2: Decellularized human corneal stroma transplantation (5 patients)
Group 3: Autologous ADASCs + decellularized human corneal stroma transplantation (4 patients)

Thirteen patients completed the study, only one abandoned it due to independent personal reasons.

24.2.2 Methods

24.2.2.1 Description of the Confocal Microscope Used: (HRT3 RCM Device from Heidelberg)

With confocal microscopy using optical sectioning, the microstructure of the cornea can be observed under better conditions than with previously available devices. For instance, the utilization of coherent light has allowed the improvement of contrast and the quality of the images of the stroma that is observed under the confocal microscope [2].

Considered as a noninvasive technique, confocal microscopy allows in vivo observation of the microstructure of the cornea and a more accurate quantification of keratocyte density (Fig. 24.1 and Table 24.1).

24.2.2.2 Preparation of the Confocal Microscope

While the device is turned off, the Rostock Cornea Module (RCM) objective must be set at +12 D (Fig. 24.2). Then, a drop of contact gel is applied on the front surface of the microscope's lens of the RCM. The gel must not contain air bubbles (Fig. 24.3). The TomoCap is then placed on top of the RCM objective (Fig. 24.4). The camera is placed on the side of the examined eye [11].

After getting the consent of the patient, making sure there is no allergy towards the gel and anesthetic applied, and informing how the examination will be performed, the patient is prepared by applying a drop of topical anesthetic in the eye to be examined. Then, a gel tear substitute is applied in both eyes. The gel is also applied on the outer surface of the TomoCap in order to improve the contact surface between the cap and the eye of the patient. Heidelberg Engineering recommends using the same high viscosity gel for both applications on the eye of the patient and the TomoCap in order to prevent any confusion between the gels, since two different gels can be used in each application. We recommend preserving the gel at 4 °C for a period of time before

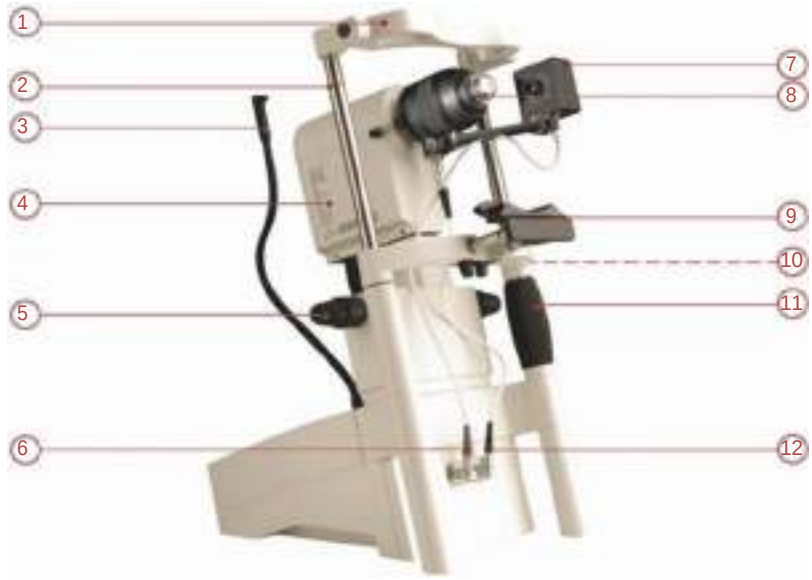

Fig. 24.1 The HRT3 RCM device from Heidelberg [11].

Table 24.1 Illustration of the confocal microscope with detailed description of its different parts [11].

1	Forehead rest	7	CCD camera
2	Headrest column with red marks	8	RCM objective
3	External fixation light	9	Chin rest
4	Camera head	10	Adjustment screw for camera position
5	Adjustment screw for vertical and horizontal camera position	11	Adjustment screw for chin rest
6	CCD camera cable	12	RCM objective cable

its use and maintaining the environment of the examination room at a relatively low temperature.

Before proceeding with the examination, the patient must remain stable, comfortable, and aligned with the lens of the confocal microscope. Afterwards, the patient is instructed not to move the eyes, to keep on looking at the light inside the lens, not to blink, and not to look outside the lens in order not to hinder the observations made with the microscope [11].

Afterwards, the CCD camera is adjusted perpendicularly to the optical axis of the scanning laser camera. The RCM objective and the focal plane are adjusted to the ocular surface of the

Fig. 24.2 RCM objective set at +12 D [11].

TomoCap, and then the focal plane position is set to "0" by clicking on "reset" the focal section (Fig. 24.5). Resetting the focal position to "0" at the superficial epithelial cells of the examined eye is crucial to measure the depth of the corneal cell layer relative to the corneal surface. Following this, the scanning laser camera is slowly moved towards the patient's eye

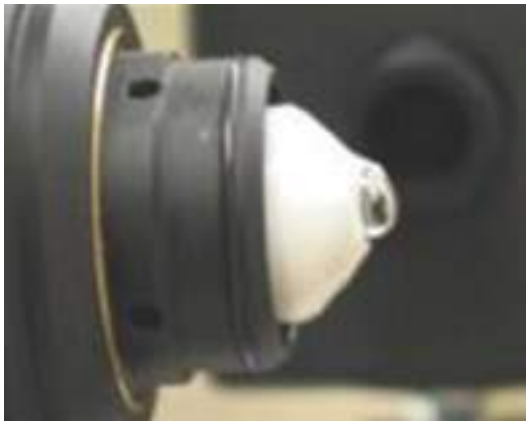

Fig. 24.3 Front surface of the contact lens of the micro-scope where the gel is applied [11].

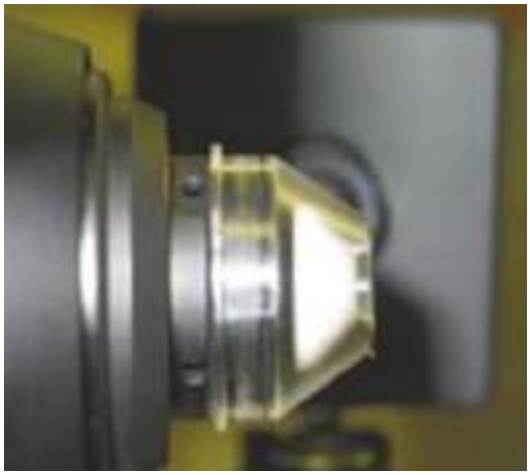

Fig. 24.4 TomoCap attached to the objective [11].

(Fig. 24.6). It is advised to apply gel on the exterior face of the TomoCap to improve the contact between the cap and the patient's cornea. At this point, the patient is asked to widely open the eye, and the scanning camera is slowly moved towards the eye until the TomoCap touches the patient's cornea. The RCM is turned clockwise or counterclockwise, and the focal plane is adjusted to the desired cell layer once a contact between the patient's cornea and the TomoCap has been made. The headrest must not be moved transversally. Finally, an image is obtained by pressing the foot switch [11].

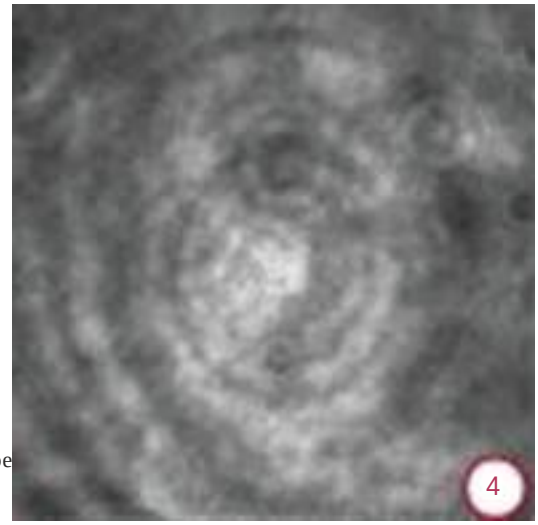

Fig. 24.5 Image seen after adjustment of the focal planeto the ocular surface of the TomoCap [11].

Fig. 24.6 Reflection of the laser from the confocal microscope in the center of the pupil indicating the right alignment between the microscope and the eye of the patient [11].

24.2.2.3 Difficulties in Handling the Confocal Microscope

The use of the confocal microscope for the study of the cornea is always somehow cumbersome for both the patient and the examiner.

The patient must be able to collaborate with the examiner in maintaining a stable posture, a good fixation, and a wide palpebral opening of the eye in order to allow contact between the TomoCap and the eye [11].

The feeling of contact of the TomoCap with the eye of the patient may cause tearing and photophobia in some patients, which increases the difficulty of the examination.

24.2.2.4 Confocal Sampling of the Corneal Stromal in Advanced Keratoconus

In confocal microscopic investigations of keratoconic patients, superficial epithelial cells that are elongated in oblique direction, are consistently found alongside highly reflective (Fig. 24.7), pathological alterations are found in principle at the fourth stage of the disease in the central area of the cornea, as reported by various authors [12].

In our experience, we also found (Figs. 24.7 and 24.8) that in the epithelial layer, superficial cells are elongated and distorted in an oblique direction instead of them being presented as a mosaic form of regular polygonal surface [13]. Unlike in normal epithelial tissues, it can be difficult to distinguish the borders between the epithelial cells, and the basal epithelium shows distortions and irregularities (Figs. 24.9, 24.10, and 24.11) [13].

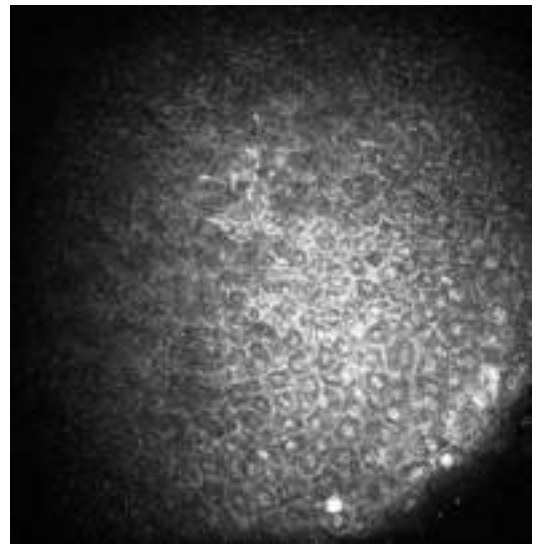

Fig. 24.8 Superficial epithelium cells at −1 μm from a 34-year-old keratoconic female patient show different sizes of superficial epithelial cells and an elongated one in oblique direction.

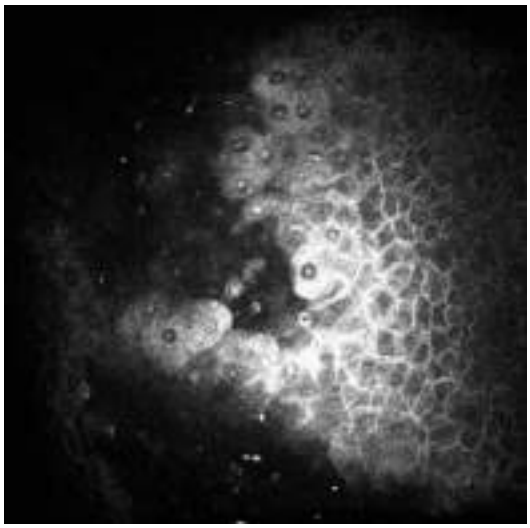

Fig. 24.7 Superficial epithelium cells at −3 μm from a 34-year-old keratoconic female patient. It shows elongated cells in oblique direction, highly reflective with evident area of missing cells.

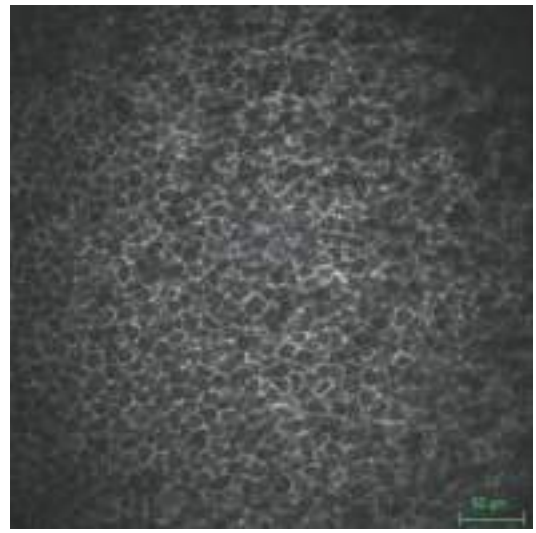

Fig. 24.9 Corneal epithelium at 32 μm from a keratoconic female patient.

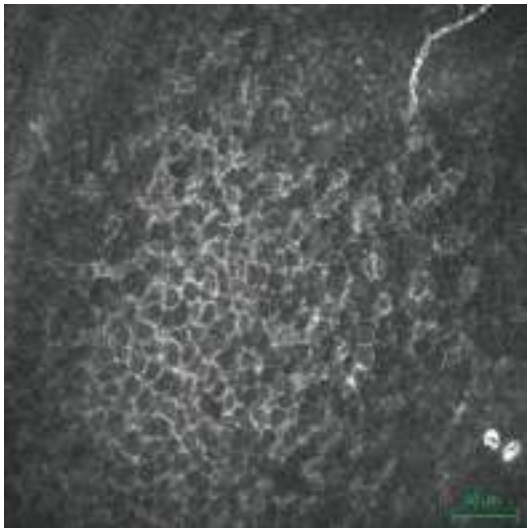

Fig. 24.10 Corneal epithelium at 50 μm from a keratoconic female patient showing the nerve plexus, irregular and distorted epithelial cells and small area of missing cells.

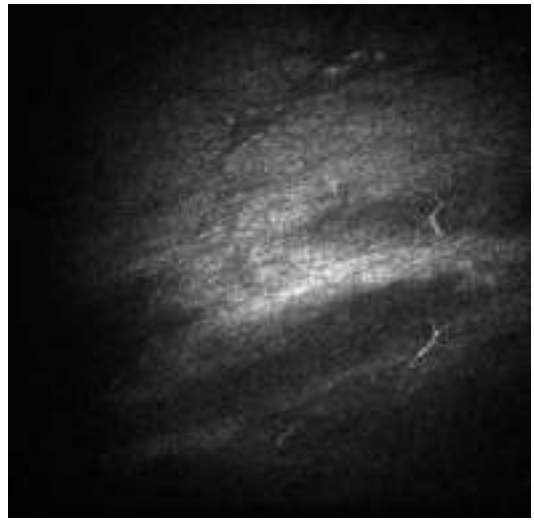

Fig. 24.12 Bowman's membrane of a 34-year-old female with advanced keratoconus shows a visible dark striae at 61 μm.

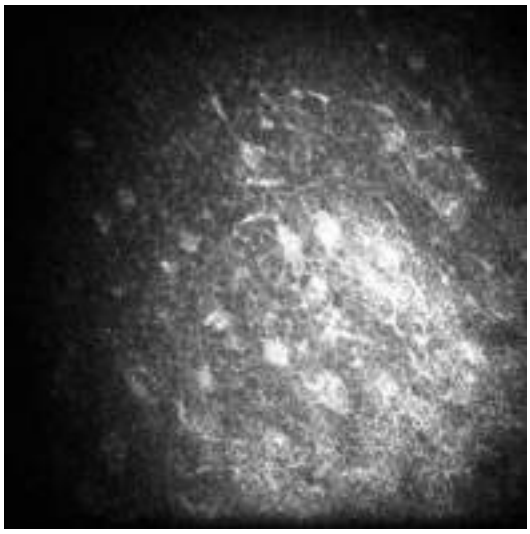

Fig. 24.11 Basal epithelium cells at 61 μm from a 32-year-old keratoconic female patient. It shows highly reflective nodules related to scar tissue at the level of Bowman's membrane, with areas of missing cells.

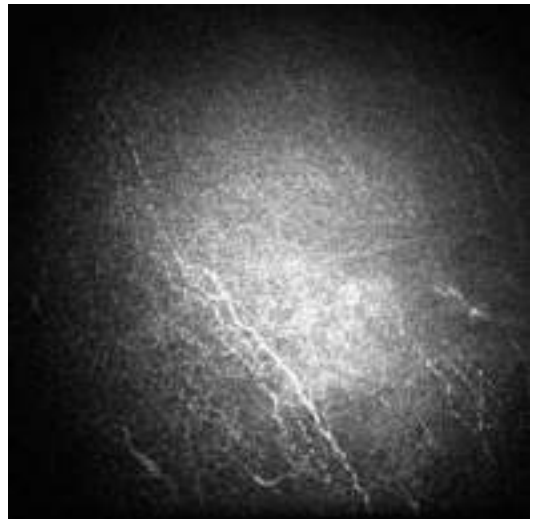

Fig. 24.13 Basal epithelium, Bowman's membrane, and subepithelial plexus nerve of a 31-year-old male patient; the fibers are disposed in oblique direction and display fine irregularity.

Extending from the basal membrane to the immediate stroma beneath it, ruptures in Bowman's membrane are represented by a highly reflective scar tissue [13]. Presence of striae (Fig. 24.12) has also been described in other studies that found that there is a reflection of bright background illumination underneath Bowman's membrane due to a disarrangement of collagen

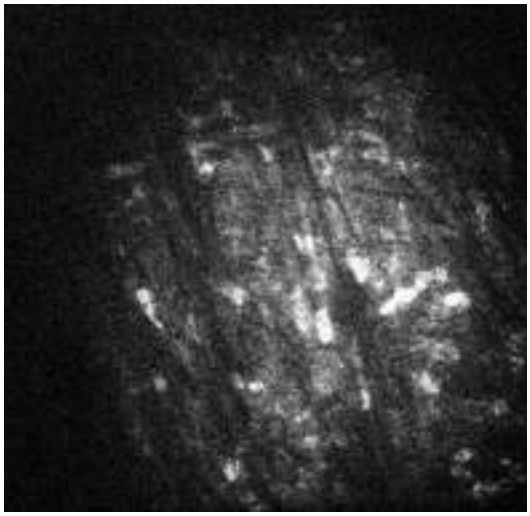

Fig. 24.14 Preoperative corneal anterior stroma at 158 μm of a 35-year-old keratoconic female patient showing oblique dark striae with a moderate number of reflective keratocytes.

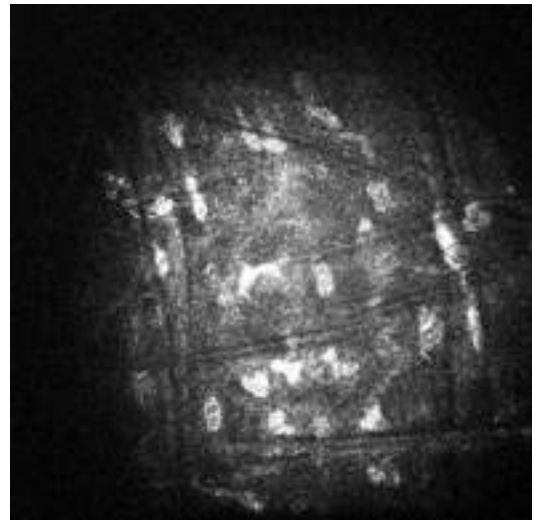

Fig. 24.15 Deep corneal stroma at 396 μm from a 50-year-old keratoconic female patient showing oblique, vertical, and horizontal dark striae with a moderate number of hyperreflective keratocytes.

fibers [12]. Sometimes, the thin nerve fibers present in the area of corneal protrusion, disposed in an oblique horizontal pattern that is coherent with the direction of the stretched epithelial cells (Fig. 24.13) [13]. In addition, an elevation in the anterior stroma and Vogt's striae in the posterior stroma's reflectivity are consistent with pathological processes of the corneal stroma [14]. One of the main abnormalities of the stroma is the presence of microstriae that are evident in the whole stroma of the cornea, which also appear as multiple dark and thin lines in comparison with the brighter stromal reflectivity (Fig. 24.14). These microstriae could possibly result from the degenerative process that leads to changes in the extracellular collagen lamellae of the cornea [13]. These microstriae can appear as horizontal, vertical, oblique, or reticular lines (Fig. 24.15), and they appear to extend from the most anterior stroma to Descemet's membrane [13].

Morphology of keratocytes changes from the anterior to the posterior stroma. They have thin and consistent nuclei in the anterior stroma (Fig. 24.16), some stromal cells have a dendritic

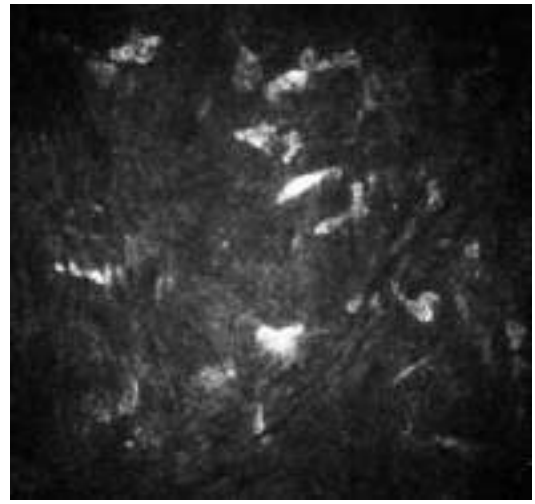

Fig. 24.16 Anterior corneal stroma at 63 μm from a 33-year-old keratoconic female patient, with a reduced number of keratocytes and thin nuclei content.

shape (Fig. 24.17), and more consistent and bigger nuclei size in the mid of stroma (Fig. 24.18). The morphology of the keratocytes in the posterior stroma is similar to the one in the

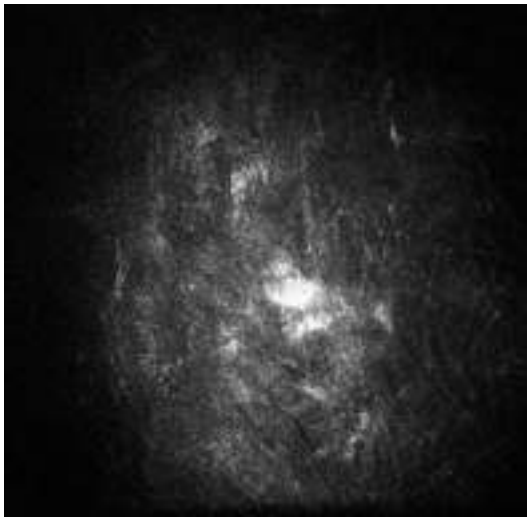

Fig. 24.17 Preoperative mid-stroma at 217 μm from a 31-year-old keratoconic male patient. It shows keratocytes in dendritic form.

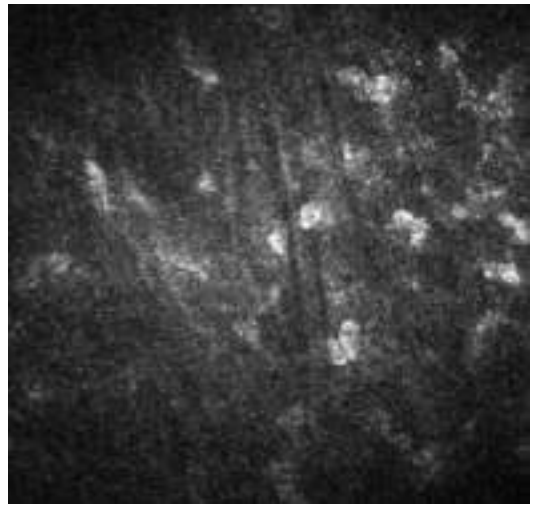

Fig. 24.19 Deep corneal stroma at 439 μm from a 33-year-old keratoconic female patient, with a significant decrease in the number of keratocytes, and less reflective and dense nuclei.

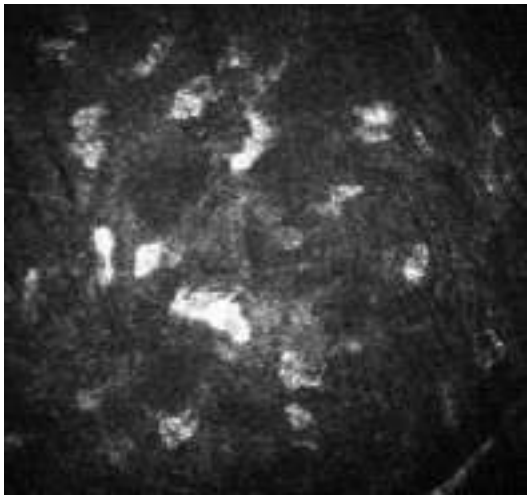

Fig. 24.18 Mid-stroma at 220 μm from a 33-year-old keratoconic female patient, with a reduced number of keratocytes with more dense nuclei.

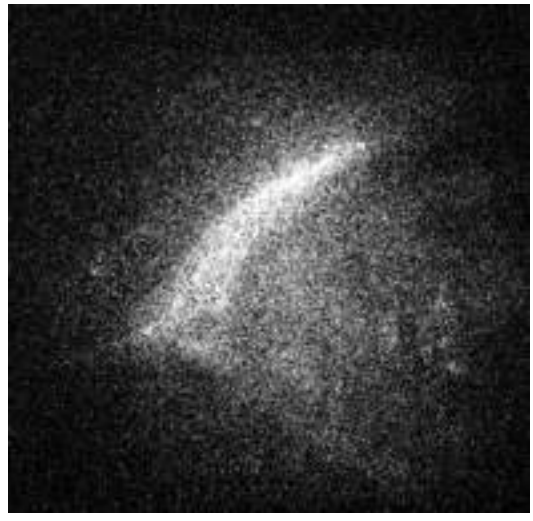

Fig. 24.20 Descemet's membrane from a 31-year-old keratoconic male patient, showing an acellular layer with a highly reflective zone.

middle stroma, but they are smaller and less bright (Fig. 24.19).

Finally, the descemet membrane appears completely acellular (Fig. 24.20) and the endothelial cell layer might show changes such as an increase in cell area, a decrease in cell density, polymegathism, and pleomorphism depending on the progression of the disease (Fig. 24.21) [13].

24.2.2.5 Methods of Cell Counting

Automated Cell Counting of Keratocytes

The automatic count that is calculated by confocal corneal microscopy devices usually is not precise, which leads to an increase in errors when calculating the number of cells. Therefore, for the purpose of this investigation, we preferred to perform a manual cell count of the keratocytes of the corneal stroma [11].

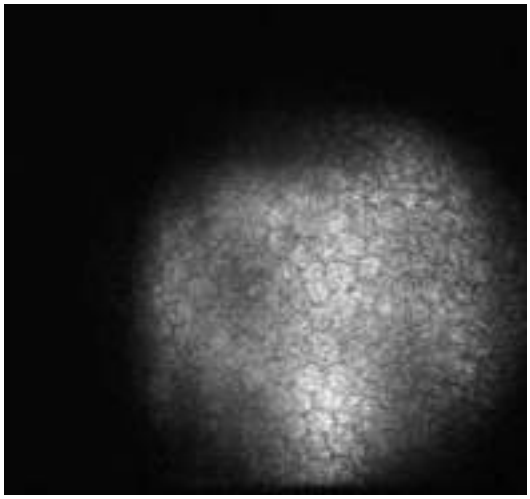

Fig. 24.21 Endothelium at 531 μm from a 24-year-old keratoconic male patient with mild pleomorphism.

Method for Manual Cell Countingof Keratocytes

First, an image of the corneal stroma of a patient is selected. The image has to have a good quality of contrast and illumination, and must contain keratocytes. An area known as the region of interest (ROI) is determined. This region has plenty of cells. It is advised to choose the same approximation of ROI (e.g., 0.1000 mm^2) for all cell counts in all layers of the corneal stroma [2, 11].

The cell count begins with mid brightness and contrast. At this point, the cells that are more illuminated and more refringent [5, 6] are selected with the marker of the device, which usually is either white or light gray and have clear borders [2]. The dark gray cells should not be taken into consideration, because these cells do not belong to the chosen plane. This high brightness is usually attributed to the nuclear content in these cells, and they have irregular oval-shaped bodies (Fig. 24.22) [5], while the difference in brightness is due to the metabolic activation and the direction of incidence of the laser light [5].

After the first count is done, the contrast is increased to the maximum, and the brightness is decreased to the minimum. Keratocytes that disappear from the chosen plane are eliminated, and only the ones that remain are used for the final

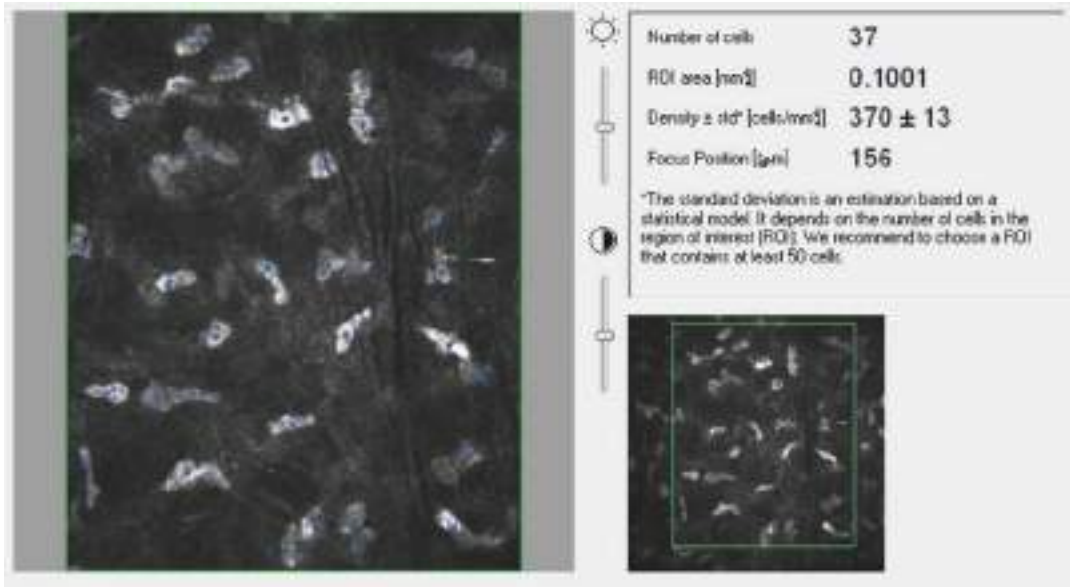

Fig. 24.22 Cell count performed with mid brightness and contrast; the keratocytes are marked in blue.

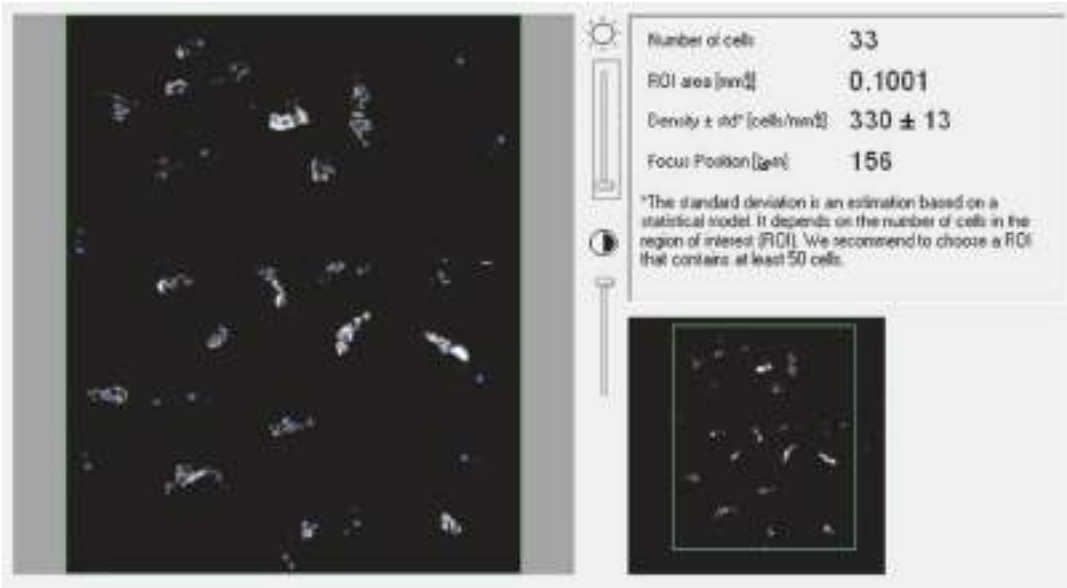

Fig. 24.23 Elimination of keratocytes that do not belong to the plane under observation using low brightness and highcontrast settings.

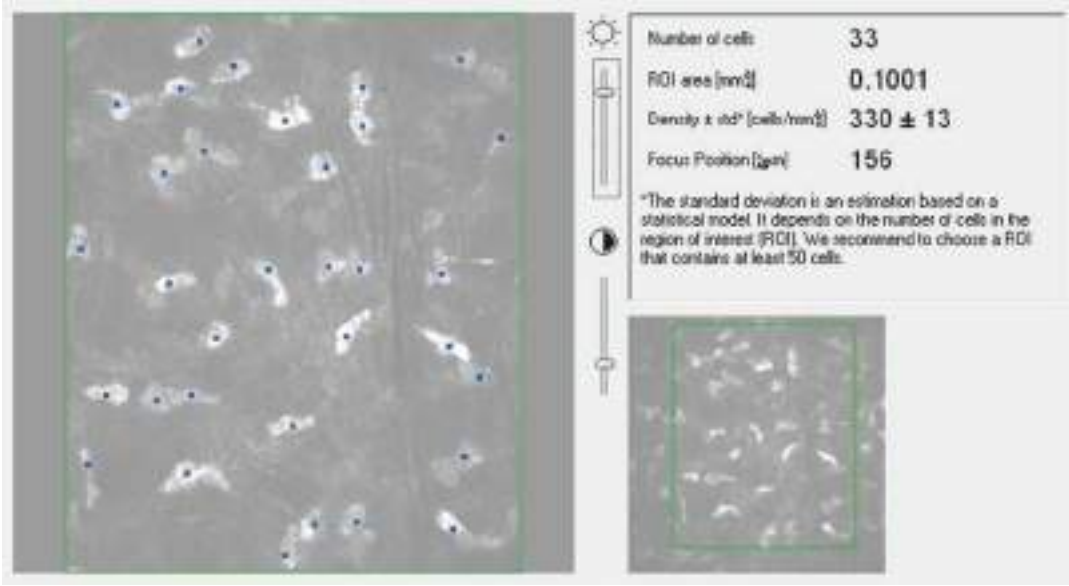

Fig. 24.24 Refining of the cell count using three-quarter high brightness and a quarter low contrast at which the imageappears in grayscale.

count of cells even if they are faintly identified in the image (Fig. 24.23).

Finally, the contrast is decreased to a quarter, and the brightness is increased to three quarters (Fig. 24.24). In this newly adjusted image, the plane becomes grayscale, and the keratocytes become highly illuminated, which allows a final refinement of the cell count.

When the images are very dark, it is recommended to increase the contrast to the maximum and the brightness to three quarters (Fig. 24.25). This facilitates the count of the

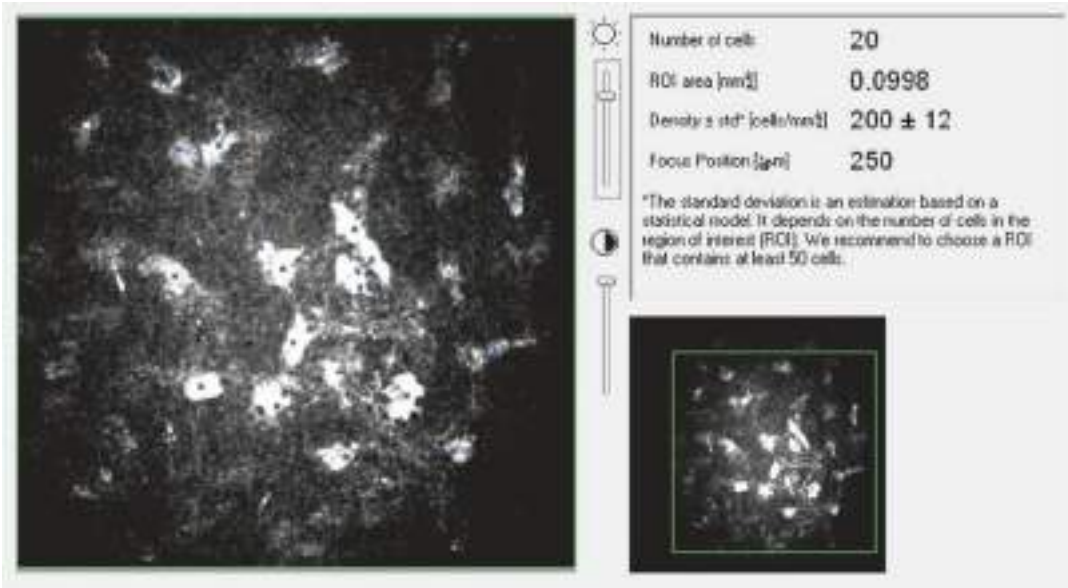

Fig. 24.25 Maximum contrast and three-quarter brightness is used in the case of very dark images.

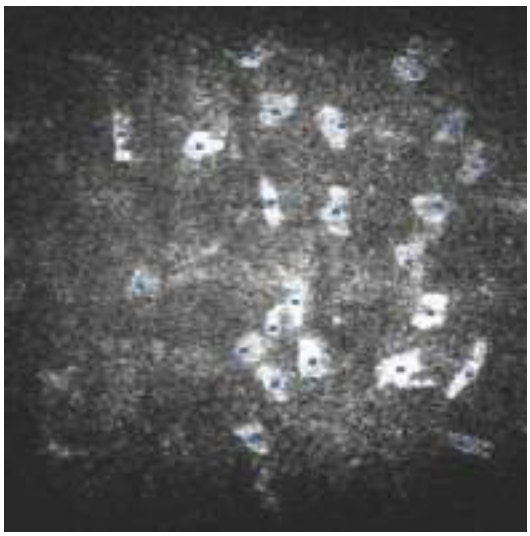

Fig. 24.26 Count of ADASCs and keratocytes, 1 month following surgery of a 33-year-old keratoconic patient. The cells are marked in blue.

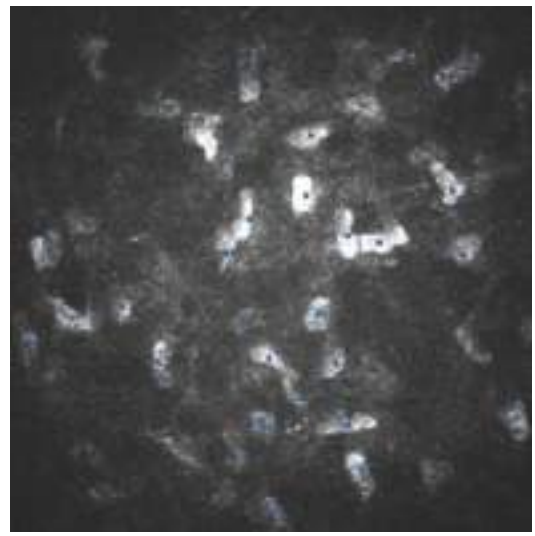

Fig. 24.27 Count of cells for the same patient 1 year after surgery.

keratocytes, and the cell count can be resumed as mentioned above.

Cell Counting of ADASCs

The counting method for transplanted ADASCs is done similarly to the way normal kerato- cytes of the corneal stroma are counted. The only difference between the two methods is that in the first 6 months after the surgery, the ADASCs have a round shape and are more luminous and refringent than normal keratocytes (Fig. 24.26) [8]. After these 6 months, the ADAS cells assimilate a shape similar to normal keratocytes [8], thus reducing any morphological differences between them (Fig. 24.27). Therefore, the cell count becomes the same for both kinds of cells.

Cell Count on a Decellularized Lamina

The images provided by the confocal microscope shows that the lamina appears totally acellular in the first month (Fig. 24.28) but the newly colonized transplanted lamina by the keratocytes of the patient's corneal stroma show that these cells differ in morphology from the native keratocytes of the cornea. This is caused by the reduced transparency of the lamina right after it is transplanted (Fig. 24. 29). Thus, the images of these cells lack the depth seen in the normal corneal keratocytes of the patient. Three months after the surgery, the morphology of patients' cells colonized on the lamina started to show some new keratocyte appearance (Fig. 24.29). The shape of these cells at 6 months became more similar to the keratocytes (Fig. 24.30) [9], before fully developing into cells that have the same morphology of keratocytes 1 year post-operation (Fig. 24.31) [10]. Therefore, it is

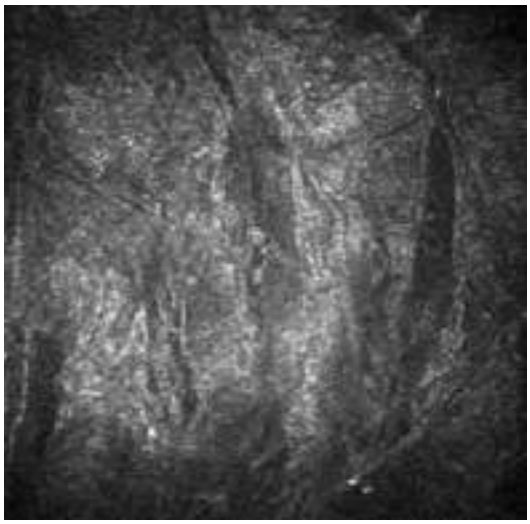

Fig. 24.28 Anterior aspect of a decellularized lamina ofa female, which appears to be without cells 1 month post-operation.

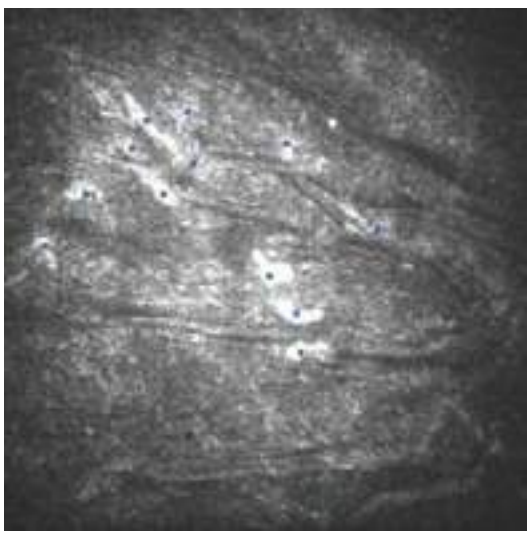

Fig. 24.29 Cell count of a 24-year-old keratoconic patient 3 months post-operation on the posterior aspect of the lamina.

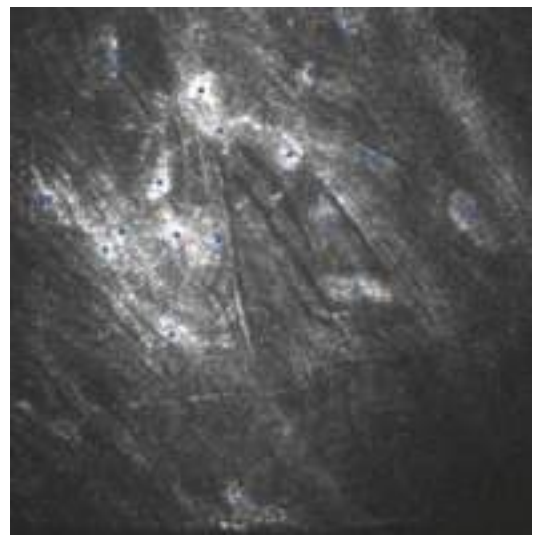

Fig. 24.30 Cell count in the anterior aspect of the lamina in a 29-year-old keratoconic patient, 6 months post-operation.

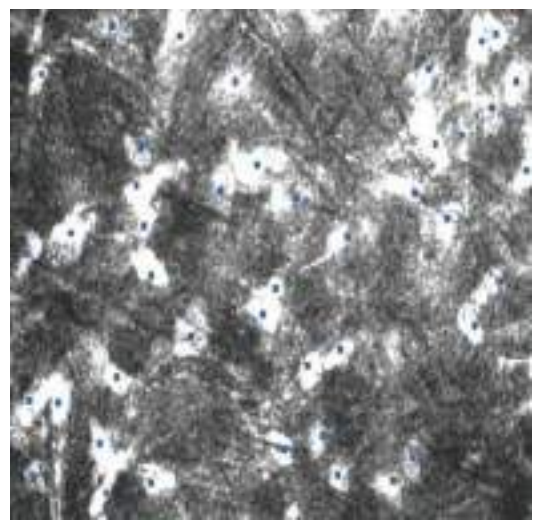

Fig. 24.31 Cell count on the anterior aspect of the lamina of a 31-year-old patient, 1 year after the surgery.

important to identify the change in morphology of these cells throughout the months, which helps in achieving a more accurate cell count.

Cell Count on a Recellularized Lamina

The cell count on a recellularized lamina is relatively similar to the one made on a decellularized one. In this case, a few ADASCs can be seen within the lamina at 1 month after the surgery in two of the four patients. In addition, the recellularized lamina consistently contained a higher number of keratocytes than in the decellularized one, when observed 3–12 months after the surgery [10].

24.2.2.6 Corneal Density Calculation

To obtain cell density, the examiner must use the cellular counting software in the confocal microscope [11] and delimit a fixed area depending on the images measured by the specialist, with a periphery that contains abundant keratocytes. Since it is difficult to achieve great corneal contact between the TomoCap and the patient, the specialist is required to select an area that contains abundant cells.

The following data appear on the software screen:

- Number of cells: Which are the number of cells counted by the observer
- ROI (mm^2): The area chosen by the same observer

Density +/− std (cell in mm^2): Density calculated by mm^2 by the same device with an error of more or less the number of cells in the area [6, 11].

For example:

$$\text{Density}\left(\text{cells in } mm^2\right) = 200 \pm 12$$

24.3.1.1 Difficulties in Cell Counting During our experience in counting keratocytes, we encountered difficulties until we established specific criteria and methodology for the purpose of cell counting. We recommend the following:

- The cells that appear in the captured images as if they belonged to the same plane of 50 micron of depth cannot be counted. These cells appear with a faded gray color. At this point, it is advisable to lower the illumination to 0% and increase the contrast to 100% as indicated in (Fig. 24.23).
- If the images have low resolution, the contrast must be modified towards 25%, and the illumination is raised to approximately 75%. By doing so, this image is seen in the clear background, and the keratocytes appear with distinguished border and are clearly illuminated. Therefore, they can be marked more easily. We call this regulation the grayscale (Fig. 24.24).
- If the confocal images are very dark, it is advisable to set the illumination to 75% and the contrast to 100% (Fig. 24.25).
- If a line of separation between both structures of attached cells is not clear, it is advisable to interchange between the contrast and illumination until a discrimination of the orientation of the nuclear content of both cells can be made. If the content appears parallel, it is more likely that they belong to the same nucleus. However, if the nuclear contents of the two cells are in different directions, then they belong to two different cells.
- If the cells at the edge of the selected plane are not seen in their complete shape, every two halves of cells are counted as one single cell.

When observing the transplanted laminas, it was noticed that their morphology is either decellularized or recellularized; has an extracellular matrix characterized by the presence of abundant streaks, which are larger in size and are more profound; and has changed during the next months after the transplant. This changed morphology remained constant afterwards.

24.3 Results

24.3.1 Confocal Microscopy of the Corneal StromaFollowing the Stromal Enhancement Intervention

24.3.1.1 Patients with Transplanted ADASCs

One to three months following the implantation surgery, the transplanted ADASCs were round in shape and more refringent [8], in comparison to the

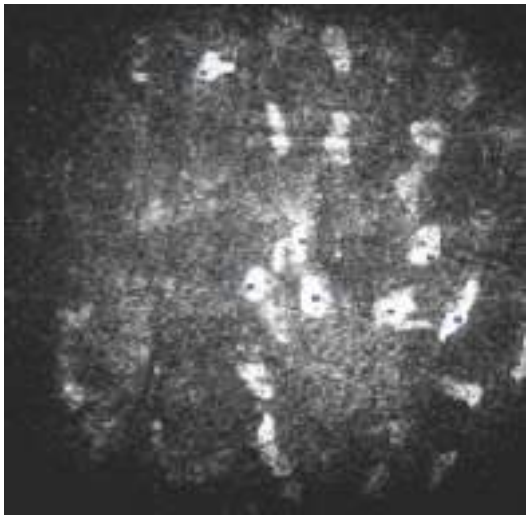

Fig. 24.32 Confocal microscopy of corneal stroma froma 33-year-old keratoconic female patient at 265 μm1 month after transplantation of ADASCs.

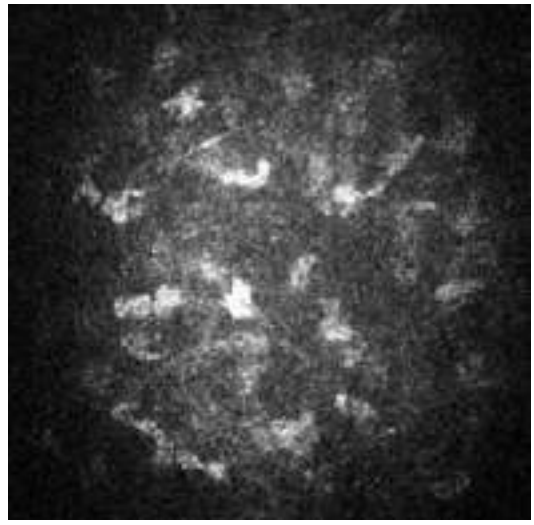

Fig. 24.34 Morphological change in the shape of ADASCs, from round to fusiform in the same 273 μm, of a 33-year-old female patient 6 months after the operation.

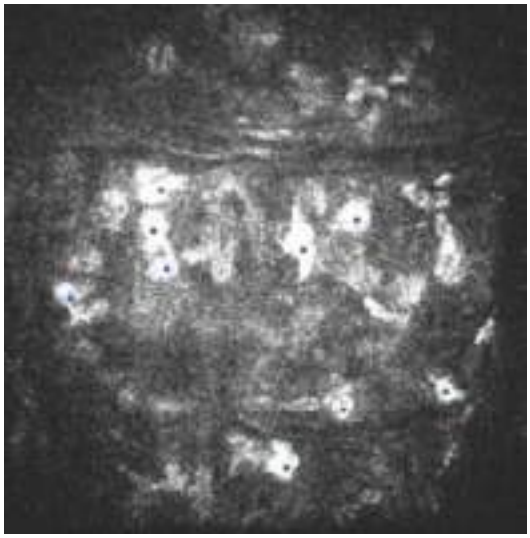

Fig. 24.33 Confocal microscopy at 273 μm from a 33-year-old keratoconic female patient 3 months after transplantation of ADASCs. The blue dots show the transplanted cells in the plane of the lamellar pocket. They have a round morphology and are more refringent than the original keratocytes of the patient's stroma.

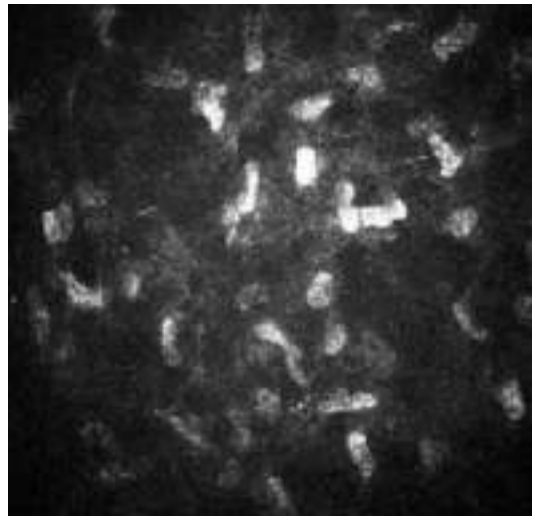

Fig. 24.35 Keratocytes in the surgical plane at 250 μm, 1 year after the transplant.

fusiform morphology of the keratocytes [5], present in the recipient cornea (Figs. 24.32 and 24.33). However, the shape of ADASCs changed from round to fusiform 6 months after the operation [8], and they assimilated a morphology similar to that of the original keratocytes of the patient's cornea (Fig. 24.34). The round morphology of these cells is a strong indicator of their ability to survive, especially during the early postoperative period [8]. We also found that the number of keratocytes increased 6 months after the operation [9]. One year after the surgery, it is noticeable that the number of keratocytes increased even more (Fig. 24.35) [10]. A gradual increase (*P* value = 0.07) in the density

Table 24.2 Evolution of the density of keratocytes of the patients over 1 year

	Preop			*6 months*			*12 months*		
	Group 1	Group 2	Group 3	Group 1	Group 2	Group 3	Group 1	Group 2	Group 3
Anterior stroma (cells/mm^2)	236.45 (220, 280)	222.6 (163.3, 286.6)	187.6 (176.6, 198)	254.15 (210, 306.6)	215.3 (190, 273.3)	286.6 (210, 356.6)	288.5 (210, 340)	441.2[a] (392.5, 474)	467.4 (333.3, 594)
Posterior stroma (cells/mm^2)	202.5 (190, 225)	181.8 (136.6, 216)	192.8 (174, 203.3)	255.8 (190, 320)	239.16 (213.3, 265)	237.4 (163.3, 293.3)	322.5 (290, 340)	459.7[a] (376.6, 540)	416.5 (388, 447.5)

Keratocyte cellular density (mean value and range) for G 1 (autologous ADASCs implantation; *n*:4), G 2 (decellularizedhuman corneal stroma implantation; *n*: 5) and G 3 (autologous ADASCs recellularized human corneal stroma implanta- tion; *n*: 4) before, 6 and 12 months after surgery [10]. [a]Shows statistically significant ($P \leq 0.05$) differences between the preoperative and 12 months postoperative values foreach parameter and for each study group separately (for mid-stroma, this comparison is between 6 and 12 months post-operation).

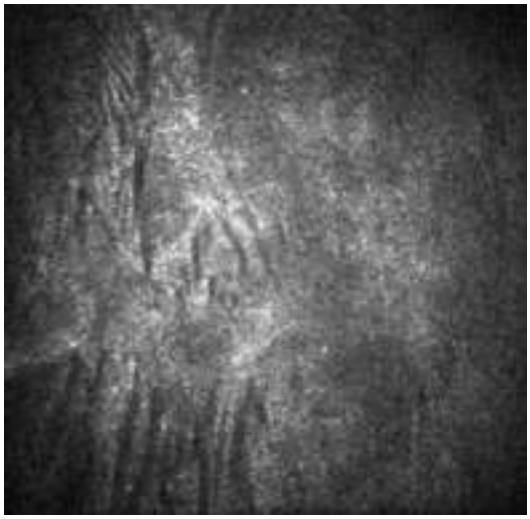

Fig. 24.36 Posterior face of a decellularized lamina of a 31-year-old male, 1 month after the operation, seen at 289 μm. The lamina appears to be almost acellular.

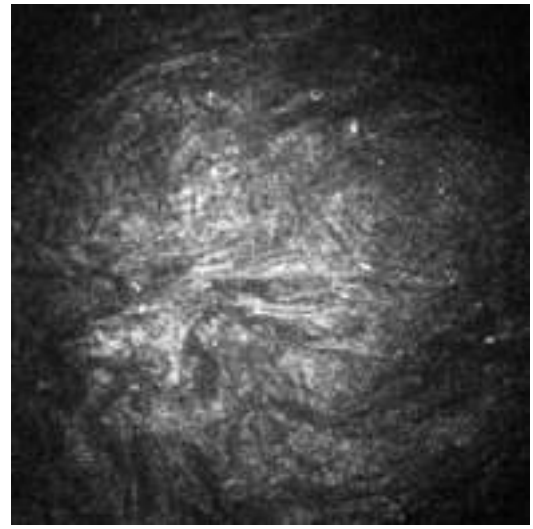

Fig. 24.37 Anterior face of the decellularized lamina of the same patient, 3 months after the operation, seen at 207 μm, showing early colonization of the keratocytes to the lamina.

of cells was evident in the anterior, middle, and posterior stroma of the patients 1 year after the operation, in comparison to the density level preoperative (Table 24.2).

24.3.1.2 Patients with Decellularized Lamina

One month after the surgery, the transplanted lamina generally remained acellular in most of the patients (Fig. 24.36) [9]. However, two out of five patients showed in the anterior aspect of the lamina the beginning of keratocyte colonization, which is a change normally seen 3 months after the surgery (Fig. 24.37). On the other hand, the posterior aspect of the lamina appeared to be clearly colonized by some keratocytes at the same time of examination in three of the five patients (Fig. 24.38). Six months after the transplant, the anterior aspect of the lamina was clearly colonized by keratocytes in some patients (Fig. 24.39), while the posterior aspect was more abundant in these cells (Fig. 24.40). Moreover, 1 year after the operation, both the anterior and posterior aspects became fully colonized by keratocytes (Figs. 24.41 and 24.42) [10]. The density of cells on the lamina

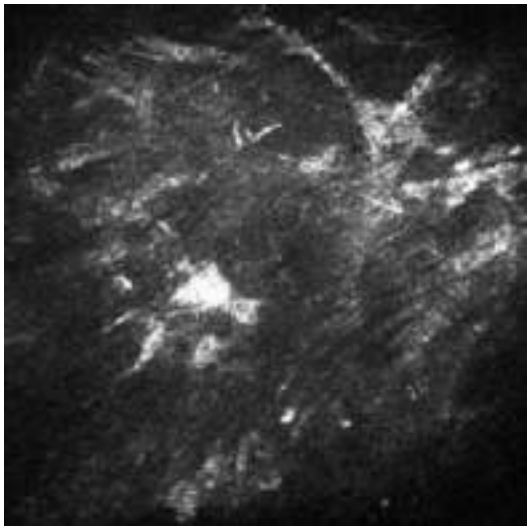

Fig. 24.38 Posterior face of the lamina at 271 μm, 3 months after the operation clearly colonized by the surrounding keratocytes.

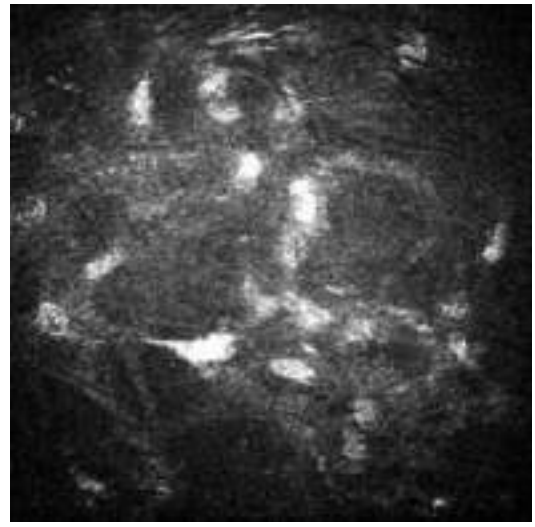

Fig. 24.40 Posterior face of the lamina that is highly colonized by keratocytes from the cornea 6 months after the operation.

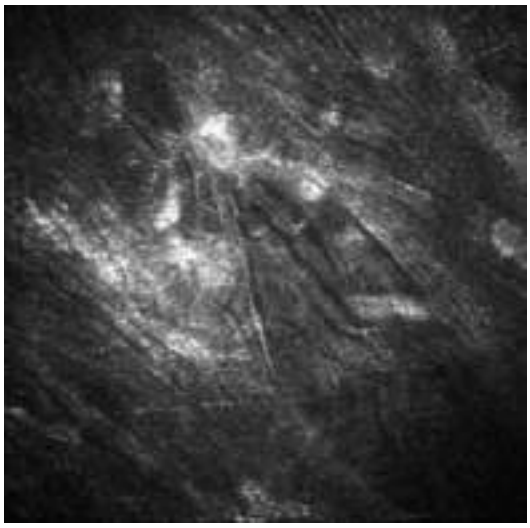

Fig. 24.39 Colonized anterior face of the lamina at 176 μm at 6 months.

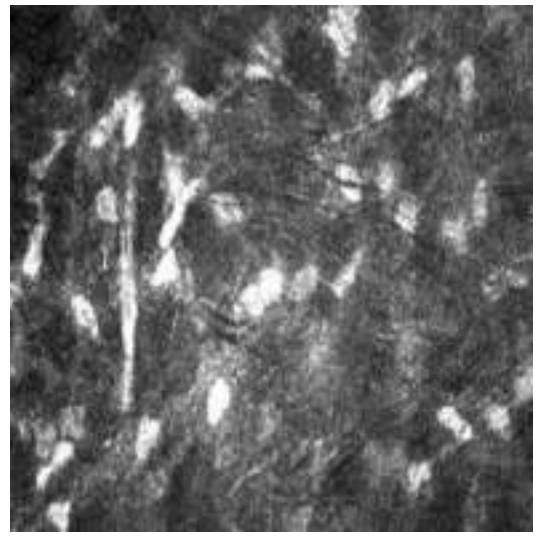

Fig. 24.41 Anterior face of the lamina showing high quantity of keratocytes 12 months after the surgery.

was similar to what is expected in a normal cornea. We were able to demonstrate that there was a significant increase in keratocytes within the lamina and keratocyte density in both the anterior and posterior stroma was statistically significant (*P* value = 0.008) 1 year after the operations were performed (Table 24.2).

The collagen matrix morphology of the decellularized lamina differs from the collagen matrix of the patient's stroma. It shows clear and abundant dark striae, some of which have considerable thickness and have vertical, horizontal, and oblique directions (Figs. 24.43 and 24.44).

We observed at the periphery and border of the lamina highly reflective structures that are caused by the mechanical trauma during the surgery (Figs. 24.45 and 24.46). The transition zone between the lamina and the corneal stroma

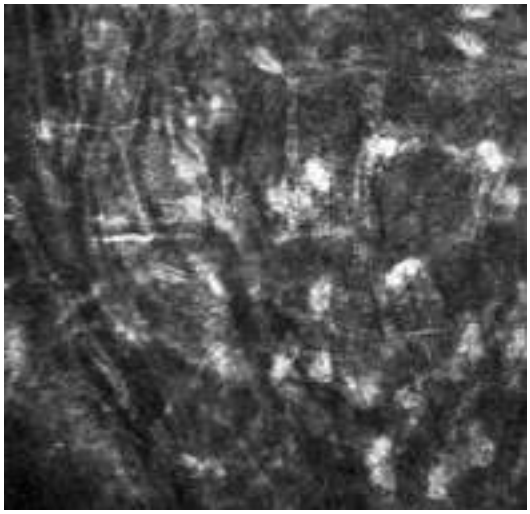

Fig. 24.42 Posterior face of the lamina colonized by high numbers of keratocytes 12 months after theoperation.

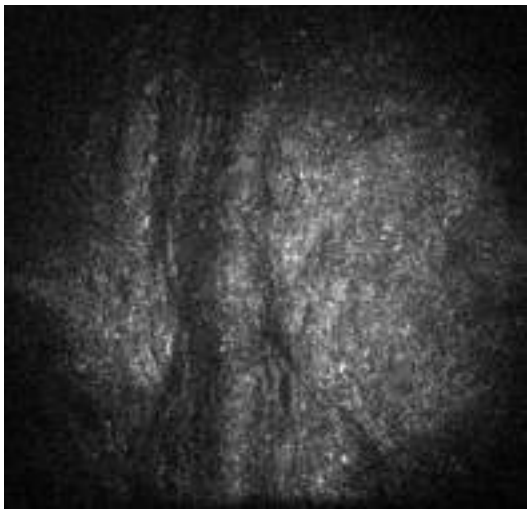

Fig. 24.43 Anterior face of the decellularized lamina ofa 31-year-old male patient, 3 months postoperatively, seenat 154 μm, showing striae that are darker and larger than the ones present in a normal stroma.

can be easily differentiated (Fig. 24.47); also, the lamina's border has, in addition, a reflective structure (Fig. 24.47). We observe as well a clear keratocyte migration from the corneal stroma to the decellularized lamina (Fig. 24.48). Also, the lamina's light reflectivity is higher than the matrix' corneal stroma (Figs. 24.44 and 24.48).

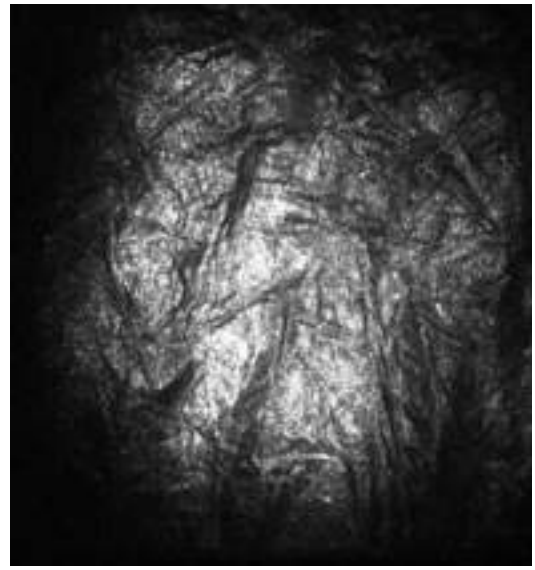

Fig. 24.44 Anterior face of the decellularized lamina ofa 35-year-old keratoconic female patient showing dark and abundant striae. The matrix is clearer than the normal stroma and more reflective.

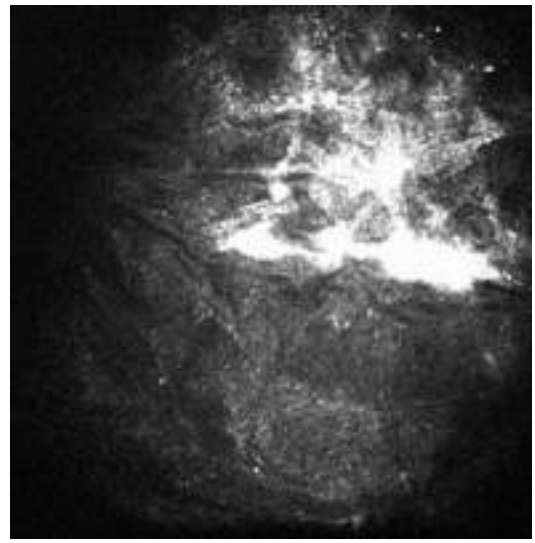

Fig. 24.45 Anterior face of the decellularized lamina ofa 34-year-old female, 1 month post-operation, shows highly reflective peripheral structures on the lamina due to mechanical trauma.

Twelve months after the operation, both anatomy of the corneal anterior and posterior stroma and the keratocyte density did not differ in patients to the normal corneal stroma at the confocal microscopy level (Figs. 24.49 and 24.50) [10].

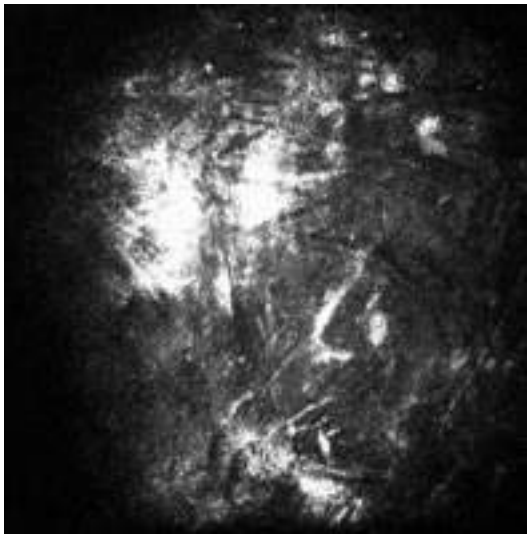

Fig. 24.46 Decellularized lamina present at 272 μm, of a 31-year-old male, 3 months after surgery, showing reflective peripheral structures, due to the mechanical surgical trauma, needle-shaped bodies, and some keratocytes with morphological change.

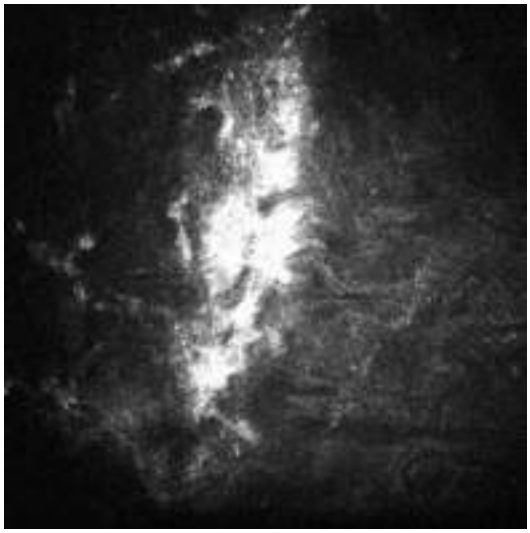

Fig. 24.47 Transition zone at 190 μm between the border of the anterior face of the decellularized lamina and the corneal stroma, 3 months post-operation, for a 35-year-old female showing highly reflective structures, with a few dendritical keratocytes.

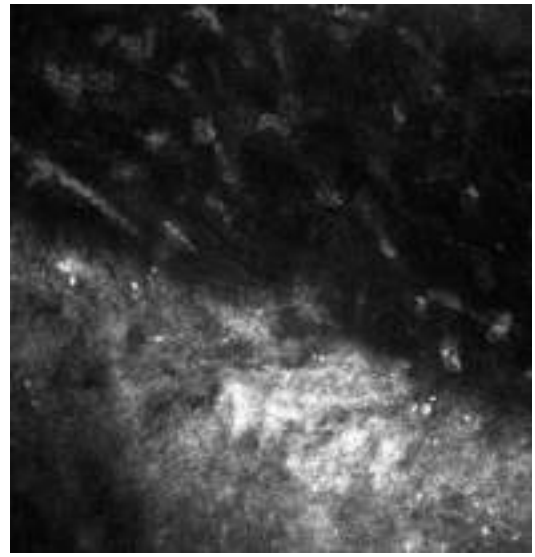

Fig. 24.48 Transition zone at 306 μm between the posterior face of the decellularized lamina and the recipient stroma with a number of migrating keratocytes with dendritical shapes and the corneal stroma with a number of keratocytes, 12 months post-operation of a 35-year-old female patient.

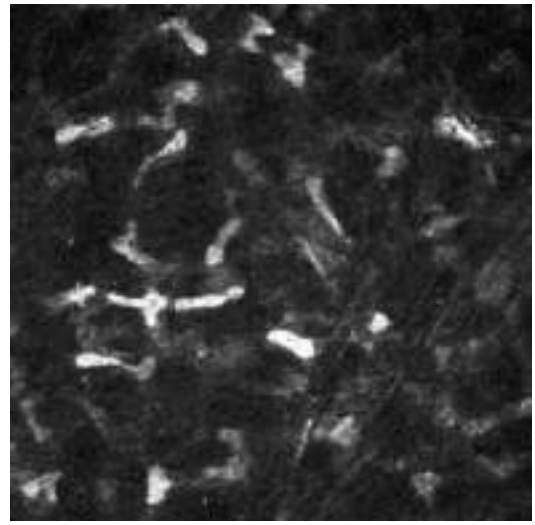

Fig. 24.49 Anterior stroma at 103 μm of a 24-year-old patient, 12 months after the surgery.

24.3.1.3 Patients with Recellularized Lamina

One month after the surgery, both the anterior and posterior faces of the patients' laminas showed in two of the four patients the presence of a few number of ADASCs on their surface, which are smaller than normal keratocytes in the ante- rior face of the lamina (Figs. 24.51 and 24.52), but they are more similar to them in the posterior face, unlike the decellularized laminas, which were completely acellular. At 3 months, the

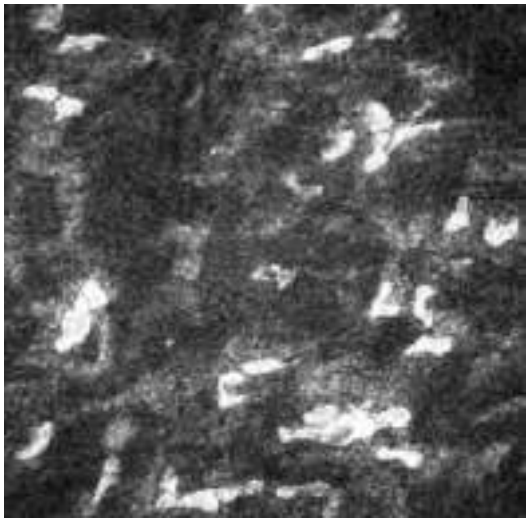

Fig. 24.50 Posterior stroma at 410 μm of the same24-year-old patient, 12 months after the surgery.

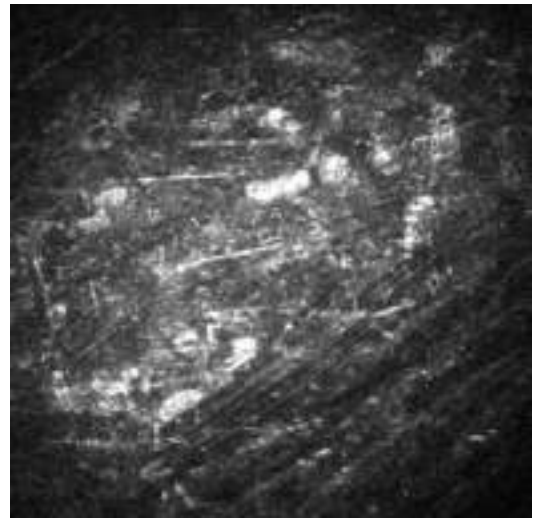

Fig. 24.52 Aspect of the posterior face of the lamina at275 μm, 1 month post-operation.

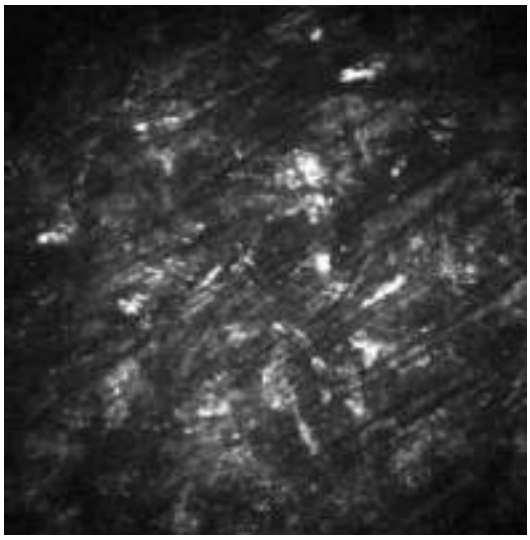

Fig. 24.51 Anterior face of a recellularized lamina at 174 μm of a 50-year-old patient, 1 month after the operation.

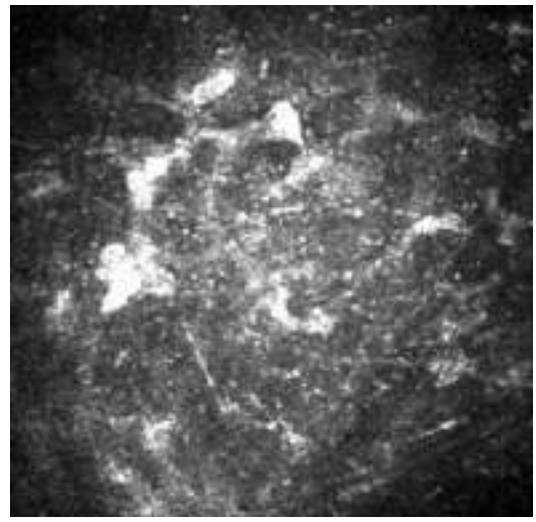

Fig. 24.53 Anterior face of the recellularized lamin at195 μm, 6 months after the surgery.

number of cells increased slightly, and all the patients showed a few number of cells similar to keratocytes, some of them presenting with dendritical shapes. Six and twelve months after the operation, the number of cells that colonized the laminas was higher in the recellularized laminas than in the decellularized ones (Figs. 24.53, 24.54, 24.55, and 24.56) [9, 10].

The histology of the anterior and posterior corneal stroma showed a very high number of keratocytes [10], similar to that in a normal cornea (Figs. 24.57 and 24.58). Results derived from the anterior stroma (P = 0.008) and posterior stroma (P = 0.008) showed a statistically significant increase in the keratocytes' density of the patients from the G2 + G3 (Table 24.2). In addition, we could demonstrate that there was a significant increase in keratocytes within the recellularized lamina more higher in the group 3 than the group 2.

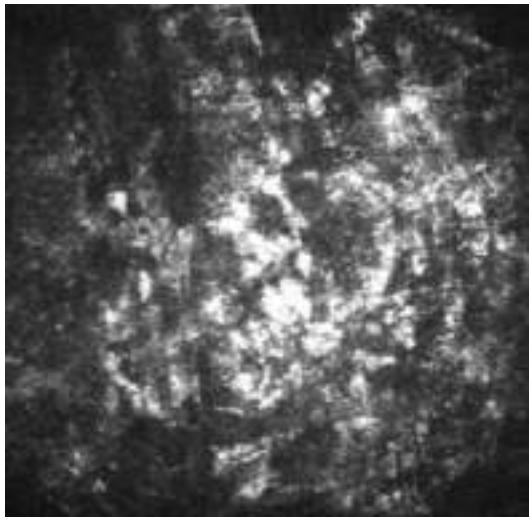

Fig. 24.54 Posterior face of the lamina 6 months post-operation with a high number of keratocytes.

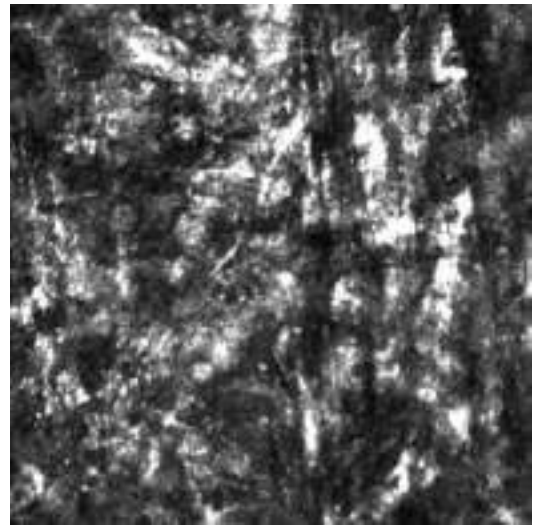

Fig. 24.56 Posterior face of the lamina at 299 μm, 12 months post-operation. It shows a very high number of keratocytes.

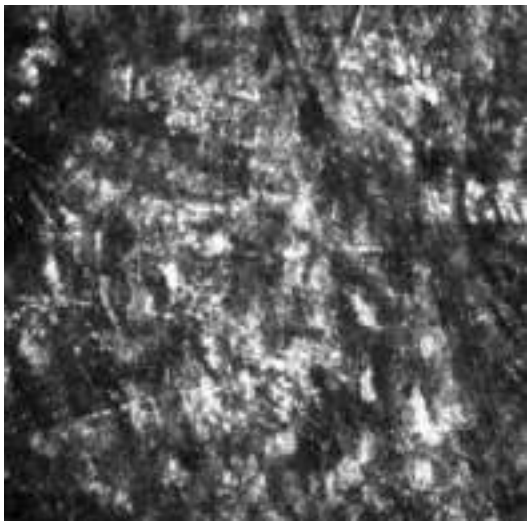

Fig. 24.55 Anterior face of the recellularized lamina at 215 μm 12 months after the surgery.

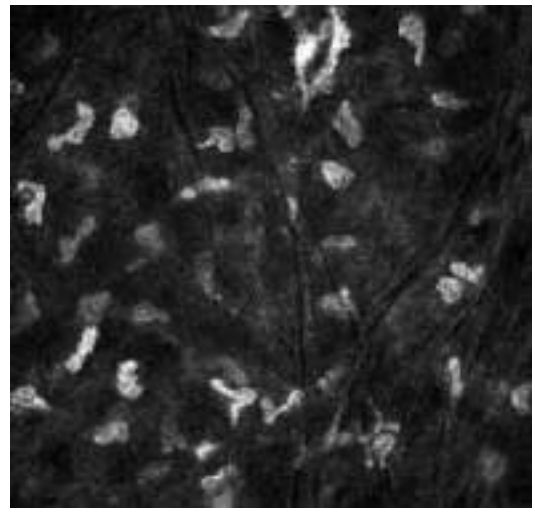

Fig. 24.57 Anterior corneal stroma with abundant keratocytes in a 33-year-old female patient, 12 months after the operation, seen at 106 μm.

24.4 Discussion

These sets of experiments represent the first attempt at using stem cell therapy for human corneal stroma in patients affected by advanced keratoconus.

We have previously reported that after the injection of autologous stem cells (ADASCs) in thestroma of the cornea, there was an increase in the density of corneal keratocytes. This favored the production of new collagen, which resulted in an improved corneal thickness [9]. In addition, this study showed that the implantation of a decellularized lamina, either colonized or not by ADASCs, also produced changes in the corneal topography, thickness, and corneal regularity that may be con- sidered as therapeutic with a potential application to the treatment of keratoconus [9, 10].

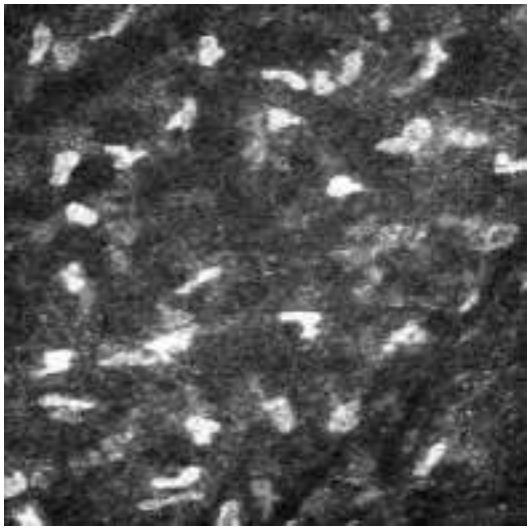

Fig. 24.58 Posterior corneal stroma at 507 μm with high number of keratocytes for the same 33-year-old patient.

In this innovative study, we have reported the outcomes of the use of corneal confocal microscopy for the observation of ADASCs in the selected surgical plane in vivo, which allowed a qualitative and quantitative assessment of them along the experience. Moreover, it allowed moni- toring of the progressive morphological changes that occurred in the decellularized and recellular-ized laminas throughout the observation and assisted in determining the change in the cell densities in the grafted tissue as well as in all the corneal stroma.

Confocal corneal microscopy has shown to be an essential tool in the assessment and "in vivo" follow-up of the corneas implanted with mesenchymal cells for corneal regeneration purposes. Corneal bioconfocal microscopy demonstrates an increase in the cellularity of the anterior and posterior stroma following the implantation of ADASCs into the corneal pockets created using a femtosecond laser.

Relevant changes in the morphology were observed in the implanted cells from the moment of their implantation into the corneal pocket, showing changes from clusters around the individual cells to their development into adult keratocytes. These findings occurred in the anterior, mid, and posterior stroma of the implanted corneas. Moreover, changes inside the acellular lamina were also observed. The decellularized lamina was colonized by the patient's own keratocytes from the first month. After 12 months, the lamina was completely recellularized.

Confocal microscopy of the cornea during the study has been able to show us from the first postoperative month the following findings: accumulations of the mesenchymal cells implanted on the lamina, cell morphological changes have been clearly seen first on the posterior face followed by the anterior face, and the number of cells has increased statistically and significantly between immediately after the surgery and a 12-month period.

Confocal microscopy is considered a noninvasive technique [6]. But difficulties can arise when patients are being examined, especially when the contact between the TomoCap and the cornea of the patient must not cause any harm for the patient. The fragility of the operated cornea is also a concern when examining a patient with the confocal microscope. Before performing the test with the confocal microscope, it is advisable to introduce a silicone hydrogel disposable contact lens, which improves the contact between the eye and the TomoCap. This lens prevents the gel from leaking. In the absence of this lens, the gel dries out with time or dissipates outside the eye. In such case, the examination is interrupted, and additional gel must be reapplied in the eye of the patient. Also, the addition of this lens reduces corneal sensitivity, which allows the patient to keep the eye open for a longer time, which ultimately facilitates the examination process. In addition, sterilization must be maintained throughout the process in order to prevent any contamination in the patient's eye, to reduce error that may hinder the results obtained from the observation, and to preserve the quality of the images obtained by the confocal microscope (Figs. 24.59 and 24.60).

One of the limitations of this study is the method used for counting cells as it was performed with a manual method. Although it was performed by two independent observers in all cases following the same guidelines, this method may introduce a certain amount of subjectivity and interpretation bias. However, this method yields at present moment more accurate

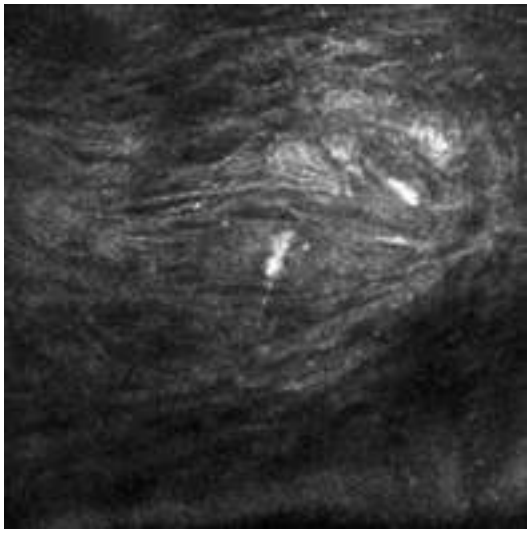

Fig. 24.59 Anterior face of decellularized lamina at 155 μm in a 33-year-old patient, 12 months after the surgery; image taken with silicone hydrogel contact lenses.

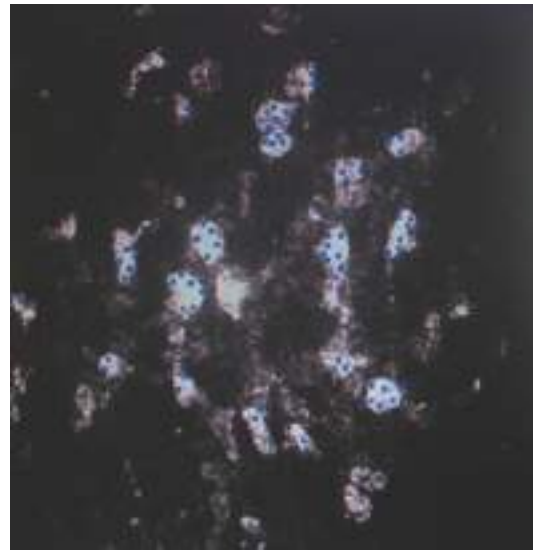

Fig. 24.61 Confocal microscopy automatic cell counting of corneal stroma, from a 33-year-old female with keratoconus at 151 μm seen 12 months after transplantation of ADASCs.

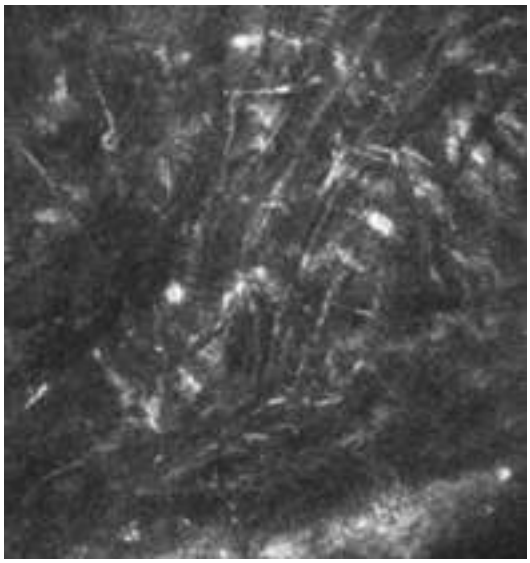

Fig. 24.60 Posterior face of decellularized lamina at 280 μm in a 33-year-old patient, seen 12 months after the surgery; image taken with silicone hydrogel contact lenses.

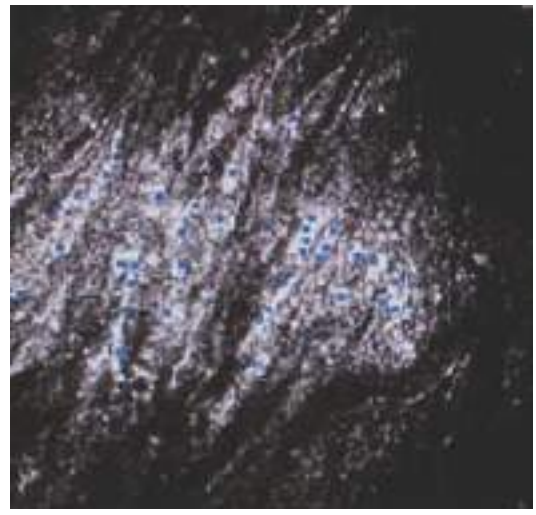

Fig. 24.62 Anterior face of the recellularized lamina at 195 μm of a 35-year-old female, 6 months after the surgery, demonstrates automatic cell counts with high and abnormal number of cells.

results than an automated cell counting microscope which are affected by a large variability and misinterpretations. We performed a refined automatic cell count, and we observed a bias towards high and abnormal number of cells that were counted for the normal structure of the cornea, and a considerable number of cells that should have been counted within the corneal stroma were not accounted for by the device (Fig. 24.61) on both sides of the transplanted lamina (Fig. 24.62). An artifacted result on the lamina's border in the transition zone between the lamina and stroma was seen with this device as well (Fig. 24.63).

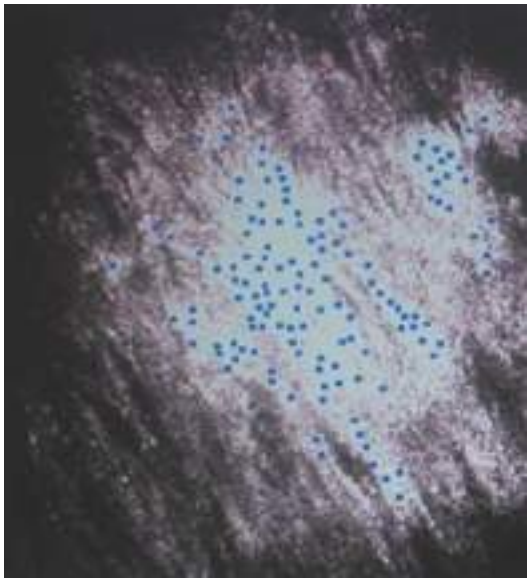

Fig. 24.63 Transition zone at 154 μm between the border of the anterior face of the decellularized lamina and the corneal stroma, 6 months post-operation, for a 31-year-old male, showing highly reflective structures, the blue dots are generated by automatic count cells.

24.5 Future Perspectives

In our study, confocal microscopy was very useful for keratocyte cell counting and determining the evolution of the implanted cells in terms of morphology and densities along the follow-up time of the experience.

Although only 14 patients participated in this study, sufficient statistical significance levels of confidence were obtained that allow us to confirm differences among the clinical groups, which demonstrates the importance of the study established by the confocal microscope. However, it is necessary to increase in future experiences the clinical number of participants in order to strengthen the statistical significances found in the present study.

Further research should be carried out to answer questions like if all morphological changes begin in the posterior stroma and then in the anterior, just as it was observed in our study, which seems to be a specific finding of this investigation.

Comparisons between the recellularized laminas containing Bowman's membrane and decellularized laminas should be made, alongside the growth of keratocytes in the corneal stroma in both types of transplants, and relate it to the improvement of the visual acuity of the operated patients.

Furthermore, comparisons among different morphologies of keratocytes should be established, comparing non-dendritic cells, with others that have a high dendritic shape and investigate the biological implications that such morphological changes may have.

A particular interest has been for the observation of hyper-reflective area, acellular or with very few cells within the corneal stroma studied by the confocal microscope. Further investigation should verify if this fact is due to secondary reactions caused by mechanical manipulation after surgery, or to the formation of new collagen related to the ADASCs implanted in the surgical plan.

Comparisons of studies between different age, sex, and ethnic groups can yield many explanations about prevalence and frequencies in the population. We believe that it is necessary to establish a more objective method of cell counting based on image processing programs, where one can edit the contrast and illumination and use different specialized filters to optimize the visualization of keratocyte cells and to better calculate their size.

In addition, the use of digital cameras capturing at high frames per second and high resolution in the future can reduce the examination time and provide a more reliable measurement of the thickness evolution of the cornea and the newly implanted corneal layers, with fewer errors caused by the movement of the patient's eye. Also, the development of a new TomoCap that has a biconcave or planoconcave silicone hydrogel lens fixated to its top, with the lens made of a specific thickness containing a viscous gel, may shorten and provide more comfort in the confocal exam of the implanted patients. Also, it would be very interesting to have a new RCM objective that can be applied on the eye, while the patient is lying down on his back. This would restrict the patient's body and head movements. In this case, a better fixation of the laser that is projected on the cornea can be made, which can provide better images of the different layers of the cornea and

less error while measuring the pachymetry of the cornea. This innovative biomicroscope objective would allow more comfortable and probably precise study of the confocal cornea microscopy evolution of the experience, as it may allow to study the collagen fibers the implanted laminas as they are added to the collagen matrix structure of the patient's cornea.

Acknowledgments The authors would like to thank Jorge L. Alió del Barrio, MD, PhD; Ziad Abdul Jawad, Od; Peggy Saba, Od; María P. de Miguel, PhD; Nehman Makdissy, PhD; Francisco Arnalich, MD, PhD; and Ibrahim Achkar, MD, for their essential contribution to the clinical and cell biology part of this study.

References

1. Piñero D, Alio J, Barraquer R, Michael R, Jiménez R. Corneal biomechanics, refraction, and corneal aberrometry in keratoconus: an integrated study. Invest Opthalmol Visual Sci. 2010;51(4): 1948.
2. Ku J, Niederer R, Patel D, Sherwin T, McGhee C. Laser scanning in vivo confocal analysis of keratocyte density in keratoconus. Ophthalmology. 2008;115(5):845–50.
3. Alió J. Keratoconus: recent advances in diagnosis and treatment. In: Keratoconus pathology to pathogenesis: Springer; 2017.
4. Alió J, Piñero D, Alesón A, Teus M, Barraquer R, Murta J, et al. Keratoconus-integrated characterization considering anterior corneal aberrations, internal astigmatism, and corneal biomechanics. J Cataract Refract Surg. 2011;37(3):552–68.
5. Mastropasqua L, Nubile M. Normal corneal morphology. In: Confocal microscopy of the cornea. Thorofare: SLACK; 2002.
6. Javadi M, Kanavi M, Mahdavi M, Yaseri M, Rabiei H, Javadi A, et al. Comparison of keratocyte density between keratoconus, post-laser in situ keratomileusis keratectasia, and uncomplicated post-laser in situ keratomileusis cases. A Confocal Scan Study. Cornea. 2009;28(7):774–9.
7. Edmund C. Assessment of an elastic model in the pathogenesis of keratoconus. Acta Ophthalmol. 2009;65(5):545–50.
8. Alió del Barrio J, El Zarif M, de Miguel M, Azaar A, Makdissy N, Harb W, et al. Cellular therapy with human autologous adipose-derived adult stem cells for advanced keratoconus. Cornea. 2017;36(8):952–60.
9. Alió del Barrio J, El Zarif M, Azaar A, Makdissy N, Khalil C, Harb W, et al. Corneal stroma enhancement with decellularized stromal laminas with or without stem cell recellularization for advanced keratoconus. A J Ophthal. 2018;186:47–58.
10. Alió J, Alió del Barrio J, El Zarif M, Azaar A, Makdissy N, Khalil C, et al. Regenerative medicine of the corneal stroma for advanced keratoconus: one year outcomes. (Not published).
11. Guthoff R. Rostock cornea modul. Klinische Monatsblätter für Augenheilkunde. 2005;222(S 3).
12. Wygledowska-Promienska D, Rokita-Wala I, Gierek-Ciaciura S, Piatek-Koronowska G. The alterations in corneal structure at III/IV stage of keratoconus by means of confocal microscopy and ultrasound biomicroscopy before penetrating keratoplasty. Klin Ocz. 1999;101(6):427–32.
13. Mastropasqua L, Nubile M. Confocal microscopy in keratoconus. In: Confocal microscopy of the cornea. Thorofare: SLACK; 2002.
14. Somdi S, Hahnel C, Slowik C, Richter A, Weiss DG, Guthoff R. Confocal in vivo microscopy and confocal laser-scanning fluorescence microscopy in keratoconus. Ger J Ophthalmol. 1996;5(6):518–25.

10. 10. Alió J.L., **El Zarif M**, Alió del barrio J.L., **Cellular therapy of the corneal stroma: a new type of corneal surgery for keratoconus and corneal dystrophies a translational research experience.** 1st ed. Elsevier. (Accepted in 2020. Ahead of print).

Cellular Therapy of the Corneal Stroma: A New Type of Corneal Surgery for Keratoconus and Corneal Dystrophies

A Translational Research experience

Jorge L. Alió MD, PhD, FEBO [1,2*], Mona Zarif MSc OD PhD[2], Jorge L. Alió del Barrio MD, PhD, FEBOS-CR [1,2]

1. Cornea, Cataract and Refractive Surgery Unit, Vissum Corporación, Alicante, Spain.
2. Division of Ophthalmology, Universidad Miguel Hernández, Alicante, Spain

* Corresponding author

Author address for correspondence and reprint: Dr. Jorge L. Alió MD PhD, Avda de Denia s/n, Vissum, Instituto Oftalmologico de Alicante 03016 Alicante, Spain, Tel. +34 965150025, jlalio@@gmailcom

Conflict of interest

The authors, their families, their employers and their business associates have no financial or proprietary interest in any product or company associated with any device, instrument or drug mentioned in this article. The authors have not received any payment as consultants, reviewers or evaluators for any of the devices, instruments or drugs mentioned in this article.

Funding/Support

This study has been supported in part by the Red Temática de Investigación Cooperativa en

Salud “OFTARED” – Referencia RD16/0008/0012 and by Instituto de Salud Carlos III/Agencia Estatal de Investigación y por el Fondo Europeo de Desarrollo Regional (FEDER) “Una manera de hacer Europa”, SPAIN.

ABSTRACT

Cellular therapy of the corneal stroma, with either ocular or extraocular stem cells, has been gaining a lot of interest over the last decade. Multiple publications from different research groups are showing its potential benefits in relation to its capacity to improve or alleviate corneal scars, improve corneal transparency in metabolic diseases by enhancing the catabolism of the accumulated molecules, generate new organized collagen within the host stroma, and its immunosuppressive and immunomodulatory properties. Autologous extraocular stem cells do not require a healthy contralateral eye and they do not involve any ophthalmic procedures for their isolation. Mesenchymal stem cells have been the most widely assayed and have the best potential to differentiate into functional adult keratocytes *in vivo* and *in vitro*. While embryonic stem cells have been partially abandoned due to ethical implications, the discovery of the induced pluripotent stem cells (iPSC) has opened a new and very promising field for future research as they are pluripotent cells with the capacity to theoretically differentiate into any cell type, with the special advantage that they are obtained from adult differentiated cells. Cellular delivery into the corneal stroma has been experimentally assayed *in vivo* in multiple ways: systemic versus local injections with or without a carrier.

For the first time, Alió et al carried out the first clinical, interventional prospective, consecutive, randomized, comparative series of cases on corneal stroma of 14 patients with advanced keratoconus. The selected patients were divided into 3 experimental groups. Group 1 (G-1) patients underwent implantation of (ADASCs) alone (3x 10^6cells/1 mL) (n = 5).

Group 2 (G-2), patients received decellularized donor corneal stroma lamina with (120 µm thickness) (n =5). Group 3 (G-3), patients received implantation of recellularized donor lamina with (ADASCs) ($1x10^6$cells/1 mL) with direct injecting of ($1x10^6$ cells/1 mL) during the surgery (n = 4), ADASCs were obtained by elective liposuction. Implantation was performed into a femtosecond-assisted 9.5-mm diameter lamellar pocket, under topical anesthesia. Follow-up data of 36 months are obtained, with all the cases no adverse reaction was observed, such as haze, infection, or allogeneic graft rejection. Clinical improvement at 3 years was detected in all cases in their Unaided distance visual acuity (**UDVA**), corrected distance visual acuity (**CDVA**), Refractive sphere (**Rx Sphr**) (D). Meanwhile, refractive cylinder (**Rx Cyl**) (D) presented a few deterioration regarding the preoperative mean values. Also, an increased in mean values of OCT-Visante: Central corneal thickness (**Visante CCT**) (µm), Pentcam Thinnest point (**Thinnest point**) (µm) and Cornea Volume (**CV**) (mm^3) was obtained at 3 years concerning the preoperative mean values. As well third order aberration RMS (**3rd order RMS**) (µm), fourth order aberration RMS (**4th order RMS**) (µm), high order aberration RMS (**HOA RMS**) (µm) and Low order aberration RMS (**LOA RMS**) (µm) showed an improvement in mean values with all the groups.

In conclusion, advanced stem cellular therapy with implantation of autologous ADASCs, decellularized human corneal stroma, showed initially to be potentially effective for the treatment of advanced keratoconus. At the light of the present evidence available, it can be said that the era of corneal stromal regeneration therapy has been already started.

Key Words: stem cells, regenerative medicine, corneal transplant, decellularized cornea, cornea, corneal stroma, cellular therapy, MSC, mesenchymal stem cells, corneal surgery, corneal transplantation.

1. BACKGROUND: FROM THE LAB TO THE PATIENT

The stroma constitutes more than 90% of the corneal thickness. Many features of the cornea, including its strength, morphology and transparency are attributable to the anatomy and properties of the corneal stroma (1). Many diseases such as corneal dystrophies, scars or ectatic disorders induce a distortion of its anatomy or physiology leading to loss of transparency and subsequent loss of vision. In the last decade, enormous efforts have been put into replicating the corneal stroma in the laboratory to find an alternative to classical corneal transplantation, but this has still not been accomplished due to the extreme difficulty in mimicking the highly complex ultrastructure of the corneal stroma, obtaining substitutes that either do not achieve enough transparency or strength (2, 3).

In the last few years, interest for cellular therapy of the corneal stroma using mesenchymal stem cells (MSCs) from either ocular or extraocular sources has gained a lot of interest; studies show that MSCs are capable of differentiating into adult keratocytes *in vitro* and *in vivo* (1). Several authors, including reports from our research group, have demonstrated (4-6) that these stem cells can not only survive and differentiate into adult human keratocytes in xenogeneic scenarios without inducing any inflammatory reaction, but also: i) produce new collagen within the host stroma (4,7), ii) modulate preexisting scars by corneal stroma remodeling (8,9), and iii) improve corneal transparency in animal models for corneal dystrophies by collagen reorganization as well as in animal models for metabolopathies by the catabolism of accumulated proteins (10-13). Mesenchymal stem cells have also shown immunomodulatory properties in syngeneic, allogeneic and even xenogeneic scenarios (13, 14). The first clinical data regarding the safety and preliminary efficacy of cellular therapy of the corneal stroma from Phase 1 human clinical trials is now available (15 , 16), which may end up providing a real alternative treatment option for corneal diseases in the near future.

Considering existing scientific evidence, it seems that all types of MSCs have similar behavior *in vivo* (Table 1), and thus are able to achieve keratocyte differentiation and modulate the corneal stroma with immunomodulatory properties (17). It has also been recently reported that MSCs secrete paracrine factors such as vascular endothelial growth factor (VEGF), platelet-derived growth factor (PDGF), hepatocyte growth factor (HGF), and transforming growth factor beta 1 (TGFβ1). Although the precise actions of the different growth factors for cornea wound healing are not fully understood, overall, they seem to promote cell migration, keratocyte survival by apoptosis inhibition, and upregulate the expression of extracellular matrix (ECM) component genes in keratocytes, subsequently enhancing corneal re-epithelialization and stromal wound healing (18). MSCs can be obtained from many human tissues, including adipose tissue, bone marrow, umbilical cord, dental pulp, gingiva, hair follicle, cornea and placenta (19, 20).

Table 1: Stem cells assayed for corneal stroma regeneration: evidence of keratocyte or keratocyte-like differentiation and their potential autologous application.

	CSSC	**BM-MSC**	**ADASC**	**UMSC**	**ESC**	**iPSC**
Keratocyte differentiation *in vitro* demonstrated	Yes	Yes	Yes	Yes	Yes	Yes
Keratocyte differentiation *in vivo* demonstrated	Yes	Yes	Yes	Yes	No	No
Possible autologous use	Yes/No	Yes	Yes	Yes/No	No	Yes

CSSCs, corneal stroma stem cells; **MSC**, mesenchymal stem cell; BM, bone marrow; **ADASC**s, adipose-derived adult stem cell; **UMSC**, umbilical MSC; **ESC**, embryonic stem cell; **iPSC**, induced pluripotent stem cell.

Corneal stroma stem cells (CSSCs) are a promising source for cellular therapy as the isolation technique and culture methods have been optimized and refined (21); presumably, they should be efficient in differentiating into keratocytes as they are already committed to the corneal lineage. On the other hand, isolating CSSCs autologously is more technically demanding considering the small amount of tissue that they are obtained from. Furthermore, this technique still requires a contralateral healthy eye, which is not always available (bilateral disease). Therefore, these drawbacks may limit its use in clinical practice. Allogeneic CSSC use requires living or cadaveric donor corneal tissue.

Human adult adipose tissue is a good source of autologous extraocular stem cells as it satisfies many requirements: easy accessibility to the tissue, high cell retrieval efficiency and the ability of its stem cells (h-ADASCs) to differentiate into multiple cell types (keratocytes, osteoblasts, chondroblasts, myoblasts, hepatocytes, neurons, etc) (4). This cellular differentiation occurs due to the effect of very specific stimulating factors or environments for each cell type, avoiding the mix of multiple kinds of cells in different niches.

Bone marrow MSCs (BM-MSCs) are the most widely studied MSCs, presenting a similar profile to ADASCs, but their extraction requires a bone marrow puncture, which is a complicated and painful procedure requiring general anesthesia.

Umbilical MSCs (UMSCs) present an attractive alternative, but their autologous use is currently limited as the umbilical cord is not generally stored after birth.

Embryonic stem cells have great potential, but also present important ethical issues. However, the use of iPSC technology (22) could solve such problems, and their capability to generate adult keratocytes has already been proven *in vitro* (23).

Finally, it is important to remark that the therapeutic effect of MSCs in a damaged tissue is not always related to the potential differentiation of the MSCs in the host tissue as multiple

mechanisms might contribute simultaneously to this therapeutic action for example, secretion of paracrine trophic and growth factors capable of stimulating resident stem cells, reduction of tissue injury and activation of immunomodulatory effects, in which case the direct cellular differentiation of the MSCs might not be relevant and could even be non-existent (17, 24-25).

We will review the different types of stem cells (mesenchymal and others) that have been proposed for the regeneration of the corneal stroma as well as the current *in vitro* or *in vivo* evidence. Finally, we will review the different surgical approaches that have been suggested (*in vivo*) for the application of stem cell therapy to regenerate the corneal stroma.

2. TRANSLATIONALITY TO A NEW TYPE OF ADVANCED CORNEAL THERAPY

2.1 Stem Cell Sources used for Corneal Stroma Regeneration.

2.1.1 Bone Marrow Mesenchymal Stem Cells (BM-MSCs).

Park et al reported that human BM-MSCs differentiate *in vitro* into keratocyte-like cells when they are grown in specific keratocyte differentiation conditions (26). They demonstrated a strong expression of keratocyte markers such as lumican and ALDH (aldehyde dehydrogenase) along with the loss of expression of MSC markers such as α-smooth muscle actin. However, they could not demonstrate an evident expression of keratocan on these differentiated cells (26). Trosan et al showed that mice BM-MSCs cultured in corneal extracts and insulin-like growth factor-I (IGF-I), efficiently differentiate into corneal-like cells with expression of corneal specific markers, such as cytokeratin 12, keratocan, and lumican (27). The survival and differentiation of human BM-MSCs into keratocytes has also been

demonstrated *in vivo* when these cells are transplanted inside the corneal stroma. Keratocan expression was observed without any sign of immune or inflammatory response (28).

2.1.2 Adipose-derived Adult Mesenchymal Stem Cells (ADASCs).

Human ADASCs (h-ADASCs) cultured *in vitro* (Fig. 1 A, 1B) under keratocyte differentiation conditions express collagens and other corneal-specific matrix components. This expression is quantitatively similar to that achieved by differentiated h-CSSCs (29).

The differentiation of h-ADASCs in functional human keratocytes has also been demonstrated *in vivo*, for the first time, in a previous study by our group using the rabbit as a model (4). These cells, once implanted intrastromally, express not only collagens type I and VI (the main components of corneal extracellular matrix), but also keratocyte specific markers such as keratocan or ALDH, without inducing an immune or inflammatory response. These findings were later reproduced and confirmed by other authors in several research papers (17).

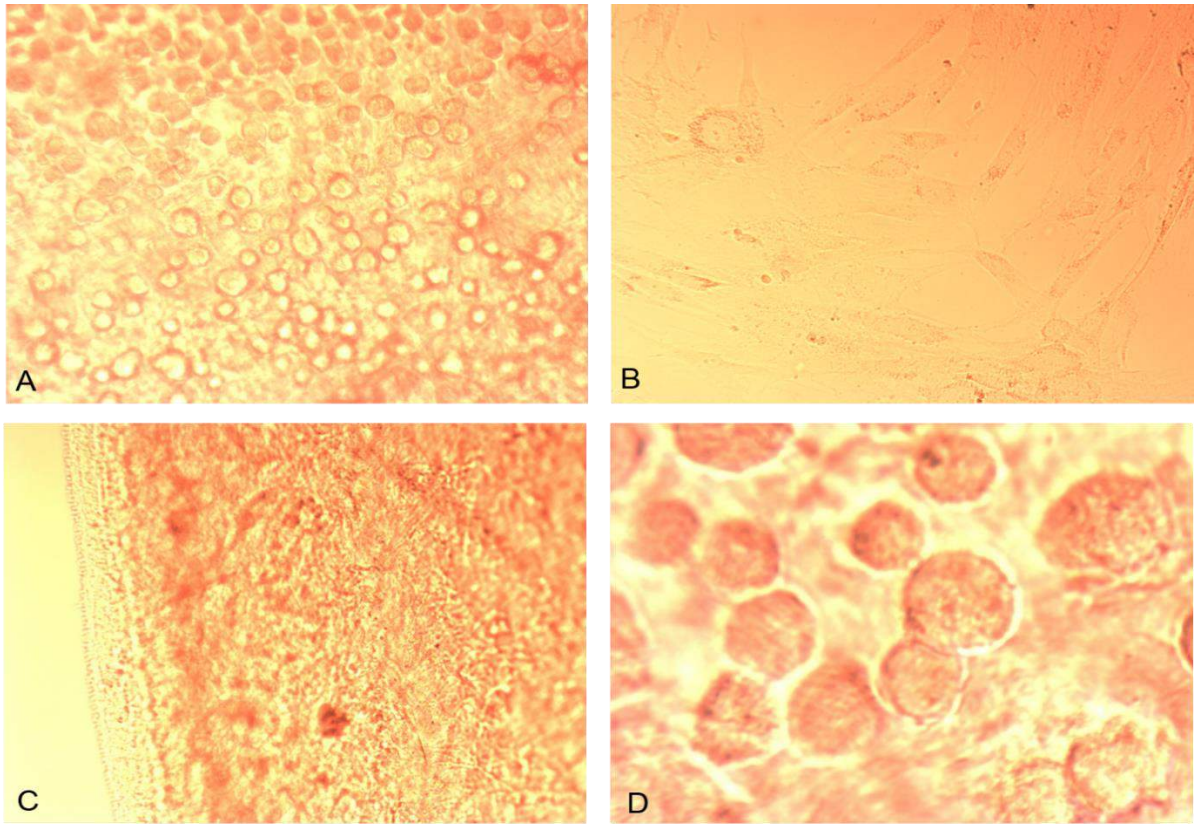

Figure 1. (A) Microscopic appearance (phase-contrast photograph) of human ADASCs (10× magnification). **(B)** Human ADASC in culture. **(C)** Decellularized human corneal lamina (10 X magnification). **(D)** Recellularized human cornal lamina with ADASCs (0.5 × 10^6 cells were cultured on each side of the laminas) (10× magnification).

2.1.3 Umbilical Cord Mesenchymal Stem Cells (UCMSCs).

Human MSCs isolated from neonatal umbilical cords have exhibited similar differentiation behavior to other types of MSCs when transplanted inside the corneal stroma *in vivo*, expressing keratocyte-specific markers such as keratocan without inducing immune or rejection responses (30). Liu et al reported that the injection of these cells inside the corneal stroma of lumican null mice improved corneal transparency and increased stromal thickness with a reorganized collagen lamellae, and also improved host keratocyte function through enhanced expression of keratocan and ALDH in these mice (11). These data are encouraging, although to date, autologous use of UCMSCs is not possible as the umbilical cord from new births is not generally stored.

2.1.4 Embryonic Stem Cells (ESCs).

Current experience with these human pluripotent stem cells for the corneal stroma regeneration is much more limited. Chan et al reported that differentiation of these cells into a keratocyte lineage can be induced *in vitro,* demonstrating an upregulation of keratocyte markers including keratocan (31).

To the best of our knowledge, no *in vivo* studies with these cells have been performed in the field of regenerative medicine for the corneal stroma. The use of these cells also raises many ethical issues, and together with the lack of *in vivo* data, discourages their current use in a clinical setting.

2.1.5 Induced Pluripotent Stem Cells (iPSCs).

As already discussed, the use of embryonic stem cells has been partially abandoned because of ethical concerns and especially since the discovery of iPSCs (22), which are derived from adult cells. In 2012, Shinya Yamanaka from Japan and John B. Gurdon from the UK received the Nobel Prize for Medicine for discovering that mature, specialized cells can be reprogrammed to an immature or stem cell state and then redirected to the required cell lineage using specific factors and environmental stimuli. iPSCs promise to be the future of tissue and cellular engineering.

Regarding their application in the regeneration of the corneal stroma, human iPSCs have shown the capability to differentiate into neural crest cells (the embryonic precursor to keratocytes). By culturing them on cadaveric corneal tissue, it promotes their keratocyte differentiation by acquiring a keratocyte-like morphology to express markers similar to corneal keratocytes (23). It has also been shown that iPSC-derived MSCs exert immunomodulatory properties in the cornea similar to those observed with BM-MSCs (32).

To the best of our knowledge, no studies have been published reporting the capability of iPSCs to differentiate into adult keratocytes *in vivo* in the animal model.

2.1.6 Corneal Stromal Stem Cells (CSSCs).

The limbal palisades of Vogt form a niche that contains both limbal epithelial stem cells (LESCs) and corneal stromal stem cells (CSSCs) (33). CSSCs express genes typical of descendants of the neural ectoderm such as PAX6, adult stem cell markers such as ABCG2 and MSC markers such as CD73 and CD90 (33, 34). They exhibit clonal growth, self-renewal properties and a potential for differentiation into multiple distinct cell types. Unlike keratocytes, human CSSCs (h-CSSCs) undergo extensive expansion *in vitro* without losing their ability to adopt a keratocyte phenotype (33, 34). These corneal MSCs have a demonstrated potential for differentiation into corneal epithelium and adult keratocytes *in vitro* (33, 35). When cultured on a substratum of parallel aligned polymeric nanofibers, h-CSSCs produce layers of highly parallel collagen fibers with packing and fibril diameter indistinguishable from that of the human stromal lamellae (36). The ability of h-CSSCs to adopt a keratocyte function has been even more striking *in vivo*. When injected into the mouse corneal stroma, h-CSSCs express keratocyte mRNA and protein, replacing the mouse ECM with human matrix components. These injected cells remain viable for many months, apparently becoming quiescent keratocytes (10).

All these experimental data have raised interest in this novel cell-based therapy for corneal stromal diseases, however, before its application in clinical practice, its efficacy and safety need to be well proven in human clinical trials, while other limitations such as the high laboratory costs and potential therapeutic efficacy differences among different donors have to be given serious consideration.

2.2 Corneal Stroma Regeneration Techniques: Early Application in the Clinical Practice.

All these types of stem cells have been used in various ways in several research projects in order to find the optimal procedure to regenerate the human corneal stroma. Corneal MSC implantation has been assayed and studied by direct intrastromal transplantation or after implantation from the ocular surface, intravenously and the anterior chamber where cellular migration within the stroma is to be expected. Different cellular carriers have been analyzed in order to enhance the potential benefits of this therapy.

2.2.1 Ocular Surface Implantation of Stem Cells.

Surface implantation of MSCs would be the optimal approach for ocular surface reconstruction and corneal epithelium/limbal stem cell niche regeneration (not the aim of this review). However, surface implantation of MSCs would still play a role in the prevention or modulation of anterior stromal scars after an ocular surface injury (like a chemical burn). As discussed previously, MSCs secrete paracrine factors that enhance corneal re-epithelialization and stromal wound healing (18). Thus, the benefit of MSCs on the ocular surface may be more justified by these paracrine effects rather than by direct differentiation of the MSCs into epithelial cells, as the evidence for the latter is controversial. In this respect, Di et al assayed *subconjunctival injections* of BM-MSCs in diabetic mice and reported an increased corneal epithelial cell proliferation as well as an attenuated inflammatory response mediated by tumor necrosis factor-α-stimulated gene 6 (TSG6) (37).

Holan et al suggested MSC application on the ocular surface using *nanofiber scaffolds*. They reported that BM-MSCs grown on these scaffolds can enhance re-epithelialization, suppress neovascularization and local inflammatory reaction when applied on an alkali-injured eye in a rabbit model, and these results were comparable to those obtained with limbal epithelial stem cells, and both were better than those obtained with ADASCs (38). The same group

suggested that these results can be improved when these nanofiber scaffolds seeded with rabbit BM-MSCs are covered with cyclosporine-A (CSA) loaded nanofiber scaffolds, observing an even greater scar suppression and healing results with the combination of both nanofibers (MSC and CSA) (39).

Topical application of a suspension of autologous ADASCs has been reported in an isolated clinical case report where authors describe the healing of a neurotrophic ulcer that is not responsive to conventional treatment (40). The lack of further scientific evidence for this delivery method since 2012 raises questions about its real efficacy.

Finally, Basu et al suggested the delivery of MSCs using *fibrin glue* (21). They resuspended CSSCs in a solution of human fibrinogen, and this was added onto a wounded ocular surface with thrombin on the wound bed. Subsequently the fibrinogen gels. Using this application, they demonstrated the prevention of corneal scarring in the mouse model together with the generation of new stroma with a collagen organization indistinguishable from that of native tissue. Currently, this group is enrolled in a clinical trial to validate these findings, using autologous and heterologous CSSCs from limbal biopsies for cases of chemical burns, neurotrophic ulcers and established scars. Preliminary report showed an improvement in visual parameters, corneal epithelization, corneal neovascularization and corneal clarity (41).

2.2.2 Intrastromal Implantation of Stem Cells Alone.

Direct *in vivo* injection of stem cells inside the corneal stroma has been assayed in some studies, demonstrating the differentiation of stem cells into adult keratocytes without signs of immune rejection. In our study, we also demonstrated the production of human ECM by immunohistochemistry when h-ADASCs were transplanted inside the rabbit cornea (Fig. 1A, 1B) (Fig. 2A-2B) (4). As expected, collagen types I and VI were found to be expressed in the rabbits' corneal stroma as well as in the transplanted h-ADASCs; collagen types III and IV,

not normally expressed in the corneal stroma, were not detected either in the host corneal stroma or in the transplanted h-ADASCs (Fig. 2C). Du et al (10) reported restoration of corneal transparency and thickness in lumican null mice (thin corneas, haze and disruption of normal stromal organization) three months after intrastromal transplant of human CSSCs. They also confirmed that human keratan sulphate was deposited in the mouse stroma and the host collagen lamellae were reorganized, concluding that delivery of h-CSSCs to the scarred human stroma may alleviate corneal scars without requiring surgery (10). Very similar findings were reported by Liu et al who utilized h-UMSCs using the same animal model (11). Coulson-Thomas et al found that, in a mouse model for mucopolysaccharidosis, transplanted h-UMSCs participate both in extracellular glycosaminoglycans (GAG) turnover and enable host keratocytes to catabolize accumulated GAG products (12).

Recently, our group has published the first clinical trial in which the preliminary safety and efficacy of the cellular therapy of the human corneal stroma is reported (15, 42). In this pilot clinical trial, we implanted autologous ADASCs (obtained by elective liposuction) in a mid-stroma femtosecond laser-assisted lamellar pocket in patients with advanced keratoconus (Fig. 1A, 1B). No signs of inflammation or rejection were observed, confirming all previous evidence reported in the animal model (15, 42).

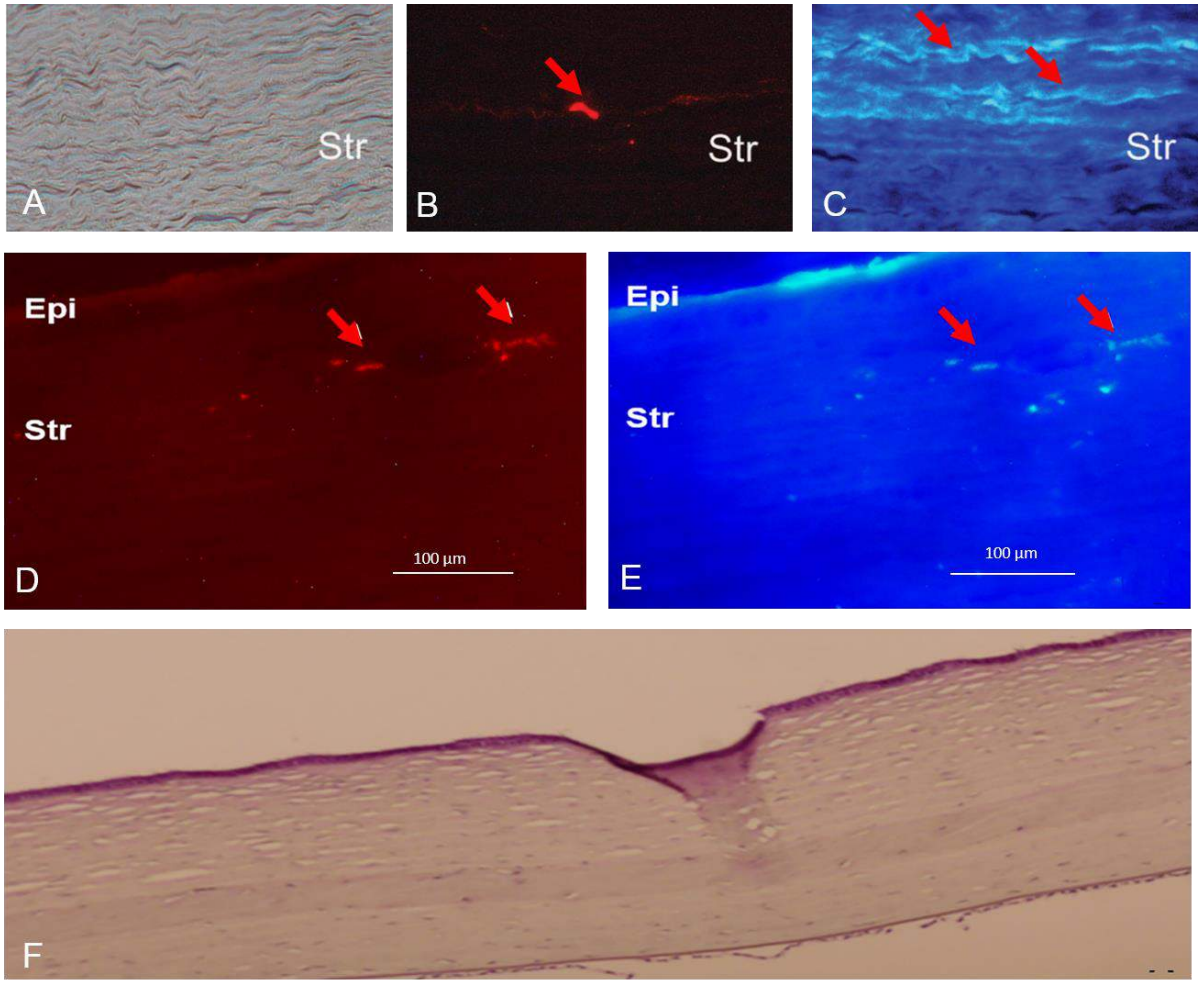

Figure 2. (A, B, C) Transplantation of human ADASCs into the thickness of the rabbit stroma in vivo. **(A)** Phase contrast photo showing a morphologically intact stroma 3 months after transplantation. **B)** Same section showing the survival of the implanted cells by detecting the Vybrant CM-DiL dye (red arrow). (**C)** Same section showing the expression of new human type I collagen inside the rabbit stroma (Str: stroma; magnification, 400X) (red arrows. Abbreviation: Str: storma **(D, E, F)** Corneal stroma enhancement with decellularized human corneal stroma with h-ADASC recellularization in the rabbit animal model. **(D)** Human cells (red arrows), labelled with CM-DiI, around and inside the implant confirming the presence of living human cells inside the rabbit corneal stroma. **(E)** Same section showing human keratocan and their eventual differentiation into human keratocytes (red arrows) (magnification 400 X); abbreviation: Epi: epithelium. **(F)** Hematoxylin-eosin staining of a rabbit cornea with an implanted graft of decellularized human corneal stroma with h-ADASC colonization; (magnification 200 X).

2.2.3 Intrastromal Implantation of Stem Cells Together with a Biodegradable Scaffold.

To enhance the growth and development of the stem cells injected into the corneal stroma, transplantation together with biodegradable synthetic ECM has been performed. Espandar et al injected h-ADASCs with a semisolid hyaluronic acid hydrogel into the rabbit corneal

stroma and reported better survival and keratocyte differentiation of the h-ADASCs when compared with their injection alone (Fig. 3 A, 3B) (7). Ma et al used rabbit ADSCs with a polylactic-co-glycolic (PLGA) biodegradable scaffold in a rabbit model of stromal injury wherein they observed newly formed tissue with successful collagen remodeling and less stromal scarring (Fig. 3A-3C) (43). At three months a high extrusion rate of the implant was observed (Fig. 3D, 3E). Initial data show that these scaffolds could enhance stem cell effects on corneal stroma, although further research is required and warranted.

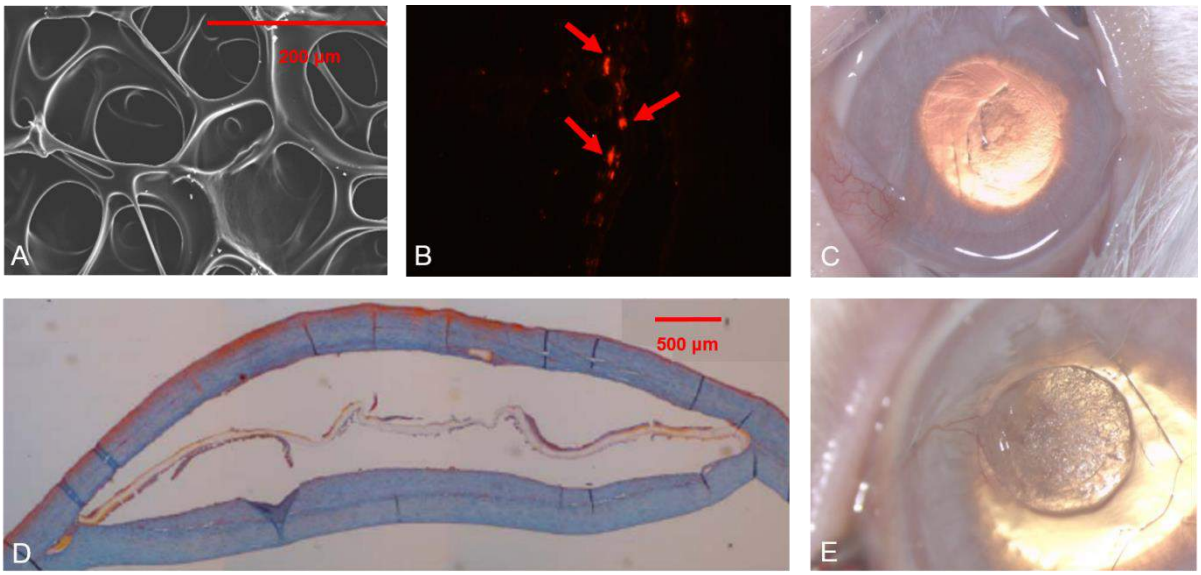

Figure 3. Transplantation of macroporous polyethylacrylate (PEA) membranes together with human ADASC into the rabbit stroma in vivo. **(A)** Electron microscopy image of the PEA. **(B)** ADASC survivors after 3 months (red arrows). **(C)** Intrastromal implant in vivo, note its transparency. **(D)** The absence of a real biointegration leads to the detachment of the sheet of PEA from the surrounding stroma in the histological sections. **(E)** A high extrusion rate of the implant was observed.

2.2.4 Intrastromal Implantation of Stem Cells with a Decellularized Corneal Stroma Scaffold

The complex structure of the corneal stroma has still not been replicated and there are well-known drawbacks to the use of synthetic scaffold-based designs: i) strong inflammatory

responses induced on their biodegradation and ii) nearly all polymer materials cause a nonspecific inflammatory response (44).

Recently, several corneal decellularization techniques have been described, which provide an acellular corneal ECM (Fig. 1C) (45). These scaffolds have gained attention in the last few years as they provide a more natural environment for the growth and differentiation of cells when compared with synthetic scaffolds. In addition, components of the ECM are generally conserved among species and are well tolerated by xenogeneic recipients. Moreover, keratocytes are essential for remodeling the corneal stroma and for normal epithelial physiology (46). This highlights the importance of transplanting a cellular substitute together with the structural support (acellular ECM) to undertake these critical functions in corneal homeostasis. To the best of our knowledge, all attempts to repopulate decellularized corneal scaffolds have used corneal cells (47-49), but as already discussed, these cells have significant drawbacks that limit their autologous use in clinical practice (damage to the donor tissue, lack of cells and more difficult cell subcultures), thus redirecting efforts to find an extraocular source of autologous cells. In a previous study by our group, we showed the perfect biointegration of human decellularized corneal stromal sheets (100 μm thickness) with and without h-ADASC colonization inside the rabbit cornea (Fig 2D-2F) and observed no rejection response despite the graft being xenogeneic (6). We also demonstrated the differentiation of h-ADASCs into functional keratocytes inside these implants *in vivo*, which then achieved their proper biofunctionalization (Fig. 2D, 2E). In our experience, decellularization of the whole (~500 μm) corneal stroma (using sodium dodecyl sulfate anionic detergent) lacks efficacy, as it not possible to completely remove the whole cellular component. However, we demonstrated that this method completely removes the cellular component and preserves the tissue integrity of the corneal stroma when thinner lenticules are treated; a method that has been later confirmed by other authors with the use of electron

microscopy (6, 50-51). Others have also assayed the integration of decellularized pig articular cartilage ECM colonized with mice BM-MSCs in the rabbit corneal stroma and reported similar findings, although the transparency of these decellularized scaffolds was not clearly reported (52).

In our opinion, the implantation of MSCs together with decellularized corneal ECM would be the best technique to effectively restore the thickness of a diseased and severely weakened human cornea because the implantation of MSCs alone only achieves a limited new ECM formation and thickness restoration (4, 15). Moreover, through this technique, and by using autologous MSCs from a given patient, it is theoretically possible to transform allogenic grafts into functional autologous grafts, thus avoiding any risk of rejection. Following this research line, we have recently published the first clinical trial using these decellularized human corneal stroma scaffolds (120 µm thickness and 9.0 mm diameter laminas), with or without autologous ADASC recellularization, in patients with advanced keratoconus (Fig. 1C,1D) (16, 42, 61, 62).

Decellularized tissues have the drawback of requiring specific laboratory equipment, although eye banks could potentially do it and deliver such grafts to different clinical centers. Keratophakia (intrastromal insertion of an allogeneic lenticule) was described by Barraquer in 1964, but was abandoned due to the unpredictability of the refractive outcome and the relatively high frequency of interface haze development (53). The lack of haze observed in our pilot clinical trial could be in relation with the absence of donor keratocytes that could potentially activate postoperatively and generate scar tissue. Moreover, rejection episodes have already been described after the implantation of allogeneic lenticules, a risk that is theoretically avoided by the use of decellularized grafts (51). We should consider that as long as human decellularized tissue is used, there will be no risk for zoonotic diseases.

2.2.5 Anterior Chamber Injection of Stem Cells.

Demirayak et al reported that BM-MSCs and ADASCs, suspended in phosphate-buffered solution (PBS) and injected into the anterior chamber after a penetrating corneal injury in a mouse model, are able to colonize the corneal stroma and increase the expression of keratocyte specific markers such as keratocan, with a demonstrated increase in keratocyte density by confocal microscopy (9). Conversely, the possible side effects of this MSC injection into the anterior chamber for the lens epithelium and trabecullum is highly questionable as it may induce scarring and a subsequent glaucoma. Considering this, the potential clinical use of this approach, in our opinion, is limited.

2.2.6 Intravenous Injection of Stem Cells.

Systemic use, by intravenous injection, of MSCs has also been tested. Intravenous injection of BM-MSCs in mice after an allograft corneal transplant was be able to colonize the transplanted cornea and conjunctiva (inflamed ocular tissues) but not the contralateral ungrafted cornea, simultaneously decreasing immunity and significantly improving allograft survival rate (54). Yun et al recently reported similar findings with the intravenous injection of iPSC-derived MSCs and BM-MSCs after a surface chemical injury, where they observed that the corneal opacity, inflammatory infiltration and inflammatory markers in the cornea were markedly decreased in the treated mice, without significant differences between both MSC types (32). In contrast, our group did not observe any benefit in corneal allograft survival and rejection rates after systemic injection of rabbit ADASCs prior to surgery, during surgery, and at various times after surgery in rabbits with vascularized corneas (model more similar to human corneal transplants than those reported in mice). A shorter graft survival compared with the non-treated corneal grafts was noted (55).

2.3 Autologous versus Allogenic MSC.

A critical question for future clinical trials to further assess the feasibility of cellular therapy of the corneal stroma, is whether the use of autologous MSCs is really necessary and whether allogenic MSCs could achieve the same benefit without any risk of inflammation or rejection. If we consider all published evidence in the animal model where human MSCs were implanted in the corneal stroma, despite being a xenogeneic transplant, no signs of rejection or inflammation have ever been reported (4-13). This coincides with the strong evidence regarding the immunomodulatory and immunosuppressive properties of MSCs, which help them to evade host immune rejection and survive by inhibiting adhesion and invasion, and inducing cell death of inflammatory cells, partially due to a rich extracellular glycocalyx that contains tumor necrosis factor-α-stimulated gene 6 (TSG6) (14, 56). TSG6 has been demonstrated to play a critical role in the immunosuppressive properties exhibited by MSCs (13, 32, 37). Taken together, the use of allogenic MSCs would greatly simplify the clinical application of MSCs, as clinical application centers would not need any specific equipment because potential MSC banks could store and supply stem cells for their use in patients. There are already low-cost systems available that are capable of enhancing the preservation of MSCs at hypothermic temperatures, while maintaining their normal function, thereby widening the time frame for distribution between the manufacturing site and the clinic, and reducing the waste associated with the limited shelf life of cells stored in their liquid state (57). Funderburgh et al recently reported that MSCs from different donors may have different immunosuppressive properties, and consequently, different abilities to regenerate and relieve stromal scars (58). Considering this important finding, the best donors could be selected by MSC banks in order to expand and supply only those MSCs with the highest immunosuppressive and regenerative capacity, so autologous cells would not be necessary. We should also consider that adult keratocytes obtained from autologous MSCs may still

carry the same genetic defect that led to the corneal disease such as in the case of corneal dystrophy. In this scenario, the use of allogenic instead of autologous MSCs would be interesting. A recent study observed gene expression differences between the iPSC-derived keratocytes generated from fibroblasts of both keratoconic and normal human corneal stroma, influencing cellular growth and proliferation, confirming that, at least in keratoconus cases, adult cells obtained from MSCs may still not be functionally normal (59).

2.4 MSC Exosomes.

Exosomes are nano-sized extracellular vesicles that originate from the fusion of intracellular multivesicular bodies with cell membranes and are released into extracellular spaces (56). They have been implicated in the ability of MSCs to repair damaged tissue. Funderburgh et al recently showed that exosomes isolated from the culture media of human CSSCs had similar immunosuppressive properties and also significantly reduced stromal scarring in wounded corneas *in vivo* (60). This finding suggests that for some diseases, such as prevention or reduction of corneal scars, MSC exosomes may provide a non-cell based therapy (58). Zhang et al suggested that exosomes released by transplanted UCMSCs in the diseased cornea are able to enter into host corneal keratocytes and endothelial cells, on the way to enhance their functions (56). Authors experimented *in vitro* using mucopolysaccharidosis VII mice, they discovered that UCMSC-secreted exosomes assisted in the recycling process of accumulated glycosaminoglycans (GAGS) in the lysosomes of diseased cells (12). These findings open an exciting new field for research as the use of exosomes may overcome some of the limitations and risks associated to intrastromal cellular injection, given that exosomes can be potentially applied topically (30).

3. FIRST CLINICAL HUMAN EXPERIENCE IN ADVANCED KERATOCONUS CASES

Recently our group performed the implantation of ADASCs and decellularized/recellularized laminas in 14 patients with advanced keratoconus. This clinical experience open a new and exciting line of therapy for research. As mentioned, the production of new ECM by the implanted MSCs occurs, but is not quantitatively enough to be able to restore the thickness of a severely diseased human cornea (as in extreme keratoconic corneas). Meanwhile the implantation of decellularized/recellularized laminas could restore the corneal thickness and the keratometric parameters. However, the direct injection of stem cells may provide a promising treatment modality for corneal dystrophies, corneal stroma progressive opacification in the context of systemic metabolic disorders, and for the modulation of corneal scarring.

3.1. Study Approval, Design, and Subjects.

This investigation was a prospective consecutive series of cases. The study was conducted in strict adherence to the tenets of the Declaration of Helsinki and it was registered in *ClinicalTrials.gov* (Code: NCT02932852).

Fourteen patients was enrolled in the study, operated within an interval of three month and were randomly distributed into three study groups: Group 1 patients were treated with Autologous ADASC implantation (n = 5 patients); group 2 received decellularized human corneal stroma transplantation (n = 5 patients) and group 3 received autologous ADASC recellularized human corneal stroma transplantation (n = 4 patients).

Thirteen patients attended the clinical follow-up, only one patient from G-1 after the first postoperative month was lost because of inability to attend further follow-up for reasons unrelated to the study.

Inclusion and exclusion criteria's was defined in previous articles (15,16,42,61,62). As well clinical monitoring of the study of the patients was established for safety purposes at 1 week, 1,3,6 ,12 and 36 months for the purpose of the clinical outcomes of the investigation and to observe implant safety for a long time.

3.2 Methodology

3.2.1 Autologous ADASC Isolation, Characterization and Culture.

Patients underwent standard liposuction. Approximately 250 ml of fat mixed with local anesthesia were obtained from each patient. The adipose tissue was processed according to the methods described in the previous articles (Fig. 1A, 1B) (4,63-65).

3.2.2 Laminas.

Human corneal stroma of donor corneas with non-viable endothelium but with negative viral serology was used. The corneas were provided by the eye bank. The quality and safety standards for donation, procurement, testing, processing, conservation, storage and testing of human cells and tissues were followed. Donor corneas were dissected with IntraLase iFS femtosecond laser (AMO, Santa Ana, CA), 2-3 consecutive laminas of 120 (μm) thick and 9.0 mm in diameter were obtained. The decellularization protocol was based on previous publications (Fig. 1C) (6,45,66).Twenty-four hours before implantation, the laminas for patients who received recelularized tissue were placed in tissue culture wells for recelularization with autologous ADASC (0.5×10^6 cells per 1ml of PBS were cultured on each side of the laminas). Than the laminas were submerged in PBS at room temperature and transferred to implantation (Fig. 1D) (16,42,62).

3.2.3 Surgical Procedure:

Autologous ADASC implantation

The method for the implantation of the mecsenchymal stem cells have been previously described (15). Topical anesthesia was used. 60 Khz IntraLase iFS femtosecond laser (AMO Inc, Irvine, CA) was used in single pass mode for the recipient corneal lamellar dissection. An intrastromal laminar cut of 9.5 mm in diameter was created at medium depth of the thinnest preoperative pachymetry point measured by the Visant OCT (Carl Zeiss, Germany). 3 million autologous ADASCs contained in 1 ml PBS were injected into the pocket (Fig. 4A,4B).

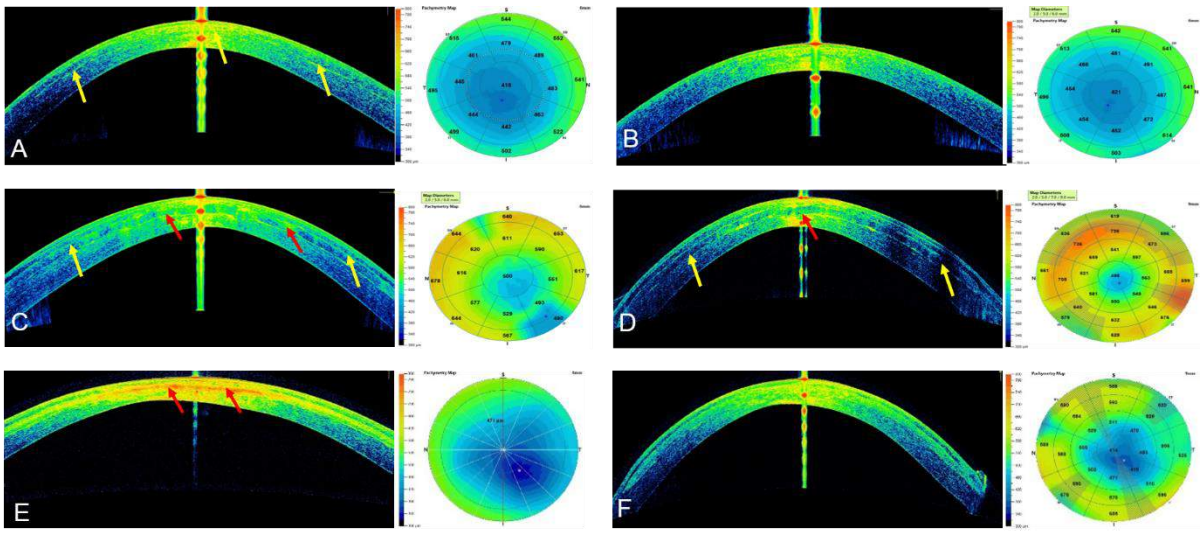

Figure 4. Anterior segment OCT-Visante (Visante **OCT). (A, B**) G-1, case 1. **(A)** At 1 month postoperative, a formation of few neo-collagen in the dissected pocket (yellow arrows) can be seen. **(B)** OCT at 12 months post-op of the case 1, notice the transparency of cornea. Observe the stability of the pachymetric parameters. And the modest improvement **(C,D)** G-2, case 7 **(C)** at 12 months postoperative and **(D)** at 36 post-op. The improvement of the reflective band of neo-collagen in the periphery of the implanted lamina (yellow arrows) can be seen. (red arrows) represent the reflectance of the neo-collagen band. Observe the improvement of the reflectance of this band from 12 months till 3 years postoperative. **(E,F)** G-3, case 11. **(E)** At 1 month post-op. The high reflectance of the neo-collagen band can be seen (red arrow). Capture of the pachymetric map was not very possible. **(F)** At almost 3 years post-op. The enhancement of the integration of the lamina in the host corneal stroma can be observed. The high reflectance of the band of neo-collagen disappeared, an enhancement of the pachymetric map can be noticed.

Lenticule implantation

Topical anesthesia was applied with oral sedation for all surgeries, the 60-kHz IntraLase iFS femtosecond laser was used in single-pass mode. Assisted corneal dissection was done with a 50^0 anterior cut. After opening the corneal intrastromal pocket, the lamina was inserted, centered and unfolded through gentle taping and massaging from the epithelial surface of the host. Also before implantation, a temporary limbal paracentesis was performed to reduce intraocular pressure (Fig. 4C, 4D). In those cases that received a recellularized lamina (G-3) (Fig. 4E, 4F), in order to compensate the cellular damage expected by the implantation process, the pocket was irrigated immediately before and after insertion with a solution containing an additional 1 million autologous ADASc in 1 ml of PBS with a 25G cannula. The incision was then closed with an interrupted 10/0 nylon suture (16, 45).

3.2.4 Postoperative care and follow-up schedule.

Postoperatively, the patients were evaluated monthly in order to record any evidence of subjective discomfort, ocular inflammation or sudden unexpected visual loss. For the purpose of the evaluation of the other clinical parameters, the patients were followed at 1 day, 1 week and at 1,3, 6, 12 and 36 months postoperative unaided distance visual acuity **(UDVA)**, corrected distance visual acuity **(CDVA)**, rigid contact lens visual acuity **(CLVA) in** (decimal equivalent to the logMar sacle). Refractive sphere (**Rx Sphr**) (D) and refractive cylinder (**Rx Cyl**) (D). Anterior segment OCT-Visante: Central corneal thickness (**Visante CCT**) (μm) (Carl Zeiss). Pentacam Thinnest point **(Thinnest point)** (μm), cornea Volume (**CV**) (mm^3) and corneal aberrometry with maximum diameter of 6-mm pupils (Pentacam; Oculus Inc., Wetzlar, Germany): Anterior mean keratometry **(Anterior Km)** (D), maximum keratometry **(Kmax)** (D).

Confocal microscopy up to 12 months postoperative, HRT3 RCM (Heidelberg) with Rostock Cornea Module was used and slit lamp **biomicroscopy**.

3.2.5 Confocal Microscopy study: Methodology of count of cells.

HRT3 confocal microscope with a Rostock Cornea Module RCM (Heidelberg Engineering, Heidelberg, Germany) was used (67). Brightness and contrast was adjusted to 50%. Nuclei cells were selected with the marker of the device and marked in blue, these nuclei were more illuminated and more refringent (Fig. 5A, 5B) (61,68,69,70). **T**he selected nucleus had clear well-defined edges (61,70,71).

The counting of transplanted ADASCs was performed in a similar way of normal keratocytes (Fig. 5C). Meanwhile; when the decellularized (G-2) or recellularized (G-3) laminas appeared without well-defined cell structures, they were considered totally acellular in the defined chosen area (Fig. 6 A). All structures that appeared on the anterior surface, posterior surface and in the mid stroma of the lamina, showing similar morphology to a keratocyte nucleus with well-defined edges were counted as a cell nucleus (Figs. 6B, 7A-7E) (61,70).

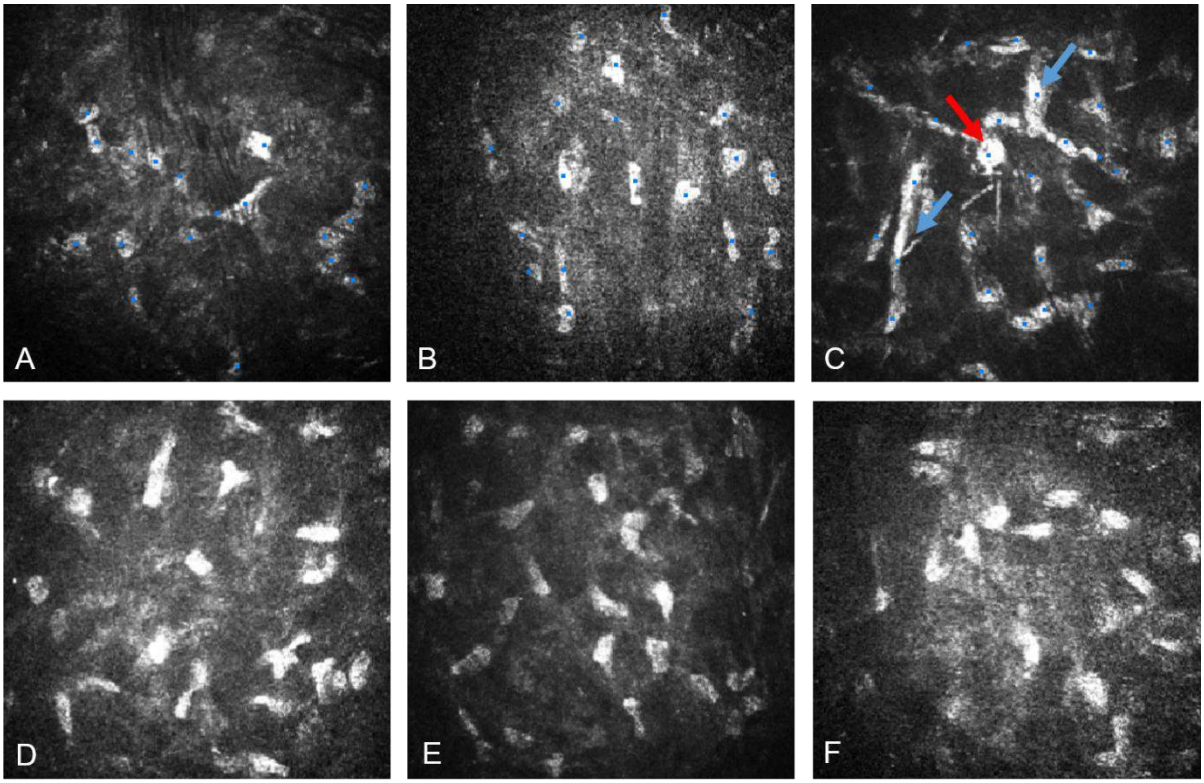

Figure 5. Confocal microscopy findings in G-1 with implantation of ADASCs. **(A, B)** Shows the few number of keratocytes at the Preoperative in case 1. **(A)** Anterior stroma, **(B)** Mid of stroma. **(C)** Confocal microscopy in the surgical plane at 3 months postoperative in case 4, shows the morphology of implanted ADASCs rounded in shape (red arrow) , more refringent and voluminous (blue arrows) . **(D)** Shows the high number of keratocytes in case 1, at 12

months post-op in the mid corneal stoma, with morphology similar to normal corneal cells. **(E, F)** Shows the high number of keratocytes in the anterior and posterior stroma respectively in case 2. Notice the different morphology of keratocytes among the preoperative time and 12 months after surgery.

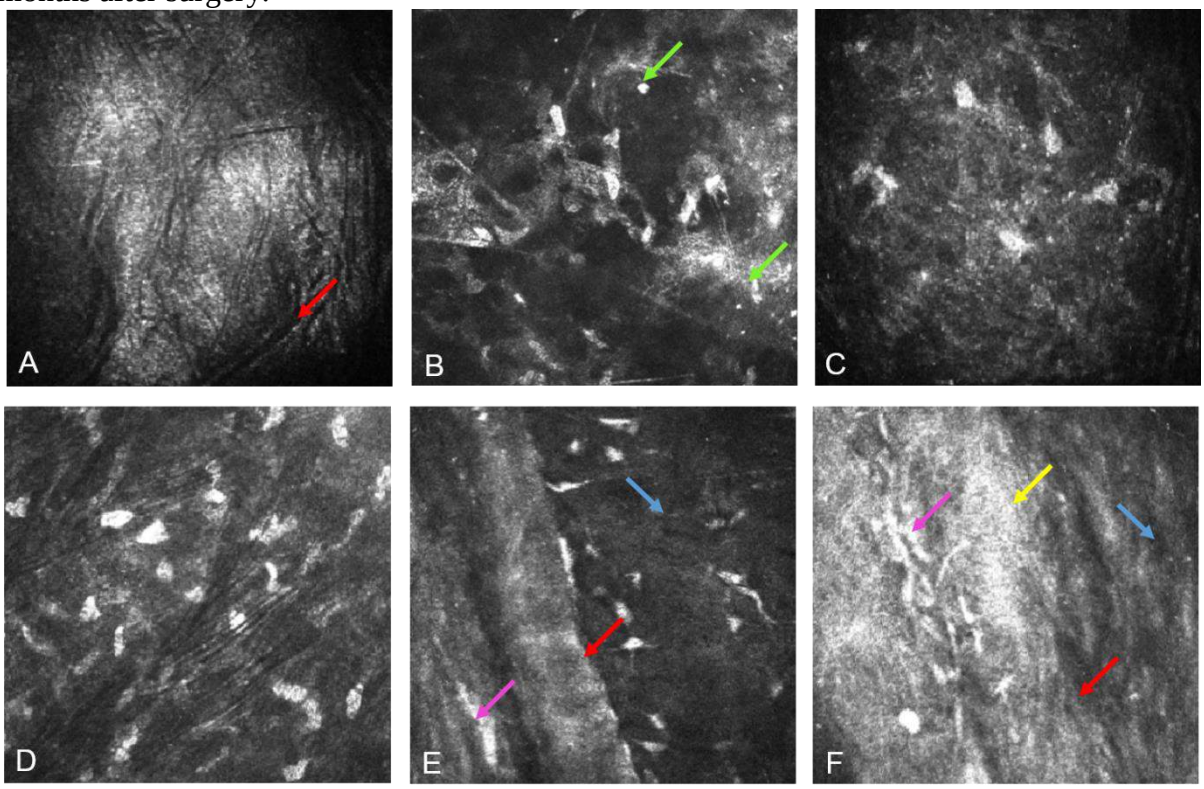

Figure 6. Confocal microscopy findings with implantation of decellularized laminas in G-2. **(A)** Anterior surface of the decellularized lamina in Case 7 at 1 month postoperative. Observe the acellular aspect of the laminas. (**B)** Shows the posterior surface of the decellularized lamina with case 5 at 12 months postoperative with high number of cells type-Keratocytes. (Green arrows) show the presence of highly reflective dots. **(C)** Shows the anterior stoma in case 5 with a very few number of keratocytes at the preoperative**. (D)** Shows the anterior stoma in case 5 with a very high number of keratocytes at 12 months postoperative. Notice the different morphology of keratocytes between **(C)** & **(D). (E, F)** Transition area between the decellularized lamina (red arrows) and the host stroma (blue arrows) in case 7, at 12 months postoperative. Observe the migrating keratocytes (Pink arrows) from the host stroma toward the decellularized implanted tissue. **(E)** Shows the absence of fibrotic tissue on the periphery of the lamina. **(F)** Shows the presence of the fibrotic tissue (yellow arrow).

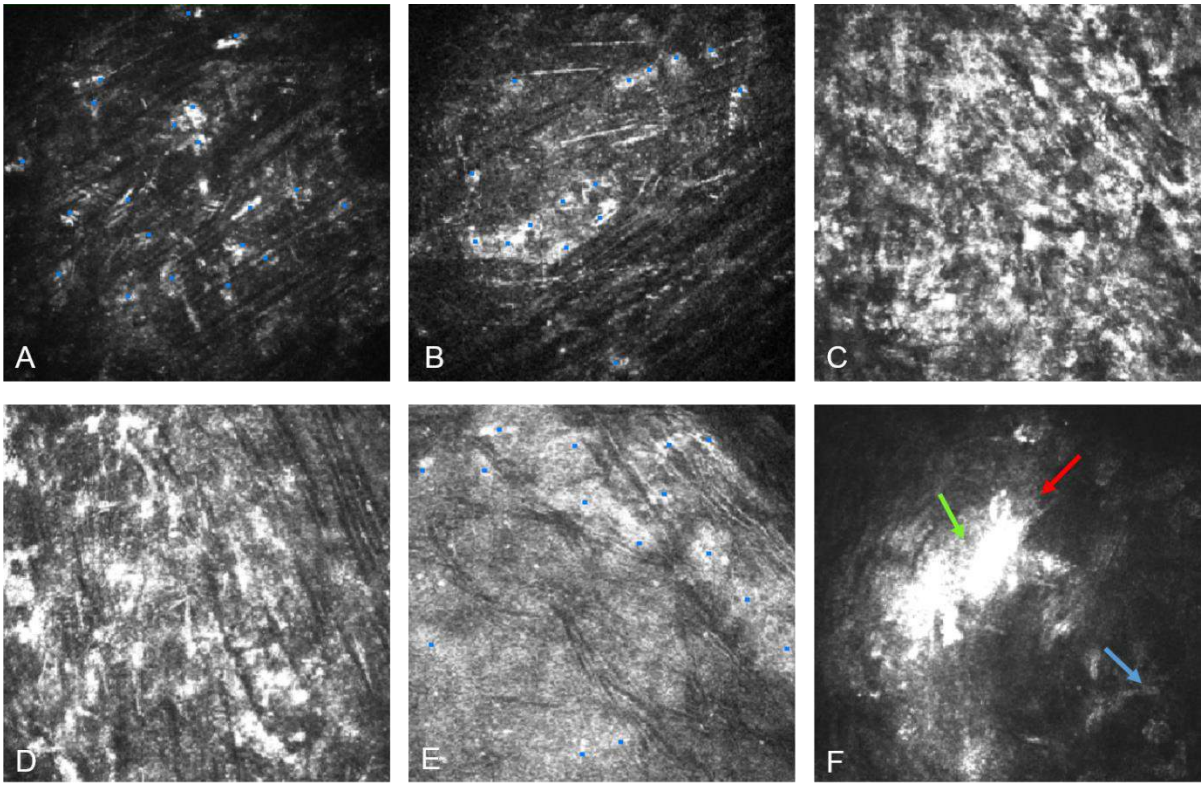

Figure 7. Confocal microscopy findings with implantation of recellularized laminas in G-3. (A,B,C,D) Confocal findings of case 13. (A) Anterior surface of the recellularized lamina at 1 month postoperative. Observe the presence of few ADASCs (marked in blue). (B) Posterior surface of the recellularized lamina 1 month after surgery: Notice the presence of few ADASCs, more similar in morphology to keratocytes. (C) Anterior surface of the recellularized lamina at12 months postoperative: Observe the abundant number of stromal cells. (D) Posterior surface of the recellularized lamina at 12 months after surgery: Observe the high number of stromal cells. (E) Mid stroma of the lamina in case 11 at 12 months postop. Observe the presence of keratocytes (marked in blue). The light gray reflective color of the lamina (yellow arrows) indicates the formation of neocollagen. (F) Transition area between the recellularized lamina (red arrows) and the host stroma (blue arrows) in case 10, at 3 months postoperative. Observe the high refective fibrotic tissue with presence of fibroblasts or myofibroblasts (active state of keratocytes).

4. RESULTS

4.1 Autologous ADASc implantations: Clinical results

No complications were observed during the 3-years follow-up so far. No adverse events such as haze, infection, were encountered. Full corneal transparency was recovered within the first post-operative day in all patients (Figs. 4A, 4B, 8A, 8B). No patient lost lines of visual acuity. All cases presented an improvement in their visual acuity 6,12 and 36 months

postoperative. All cases enhanced 1-2 lines in LogMar scale at 36 months post-operative regarding the preoperative values in their unaided distance visual acuity (**UDVA**), corrected distance visual acuity (**CDVA**) and rigid contact lens visual acuity (**CLVA**). A significant improvement in mean values was recorded comparing G-2 & G-3 with G-1 with all the cases at 36 months postoperative regarding the preoperative mean values, p-values and standard deviation was presented in (Table 2) (62) .

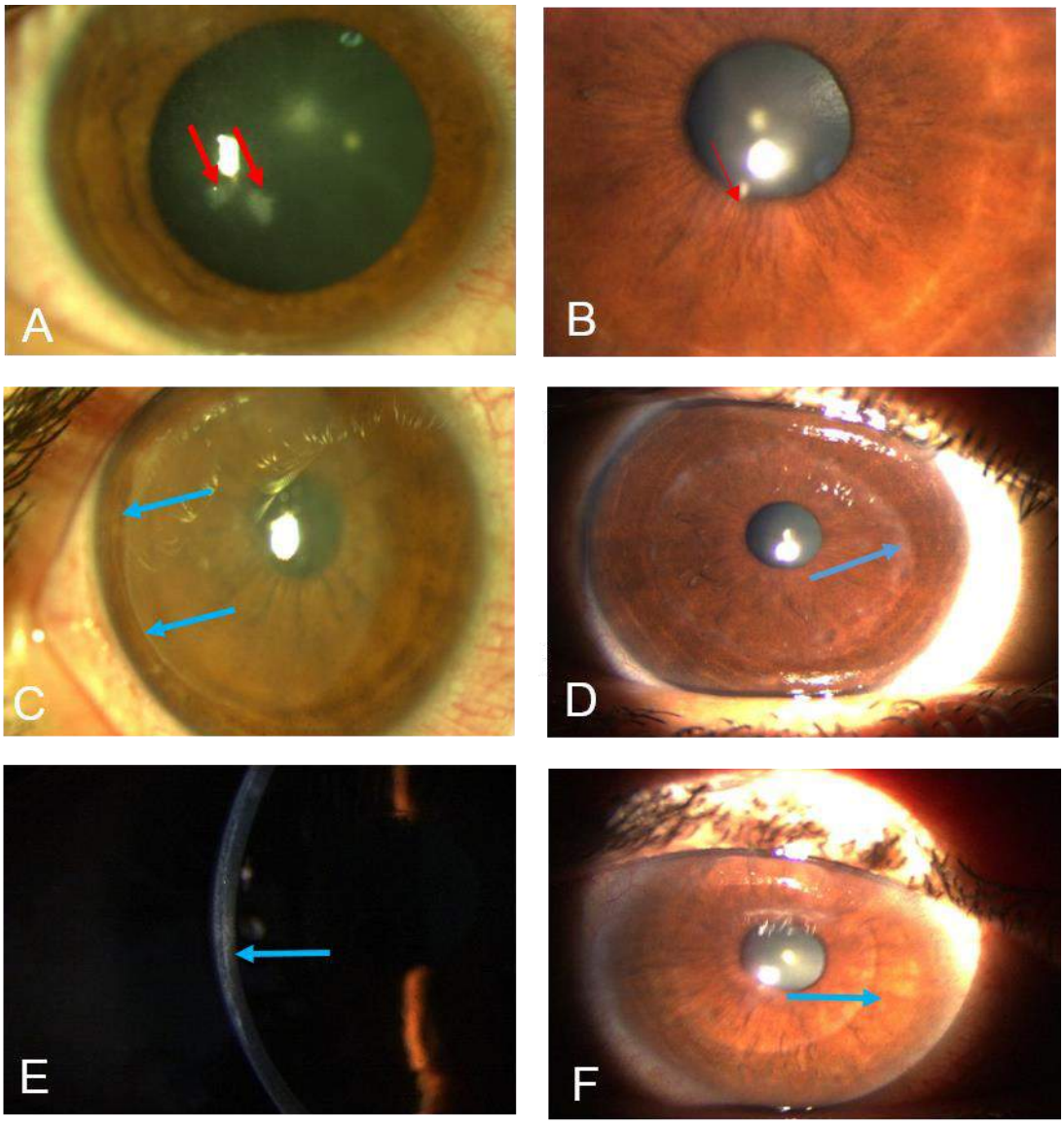

Figure 8. Biomicroscopic changes between the preoperative and up to 36 months post-operative in G-1, G-2 & G-3. **(A)** Case 2, G-1. Observe the presence of paracentral scars (red arrows) at the pre-operative time. **(B)** Case 2, G-1 at 36 months post-op, shows the transparency of the cornea and the marked improvement of the para-central scars (red arrow). **(C)** Case 5, G-2, 1 day post-op, shows the reduced transparency of the implanted lamina,

(blue arrows) represent the border of the lamina. **(D)** Case 5, G-2, 36 months post-op, presents improving of the transparency of the implanted tissue. (Blue arrow) represent the border of the lamina. **(E)** G-3, case 12, at 12 months post-op. The (blue arrow) indicates the implanted recellularized lamina. **(F)** G-3, case 12, at 36 months post-op. The (blue arrow) indicates the periphery of the recellularized lamina. Notice the improvement of the transparency of the implanted tissue.

Table. 2 P values of the results of three years clinical outcomes among G-2 / G-1, G-3 / G-1, G-2 / G-3 and standard deviation (σ) regarding the preoperative time.

	(G-2) / (G-1)	**(G-3) / (G-1)**	**(G-2) / (G-3)**	**σ**
UDVA	[P= 0.054]	[P= 0.069]	[P= 0.986]	0.116
CDVA	[P< 0.001]	[P< 0.001]	[P= 0.900]	0.151
CLVA	[P< 0.001]	[P= 0.090]	[P= 0.010]	0.180
Rx Sphr (D)	[P= 0.892]	[P= 0.863]	[P= 0.747]	2.691
Rx Cyl (D)	[P< 0.001]	[P= 0.014]	[P= 0.086]	0.824
Visante CCT (µm)	[P= 0.012]	[P< 0.001]	[P= 0.055]	62.940
Thinnest point (µm)	[P= 0.007]	[P= 0.001]	[P= 0.465]	67.966
CV (mm^3)	[P< 0.001]	[P< 0.001]	[P= 0.948]	3.757
Kmax (D)	[P= 0.949]	[P= 0.387]	[P= 0.391]	8.250
RMS N=3 (µm)	[P< 0.001]	[P= 0.009]	[P= 0.376]	4.571
RMS N=4 (µm)	[P= 0.074]	[P= 0.817]	[P= 0.004]	2.515
RMS HOA (µm)	[P< 0.001]	[P= 0.038]	[P= 0.091]	4.530
RMS LOA (µm)	[P= 0.617]	[P= 0.870]	[P= 0.491]	27.299

Unaided visual acuity **(UDVA)**, corrected distance visual acuity **(CDVA)**, rigid contact lens visual acuity **(CLVA) in** (decimal equivalent to the logMar sacle). Refractive sphere (**Rx Sphr**) (D) and refractive cylinder (**Rx Cyl**) (D). Anterior segment OCT-Visante: Central corneal thickness (**Visante CCT**) (µm) (Carl Zeiss). Pentacam Thinnest point **(Thinnest point)** (µm), cornea Volume (**CV**) (mm^3). Corneal aberrometry (Pentacam; Oculus Inc., Wetzlar, Germany): Third order aberration RMS **(3^{rd} order RMS)** (µm)**,** fourth order aberration RMS **(4^{th} order RMS)** (µm)**,** high order aberration RMS **(HOA RMS)** (µm) and

Low order aberration RMS **(LOA RMS)** (µm). Anterior mean keratometry **(Anterior Km)** (D), posterior mean keratometry **(Posterior Km)** (D), maximum keratometry **(Kmax)** (D) and Topographic cylinder **(Topo Cyl) (D)** (Pentacam; Oculus Inc., Wetzlar, Germany).

On the other hand the Refractive sphere (**Rx Sphr**) (D) presented a significant improvement at 6,12 and 36 months post-operative regarding the preoperative mean values, meanwhile; refractive cylinder (**Rx Cyl**) (D) remained almost stable till 12 months post-operative followed by a change of 0.5 (D) till 36 months post-operative regarding the pre-operative mean values, p values were presented in (Table 2) (62) .

Results of OCT-Visante: Central corneal thickness (**Visante CCT**) (µm) (Fig. 4A, 4B), Pentcam Thinnest point **(Thinnest point)** (µm) and Cornea Volume **(CV**) (mm^3) (Fig. 9A, 9B), showed a significant increase in mean values, all results was statistically significant better comparing G-2 & G-3 with G-1 at 36 months concerning the preoperative mean values (Table 2) (62).

Also, the mean values in third order aberration RMS **(3^{rd} order RMS)** (µm)**,** high order aberration RMS **(HOA RMS)** (µm) were statistically significant better comparing G-2 & G-3 with G-1, mean values aberration of fourth order aberration RMS **(4^{th} order RMS)** (µm) and Low order aberration RMS **(LOA RMS)** (µm) presented an enhancement at 36 months post-operative regarding the preoperative mean values (Table 2) (**62).**

Additionally, results of anterior mean keratometry (**Anterior Km**) (D) presented an improvement of a mean values of 1 (D) till 12 months post-operative and other 1 (D) at 36 months post-operative regarding the pre-operative mean values. Nevertheless; a flattening in mean values of 2 (D) in maximum keratometry (**Kmax**) (D) was found till 12 months post-operative, followed by 1 (D) till 36 months post-operative regarding the pre-operative mean values, more results were recorded in previous publications (62).

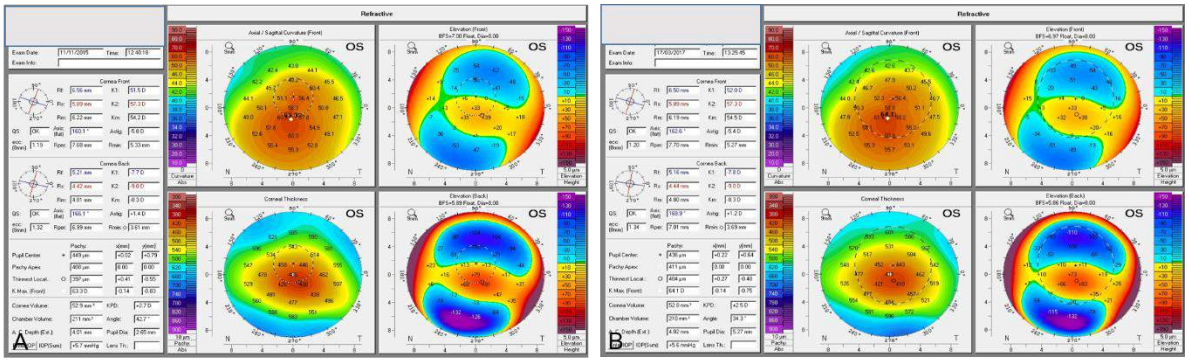

Figure 9. 4 maps corneal topography (Pentacam) comparison between the preoperative in G-1 and 12 months post-op. (A,B) 4 maps Corneal topography (Pentacam), G-1, case 4. (A) At the preoperative (B) 12months post-op, a modest improvement in the pachymetric parameters and almost stability in the Keratometric results can be noticed.

4.2 Results with lamina's implantation: Clinical Results.

No complications was recorded during the 3-years follow-up, with the exception that the implanted laminas showed a mild early haziness during the first postoperative month, this issue was related to a mild lenticular edema. Corneal recovery and full transparency was observed within the third post-operative month in all patients. No adverse events of any type were observed along the 3 years follow up (Figs. 4C-4F, 8C-8F) (62).

All patients with decellularized or recellularized laminas obtained an improvement at 6,12 and 36 months post-operative in mean values regarding the pre-operative values, enhancement results of unaided distance visual acuity (**UDVA**) were up to 0.13 in decimal values nearly equivalent to one line in loghMar scale with decellularized and recellularized laminas, corrected distance visual acuity (**CDVA**) were up to 0.2 with decellularized and recellularized laminas, equivalent to 2 lines in LogMar scale, as well rigid contact lens visual acuity (**CLVA**) mean improvement was up to 0.23 with decellularized and recellularized laminas, nearly equivalent to 2 lines in LogMar sacle. Also mean results of Cornea Volume (**CV**) (mm^3) demonstrated an improvement in mean values of 2-3 (mm^3) in both laminas' groups at 6,12, and 36 months post-operative regarding the pre-operative values (62).

Besides the Refractive sphere (**Rx Sphr**) (D), refractive cylinder (**Rx Cyl**) (D), OCT-Visante: Central corneal thickness (**Visante CCT**) (µm) (Fig. 4C-4F), Pentcam Thinnest point (**Thinnest point**) (µm) (Figs. 10, 11), Third order aberration RMS **(3rd order RMS)** (µm)**,** fourth order aberration RMS **(4th order RMS)** (µm)**,** high order aberration RMS **(HOA RMS)** (µm) (Fig. 12) and Low order aberration RMS **(LOA RMS)** (µm). Anterior mean keratometry (**Anterior Km**) (D) (Figs 10B, 11A) , posterior mean keratometry (**Posterior Km**) (D), maximum keratometry (**Kmax**) (D) and topographic cylinder (**Topo Cyl**) (D) with decellularized and recellularized laminas showed results close to patients' results with implantation of ADASCs (62).

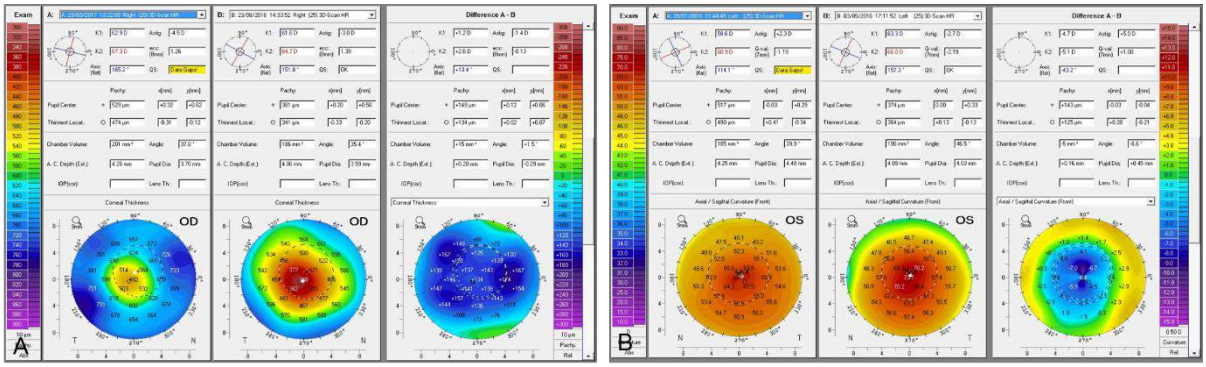

Figure 10. Corneal topography (Pentacam) comparison pachymetric exams between preoperative in G-2, 12 and 36 months postoperative. **(A)** Corneal topography (Pentacam) comparison (right image) among the preoperative (middle image) and almost 12 months postoperative (left image) in patient case 9, G-2. Detect the enhancement of the pachymetric parameters. **(B)** Corneal topography (Pentacam) comparison (right image) among the preoperative (middle image) and almost 3 years post-op (left image), respectively, in patient case 7, G-2. Notice the enhancement of the keratometric parameters**.**

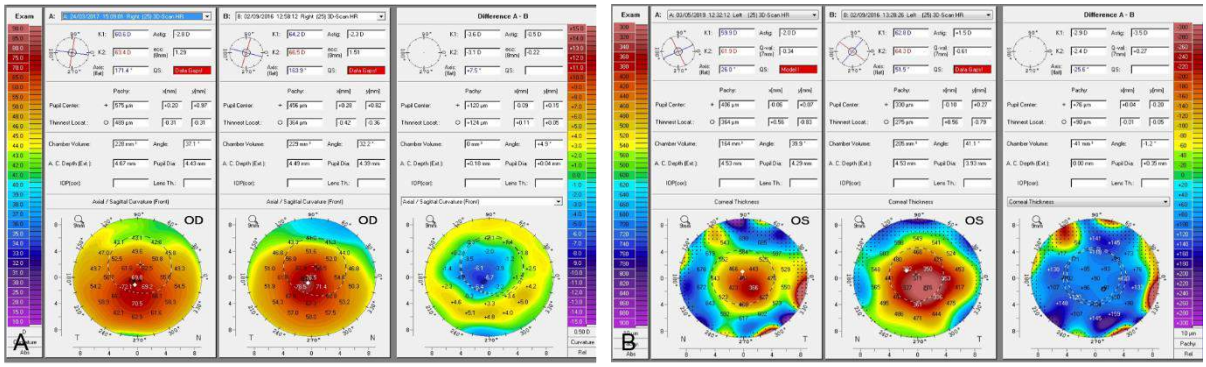

Figure 11. Corneal topography (Pentacam) comparison pachymetric exams between preoperative in G-3, 12 and 36 months postoperative. **(A)** Corneal topography (Pentacam) comparison between preoperative, 12 months in patient case 12, G-3. Notice the enhancement of the keratometric parameters**. (B)** Corneal topography (Pentacam) comparison between preoperative, and almost 3 years post-op, in patient case 12, G-3. Notice the enhancement of the pachymetric parameters**.**

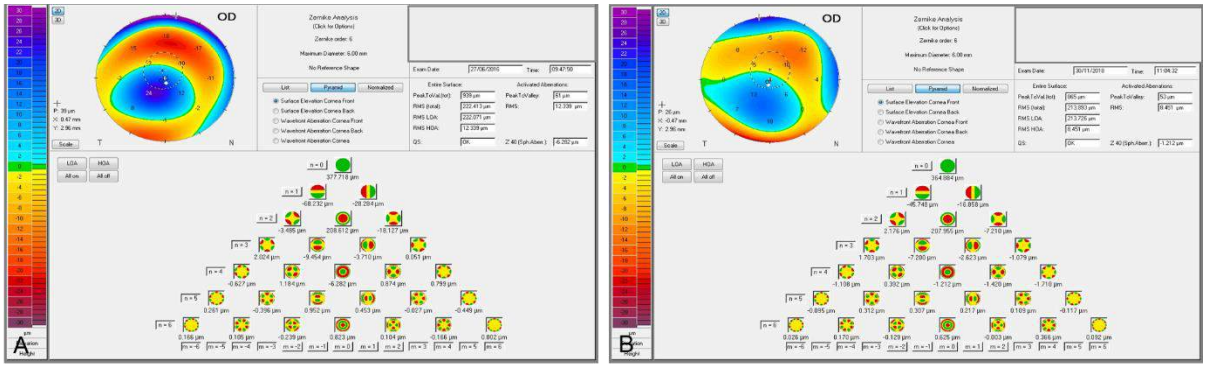

Figure 12. Corneal aberrometries (Pentcam) in G-2, case 5. **(A)** Preoperatory high order aberration RMS **(HOA RMS). (B)** Almost 3 postoperative years **HOA.** Notice the enhancement of 3.888 (µm).

4.3 Confocal Microscopy Study.

4.3.1 ADASc Results.

Morphological results: the ADASCs showed to be rounded in shape, voluminous, more refringent and more luminous comparing to the host keratocytes in the G-1 (Fig 5C). However, the shape of ADASc changed from round to fusiform six months after surgery (Fig 5D).

Also, change in morphology of the host keratocytes was observed in the anterior mid and posterior stroma, corneal cells acquired more fusiform shape, very similar to the keratocytes of a normal corneal stroma (Fig. 5D-5F) (15,61,70).

Moreover; confocal microscopy study showed the presence of a small fibrotic tissue at 3 months post-operative in 2 of 4 patients, then a full recovery of the corneal stroma was noted at 12 months follow up (61).

Statistical results: showed a gradual statistically significant increase in the cellular density at 12 months after the surgery at the anterior, mid and posterior host stroma comparing with the preoperative values (Table 3) (61).

Table3. Statistical results of cell density in G-1, G-2 & G-3. P value at 12 months after surgery/ preoperative time.

	Anterior Stroma (cells/mm^2)	**Mid stroma (cells/mm^2)**	**Posterior Stroma (cells/mm^2)**	**Anterior surface of the lamina (cells/mm^2)**	**Mid stroma of the lamina (cells/mm^2)**	**Posterior surface of the lamina (cells/mm^2)**
Group 1	[P value <0.001]	[P value <0.001]	[P value <0.001]	NA	NA	NA
Group 2	[P value <0.001]	NA	[P value <0.001]	[P value <0.001]	[P value <0.001]	[P value <0.001]
Group 3	[P value <0.001]	NA	[P value <0.001]	[P value <0.001]	[P value <0.001]	[P value <0.001]
G-1/G-2/G-3	[P= 0.025]	NA	[P= 0.311]	NA	NA	NA
G-2/G-3	[P= 0.025]	NA	[P= 0.311]	[P= 0.011]	[P= 0.011]	[P= 0.029]

P values in G-3 > G-2 > G-1 G-3 > G-2.

4.3.2 lamina's Results

Morohological results: decellularized laminas appeared acellular at the first months (Fig. 6A), unlike the recellularized ones that showed in some determined areas of interest a similar structures to corneal keratocytes (Fig. 7A,7B) The number of cells increased during the 12 months follow-up, the anterior, mid and posterior surfaces of the decellularized and recellularized laminas became more colonized by keratocyte-type cells, until they showed similar morphology of normal corneal keratocytes (Figs. 6B, 7C-7E) (61,70). We could differentiate the morphology of the lamina from the host stroma, by the presence of more abundant, dark and profound striaes (Fig. 6A) (70). Also some laminas matrix was observed

with a light gray color, reflecting more light, this fact could be attributed to the formation of the new layer of neocollagen after the implant of the laminas in the corneal stroma (Fig.7E).

The morphology and number of cells at the anterior and posterior stroma increased during the 12 months follow-up, then cell density became much closer to normal corneal keratocytes (Fig. 6C, 6D) (61,70).

Also, confocal microscopy findings showed the presence of fibrotic tissue in almost all the cases of G-2 & G-3 during the 12 months follow up (Figs. 6F, 7F). All detected fibrotic tissue corresponded with some paracentral areas of the decellularized or recellularized implanted laminas. The fibrotic tissue was absent in the central visual axis of the cornea with all the patients from G-2 & G-3 (Figs. 6E, 6F, 7F) (61).

Statistical results: at twelve months after surgery, with G-2 & G-3 cellular density in the anterior and posterior corneal stroma showed a statisticaly significance differences regarding the preoperative values (Table. 3) (61). Also, on the anterior surface, posterior surface and mid decellularized and recellularized laminas cellular densities was statistically significant, close to that found in a normal cornea (Table. 3) (61).

One the other hand, the statistical results of the fibrotic tissue, did not demonstrated a direct and significant association between the recelularization and the presence of such fibrotic tissue on the periphery of the decellularized or recellularized laminas (61).

4.3.3 Confocal microscopy study: comparison of results among G-1, G-2 & G-3.

A statistical significance differences was obtained among the three groups in the anterior stroma, G3 having the highest, followed by G2, and then G1. However, in the posterior stroma, the results in cell density was not statistically significant among the three groups (Table. 3) (61).

In addition, at 12 months postoperative, cell densities in the anterior surface, posterior surface and within the laminas was statistically significantly higher with the recellularized laminas than the decellularized ones (Table. 3) (61).

4.4. Slit Lamp Biomicroscopy.

Before surgery only one patient from each group presented a mild preoperative paracentral anterior stromal scars (case-2, case-9 and case-11) (Fig 8A). During the 36 months follow up, all corneas didn't show any posterior stromal or predescemetic scars and presented a fully transparent visual axis (Figs 4, 8B-8F). No case presented any complications such as inflammation or rejection throughout the follow-up period (Figs. 4, 8B-8F). The transparency of the cornea in G-1 was completely recovered within 24 hours after surgery, and it was maintained throughout the 36 months follow-up period (Figs. 4A,4 B, 8A, 8B). As described in our previous interim report (15,42,61,62). Case-2 from G-1 presented paracentral anterior stromal scars at the preoperative time, we observed progressive improvement of those scars during the following 12 and 36 months follow-up after surgery (Fig. 8B) (15, 61,62). In G-2 and G-3, the implanted laminas showed a mild early clinical haziness during the first postoperative month that was related to a mild lenticular edema (Fig. 8C). Then, corneal transparency improved progressively, a complete restoration was observed in all cases toward the 3rd month of follow-up. No patient showed visually significant corneal haze or scarring (Figs. 4, 8D-8F). In G-3 with case-11, we could detect an improvement in the paracentral scar at 36 months postoperative comparing with the pre-operative examination, more findings were already described in our previous interim publications (61,62).

5. DISCUSSION & CONCLUSIONS

The research Alió et al demonstrated for the first time the feasibility of the implantation of ADASCs into the corneal stromal pocket in cases of advanced keratoconus, they confirmed the appearance of new collagen in the injected areas, this new collagen could be useful for repair the corneal dystrophies, scars and increase slightly the corneal thickness, but this enhancement is not sufficient to restore the corneal disease in advanced keratoconus (15).

Also, they demonstrated for the first time that decellularized laminas of a human corneal stroma, colonized or not by autologous ADASCs, can be implanted for a clinical basis in the corneal stroma for therapeutic purposes. Also, such studies demonstrated the safety and the feasibility of the use of femtosecond laser to dissect the cornea in advanced keratoconus, even when a large 9.5 mm corneal pocket was performed in the middle of the corneal stroma (16,42,62). After three years follow up, no patient showed inflammation, rejection or any evidence of scarring or haze (Figs. 4, 8). Furthermore; there was an improvement with all the cases after three years follow up in all the visual parameters with 1-2 lines in LogMar. A significant increase in central corneal thickness, in thinnest corneal point and in corneal volume was obtained, the results was statistically significant better with the groups with implanted decellularized or recellularized laminas comparing with the group of implanted ADASCs alone. There was also an improvement in all the corneal aberrations (Fig. 12) and stability or enhancement corneal topographic parameters (Figs. 9-11) (62).

The Confocal microscopy was an essential tool for the evaluation and monitoring in "in vivo" of the evolution of ADASC nucleus and their morphological changes, being rounded shape and highly refringent cells up to 6 months, to fusiform structures and less nucleus refringent up to 12 months. These findings demonstrate in the human clinical model that the ADASCs implanted in the corneal human pocket have survived and have been able to differentiate into

keratocytes (Fig. 5.C) (61,70). Such findings confirm the previous animal studies in which the post-mortem analysis demonstrated the survival of these human cells and there capacity to produce a human collagen in the rabbit cornea (Figs. 2B-2D, 3B) (4,44). Confocal microscopy as well; allowed observing of the progressive morphological changes that occurred in the decellularized and recellularized laminas, it assisted in determining the change in the cells densities in the grafted tissue as well as in all the corneal stroma (Figs. 6A-6D, 7A-7E) (61,70).

En conclusion, cellular therapy of the corneal stroma is a novel treatment modality for stromal diseases, which even though further studies are still required in the form of clinical trials with larger sample sizes in order to definitely establish its safety and efficacy for different stromal diseases, the initial results obtained from the first few pilot clinical trials are encouraging. In our opinion, the creation of cellular banks storing and expanding stem cells or their exosomes, and their shipping and delivery to the different clinical centers for their use may be the future for this promising treatment modality, although prior to this, there is still a lot of research work to be undertaken.

Declarations

Availability of data and materials

Not applicable

Competing interests

The authors declare that they have no competing interests.

Funding

Not applicable

Authors' contributions

(J.L.A.), (M.E.Z.), (J.L.A.DB), have participated in the review of the literature, and drafted the manuscript.

All authors have participated in the reading, correction and approval of the final manuscript.

Acknowledgements

Not applicable

6. BIBLIOGRAPHY

1. De Miguel MP, Casaroli-Marano RP, Nieto-Nicolau N, et al. Frontiers in Regenerative Medicine for Cornea and Ocular Surface. In: Rahman A , Anjum S. Frontiers in Stem Cell and Regenerative Medicine Research. 1st ed. PA: Bentham e-Books, Vol. 1, 2015: 92-138.
2. Ruberti JW, Zieske JD. Prelude to corneal tissue engineering—Gaining control of collagen organization. Prog Retin Eye Res. 2008;27:549–77.
3. Isaacson A, Swioklo S, Connon CJ. 3D bioprinting of a corneal stroma equivalent. Exp Eye Res. 2018;173:188-93.
4. Arnalich-Montiel F, Pastor S, Blazquez-Martinez A, Fernandez-Delgado J, Nistal M, Alio JL, et al. Adipose-derived stem cells are a source for cell therapy of the corneal stroma. Stem Cells. 2008;26:570–9.
5. Alió del Barrio JL, Chiesa M, Gallego Ferrer G, Garagorri N, Briz N, Fernandez-Delgado J, et al. Biointegration of corneal macroporous membranes based on poly(ethyl acrylate) copolymers in an experimental animal model. J Biomed Mater Res A. 2015;103:1106–18.
6. Alió del Barrio JL, Chiesa M, Garagorri N, Garcia-Urquia N, Fernandez-Delgado J, Bataille L, et al. Acellular human corneal matrix sheets seeded with human adipose-derived mesenchymal stem cells integrate functionally in an experimental animal model. Exp Eye Res. 2015;132:91–100.
7. Espandar L, Bunnell B, Wang GY, Gregory P, McBride C, Moshirfar M. Adipose-derived stem cells on hyaluronic acid-derived scaffold: a new horizon in bioengineered cornea. Arch Ophthalmol. 2012;130:202–8.
8. Mittal SK, Omoto M, Amouzegar A, Sahu A, Rezazadeh A, Katikireddy KR, et al. Restoration of corneal transparency by mesenchymal stem cells. Stem Cell Reports. 2016;7:583-90.
9. Demirayak B, Yüksel N, Çelik OS, Subaşı C, Duruksu G, Unal ZS, et al. Effect of bone marrow and adipose tissue-derived mesenchymal stem cells on the natural course of corneal scarring after penetrating injury. Exp Eye Res. 2016;151:227-35.

10. Du Y, Carlson EC, Funderburgh ML, Birk DE, Pearlman E, Guo N, et al. Stem cell therapy restores transparency to defective murine corneas. Stem Cells. 2009;27:1635–42.
11. Liu H, Zhang J, Liu CY, Wang IJ, Sieber M, Chang J, et al. Cell therapy of congenital corneal diseases with umbilical mesenchymal stem cells: lumican null mice. PLoS One. 2010;5:e10707.
12. Coulson-Thomas VJ, Caterson B, Kao WW. Transplantation of human umbilical mesenchymal stem cells cures the corneal defects of mucopolysaccharidosis VII mice. Stem Cells. 2013;31:2116–26.
13. Kao WW, Coulson-Thomas VJ. Cell Therapy of Corneal Diseases. Cornea 2016; 35 Suppl 1:S9-S19.
14. De Miguel MP, Fuentes-Julián S, Blázquez-Martínez A, Pascual CY, Aller MA, Arias J, et al. Immunosuppressive properties of mesenchymal stem cells: advances and applications. Curr Mol Med. 2012;12:574-91.
15. Alió del Barrio JL, El Zarif M, de Miguel MP, Azaar A, Makdissy N, Harb W, et al. Cellular therapy with human autologous adipose-derived adult stem cells for advanced keratoconus. Cornea. 2017;36(8):952-60.
16. Alió Del Barrio JL, El Zarif M, Azaar A, Makdissy N, Khalil C, Harb W, et al. Corneal stroma enhancement with decellularized stromal laminas with or without stem cell recellularization for advanced keratoconus. Am J Ophthalmol. 2018;186:47-58.
17. Harkin DG, Foyn L, Bray LJ, Sutherland AJ, Li FJ, Cronin BG. Concise reviews: can mesenchymal stromal cells differentiate into corneal cells? A systematic review of published data. Stem Cells. 2015;33(3):785-91.
18. Jiang Z, Liu G, Meng F, Wang W, Hao P, Xiang Y, et al. Paracrine effects of mesenchymal stem cells on the activation of keratocytes. Br J Ophthalmol. 2017;101(11):1583-90.
19. Hendijani F. Explant culture: An advantageous method for isolation of mesenchymal stem cells from human tissues. Cell Prolif. 2017;50(2). doi: 10.1111/cpr.12334.
20. Górski B. Gingiva as a new and the most accessible source of mesenchymal stem cells from the oral cavity to be used in regenerative therapies. Postepy Hig Med Dosw (Online). 2016;70(0):858-71.
21. Basu S, Hertsenberg AJ, Funderburgh ML, Burrow MK, Mann MM, Du Y, et al. Human limbal biopsy-derived stromal stem cells prevent corneal scarring. Sci Transl Med. 2014; 6(266):266ra172.
22. Takahashi K, Yamanaka S. Induction of pluripotent stem cells from mouse embryonic and adult fibroblast cultures by defined factors. Cell. 2006;126:663-76.
23. Naylor RW, McGhee CN, Cowan CA, Davidson AJ, Holm TM, Sherwin T. Derivation of corneal keratocyte-like cells from human induced pluripotent stem cells. PLoS One. 2016;11(10):e0165464.
24. Yao L, Bai H. Review: Mesenchymal stem cells and corneal reconstruction. Mol Vis. 2013;19:2237–43.
25. Caplan AI. Mesenchymal stem cells: Time to change the name! Stem Cells Transl Med. 2017;6(6):1445-51.
26. Park SH, Kim KW, Chun YS, Kim JC. Human mesenchymal stem cells differentiate into keratocyte-like cells in keratocyte-conditioned medium. Exp Eye Research. 2012;101: 16-26.
27. Trosan P, Javorkova E, Zajicova A, Hajkova M, Hermankova B, Kossl J, et al. The Supportive role of insulin-like growth factor-I in the differentiation of murine mesenchymal stem cells into corneal-like cells. Stem Cells Dev. 2016;25(11):874-81.

28. Liu H, Zhang J, Liu CY, Hayashi Y, Kao WW. Bone marrow mesenchymal stem cells can differentiate and assume corneal keratocyte phenotype. J Cell Mol Med. 2012;16: 1114-24.
29. Du Y, Roh DS, Funderburgh ML, Mann MM, Marra KG, Rubin JP, et al. Adipose-derived stem cells differentiate to keratocytes *in vitro*. Mol Vis. 2010;16:2680-9.
30. Ziaei M, Zhang J, Patel DV, McGhee CNJ. Umbilical cord stem cells in the treatment of corneal disease. Surv Ophthalmol. 2017;62(6):803-15.
31. Chan AA, Hertsenberg AJ, Funderburgh ML, Mann MM, Du Y, Davoli KA, et al. Differentiation of human embryonic stem cells into cells with corneal keratocyte phenotype. PloS One. 2013;8:e56831.
32. Yun YI, Park SY, Lee HJ, Ko JH, Kim MK, Wee WR, et al. Comparison of the anti-inflammatory effects of induced pluripotent stem cell-derived and bone marrow-derived mesenchymal stromal cells in a murine model of corneal injury. Cytotherapy. 2017;19(1):28-35.
33. Pinnamaneni N, Funderburgh JL. Concise review: Stem cells in the corneal stroma. Stem Cells. 2012;30(6):1059-63.
34. Du Y, Funderburgh ML, Mann MM, SundarRaj N, Funderburgh JL. Multipotent stem cells in human corneal stroma. Stem Cells. 2005;23(9):1266-75.
35. Katikireddy KR, Dana R, Jurkunas UV. Differentiation potential of limbal fibroblasts and bone marrow mesenchymal stem cells to corneal epithelial cells. Stem Cells. 2014;32(3):717-29.
36. Wu J, Du Y, Watkins SC, Funderburgh JL, Wagner WR. The engineering of organized human corneal tissue through the spatial guidance of corneal stromal stem cells. Biomaterials. 2012;33(5):1343-52.
37. Di G, Du X, Qi X, Zhao X, Duan H, Li S, et al. Mesenchymal stem cells promote diabetic corneal epithelial wound healing through TSG-6-dependent stem cell activation and macrophage switch. Invest Ophthalmol Vis Sci. 2017;58(10):4344–54.
38. Holan V, Trosan P, Cejka C, Javorkova E, Zajicova A, Hermankova B, et al. A comparative study of the therapeutic potential of mesenchymal stem cells and limbal epithelial stem cells for ocular surface reconstruction. Stem Cells Transl Med. 2015;4(9):1052-63.
39. Cejka C, Cejkova J, Trosan P, Zajicova A, Sykova E, Holan V. Transfer of mesenchymal stem cells and cyclosporine A on alkali-injured rabbit cornea using nanofiber scaffolds strongly reduces corneal neovascularization and scar formation. Histol Histopathol. 2016;31(9):969-80.
40. Agorogiannis GI, Alexaki VI, Castana O, Kymionis GD. Topical application of autologous adipose-derived mesenchymal stem cells (MSCs) for persistent sterile corneal epithelial defect. Graefes Arch Clin Exp Ophthalmol. 2012;250(3):455-7.
41. Basu S. Limbal stromal stem cell therapy for acute and chronic superficial corneal pathologies: early clinical outcomes with the Funderburgh technique. Oral presentation at The Association for Research in Vision and Ophthalmology (ARVO) Annual meeting; 2017; Baltimore (USA).
42. Alió J, Alió Del Barrio J, El Zarif M, Azaar A, Makdissy N, Khalil C, et al. Regenerative Surgery of the Corneal Stroma for Advanced Keratoconus: 1-Year Outcomes. Am J Ophthalmol. 2019;203:53–68.
43. Ma XY, Bao HJ, Cui L, Zou J. The graft of autologous adipose-derived stem cells in the corneal stromal after mechanic damage. PloS One. 2013;8:e76103.
44. Alió del Barrio JL, Chiesa M, Gallego Ferrer G, Garagorri N, Briz N, Fernandez-Delgado J, et al. Biointegration of corneal macroporous membranes based on poly(ethyl acrylate) copolymers in an experimental animal model. J Biomed Mater Res A. 2015;103:1106-18.

45. Lynch AP, Ahearne M. Strategies for developing decellularized corneal scaffolds. Exp Eye Research. 2013;108:42-7.
46. Wilson SE, Liu JJ, Mohan RR. Stromal-epithelial interactions in the cornea. Prog Retin Eye Res. 1999;18:293-309.
47. Choi JS, Williams JK, Greven M, Walter KA, Laber PW, Khang G, et al. Bioengineering endothelialized neo-corneas using donor-derived corneal endothelial cells and decellularized corneal stroma. Biomaterials. 2010;31:6738-45.
48. Shafiq MA, Gemeinhart RA, Yue BY, Djalilian AR. Decellularized human cornea for reconstructing the corneal epithelium and anterior stroma. Tissue Eng Part C Methods. 2012;18:340-8.
49. Gonzalez-Andrades M, de la Cruz Cardona J, Ionescu AM, Campos A, Del Mar Perez M, Alaminos M. Generation of bioengineered corneas with decellularized xenografts and human keratocytes. Invest Ophthalmol Vis Sci. 2011;52:215-22.
50. Yam GH, Yusoff NZ, Goh TW, Setiawan M, Lee XW, Liu YC, et al. Decellularization of human stromal refractive lenticules for corneal tissue engineering. Sci Rep. 2016;6:26339.
51. Liu YC, Teo EPW, Ang HP, Seah XY, Lwin NC, Yam GHF, et al. Biological corneal inlay for presbyopia derived from small incision lenticule extraction (SMILE). Sci Rep. 2018; 8(1):1831.
52. Bai H, Wang LL, Huang YF, Huang JX. An experimental study of mesenchymal stem cells in tissue engineering scaffolds implanted in rabbit corneal lamellae to increase keratoprosthesis biointegration. Zhonghua Yan Ke Za Zhi. 2016;52(3):192-7.
53. Barraquer JI. Keratophakia. Trans Ophthalmol Soc U K. 1972;92: 499-516.
54. Omoto M, Katikireddy KR, Rezazadeh A, Dohlman TH, Chauhan SK. Mesenchymal stem cellshome to inflamed ocular surface and suppress allosensitization in corneal transplantation. Invest Ophthalmol Vis Sci. 2014;55(10):6631-8.
55. Fuentes-Julián S, Arnalich-Montiel F, Jaumandreu L, Leal M, Casado A, García-Tuñon I, et al. Adipose-derived mesenchymal stem cell administration does not improve corneal graft survival outcome. PLoS One. 2015;10(3):e0117945.
56. Zhang L, Coulson-Thomas VJ, Ferreira TG, Kao WW. Mesenchymal stem cells for treating ocular surface diseases. BMC Ophthalmol. 2015;15 Suppl 1:155.
57. Swioklo S, Constantinescu A, Connon CJ. Alginate-encapsulation for the improved hypothermic preservation of human adipose-derived stem cells. Stem Cells Transl Med. 2016;5(3):339-49.
58. Funderburgh JL. Assessing the Potential of Stem Cells to Regenerate Stromal Tissue. Oral presentation at The Association for Research in Vision and Ophthalmology (ARVO) Annual meeting; 2017; Baltimore (USA).
59. Joseph R, Srivastava OP, Pfister RR. Modeling keratoconus using induced pluripotent stem cells. Invest Ophthalmol Vis Sci. 2016;57:3685-97.
60. Shojaati G. Regenerative Potential of Stem cell-Derived Exosomes. Oral presentation at The Association for Research in Vision and Ophthalmology (ARVO) Annual meeting; 2017; Baltimore (USA).
61. El Zarif M, Abdul Jawad K, Alió del Barrio JL, Abdul Jawad Z, Palazón-Bru A, De Miguel MP, et al. Corneal stroma cell density evolution in keratoconus corneas following the implantation of adipose mesenchymal stem cells and corneal laminas: an in vivo confocal microscopy study. IOVS. 2020;61(4):22.
62. El Zarif M, Alió J, Alió del Barrio J, Abdul Jawad K, Palazón-Bru A, Abdul Jawad Z, et al. Corneal stromal regeneration therapy for advanced keratoconus: long-term outcomes at 3 years. Cornea. 2021;40(6):741–54.
63. Zuk P, Zhu M, Mizuno H, Huang J, Futrell J, Katz A, et al. Multilineage cells from

human adipose tissue: implications for cell-based therapies. Tissue Eng. 2001;7(2):211–28.
64. Zuk P, Zhu M, Ashjian P, De Ugarte D, Huang J, Mizuno H, et al. Human adipose tissue is a source of multipotent stem cells. Mol Biol Cell. 2002;13(12):4279–95.
65. Bourin P, Bunnell B, Casteilla L, Dominici M, Katz A, March K, et al. Stromal cells from the adipose tissue-derived stromal vascular fraction and culture expanded adipose tissue-derived stromal/stem cells: a joint statement of the International Federation for Adipose Therapeutics and Science (IFATS) and the International So. Cytotherapy. 2013;15(6):641–8.
66. Ponce Márquez S, Martínez V, McIntosh Ambrose W, Wang J, Gantxegui N, Schein O, et al. Decellularization of bovine corneas for tissue engineering applications. Acta Biomater. 2009;5(6):1839–47.
67. Guthoff R, Klink T, Schlunck G, Grehn F. Die sickerkissenuntersuchung mittels konfokaler in-vivo mikroskopie mit dem rostocker cornea modul - erste erfahrungen. Klin Monatsbl Augenheilkd. 2005;222-R8.
68. Ali Javadi M, Kanavi M, Mahdavi M, Yaseri M, Rabiei H, Javadi A, et al. Comparison of keratocyte density between keratoconus, post-laser in situ keratomileusis keratectasia, and uncomplicated post-laser in situ keratomileusis cases. A confocal scan study. Cornea. 2009;28(7):774–9.
69. Mastropasqua L, Nubile M. Normal Corneal Morphology. In: Confocal Microscopy of the Cornea. Thorofare, NJ: SLACK. 2002. 7–16 p.
70. El Zarif M, Abdul Jawad K, Alió JL. Corneal Regeneration therapy and surgery. 1st ed. Alió JL, Alió del Barrio JL, Arnalich-Montiel F, editors. Springer; 2019. 363–386 p.
71. Ku J, Niederer R, Patel D, Sherwin T, McGhee C. Laser scanning in vivo confocal analysis of keratocyte density in keratoconus. Ophthalmology. 2008;115(5):845–50.

10. 11. Alió del Barrio, J.L., El Zarif, M., Alió, J.L., 2021. Anterior segment OCT: observations in corneal stroma regeneration, in: Alió, J.L., Alio del Barrio, J. (Eds.), Text and Atlas of Anterior Segment OCT. Springer Nature, Cham, Switzerland, pp. 207–210. https://doi.org/10.1007/978-3-030-53374-8_9

Anterior Segment OCT: Observations in Corneal Stroma Regeneration

Jorge L. Alió del Barrio, Mona El Zarif, and Jorge L. Alió

INTRODUCTION

Corneal grafting is one of the most common and successful forms of human tissue transplantation in the world, but the need for corneal grafting is growing and availability of human corneal donor tissue to fulfill this increasing demand is not assured worldwide. The stroma is responsible for many features of the cornea, including its strength refractive power, and transparency, so enormous efforts have been put into replicating the corneal stroma in the laboratory to find an alternative to classical corneal transplantation [1]. Unfortunately,this has not been yet accomplished due to the extreme difficulty in mimicking the highly complex ultrastructure of the corneal stroma, and none of the obtained substitutes that have been assayed has been able to replicate this complexity yet [2]. In general, they can neither match the mechanical properties nor recreate the local nanoscale organization and thus the transparency and optical properties of a normal cornea.

In this context, there is an increasing interest in the cellular therapy of the corneal stroma using stem cells (SCs) such as induced pluripotent stem cells (iPSCs) or mesenchymal stem cells (MSCs) from either ocular or extraocular sources, as they have proven to be capable of producing new collagen within the host stroma, modulate preexisting scars, and enhance transparency by corneal stroma remodeling [1]. However, new collagen production by these stem cells, once implanted within the stroma, is expected to be limited and insufficient for those corneas severely damaged with significant tissue loss (as in advanced keratoconus) [3]. For that reason, it has been suggested to provide this cellular component together with a carrier that could restore efficiently the anatomy and integrity of the corneal stroma without the inherent risks of allograft implants such as rejection [4]. In this scenario, several corneal decellularization techniques have been described, which provide an acellular corneal extracellular matrix [5]. These scaffolds have gained attention in the last few years as they provide a more natural environment for the growth and differentiation of cells when compared with synthetic scaffolds. Moreover, through this technique, and by using autologous SCs from a given patient, it is theoretically possible to transform allogenic grafts into functional autologous grafts, thus avoiding any risk of rejection.

Following this research line, our group has recently published the first clinical trial using such concepts of cellular therapy for the regeneration of the corneal stroma in patients with advanced (stage IV) keratoconus [6–8]. This trial assayed three different techniques, which will be reviewed in the current chapter focusing mainly on their AS-OCT findings.

INTRASTROMAL IMPLANTATION OF AUTOLOGOUS MSCS ALONE

A suspension of autologous adipose-derived adult stem cells (ADASCs), obtained by elective liposuction, was implanted into a mid-stroma femtosecond laser-assisted lamellar pocket in patients with advanced keratoconus (already candidates for corneal transplantation; n = 5) [6,8]. No signs of inflammation or rejection were observed, confirming previous evidence obtained in

the animal model. AS-OCT demonstrated the production of new collagen in the area of the MSC implantation (Fig.1A), inducing a mild central pachymetric improvement of 15 µm (mean: 14.5 ± 27 µm 12 months postop; p = 0.47) (see Fig.1C). This neo-collagen band, seen in AS-OCT as a hyperreflective band not homogeneously distributed along the surgical plane (see Fig. 1A, B), did not induce any clinical haze. One year after surgery, some of these patients showed a partial normalization of the reflectance
of this neo-collagen band (see Fig.1B). All patients moderately improved their visual function (mean improvement of two lines in all visual parameters), while keratometric values remained stable (see Fig. 1C) [6, 8]. Further studies with larger samples are required in order to confirm this preliminary data, but encouraging results were observed, thus opening a new and exciting line of therapy for research. As mentioned before, the production of new extracellular matrix (ECM) by the implanted MSCs occurs, but is not quantitatively enough to be able to restore the thickness of these advanced keratoconic corneas.

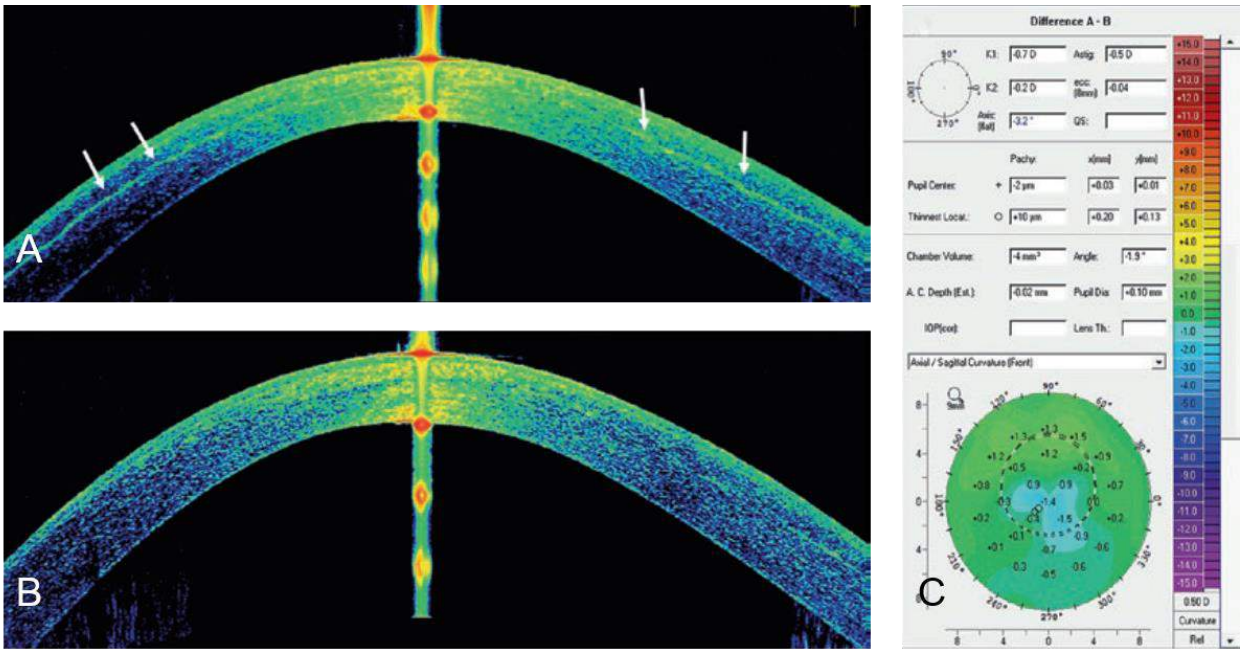

Figure 1. Cornea OCT pictures (Visante) after autologous ADASCs implantation. (**A**) Observe the hyperreflective band of neo collagen at the level of the stromal pocket 6 months after surgery. (**B**) Same patient 1 year after surgery, showing a partial normalization of the reflectance of the neo-collagen band. (**C**) Corneal topography (Pentacam) comparison map between preop and 12 months after surgery. Observe the stability of the keratometric parameters with minimal central thickening.

INTRASTROMAL IMPLANTATION OF DECELLULARIZED HUMAN CORNEAL STROMA WITH OR WITHOUT REPOPULATION BY AUTOLOGOUS MSCS

We assayed the implantation of decellularized human corneal stroma lenticules (planar, 120 µm thickness, and 9.0 mm diameter laminas), with or without autologous ADASCs recellularization, in patients with advanced keratoconus (n = 10) [7,8]. We demonstrated a moderate but significant improvement in all visual parameters (about two lines of improvement), together with a reduction in refractive sphere, significant anterior keratometric flattening (Fig. 2C), and improvement in corneal aberrations, especially the spherical aberration [7, 8]. Complete corneal transparency

without significant haze was obtained 3 months after the procedure, and all pachymetric parameters improved over 100 μm as expected (see Fig. 1C), anatomically restoring these advanced keratoconic corneas. Transplanted laminas were clearly visible by AS-OCT, showing a moderate early postoperative hyper-reflectance during the
first postoperative month (see Fig. 1A) that correlated with an early transient clinical corneal haze and early visual loss. After the third postoperative month, the lamina already presented a normal reflectance, equivalent to the surrounding recipient stroma (see Fig. 2B). No clinical or anatomical differences could be demonstrated between the decellularized and recellularized implants. No obvious areas of new collagen production could be observed in those cases with recellularized implants [7, 8].

CONCLUSION

In conclusion, cellular therapy of the corneal stroma is a novel treatment modality for stromal diseases. Despite further studies are still required in the form of clinical trials with larger sample sizes in order to definitely establish its safety and efficacy for different stromal diseases, the initial results obtained from the first few pilot clinical trials are encouraging. AS-OCT becomes a critical tool in order to postoperatively monitor the anatomical changes that occur within the corneal stroma with time. Actually, modern AS-OCT devices provide an axial resolution up to 4 microns, which will help to understand even better the long-term behavior of these implants and the stability of the neo-collagen generated by these stem cells.

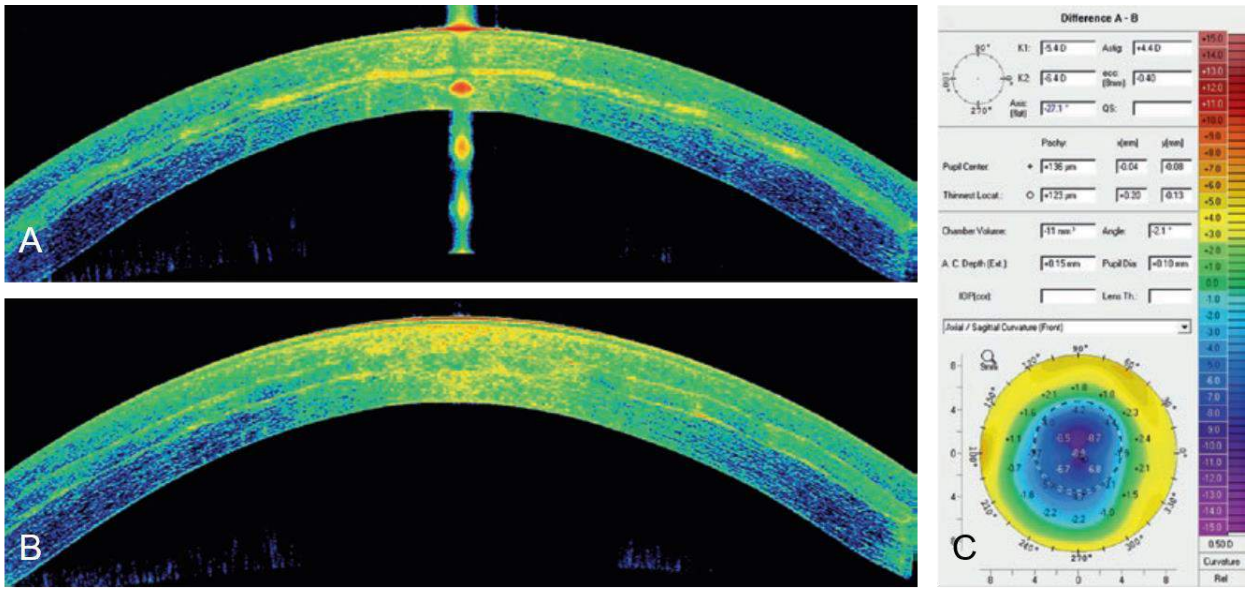

Figure 2. Cornea OCT pictures (Visante) after corneal stroma enhancement with planar lenticules of decellularized human corneal stroma. One year after surgery (**B**) is observed a normalization of the early postoperative increased reflectance of the implanted lamina (**A**). (**C**) Corneal topography (Pentacam) comparison map between preop and 12 months after surgery. Observe the significant flattening of the central keratometry and the important improvement in all thickness parameters.

Compliance with Ethical Requirements

The authors, their families, their employers, and their business associates have no financial or proprietary interest in any product

or company associated with any device, instrument, or drug mentioned in this article. The authors have not received any payment as consultants, reviewers, or evaluators for any of the devices, instruments, or drugs mentioned in this article.

REFERENCES

1. Alió Del Barrio JL, Alió JL. Cellular therapy of the corneal stroma: a new type of corneal surgery for keratoconus and corneal dystrophies. Eye Vis (Lond). 2018;5:28.
2. Ruberti JW, Zieske JD. Prelude to corneal tissue engineering—gaining control of collagen organization. Prog Retin Eye Res. 2008;27:549–77.
3. Arnalich-Montiel F, Pastor S, Blazquez-Martinez A, Fernandez-Delgado J, Nistal M, Alió JL, et al. Adipose-derived stem cells are a source for cell therapy of the corneal stroma. Stem Cells. 2008;26:570–9.
4. Alió Del Barrio JL, Chiesa M, Garagorri N, Garcia-Urquia N, Fernandez-Delgado J, Bataille L, et al. Acellular human corneal matrix sheets seeded with human adipose-derived mesenchymal stem cells integrate functionally in an experimental animal model. Exp Eye Res. 2015;132:91–100.
5. Lynch AP, Ahearne M. Strategies for developing decellularized corneal scaffolds. Exp Eye Res. 2013;108:42–7.
6. Alió Del del Barrio JL, El Zarif M, de Miguel MP, Azaar A, Makdissy N, Harb W, et al. Cellular therapy with human autologous adipose-derived adult stem cells for advanced keratoconus. Cornea. 2017;36(8):952–60.
7. Alió Del Del Barrio JL, El Zarif M, Azaar A, Makdissy N, Khalil C, Harb W, et al. Corneal stroma enhancement with decellularized stromal laminas with or without stem cell recellularization for advanced keratoconus.Am J Ophthalmol. 2018;186:47–58.
8. Alió JL, Alió Del Barrio JL, El Zarif M, et al. Regenerative surgery of the corneal stroma for advanced keratoconus: one year outcomes. Am J Ophthalmol. 2019;203:53–68.

10. 12. **El Zarif M**, Alió J.L., Alió del Barrio J.L., **Advanced therapy of the human corneal stroma in keratoconus with stem cells.** (Accepted in 2021. Ahead of print).

ADVANCED THERAPY OF THE HUMAN CORNEAL STROMA WITH STEM CELLS IN KERATOCONUS

Mona El Zarif OD, MSc[1,3,4,5], Jorge L. Alió MD, PhD, FEBOphth [2,3*], Jorge L. Alió del Barrio MD, PhD FEBOS-CR[2,3]

1. Optica General, Saida, Lebanon.
2. Cornea, Cataract and Refractive Surgery Unit, Vissum (Miranza Group), Alicante, Spain.
3. Division of Ophthalmology, Universidad Miguel Hernández, Alicante, Spain.
4. Lebanese University, Faculty of Sciences, GSBT Genomic Surveillance and Biotherapy Team, Mont Michel Campus, Lebanon.
5. Lebanese University, Doctoral School of Sciences and Technology, DSST of biotechnology, Hadath Lebanon.

* Corresponding author: Prof. Dr. Jorge L. Alió MD PhD FEBOphth

Email: jlalio@vissum.com

Vissum, Calle Cabañal, 1, 03016 Alicante . SPAIN.

Funding/Support

This study has been financed by Optica General, Saida Lebanon, and Vissum ophthalmological institute of Alicante, Spain. It was also supported in part by the Red Temática de Investigación Cooperativa en Salud (RETICS), reference number RD16/0008/0012, financed by the Instituto Carlos III – General Subdirection of Networks and Cooperative Investigation Centers (R&D&I

National Plan 2008-2011) and the European Regional Development Fund (Fondo Europeo de Desarrollo Regional FEDER).

Financial disclosures: None specific for this report.

ABSTRACT

In recent years, the idea of using advanced therapies with stem cells to reconstruct the cornea structure has gained interest. Important preclinical experimental evidence is available demonstrating the feasibility of such advanced new therapies and surgeries. The corneal stroma is one of the targets that may as preclinical studies have shown the capability of stem cells to differentiate into functional adult keratocytes so that they are capable of naturally reproducing this complex tissue.

Recently, the outcomes of the first clinical experience with stem cells therapy on corneal stroma regeneration in patients with advanced keratoconus were reported by our research group.

14 patients with advanced keratoconus were distributed in three experimental groups: Group 1 (G-1) patients underwent implantation of autologous adipose-derived adult stem cells (**ADASC**s) alone, Group 2 (G-2) patients received decellularized donor corneal stroma laminas with 120 µm thickness, and group 3 (G-3) implantation of recellularized donor laminas with (**ADASCs**). Implantation of the laminas or **ADASCs** injection was performed into a 9.5 mm femtosecond-assisted created corneal pocket. 36 months of clinical follow-up data and 12 months of confocal microscopy study have been already reported. Clinical improvement was observed in almost all studied mean values of primary and secondary outcomes with all cases of the study, and also an increase in cell density was obtained in the anterior mid and posterior corneal stroma, as well in the implanted tissue.

In conclusion, advanced stem cell therapy with implantation of autologous **ADASCs**, decellularized human corneal stroma with or without **ADASCs** demonstrated to be feasible, and safe, an allogenic corneal laminas were transformed into the autologous implant and implanted in mid of the cornea in cases with advanced keratoconus, no inflammation or rejection was observed, while transplantation of allogenic corneal lenticules as stroma inlays and to a lesser extent recombinant Cross-linked Collagen have shown initially to be potentially effective for the treatment of advanced keratoconus, but still having heterologous stromal cells, and should be considered as a new form of corneal stroma transplantation.

In the light of the current evidence available, it can be said that with these innovative studies, the era of corneal stromal regeneration therapy has already begun, and a new stage in keratoconus surgery is approaching soon.

KEYWORDS: stem cells, regenerative medicine, corneal stem cell therapy, corneal bioengineering, cornea surgery, corneal transplant, keratoconus, autologous adipose-derived adult stem cells (**ADASCs**), corneal stromal transplantation.

1. INTRODUCTION

The corneal stroma constitutes more than 90% of the corneal thickness, Many characteristics of the cornea, including its strength, morphology, and transparency (1), biomechanics, and optical behavior (2) are all attributable to the anatomy and properties of the corneal stroma.

Many diseases such as corneal dystrophies, scars, or ectatic disorders induce a distortion of its anatomy or physiology leading to loss of transparency and subsequent loss of vision. Keratoconus is the most common corneal dystrophy, with a diverse prevalence in the population, from 0.05-2.3 %. Being a relatively prevalent disease, it is more observed today than before due to the more advanced diagnostic tools that are available for the diagnosis of early keratoconus (3).

Consistant efforts have been put into replicating the corneal stroma in the laboratory to find an alternative to classical corneal transplantation, but mimicking the highly complex anatomical, and optical ultrastructure of the corneal stroma led to not achieving sufficient transparency or strength of such imitated tissue (4,5).

In the last few years, interest in cellular therapy of the corneal stroma using mesenchymal stem cells (MSCs) from either ocular or extraocular sources has gained a lot of importance; studies show that MSCs are capable of differentiating into adult keratocytes *in vitro* and *in vivo* (1). Numerous authors, including reports from our research group, have demonstrated (6–8) that these stem cells, in xenogeneic scenarios, can survive and differentiate into adult human keratocytes without inducing an inflammatory reaction, and also: 1) produce new collagen within the host stroma (6,9), 2) they can modulate preexisting scars (10,11), and 3) to improve corneal transparency in animal models with corneal dystrophies due to collagen reorganization, as well as in animal models for metabolic diseases due to catabolism of accumulated proteins (12–15). **MSCs** have also shown

immunomodulatory properties in syngeneic, allogeneic, and even xenogeneic scenarios (15,16). Taking into consideration the existing scientific evidence, it appears that all types of MSCs behave similarly in vivo (Table 1) and therefore achieve keratocyte differentiation and can modulate the corneal stroma with immunomodulatory properties (17).

Table 1: Stem cells assayed for corneal stroma regeneration: evidence of keratocyte or keratocyte-like differentiation and their potential autologous application.

	CSSCs	**BM-MSCs**	**ADASCs**	**UMSCs**	**ESCs**	**iPSCs**
Keratocyte differentiation *in vitro* demonstrated	Yes	Yes	Yes	Yes	Yes	Yes
Keratocyte differentiation *in vivo* demonstrated	Yes	Yes	Yes	Yes	No	No
Possible autologous use	Yes/No	Yes	Yes	Yes/No	No	Yes

CSSCs, corneal stroma stem cells; **MSCs**, mesenchymal stem cell; **BM,** bone marrow; **ADASC**s, adipose-derived adult stem cell; **UMSCs**, umbilical MSC; **ESCs**, embryonic stem cell; **iPSCs**, an induced pluripotent stem cell. Table is taken from the chapter of Alió JL et al (18).

2. FROM THE PRECLINICAL STUDIES TO THE PATIENTS

Our group reported recently the first human clinical trials using an extraocular source of **MSCs** for corneal stem cell therapy in advanced keratoconus (19–24), based on previous successful animal studies accomplished by the same research group (6,9), it has been demonstrated that adult **MSCs** from human adipose tissue form an ideal source since they are easy to access, they have a high cell retrieval efficiency and high differentiation capacity. They are known as "Human Adipose-Derived Adult Stem Cells " (**h-ADASCs**), these cells can be differentiated into different cell types, such as keratinocytes, chondroblasts, osteoblasts, hepatocytes, myoblasts, neurons,

among others (6,25). Moreover, these cells have shown immunomodulatory properties in autologous, allogenic, and xenogeneic scenarios (15,16).

In our previous preclinical studies, we transplanted **h-ADASCs** into damaged rabbit corneas, we demonstrated that these cells were able to differentiate into corneal keratocytes, produced collagen and keratocan which are characteristics of the corneal stroma (6). To provide an adequate volume of collagen to restore the thickness of the cornea, protocols have been performed to obtain decellularized corneal matrices, since they provide an environment for the growth and differentiation of **MSCs** much more natural compared to synthetic scaffolds (7,8,26). The effectiveness of sodium dodecyl sulfate decellularization on the human donor cornea has also been demonstrated in previous studies (8,20,21,26). In the experimental animal model, the **h-ADASCs** demonstrated their capacity to repopulate scaffolds (6,8,9,26) and were able to survive at least 12 weeks after transplantation, and they also differentiate into human keratocytes (8).

The experimental studies opened the translational of this concept from the animal into the human, from the laboratory to a new therapy for human corneal disease, using the advanced keratoconus disease as a model for this type of advanced regenerative therapy.

3. FIRST CLINICAL HUMAN EXPERIENCE OF THE CORNEAL STROMA IN KERATOCONUS

Our group has recently performed, and reported with 14 patients with advanced keratoconus a new type of regenerative corneal surgery. This clinical experience opens a new and exciting line of therapy for research for corneal dystrophies such as keratoconus.

3.1. Study Approval, Design, and Subjects.

This study was a prospective interventional randomized, non-masked series of cases, based on the cooperation between the Research, Development, and Innovation Department of Vissum Instituto Oftalmologico de Alicante, Miguel Hernandez University, Alicante (Spain), Optica General (Saida, Lebanon), REVIVA Research and Application Center (Middle East Hospital, Beirut, Lebanon), and Laser Vision Center (Beirut, Lebanon). The Institutional Review Board (IRB) Ethical committee of Reviva Research and Application Center (Lebanese University, Beirut, Lebanon), prospectively approved this study. All patients signed informed written consent for all procedures described in this study. The study was conducted in strict adherence to the tenets of the Declaration of Helsinki, and it was officially registered in *ClinicalTrials.gov* (Code: NCT02932852).

Fourteen patients were selected and enrolled in the study following the inclusion criteria and were randomly distributed into three groups: Group 1 (**G-1**), five patients received an implant of autologous adipose-derived adult stem cells (**ADASCs**) alone 3x 10^6cells/1 mL of phosphate-buffered saline (**PBS**); Group 2 (**G-2**), five patients received 120 µm thick decellularized human corneal stroma laminas implants, and Group 3 (**G-3**), four patients received 120 µm thick (**ADASCs**)-recellularized human corneal stroma laminas 1x10^6cells/1 ml of **PBS**. **ADASCs** were obtained by elective liposuction. Superficial laminas with Bowman´s membrane (**BM**) or deep

laminas without **BM** were randomly distributed among the patients of **G-2** and **G-3** after the decellularization procedure.

3.2 Autologous ADASCs Isolation, Characterization, and Culture.

Approximately 250 ml of fat mixed with local anesthesia was obtained by standard liposuction from each patient. The adipose tissue was processed according to the methods described in our previous reports (6,8,27–29). From sixty to eighty hours before transplantation, the quiescence of the **ADASCs** was induced by decreasing the amount of serum in the culture media to 0.5% to transplant them in a non-proliferative physiological state, closer to natural stromal keratocytes. The inactivity, the absence of apoptosis, the aneuploidy, as well as the blocking properties of pro-inflammatory and inducing anti-inflammatory ADSCs, and the absence of infection were verified as quality controls, as described by the authors in previous publications. and 3×10^6 Cells in 1 ml of **PBS**. Such concentration was established based on previous experimental studies, and since cell loss was expected after cell implantation due to leakage of the cell solution out of the cornea (7,8,19–24), and the cells were transplanted directly in situ (Figures. 1A, 1B).

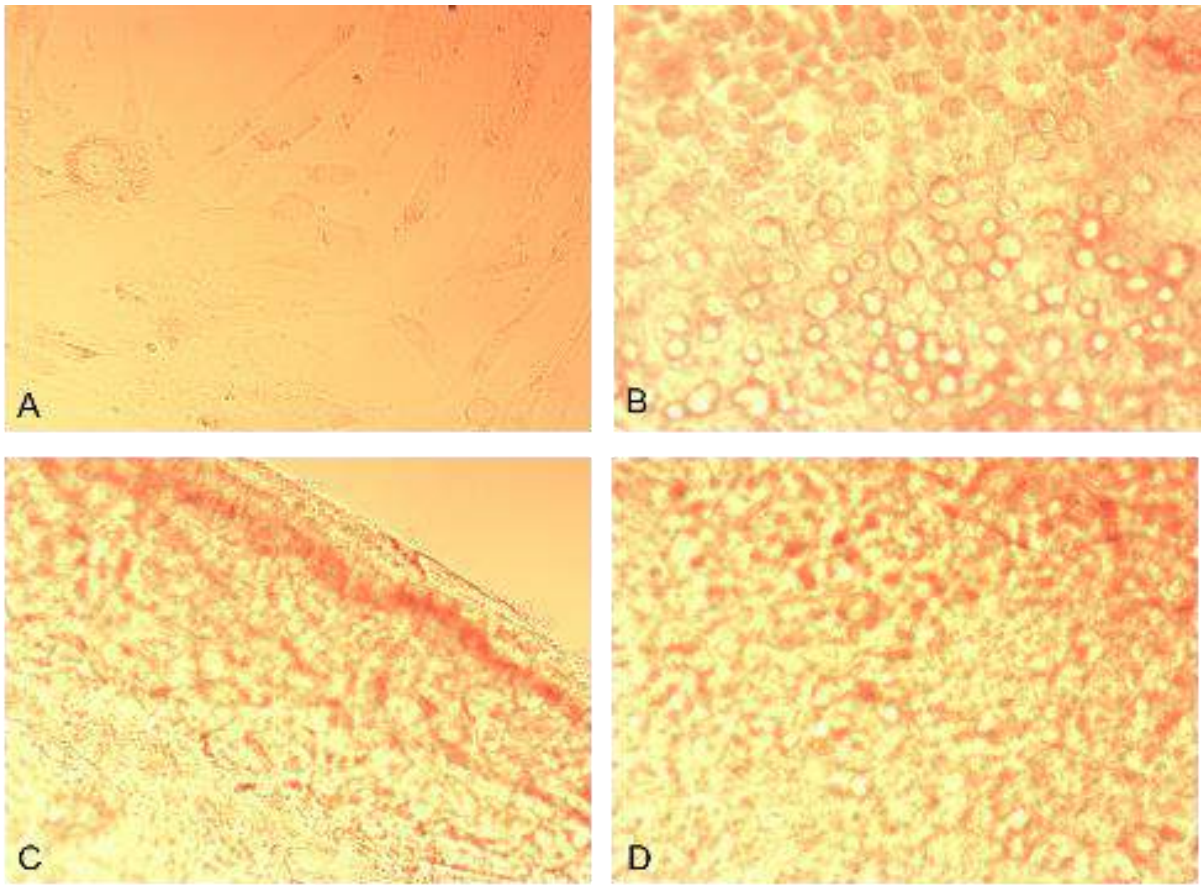

Figure 1. (A) Human ADASC in culture. **(B)** Microscopic appearance (phase-contrast photograph) of human ADASCs (10× magnification). **(C)** Decellularized human corneal lamina (10× magnification). **(D)** Recellularized human corenal lamina with ADASCs (0.5×10^6 cells in 1 ml of PBS were cultured on each side of the laminas) (10× magnification).

3.3 Decellularization and Recellularization method of Human Corneal Stroma Laminas

In this phase 1 of our clinical trial in advanced keratoconus. A human donor's corneal stroma with non-viable endothelium (without scars) but with negative viral serology was useful for human use and was selected for this investigation. The epithelium was removed mechanically, the anterior corneal stroma was cut by 60 kHz IntraLase **IFS** femtosecond laser (AMO, Santa Ana, CA). 2-3 consecutive laminas 120 µm thick and 9.0 mm in diameter were obtained, a superficial lamina that contains the Bowman membrane and a deeper one without this layer. The decellularization protocol was based on previous publications (Figure. 1C) (8,20,21,24,30). The laminas were randomly distributed on the patients of G-2, and G-3. In (**G-3**), the **ADASCs** were harvested by

trypsinization (Sigma-Aldrich), 24 hours before implantation and 0.5×10^6 cells per 1ml of **PBS** were cultured for 24 and 12 hours on each surface of the decellularized corneal stroma lamina, respectively (Figure. 1D) (19–21,24). Five patients received decellularized human corneal stroma laminas only, and four patients received human corneal stroma recellularized with autologous **ADASCs**.

3.4 Surgical Procedures.

3.4.1 Autologous ADASCs Alone.

Topical anesthesia was applied. **IFS** femtosecond laser (AMO Inc, Irvine, CA) 60 Khz. IntraLase was used in a single-pass mode for the recipient corneal lamellar dissection. At the medium depth of the thinnest preoperative pachymetry point measured by an anterior segment optical coherence tomography (**AS-OCT)** (Visante, Carl Zeiss, Germany), an intrastromal laminar cut of 9.5 mm of diameter was created and dissected, the femtosecond laser-assisted corneal dissection ended with a 30^0 anterior side cut as a corneal incision, and the arc length incision was 3mm. to reduce the intraocular pressure and allow the higher volume to be injected into de stromal pocket. Previous to the cellular injection, to reduce the intraocular pressure and allow the higher volume to be injected into the stromal pocket, a 1 mm corneal paracentesis was performed. An injection of 3 million autologous **ADASCs** in 1 ml **PBS** in the stroma pocket using a 25-G cannula was performed. No corneal sutures were used (Figure. 2) (19).

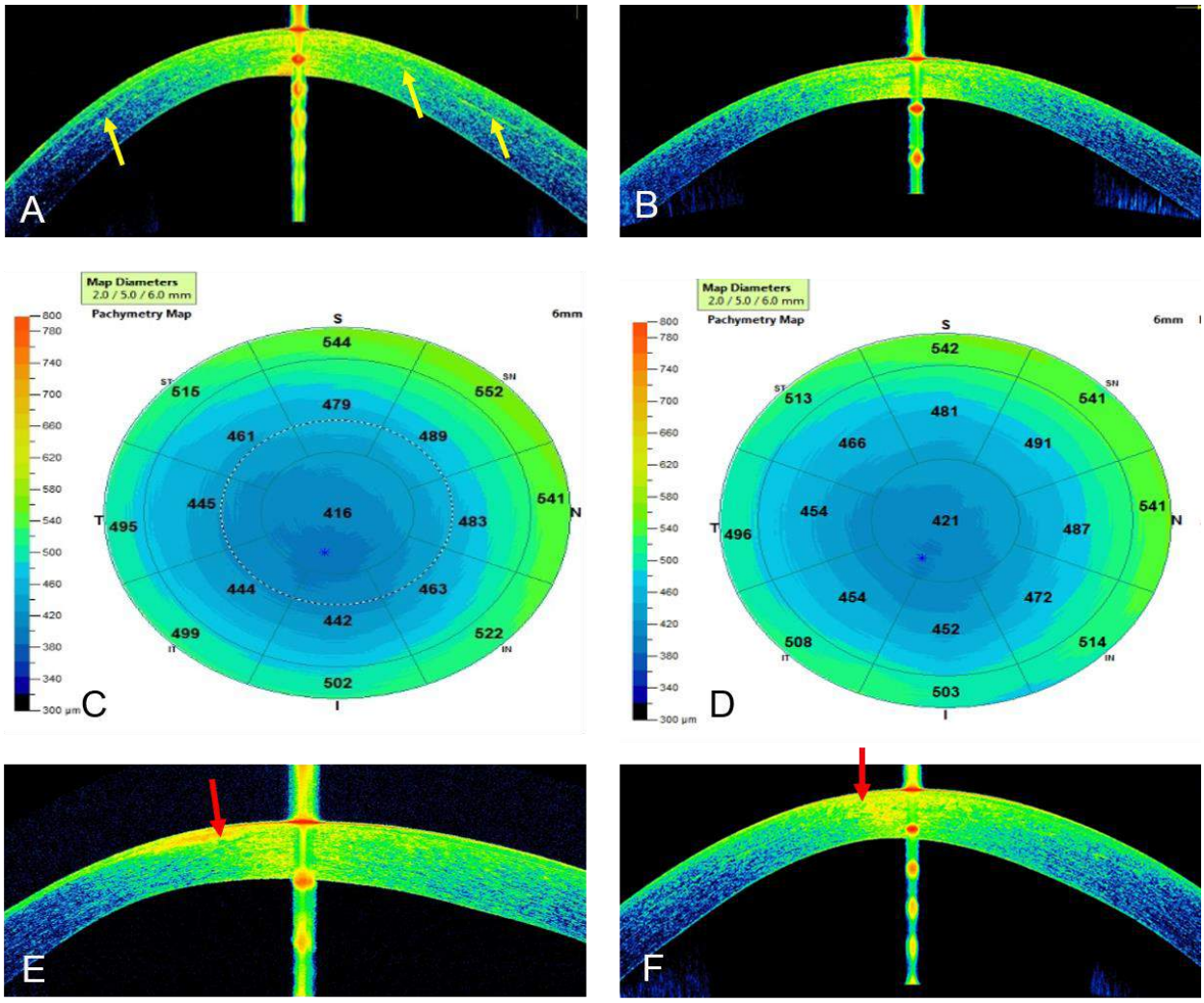

Figure. 2 Anterior segment OCT-Visante (**Visante OCT**). **(A, B)** G-1, case 1. (A) At 1 month postoperative, a formation of a few neo-collagen in the dissected pocket (yellow arrows) can be seen. **(B) OCT** at 12 months post-op of case 1, notice the transparency of the cornea. **(C, D)** Same anterior case. Observe the stability of the paquimetric parameters among one-month postoperative **(C)** and **(D)** 12 months postoperative. **(E)** G-1 case 2, observe the high reflectance corresponded to paracentral scars. **(F)** Same case 2, at 3 years postoperative. Observe the enhancement of the paracentral scars.

3.4.2 Decellularized/or Recellularized Human Corneal Stroma Laminas.

Topical anesthesia was applied with oral sedation for all surgeries. The 60-kHz IntraLase **IFS** femtosecond laser was used in single-pass mode. Assisted corneal dissection was done with a 50^0 anterior cut, and the arc length incision was 4 mm, and through the corneal intrastromal pocket the lamina was inserted, then centered and unfolded through the application of gentle tapping and

massaging from the epithelial surface of the cornea. Only with the cases of the G-3, In those cases that received a recellularized lamina, the pocket was irrigated immediately before and after insertion with a solution containing an additional 1 million autologous **ADASCs** in 1 ml of **PBS** using a 25-G cannula. One interrupted 10/0 nylon suture was performed and was then removed one week after the operation. Topical antibiotics and steroids were applied at the end of the surgery. (Figure. 3, 4) (20).

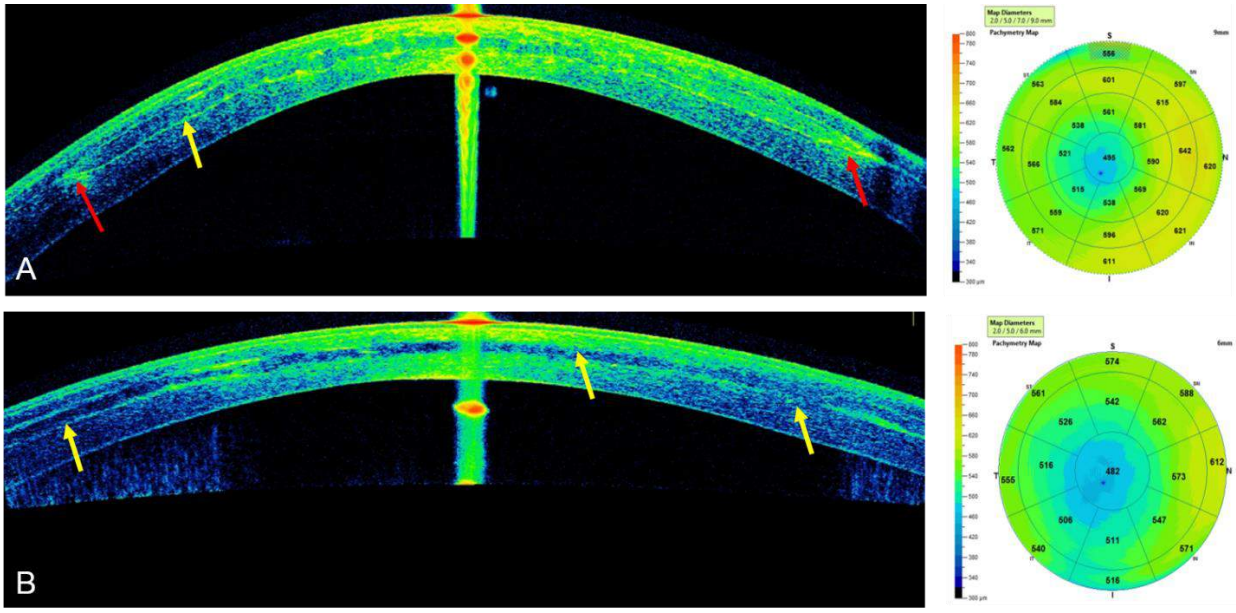

Figure 3. Anterior segment OCT-Visante (**Visante OCT**). G-2, case 5. **(A)** At 6 months postoperative, (red arrows) represent the reflectance of the periphery of the implanted lamina. (Yellow arrow) represents the improvement of the reflective band of neo-collagen. **(B)** At 36 postoperative, (yellow arrows) represent the improvement of the reflective band of neo-collagen of the implanted lamina. Observe the enhancement in the reflectance of this band from 6 months till 3 years postoperative. Notice the few changes in the pachymetric map among 6 months and 3 years postoperative, this due to the enhancement of the integration, homogeneity, and the improvement of the densimetry of the implanted tissue over time.

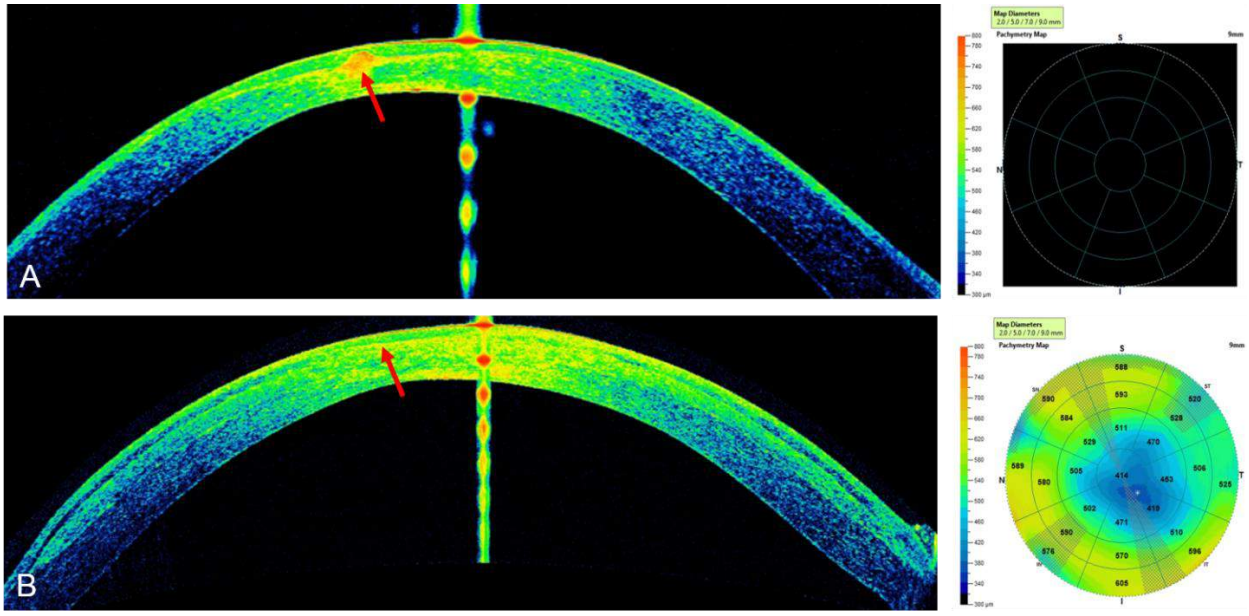

Figure 4. Anterior segment OCT-Visante (**Visante OCT**). G-3, case 11 very advanced keratoconus. **(A)** Preoperative time. The high reflectance can be seen (red arrow) due to a paracentral scar. The capture of the pachymetric map was not possible. **(B)** At almost 3 years postoperative. The enhancement of the integration of the lamina in the host corneal stroma can be observed. A noticeable improvement of the pachymetric map was obtained. As well an enhancement in the corneal densimetry was noticed. Observe the paracentral preoperative sacar has disappeared (red arrow).

3.5 Confocal microscopy study.

3.5.1 Methodology

The confocal microscope HRT3 RCM (Heidelberg) with Rostock Cornea Module was used. An area is known as the "region of interest" was determined (23,31). Almost the same area of (0.1 mm^2) was taken in all the studied pictures. The count of Nuclei cells was performed with 50% brightness and contrast, the nucleus of cells that had well-defined edges were selected with the blue marker of the device, that cell nucleus was more illuminated, and more refringent (23,32).

ADASCs Counting

The counting method for transplanted **ADASCs** at one month after surgery was performed similarly to the normal corneal keratocytes. **ADASCs** appeared rounded in shape, more voluminous, and refringent (Figure 5A) (23).

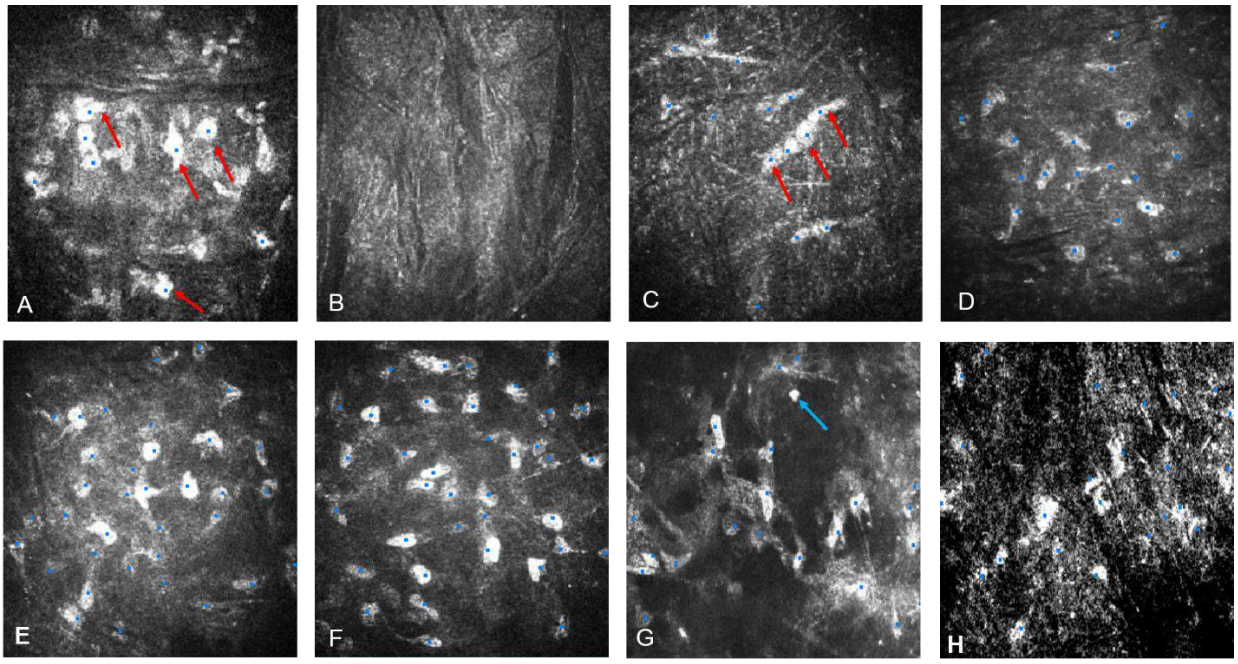

Figure 5. Confocal microscopy findings in G-1, G-2, and G-3. **(A)** G-1, case 1 at 3 months, at the level of the stromal pocket, ADASCs (red arrows) have a rounded shape, more luminous, and more refringent than the normal keratocytes. **(B)** G-2, case 5, observe the acellular anterior surface of the decellularized lamina at 1 month. **(C)** G-3, case 12, notice the anterior surface of a recellularized lamina at 1 month; few ADASCs can be seen (red arrows). **(D)** G-1 case 2, shows the anterior stroma at the preoperative time. **(E)** Same case 2, in the anterior stroma at 12 months, shows an increase in cell density statistically significant. **(F)** G-1, case 1 at the stromal pocket, an increase in cell density statistically significant was obtained at 12 months. **(G)** G-2, case 5, at the posterior surface of the decellularized lamina, an increase in cell density statistically significant was obtained after 12 months. The (blue arrow) shows highly reflective dots. **(H)** G-3, case 12, notice the posterior surface of the lamina at 12 months with an increase of cell density statistically significant.

Cell count on decellularized and recellularized laminas

One month after surgery, the decellularized laminas appeared without the presence of well-defined cell structures, then they were considered acellular (Figure 5B). Unlike the recellularized laminas that appeared with the presence of structures similar to the host keratocytes, so these structures were counted as cell nuclei (Figure 5C) (23).

4. RESULTS

4.1. Autologous ADASCs Implantation.

4.1.1 Clinical Results.

No complications were recorded such as haze or infection during the 3-year follow-up. In this group of **ADASCs** implantation, full corneal transparency was observed within the first postoperative day in all the cases. Besides, as described in our previous reports case-2 from G-1 presented in the anterior stroma with preoperative paracentral scars, but we observed an evident enhancement of those scars, with continuous improve over the 36 months of follow-up (Figures 6A,6B). At the level of the stromal pocket, new collagen production was noted as patchy hyperreflective areas (Figure 2 A,B) (19,21). No patient lost lines of visual acuity. All cases presented an enhancement in their visuals outcomes: The improvement was in the Unaided distance visual acuity (**UDVA**) of (0.08,0.14,0.12) (Figure 7A; Table 2), in the corrected distance visual acuity (**CDVA**) was (0.11,0.2,0.18) (Figure 7B; Table 2), and in the rigid contact lens visual acuity (**CLDVA**) was (0.11,0.19,0.23) (Figure 7C; Table 2), in decimal lines mean value equivalents in LogMar scale at 6, 12 and 36 months of follow up (24).

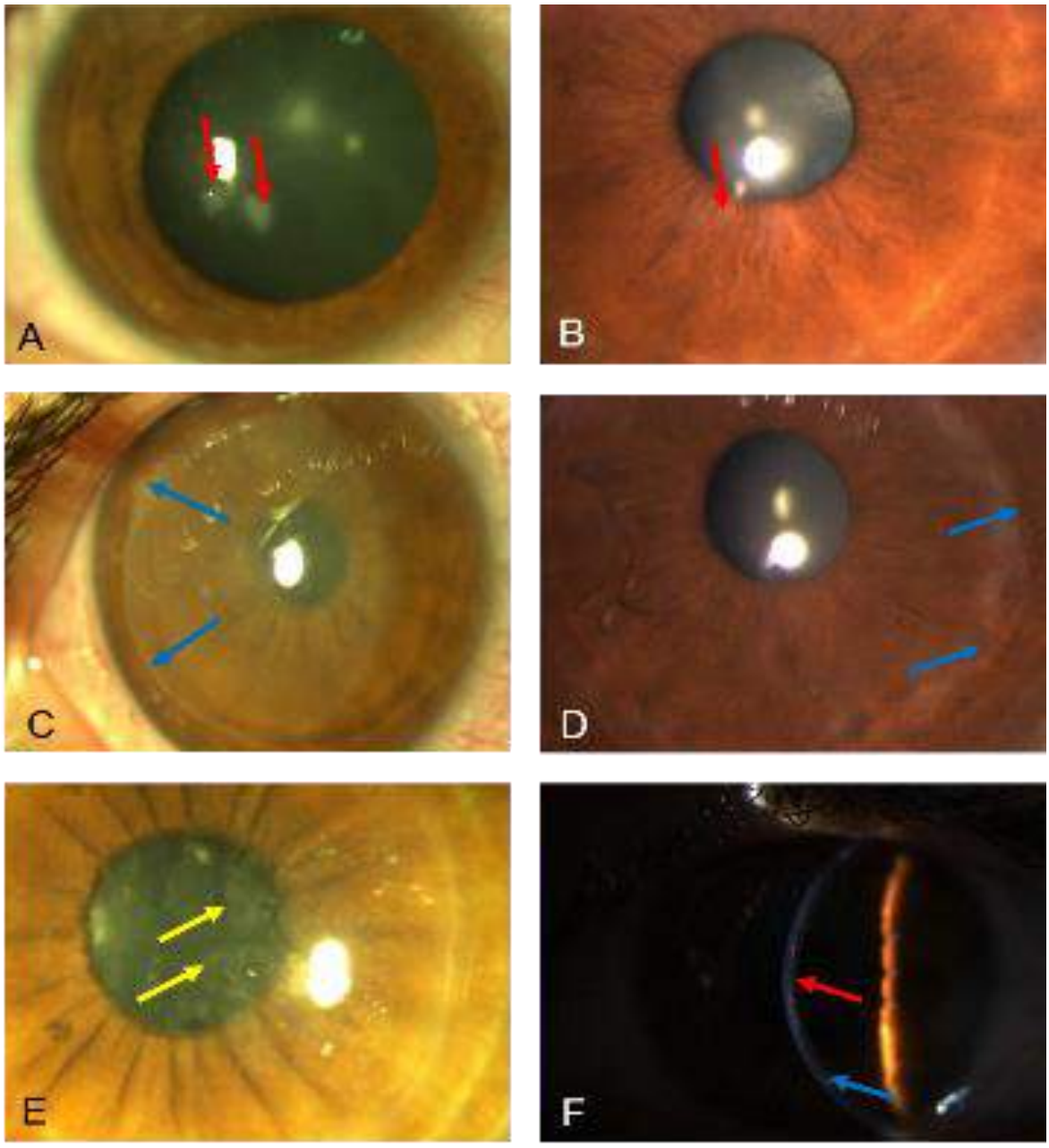

Figure 6. Biomicroscopic changes between the preoperative and up to 36 months post-operative in G-1, G-2 & G-3 **(A)** Case 2, G-1. Observe the presence of paracentral scars (red arrows) at the preoperative time. **(B)** Case 2, G-1 at 36 months postoperative, shows the transparency of the cornea and the marked improvement of the para-central scars (red arrow). **(C)** Case 5, G-2, 1 day postoperative, shows the reduced transparency of the implanted lamina, (blue arrows) represent the border of the lamina. **(D)** Case 5, G-2, 36 months post-op, presents improving the transparency of the implanted tissue. (Blue arrow) represent the border of the lamina. **(E)** G-3, case 10, at one month postoperative. The (yellow arrows) indicate the reduced transparency of the implanted recellularized lamina. **(F)** G-3, case 10, at 12 months post-op. The (blue arrow) indicates the periphery of the recellularized lamina. Notice the improvement of the transparency of the implanted tissue (red arrow).

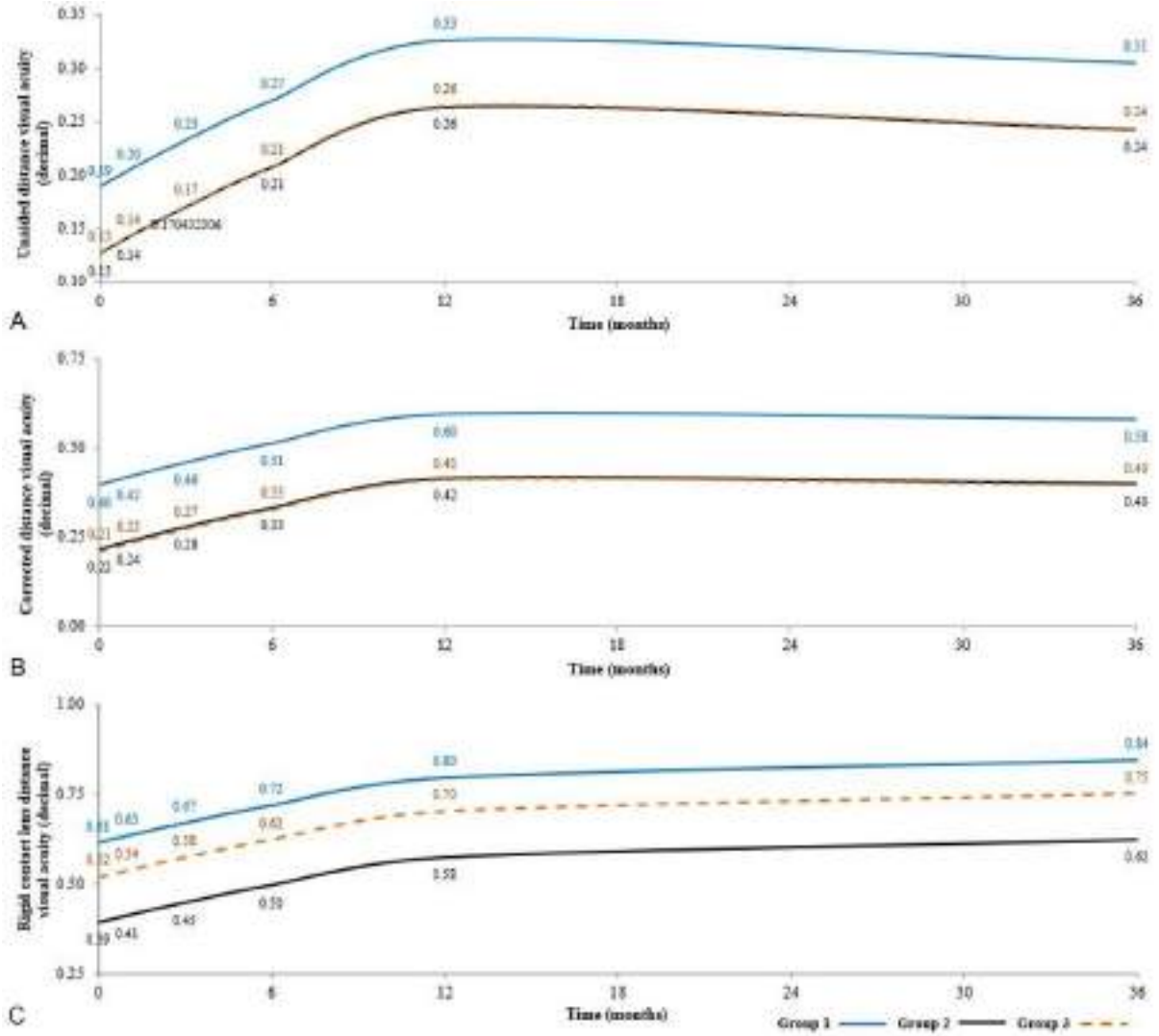

Figure 7. Demonstrated the statistical mean results after 36 months follow-up in G-1, G-2 & G-3, and Shows the improvement in **(A)** Unaided visual acuity **(UDVA), (B)** corrected distance visual acuity **(CDVA), (C)** rigid contact lens visual acuity **(CLDVA)** in decimal (equivalent to Loghmar scale) from the preoperative till 36 months.

Table 2: Difference in mean values of the variables of this study among the three groups.

	(G-1) – (G-2)	(G-1) – (G-3)	(G-2) – (G-3)
UDVA	0.07	0.07	0.00
CDVA	0.18*	0.19*	0.01
CLDVA	0.22*	0.10	-0.12*
Visante CCT (µm)	-44.00*	-77.00*	-33.00
Thinnest point (µm)	-51.00*	-65.00*	-14.00
CV (mm^3)	-5.00*	-5.00*	0.00
Rx Sphr (D)	0.10	-0.10	-0.20
Rx Cyl (D)	-1.00*	-0.60*	0.40
Anterior Km (D)	-3.00	1.00	4.00
Kmax (D)	0.00	2.00	2.00
Posterior Km (D)	1.3*	0.2	-1.1*
Topo Cyl (D)	1.1	0.9	-0.2
3rd order RMS	4.65*	3.54*	-1.11
4th order RMS	1.28	-0.17	-1.45*
HOA RMS	4.9	2.78	-2.12
LOA RMS	-3.87*	1.32*	5.19

* Indicates a statistically significant difference between the compared groups. (G-1) – (G-2) = difference in mean values between G-1 and G-2. (G-1) – (G-3) = differencein mean values between G-1 and G-3. (G-2) – (G-3) = difference in mean values between G-2 and G-3.

The Central corneal thickness (**CCT**) (µm) was measured by **AS-OCT** (Visante, Carl Zeiss), the thinnest point (**Thinnest point**) (µm), and Cornea Volume **(CV**) (mm^3) were measured by Scheimpflug corneal topography. An increase in mean values with all patients of this group in **CCT** by (36,59,30) (µm**)** (Figures 2, 8A**), in the Thinnest point** (29,48,31) (µm) (Figures 8B, 9A), and the **CV** (3,4,3) (mm^3) were obtained during the 6,12 and 36 months of follow-up ((24). Besides, the Refractive sphere (**Rx Sphr**) (D) presented an improvement of (0.8,1.3,1.1) myopic diopters during the 3-year follow-up, meanwhile, the refractive cylinder (**Rx Cyl**) (D) remained almost stable up to 12 months post-operative, then it was followed by a change of 0.5 (D) until 36 months post-operative regarding the pre-operative mean values (Table 2) (24).

Also, an improvement in mean values was observed during the 3-year follow up in the following aberrations: Third-order aberration RMS **(3^{rd} order RMS)** (µm)**,** fourth-order aberration RMS **(4^{th} order RMS)** (µm)**,** high order aberration RMS **(HOA RMS)** (µm) and Low order aberration RMS **(LOA RMS)** (Table 2) (24).

The results of Anterior mean keratometry (**Anterior Km**) (D) (Figure 8C) presented a modest improvement of mean values of 2 (D) during the 3-year follow-up. Meanwhile, stability in mean values of Posterior mean keratometry (**Posterior Km**) (D) was detected up to 36 months post-operative. Nevertheless, the authors found a flattening in mean values of 3 (D) in maximum keratometry (**Kmax**) (D) (Figure 8D) during the 36 months follow-up. Finally, a mild deterioration of -0.3 (D) was obtain**ed** at 12 months post-operative in the topographic cylinder **(Topo Cyl)** (D)**,** at 3 years post-operative, they obtained the same pre-operative mean values (24).

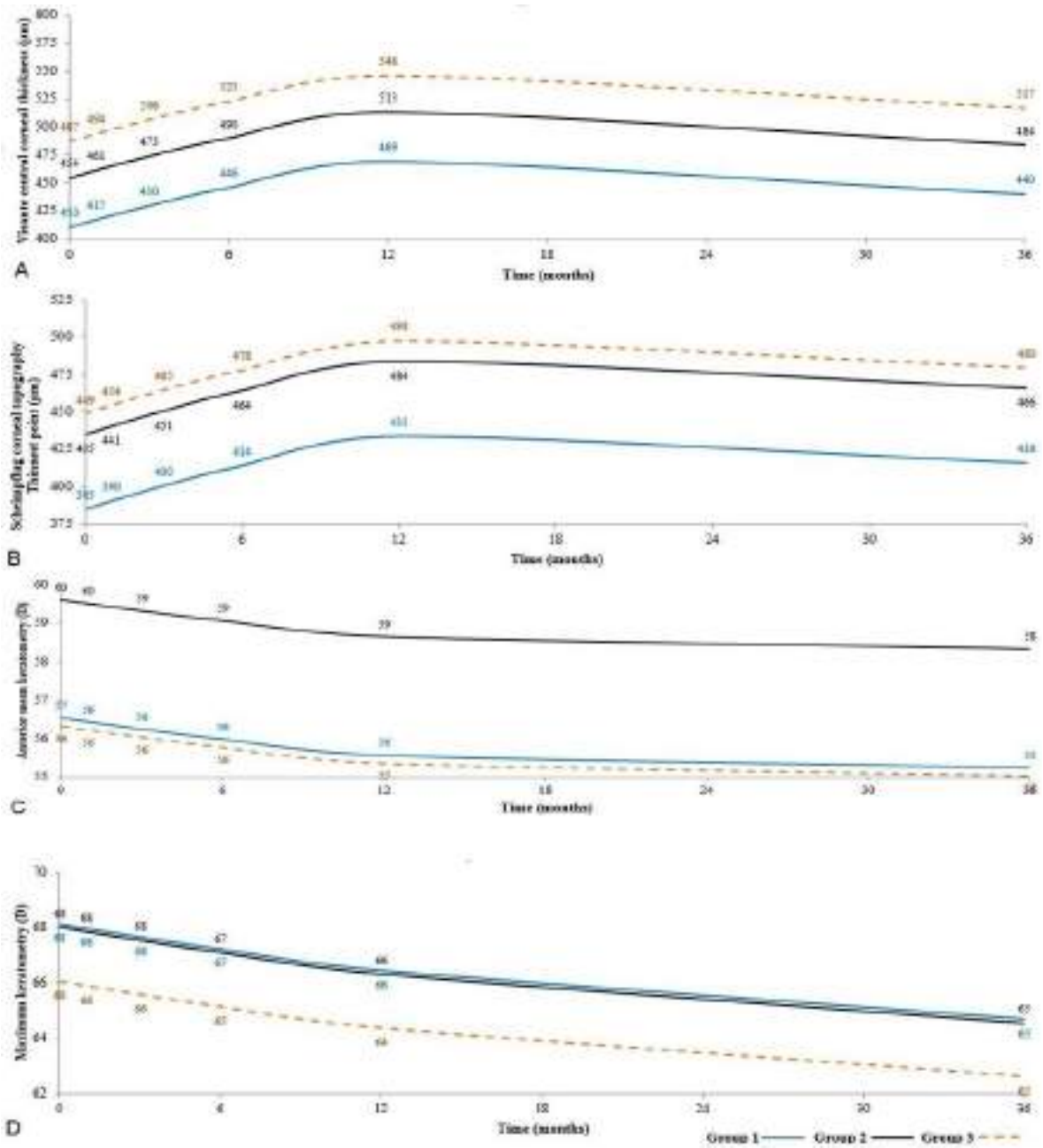

Figure 8. Paquimetric and keratometric outcomes after 3 years of follow-up in G-1, G-2 & G-3. **(A)** Presents central corneal thickness **(CCT)** (µm), was measured with **AS-OCT** Visante. **(B)** Scheimpflug corneal topography thinnest point **(Thinnest point)** (µm). Observe the increase in mean values from the pre-operative, till reached a maximum at 12 months and they were established with a slow decrease at 36 months. A statistically significant improvement in the mean values was obtained in **(CCT),** and **(Thinnest point)** in G-2 & G-3 when compared to G-1. **(C)** shows mean values of anterior mean keratometry (**Anterior Km)** (D). Notice the improvement of 2 diopters of flattening till 36 months. **(D)** Maximum keratometry **(Kmax)** (D): there was a mean flattening of 3 diopters at 36 months.

4.1.2 Confocal Microscopy Results.

Morphological results showed up to 6 months post-operative that **ADASCs** appeared rounded in shape, more voluminous, and refringent than the host corneal keratocytes (Figure 5A). Besides, statistical results at 12 months post-operative demonstrated a gradual statistically significant increase in the cell density at the anterior (Figures 5D,5E) , mid (Figure 5F), and posterior corneal stroma when compared to the preoperative values (23). Also, the authors performed a study to detect any appearance of fibrotic tissue, they found at 3 months postoperative in 2 out of the 4 patients presence of small fibrotic structures, but a full recovery of the corneal stroma was observed at 12 months follow-up (23).

4.2 Decellularized and Recellularized Corneal Human Laminas Implantation.

4.2.1 Clinical Results.

The authors did not observe any complications during the 3-year follow-up, only during the first postoperative month, the implanted lamina's showed a mild early haziness, this matter was related to mild lenticular edema. Corneal recovery and full transparency were recuperated within the third post-operative month with all the cases. Aside, no adverse events were recorded over the 3 years (Figures 6C-6F) (24).

All cases in the G-2, and G-3 showed an improvement in their clinical outcomes during 6,12 and 36 months of follow up, the enhancement in **UDVA** was (0.08,0.13.0.11) in decimal values almost equivalent to one line in logMar scale with decellularized and recellularized laminas (Figure 7A; Table 2), all patients upgrade their **CDVA** with the following the decimal values (0.11,0.2,0.18) with decellularized lamina and (0.12,0.2,0.19) with recellularized ones, equivalent to 1-2 lines in LogMar scale (Figure 7B; Table 2), as well **CLDVA** means improvement was (0.11,0.19,0.23) in

decimal values with decellularized laminas, and (0.1,0.18,0,23) in decimal values with recellularized ones (Figure 7C; Table 2), equivalent to 1-2 lines in LogMar scale.

The mean values of **CCT** (µm) (Figure 8A)**, Thinnest point** (µm) (Figure 8B) showed an enhancement of (36,59,30) (µm)**,** and (29,49,31) (µm) respectively, also, mean value results **of CV** (mm^3) revealed an increase of (2,3,2) (mm^3) in both laminas' groups at 6,12 and 3-year of follow up (24). The results were statistically significantly better in G-2 and G-3 comparing with G-1 (Table 2).

Besides the **Rx Sphr** (D), **Rx Cyl** (D), Results of **3rd order RMS** (µm)**, 4th order RMS** (µm), **HOA RMS** (µm)**,** and **LOA RMS** (µm). **Anterior Km** (D) (Figure 8C), **Posterior Km** (D), **Kmax** (D) (Figure 8F)a, and **Topo Cyl** (D) with the groups of decellularized and recellularized laminas, the authors obtained results close to patients' results of the group with implantation of **ADASCs** alone (Table 2) (24).

More information about the comparative results among the three groups was summarized in (Table 2).

4.2.2 Confocal Microscopy Results.

One month after the surgery, the implanted decellularized laminas remained acellular in most of the patients (Figure 5B) (20)(21), unlike the recellularized ones, few **ADASCs** were seen on the anterior surface of the laminas, they were smaller than the normal keratocytes (Figure 5C). Three months after surgery, the patient's host cells started colonizing the laminas, the number of cells on the laminas increase progressively over time. Up to 12 months follow-up, the anterior, mid, and posterior surfaces of the decellularized and recellularized laminas became more colonized by keratocyte-type cells, they showed similar morphology to normal corneal keratocytes (Figures 5G,5H), and the cell density was statistically significantly highest then the one obtained at the first

postoperative month. Besides, one year after surgery, the cell density of the anterior, and posterior corneal stroma showed a statistically significant increase in the number of keratocytes, these results were close to that found in a normal cornea (23). The confocal microscopy study also demonstrated the presence of fibrotic tissue in non-central corneal areas, almost all of the cases implanted with decellularized lamina's and recellularized ones showed the presence of such fibrotic structures, the statistical study demonstrated that no significant association was found between recellularization and the presence of such fibrotic tissue on the periphery of the decellularized or recellularized laminas (23).

5. DISCUSSION: ADVANCED STEM CELL THERAPIES vs TECHNOLOGIES ALLOGENIC STROMAL TRANSPLANATION AND RECOMBINANT CORNEAL COLLAGEN

Our research group demonstrated for the first time the viability of a new type of regenerative al corneal surgeries, authors implanted autologous **ADASCs** into the medium depth of the thinnest preoperative pachymetry in cases with advanced keratoconus, also they confirmed the appearance of new collagen in the injected stromal pocket, that could be useful for repairing the corneal scars, and dystrophies, and may also slightly increase the corneal thickness, but this amount of collagen is not enough to restore corneal disease in cases with advanced keratoconus (18,19,21,24,33,34)Also, we could demonstrate that decellularized laminas of a human corneal stroma, embedded or not by autologous **ADASCs**, can be implanted in the mid stroma of patients with advanced keratoconus for therapeutic purposes (Figures 2,3,4,9). 3-year of follow-up, in no

case we detected inflammation, rejection, or any evidence of scarring or haze (Figures 2,3,4,6) (18,20,21,23,24,33,34).

Besides, an improvement in all the visual parameters with 1-2 lines in LogMar was obtained (Figure 7). In G-1, we obtained an improvement in mean results of 30 (µm), 31 (µm), and 3 (mm^3) in **CCT** (Figure 8A), **thinnest point** (Figure 8B), and **CV** respectively, comparing the results at 36 months of the G-2, and G-3 with the G-1, we obtained statistical differences significantly better in patients with implanted laminas. The **CCT** mean the difference among G-1/G-2 was 44 (µm), however, when comparing G-1/G-3 this mean difference was 77 (µm) (Figure 8A; Table 2). In the **thinnest point,** the mean difference was 51 (µm) among G-1/G-2 and 65 (µm) among G-1/G-3 (Figure 8B; Table 2). In **CV the** mean differences were 5 (mm^3) when comparing G-1/G-2, and G-1/G-3 (Table 2) (18,24,33,34).

We obtained also, an improvement in the corneal aberrometry, and corneal topographic parameters (Figure 9) (18,24,33,34).

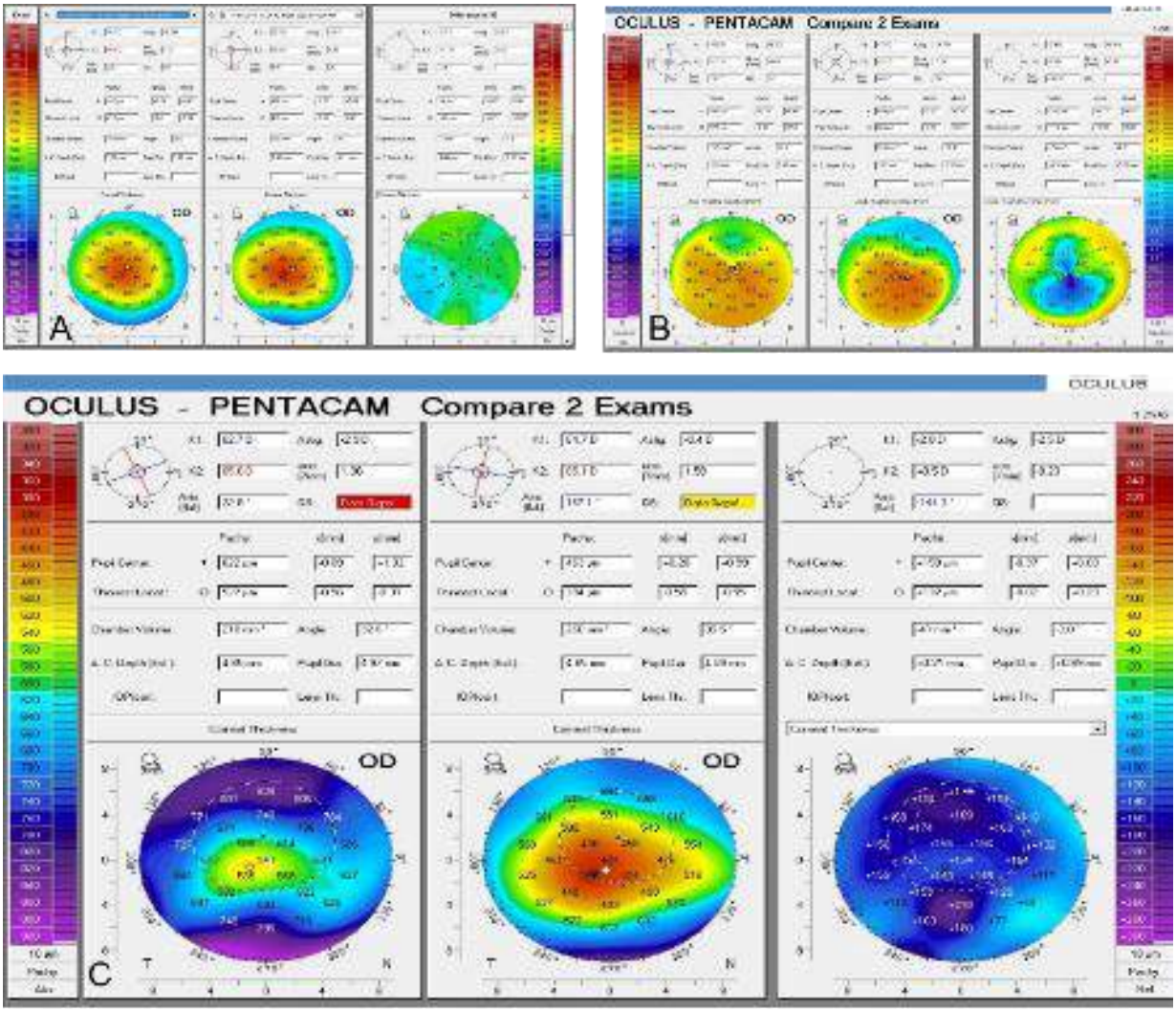

Figure 9. Corneal topography (Pentacam), comparative examinations among the preoperative, 12 and 36 months post-op. **(A)**) G-1, case 1. Preoperative topography (middle), and 12 months post-op (left side). Comparative paquimetric results (right side). Observe the modest enhancement of the corneal thickness. **(B)** G-2, case 6. Preoperative (middle), at36 months post-op (left side), and the sagittal curvature comparative results (right side). Observe the enhancement in the keratometric parameters of the cornea. **(C)** Comparative pachymetric results (right side), the preoperative (middle), and 3 years postoperative (left side) in G-3, case 12. The enhancement of the pachymetric parameters can be noticed.

The confocal microscopy findings at 12 months follow up, showed an evolution of **ADASCs** nuclei and morphological changes. Up to six months, **ADASCs** were rounded shape, more voluminous, and highly refringent, after 6 months the structures of these cells changed to fusiform shape and less nucleus refringent. As in human beings, we can not perform a post-mortem analysis, these findings demonstrate in the human clinical model that the **ADASCs** implanted in the corneal human pocket have survived and have been able to differentiate into keratocytes (Figures 5A,5F) (18,23,33,34).

One year after the surgery, in the anterior, mid, and posterior stroma in G-1, a gradual and significant increase (P-value <0.001) was obtained in the cell density, as well in the anterior, and posterior stroma, and among the implanted decellularized/ or recellularized tissue when comparing the outcomes with the preoperative density level (18,23,33,34). Such findings confirm the previous animal studies, in which a post-mortem analysis was performed, and demonstrated the presence and survival of these human cells and the production of human collagen into the rabbit cornea (6,8).

Other alternatives being studied by other researchers in the collagen production line, and SMILE lenticule corneal inlay grafts, have been transplanted into the corneal stroma without having been subjected to decellularization protocols, they should be considered as a variant of corneal stromal transplantation (34). Jorge Alio et al with another group in Tehran (35), performed a prospective study, and reported a novel method with customized **SMILE** lenticule implantation, 22 cases of advanced keratoconus received this new surgery (shape of the lenticule was compound form or necklace). They obtained a mean enhancement of 100.4 µm of corneal thickness at the thinnest point measured by **AS-OCT**. An improvement in visual outcomes was observed, at six months with all the patients, the best **CDVA** improved from 0.70 (range 0.4–1) to 0.49 (range 0.3–0.7),

this fact was consistent with the decline in corneal aberration, also some flattening was obtained by a decrease in keratometry from 54.68 ± 2.77 to 51.95 ± 2.21 (D). This study needs more follow-up to ensure long-term results, also, the laminas contains allogenic cells, meanwhile with the planner decellularized laminas the implant is safer, no rejection is expected because the implant was autologous, and does not contain heterologous cells (18,20,21,23,24,33,34).

Using other approaches, different authors have been proven in an ex vivo and in vivo the feasibility of allogenic small incision lenticule extraction **(SMILE)** implantation in cases with advanced keratoconus, they proved that the implantation of negative meniscus shaped lenticules was safe, and efficacy in the treatment of thinning disorders such as keratoconus. Mastropasqua et al (36,37) obtained a flattening of the cone, and a decrease of **Anterior Km** from 58.69 ± 3.59 (D) to 53.59 ± 3.50 (D) was obtained at 6 months after surgery. Ganesh et al evaluated the outcomes of femtosecond intrastromal lenticular implantation (**FILI**) from corneal stroma donor tissue, combined with accelerated collagen cross-linking (**CXL)** (38,39), they obtained a flattening of **Km** in 3-mm and 5-mm zones by 3.42 (D) and 1.70 (D), respectively. Meanwhile, with Jorge Alio et al the (18,24,33,34) flattening in the keratometric values was almost 2 (D) in the **Anterior Km,** and 3 (D) **in Kmax** at 36 months after the surgery.

Reinstein et al (40), using a different approach, proposed femtosecond laser-assisted small incision sutureless intrasotromal lamellar keratoplasty (**SILK**), and obtained a flattening of 7,34 (D) in **Kmax**. These results were planar than the lenticules implanted by Alió et al (18,24,33,34), but it was obtained with only one case report (40).

Other comparatives surgical procedures (41), small-incision femtosecond laser-assisted intracorneal concave lenticule implantation **SFII,** and penetrating keratoplasty **PKP** resulted in a

stable corneal volume and improved visual acuity during the 24-month study period. **SFII** was less invasive and more efficient when compared with **PKP**. Using concave lenticule implantation improved the maximum central keratometry of (-4.65 ± 2.04) (D), this outcome was more planner than the laminas implanted with Alio et al (18,24,33,34,41).

Using planner lenticules, the increase in corneal thickness (18–21,24,33,34) is higher than the one using allogenic **SMILE** lenticule corneal inlay implantation combined or not with collagen **CXL** (37,39,41). Besides, the planner laminas improved aberrometry parameters during 3-year follow-up in almost all the study cases. Meanwhile, donut-shaped lenticules or negative meniscus-shaped lenticules are only suggested for pure central cones, as for eccentric cones which are more frequent in this disease they would generate non-acceptable aberrations within the visual.

The use of customized positive meniscus lenticules in keratoconus corneas is debatable (35,39), as could worsen myopia usually encountered in such patients, and so planar or negative meniscus lenticules are always preferable for such purpose. The visual acuity enhancement has been slightly better with the negative meniscus lenticules implant than with the implant of planar laminas (24,37,39,41), but the goal of our regenerative surgery is not only to improve visual acuity but also at the same time, increase significantly the corneal pachymetry in patients with advanced keratoconus, this fact was carried out in our study, although with a small sample (18,20,21,23,24,33,34). Further studies are needed to increase the clinical number, and enhance the results.

The use of recombinant human collagen, synthesized in yeast and chemically cross-linked demonstrated to be feasible (42,43), improved the visual acuity, nevertheless, a large variation of corneal thickness was obtained among the cases of this study up to 24 months of follow-up, and high presence of fibrosis was observed. With the implantation of decellularized or recellularized

laminas, the presence of fibrotic tissue was detected, but always in the periphery of the implanted laminas, a fact that may be due to the impact of the **IFS** femtosecond laser on the periphery of the cut laminas, as well as in the periphery of the created corneal pocket (18,20,21,23,24,33,34).

The use of acellular laminas (20,21,23,24), in which the lack of cells makes the experience out from being considered as a corneal graft, and by using autologous **MSCs** from a given patient, it was possible to transform allogenic grafts into functional autologous grafts, thus avoiding any risk of rejection. So far, the long-term follow-up did not show any complications with all the cases (24).

6. CONCLUSION

In conclusion, cellular therapy of the corneal stroma is a novel treatment for stromal diseases such as keratoconus, even though, further clinical studies are still essential with larger sample sizes to ensure the safety, and effectiveness of this surgery for different corneal stromal diseases, the initial results obtained from this first clinical trials are encouraging. In our belief, the creation of cellular banks for storing, shipping, and delivery of the stem cells or their exosomes to the different clinical centers for their use, could be a very promising treatment modality. Although, the treatment of the diseased corneas with the implantation of the decellularized or recellularized corneal stromal laminas, along with those of allogeneic stromal transplantation are shown as viable short-term alternatives in the treatment of keratoconus. further studies will be needed to expand the potential of the application of this new therapy in the treatment of corneal stromal diseases.

ABBREVIATIONS

ADASCs: Adipose-derived adult stem cells.

SMILE: Small incision lenticule extraction**.**

PKP: Penetrating keratoplasty.

SFII: Femtosecond laser-assisted intracorneal concave lenticule implantation.

SILK: Small incision sutureless intrasotromal lamellar keratoplasty.

UDVA: Unaided distance visual acuity.

CDVA: Corrected distance visual acuity.

MSCs: Mesenchymal stem cells.

h-ADASCs: Human Adipose-Derived Adult Stem Cells.

PBS: Phosphate-buffered saline.

IFS: IntraLase femtosecond laser

AS-OCT: Anterior segment optical coherence tomography.

CLVA: Contact lens visual acuity**.**

CCT: Central corneal thickness.

Thinnest point: Scheimpflug corneal topography Thinnest point.

CV: Cornea Volume**.**

Rx Sphr: Refractive sphere**.**

Rx Cyl: Refractive cylinder**.**

3rd order RMS: Third-order aberration RMS**.**

4th order RMS: Fourth-order aberration RMS**.**

HOA RMS: High order aberration RMS.

LOA RMS: Low order aberration RMS**.**

Anterior Km: Anterior mean keratometry**.**

Posterior Km: Posterior mean keratometry**.**

Kmax: Maximum keratometry**.**

Topo Cyl: Topographic cylinder.

FILI: Femtosecond intrastromal lenticular implantation.

CXL: Cross-linking.

COMPLIANCE WITH ETHICS GUIDELINES

Conflict of interest: the authors, their families, their employers, and their business associates have no financial or proprietary interest in any product or company associated with any device, instrument, or drug mentioned in this study. The authors have not received any payment as reviewers, consultants, or evaluators of any of the instruments, devices, or drugs mentioned in this study.

BIBLIOGRAPHY

1. De Miguel MP, Casaroli-Marano RP, Nieto-Nicolau N, Martínez-Conesa EM, Alió del Barrio JL, Alió JL, et al. Frontiers in regenerative medicine for cornea and ocular surface. In: Rahman A, Anjum S, editors. Frontiers in Stem Cell and Regenerative Medicine Research. 1st ed. Bentham e-Books; 2015. p. 92–138.

2. Alió J, Piñero D, Alesón A, Teus M, Barraquer R, Murta J, et al. Keratoconus-integrated characterization considering anterior corneal aberrations, internal astigmatism, and corneal biomechanics. J Cataract Refract Surg. 2011;37(3):552–68.

3. Alio J. Keratoconus: recent advances in diagnosis and treatment. Alió JL, editor. Springer; 2017.

4. Ruberti J, Zieske J. Prelude to corneal tissue engineering - gaining control of collagen organization. Prog Retin Eye Res. 2008;27(5):549–77.

5. Isaacson A, Swioklo S, Connon CJ. 3D bioprinting of a corneal stroma equivalent. Exp Eye Res. 2018;173:188–93.

6. Arnalich-Montiel F, Pastor S, Blazquez-Martinez, A Fernandez-Delgado J, Nistal M, Alio J, De Miguel M. Adipose-derived stem cells are a source for cell therapy of the corneal stroma. Stem Cells. 2008;26(2):570–9.

7. Alió del Barrio J, Chiesa M, Ferrer GG, Garagorri N, Briz N, Fernandez-Delgado J, et al. Biointegration of corneal macroporous membranes based on poly(ethyl acrylate) copolymers in an experimental animal model. J Biomed Mater Res A. 2015;103(3):1106–18.

8. Alio del Barrio J, Chiesa M, Garagorri N, Garcia-Urquia N, Fernandez-Delgado J, Bataille L, et al. Acellular human corneal matrix sheets seeded with human adipose-derived mesenchymal stem cells integrate functionally in an experimental animal model. Exp Eye Res. 2015;132:91–100.

9. Espandar L, Bunnell B, Wang G, Gregory P, McBride C, Moshirfar M. Adipose-derived stem cells on hyaluronic acid-derived scaffold: A new horizon in bioengineered cornea. Arch Ophthalmol. 2012;130(2):202–8.

10. Mittal SK, Omoto M, Amouzegar A, Sahu A, Alexandra R, Katikireddy KR, et al. Restoration of corneal transparency by mesenchymal stem cells. Stem Cell Reports. 2016;7(4):583–590.

11. Demirayak B, Yüksel N, Çelik O, Subaşı C, Duruksu G, Unal Z, et al. Effect of bone marrow and adipose tissue-derived mesenchymal stem cells on the natural course of corneal scarring after penetrating injury. Exp Eye Res. 2016;151:227–35.

12. Du Y, Carlson E, Funderburgh M, Birk D, Pearlman E, Guo N, et al. Stem cell therapy restores transparency to defective murine corneas. Stem Cells. 2009;27(7):1635–42.

13. Liu H, Zhang J, Liu C-Y, Wang I-J, Sieber M, Chang J, et al. Cell therapy of congenital corneal diseases with umbilical mesenchymal stem cells: lumican null mice. PLoS One. 2010;5(5):e10707.

14. Coulson Thomas VJ, Caterson B, Kao W. Transplantation of human umbilical mesenchymal stem cells cures the corneal defects of Mucopolysaccharidosis VII mice. Stem Cells. 2013;31(10):2116–2126.

15. Winston W-Y K, Vivien J. CT. Cell therapy of corneal diseases. Cornea. 2016;35(Suppl

1):S9–S19.

16. De Miguel M, Fuentes-Julián S, Blázquez-Martínez A, Pascual C, Aller M, Arias J, et al. Immunosuppressive properties of mesenchymal stem cells: advances and applications. Curr Mol Med. 2012;12(5):574–91.

17. Harkin D, Foyn L, Bray L, Sutherland A, Li F, Cronin B. Concise reviews: can mesenchymal stromal cells differentiate into corneal cells? A systematic review of published data. Stem Cells. 2015;33(3):785–91.

18. Alió JL, El Zarif M, Alió del Barrio JL. Cellular therapy of the corneal stroma: a new type of corneal surgery for keratoconus and corneal dystrophies a translational research experience. 1st ed. Elsevier; 2020.

19. Alió Del Barrio J, El Zarif M, De Miguel M, Azaar A, Makdissy N, Harb W, et al. Cellular therapy with human autologous adipose-derived adult stem cells for advanced keratoconus. Cornea. 2017;36(8):952–60.

20. Alió Del Barrio J, El Zarif M, Azaar A, Makdissy N, Khalil C, Harb W, et al. Corneal stroma enhancement with decellularized stromal laminas with or without stem cell recellularization for advanced keratoconus. Am J Ophthalmol. 2018;186:47–58.

21. Alió J, Alió Del Barrio J, El Zarif M, Azaar A, Makdissy N, Khalil C, et al. Regenerative surgery of the corneal stroma for advanced keratoconus: 1-year outcomes. Am J Ophthalmol. 2019;203:53–68.

22. Alió J, Alió del Barrio J. Cellular therapy with human autologous adipose-derived adult stem cells for advanced keratoconus: reply to the letter to editor. Cornea. 2017;36(12):e37.

23. El Zarif M, Abdul Jawad K, Alió del Barrio J, Abdul Jawad Z, Palazón-Bru A, De Miguel M, et al. Corneal stroma cell density evolution in keratoconus corneas following the implantation of adipose mesenchymal stem cells and corneal laminas: an in vivo confocal microscopy study. IOVS. 2020;61(4):22.

24. El Zarif M, Alió J, Alió del Barrio J, Abdul Jawad K, Palazón-Bru A, Abdul Jawad Z, et

al. Corneal stromal regeneration therapy for advanced keratoconus: long-term outcomes at 3 years. Cornea. 2021;40(6):741–54.

25. De Miguel M, Alio J, Arnalich-Montiel F, Fuentes-Julian S, de Benito-Llopis, L Amparo F, Bataille L. Cornea and ocular surface treatment. Curr Stem Cell Res Ther. 2010;5(2):195–204.

26. Lynch A, Ahearne M. Strategies for developing decellularized corneal scaffolds. Exp Eye Res. 2013;108:42–7.

27. Zuk P, Zhu M, Mizuno H, Huang J, Futrell J, Katz A, et al. Multilineage cells from human adipose tissue: implications for cell-based therapies. Tissue Eng. 2001;7(2):211–28.

28. Zuk PA, Zhu M, Ashjian P, De Ugarte D, Huang J, Mizuno H, et al. Human adipose tissue is a source of multipotent stem cells. Mol Biol Cell. 2002;13(12):4279–95.

29. Bourin P, Bunnell B, Casteilla L, Dominici M, Katz A, March K, et al. Stromal cells from the adipose tissue-derived stromal vascular fraction and culture expanded adipose tissue-derived stromal/stem cells: a joint statement of the International Federation for Adipose Therapeutics and Science (IFATS) and the International So. Cytotherapy. 2013;15(6):641–8.

30. Ponce Márquez S, Martínez V, McIntosh Ambrose W, Wang J, Gantxegui N, Schein O, et al. Decellularization of bovine corneas for tissue engineering applications. Acta Biomater. 2009;5(6):1839–47.

31. Guthoff R, Klink T, Schlunck G, Grehn F. Die sickerkissenuntersuchung mittels konfokaler in-vivo mikroskopie mit dem rostocker cornea modul - erste erfahrungen. Klin Monatsbl Augenheilkd. 2005;222:R8.

32. Ku J, Niederer R, Patel D, Sherwin T, McGhee C. Laser scanning in vivo confocal analysis of keratocyte density in keratoconus. Ophthalmology. 2008;115(5):845–50.

33. El Zarif M, Alió del Barrio JL, Arnalich-Montiel F, De Miguel MP, Makdissy N, Alió JL. Corneal stroma regeneration: new approach for the treatment of cornea disease. APJO.

2020;9(6):571–9.

34. El Zarif M, Alió JL, Alió del Barrio JL, De Miguel MP, Abdul Jawad K, Makdissy N. Corneal stromal regeneration: a review on human clinical studies for treatement of keratoconus. Front Med. 2021;8:650724.

35. Doroodgar F, Jabbarvand M, Niazi S, Karimian F, Niazi F, Sanginabadi A, et al. Customized stromal lenticule implantation for keratoconus. J Refract Surg. 2020;36(12):786–94.

36. Mastropasqua L, Nubile M. Corneal thickening and central flattening induced by femtosecond laser hyperopic-shaped intrastromal lenticule implantation. Int Ophthalmol. 2017;37(4):893–904.

37. Mastropasqua L, Nubile M, Salgari N, Mastropasqua R. Femtosecond laser-assisted stromal lenticule addition keratoplasty for the treatment of advanced keratoconus: a preliminary study. J Refract Surg. 2018;34(1):36–44.

38. Ganesh S, Brar S, Rao P. Cryopreservation of extracted corneal lenticules after small incision lenticule extraction for potential use in human subjects. Cornea. 2014;33(12):1355–62.

39. Ganesh S, Brar S. Femtosecond intrastromal lenticular implantation combined with accelerated collagen cross-linking for the treatment of keratoconus-- initial clinical result in 6 eyes. Cornea. 2015;34(10):1331–9.

40. Pradhan K, Reinstein D, Vida R, Archer T, Dhungel S, Moptom D, et al. Femtosecond laser–assisted small incision sutureless intrastromal lamellar keratoplasty (SILK) for corneal transplantation in keratoconus. J Refract Surg. 2019;35(10):663–71.

41. Jin H, He M, Liu H, Zhong X, Wu J, Liu L, et al. Small-incision femtosecond laser–assisted intracorneal concave lenticule implantation in patients with keratoconus. Cornea. 2019;38(4):446–453.

42. Gahmberg C, Fagerholm S, Nurmi S, Chavakis T, Marchesan S, Grönholm M. Regulation

of integrin activity and signalling. Biochim Biophys Acta. 2009;1790(6):431–44.

43. Fagerholm P, Lagali N, Merrett K, Jackson W, Munger R, Liu Y, et al. A biosynthetic alternative to human donor tissue for inducing corneal regeneration: 24-month follow-up of a phase 1 clinical study. Sci Transl Med. 2010;2(46):46ra61.